METEOR-BERICHTE

98-2

Nordatlantik 1996

Cruise No. 36
6 June 1996 - 4 November 1996

Edited by:
Jürgen Mienert, Gerhard Graf, Christoph Hemleben, Klaus Kremling, Olaf Pfannkuche, Detlef Schulz-Bull

Editorial Assistance:
Frank Schmieder
Fachbereich Geowissenschaften, Universität Bremen
Manon Wilken, Keiko Kähler-Mähl, Marcia Schwartz
GEOMAR, Universität Kiel

Leitstelle METEOR
Institut für Meereskunde der Universität Hamburg

1998

Table of Contents

		Page
Abstract		ix
Zusammenfassung		ix
1	Research Objectives	1
1.1	Leg M 36/1	1
1.2	Leg M 36/2	1
1.3	Leg M 36/3	1
1.4	Leg M 36/4	2
1.5	Leg M 36/5	2
1.6	Leg M 36/6	2
2	Participants	6
3	Research Programme	17
3.1	Leg M 36/1	17
3.1.1	International Intercomparison of underway pCO_2 Systems	18
3.1.2	Organic Tracers	18
3.1.3	Trace Elements	18
3.1.4	Hydrography	19
3.2	Leg M 36/2	19
3.2.1	Hydrography	19
3.2.2	Marine CO_2 System	19
3.2.3	Organic Tracer	20
3.2.4	Trace Elements	21
3.2.5	Natural Radionuclides	21
3.2.6	Dissolved Organic Matter	22
3.2.7	Planktology	22
3.2.8	Planktonic Foraminifers	23
3.3	Leg M 36/3	23
3.3.1	European North Atlantic Margin (ENAM)	23
3.3.2	Geophysical Signals in Sediments	24

		Page
3.3.3	Pelagic Processes and Particle Flux from the Pelagic Region to the Ice Edge	24
3.3.4	Settlement Pattern and Material Deposit in the Benthal	25
3.3.5	Metabolism and Diagenetical Modification of Production and Environment Factors	26
3.3.6	Chronostratigraphy and Palaeoceanography by Isotopes: Quantitative Reconstruction of Models	27
3.3.7	Palaeontology of the Pelagic Changes in the late Quaternary	27
3.4	Leg 36/4	28
3.4.1	Particle Flux in the Benthic Boundary Layer, Benthic Foraminiferal Habitats and early Diagenetic Processes in Deep-Sea Environments (BIGSET)	28
3.4.2	Carbon Remineralization by the Benthic Community	28
3.4.3	Processes within the Nepholoid Layers and in the Sediment	29
3.4.4	Organic Matter Degradation, Denitrification and Trace Metal Diagenesis	29
3.4.5	Particle Flux and in-situ Aggregate Studies at the Continental Margin	30
3.4.6	Distribution of Methane $\delta^{13}C$ of TCO_2	30
3.5	Leg M 36/5	30
3.5.1	Physical Oceanography	30
3.5.2	Chemical Oceanography	31
3.5.3	Biological Oceanography - Planktology and Microbiology	31
3.5.4	Population Dynamics and Flux of Calcareous Zoo- and Phytoplankton in the North Atlantic	32
3.5.5	Molecular Genetic Differentiation among Planktic Foraminifera as Indicators of Water Masses	32
3.6	Leg M 36/6	33
3.6.1	Preservation Potential of the Primary Climatic and Environmental Signals in Deep-Sea Sediments	33
3.6.2	Particle Flux in the Benthic Boundary Layer, Benthic Foraminiferal Habitats and early Diagenetic Processes in Deep-Sea Environments	34
3.6.3	Benthic Remineralization and Activity Rates	34
3.6.4	Microbial Degradation Processes in the Sediment	34
3.6.5	Trophic Relationships and Biological Fluxes in the Bathy- and Benthopelagic Zone	35
3.6.7	Geochemical Investigations of Organic Matter Degradation in Surface Sediments	36

Page

3.6.8 Interaction of Seasonally Variable Benthic Turnover Rates and Distribution of Trace Elements in Deep-Sea Sediments 37

4 Narrative of the Cruise 38

4.1 Leg M 36/1 (D. Schulz-Bull) 38

4.2 Leg M 36/2 (K. Kremling) 40

4.3 Leg M 36/3 (J. Mienert) 44

4.4 Leg M 36/4 (G. Graf) 48

4.5 Leg M 36/5 (C. Hemleben) 48

4.6 Leg M 36/6 (O. Pfannkuche) 51

5 Preliminary Results 55

5.1 Leg M 36/1 55
5.1.1 Physical Oceanography (J. Waniek) 55
5.1.1.1 Shipboard Results 55
5.1.2 First International At-Sea Intercomparison of Underway pCO_2 Systems (A. Körtzinger, L. Mintrop) 59
5.1.2.1 Scientific Background of the Exercise 59
5.1.2.2 Technical Aspects of the Exercise 62
5.1.2.3 Shipboard Results 63

5.2 Leg M 36/2 67
5.2.1 Physical Oceanography (J. Waniek, P. Schröder) 67
5.2.1.1 Shipboard Results 69
5.2.2 Chemical Oceanography 72
5.2.2.1 Marine CO_2 System, Dissolved Oxygen, and Nutrients (L. Mintrop, S. Schweinsberg, F. Malien) 72
5.2.2.2 Shipboard Results 73
5.2.2.3 Amino Acids: Shipboard Results (U. Lundgreen) 79
5.2.2.4 Trace Element: Shipboard Results (J. Kuss, P. Streu, A. Prang, K. Kremling) 85
5.2.2.5 Distribution of Natural Radionuclides in the Water Column: Shipboard Results (J. Scholten, S. Vogler, K. Schmikale) 90
5.2.3 Biological Oceanography: Shipboard Results 91

			Page
	5.2.3.1	Dissolved Organic Carbon and Nitrogen (DOC and DON) (P. Kähler)	91
	5.2.3.2	Upper Ocean Biology along a Transect at 20°W during Summer 1996 (W. Koeve, M. Schroeter, C. Sellmer, C. Reineke, W. Gaul)	97
	5.2.3.3	Production and Flux of Biogenous Calcareous Particles in the Eastern North Atlantic (R. Schiebel, A. Zeltner, A.-B. von Gyldenfeldt)	101
		Shipboard Results	103
5.3	Leg M 36/3		105
5.3.1	Geology (O. Costello, D. Dreger, J. Simstich, E. Steen)		105
	5.3.1.1	Faeroe-Shetland Channel	105
	5.3.1.2	Sampling of Box Cores	105
	5.3.1.3	Sampling of Diatoms from Sediments and Surface Water	108
	5.3.1.4	Sampling of the Water Column for Isotopic Analysis	108
	5.3.1.5	Coring Devices	108
5.3.2	Geophysics: HF-OBH Wide Angle Experiments (J. Mienert, J. Posewang, M. Baumann, X. Liu)		110
	5.3.2.1	Seismic Source and OBH Deployments	112
	5.3.2.2	HF-OBH Measurements and PARASOUND and DTB Profiles at HF-OBH Stations	113
5.3.3	Geophysics: Parasound and Hydrosweep Profiling (F.-J. Hollender, X. Liu, J. Posewang, O. Bothmann, J. Simstich, D. Dreger, O. Costello)		120
	5.3.3.1	Faeroe-Shetland Channel and North Sea Fan	120
	5.3.3.2	Northern Voering Plateau	122
	5.3.3.3	Greenland Basin and Denmark Strait	132
5.3.4	High-Resolution Deep-Tow Boomer Profiling in the Region of the Traendjupet Slide off Mid-Norway (D. Evans, D.G. Wallis, N.C. Campbell)		136
	5.3.4.1	Geological Background	137
	5.3.4.2	Operations	139
	5.3.4.3	The Deep-Tow Boomer (DTB) System	139
	5.3.4.4	Mobilisation	141
	5.3.4.5	Deployments	141
	5.3.4.6	Preliminary Interpretation of Data	143
5.3.5	Palaeontology of the Pelagic Realm (H. Andruleit, S. Jensen)		149
	5.3.5.1	Shipboard Results	150

Page

5.3.6 Planktology
(O. Haupt, E. Bauernfeind, M. Krumbholz, G. Donner) 151
5.3.6.1 Shipboard Results 151
5.3.7 Bentho-Pelagic Coupling in the Northern North Atlantic
(J. Berg, O. Bothmann, W. Ritzrau, A. Scheltz, D. Seiler) 153
5.3.8 Marine Geochemistry
(J. Maaßen, A. Flügge, A. Lunau, T. Körner) 156
5.3.8.1 Shipboard Results: Organic Chemistry 156
5.3.8.2 Shipboard Results: Sea Floor Oxygen in-situ Analyser (FLOORIAN) 159
5.3.8.3 Shipboard Results: Nutrients and Dissolved Oxygen 159
5.3.9 CTD Deployments on M 36/3 (H. Beese, O. Haupt) 160

5.4 Leg M 36/4 168
5.4.1 CTD Deployments (T. Viergutz) 168
5.4.2 Hydrosweep (T. Schillhorn, L. Thomsen) 168
5.4.3 Parasound (T. Schillhorn, L. Thomsen) 168
5.4.4 Microbiology in the Benthic Boundary Layer
(K.-P. Witzel, W. Ritzrau) 170
5.4.5 Distribution of Methane and $\delta^{13}C$ of total CO_2 (M. Friedrichs) 171
5.4.6 Processes in the Benthic Boundary Layer at the Whittard Canyon (L. Thomsen, G. Graf) 172
5.4.6.1 Shipboard Results 172
5.4.7 BENGAL: Benthic Bioturbation and Bioirrigation
(R. Turnewitsch, G. Graf) 174
5.4.8 Benthic Foraminiferal Habitats and early Diagenetic Processes in Deep-Sea Environments (A. Keller) 175
5.4.8.1 Shipboard Results 176
5.4.9 Oxygen and Phytopigment Distribution in the Sediment
(J.J.M. Belgers) 176
5.4.10 Organic Matter Degradation, Denitrification and Trace Metal Diagenesis (S. Otto, T. Stöver, C. Maeß) 180
5.4.10.1 Shipboard Results 181

5.5 Leg M 36/5 181
5.5.1 Hydrographical Studies
(T.P. Zeitzschel, J. Waniek, K. Bülow, P. Schröder) 181
5.5.1.1 Shipboard Results 182
5.5.2 Dissolved Inorganic Carbon Measurements (C.C. Neill) 185
5.5.2.1 Shipboard Results 188
5.5.3 Alkalinity and pH Measurements (J.M.G. Pineiro) 188

Page

5.5.4 Bacterial Degradation of Organic Matter (C. Petry, D. Setzkorn) 195
5.5.4.1 Shipboard Results 195
5.5.5 Planktological Studies (T.P. Zeitzschel, C. Sellmer, U. Fehner, K. Nachtigall, C. Reineke, P. Fritsche, K. Lisok, B. Obermüller, D. Adam) 197
5.5.5.1 Shipboard Results 198
5.5.5.2 First Results from Microscopic Studies of the Net Samples 198
5.5.5.3 Shipboard Results from Experimental work for Production Measurements (^{14}C and ^{15}N uptake) 199
5.5.6 Primary Production- P vs I Experiments (B. Irwin) 201
5.5.7 Zooplankton (U. Zeller) 201
5.5.7.1 Shipboard Results 201
5.5.8 Calcareous Zoo- and Phytoplankton (C. Hemleben, R. Schiebel) 204
5.5.8.1 Shipboard Results 204
5.5.9 Molecular Genetic Differentiation among Planktic Foraminifera as Indicators of Water Masses (M. Langer, C. Hemleben) 204
5.5.9.1 Shipboard Results 208

5.6 Leg M 36/6 208
5.6.1 Benthic Standing Stock and Activity in the Benthic Boundary Layer at the BIOTRANS and BENGAL Site (O. Pfannkuche, B. Springer, R. Turnewitsch, A. Cremer, A. Kähler, T. Viergutz) 208
5.6.1.1 Shipboard Results: Standing Stock and Activity of Small Benthic Size Classes 208
5.6.1.2 Shipboard Results: Benthic Respiratory Activity 212
5.6.1.3 Shipboard Results: Bioturbation and Bioirrigation 212
5.6.1.4 Shipboard Results: Benthic Boundary Layer Activity 214
5.6.2 Meiofauna Sampling at the BENGAL and BIOTRANS Station (T. Mutch) 215
5.6.3 Benthic Foraminifera at the BENGAL and BIOTRANS Station (P. Heinz, F. Kurbjeweit) 216
5.6.3.1 Experiments 217
5.6.3.2 Shipboard Results 217
5.6.4 Microbial Enzyme Activities in the NE Atlantic Deep-Sea (A. Boetius, C. Chwieralski) 218
5.6.4.1 Shipboard Results 218
5.6.5 Bacterial Biomass and Community Structure (D. Eardly) 220
5.6.6 Benthopelagic Fauna (B. Christiansen) 222
5.6.7 Geochemistry (D. Rickert, H. Schale, S. Grandel, A. Bleyer) 223

Page

5.6.7.1 Shipboard Results: Sediment Geochemistry and Nutrients in the Water Column 224
5.6.8 Biogeochemistry of Sediments and Megafauna of the Porcupine Abyssal Plain (I. Horsfall) 228
5.6.9 Geochemical Analysis of Near Bottom Water and Sediments (D. Panagiotaras) 229
5.6.10 Particle Flux and Organic Geochemistry of Sediments and Pore Waters (P. Schäfer, N. Lahajnar) 229
5.6.10.1 Shipboard Results of Sediment Trap Analysis 229

6 Ship's Meteorological Station 234
6.1 Weather and Meteorological Conditions during Leg M 36/1 (C. Joppich) 234
6.2 Weather and Meteorological Conditions during Leg M 36/2 (G. Kahl, H.-P. Lambert) 234
6.3 Weather and Meteorological Conditions during Leg M 36/3 (G. Kahl, H.-P. Lampert) 235
6.4 Weather and Meteorological Conditions during Leg M 36/4 (G. Kahl, W.-T. Ochsenhirt) 237
6.5 Weather and Meteorological Conditions during Leg M 36/5 (H. Weiland) 237
6.6 Weather and Meteorological Conditions during Leg M 36/6 (D. Bassek, H. Weiland) 238

7 Lists 239

7.1 Leg M 36/1 239
7.1.1 List of Stations 239

7.2 Leg M 36/2 240
7.2.1 List of Stations 240

7.3 Leg M 36/3 248
7.3.1 List of Stations 248

7.4 Leg M 36/4 256
7.4.1 List of Stations 256
7.4.2 HS and PS Profiles 260

7.5 Leg M 36/5 261
7.5.1 List of Stations 261
7.5.2 Water Sample Data Summary Database 271

		Page
	7.5.3 Stations and Depths Analysed	287
	7.5.4 Samples Collected at Stations	288
7.6	Leg M 36/6	290
	7.6.1 Pore Water Profiles	290
	7.6.2 List of Stations	294
8	Concluding Remarks	298
9	References	299

Abstract

The METEOR cruise no. 36 included six legs and five major research programmes in which 37 institutes participated to study recent and past changes of North Atlantic environments (Fig. 1a, Tab. 3). On legs 1 and 2 the measurements of chemical parameters of the upper water mass layer contributed to the international Joint Global Ocean Flux Study (JGOFS). In a transect from the Bermudas to the Canary Islands and to the Northeast Atlantic they accomplished measurements of organic and inorganic traces and how much of the dissolved organic carbon (DOC) contributes to the carbon export. Second, international pCO_2 intercomparisons during the cruises were aimed to improve estimations of the oceanic uptake of anthropogenic CO_2. During leg 3 biological and hydrographical long-term stations on the Voering Plateau, the Norwegian Basin and East Greenland contributed to the goals of the SFB 313 and aided in understanding changes in the vertical particle fluxes in the water column and the transport of organic carbon to the upper sediment layer. Geophysical studies of submarine gas hydrates, a major carbon reservoir, focused on the European North Atlantic Margin programme (ENAM) and aimed towards a better understanding of slope instabilities and their climatic relevance on the mid-Norwegian margin. Legs 4, 5 and 6 contributed mainly to studies of Bio-Geochemical Transports of Matter and Energy in the Deep Sea (BIGSET) and the Benthic Biology and Geochemistry of a Northeastern Atlantic Abyssal Locality (BENGAL). While the fate of sediment organic matter and the role of different ecological groups and their interactions are key questions for the quantification of biochemical and geochemical fluxes within the benthic boundary layer (BBL), the modification of the incoming chemical signal from the overlying surface waters by a combination of physical, chemical and biological processes are key questions for the quantification and characterisation of the ultimate deposition.

Zusammenfassung

Die METEOR Forschungsfahrt Nr. 36 bestand aus sechs Fahrtabschnitten und fünf großen Forschungsprogrammen, an denen 37 Institute teilgenommen haben, um gegenwärtige und vergangene Umweltveränderungen des Nordatlantiks zu erforschen (Abb. 1a, Tab. 3). Während des 1. und 2. Fahrtabschnittes dienten Messungen von chemischen Parametern der oberen Wassermassenschicht als Beitrag zum internationalen Forschungsprogramm Joint Global Ocean Flux Study (JGOFS). In einem Transekt von den Bermudas zu den Kanarischen Inseln und zum Nordostatlantik wurden Messungen organischer und anorganischer Spurenstoffe vorgenommen. Es wurde untersucht, wieviel vom gelösten organischen Kohlenstoff (Dissolved Organic Carbon, DOC) zum Kohlenstoffexport beiträgt. Außerdem wurden während der Fahrten internationale pCO_2-Vergleichsmessungen durchgeführt mit dem Ziel, Abschätzungen der ozeanischen Aufnahme von anthropogenem CO_2 zu standardisieren und zu verbessern. Während des 3. Fahrtabschnittes wurden biologische und hydrographische Langzeitstationen am Vøring-Plateau, dem Norwegenbecken und im Ostgrönlandbecken für den Sonderforschungsbereich 313 (SFB 313) durchgeführt, die dem Verständnis von Veränderungen im vertikalen Partikelfluß in der Wassersäule sowie des Transports des

organischen Kohlenstoffs in die obere Sedimentschicht dienen. Das ENAM-Programm (European North Atlantic Margin) konzentrierte sich auf geophysikalische Studien von Gashydraten. Sie sind ein wichtiger Kohlenstoffspeicher und für ein besseres Verständnis von Kontinentalabhangs-Instabilitäten und deren Klimarelevanz von Bedeutung. Die Fahrtabschnitte 4, 5 und 6 dienten hauptsächlich als Beitrag zu Studien des BIGSET- (Bio-Geochemical Transports of Matter and Energy in the Deep Sea) und des BENGAL-Projektes (Benthic Biology and Geochemistry of a Northeastern Atlantic Abyssal Locality). Während der Verbleib von sedimentorganischen Substanzen und die Rolle verschiedener ökologischer Gruppen sowie ihrer Interaktion wichtig für die Quantifizierung biochemischer und geochemischer Flüsse innerhalb der benthischen Grenzschicht (Benthic Boundary Layer, BBL) sind, ist die weitere Modifikation des eingehenden geochemischen Signals durch eine Kombination physikalischer, chemischer und biologischer Prozeßabläufe von Bedeutung für eine Quantifizierung der Abbauraten.

1 Research Objectives

1.1 Leg M 36/1

M 36/1 was aimed to contribute to the international Joint Global Ocean Flux Study (JGOFS). JGOFS is a long-term programme to determine and understand on a global scale the processes controlling the time varying fluxes of carbon and associated elements in the ocean. During leg 1 several chemical parameters of the upper water mass layer in a transect of the North Atlantic, from Hamilton (Bermudas) - 47°N, 42°W to the Canary Islands were determined, especially the organic and inorganic traces and the components of the CO_2 system. A second aim was the international pCO_2 intercomparison exercise with 10 groups from 6 nations.

1.2 Leg M 36/2

The objectives of leg 2 were to continue research activities in the framework of the German JGOFS projects with their main project "Long-term studies on the variability of particle flux in the North Atlantic". The aim of this study is to determine and understand the processes controlling the short-term, seasonal and interannually varying fluxes of carbon and associated (trace) biogenic elements and compounds in different climatic regions of the North Atlantic. Another important aspect of the German JGOFS programme during leg 2 were measurements on the CO_2 system in the North Atlantic (see also M 36/1). The intention was to improve estimations of the oceanic uptake of anthropogenic CO_2. These investigations were accompanied by studies on how much of the dissolved organic carbon (DOC) contributes to the carbon export and by observations on the population dynamics and flux of calcareous phyto- and zooplankton in the northeast Atlantic.

1.3 Leg M 36/3

Based on results of several earlier expeditions M 36/3 continued research of the SFB 313 along the Norwegian and East Greenland continental slope. The goals included biological and hydrographical long-term studies on the Voering Plateau, Norwegian Basin and East Greenland Basin and served to understand the changes in vertical particle fluxes in the water column, e.g. the transport of organic carbon to the upper sediment layer. Geophysical studies of the SFB 313 and ENAM focused on sediment mass wasting areas along the Norwegian continental slope. A better understanding of slope instabilities and gas hydrate instabilities and their climatic relevance will lead to a better understanding of large scale margin sedimentary processes and their likelihood of climatic impacts.

1.4 Leg M 36/4

M 36/4 contributed to BENGAL an international deep-sea programme which has the aim to study the long-term variability, seasonality of fluxes to the sea floor, and especially the particle exchange between the benthic nepheloid layers and the sediments down to the bioturbation depth. The studies also contributed to the Ocean Margin Exchange (OMEX) programme which is also funded by the EU. The aim was to investigate the cross shelf edge transport of particles, which is topographically channelled through canyons. The Whittard Canyon on the Celtic-Irish continental slope was chosen as an example.

1.5 Leg M 36/5

Major tasks relate to the JGOFS programme, primarily to the long-term particle study of the North Atlantic during autumn. The work was mainly conducted at the central BIOTRANS station. Continual surface examinations as well as highly dissolvable vertical profiles of the water column up to a depth of 2500 m were carried out. Apart from the JGOFS work in the pelagic region, tasks related to BIGSET and the new long-term station BENGAL were accomplished.

1.6 Leg M 36/6

The sixth cruise leg was dedicated to the research programmes „Biogeochemical transports of matter and energy in the deep sea" (BIGSET) and „High resolution temporal and spatial study of the Benthic biology and Geochemistry of a northeastern Atlantic abyssal Locality" (BENGAL).

BIGSET is concerned with the biogeochemical processes in the ecosystem of the deep sea. The main objective is the fate of sedimenting organic matter. Investigations concentrate on the abyssopelagic and benthic realm with the benthic boundary layer (BBL) as a focal point. The BBL is defined as a zone extending from the clear water minimum to about one metre into the sediment, containing the nepheloid layer, the bottom contact water and the bioturbated sediment horizons. The quantification of biochemical and geochemical fluxes (esp. carbon compounds and opal) within the BBL, the identification of the role of different ecological groups and their interactions are key questions. The investigations increased our knowledge of deep ocean fluxes and the early diagenesis of pelagic sediments, thus also being important for a better interpretation of the geological record.

BENGAL aims to quantify and characterise the incoming flux (with time-lapse sediment traps and midwater particle cameras), its resuspension (with transmissometers and current meters) and its ultimate deposition (with chemical analysis of core samples and time-lapse sea bed photography). Once on the sea floor, the diagenesis of the incoming flux and its incorporation into the sediment was studied with benthic landers to measure solute fluxes across the sediment

water interface and to conduct in-situ manipulations. Photographic sediment profile imaging was used extensively here for the first time in the deep sea. The resulting data will be employed to develop a number of models with predictive capabilities for the effect of the pulsed incoming flux on the BBL and vice versa.

Tab. 1: Legs and chief scientists of METEOR cruise No. 36

Leg M 36/1

6 June 1996 - 19 June 1996
Bermuda/United Kingdom - Las Palmas/Canary Islands
Chief Scientist: Dr. D. Schulz-Bull

Leg M 36/2

21 June 1996 - 18 July 1996
Las Palmas/Canary Islands - Bergen/Norway
Chief Scientist: Dr. K. Kremling

Leg M 36/3

21 July 1996 - 17 August 1996
Bergen/Norway - Reykjavik/Iceland
Chief Scientist: Dr. J. Mienert

Leg M 36/4

20 August 1996 - 5 September 1996
Reykjavik/Iceland - Lisbon/Portugal
Chief Scientist: Prof. Dr. G. Graf

Leg M 36/5

7 September 1996 - 6 October 1996
Lisbon/Portugal - Vigo/Spain
Chief Scientist: Prof. Dr. C. Hemleben

Leg M 36/6

9 October 1996 - 4 November 1996
Vigo/Spain - Viana do Castelo/Portugal
Chief Scientist: Dr. O. Pfannkuche

Masters (FS METEOR):

Captain M. Kull (M 36/1 - M 36/4)
Captain D. Kalthoff (M 36/5 - M 36/6)

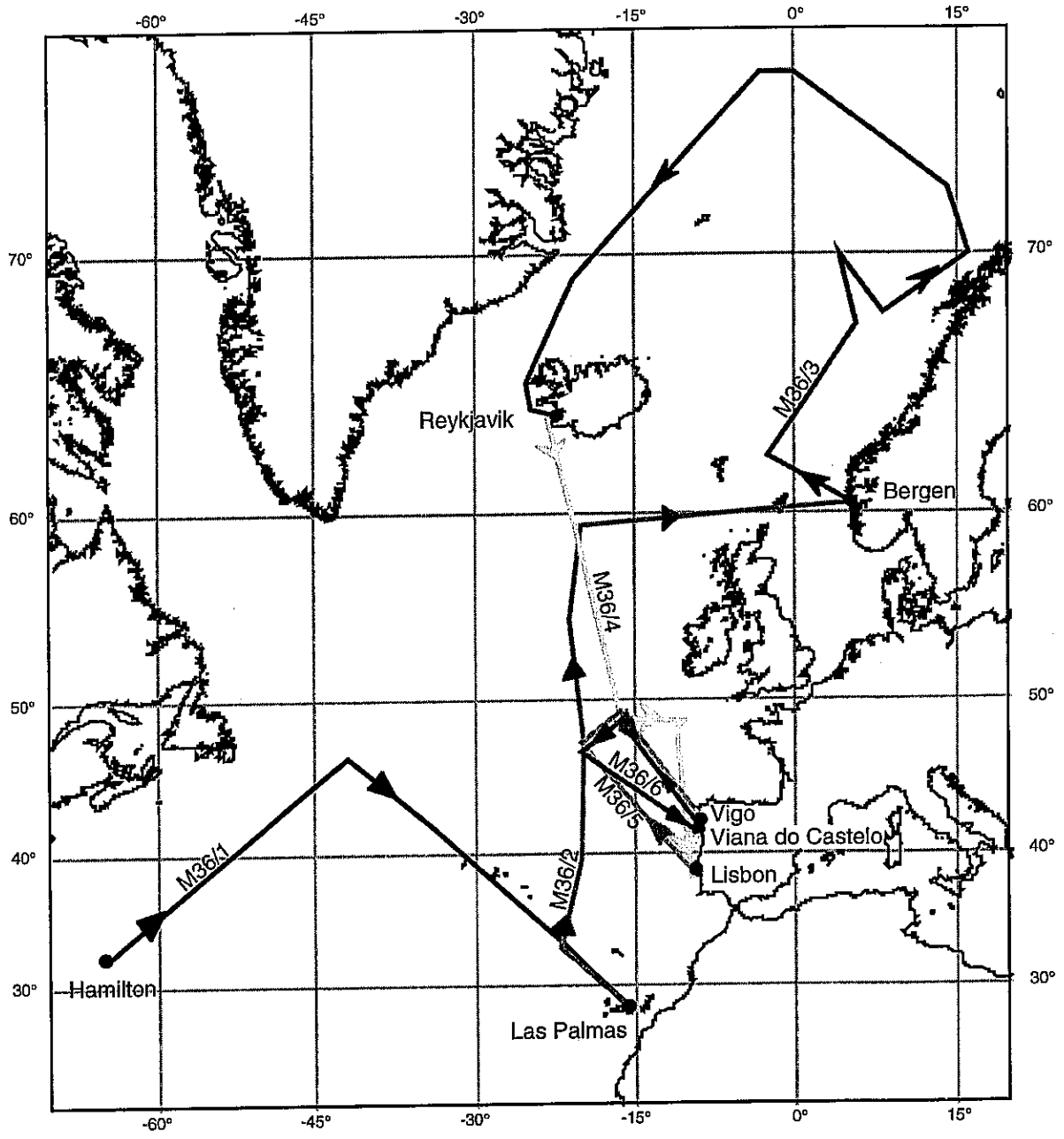

Fig. 1a: Ship's track of METEOR cruise M 36/1 - M 36/6

2 Participants

Tab. 2: Participants of METEOR cruise No. 36

Leg M 36/1

Name	Speciality	Institute
Schulz-Bull, Detlef, Dr. (Chief Scientist)	Marine Chemistry	IfMK
Brunet, Christian	Marine Chemistry	UP&MC
Eischeid, Greg	Marine Chemistry	WHOI
Ishii, Masao, Dr.	Marine Chemistry	MRI
Johnson, Kenneth	Marine Chemistry	BNL
Joppich, Christoph	Meteorology	DWD
Körtzinger, Arne, Dr.	Marine Chemistry	IfMK
Kuß, Joachim, Dr.	Marine Chemistry	IfMK
Lambert, Hans-Peter	Meteorology	DWD
Lembrecht, Anette,	Marine Chemistry	IfMK
Lundgreen, Ulrich, Dr.	Marine Chemistry	IfMK
Maaßen, Jörg, Dr.	Marine Chemistry	IfMK
Malien, Frank	Marine Chemistry	IfMK
Mintrop, Ludger, Dr.	Marine Chemistry	IfMK
Neill, Craig	Marine Chemistry	BNL
Ohtaki, Eiji, Prof.	Marine Chemistry	OU
Parks, Justine	Marine Chemistry	SIO
Pineiro, Jesus Gago	Marine Chemistry	IIM
Prang, Angela	Marine Chemistry	IfMK
Schauer, Bernard	Marine Chemistry	UP&MC
Schweinsberg, Susanne	Marine Chemistry	IfMK
Streu, Peter	Marine Chemistry	IfMK
Torres, S. Rodrigo	Marine Chemistry	NBI
Towler, Philip, Dr.	Marine Chemistry	CSIRO
Waniek, Joanna	Oceanography	IfMK
Yamashita, Eiji, Dr.	Marine Chemistry	OU
Yoshikawa, Hisayuki, Dr.	Marine Chemistry	MRI

Tab. 2: continued

Leg M 36/2

Name	Speciality	Institute
Kremling, Klaus, Dr. (Chief Scientist)	Marine Chemistry	IfMK
Anders, Tania-Maria, Dipl.-Geol.	Geology	SFB 313
Gaul, Wilhelm, Student	Planktology	IfMK
Kahl, Gerhard, Dipl.-Geogr.	Meteorology	DWD
Kähler, Paul, Dr.	Planktology	IOW
Koeve, Wolfgang, Dr.	Planktology	IfMK
Kuß, Joachim, Dr.	Marine Chemistry	IfMK
Lambert, Hans-Peter, Technician	Meteorology	DWD
Lembrecht, Anette, Technician	Marine Chemistry	IfMK
Lundgreen, Ulrich, Dr.	Marine Chemistry	IfMK
Malien, Frank, Technician	Marine Chemistry	IfMK
Mintrop, Ludger, Dr.	Marine Chemistry	GEOB
Osterroht, Christoph, Dr.	Marine Chemistry	IfMK
Petersen, Johannes, Technician	Marine Chemistry	IfMK
Prang, Angela, Technician	Marine Chemistry	IfMK
Reineke, Cornelia, Technician	Planktology	IfMK
Rosell-Melé, Antoni, Dr.	Marine Chemistry	UOB
Schankin, Holger, Student	Planktology	IOW
Schmikale, Karen, Technician	Geochemistry	GPIK
Schröder, Petra, Student	Planktology	IfMK
Schroeter, Marcel, Student	Planktology	IfMK
Schweinsberg, Susanne, Technician	Marine Chemistry	IfMK
Sellmer, Claudia, Dipl.-Biol.	Planktology	IfMK
Streu, Peter, Technician	Marine Chemistry	IfMK
v. Gyldenfeldt, Anna, Dipl.-Oz.	Paleontology	GPIT
Vogler, Sven, Dipl.-Phys.	Geochemistry	AKWH
Waniek, Joanna, Dipl.-Oz.	Oceanography	IfMK
Will, Stefan, Technician	Marine Chemistry	IfMK
Zeltner, Alexandra, Dipl.-Oz.	Paleontology	GPIT

Tab. 2: continued

Leg M 36/3

Name	Speciality	Institute
Mienert, Jürgen, Dr. (Chief Scientist)	Geophysics	SFB 313/ GEOMAR
Andruleit, Harald, Dr.	Micropaleontology	SFB 313
Baumann, Marlyse, Dr.	Geophysics	GEOMAR
Beese, Helmut, Technician	Electronics	SFB 313
Berg, Jörg Stefan	Benthology	SFB 313
Bothmann, Oliver, Technician	Benthology	
Brett, Colin, Technician	Geophysics	BGS
Costello, Oran	Micropaleontology	SFB 313
Donner, Gabi	Planktology	SFB 313
Dreger, Derek	Micropaleontology	SFB 313
Evans, Dan, Dr.	Geophysics	BGS
Flügge, Arnim	Marine Chemistry	SFB 313
Gedamke, Michael	Benthology	SFB 313
Haupt, Olaf, Dr.	Planktology	SFB 313
Hollender, Franz-Josef, Dr.	Geophysics B1	SFB 313
Jensen, Stefan	Micropaleontology	SFB 313
Kahl, Gerhard	Meteorology	DWD
Körner, Thomas	Marine Chemistry	SFB 313
Krumbholz, Marita	Planktology	SFB 313
Lambert, Hans-Peter	Meteorology	DWD
Liu, Xanxia, Dr.	Geophysics	GEOMAR
Lunau, Angela, Technician	Marine Chemistry	SFB 313
Maaßen, Jörg, Dr.	Marine Chemistry	SFB 313
Posewang, Jörg, Dr.	Geophysics B1	SFB 313
Ritzrau, Will, Dr.	Benthology	SFB 313
Scheltz, Annette	Benthology	SFB 313
Seiler, Dan	Benthology	SFB 313
Simstich, Johannes, Dr.	Geology	SFB 313
Steen, Eric, Technician	Core Sampling	SFB 313
Wallis, David G.	Geophysics	BGS

Tab. 2: continued

Leg M 36/4

Name	Speciality	Institute
Graf, G., Prof. Dr. (Chief Scientist)	Benthology	GEOMAR
Belgers, Jan, Dr.	Benthology	GEOMAR
Boldt, Andrea, Student	Benthology	GEOMAR
Friedrichs, Michael, Dipl. Biol.	Benthology	GEOMAR
Gutthann, Franziska, Student	Benthology	GEOMAR
Kahl, Gerhard, Dipl. Meteor.	Meteorology	DWD
Kähler, Anja, Technician	Biogeochemistry	GEOMAR
Keller, Angela, Dr.	Micropaleontology	GPIT
Knuth, Erich, Dipl.-Met.	Meteorology	DWD
Maeß, Christian, Dipl. Chem.	Marine Chemistry	UBMCh
Ochsenhirt, Wolf-Thilo, Techn.	Meteorology	DWD
Otto, Sabine, Dipl. Chem.	Marine Chemistry	UBMCh
Queisser, Wolfgang, Techn.	Benthology	GEOMAR
Ritzrau, Will, Dr.	Benthology	SFB 313
Sanders, Dirk, Dipl. Chem.	Marine Chemistry	IfMK
Schillhorn, Thies, Dipl. Geophy.	Geophysics	GEOMAR
Stöver, Tatjana, Student	Marine Chemistry	UBMCh
Thomsen, Laurenz, Dr.	Benthology	GEOMAR
Treude, Tina, Student	Benthology	GEOMAR
Turnewitsch, Robert, Dipl. Biol.	Benthology	GEOMAR
Viergutz, Thomas, Technician	Electronics	GEOMAR
Witzel, Karl-Paul, Dr.	Microbiology	MPI

Tab. 2: continued

Leg M 36/5

Name	Speciality	Institite
Hemleben, Christoph, Prof. Dr. (Chief Scientist)	Micropaleontology	GPIT
Adam, Dorothee, Student	Planktology	IfMK
Bayer, Magret, Technician	Micropaleontology	GPIT
Boldt, Andrea, Student	Benthosbiology	GEOMAR
Bülow, Katherina, Dipl.-Oz.	Oceanography	IfMK
Fehner, Uwe, Dipl.-Biol.	Planktology	IfMK
Flaiz, Sabine, Technician	Micropaleontology	GPIT
Forberich, Björn, Meteorologist	Meteorology	DWD
Fritsche, Peter, Technician	Planktology	IfMK
Irwin, Brian, Dr., Biol.	Planktology	BIC
Lisok, Katrin, Student	Planktology	IfMK
Kahl, Gerhard, Dipl. Meteor.	Meteorology	DWD
Karpen, Volker, Student	Benthosbiology	GEOMAR
Langer, Martin, Dr. Mikropal.	Molecularbiology	GPIT
Nachtigal, Kerstin, Technician	Planktology	IfMK
Neill, Craig, Dr.	CO_2	BNL
Obermüller, Birgitt, Student	Planktology	IfMK
Ochsenhirt, Wolf-Thilo, Techn.	Meteorology	DWD
Petry, Carolin, Dipl.-Biol.	Microbiology	IOW
Pineiro, Jesus Manuel Gago	Alkalinity	IIM
Reineke, Cornelia, Technician	Planktology	IfMK
Schankin, Holger, Student	Microbiology	IOW
Schröder, Petra, Student	Planktology	IfMK
Sellmer, Claudia, Dipl.-Biol.	Planktology	IfMK
Setzkorn, Dorothea	Microbiology	IOW
Waniek, Joanna, Dipl.-Oz.	Oceanography	IfMK
Zeller, Ute, Dr. Diol.	Planktology	IfMK

Tab. 2: continued

Leg M 36/6

Name	Speciality	Institute
Pfannkuche, Olaf, Dr. (Chief Scientist)	Benthic Biology	GEOMAR
Bassek, Dieter	Meteorology	DWD
Berg, Stefan	Benthic Biology	SFB 313
Bleyer, Anke, Technician	Geochemistry	GEOMAR
Boetius, Antje, Dr.	Microbiology	IOW
Bülow, Katharina	Physical Oceanography	IfMK
Christiansen, Bernd, Dr.	Planktology	IHF
Chwieralski, Caroline	Microbiology	IOW
Cremer, Axel, Dipl.-Ing.	Electronics	GEOMAR
Eardly, Donal, Dr.	Microbiology	UCG
Fehner, Uwe	Planktology	IfMK
Gaul, Wilhelm	Planktology	IfMK
Grandel, Sibylle	Geochemistry	GEOMAR
Heinz, Petra	Paleontology	GPIT
Horsfall, Ian, Dr.	Biogeochemistry	UCG
Janßen, Felix	Benthic Biology	GEOMAR
Janßen, Silke	Planktology	IHF
Kähler, Anja, Technician	Benthic Biology	GEOMAR
Kurbjeweit, Frank, Dr.	Paleontology	GPIT
Lahajner, Niko	Biogeochemistry	IBM
Lunau, Angela	Benthic Biology	GEOMAR
Mutch, Thomas James, Dr.	Benthic Biology	SOC
Panagiotaras, Dionisos	Geochemistry	GUP
Rickert, Dirk	Geochemistry	GEOMAR
Schäfer, Petra, Dr.	Geochemistry	IBM
Schale, Holger	Biogeochemistry	CBM
Springer, Barbara, Dr.	Benthic Biology	GEOMAR
Turnewitsch, Robert, Dr.	Benthic Biology	GEOMAR
Viergutz, Thomas, Technician	Electronics	GEOMAR
Weiland, Hans	Meteorology	DWD

Tab. 3: Participating Institutes

AKWH	Akademie der Wissenschaften Heidelberg Im Neuenheimer Feld 336 69120 Heidelberg Germany
BGS	British Geological Survey Kingsley Dunham Centre Keyworth Nottingham, NG 12 5GG United Kingdom
BIC	Marine Ecology Laboratory Bedford Institute of Oceanography Dartmouth Nova Scotia, B2Y4A2 Canada
BNL	Brookhaven National Laboratory Oceanographic and Atmospheric Sciences Division Upton Long Island, NY 11973 USA
CBM	Institut für Chemie und Biologie des Meeres Universität Oldenburg Carl-von-Ossietzky Straße 9-11 26111 Oldenburg Germany
CSIRO	Commonwealth Scientific and Industrial Research Organisation Division of Oceanography Castry Esplanade Hobart TAS 7001 Australia

Tab. 3: continued

DWD	Deutscher Wetterdienst Geschäftsfeld Seeschiffahrt Postfach 30 11 90 20304 Hamburg Germany
GEOB	Fachbereich Geowissenschaften Universität Bremen Postfach 33 04 40 28359 Bremen Germany
GEOMAR	Forschungszentrum für marine Geowissenschaften der Christian-Albrechts Universität zu Kiel Wischhofstr. 1-3 24148 Kiel Germany
GPIK	Geologisch-Paläontologisches Institut und Museum der Christian-Albrechts Universität zu Kiel Olshausenstr. 40 24118 Kiel Germany
GUP	Department of Geology University of Patras 26110 Patras Greece
GPIT	Institut und Museum für Geologie und Paläontologie Universität Tübingen Sigwartstraße 10 72076 Tübingen Germany

Tab. 3: continued

IBM	Zentrum für Meeres- und Klimaforschung Institut für Biogeochemie und Meereschemie Universität Hamburg Bundesstr. 55 20146 Hamburg Germany
IfMK	Institut für Meereskunde an der Universität Kiel Düsternbrooker Weg 20 24105 Kiel Germany
IHF	Institut für Hydrobiologie und Fischereiwissenschaften Universität Hamburg Zeiseweg 9 22765 Hamburg Germany
IIM	Instituto de Investigacions Marinas Eduardo Cabello 6 36208 Vigo Spain
MPI	Max-Planck-Institut August-Thienemann-Str. 2 24306 Plön Germany
IOW	Institut für Ostseeforschung Warnemünde Seestraße 15 18119 Rostock-Warnemünde Germany

Tab. 3: continued

MRI	Meteorological Research Institute Nagamine 1-1 Tsukuba, Ibaraki 305 Japan
NBI	Niels Bohr Institute for Astronomy Physics and Geophysics University of Copenhagen Juliane Maries Vej 30 Copenhagen Denmark
NIOZ	Netherlands Institute of Sea Research P.O.Box 59 Den Burg (Texel), 1790 AB The Netherlands
OU	Okayama University Faculty of Environmental Science and Technology Tsushima-Naka 2-1-1 Okayama 700 Japan
SIO	Scripps Institution of Oceanography Marine Physical Laboratory 9500 Gilman Drive La Jolla, CA 92093-0902 USA
SFB 313	Sonderforschungsbereich 313 der Universität Kiel Heinrich-Hecht-Platz 10 24118 Kiel Germany

Tab. 3: continued

SOC	Southampton Oceanographic Centre Empress Dock Southampton, SO 143 ZH United Kingdom
UBMCh	FB 2 Meereschmie Universität Bremen Postfach 33044028334 Bremen Germany
UCG	The Martin Ryan Marine Science Institute University College, Galway Ireland
UOB	Environmental and Analytical Section University of Bristol School of Chemistry Cantocks Close, Bristol BS8 1TS United Kingdom
UP&MC	Université Pierre et Marie Curie (Paris VI) Laboratoire Physique et Chimie Marines 4 Place Jussieu, Tour 24-25 5230 Paris, Cedex 05 France
WHOI	Woods Hole Oceanographic Institution Department of Marine Chemistry and Geochemistry 360 Woods Hole Road Woods Hole, MA 02543 USA

3 Research Programme

3.1 Leg M 36/1

3.1.1 International Intercomparison of underway pCO_2 Systems

Currently different concepts are used in order to quantify the oceanic uptake of CO_2. These efforts are being undertaken in light of the atmospheric perturbation and its possible impact on the climate. One important concept is based on the determination of the partial pressure difference (ΔpCO_2) between surface seawater and the overlying air, which is the driving force for any net exchange of CO_2. By means of a transfer coefficient, this measured ΔpCO_2 can be converted into a momentary net flux of CO_2 across the air/sea interface. Keeping in mind the strong variation of pCO_2 in time and space, this concept has to come up with representative mean ΔpCO_2 values on a global grid. If this concept is to be successful, the combined effort of research groups all over the world is necessary. One important requirement, however, is a good inter-laboratory comparability of the data sets, which are derived from quite different types of analytical systems. While the present precision of the various systems is of the order of 1 µatm, not much is known about the comparability between the laboratories.

As a first important step to assess the current state of this parameter, an international shore-based intercomparison exercise was carried out in June 1994 at the Scripps Institution of Oceanography, La Jolla/USA. However, the general consensus was that a necessary second step would be an at-sea intercomparison under realistic operation conditions.

The first leg of METEOR cruise No. 36 was perfectly suited for such an exercise. 10 groups from 6 nations participated in the important exercise. Underway samples from the surface layer (7 m depth) were taken continuously by the Kiel pumping system for the measurements of chemical parameters. The following investigations were planned:

- Continuous measurements of partial pressure of CO_2, alkalinity and pH by about 10 groups;
- collection of suspended particulate matter using an ultracentrifuge for the analysis of trace elements and organic compounds (amino acids, alkenones, PCB and other);
- registration of salinity, temperature and nutrient concentration;
- measurements of DOC and DON.

All participating groups operated their underway pCO_2 systems simultaneously on a special seawater pumping system and a consistent set of calibration gases. Measurements of various other parameters were carried out to provide a broad data base, which provides the necessary background information and strongly enhances interpretation of the exercise's results. Additional measurements included the following parameters: Total dissolved inorganic carbon, alkalinity, and partial pressure of CO_2 in discrete samples, pH continuity in surface waters, pH in discrete samples, temperature and salinity of the surface water, as well as nutrients.

3.1.2 Organic Tracers

The major aim of the organic studies was to get information about the biological influence on the chemical composition of the particulate material. During leg M 36/1, investigations were carried out on horizontal distribution of biogenic markers (amino acids, alkenones and alkanes) and on anthropogenic tracers (e.g. PCB). Large volume samples of surface SPM were collected from the steaming ship with the Kiel pumping system. The dissolved organics were extracted from seawater by XAD resins.

During the first leg of METEOR cruise 36, we concentrated on the sampling of suspended particulate matter (SPM) in the water column. The surface was sampled by means of the Kiel pumping system (KPS) and SPM was trapped in a continuous flow centrifuge. Analyses of the amino acid content of the collected matter will be performed after freeze-drying in conjunction with the trace elements group in the home laboratory.

Water profiles were obtained from in-situ pumping systems, which can filtrate up to 2000 l of water. The filtrates will be subsampled for the analysis of amino acids, the rest will be analysed for the organic tracers POC/PON.

The aim of the investigation is to get information about the variability of SPM amino acid content and composition in dependence on the physical-biological state of the water column. How will the amino acid content respond to a change in the phyto-plankton/zooplankton ratio caused by passing different water masses during the ship's course?

3.1.3 Trace Elements

One fundamental problem of chemical oceanography is the strikingly low concentrations of trace elements in seawater. So far they can only be explained by sorption on and sedimentation with biogenic particles. The distribution of trace elements between water and suspended particulate matter (SPM) and its variability in relation to biological processes in the surface layer has to be investigated in different climatic regions. As a comparison, the composition of SPM in different depths of the water column is investigated. In this context, the special purposes for the first cruise leg were as follows:

- Study of the chemical composition of suspended particulates in dependence on depth, time, space and physical and biological "events"
- Is the binding of trace elements to organic material biologically controlled?
- How fast does the remineralization follow changes in the biological and chemical parameters within the water column?
- How do plankton blooms influence trace elements delivered to the sea by atmospheric deposition?

3.1.4 Hydrography

The objective of the hydrographic programme during leg 1 was the detailed description of the surface physical environment along the cruise track in selected areas of the subtropical and moderate North Atlantic.
Special emphasis during this leg was focused on the documentation of the variability of the temperature field at sea surface and at depth. The spatial and vertical variability of the temperature field was investigated by XBT drops (Expandable Bathythermographs) every 40 nm down to 1800 m depth. At several positions a few CTD casts were also made (Fig. 2). From the temperature profiles, the depth of the mixed layer and characteristics of the eddy field can be estimated.

3.2 Leg M 36/2

3.2.1 Hydrography

The objective of the programme during leg 2 was the detailed description of the physical environment along 20°W in selected areas of the subtropical, moderate and subarctical North Atlantic and are, therefore, a substantial precondition for the interpretation of biological and chemical results.

Special emphasis during this leg was placed on the documentation of the variability of the mixed layer in relation to the circulation patterns at greater depth of several main stations. In addition, diurnal changes in the mixed layer depth and their forcing functions (insulation, air temperature and wind stress) were monitored using CTD-O_2-fluorescence profiles and shipborne sensors.

The spatial and vertical variability of the hydrographic field between the main CTD stations was investigated by short CTD casts (upper 500 m). The spatial variability of the temperature field was monitored by XBT drops (upper 1800 m of the water column). The depth of the mixed layer and characteristics of eddies can be estimated from the temperature profiles. The work at the mooring positions is concentrated on the first analysis of the physical data (acoustical and mechanical current meters, inclinometer) and on the maintenance of equipment for the next deployment.

3.2.2 Marine CO_2 System

The CO_2 project's field work is based on the full analytical determination of the marine CO_2 system as well as ancillary measurements of nutrients and dissolved oxygen. The generated data sets allow the use of different concepts for the quantification of the oceanic uptake of anthropogenic CO_2. The coupling of hydrographic, chemical and biological factors with the

marine CO_2 system as well as the degree of disequilibrium with respect to CO_2 between surface seawater and overlying air are important objectives of the scientific strategy.

Based on the measurements, we focus on two different concepts for the quantification of the oceanic uptake of anthropogenic CO_2. One is the calculation of the net flux of CO_2 across the air-sea interface from the knowledge of the partial pressure difference (ΔpCO_2) between the two bulk layers and the transfer coefficient. The second is a back-calculation technique to quantify the anthropogenic part of the total dissolved inorganic carbon content in seawater. Results of the distribution pattern of anthropogenic CO_2 in the ocean also serve as an important tool in the validation of distributions derived from General Circulation Models, which simulate only the anthropogenic component of the total dissolved inorganic carbon. This parameter, however, is not susceptible to direct measurement.

3.2.3 Organic Tracers

The JGOFS Kiel organic chemistry group is studying the long- and short-term variation in the vertical flux of particulate organic compounds. The major aim was to get information about the biological influence on chemical composition and on degradation and changing processes of organic particles in the water column.

During leg M 36/2, investigations were carried out on formation and transport of naturally occurring organic substances (amino acids, alkenones and pigments, in co-operation with the University of Bristol) and on anthropogenic tracers (hydrocarbons like PCB, PAH and pesticides) in different climatic regions.

Large volume samples of surface suspended particulate matter (SPM) were collected while the ship was steaming using the Kiel pumping system (KPS). The chemical composition of particulates will be studied in collaboration with the Trace Elements group.

During the second leg, the following questions were of special interest:

- Are the changes in the composition of sedimenting organic matter in relation to time, space, particle size and physical or biological events in the surface layer?
- How do the composition of particulate and dissolved organic matter change with water depth?
- What are the particulate 'biomarkers' that may provide information about biological composition of the remote ocean?
- What kind of vertical concentration profiles exist for dissolved anthropogenic traces (e.g. PCB) and what is the concentration in suspended particulate matter (SPM)?
- What is the relationship between organic tracers and trace elements?

In addition, during this cruise investigations on dissolved organic acids in North Atlantic surface waters were continued. The results shall be discussed in relationship to other variables

(e.g. concentration of nutrients, dissolved organic carbon (DOC)/dissolved organic nitrogen (DON) contents) and will be compared with measurements taken during cruise M 26/1.

3.2.4 Trace Elements

The vertical flux of particulate trace elements (TE) and its short- and long-term variations were investigated. This study was related to the investigations of particulate organic compounds and particulate natural radionuclides.

The programme of leg 1 was continued. A major aim during M 36/2 cruise was to investigate the vertical flux of trace elements and its variability in relation to biological processes in the surface layer in different climatic regions. In this context, the special supplementary studies for the second cruise leg are as follows:

- Investigation of seasonal variations of trace element fluxes using sediment traps.
- Is the binding of trace elements to organic material biologically controlled?
- How fast does the remineralization follow changes in the biological and chemical parameters within the water column?
- How do plankton blooms influence the flux of trace elements delivered to the sea by atmospheric deposition?
- What are the compositional differences between suspended particulate matter (SPM) and sedimenting particles?

3.2.5 Natural Radionuclides

This JGOFS project studies the distribution of natural radionuclides (^{234}Th, ^{232}Th, ^{230}Th, ^{231}Pa, ^{210}Po, ^{210}Pb) in the water column and the seasonal and spatial variations of radionuclide fluxes in sediment traps.

One aim of the project is to examine the exchange rates of particles in the water column. By means of Th-scavenging models the exchange rates between dissolved phases and suspended particles (adsorption and desorption), as well as the exchange rates between suspended and sinking particles (aggregation and disaggregation), shall be determined. In this context, the terms of chemical modification of sinking particles are of further interest.

Another objective is to investigate the trapping efficiency of the sediment traps, which is an important factor for the determination of oceanic fluxes and mass balances. In measuring the distribution of radionuclides in the water column and in sediment traps the trapping efficiency can be calculated.

The investigations will also include radionuclide measurements in surface sediments and in near bottom nepheloid layers in order to evaluate the advective sediment supply and to compare fluxes in sediment traps with those in sediments.

3.2.6 Dissolved Organic Matter

During leg 2 the seasonal cycle of DOC and DON concentrations, which has been measured at 47°N/20°W during the past years, should be completed with measurements during summer and autumn seasons. It could be shown that DOC contributes little to the long-term carbon export in the ocean. Accumulation of DOC in surface waters, however, can be considerably high during the summer season, with major consequences for the seasonal carbon balance.

The programme consists of DOC and DON measurements in horizontal transects and vertical profiles. Experiments with bacteria growing with dissolved organic matter (DOM) as the sole carbon source were carried out. The following aspects were studied:

- Divergences in the uptake ratio of CO_2 and dissolved inorganic nitrogen (DIN) from the Redfield ratio;
- availability of deep-water DOM to bacteria;
- nutrient requirement for bacterial degradation of DOM;
- carbon export from the surface via DOC;
- measurement of DOC/DON in sediment trap supernatants to correct particulate organic carbon (POC)/particulate organic nitrogen (PON) particle flux data.

3.2.7 Planktology

During leg 2 the planktological work group studied characteristic summer-like features of optical and biological properties of the epipelagic system in the northeast Atlantic. This study is intended to extend detailed observations from a two ship experiment in 1993 at the BIOTRANS site (47°N/20°W) along the 20th meridian. Furthermore, data collected during this cruise will contribute to an extensive data base covering almost the whole annual cycle.

Profiling optical measurements and sampling for a diverse number of planktological measurements using a CTD/rosette system were carried out at the three long-term mooring positions and at about 15 additional stations. The measurements should help to describe typical vertical structures of the three different domains of productivity (subtropical-oligotrophic, mesotrophic and subarctic-eutrophic) that were passed during the cruise. It was intended to concentrate on measurements of size fractionated 'new production' and biomass and on biomass distribution and production of nanoplanktic calcified autotrophs.

Additional sampling for other JGOFS level one parameters was carried out. Surface sampling along the south-north transect between the Canary Islands and Bergen completed the planktological programme. Chl.-a measurements were carried out at distances of about 10 nm. These measurements are thought of as a contribution to the calibration data set for the SeaWifs satellite, which is expected to be launched in May 1996.

3.2.8 Planktonic Foraminifers

The major topics were the population dynamics and the flux of calcareous phyto- and zooplankton in the northeast Atlantic. The population dynamic of pteropods and planktic foraminifers in conjunction with processes, controlling the export of calcareous skeletons, determine the skeleton distribution in the water column and in the sediment. The objectives of this part of the cruise were to quantitatively describe the temporal and the spatial distribution of the planktic calcareous flora and fauna and the calcareous particle flux. By comparing multinet and water sampler material with sediment trap samples, a detailed recording of the investigated flora and fauna is possible.

Earlier METEOR and POSEIDON cruises serve as a data base for the long-term study continued by this cruise. Additional investigation of coccolithophorids will help to complete our studies on the calcareous bioproduction. Processes in the productive zone and the water column down to 2500 m water depth were investigated mainly at the three JGOFS sites L1, L2, and L3. Process studies and long-term surveys were intended to investigate the fate of carbon and calcium in the water column and increased our understanding of climate change (historical sedimentary record).

3.3 Leg M 36/3

3.3.1 European North Atlantic Margin (ENAM)

The cruise on the one hand followed aims by the SFB 313 "Changes in the environment: The northern North Atlantic" and on the other hand those of ENAM (European North Atlantic Margin).

The overall objectives of ENAM II are to quantify and model large-scale sedimentary processes and material fluxes and to assess their relation to the variability of oceanic and cryospheric processes. The timing, causes and flow behaviour of mass wasting events and the relationship between mass wasting events and deep-sea fan developments were to be determined in order to understand the spatial and temporal variability of marine systems from the shelf edge to the continental slope and the deep sea. The work areas encompass, from north to south, three major mass wasting and high-sedimentation rate areas between Spitsbergen and the Voering Plateau. These key regions have been selected where basic morphodynamic features and sedimentary processes of the ocean margin allow high-resolution studies of the formation and timing of the processes and their products. Seismic (reflection) high-resolution deep-towed lines were to be made along and transverse to the mass wasting areas, and high-sediment accumulation rate areas along the northeastern Atlantic margin. Seismic data should be collected to establish sufficiently dense data coverage for quantifying processes and material fluxes and particularly to tie together existing data from stable and high accumulation rate regions. Based on this information the frequencies of large-scale events should be determined for each of the three margin sectors. Existing and new long-range side-scan sonar image data (GLORIA) should be

combined with seismic data to provide the needed morphological and seismic stratigraphic context. Detailed geophysical investigations in the vicinity of the sediment slides were made in selected areas with high-frequency ocean-bottom seismometers. As a result, high-resolution geophysical information about the propagation of sound in sea-floor sediments help determine (1) whether free gas and/or gas hydrates exist in sea-floor sediments and (2) how it influences sediment slope stabilities.

3.3.2 Geophysical Signals in Sediments

Project B1 of the SFB 313 concentrated on geophysical determinations of sea floor physical properties of the continental slopes of Norway and East Greenland. Morphological-physical sea floor data were used to deduct from it first, the main transport pathways of bottom water currents and sediments, and second, the potential for sediment instability on continental slopes. The examination of gas hydrates and free gas in sediments is of crucial importance for the determination of the instability of sediment layers. A number of different geophysical examination methods were used to determine the potential for slope instability. Apart from seismic profiling and sediment core investigations, the HF Ocean Bottom Hydrophone (HF-OBH) was deployed. The HF-OBH measures the propagation velocity of compressional waves in sediments below the depth reached by gravity cores. It is, therefore, well suited to determine free gas (low pressure velocity) or gas hydrate zones (high pressure velocity) which occurred in the upper 300 m of the sediment column on the Mid-Norwegian margin. High resolution seismic profile lines with a deep-towed seismic boomer ideally allow to combine the results of the wide-angle HF-OBH's measurements and seismic profiles. All of these projects were in collaboration with ENAM of the European Union.

3.3.3 Pelagic Processes and Particle Flux from the Pelagic Region to the Ice Edge

The investigations aimed at elucidating the relationship between the pelagic cycling of matter and particle exports in the Norwegian Greenland Sea. The participation in the METEOR cruise enabled us to conduct research in the ice-free area of this region and to compare results with those obtained during the same season in the ice-edge system further north in the East Greenland current and adjacent waters (POLARSTERN cruise, 1994). We postulated differences between both production regimes with respect to quantity and quality of suspended particles and particle exports from the euphotic zone. In summer there are stratified waters with low nutrient concentrations. We expected a smaller particle load in the water column with a restricted diatom contribution to the autotrophic biomass and a more intense coupling between autotrophs and heterotrophs than in the ice-edge pelagic system. This should result in a low particle flux that is mainly controlled by heterotrophs. The sampling programme also aimed at documenting the production and particle flux potential that leaves the Greenland Sea during summer via southward moving currents. In the framework of the SFB 313, the investigations provide information about the transfer of organic matter and organisms to the sea floor and,

hence, contribute to understanding of the pelagic-benthic coupling and the micro palaeontological record.

3.3.4 Settlement Pattern and Material Deposit in the Benthal

The benthos work focused on interactions between the bottom nepheloid layer (BNL) and the upper sediment layer.

Recent investigations indicate that biological and physical resuspension result in elevated particle concentrations in the BNL. Even at low flow velocities the lateral advective particle flux exceeds the vertical flux arriving at the sea floor. For this reason, the final incorporation of particles into the sediment depends not only on the arriving particle flux, but also on bottom topography as well as the density and composition of the benthic community, which actively intercepts particles and incorporates them into the sediment by biodeposition.

The focus of our work was on the interaction of the amount, the composition and the flux of particles in the BNL and the dispersion patterns and activity of benthic communities.

Our proposed programme included:
- investigations on the distribution and structure of macrobenthic communities, at the sea floor proper and in the BNL;
- the assessment of micro- and mesoscale dispersion patterns of benthic populations;
- the analyses of BNL characteristics in terms of the amount and composition of particles in relation to near-bed current velocities and direction;
- measurements of the metabolic performance of the sediment community as well as of individual macro benthos organisms;
- evaluation of biodeposition and bioentrainment rates of benthic communities along the main outflow region of the northern North Atlantic;
- investigation of benthospelagic coupling at a mooring position where measurements of the annual sedimentation pattern were estimated by the SFB-plankton group.

These goals were planned to be accomplished by completing two transects in the Denmark Strait (work area 4). The spatial distribution, structure and activity of benthic communities as well as particle characteristics of the BNL in the main outflow area of the northern North Atlantic were proposed to be studied on a transect which would cover the Denmark Strait from the Icelandic to the Greenland shelf. One transect along the present current direction in the Denmark Strait will allow to elucidate interactions between the BNL and benthic communities and the influence of benthic organisms on the lateral particle flux, i.e. the potential near-bottom export of particulate matter from the northern North Atlantic.
Additional focus was set towards the bentho-pelagic coupling by revisiting stations of SFB moorings at 75°N/3°W (work area 3).

To achieve the given goals, we wanted to deploy the following equipment:

For the inventory of mega epibenthos, a remodelled epibenthic sledge should be deployed. Additionally, the macrobenthic epi- and infauna should be collected using a box corer. The vertical distribution of chemical and biogeochemical parameters should be assessed by deploying a multiple corer. For the characterisation of the BNL a newly designed bottom-water sampler retrieved water samples and gave information on current velocity and direction within the last metre of the BNL, i.e. just above the sediment/water interface.

3.3.5 Metabolism and Diagenetical Modification of Production and Environment Factors

Particulate matter plays a major role in the biogeochemical cycle of carbon in the oceans. The main aim on M 36 was early diagenesis investigations of organic biomarkers (n-alkanes, isoprenoids, alkenones), anthropogenic tracers (PCBs) as well as primary productivity indicators like opal and barium within the water column and fluxes through the water/sediment interface. Investigations for the understanding of the decrease of organic carbon in surface sediments were planned with a newly developed in-situ O_2 profiler recording high-resolution (50-100 µm) profiles of oxygen in surface sediment samples. Measurements of nutrients complete the geochemical and organo-chemical studies.

From these measurements, in combination with mooring experiments, hints for the reconstruction of productivity ratios from sedimentary recorded accumulation rates of organic markers, i.e. organism specific biomarkers of Prymnesiophyceen (C37, C38-alkenones), were expected. In comparison with the characterisation and quantification of seasonal variations of the chemical marker composition of sinking particles, the organic matter flux should be correlated to the input and decrease of organic carbon.

Investigations concentrating on water column and surface sediments should be taken mainly at the long-time mooring position NB9 (70°N/4°E) in the Norwegian Basin and the main SFB work area in the Denmark Strait. In addition, samples at selected SFB stations around 75°N should be collected. Surface water sampling should be carried out by a snorkelling system attached to the hydrographic dome. Vertical profiles of the water column are obtained from a series of in-situ deep-sea pumps. Measurements of organic biomarkers (isoprenoides, alkanes and alkenones), anthropogenic tracers (PCBs) and nutrients were planned. The long-time mooring at 70°N/4°E (NB9), which was changed in 1995 on POSEIDON Cruise 209/3, should be changed.

In addition to sampling in the water column, investigations at the water/sediment interface should take place at all sites. At this interface strong gradients in physical, chemical and biological properties occur. The O_2 gradients within the upper sediment centimetres should be measured by a high-resolution (50-100 µm) in-situ O_2/pH profiler. Besides the use of the in-situ O_2 profiler, surface sediment samples should be taken by multicorer and box corer. Organic biomarker gradients, as a key to the understanding of the different processes and the nature of the complex chemical composition of organic matter, should be obtained from these samples.

During the cruise the collected labile organic material should be prepared for subsequent analysis onshore.

3.3.6 Chronostratigraphy and Palaeoceanography by Isotopes: Quantitative Reconstruction of Models

Project B2 aims at a data basis for a high-resolution time scale in the region of the Faeroe-Shetland sill. This area between the Norwegian-Greenland Sea and the North Atlantic is very well suited for the reconstruction of the thermohaline circulation and abrupt climatic oscillations. The expected chronostratigraphy of the core transect should provide an important data base for high-resolution palaeoceanographic studies.

3.3.7 Palaeontology of the Pelagic Changes in the late Quaternary

Until now, investigations on living siliceous (radiolarians, diatoms), calcareous (coccolithophorids, planktonic foraminifera) and organic-walled microplankton (dinoflagellate-cysts) from the water masses of the northern North Atlantic were seldom.

In recent years, systematic investigations on the occurrence and distribution of these plankton groups in the water column of the northern North Atlantic were carried out and are to be continued on M 36/3. The western and southwestern part (Denmark Strait) of the Norwegian-Greenland Sea was the main work area. Additionally, the water column at the long-term mooring station of the SFB (NB9) should be sampled. Investigations should be extended to the southern, ice-free areas of the Denmark Strait. Regional and vertical changes in the composition of plankton assemblages were of major interest.

In 1994 (ARK X) a documentation of living dinoflagellates in the northern North Atlantic was started in cooperation with Prof. J. Dodge (University of London) and was continued during M 36/3. Sampling took place in the above mentioned work area. Continuous sampling using the "membrane pump" was planned.

Sediment trap investigations revealed that selected radiolarians are typical deep-water species. This is of special interest for the reconstruction of the former vertical structure of the water column. Therefore, the investigations on the vertical distribution of radiolarians and, additionally, planktonic foraminifera should be continued with open/closing nets (down to 2000 m depth).

3.4 Leg M 36/4

3.4.1 Particle Flux in the Benthic Boundary Layer, Benthic Foraminiferal Habitats and early Diagenetic Processes in Deep-Sea Environments (BIGSET)

Benthic foraminifera are sensitive to the input of organic carbon and, therefore, they are a proper proxy for the evaluation of the benthic-pelagic coupling. Variations in the flux of organic particles result in changes of the faunal structure of benthic foraminifera and ostracods. The particle flux within the benthic boundary layer should be measured and its impact on benthic microhabitats described. Changes in the biomass of the benthic foraminifera, their specific behaviour (feeding, chamber formation, reproduction), and their contribution to the bioturbation (mobility of different species) should be investigated. Temporal changes in the particle composition of the sediment should be quantified. This leads to a description of the impact of benthic foraminifera and ostracods on the sediment/water interface and, therefore, to a fine-scale resolution of early diagenetic processes. The knowledge of degradation processes and their interactive relationship allows for the quantification of remineralization and of the material buried in the sediment. To fulfil the aims the following work was carried out:

- Sediment sampling by multicorer (MUC);
- Observations of living benthic foraminifera: Documentation of the sediment surface and sections for comparison with our laboratory results;
- Sediment slices of 1 cm fixed and stained with Rose Bengal;
- Transmission-Electron Microscope fixations (TEM; trophic structure);
- Sampling of sediments for cultures in Tübingen;
- Feeding experiments with benthic foraminifera under high pressure;
- Sampling of bottom water from MUC tubes (stable isotopes);
- Participation in sampling of the bottom water sampler (particle flux, stable isotopes).

3.4.2 Carbon Remineralization by the Benthic Community

Remineralization rates are the result of all carbon transport processes occurring in the water column. Parameterization of the processes acting in the benthal should be required to estimate the fraction of carbon that is recycled back into the ocean versus that which is permanently buried. A better understanding of the biological, chemical and physical processes and the measurement of the corresponding rates are required for a balance of carbon flux through the sediment.

Measurements of benthic respiration rates, biomass production and activity are necessary to estimate the role of benthic organisms for the carbon flux through the sediment. Recent results from the temperate Northeast Atlantic demonstrated a strong seasonality in benthic biomass production, respiration and activity rates which were coupled with sedimentation events. The major part of benthic carbon consumption goes into respiration, lying in the range of 80-95% of total benthic carbon consumption.

The main objective of the benthic programme was the quantification of the biologically mediated carbon flux through the sediment by following the benthic reaction (remineralization, burial rates) toward sedimentation pulses. The canyon areas should be studied additionally.

3.4.3 Processes within the Nepholoid Layers and in the Sediment

In the deep sea, high-energy events like "benthic storms" support the existence of bottom nepheloid layers. These BNLs are commonly found at continental margins. Lateral particle fluxes in the benthic boundary layer far exceed the vertical fluxes from the euphotic zone. The fluxes are dominated by fast sinking particles whereas the mass of particles consist of fine slow sinking particles.

The aim of the project is the investigation of the following processes: particle transport within internal boundary layers, especially in canyons, sedimentation, accumulation and mass fluxes of particulate matter. With the help of CTD water samplers and a transmissiometer, samples should be taken in the deep-sea and in the canyon area at the continental margin. With the help of the BIOPROBE bottom water sampler, flow velocity and light transmission should be determined and water samples at heights of 5, 10, 20 and 40 cm above the sea floor should be taken. A particle camera will take video pictures of aggregates. Gravity cores should be used to determine sediment accumulation rates.

3.4.4 Organic Matter Degradation, Denitrification and Trace Metal Diagenesis

The project contributed to the understanding of the cycling of trace elements, nitrogen and carbon at continental margins, where benthic processes are expected to play a significant role for the chemistry of the whole ocean. Necessary for the understanding of the major controls over release fluxes from boundary sediments is a detailed investigation of early diagenetic processes acting within the sediments. Therefore, it was planned to conduct extensive work on pore water chemistry and on solid sediment phases at transects across the continental margin. First the integrated rate of organic matter remineralization in near-surface sediments was quantified on transects across the continental margin by modelling the pore-water profiles of involved solutes. In dependence on both, the diagenetic redox milieu brought about by this process and the input terms, the benthic reactions and fluxes of selected trace metals should be investigated during M 36/4 to assess the significance of margin processes for the chemistry of the ocean. It was presumed that sediment regions highly intense organic matter recycling are predominantly those areas on the slope from where preferentially dissolved trace components are injected into the ocean. By analysing the trace metal content in trapped particles, suspended material, sediments and pore waters, we should contribute to finding relationships between vertical/lateral sedimentation fluxes, benthic release fluxes and burial rates of chemically differing elements. A special study should deal with sedimentary denitrification in continental margin sediments because fixed nitrogen is removed from the pool available to plants only by denitrification and

because margin sediments provide optimal conditions for this process so that ocean margins may act as a barrier for the delivery of eutrophic coastal nitrogen to the ocean.

3.4.5 Particle Flux and in-situ Aggregate Studies at the Continental Margin

A central aim of the project is to determine the flux of material both along and across the European continental margin and specifically to attempt to quantify elemental exchange between the shelf and the open ocean. The site chosen for this study lies on the Goban Spur (between 47°N-50°N and 10°W-14°W) where relatively low current speeds and a gradual continental slope make this area amenable to the deployment of sediment traps. Current speeds at all depths were lower than 15-20 cm/sec, above which the collection efficiency of sediment traps is thought to be biased. It is apparent from current meter data at 1445 m that the predominant currents on the slope flow in a poleward direction, following the depth contours in this region. At 3665 m, currents at intermediate water depth flow in an off-slope direction, presumably taking with them material from the slope. Indeed, the sediment trap at 1460 m water depth at this site shows an increase in collected material as compared to the trap 1100 m above it. Low current speeds at this site and the indication of lateral off-slope transport seem to complement the data from benthic investigations showing that the continental rise is an area of accumulation.

3.4.6 Distribution of Methane and $\delta^{13}C$ of TCO_2

In order to evaluate the role of biotic processes for the transfer of CO_2 through the upper ocean boundary, it is intended to determine the pattern of the vertical and horizontal distribution of methane and the $\delta^{13}C$ of total CO_2 in the water column. The $\delta^{13}C$ signal of total CO_2 in the water column reflects the interaction of the following processes, whose relative significance was determined: primary production, upwelling, gas exchange as well as lateral mixing and advection. Especially the role of canyons should be studied.

3.5 Leg M 36/5

3.5.1 Physical Oceanography

M 36/5 is planned to study the late summer/autumn system. Based on observations from earlier studies in the investigation area, we expect that a detailed description of the mesoscale structures is essential to understand the pelagic system during late summer/autumn. Hydrographic investigations (XBT and CTD) enable a detailed description of the physical environment in the research area and are therefore substantial preconditions for a variety of biological-chemical studies.

3.5.2 Chemical Oceanography

The main objective of M 36/5 was to aim for a better understanding of the carbon cycle. Models of the global carbon cycle indicate that approximately 30% of the anthropogenic carbon dioxyde (CO_2) are taken up by the ocean. One of the goals of JGOFS (Global Ocean Flux Studies) is to determine the processes controlling carbon fluxes between atmosphere, ocean, and sea floor and to quantify marine sinks and sources of CO_2. Apart from chemophysical dissolution and release of CO_2 by calcifying organisms, other biological processes play an important role for the distribution of CO_2 in the sea ("biological pump"). Former measurements reveal that the Northeast Atlantic represents a net CO_2 sink between summer and autumn. Thus, the aim of the M 36/5 was to investigate the hydrographical and chemophysical properties of the water column in addition to biological research in order to solve the questions above mentioned. The following parameters have been measured: temperature, salinity, CO_2, oxygen, alkalinity, transparency, nutrients (silicate, nitrogen, phosphate), calcium carbonate, dissolved organic carbon, chlorophyll, pigments, primary production, new production, photosynthesis vs. light penetration, bacterial production, phyto- and zooplankton. The scientific programmes for sampling and measurements on board were performed by members of four nations (Spain, Canada, USA and Germany). Preliminary results indicate a rather abrupt change in fertility (from low to high) in surface waters after strong winds caused a mixing of the water column. Thus, nutrients were introduced into surface layers from deeper parts of the water column. Viewed in total, the ocean summer situation has changed into a autumn situation which resembles an early spring bloom. Thus, the data may support a CO_2 sink situation during autumn.

Total alkalinity (TA) and total dissolved inorganic carbon (TIC) of seawater will be analysed onboard with the help of a potentiometric precision titration and the CO_2 coulometry. These results will be used to calculate the partial pressure of CO_2 (pCO_2) in seawater and the CO_2 flux between atmosphere and oceanic mixed layer. It is planned to apply an instrument for direct pCO_2 measurements in the mixed layer. The survey programme encompasses the continuous sampling of the mixed layer via a pump system (from approx. 7 m water depth) as well as measurements of discrete samples from the upper 1000 m of the water column.

3.5.3 Biological Oceanography - Planktology and Microbiology

The main goal of the planktological JGOFS project at IfM Kiel activities during this leg was to improve the understanding of the processes of particle formation, modification and primary particle export. Together with other German JGOFS projects, ship-intensive process studies were carried out to describe the relevant processes of the carbon cycle with an abundant number of different measurements. For the geographical focus of this work, the German JGOFS selected the BIOTRANS site (47°N/20°W). The focus on this cruise was to study in autumn a system, where we have a limited number of planktological observations at the study site in particular and the open North Atlantic in general; and testing hypotheses and the mechanism of

the physical and geomorphological control of biogeochemical processes. These results will add to a number of results carried out during other seasons at that site .

The vertical flux resulting from a phytoplankton bloom is also intensively remineralized by bacteria in the water column down to the permanent thermocline. Data of this microbial breakdown of organic matter in late summer and were rare up until the present.

The aim of the microbiological investigations was the determination of bacterial rates of degradation in the autumnal planktonic system. These studies are closely linked to the investigation of the standing stocks of the phytoplankton and of primary production. Special questions are the effect of storm mixing on sedimentation and the bacterial degradation of sinking particles.

3.5.4 Population Dynamics and Flux of Calcareous Zoo- and Phytoplankton in the North Atlantic

The objectives of this part of the cruise were to quantitatively describe the temporal and the spatial distribution of the planktic calcareous fauna (planktic foraminifera and Pteropods) and flora (Coccolithophorids) as well as the calcareous particle flux in the eastern North Atlantic. In particular the autumn plankton bloom at 47°N/20°W, and frontal systems and eddies will be studied. Comparing multinet- and water sampler material with sediment trap samples a detailed recording of the investigated fauna and flora is possible. In addition, investigation at BENGAL will begin. Processes in the productive zone and the water column down to 2500 m depth will be investigated. Process studies and long-term surveys are intended to investigate the fate of carbon and calcium in the water column and will increase our understanding of climate change (historical sedimentary record).

3.5.5 Molecular Genetic Differentiation among Planktic Foraminifera as Indicators of Water Masses

Comparative studies on DNA nucleotide sequences are important tools in evolutionary, biogeographic, ecologic and palaeobiologic inquiry that can be used in conjunction with the geologic record. The techniques are useful wherever genetic differentiation may have developed.

3.6 Leg M 36/6

3.6.1 Preservation Potential of the Primary Climatic and Environmental Signals in Deep-Sea Sediments

The transport of particulate matter and its turnover in the deep-sea benthic boundary layer was studied at two localities (BIOTRANS, BENGAL) in the western European Basin, an area of distinct seasonal sedimentation patterns. The biogeochemical turnover of matter and benthic activity rates were studied in the Benthic Boundary Layer (BBL) during a season when an expected autumn phytoplankton bloom (see chapter 5.5) may generate a sedimentation pulse to the sea floor. The distinct seasonal and regional variations of the vertical fluxes characteristic of the NE Atlantic suggest that this episodicity may also be found in benthic activity and fluxes. A comprehensive data set of long-term sediment trap deployments is available from both stations. These data sets facilitate the estimation of interannual variability in vertical fluxes.

These investigations continued the JGOFS studies of leg M 36/5 which were carried out at the same stations addressing the hydrography and biogeochemistry in the upper mixed water layer. The fields of investigation are described in the following chapters.

Biogeochemical input parameters were obtained by this sub-project for all other participating groups. Sedimenting and suspended particles were collected above and within the nepheloid layer and in the sediment. They were chemically quantified and characterised. These measurements provide information about turnover of matter in the deep sea and, furthermore, about the preservation potential of primary climatic and environmental signals from the epipelagic zone for palaeoceanographic studies:

- qualitative and quantitative characterisation of the sinking fluxes in the BBL and of suspended particles in the nepheloid layer;
- identification of factors controlling the early diagenetic changes of the organic material;
- investigation of the preservation sediments.

The transport of particulate matter and its turnover in the deep-sea benthic boundary layer was studied at two localities (BIOTRANS, BENGAL) in the western European Basin, an area of distinct seasonal sedimentation patterns. The biogeochemical turnover of matter and benthic activity rates were studied in the Benthic Boundary Layer (BBL) during a season when an expected autumn phytoplankton bloom (see chapter 5.5) may generate a sedimentation pulse to the sea floor. The distinct seasonal and regional variations of the vertical fluxes characteristic of the NE Atlantic suggest that this episodicity may also be found in benthic activity and fluxes. A comprehensive data set of long-term sediment trap deployments is available from both stations. These data sets facilitate the estimation of interannual variability in vertical fluxes.

3.6.2 Particle Flux in the Benthic Boundary Layer, Benthic Foraminiferal Habitats and early Diagenetic Processes in Deep-Sea Environments

Benthic foraminifera are sensitive to the input of organic carbon and, hence, they are a suitable proxy for the evaluation of the pelagic-benthic coupling. Variations in the flux of organic particles result in changes of the faunal structure of benthic foraminifera and ostracods. The particle flux within the benthic boundary layer will be measured and its impact on benthic microhabitats will be described. Changes in the biomass of the benthic foraminifera, their specific behaviour (feeding, building of chambers, reproduction), and their contribution to bioturbation (mobility of different species) were investigated. Changes in the particle composition of the sediment were quantified. This leads to a description of the impact of benthic foraminifera and ostracods on the sediment-water interface and, hence, to a fine-scale resolution of early diagenetic processes. The knowledge of degradation processes and their interactive relationship allows for the quantification of remineralization and of the material buried in the sediment.

3.6.3 Benthic Remineralization and Activity Rates

Investigations in the NE Atlantic (METEOR cruises M 21, M 27) demonstrated a close pelagic-abyssobenthic coupling. High sedimentation rates after phytoplankton blooms enhanced remineralization rates of the abyssal benthos. The main generators of these enhanced rates are micro-organisms (bacteria, protozoa). Within a short period, these groups can react to sedimentation pulses by activation of dormant cells or other resting stages as well as by their short generation times. The amplitude of the benthic reaction is limited by the amount of labile organic matter as shown by previous in-situ respiration measurements.

By comparing the two stations, which are characterised by different sedimentation rates, the following questions were addressed:

- How does the different seasonal input of organic carbon affect the biomass development and remineralization rates of the benthos?
- What are their effects on geochemical fluxes (ratio of remineralization rates/deposition rates)?
- What is the time lag between the sedimentation signal originating in the epi-/ mesopelagial and the benthic reactions?
- Which are the main horizons of biological degradation in the sediment column?

3.6.4 Microbial Degradation Processes in the Sediment

The vertical distribution of bacteria and of hydrolytic enzymes in the upper centimetres of the sediment gives indirect evidence of the level of food supply. When the input of organic matter increases, one of the first reactions will be an adaptive change in enzyme activity. Increase of bacterial biomass will only result with some delay when the supply of labile

organic matter is high enough. As basic microbial parameters indicative of C_{org} supply at different stations, bacterial biomass and the activity of different extracellular hydrolytic enzymes were determined.

The quantitative degradation of organic matter was investigated in experiments with different added organic substances under simulated deep-sea conditions. These experiments give estimates of microbial degradation rates in the sediment and about time scales of reaction to food input. These experiments will be interpreted in the context of the in-situ measurements of benthic oxygen demand and of vertical particle flux. Consumption of bacteria by benthic protozoa (e.g. foraminifera) was studied in pressure incubations. These data will be analysed in cooperation with the scientists of the University of Tübingen (Benthic foraminiferal habitats).

3.6.5 Trophic Relationships and Biological Fluxes in the Bathy- and Benthopelagic Zone

Zooplankton and nekton of the deep ocean interact in three ways with the carbon flux between the epipelagial and benthal:

1. Utilisation of organic carbon by ingestion, assimilation and metabolism;
2. Modification of sinking organic matter by ingestion and defecation;
3. Direct transport of carbon via vertical migration.

The investigations focused on the assessment of the organic carbon demand of bathy- and benthopelagic fauna in relation to the carbon input measured by sediment traps. This demand has to be seen also in relation to the other faunal components of the deep sea. These results, together with data on trophic relationships and vertical migrations, will be used in a model describing the carbon flux in the bathypelagial. Analysis of size spectra and the food of selected taxa provides information about the trophic structure. Budgeting the food supply (from sediment traps) and the nutritional demand will allow for an assessment of additional food sources like fast sinking, large falls of dead fish, squids, whales, salps etc. not included in sediment traps.

The following investigations were carried out:

- determination of the standing stocks and the distribution of bathy- and benthopelagic fauna with video/phototrawl (epibenthos) and MOCNESS (plankton and micronekton);
- estimation of the metabolic carbon demand from the measured biomasses and literature data on metabolism of deep-sea organisms.

3.6.6 Benthic Resuspension, Bioturbation and Bioirrigation

Particles in the benthic nepheloid layer (BNL) are generally very small and have very low sinking speeds. In the North Atlantic, a half-life of approx. 2 years is assumed for these particles. Sedimentation of large particles dominates the mass flux to the sea floor. Trapping of small particles by large ones provides the main transport for suspended small particles to the sediment. Measurements and modelling of ^{234}Th isotopes gave an estimate of the half-life of the whole size spectrum of particles in the BNL (HEBBLE area) of 23 days. These short half-life times, as well as flux data from sediment traps, indicate that a substantial mass flux occurs between sediment and BNL (resuspension loop). The aim of this investigation was to determine the rate and the mass flux of this resuspension and the rate of remineralization in the BNL. We assume that sedimentation events will also have a significant effect on the particle resuspension loop. The available information about particle fluxes will be extended by determination of aggregate sizes and sinking speeds with an in-situ particle camera. A small-scale resolution of gradients close to the bottom (0-1 m) was obtained by a bottom water sampler.

Within the sediment the circulation of particles continues through the activity of the benthic fauna, which mixes freshly sedimenting or resedimenting particles into the sediment but also transports them back to the surface again. Usually such transports are estimated via ^{210}Pb determinations. Recently it was shown that the mixing coefficients determined by the natural radioisotopes are inversely proportional to the half-life of the tracers. This supports biological observations showing that particle transport by benthic fauna is highly selective and can not be described by diffusion-analogous models particularly in deep-sea sediments. In order to assess the contribution of these fluxes to the benthic carbon budget, a tracer has to be used with a half-life in the range of benthic reactions, i.e. of a few days to weeks. For this purpose ^{234}Th seems to be a suitable tracer. Alternatively the pigments of the sedimenting matter may be used as tracers, which allow the calculation of mixing coefficients provided the decay constants are known. Determination of pigments in the sediment and incubation experiments to determine their decay constants were carried out in co-operation with other groups. These transport coefficients are basic prerequisites to model early diagenetic processes in the sediment.

3.6.7 Geochemical Investigations of Organic Matter Degradation in Surface Sediments

Recent investigations showed that oxygen and sulphate are not only used as the terminal electron acceptors in different sediment depths as previously assumed, but occur parallel in the same layer provided sufficient amounts of labile organic matter are available. Intensive exchange between oxic and suboxic or anoxic deeper sediment layers, which may be strongly enhanced by bioturbation and bioirrigation, transports furthermore substantial amounts of reduced, inorganic substances into the oxic layer. Oxygen will then be used for the oxidation of these substances and not for the aerobic remineralization of organic matter. During

oxidation of sulfidic minerals and dissolved components like ammonia, methane, H_2S, Fe^{2+} and Mn^{2+}, acids are produced and, therefore, the oxidation of reduced inorganic components contribute to an enhanced $CaCO_3$ dissolution and return of inorganic carbon into the bottom water.

The complex interplay of aerobic and anaerobic degradation processes and the local and non-local transport processes are presently not well understood. To our knowledge, no set of data yet exists which would allow to model transport, degradation as well as redox and dissolution reactions in sediments with high C_{org} inputs. The aim of these studies was to contribute to data sets which facilitate a comprehensive modelling of benthic turnover rates and fluxes. The following measurements were carried out:

- concentrations of dissolved O_2, NO_3^-, NH_4^+, Mn_2^+, Fe_2^+, SO_4^{2-}, sulphide, CH_4, alkalinity, Ca_2^+, SiO_2, PO_4^{3-} and pH in pore water of sediments and in bottom water;
- concentrations of particulate C_{org}, C_{anorg}, nitrogen, ammonium, pyrite, Fe(II), Fe(III) in sediment and in sinking particles.

3.6.8 Interaction of Seasonally Variable Benthic Turnover Rates and Distribution of Trace Elements in Deep-Sea Sediments

In co-operation with the investigations of pore water chemistry (chapter 5.6.10) high resolution analyses of the composition of solid matter were carried out in the sediments. The main aims of this project were:

- budget of trace element distribution in the system pore water/solid phase with respect to possible forcing functions, like interannual variations of particle flux, geochemical environment and rates of bioturbation and bioirrigation;
- assessment of the dynamics of dissolution and enrichment with respect to the possible use of individual trace element distributions as palaeo-indicators.

4 Narrative of the Cruise

4.1 Leg M 36/1 (D. Schulz-Bull)

METEOR cruise M 36/1 was aimed to contribute to the international JGOFS (Joint Global Ocean Flux Study) programme and served to obtain chemical parameters of the upper water mass layer in a transect of the North Atlantic, i.e. Bermuda (47°N/42°W) to the Canary Islands (30°N/20°W) (Fig. 1b). Organic and inorganic tracers and also the components of the CO_2 system were determined. A second task is the international intercomparison exercise of different underway pCO_2 systems.

METEOR left Freeport, Bermuda on June 6, 1996, at 09:00 and started the first transect of the cruise to 47°N/42°W. During the first day in calm weather and sea conditions, several groups completed their underway pCO_2 systems in the geology laboratory and the continuous pumping system for organic and inorganic chemical tracers was installed and checked. The sampling started on June 7 at 12:00 (35°01 N/60°42 W) with continuous water pumping and XBT drops (Expandable Bathythermographs) every 40 nm down to 1800 m depth.
CTD casts were made at four stations.

Large volume samples of surface particulate matter were collected with the Kieler pumping system (KPS) by high-speed ultracentrifugation. The system ran during the whole cruise without any problems. Samples will be analysed for trace metal and trace organic chemicals in the home laboratories. A total of 10 samples (9 - 22 m^3) was obtained. Additional samples were collected for the analysis of particulate organic carbon, nutrients and salinity along the cruise track.

All seven underway pCO_2 systems were operated simultaneously for most of the time between June 7 and June 17. Technical problems which occurred in some of the systems only caused short interruptions. Only one system suffered heavy damage in the infrared gas analyser and had to stop taking measurements on June 16. The two underway spectrophotometric pH systems were operated over the duration of the cruise. The newly modified coulometric SOMMA system for underway determination of C_T was tested successfully at sea and contributed 452 high-quality underway measurements along the cruise track.

In addition to the various surface measurements - whether continuous or discrete - four full depth CTD stations were carried out. Samples were drawn for measurements of all four CO_2 system parameters (pH, pCO_2, C_T, A_T) thus yielding the highest possible overdetermination of the marine CO_2 system.

The prominent physical feature during transect I (Bermuda - 47°N/42°W) was a very high variability of the measured temperature signal at sea surface (in 5 m depth). In the southern part of the section the surface waters showed an almost uniform temperature distribution with values higher than 20°C. A strong front in the temperature field was evident 700 nm away from the first underway station. The temperature difference at the surface between the front

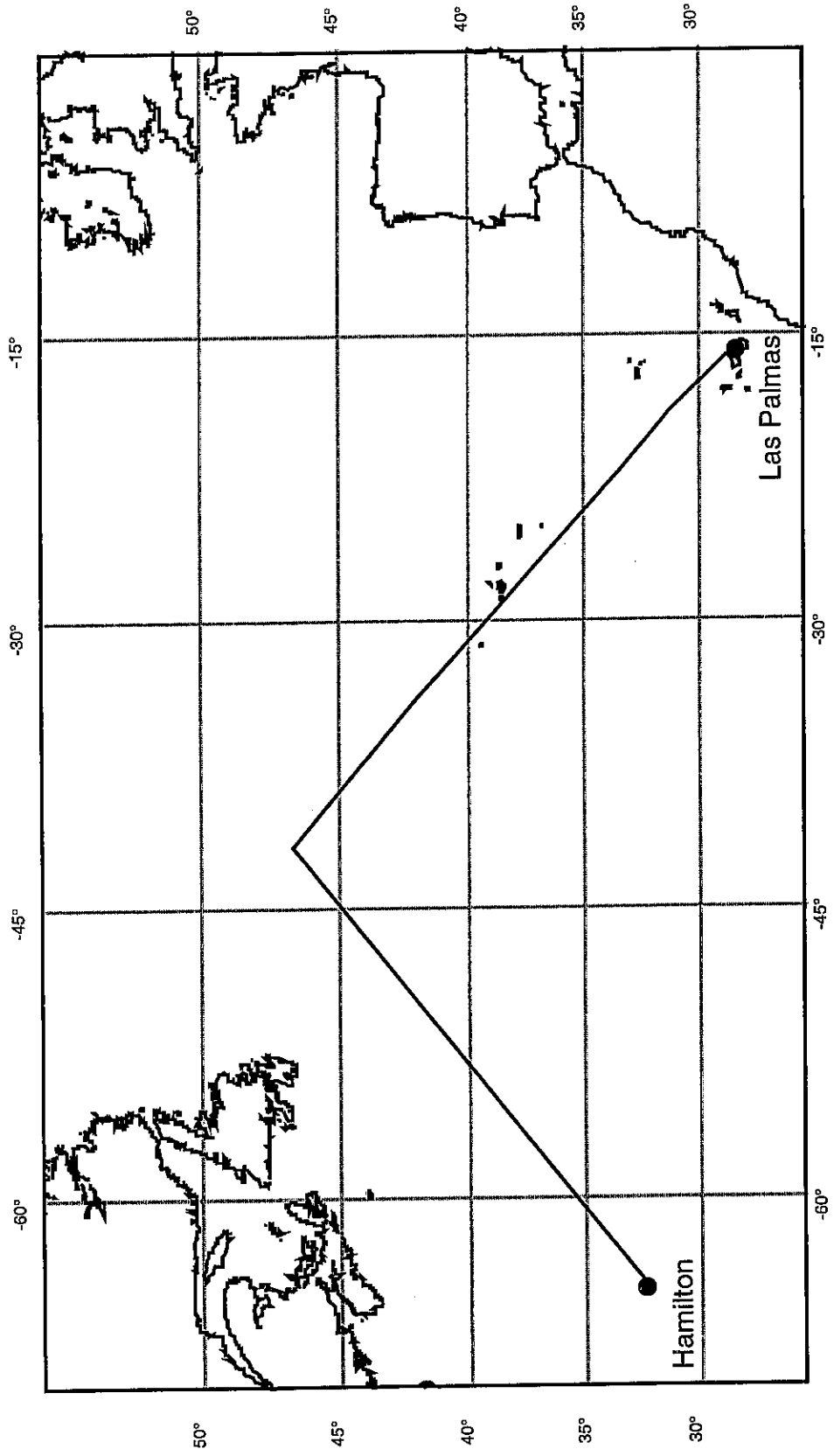

Fig. 1b: Cruise track of Leg M 36/1, Hamilton - Las Palmas

region and neighbouring stations reached 17°C. The front region itself had a spatial scale of 200 nm. The north end of the transect was characterised by a strong variability in the temperature field; the measured values ranged between 10-18°C. The variability in the sea surface temperature signal was accompanied by a similar variability in the salinity. Along the transect the salinity ranged between 36.5-36.6 in the southern part, whereas it had values near 33 in the front regime and between 34.5-36 on the north end of transect I.
The discrete measurements of nutrients (NO_2, NO_3, PO_4 and SiO_2) along the transect I showed that the upwelled waters transport water masses with higher nutrient concentrations to the surface. The concentrations reached values of 0.11 µmol/l NO_2, 2.56 µmol/l NO_3, 0.12 µmol/l PO_4 and 0.29 µmol/l SiO_2 respectively.

Along our second transect from 46°40 N/41°54 W toward Las Palmas, the measured sea surface temperature was characterised by slower variability. The temperature at sea surface increased constantly from the north (15.2°C) to the south end (> 20°C) of this transect. A similar development in salinity signal (increase from north to south end of the transect) was clearly evident.

On the morning of June 19, METEOR arrived at Las Palmas and the first leg ended as scheduled.

4.2 **Leg M 36/2** (K. Kremling)

METEOR left the port of Las Palmas shortly after 11:00 on Saturday, June 22, after a new deep-sea wire was wound up and the equipment was unloaded and stowed away. During the stay in Las Palmas, several classes of the local German school were informed about the ship and the current research projects by Captain Kull and the scientists. On board were 33 crew members and 9 scientific work groups which were specialised in the following disciplines: oceanography, geochemistry, planktology, paleontology and marine chemistry. The major topics of our cruise were mooring and station works in the North Atlantic, which will serve as components of the German contribution to the international JGOFS project (Fig. 1c).

Some instruments were tested in deep water at 30°34 N/18°35 W. On June 24, approximately 450 nm from the test site, we reached our first main station (L1) in the northern Canarian Basin, west of Madeira. At 12:50 UTC we released a mooring of over 5000 m in length which had been deployed there for one year. At about 13:15 the mooring was spotted on the surface and brought back on board complete with all instruments (4 sediment traps, 6 current meters) in approximately 3 hours. During the operation we had northwesterly winds with a speed of 5 Bft. All instruments worked perfectly except for one sediment trap, which malfunctioned due to electronical problems. The bottom current meter of the ground layer was notably damaged two weeks after the mooring (1995) by an implosion of five floats. On June 28, the mooring, which has been deployed there for three years in co-operation with the Dept. of Physical Oceanography of the IfM Kiel, could be redeployed at the same position. This is worth mentioning because the current meter mooring of this position ('Kiel-276'), which has

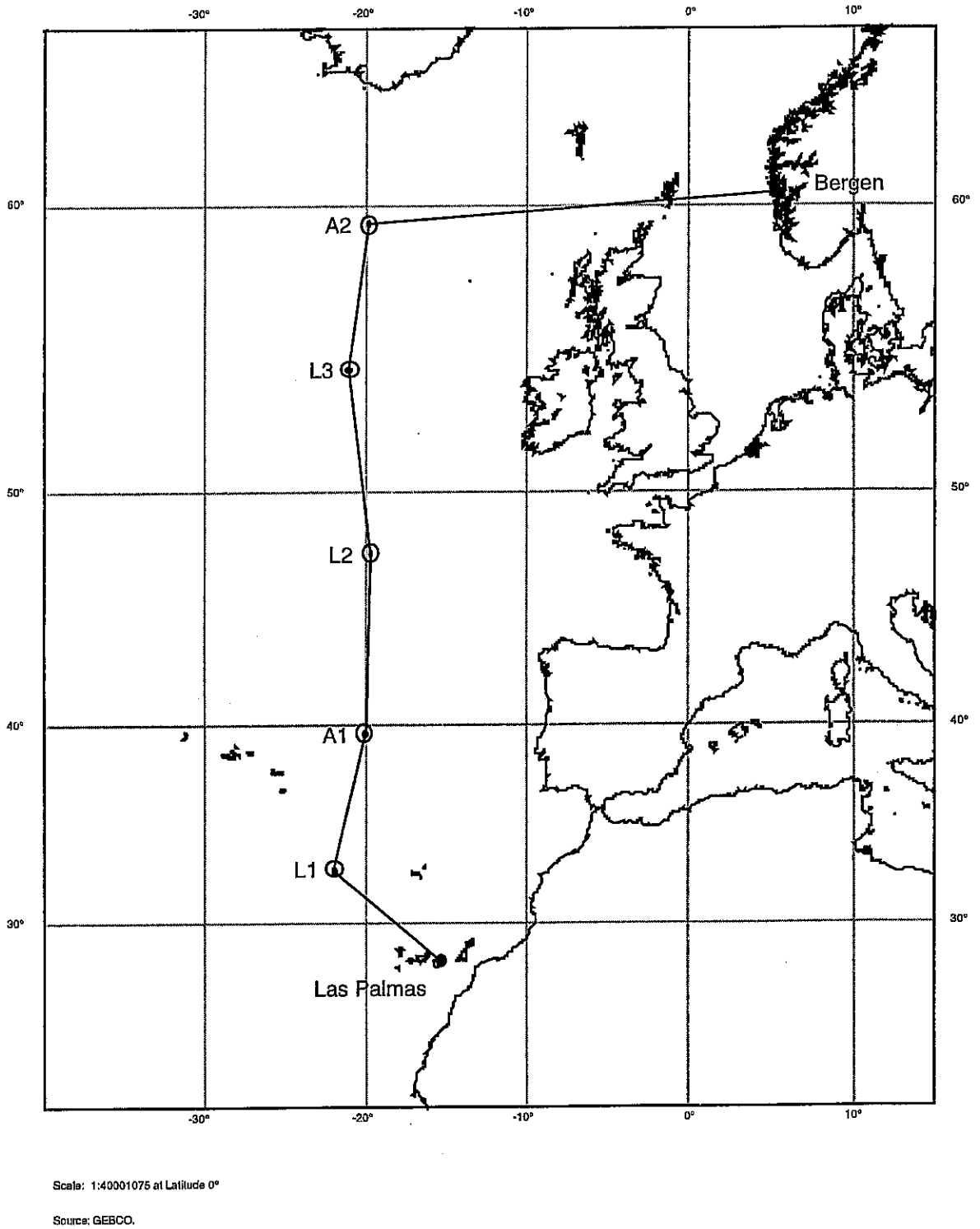

Fig. 1c: Cruise track and working areas of Leg M 36/2, Las Palmas - Bergen

been tracked for 16 years, now represents one of the few long-term stations in the North Atlantic.

Before the mooring works we had an intense sampling of the water column by the various work groups. Several CTD/rosette profiles were obtained for the examination of hydrographic standard parameters, oxygen content and CO_2 system, dissolved organic carbon and nutrient concentrations, as well as for the distribution of natural radionuclides and biological variables.

The problem of assigning the newly developed in-situ pumps for the sampling suspended particulate material (SPM) in the water column was solved so that we could carry out 12 successful experiments. Station work was concluded with a successful multiple corer hawl.

After leaving the long-term station L1, we continued the surface transect with XBT casts at intervals of 30 nm and CTD/rosette stations at intervals of approximately 2° latitude. The CO_2 partial pressure and the chlorophyll content in the top water layer were also surveyed continuously or in defined intervals through pumping systems or probes installed in the hydrographical shaft, respectively. Samples were also taken for the analysis of dissolved trace elements. A flow-through centrifuge was also connected. The centrifuge with a capacity of ca. 700 l/h enriched a large amount of SPM from the surface layer.

As we continued our meridional transect northward, not only did the wind direction change from northeast to west-northwest, but we also noticed a clear transmission from the oligotrophic area to the temperate productive latitudes of the North Atlantic. The constant analysis of phytoplankton close to the water surface showed a steady increase towards north. The Chl.-a contents showed an increase from < 0.1 µg/l at the southern stations to > 1 µg/l in the area of 47°N. The vertical distribution of nutrients and the position of the Chl.-a maximum changed correspondingly. In the south we found the nitrat cline (0.5 µmol/l NO_3) and the subsurface maximum at a depth of about 100 m (ca. 0.1% light penetration depth) in contrast to our last CTD stations, where it occurred at 40 m depth (ca. 10% light penetration depth). At the same time the CO_2 partial pressure showed a decrease from approximately 380 ppm (CO_2 content in the atmosphere is about 363 ppm) in the area of 47°N to less than 330 ppm in the area of 44°N. Towards the north the large spacial variability was especially eye-catching. The increased production became clearly visible by the rising amounts of suspended particulate material which was centrifuged from a distinct water volume.

On our way north we finally reached the JGOFS station L2 in the West European Basin (47°40 N/19°50 W) early Thursday morning with temporary head wind (up to 7 Bft) from the northwest. At 7:00 we started with the release of the first mooring, which had been deployed for one year at 4500 m depth. It appeared quickly on the surface and we could bring it back on board completely in less than two hours. This was also possible because of the favourable weather conditions with western winds of 4-5 Bft. In the afternoon of the same day, the recovery of the second mooring at a distance of 12 nm went almost as well as the first one. All instruments (4 sediment traps, 6 current meters) worked well although the lowest trap showed deviations from the preprogrammed sample intervals. Especially at 1000 and 2000 m depth we

noticed clear particle flux signals. After recovering the moorings, we began with an extensive sampling of the station (60 h), with analysis of the distribution of hydrochemical and planktological variables as well as chemical and geochemical trace elements.

We finished the station work with the redeployment of the two moorings and a multiple corer hawl. In order to enliven the social life on board, we celebrated our mid-cruise party on our passage to the next station.

We started the third week of our cruise (July 8-14) with moderate wind and two CTD/rosette stations at 49°54 and 52°17 N. We reached our next mooring position (54°41 N/21°10 W) Tuesday evening and started with station works at 19:00. Meanwhile the weather worsened, we had wind out of the southwest with 7-8 Bft and fog with a range of visibility of 300-500 m. Nevertheless, we managed to recover the annual mooring by Wednesday at noon without any major problems, but unfortunately without the surface buoy, which was torn off because of a corroded shackle. According to the pressure sensor's recording of the top current meter, we could determine that it had been torn off in April (1996). The recording instruments of the mooring, three sediment traps and four of the five current meters had worked perfectly over the whole year with very good particle catches at 500, 1000 and 2200 m depths.

During our stay at the station the weather improved remarkably and on Thursday, all cruise participants could enjoy the visit of at least a hundred pilot whales with their young. They came so close to METEOR that we had the opportunity to do some intensive "whale-watching". Since our on-board meteorologist informed us about an upcoming cyclone above Greenland we had to return to work and deployed the new mooring without any problems the same evening. We finished the 60 h lasting station works with another successful multiple corer hawl.

On Friday at noon, we headed north towards the last station with astern winds from southwest of 7 Bft. At that point we continued with the surface transect of almost 2000 nm length. Many components of these samples can only be determined ashore because of the sophisticated analytical methods. Most noticeable were the strong horizontal gradients of our north-south transect. Concerning the dissolved organic carbon (DOC), we could measure a clear accumulation towards the north which increased from 10 µmol/l in the south to more than 40 µmol/l in the area of 47°N. Contrary to that, the dissolved organic nitrogen (DON) showed quite homogeneous values of 5 µmol/l, indicating that the dissolved organic material on the surface is especially nitrogen-poor.

Between 51° and 52°N, the CO_2 partial pressure of the water reached its minimum with 290 ppm during this part of leg M 36/2. For the first time since at approx. 50°N the nutrient values were above the analytical detection limit; with a NO_3 increase of 0.30 µmol/l to 4.8 µmol/l between 50° and 57°N. These tendencies coincide with a noticeable increase of the mixed surface layer depth towards north to 70 m at 57°N.

After finishing our work at the last station A2 (59°30 N/20° W) we went on our way back

"home" to Bergen early Monday morning with nice weather of high pressure still continuing the surface transect into the northwestern European Shelf area. After passing by the Orkney and Shetland Islands we finished our surface registration on the morning of July 17. So we had one day left in order to pack and stow away our instruments before we reached Bergen on July 18. With our arrival in Bergen, we finished leg M 36/2 without any major losses or damage of instruments. It was possible to fulfill the whole working programme in the planned time schedule due to mainly good weather conditions, the good communication between the work groups, and especially the optimal support from Captain Kull and his crew members.

4.3 Leg M 36/3 (J. Mienert)

METEOR left Bergen on July 21, 1996, at 9:00 to carry out two major research programmes along the Faeroe-Shetland Channel, the Norwegian Margin and the East Greenland Margin (Fig. 1d). The overall objectives of the research programmes of the cruise were to study oceanic gas hydrates along the Norwegian Margin, and to determine the development of phytopankton and benthos in relation to sea surface and bottom water conditions off East Greenland. The research programmes are part of the DFG funded SFB 313 project "Environmental changes in the northern North Atlantic" and the EC funded "European North Atlantic Margin ENAM II" project .

We began the parasound/hydrosweep profiling and sediment gravity coring work in the Faeroe-Shetland Channel on July 22 with a relatively calm sea of Bft 4. Four sediment gravity cores were taken from a water depth between 1100 and 1600 m. The retrieved sediment cores were up to 10.7 m long. Box cores were also taken in an attempt to obtain an undisturbed upper 50 cm sediment column. Also, we successfully carried out FLOORIAN O_2 in-situ measurements. All stations were completed in time. We left the Faeroe-Shetland Channel on July 23; at 17:00, heading northward towards the work area on the Voering Plateau.

The first station on the Voering Plateau, which is a long-term SFB 313 mooring station, was reached on July 25 at 00:54. Here we started with (FLOORIAN) O_2 in-situ measurements, completed a CTD station, and carried out sea-floor sediment sampling. Unfortunately, the FLOORIAN device for O_2 in-situ measurements malfunctioned due to broken sensors. The sensors were replaced for the next station work.

The second station on the northern Voering Plateau was reached on July 25 at 17:00. At this location small-scale sediment mass movements occur in the vicinity of the Traendjupet slide off Mid-Norway. The first deep-tow boomer profiles were run for about 27 hours on a 225 km long track. The fish was towed at about 700 m below the sea surface at a speed of 4.5 knts. The record showed parallel reflector sequences and numerous debris flows and achieved a maximum penetration of about 80 ms two way travel time (TWT). The boomer profiles ended on July 27 at 03:04, a little to the west of the Traendjupet slide. The box and gravity cores retrieved sediments from water depths ranging between 1100 and 1250 m. The goal was to find hints of gas hydrate occurrences but evidently no indications exist in the area

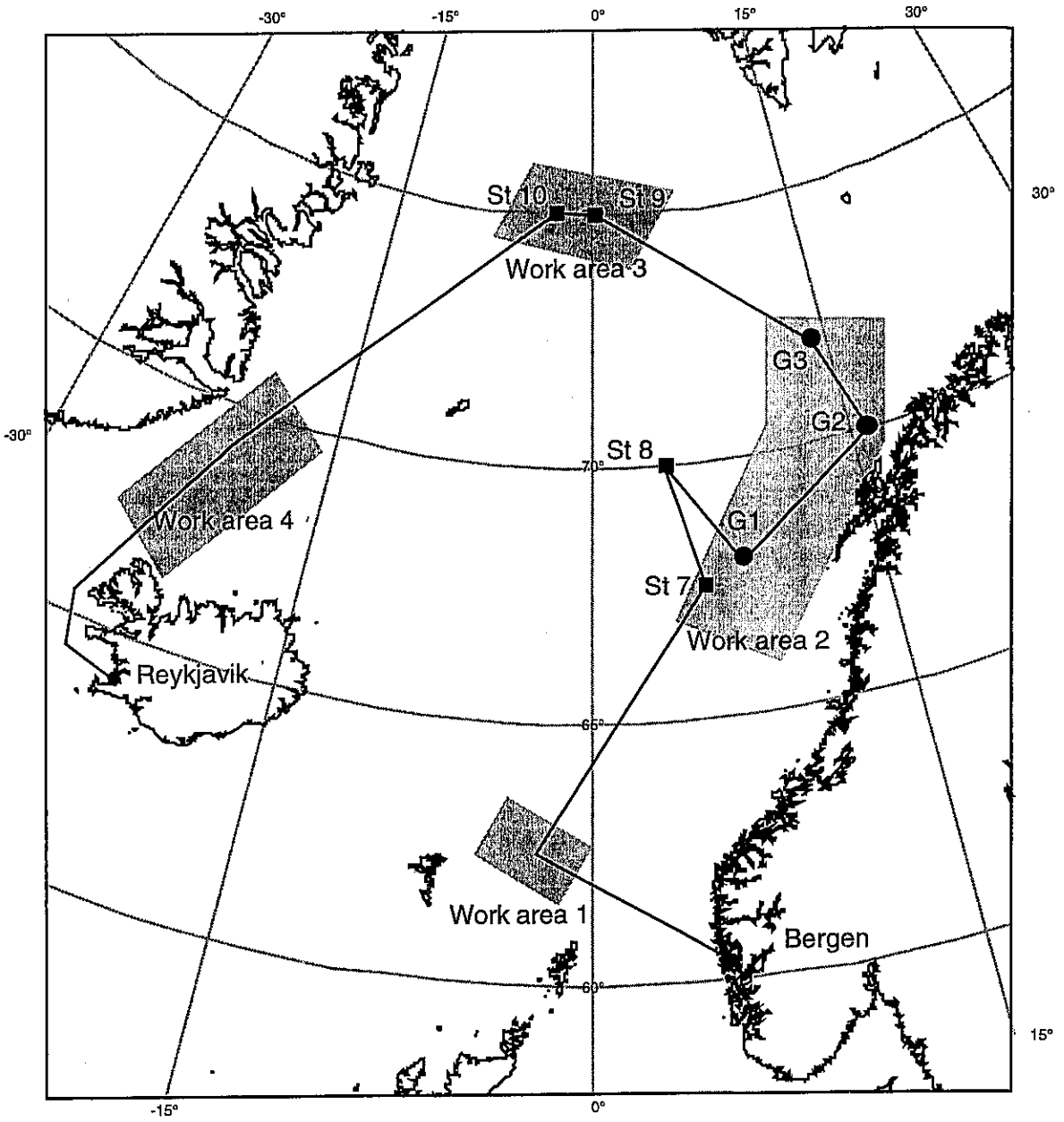

Fig. 1d: Cruise track and working areas of Leg M 36/3, Bergen - Reykjavik

investigated. This is in clear contrast to the southern Voering Plateau at the northern rim of the Storegga slide, where, between 800 and 1200 m water depth, the formation of hydrotroilite indicates the presence of methane and moreover, the seismic profiles show the existence of fluid outflow structures.

Three OBS wide-angle seismic experiments (METEOR stations 218, 225, 227) were carried out with a deep-towed source, i.e. near-vertical single channel seismic reflection profiles (BGS deep-tow boomer) in the layered sequence west of the Traendjupet slide in water depth of about 1200 m. All profiles were run directly across the OBS positions. Afterwards the deep-tow boomer and the OBS instruments were brought on board safely. The experiments ended on July 28 at 20:20 during excellent weather conditions (Bft 2).

Boomer profiling continued on July 26 at 00:32 across the sidewall scarp of Traendjupet and west of it, where several debris flows have been identified. Slide scarps, glideplanes below sediment surfaces and sea floor hyperbolaes provide evidence for areas of mass movements. The boomer was brought on deck on July 30 at 18:00. Afterwards two sediment gravity cores (23542, 23543) with a core recovery of up to 5.5 m were retrieved. The cores penetrated through the base of the glideplane and the upper debris flow. Hopefully the dating of the sediments will allow determination of the timing of the slide event.

On July 31 at 13:29 METEOR reached the Voering Plateau escarpment at DSDP site 338 (67°47 N/5°23 E). An OBS station and boomer profile were run in order to calibrate the compressional wave velocity profile. Data recording was finished at 16:50 successfully. We left the Voering Plateau and sailed towards the long-term mooring station NB9 (69°58.7 N/4°3.8 E) in the Norwegian Basin.

In the Norwegian Basin the release of the sediment trap mooring started on August 1 at 7:00. The release worked well and the acoustic range measurement showed that the mooring was coming up. The mooring surfaced and was recovered and brought on deck. The traps had partially worked well and collected high amounts of biogenic material. Afterwards a CTD, (FLOORIAN) O_2 in-situ measurement, multinet, box corer and multicorer station were completed at 3265 m. It is important to note that we discovered a rarely observable chlorophyll-rich layer on the sediment surface which provided clear evidence for an intense plankton-blooming event in surface waters. The deployment of a new sediment trap mooring (NB10) on August 2 at 04:00 at 3265 m water depth at position 69°59.35 N/ 003°59.9 E was carried out smoothly. We left the mooring station at 05:30 and sailed northwestward towards the Greenland Basin at 75°N/0°.

In the Greenland Basin the visibility decreased, the wind force was Bft 3 and the sea was calm. Both water and air temperatures were about 4°C. Under these weather conditions we started the first station on August 3 at 07:40, with a CTD, multinet, plankton net, and finally a multicorer. The preliminary interpretation of the data point towards a blooming of plankton. The second location was a sediment trap mooring station at 75°3.4 N/4°35.7 W at 3609 m water depth. We arrived at the station on August 4 at 03:06, after a 71 sm long parasound profile. The sediment

trap mooring (OG11) was successfully released, surfaced, recovered and brought on deck at 05:56. Because the mooring came up so quickly, some of the parts were tangled and one out of three sediment traps (No. 36, 1036 m water depth) surfaced upside down. However, our finding was that most of the trap beacons had worked properly and collected high amounts of biogenic material. After the mooring recovery, we started the CTD, multinet, bottom water sampler, in-situ pumping, (FLOORIAN) O_2 in-situ measurement, multicorer and box corer stations. They were completed on August 5 at 01:50. That same day, we sailed westwards towards the ice margin and deployed a sediment trap mooring (OG11) in 3465 m water depth at 74°59.69 N/6°57.39 W without seeing the ice. The top of the mooring was also not seen due to dense fog but the deployment was completed without any problems.

The next area we approached was the seamount Vesteris Banken. On this cruise, the ship proceeded to the ice as far as it could go avoiding the direct contact with the ice floes. However, Vesteris Banken proved to be unaccessible during these sea ice conditions. We turned and found our way out under dense fog and light easterly winds by first sailing varying directions but generally eastward to 74°10.2 N/0°36.5 E and then southward towards Jan Mayen Island. The water there proved to be ice-free so that the island could be passed on its western side on August 8 at 08:25. We were briefly able to see the island in the sunshine, which was a rare occasion and fully appreciated by scientists and crew members. To crown this event we spotted two whales in front of the island. As soon as we passed the island it disappeared in the fog again.

In the Denmark Strait we encountered weather conditions varying from Bft 4 to 9 often with mist to dense fog giving poor visibility. During the rare sunny intervals we saw 10 to 30 m high icebergs, whales, and during times of good visibility the coastline of East Greenland at a distance of about 55 miles westward from METEOR. On August 9 at 10:20, we started our work on the eastern slope of the Denmark Strait at 67°52.5 N/18°43.3 W at 912 m water depth with CTD, multinet, plankton net, bottom water sampler, box corer and multicorer. Afterwards, on August 10 at 01:45, we carried out a 103 sm long parasound profile in E-W and N-S directions, i.e. perpendicular and parallel to the axis of the Denmark Strait in order to provide information about the site locations. The acoustic patterns observed showed strong reflectivity on the western slope (Greenland side) with no penetration due to the erosive nature of strong southward directed bottom water currents and consequent sediment winnowing. In contrast, the eastern slope (Iceland side), where the currents are less vigorous showed parallel, reflector sequences and more than 50 m of penetration. A cross transect of 5 benthic stations was selected and completed from the western side of the channel on the Greenland Shelf at 400 m water depth to the central part of the Denmark Strait at 1532 m water depth to the eastern (Iceland) side of the channel in 1300 m water depth. The benthic stations included CTD, multinet, plankton net, bottom water sampler, box corer, multicorer and epi-benthos sledge sampling.

On August 16 we left the Denmark Strait and the floating icebergs which were always visible from the ship or on the radar. Finally the voyage ended in Reykjavik on August 17 at 08:00.

4.4 Leg M 36/4 (G.Graf)

METEOR departed Reykjavik/Iceland in the afternoon of August 19, 1996, and turned south for the BENGAL area (Fig. 1e), which is the permanent station of the new EU deep-sea programme BENGAL. It is situated right between the outlet of the Porcupine Seabight and the BIOTRANS area in a deep-sea plane of 4830 m water depth. The 1000 nm trip to this first benthic station was only interrupted by a test station, a CTD station, and water samples for methane and $\partial^{13}C$ analyses. We reached the deep-sea station on August 23 and started with CTD and water samples followed by benthic equipments such as bottom water sampler, multiple corer and box corer. At the beginning of this 36 hour station, a swell of 3 to 4 m at 8 Bft created some problems with the light gear, but at the end of the second day the situation changed and all scheduled samples were taken.

On August 25 we arrived at the OMEX area on the Irish-Celtic Continental slope. An initial hydrosweep profile demonstrated that the map delivered by the British Oceanographic Data Center (BODC) was very consistent with our measurements. Therefore, we decided to select the Whittard Canyon as major study side according to our original plan.

During the second week of our cruise, weather conditions got better and better comprising optimal conditions for the mapping of the canyon with hydrosweep and parasound profiles. The Whittard Canyon is 80 km long and starts on the shelf edge at 300 m water depth turning southeast and opens into the deep-sea plane at 3600 m. Along the axes of the canyon, small basins were detected where sediments are deposited. During this week we managed to run 6 stations along the canyon axes depicting the sorting of sediments along the depth gradient.

A second set of stations was run with the bottom water sampler, which was equipped with nepheloid-meters, CTD and particle cameras. In the canyon itself, an intermediate nepheloid layer was detected which most likely is created by the breaking of internal waves on the continental slope.

On September 2, we finished our programme with a parasound profile along the sediment fan of the canyon and headed south for Lisbon. In the afternoon of September 4, we docked in Lisbon. Although this short cruise provided only 9 days for scientific work, all participants were very happy with the samples and results of this leg.

4.5 Leg M 36/5 (C. Hemleben)

METEOR departed on September 7 from Lisbon for ocean research in the Northeast Atlantic (centered at 47°N/20°W, Fig. 1f) aiming for a better understanding of the carbon cycle. After general discussions about safety in the laboratories, we experienced optimal weather and started with XBT, surface sampling and CTD stations approximately 100 nautical miles SE of BIOTRANS station. In addition, the pumping system for CO_2 Chl.-a, particulate organic nitrogen (PON)/particulate organic carbon (POC), Psi, particulate $CaCO_3$, and HPLC

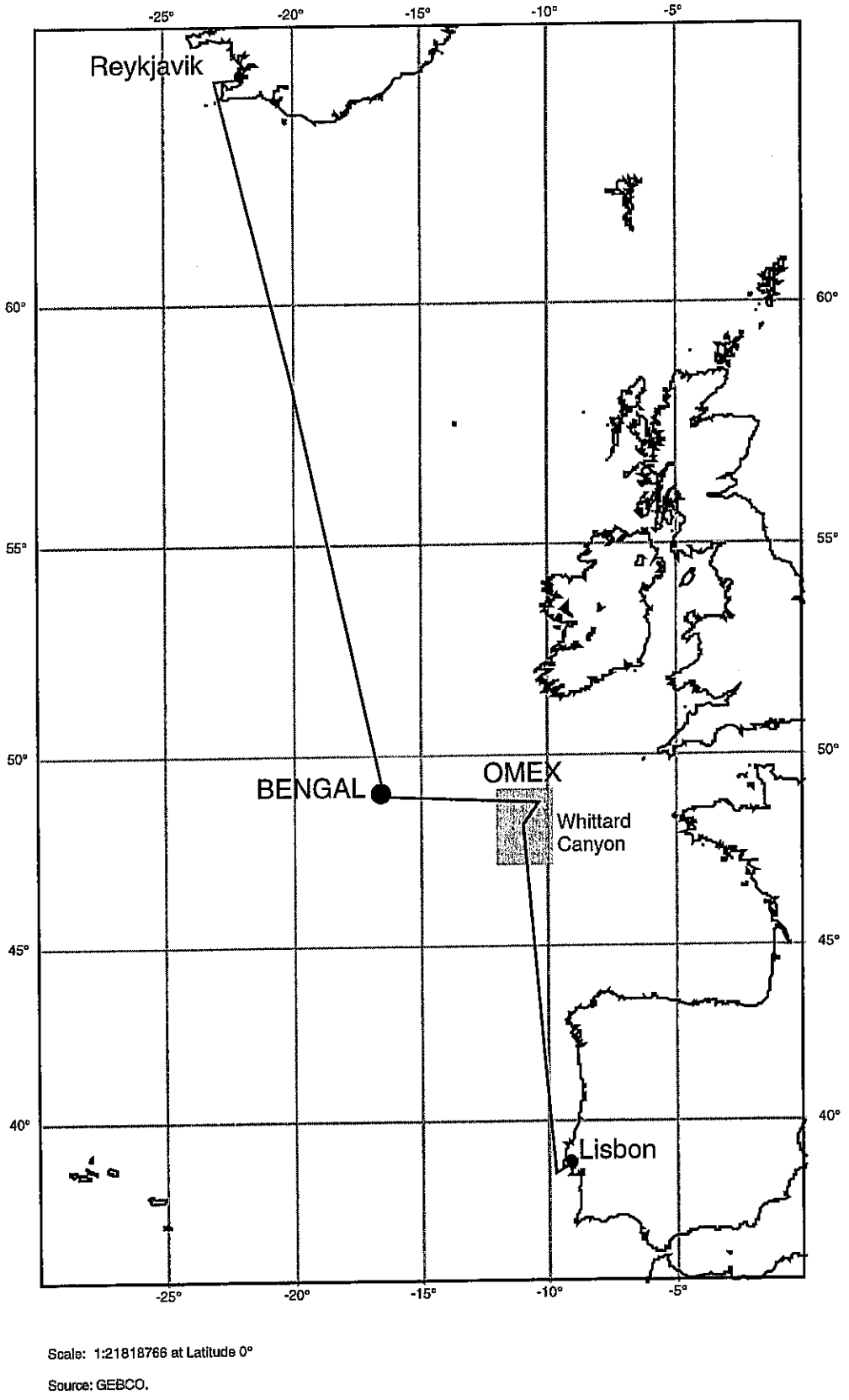

Fig. 1e: Cruise track of M 36/4 from August 19 - September 9, 1996.

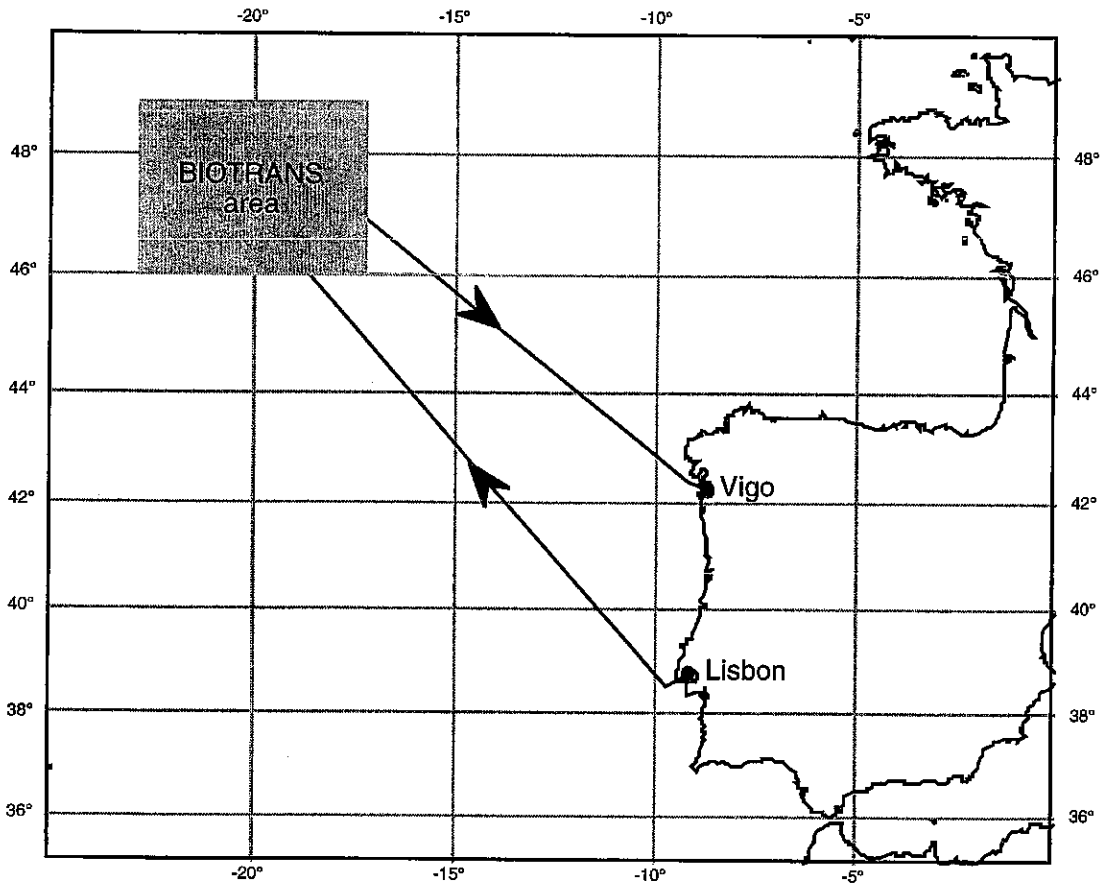

Fig. 1f: Cruise track and working areas of Leg M 36/5, Lisboa - Vigo

provided us with water samples every 10 miles. Early on September 10 we arrived at the BIOTRANS station where we ran the full programme including sediment sampling. On September 11 we departed to the NW to start our grid sampling. The grid was 180 by 180 nm with a distance of 15 nm between stations. In addition, we served the diagonals. The station work was effected by heavy winds on September 16 for several hours. However, on September 19/20 a heavy storm low (9 Bft, maximum 11 Bft) crossed our work area. Thus we ran only XBTs until we arrived at the BIOTRANS station for the second time. Because the weather was still bad, we postponed the station work until September 22 and continued to the north where we observed a different hydrographical situation: lower temperatures and a less stratified water column. The storms had changed the first observed situation, which was late summer-like, into a autumnal condition. In the north on the westside of the BIOTRANS station we found a slightly different hydrographic situation, caused by the storms. On September 26 another gale effected our work although only for a rather short time of a few hours. A longer interruption due to heavy winds occurred on September 28 and 29 where again a heavy low crossed the Atlantic. However, this was the last break before we departed for the BENGAL station. Here we sampled mostly sediments for various purposes. Because we still had some spare time we sailed back to our BIOTRANS grid to resample some stations in the eastern part of the grid to compare with the situation during our arrival in early September. Viewed in total, the ocean summer conditions have changed to a autumnal situation which resembled an early spring bloom. Thus, the data may support a CO_2 sink situation during the autumn. METEOR arrived at Vigo port early Sunday morning, October 6.

4.6 **Leg M 36/6** (O. Pfannkuche)

METEOR left the port of Vigo on October 9 under perfect weather conditions with the sun shining and all the scientific equipment being delivered on time. 28 scientists were on board representing the following scientific programmes: JGOFS (3 people), BENGAL (4 people) and BIGSET (21 people). After a life boat drill in coastal waters, METEOR headed directly for the first work area on the Porcupine Abyssal Plain at 49°N/16°30 W (Fig. 1g). This area was also sampled during the previous METEOR legs M 36/4 and M 36/5. While heading for the BENGAL station we had a CTD test on the morning of October 10, and on October 11 we took another CTD/rosette profile down to 4000 m depth in order to get some deep water for the preparation of experiments and for the calibration of sensors.

We reached the BENGAL area on October 11 at 19:30. During the night we ran the first benthos stations with the multicorer. On the morning of October 12, one sediment trap and a deep-sea pump were moored 500 m above the sea bed and afterwards we continued with the benthos sampling series. In the evening while mooring again for a short time, a baited trap chain for catching nekrophagous benthopelagic organisms was brought out. We had to break off a following plankton hawl with the 1 m^2-MOCNESS after about one hour because of an upcoming storm. On the night of October 13, the storm became worse and reached wind speeds of up to 10 Bft. On October 14, the wind slowed down to 6 Bft but the swell hardly ebbed; nevertheless we were able to run a CTD/rosette down to a water depth of 800 m.

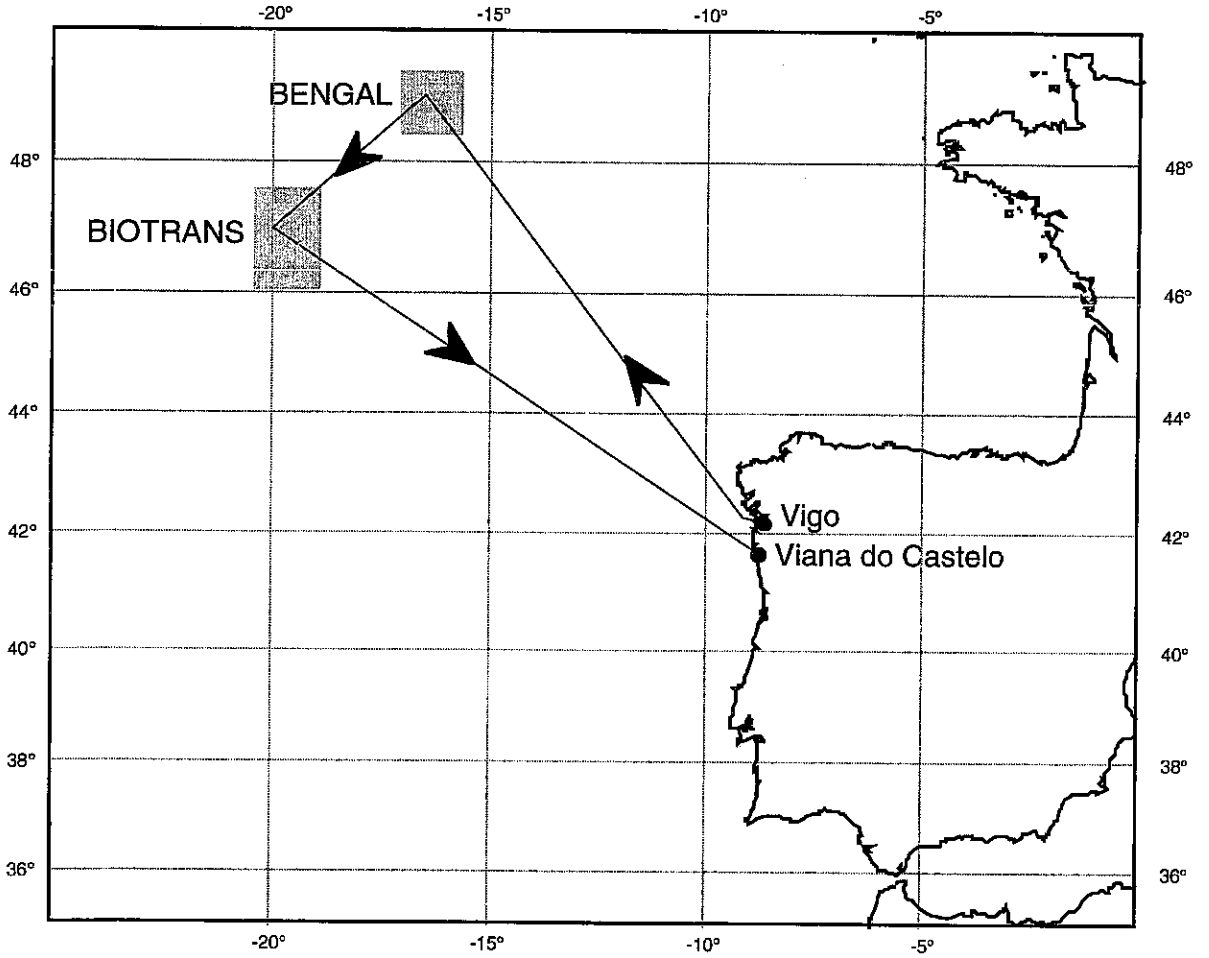

Scale: 1:18182308 at Latitude 0°

Source: GEBCO.

Fig. 1g: Cruise track and working areas of Leg M 36/6, Vigo - Viana do Castelo

The following deployment of the GEOMAR lander with benthic chambers had to be cancelled after all mooring weights were cast off at the ship's hull when the gear hung on the crane. Wind speeds again reached 8-9 Bft and the swell reached 12 m. These weather conditions forced us once again to wait for better conditions until the morning of October 16. In the morning we had wind speeds of 6 Bft but still a swell of 6 to 8 m.

We were able to successfully run a CTD/rosette as the first instrument, afterwards we recovered the trap chain and deployed the lander. Since the ship still rolled a lot, we had to break off a multinet hawl because the nets had been torn up during heaving. The rolling also had negative effects on the benthos sampling with multicorer and box corer. During all multicorer hawls only a part of the tubes was filled with sediment; two hawls were completely unsuccessful. On the night of October 17, the 1 m^2-MOCNESS was successfully towed down to 20 m above the ground.

In the morning of the next day we once again had to cancel station works until the morning of the 19 because of another storm (9 Bft) and the rising swell. Sampling started again with another benthos station; the trap chain was deployed and a CTD/rosette was taken. Afterwards the group from Tübingen was able to take a full series of multinets for the first time. On the night of October 20, the photo/videotrawl was towed for the first time. Heaving the trawl, one of the active rolls of winch No. 10 blocked during the last 1000 m of cable length. During the course on 20 October we managed to recover the sediment trap (moored at the beginning of the cruise), as well as the lander and the trap chain.

In the afternoon of October 21, we completed the station works at the BENGAL station, and METEOR headed for the second work area, the BIOTRANS station (47°11 N/19°34 W). During our transit to the next station, one of the CTD/rosette and XBT transects of the JGOFS work group from leg M 36/5 was repeated starting at 48°36 N with southern course for the examination of mesoscale structures of hydrography and nutrient distribution in the mixed surface layer. While heading for the first station, the weather once again deteriorated rapidly so that a CTD hawl was not possible and only the XBT drops could be realised. Since the wind direction changed in the afternoon of the 22nd, we were forced to abandon the hydrographic transect after approx. 100 nm. On the morning of the next day, the wind speed slowed down to 6 Bft and we headed for the central benthos station in the BIOTRANS area at 47°11 N/19°34 W. After a CTD/rosette and a multinet hawl, the sediment trap was deployed again. On the night of the 24th, a series of multicorers was taken with only moderate success, because the swell and a damage to the gear's hydraulic damping system, discovered during a later inspection of the instrument, disturbed the sampling. Consequently, only a few multicorer tubes were filled with sediment.

During the 24th, the trap chain was moored and a series of multinets and a CTD/rosette were taken. In the evening, the lander from GEOMAR was deployed again. One of its benthic chambers was provided with injection devices for tracers to investigate in-situ bioturbation rates of the benthic community (experiment: GEOMAR) as well the bioturbation and ingestion rates of foraminifers (experiment: Tübingen). The lander was supposed to be moored for 4.5 days.

On the night of the 25th, we started with another CTD/XBT transect for the JGOFS work group leaving the benthos station in a NNE direction. This transect was finished successfully. On our way back to the central benthos station we faced strong head winds so that we returned with a delay and reached the station on the evening of the 25th. On the night of the 26th, some more multicorers were taken but during this station the weather conditions once again deteriorated. While heaving the last multicorer in the morning of the 26th, we already had wind speeds of 10 Bft.

Although wind speeds smoothed during the course of the 26th, no station works were possible because of the heavy swell. In the morning of October 27, hurricane „Lilly" came upon us with wind speeds of 12 Bft. On October 28, with wind speeds of 7/8 Bft, we once again managed to start station works. We recovered the trap chain which was originally scheduled to be recovered on the 25th. After a CTD/rosette, we carried out a series of multicorer drops until the early morning of the 29th. Unfortunately, only about 40% of the corer tubes were filled because the sampling was hampered by the still very high swell. On Tuesday, October 30, the wind conditions improved and therefore we decided to recover all the remaining moorings; the lander and the sediment trap were retrieved without any problems. After the successful employment of the GEOMAR bottom water sampler, we deployed the 1 m^2-MOCNESS during the night of October 30. The successful hawl included 3 catch steps with 2 nets in the horizons 20 m, 50 m and 100 m above the sea bed. After another CTD/rosette down to 4570 m depth (10 m above sea floor), we retrieved another benthos series with multicorer and box corer at the central station at 47°11 N/19°34 W until the late evening. We continued with another hawl with the bottom water sampler which was completed successfully in the morning of October 31. Until noon a CTD/rosette followed in combination with 3 multinets. We completed our work programme at the BIOTRANS station with a multicorer on the western peak of the deep-sea mountain „Großer Dreizack". In the afternoon of the 31st, we headed for Viana do Castelo.

During our passage another hydrographic transect of the JGOFS work group from leg M 36/5 with CTD/rosette, XBT drops and Apstein-net hawls was repeated. This transect was completed at 45°36 N/17°27 W on November 1. At this position an additional multicorer was taken. With the ship station 411 scientific station works of M 36/6 ended and after a calm transit we reached Viana do Castelo, thus completing leg M 36/6 on Sunday, November 3, at 08:00.

5 Preliminary Results

5.1 Leg M 36/1

5.1.1 Physical Oceanography (J. Waniek)

The objective of the hydrographic programme during leg 1 was the detailed description of the surface physical environment along the cruise track in selected areas of the subtropical and moderate North Atlantic.
Special emphasis during this leg was focused on the documentation of the variability of the temperature field at sea surface and at depth. The spatial and vertical variability of the temperature field was investigated by XBT drops (Expandable Bathythermographs) every 40 nm down to 1800 m depth. At several positions a few CTD casts were also made (Fig. 2). From the temperature profiles, the depth of the mixed layer and characteristics of the eddy field can be estimated.

5.1.1.1 Shipboard Results

Transect I: Hamilton - 46°40 N/41°54 W
The horizontal distribution of sea surface temperature from XBT data and shipborne thermosalinograph is given in Figure 3a. The prominent feature during transect I from Hamilton to 46°40 N/41°54 W was a very high variability of the measured temperature signal at sea surface (at 5 m depth). In the southern part of the section, until 600 nm from the first underway station, the surface waters show an almost uniform temperature distribution with values higher than 20°C. The central part is occupied by surface waters with temperatures between 6-10°C. A strong front in the temperature field is evident 700 nm away from the first underway station. The temperature difference at the surface between the front region and neighboured stations reached 17°C. The front region itself has a spatial scale of 200 nm. The north end of the transect is characterised by a strong variability in the temperature field; the measured values range between 10-18°C (Fig. 3a). The variability in the sea surface temperature signal is accompanied by a similar variability in the salinity. Along the transect, the salinity ranged between 36.5-36.6 in the southern part; it has values near 33 in the front regime and between 34.5-36 on the north end of the transect (Fig. 3b).

The large spatial variability in temperature signal at sea surface along the transect is also coupled with a variability of the temperature field at depth. Figure 4 shows a section of vertical temperature distribution along transect I down to 900 m depth measured by XBT drops. Between station 1 and 15 we can see almost uniform water below the 19.2°C isotherm down to 400 m depth. Below 400 m depth the water column is well stratified. At stations 15 to 25, an upward motion of cold waters to the surface is evident. In 300 m depth we found temperatures between 5-6°C, and typical values in the southern part at the same depth level reached 17°C. The upwelled water is coming from depths below 1000 m which suggests an influence of the Gulf Stream system (Fig. 4) or evidence of a Gulf Stream ring.

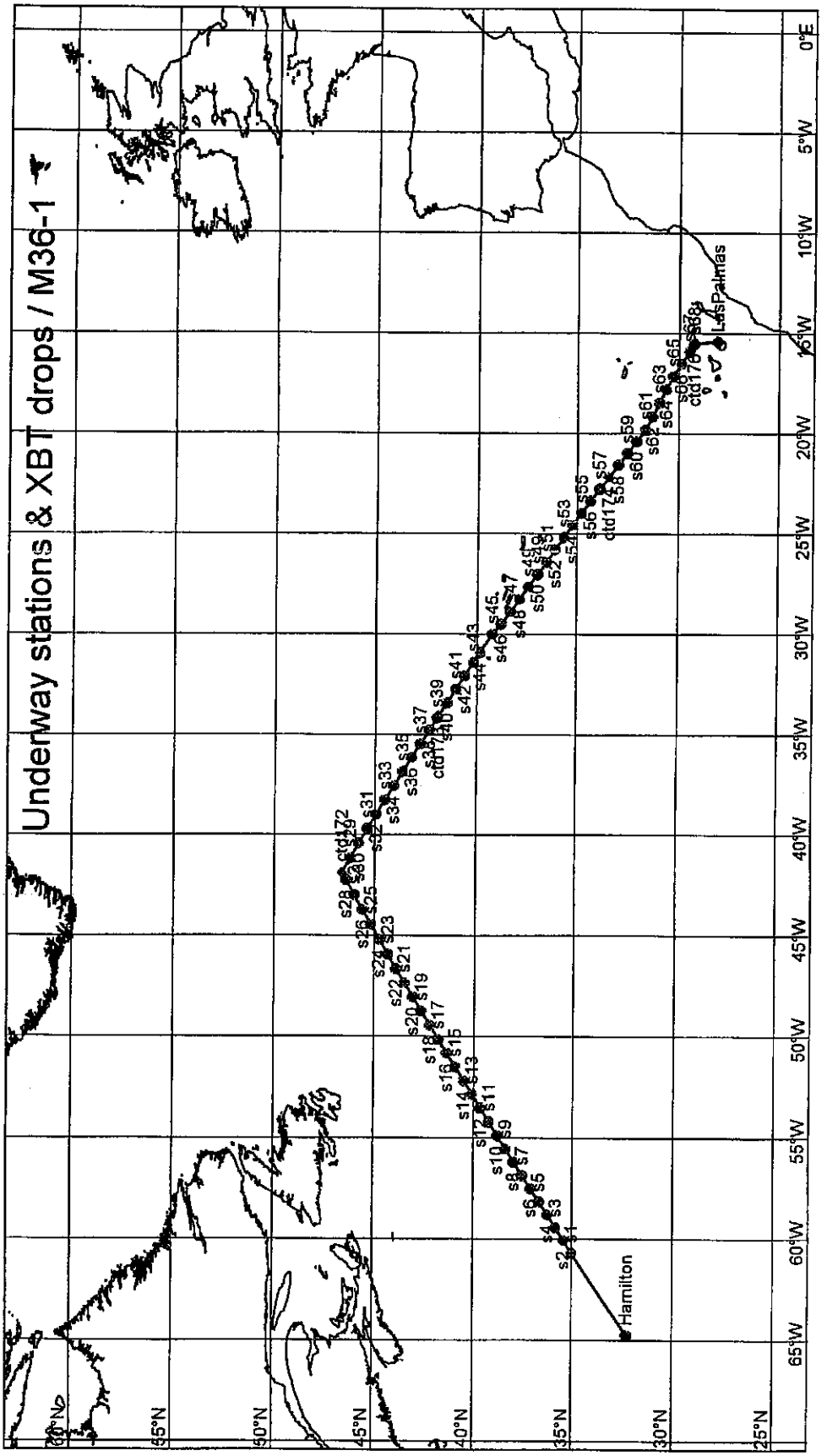

Fig. 2: Cruise track during M 36/1 and area of investigation. XBT drops are marked by circles and CTD casts by squares.

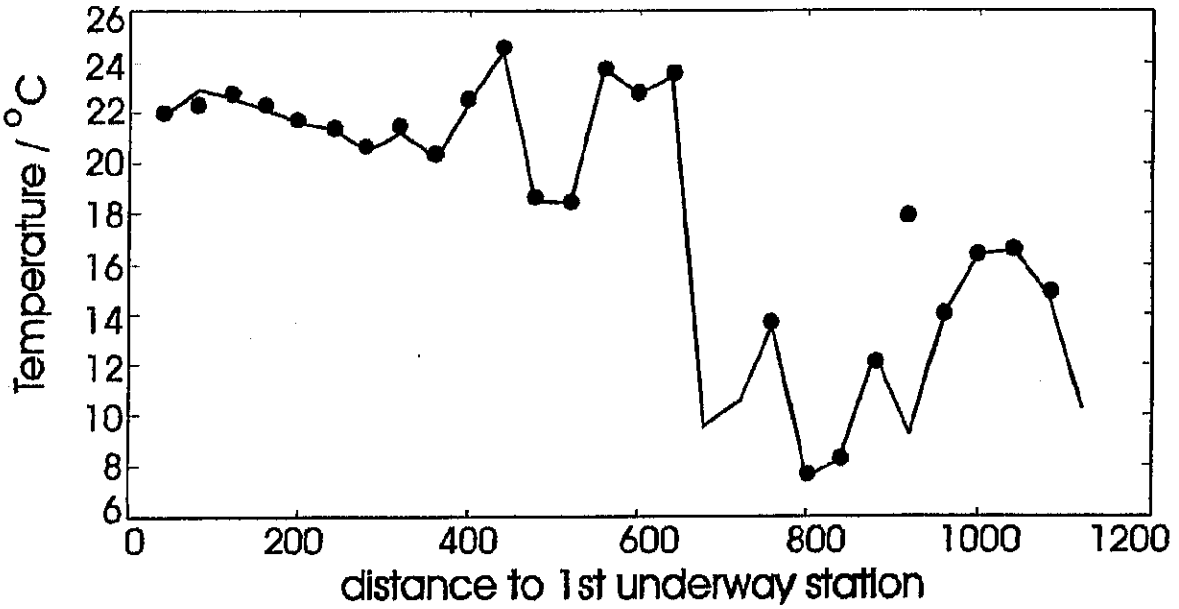

Fig. 3a: Sea surface temperature measured by shipborne thermosalinograph (solid line) compared with temperature from XBT drops (dots) along the transect from Hamilton to 46°40 N/41°54 W; both are measured at 5 m depth. The distance is calculated relative to the first underway/XBT station.

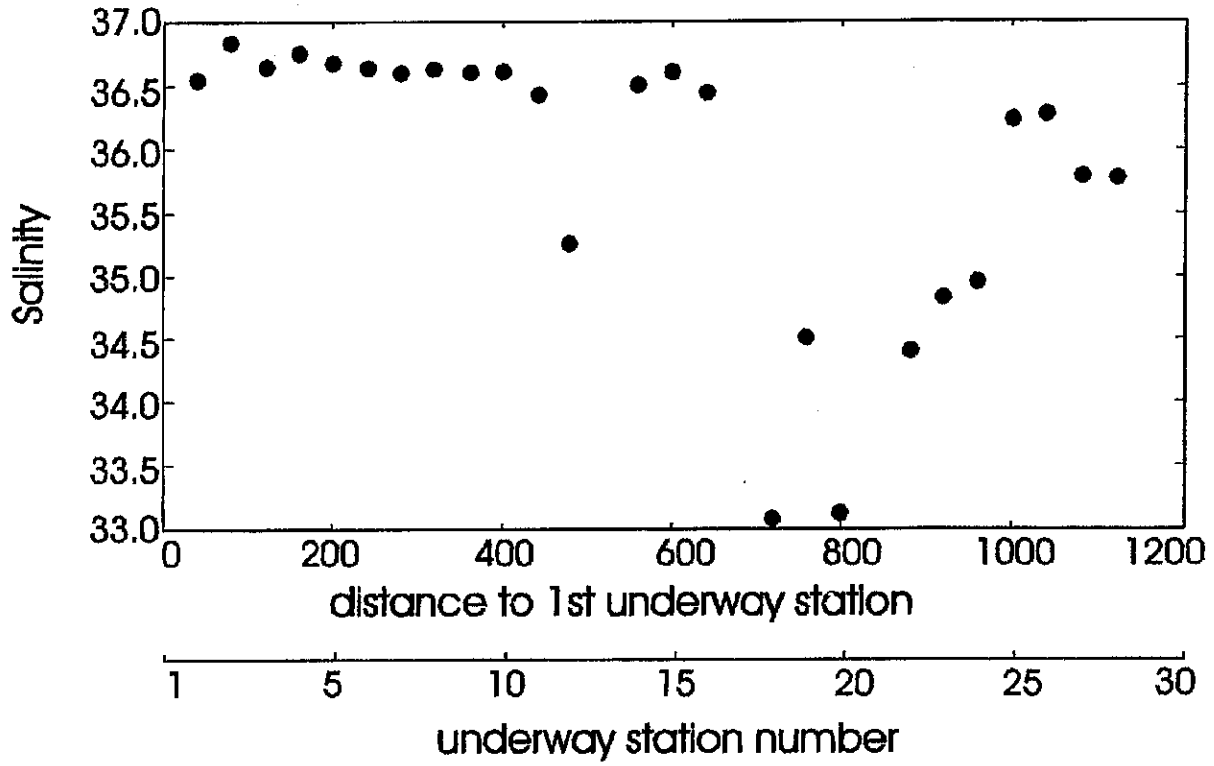

Fig. 3b: Salinity at sea surface.

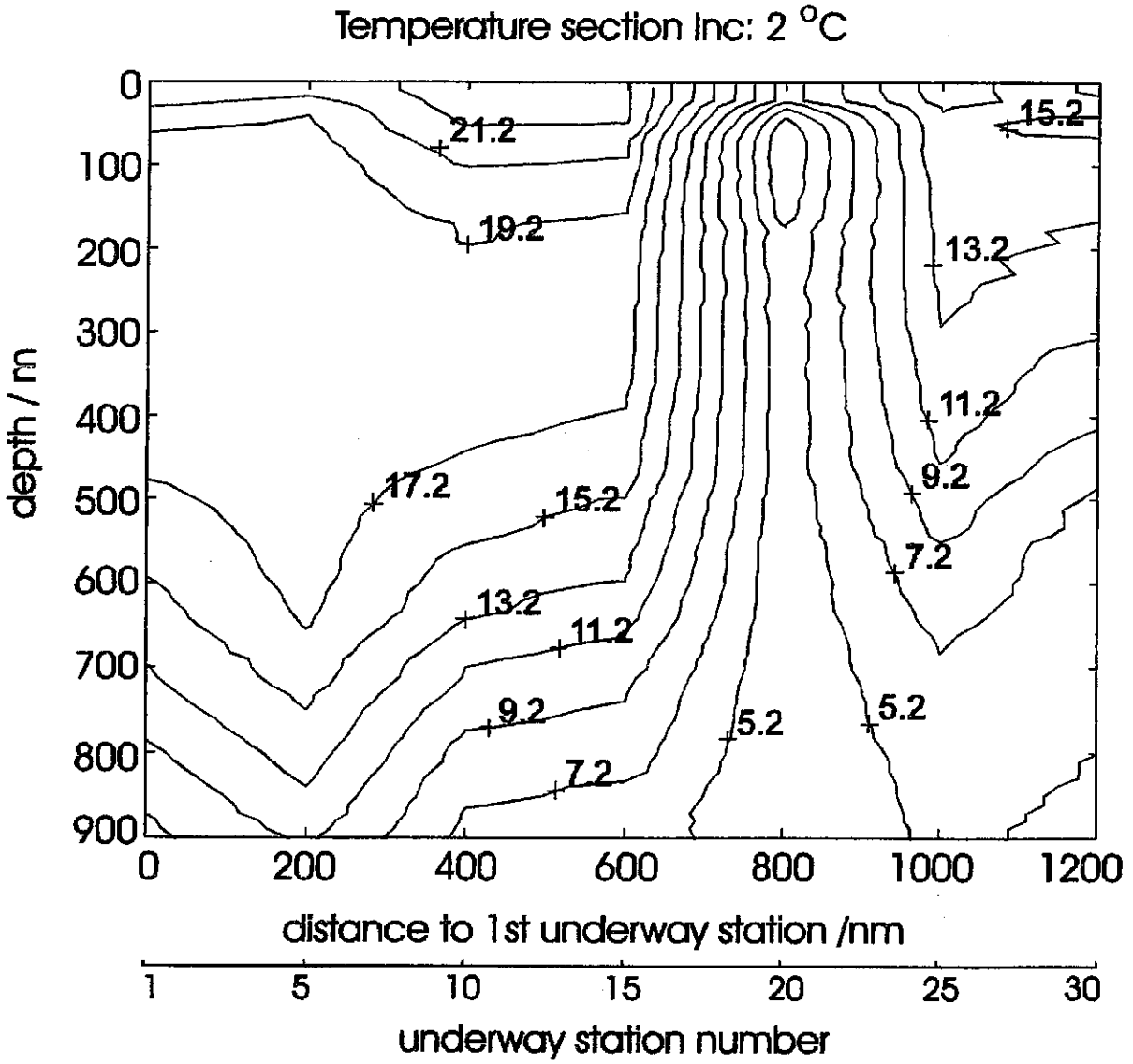

Fig. 4: Temperature section for the upper 900 m water depth from XBT data along the transect from Hamilton to 46°40 N/41°54 W. The distance is calculated relative to the first underway/XBT station. The mean distance between XBT drops was 40 nm.

Transect II: 46°40 N/41°54 W - Las Palmas

Along our second transect from 46°40 N/41°54 W directed to Las Palmas the measured sea surface temperature was characterised by slower variability (Fig. 5 or Fig. 6). The temperature at sea surface increased constantly from the north (15.2°C) to the south end (> 20°C) of this transect. This is a typical situation for a change of the hydrographic regimes between the moderate and subtropical Atlantic. A similar development in salinity signal (increase from north to south end of the transect) measured at sea surface at the XBT position is clearly evident (Fig. 5b).

5.1.2 First International At-Sea Intercomparison of Underway pCO_2 Systems

(A. Körtzinger, L. Mintrop)

5.1.2.1 Scientific Background of the Exercise

Currently different concepts are applied to quantify the oceanic uptake of CO_2. These efforts are being undertaken in the light of the atmospheric CO_2 perturbation and its possible impact on the earth's climate. One important concept is based on the determination of the partial pressure difference of CO_2 (ΔpCO_2) between surface seawater and the overlying air, which is the thermodynamic driving force for any net exchange of CO_2. By means of a transfer coefficient, a measured ΔpCO_2 can be converted into a momentary net flux of CO_2 across the air-sea interface. Given the strong spatial and temporal variability of pCO_2, this concept faces the challenge of coming up with representative mean ΔpCO_2 values on a global grid. If this concept is to be successful, the combined efforts of research groups all over the world is necessary. The IOC/SCOR Carbon Dioxide Advisory Panel is currently establishing an international inventory of all measurements that have been made so far. One important requirement in this context, however, is a good inter-laboratory comparability of the data sets, which in fact have been measured by quite different types of analytical systems. While the analytical precision of the various systems in use is of the order of 1 µatm, not much is presently known about the comparability between the different laboratories.

As a important first step to assess the current state of this parameter, an international shore-based intercomparison exercise of underway pCO_2 systems was carried out in June 1994 at the Scripps Institution of Oceanography, Marine Physical Laboratory, La Jolla/USA (Dr. Andrew Dickson) on behalf of the Joint IOC/SCOR CO_2 Panel. However, the general consensus in the scientific community was that a necessary second step would be an at-sea intercomparison under realistic and identical operation conditions.

The principal idea of the exercise was to operate as many underway pCO_2 systems simultaneously for as much time as possible. Backed up with in-situ salinity and temperature data as well as navigational and meteorological data, this data set is the mainstay of the exercise. While shore-based intercomparison exercises allow us to run special experiments which reflect extreme situations, ship-based exercises have to rely fully on the conditions which are provided by the sea. The chosen cruise track reflects the attempt to include extreme

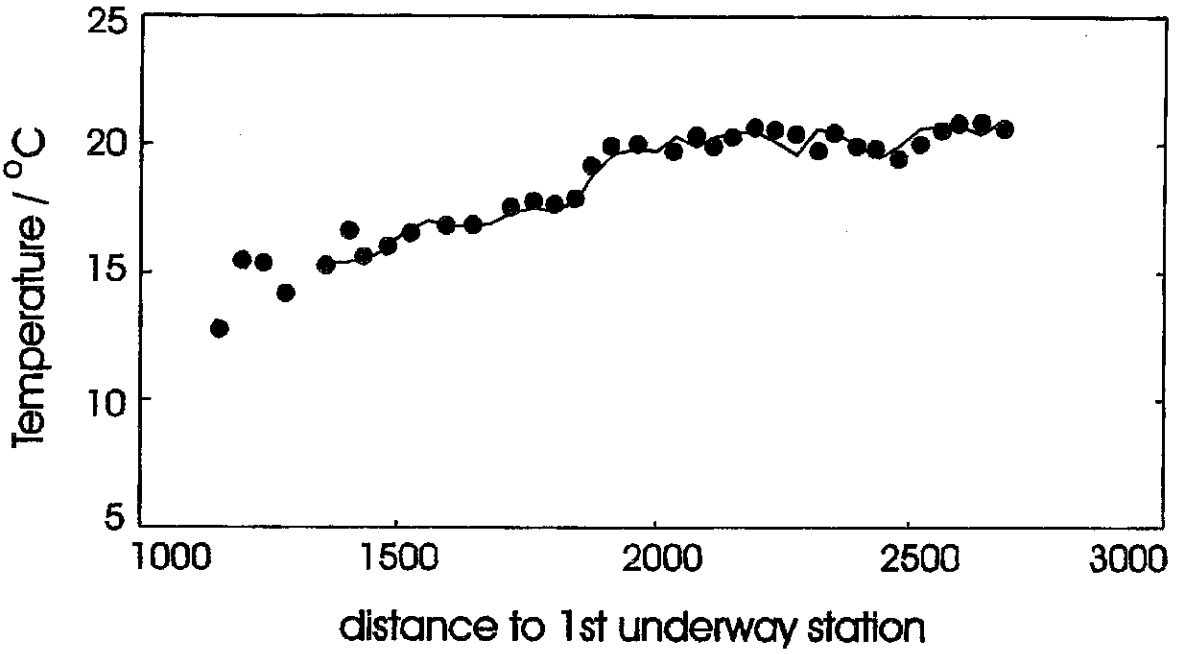

Fig. 5a: Sea surface temperature measured by shipborne thermosalinograph (solid line) compared with temperature from XBT drops (dots) along the transect from 46°40 N/41°54 W to Las Palmas; both are measured at 5 m depth. The distance is calculated relative to the first underway/XBT station.

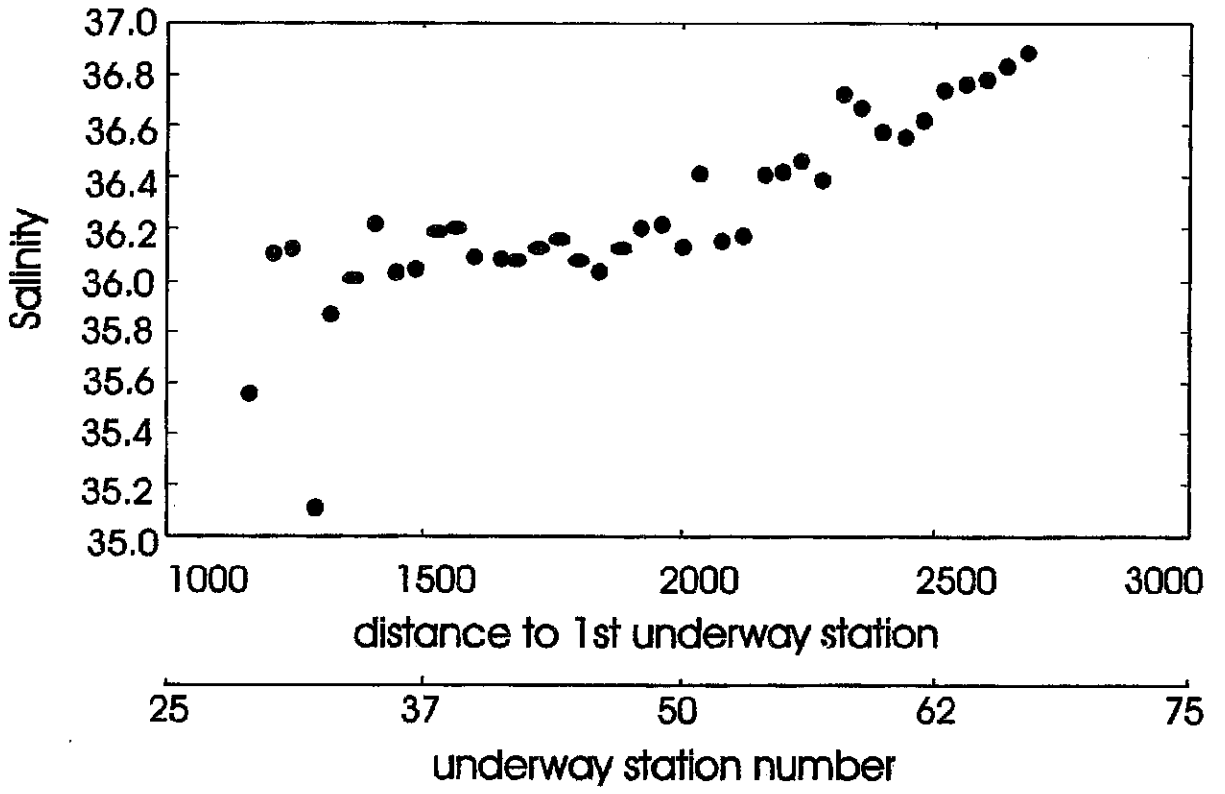

Fig. 5b: Salinity at sea surface.

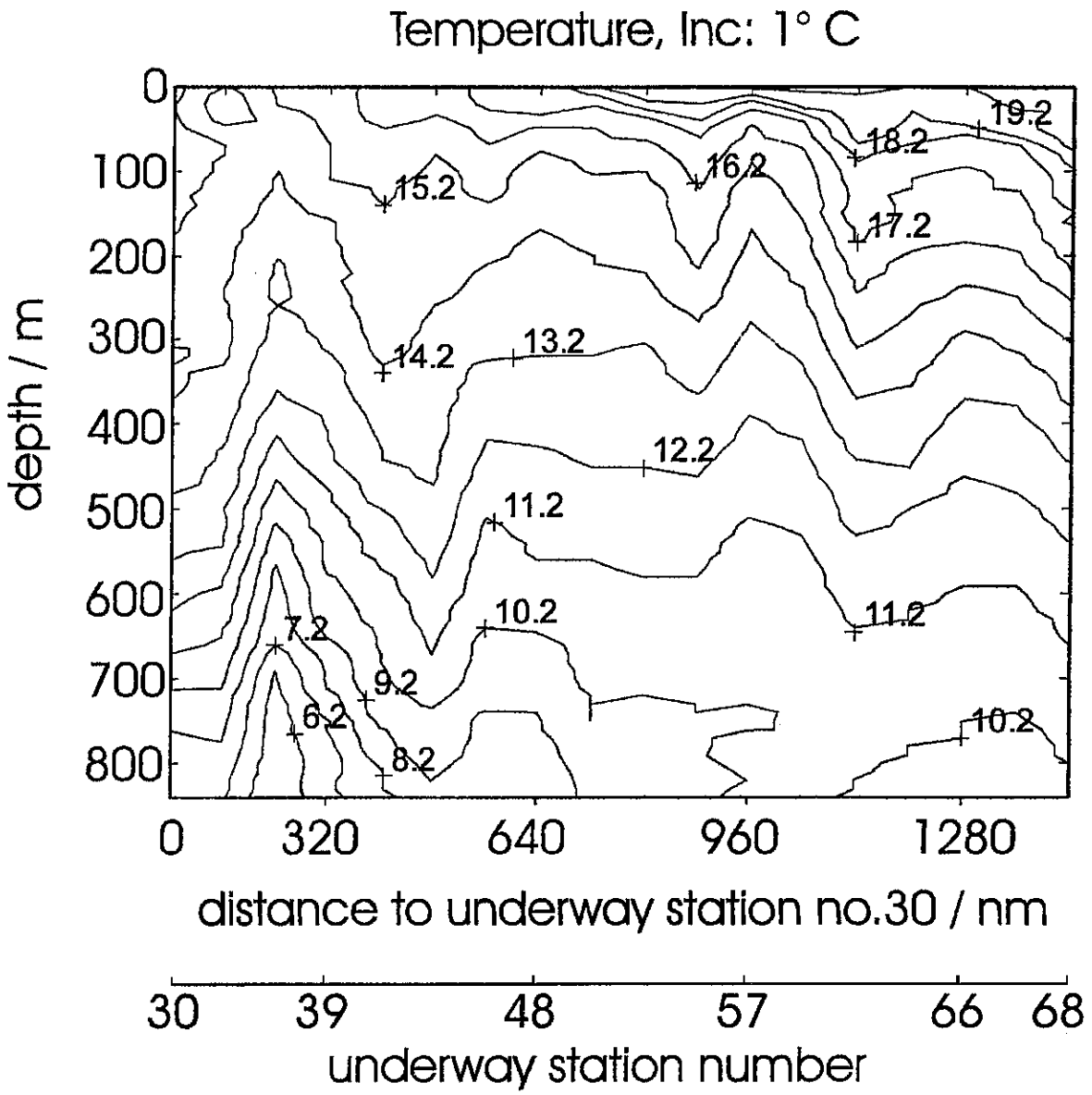

Fig. 6: Temperature section for the upper 850 m water depth from XBT data along the transect from 46°40 N/41°54 W to Las Palmas. The distance is calculated relative to the underway/XBT station number 30. The mean distance between XBT drops was 40 nm.

oceanic regimes in the exercise. While in the eastern North Atlantic, the situation was very stable with not much variability in surface seawater temperatures and salinities and likewise pCO_2, the North Atlantic drift region off Newfoundland provided extreme variability with steepest gradients. The overall temperature range during the exercise was roughly 6 to 25°C, while the salinity varied between 32.5 and 36.8. In this area our cruise track hit warm and cold ring features. Associated with them were steep frontal gradients of up to 15°C and more than three salinity units within a few nautical miles.

These different regimes allow to gain various insights into the performance and comparability of the participating systems. The stable situation allows us to detect systematic offsets between the data sets, thus providing the basic information about the inter-laboratory comparability. The strong gradient regime mimics the step experiments of shore-based intercomparison exercise. The fast change between two "batches" of seawater, which are characterised by different pCO_2 values, reveals the different time constants of the analytical systems. Fast responding systems are able to follow the signal much closer than the slow responding ones. So even if there are no systematic differences between two given systems they may have quite different response times, which is equivalent to different spatial resolution in underway work.

5.1.2.2 Technical Aspects of the Exercise

The intercomparison exercise almost entirely consisted of continuous underway sampling of surface seawater. Only four CTD stations were included in the programme. In order to encounter the widest possible range of surface seawater temperatures and salinities, a cruise track via the Flemish Cap off Newfoundland was chosen. All participating groups operated their underway pCO_2 systems simultaneously on a separate seawater pumping system and a consistent suite of calibration gases, all of which was provided by the organiser.

As most up-to-date research vessels, METEOR provides a special seawater pumping system for scientific purposes. From experience it is known that the use of this kind of pumping system for measurements of dissolved gases is hampered by a number of problems. Pump action may cause cavitation when underpressure is applied to the water flow, thus making undisturbed gas measurements nearly impossible. Due to the location of the seawater intake (i.e. bow intake on METEOR), air bubbles are also introduced into the water lines in rough sea. This again possibly biases the concentration of dissolved gases or even makes seawater sampling technically impossible. Furthermore, the unavoidable warming of seawater during its travel from the seawater intake to the user is significant. In the case of pCO_2 measurements it is desirable to have the temperature change as small as possible.

Due to the sluggish equilibration of CO_2 between gas and water phase sampling for CO_2 measurements (e.g., pCO_2, pH, C_T (total dissolved inorganic carbon)) is less susceptible to artefacts caused by imperfect pumping techniques as compared to non-reactive gases like oxygen. Nevertheless, a careful sampling technique was an important aspect of the exercise. For this reason, a simple and reliable underway pumping system (see also: KÖRTZINGER et al.,

1996) was designed for use in the "moon pool" of METEOR. The system consisted of a small conductivity-temperature-depth probe (CTD probe "ECO", ME Meerestechnik-Elektronik GmbH, Trappenkamp, Germany) for measuring seawater temperature and salinity at the intake as well as a submersible pump, both of which were installed in the bottom plate of the "moon pool". Figure 7 shows a schematic drawing of this underway pumping system. To make the system as flexible as possible, a separate GPS receiver (GPS 120, Garmin/Europe Ltd., Romsey, Hampshire, UK) was included. CTD and navigational data from the GPS system were continuously logged on a computer.
The "moon pool" of METEOR is specially designed for sampling purposes as no cooling or waste waters are emitted forward of the "moon pool". Even at full speed or in very rough sea, no air bubbles reach the "moon pool". Seawater was pumped through the "moon pool" from below the ship by means of a large submersible pump (multi-vane impeller pump CS 3060, ITT Flygt Pumpen GmbH, Langenhagen, Germany) at a pumping rate of about 350 l/min. The CTD probe was installed next to the submersible pump.

All underway pCO_2 systems were assembled in the geology laboratory of METEOR. Two seawater supply lines were teed-off from the main bypass and laid through the lab. All systems were hooked up to these supply lines which delivered the necessary flow rates of seawater (between 1 and 10 l/min). We also provided a whole suite of calibration gases. Nitrogen (99.999 %) was used by some groups for zeroing their gas analysers. Calibration gases with precisely known amounts of CO_2 in natural dry air were purchased from the NOAA Climate Monitoring Diagnostics Laboratory (CMDL) in Boulder, Colorado, U.S.A. This consistent suite of gases was used by all groups for calibrating their instruments. The common seawater and calibration gas supply were key requirements for exercise, as otherwise systematic errors most likely would have been introduced.

The waste water from the systems was collected in three 100 l carboys and disposed of through the floor drains of the geology lab. To prevent clogging of the drains due to rough sea conditions, small submersible pumps (multi-vane impeller pump GS 9565, ITT Flygt Pumpen GmbH, Langenhagen, Germany) were at hand to pump the waste water actively out of the lab. However, they did not have to be used during the cruise. According to the different power requirements the ship provided three different power sources: the standard 220 V/50 Hz system as well as two additional systems for 220 V/50 Hz (static transformer) and 220 V/60 Hz (dynamic transformer).

5.1.2.3 Shipboard Results

Right from the beginning it was considered high priority to measure as many CO_2 parameters (i.e. pH, pCO_2 (partial pressure of CO_2), C_T, A_T (total alkalinity)) as possible rather than restricting the exercise to mere pCO_2 measurements. For this purpose we followed two different sampling strategies, i.e. underway sampling and discrete sampling. As all participating pCO_2 systems (CSIRO, IfMK, MRI, NBI, OU, UP & MC, WHOI) were operated in an underway mode on the same seawater source, it was highly desirable to back up these

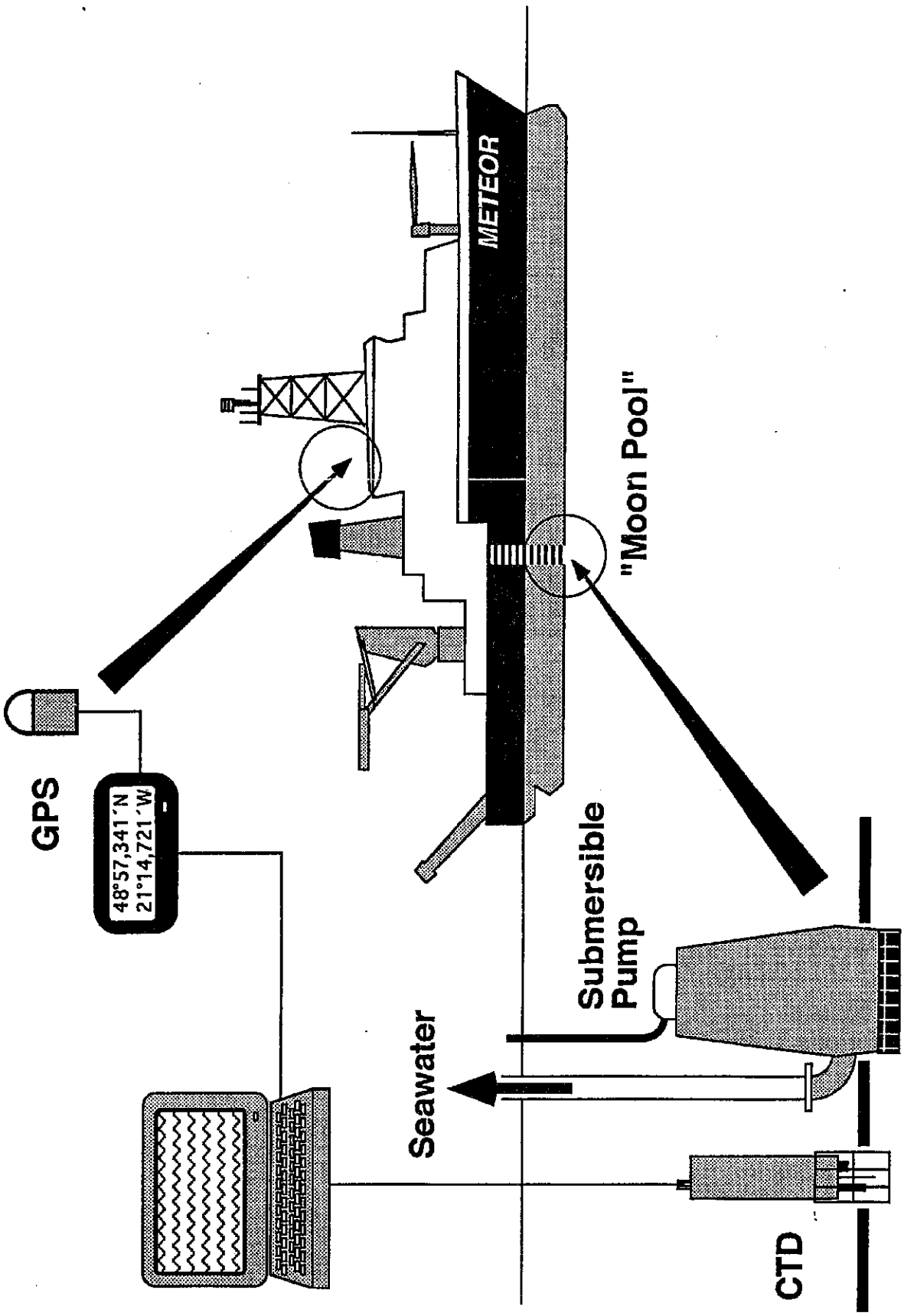

Fig. 7: Schematic drawing of the underway seawater pumping system as installed on METEOR during cruise M 36/1 from Bermuda to Las Palmas de Gran Canaria (from: JOHNSON et al., in prep.).

pCO_2 measurements with additional underway measurements of other CO_2 parameters. This was accomplished by underway pH measurements with two different spectrophotometric systems (SIO, WHOI) as well as underway C_T measurements (BNL/IfMK) with a newly modified SOMMA coulometric titration system (JOHNSON et al., in prep.), all of which were also hooked up to the seawater pumping system. The discrete samples for measurements of pCO_2 (BNL), C_T (BNL/IfMK), A_T (IfMK), salinity (IfMK) as well as nutrients (IfMK) were taken regularly during the XBT launches.

By measuring more than two CO_2 parameters, the CO_2 system in seawater is overdetermined as all parameters can be calculated from any combination of two measured parameters. This was the case for both sampling strategies. This overdetermination will allow for consistency checks on the data sets. It may also provide additional information in the controversy about the best set of thermodynamic constants for the CO_2 system. The broad CO_2 data base furthermore serves as valuable background information and strongly enhances interpretation of the results.

The exercise also included checks on ancillary measurements like temperature and barometric pressure as performed by most of the analytical systems. All temperature sensors were compared against a calibrated Pt 100 reference thermometer. The barometric pressure readings were also referenced against a high-quality digital barometer. These checks revealed offsets and miscalibrations, which will lead to differences in the final pCO_2 values. The checks will help to identify the error contribution from these sources. They will also allow all pCO_2 measurements to be corrected for these effects to reveal any other systematic differences which cannot be attributed to incorrect temperature and pressure readings.

Further checks were carried out with the calibration gases. The suite of calibration gases covered a range of CO_2 concentrations between 250 and 500 ppmv with nominal values of 250, 300, 350, 400, 450 and 500 ppmv. While every group required one or more of these calibration gases for their calibration procedure, they measured all other concentrations as unknown samples on their systems. The results provide information on the quality and reliability of the calibration procedures over the whole range from 250 to 500 ppmv. As the infrared detectors used by all groups generally show non-linear response functions, the calibration procedure is a crucial point.

All seven underway pCO_2 systems were operated simultaneously for most of the time between June 7 and June 17. Technical problems which occurred to some of the systems only caused short interruptions. Only one system suffered heavy damage in the infrared gas analyser and had to cease taking measurements on June 16. The two underway spectrophotometric pH systems were operated throughout the cruise. The newly modified coulometric SOMMA system for underway determination of C_T was tested successfully at sea and contributed 452 high-quality underway measurements along the cruise track. These data (Fig. 8) nicely show the correlation between surface seawater temperature (SST) and C_T normalized to a salinity of 35 (JOHNSON et al., in prep.). This new application of the well-known SOMMA system herewith demonstrates its potential for high-quality, high-resolution surface measurements of C_T. Synchronised with the XBT survey a total of 57 discrete samples were taken from the

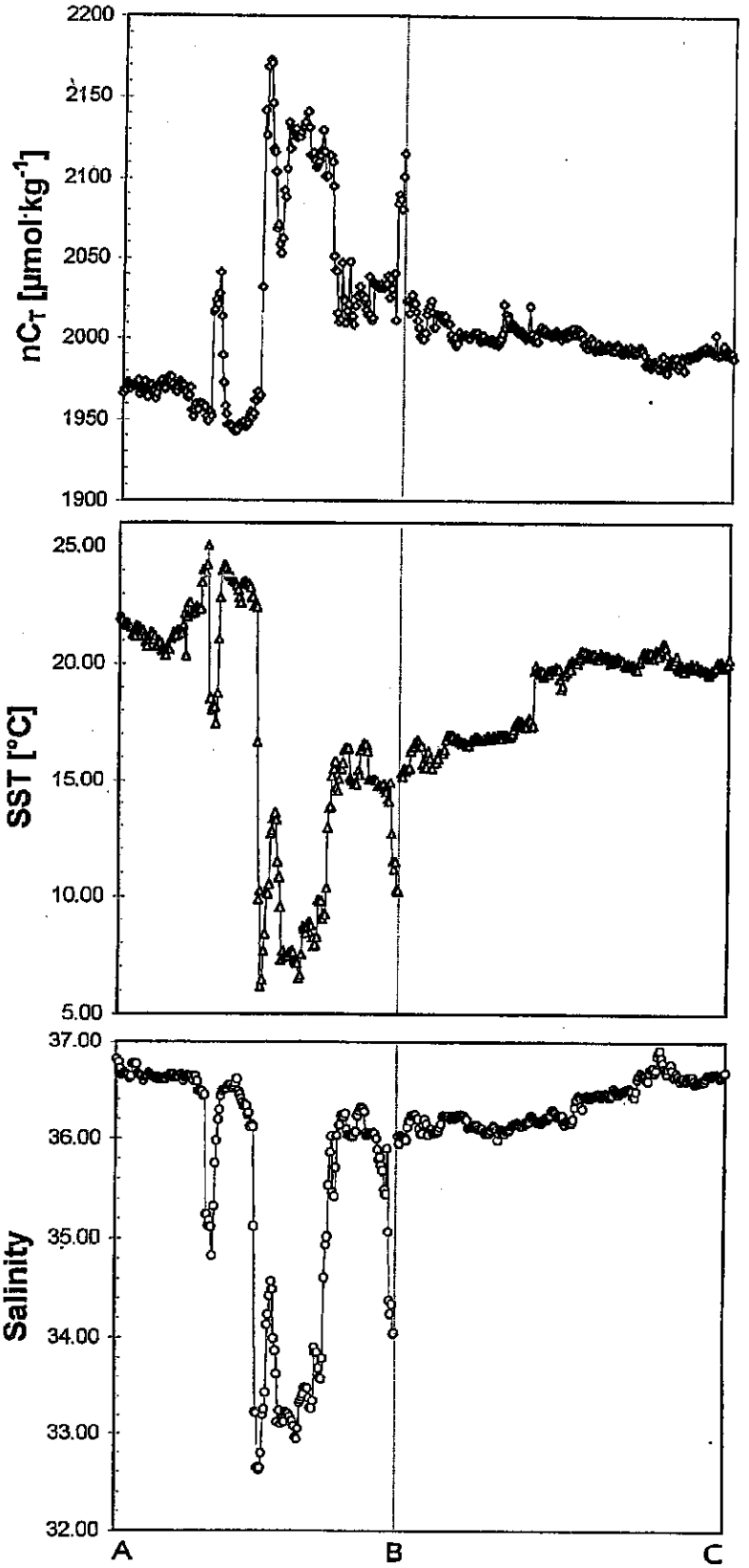

Fig. 8: Surface profiles of salinity-normalized total dissolved inorganic carbon (nC_T, top), sea surface temperature (SST, centre) and surface salinity (bottom) along cruise track of METEOR during M 36/1. The nC_T profile shows a pattern which is virtually the mirrored image of the SST pattern (from: JOHNSON et al., in prep.).

seawater supply and were analysed for C_T and A_T. The discrete pCO_2 measurements could not be carried out on the same schedule; only about 25 XBT stations samples were taken for this parameter.

In addition to the various surface measurements - whether continuous or discrete - four full depth CTD stations were carried out. Samples were drawn for measurements of all four CO_2 system parameters (pH, pCO_2, C_T, A_T) thus yielding the highest possible overdetermination of the marine CO_2 system.

Participants had all their raw data delivered to the organiser by the end of the cruise. However, final data are not yet available in most cases. These final data sets have to be submitted to the organiser by September 19, 1996. After that, much thought needs to go into teasing out the information contained in the data collected and into preparation of the final exercise report. The ultimate aim is to provide information on the comparability of data sets, which is a crucial point in the current international effort of bringing together all available pCO_2 data, and to develop recommendations for future field measurements of pCO_2.

5.2 Leg M 36/2

5.2.1 **Physical Oceanography** (J. Waniek, P. Schröder)

The objective of the hydrographic programme during leg 2 was the detailed description of the physical environment along 20°W in selected areas of the subtropical, moderate and subarctical North Atlantic and, therefore, was a substantial precondition for a variety of biological-chemical studies and for interpretation of the results. The cruise M 36/2 was planned to study the pelagic summer system along 20°W. Based on observations of earlier studies in the investigation area, we assume that a detailed description of the mesoscale structures is essential to understand the pelagic system during summer. Special emphasis during this leg was placed on the documentation of the variability in the upper 500 m of the water column in relation to the circulation patterns at greater depths. In addition, diurnal changes in the mixed layer depth and their forcing functions (insulation, air temperature and wind stress) were monitored using CTD-O_2 fluorescence system and shipborne sensors.

During good weather conditions METEOR left Las Palmas on June 22, 1996, heading for the southern mooring station at 33°N/20°W (Fig. 9a,b). From this position we started our investigations with CTD casts (spatial resolution was 140 nm) and dropping XBTs (Expendable Bathythermographs, every 30 nm) inbetween (chapter 7.2.1). The standard sampling device was a combined CTD water sampler with additional sensors for oxygen and Chl.-a fluorescence. Along the cruise track between the CTD stations, a surface pump system was used, which delivered samples for the filtration of Chl.-a, particulate organic nitrogen (PON)/particulate organic carbon (POC), particulate Si and $CaCO_3$ as well as for HPLC analysis, the determination of nutrient concentrations, the salinity and large-scale distribution of phytoplankton biomass. These investigations were supported by continuous records of

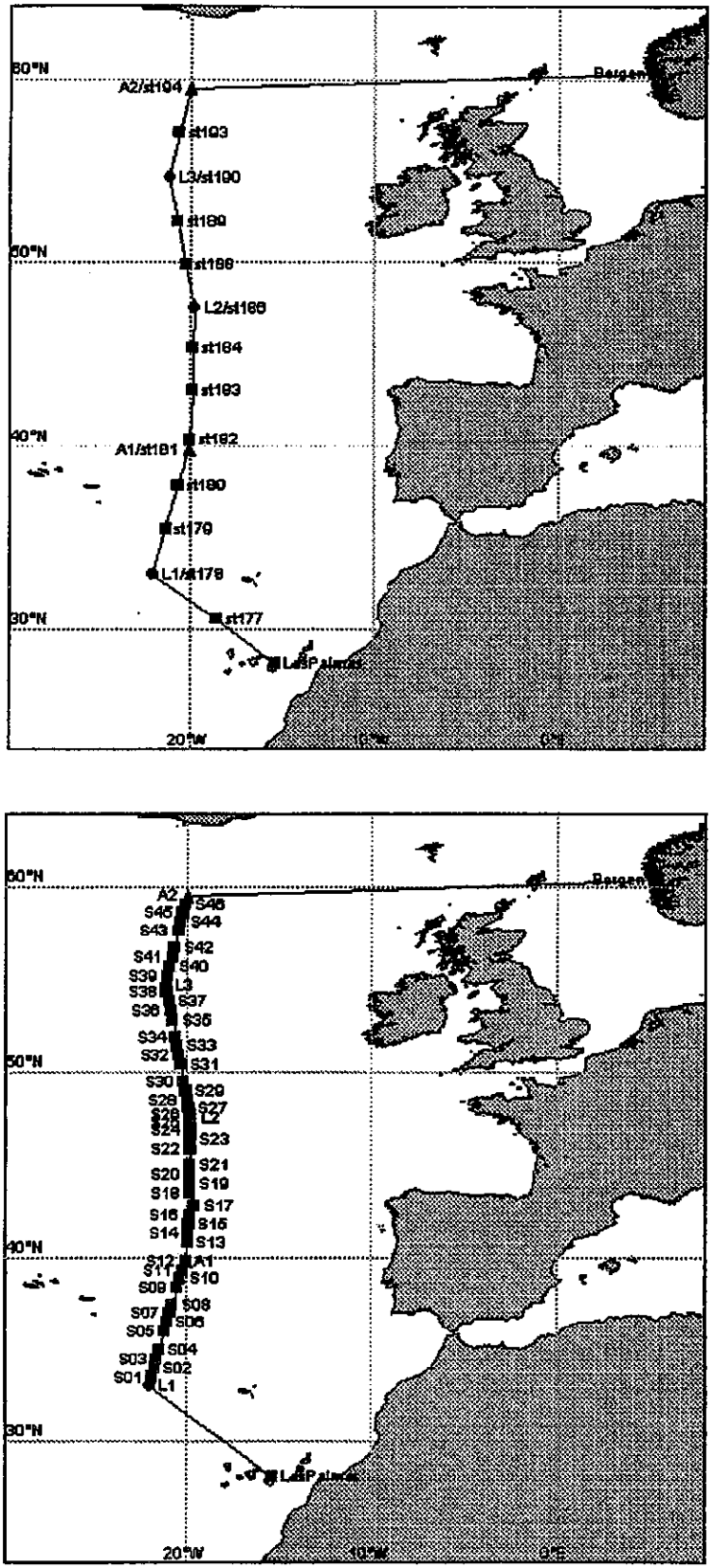

Fig. 9a,b: Cruise track and the research area during M 36/2;
(a) position of the main CTD stations and (b) mooring positions L1, L2 and L3, underway stations.

Chl.-a fluorescence, CTD (at sea surface) and ADCP (Acoustical Current Doppler Profiler) along the cruise track in the upper 300 m of the water column.

5.2.1.1 Shipboard Results

The temperature signal at sea surface measured during the second leg of M 36 showed a strong gradient from south to north along 20°W. This feature showed that the research area (section along 20°W) is dominated by a change of the hydrographical regimes: At the southern end of the section, in the region between 33°N and 40°N (Fig. 10a,b), the surface temperatures are relatively high ranging between 19-21°C (subtropical area). In the moderate North Atlantic (40°-50°N), the temperature signal ranged between 14°-18°C and sank down to 11°C at 60°N in the subarctical region. The measured salinity at sea surface is in good relationship with the temperature signal at sea surface: High salinities (> 35.6) were observed in the subtropical area south of 45°N, whereas the salinity signal decreased to 35.2 in the subarctical part of the section at 60°N (Fig. 10a,b).

The same features have been observed in the water column. The upper 100 m are dominated by the seasonal signal with a shallow mixed layer (Fig. 11a). In the subtropical region (stations 177-180), waters with high temperature signal (values between 15°-21°C) occupied the water column from the surface down to 100 m depth. In the moderate North Atlantic (station 181-188) the temperature signal decreased and reached 12°C at 100 m depth. Finally, the subarctic part of the section again showed lower temperatures with only 10°C at 100 m depth. The mixed layer, calculated from the CTD data with a criterion ΔT=0.5°C, is very shallow at all stations of this transect. For example, at station 177 the mixed layer reaches only 19 m, rises up to 12 m at stations 181-183 and deepens from station 184 to the north end of the transect (station 194) down to 60 m (Fig. 11a). The main gradient between the mixed layer and the deeper water column was 2°-3°C (seasonal thermocline).

The vertical temperature distribution down to 2000 m during M 36/2 showed a well-stratified water column below the shallow mixed layer along the whole transect. In the southern part of the section (station 177 to 180), the water column is dominated by relatively warm, salty waters. The observed temperature between the sea surface and 500 m depth ranged between 12°-21°C accompanied by a high salinity signal of 36.6 at the surface and 35.6 in 500 m depth. Below 500 m, the temperature decreased and reached values between 4°-5°C at 2000 m. In depths between 800-1100 m, the influence of waters coming from the Mediterranean Sea is evident. The temperature and salinity signal increased again; the temperature showed values around 10°C and salinity reaches values higher than 35.6 (Fig. 11b,c).

The region in the moderate part of the North Atlantic (station 182-188) is occupied by waters with lower temperature and salinity signal down to 2000 m; In comparison, the waters at 500 m depth are 2°C colder than in the subtropical region and have temperatures of only 10°-11°C. The salinity only reached values between 35.7-35. The influence of waters spreading from the Mediterranean Sea is missing. In 2000 m the water column is occupied by the North

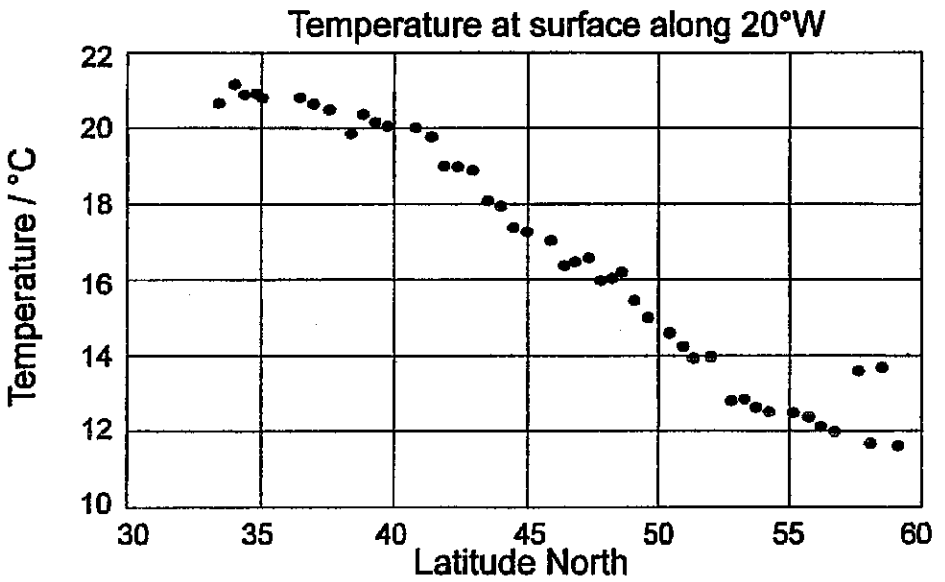

Fig. 10a: Temperature at sea surface measured at the underway stations along the cruise track from 33°N to 60°N.

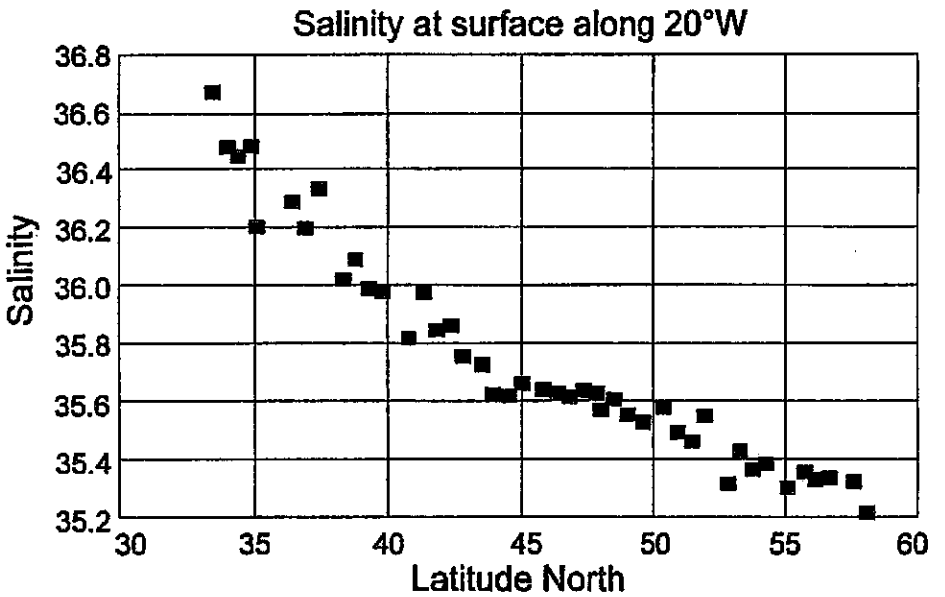

Fig. 10b: Salinity at sea surface measured at the underway stations along the cruise track from 33°N to 60°N.

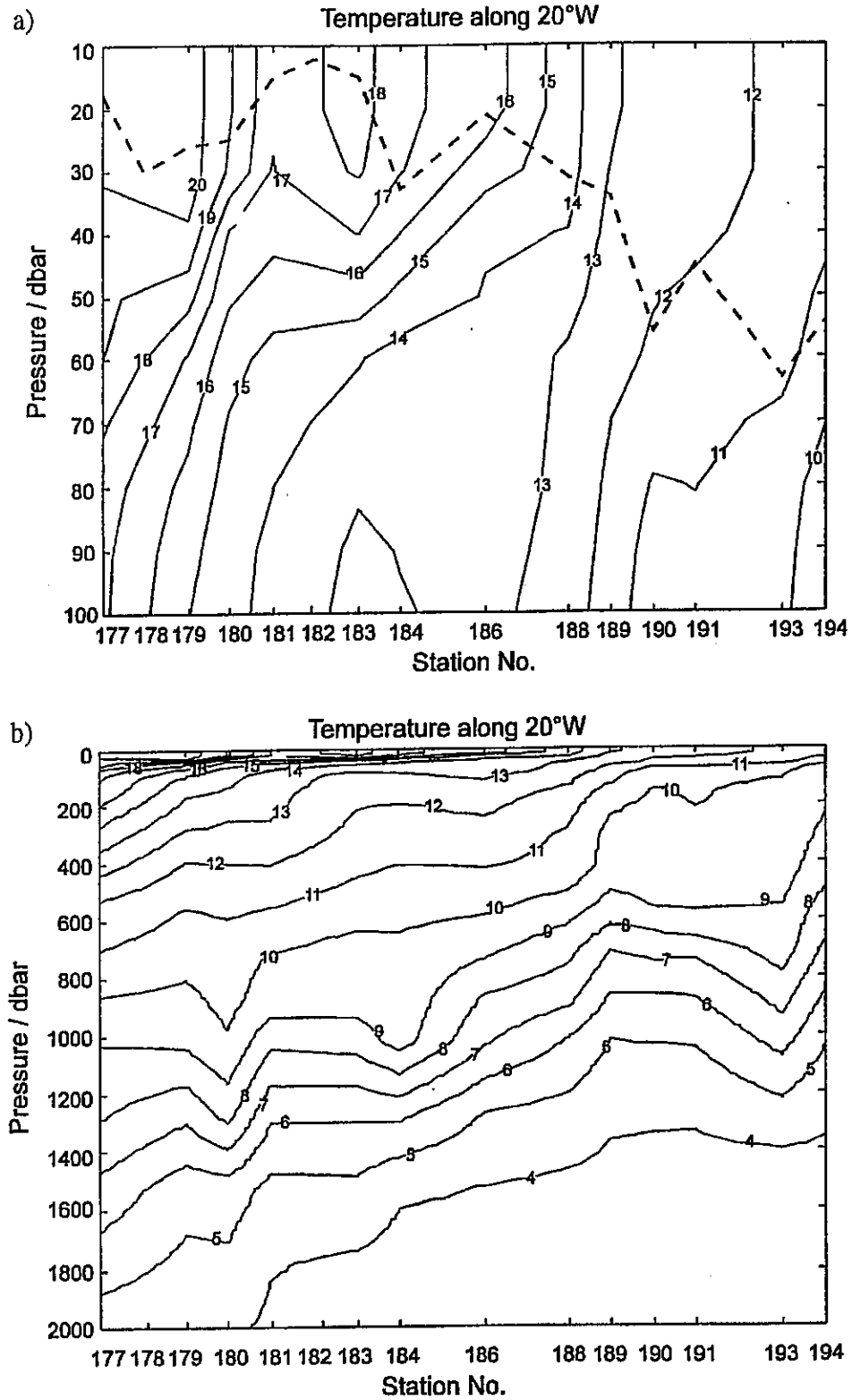

Fig. 11a,b: (a) Temperature section for the upper 100 m of the water column along the CTD section from station 177 to station 194; the line marks the mixed layer depth calculated with the criterion $\Delta T=0.5°C$ (for position of the stations see Fig. 9); (b) vertical temperature distribution down to 2000 m depth.

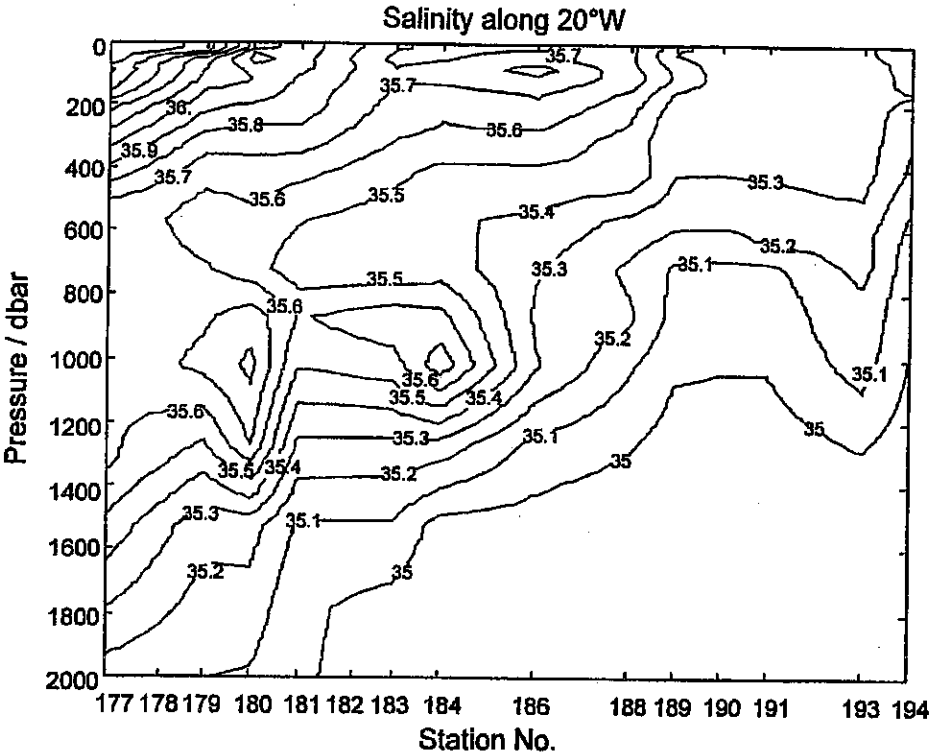

Fig. 11c: (c) Salinity section down to 2000 m depth along the CTD section from station 177 to station 194; for position of the stations see Fig. 9.

Atlantic Deep Water (NADW), which is characterised by low temperatures (< 4°C) and uniform salinity (< 35).

The most drastic differences in the vertical temperature and salinity field are evident on the northern part of our transect (subarctical region, stations 189-194). The temperature differences at 500 m depth between this region and the subtropics (stations 177-181) reached up to 3°C. The waters below 500 m are characterised by temperatures between 3°- 8°C. In the salinity field only small gradients are evident and the water column between surface and 2000 m depth is occupied by waters with salinity between 35.3 and 35.

5.2.2 Chemical Oceanography

5.2.2.1 Marine CO_2-System, Dissolved Oxygen and Nutrients

(L. Mintrop, S. Schweinsberg, F. Malien)

The work carried out by the CO_2 project basically followed two different sampling strategies. The first comprised classical discrete water sampling from 14 hydrocasts at 12 hydrographic stations. A total of 282 samples were drawn and immediately analysed for total dissolved inorganic carbon (C_T) and total alkalinity (A_T). The analytical methods involved are a coulometric titration technique for C_T (SOMMA-system, JOHNSON et al., 1993; DOE, 1994) and potentiometric titration for A_T, basically according to MILLERO et al. (1993), but carried

out in an open vessel (VINDTA-system, MINTROP, 1996, unpubl.). Due to modifications of the SOMMA system in using a smaller pipette (approx. 6 ml) than usual, C_T and A_T could be determined from the same sample bottle (approx. 250 ml). The precision (between-bottle reproducibility) as judged from regular measurements of duplicate samples was 0.5 µmol/kg for C_T and 0.5 µmol/kg for A_T. Accuracy of the data has been estimated to be about 1.5 µmol/kg for C_T and 2.0 µmol/kg for A_T.

The second sampling strategy involved the continuous determination of the partial pressure of CO_2 (pCO_2, closely equivalent to fugacity of CO_2 which more correctly takes into account the non-ideal nature of this gas) in surface seawater and overlying air. For this purpose a newly developed automated underway pCO_2 system with a non-dispersive infrared gas detection technique (KÖRTZINGER et al., 1996) was operated throughout the cruise. The continuous flow of seawater was drawn at 5 m depth. During the cruise, a data set of more than 1800 one-minute-averages for atmospheric pCO_2 and approx. 35,000 averages for surface seawater pCO_2 were generated. The comparatively short time constant of the system of 75 s even allows the small-scale variability of pCO_2 in seawater to be resolved. In the „moon pool", a CTD system was installed to allow for continuous registration of temperature and salinity close to the water intake of the pump. The data were stored on a PC which was also connected to a GPS system and the data were merged.

Dissolved oxygen was measured in the samples from the hydrocasts using standard Winkler titration. A total of 447 samples were analysed.

Nutrients (nitrite, nitrate, phosphate and silicate) were determined from hydrocast samples and from surface samples taken at certain locations (i.e. every 30-40 nautical miles) along the track. A total of 620 samples were analysed, plus about 80 samples from various experiments. Measurements were done on an autoanalyser system using classical photometric techniques.

5.2.2.2 Shipboard Results: Marine CO_2-System, Dissolved Oxygen and Nutrients

The **C_T (total carbonate)** measurements show the following: the values of total carbonate at the surface were generally around 2080-2090 µmol/kg along the track, with a slight increase towards the north. Decreasing salinity is responsible for these rather constant values, while decreasing temperature theoretically should lead to higher C_T values. If C_T values are normalized to constant salinity (35) to account for evaporation loss and precipitation gain, the normalized values show an increase from 1980 to 2060 µmol/kg/salinity 35 along the track.

Generally, depth profiles of C_T are characterised by a steep gradient from the mixed layer to a secondary maximum encountered at approx. 1000 m depth, a slight decrease further on with depth and increase below 2500 m towards the bottom, where the maximum values were found. Fig. 12a shows an isoplot of C_T values and depth (expressed as pressure in dbars, nearly equilvalent to metres) versus latitude. The secondary maximum, associated with the Mediterranean Outflow Water at approx. 1000 m depth nearly vanishes at the northern half of

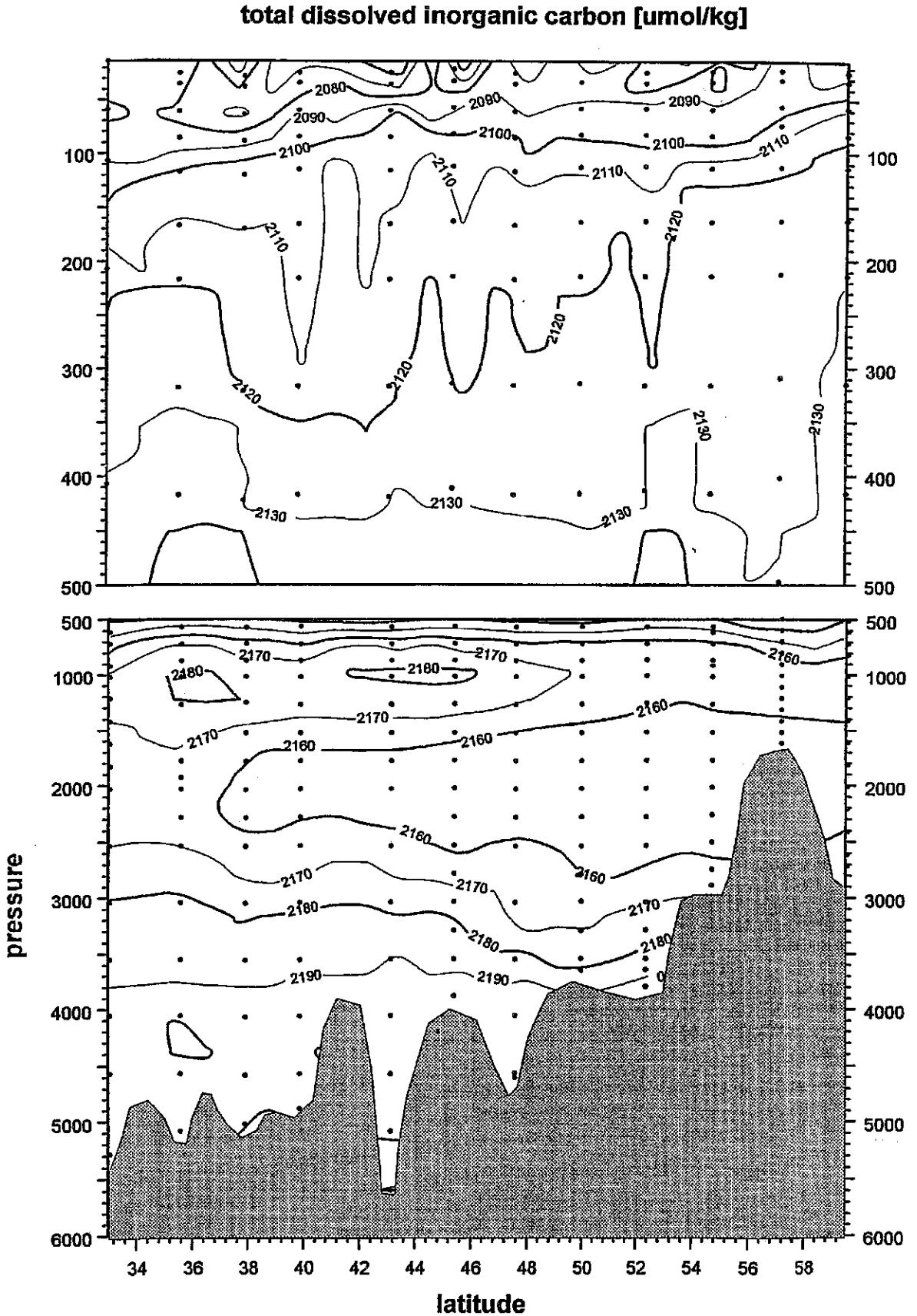

Fig. 12a: Isoplots of the measured parameter total dissolved inorganic carbon (C_T) along the cruise track (nominally 20°W). Values (preliminary) are in µmol/kg. The upper 500 m are enlarged at the upper part of the diagram.

the track, allowing for the development of a slight secondary minimum at about 2000 m depth, resulting from increasing NADW contribution. Deep water values reach more than 2190 µmol/kg. In the upper water column, enlarged at the top of the diagram, the rising of isolines with higher latitude becomes obvious.

A_T (titration alkalinity): Surface water alkalinity decreases from 2420 to 2350 µmol/kg from the southern end of the track towards approx. 45°N and stays rather constant at this level to the northern end of the track. However, normalized to salinity 35, the increase reduces from 2300 to 2325 µmol/kg/salinity 35, thus demonstrating the rather conservative behaviour of alkalinity.

Depth profiles of alkalinity show a gradual increase with depth from the mixed layer to approx. 3500 m and values remaining more or less constant towards the bottom. A secondary maximum is observed at about 1000 m depth, nearly absent after normalisation. This type of profile was found in the southern part of the track. Further north, alkalinity was nearly constant or even slightly decreasing from the mixed layer to about 500 m, further increasing with depth to about 1000 m. Minimum values were found between 1500 and 2500 m, with values increasing towards the bottom below this zone. Fig. 12b shows the isoplot of alkalinity with depth (expressed as pressure in dbars) versus latitude. Mediterranean Outflow and NADW are clearly visible by a plume of high and low values, respectively. Deep values lie below 2360 µmol/kg. In the upper part of the plot, the steep isolines from S to N are obvious, resulting in nearly uniform values for the northernmost depth profiles.

Depth profiles of both C_T and A_T very much resemble those obtained in the eastern North Atlantic Basin on the zonal transect at 47°N in November 1994, though the S-N alteration of the profiles is obvious as discussed above. However, they show distinct differences compared to those obtained in the western North Atlantic Basin on the first leg of this cruise and in November 1994.

A further discussion of C_T and A_T properties of different water masses will be accomplished after all hydrographic data have been processed in detail. Oxygen data will allow for a detailed study about the demineralisation of organic matter and the dissolution of calcite. This will also form the basis for the calculation of the penetration depth of anthropogenic carbon into the North Atlantic Ocean as previously carried out from data obtained on a zonal transect at approx. 45°N (KÖRTZINGER et al., 1996). The data of the meridional transect at 20°W obtained on this cruise will give valuable information on the north-south gradient of anthropogenic CO_2 penetration in the eastern North Atlantic Basin. The results will help to refine the estimations of the inventory of anthropogenic CO_2 (approx. 30 giga tons (Gt) for the North Atlantic north of 15°N) and to assess the importance of this ocean in the light of the global oceanic uptake of anthropogenic CO_2.

By determining two of the four parameters of the oceanic carbonate system (C_T, A_T, pH, and pCO_2), the remaining two can be calculated to result in a full specification of inorganic carbon.

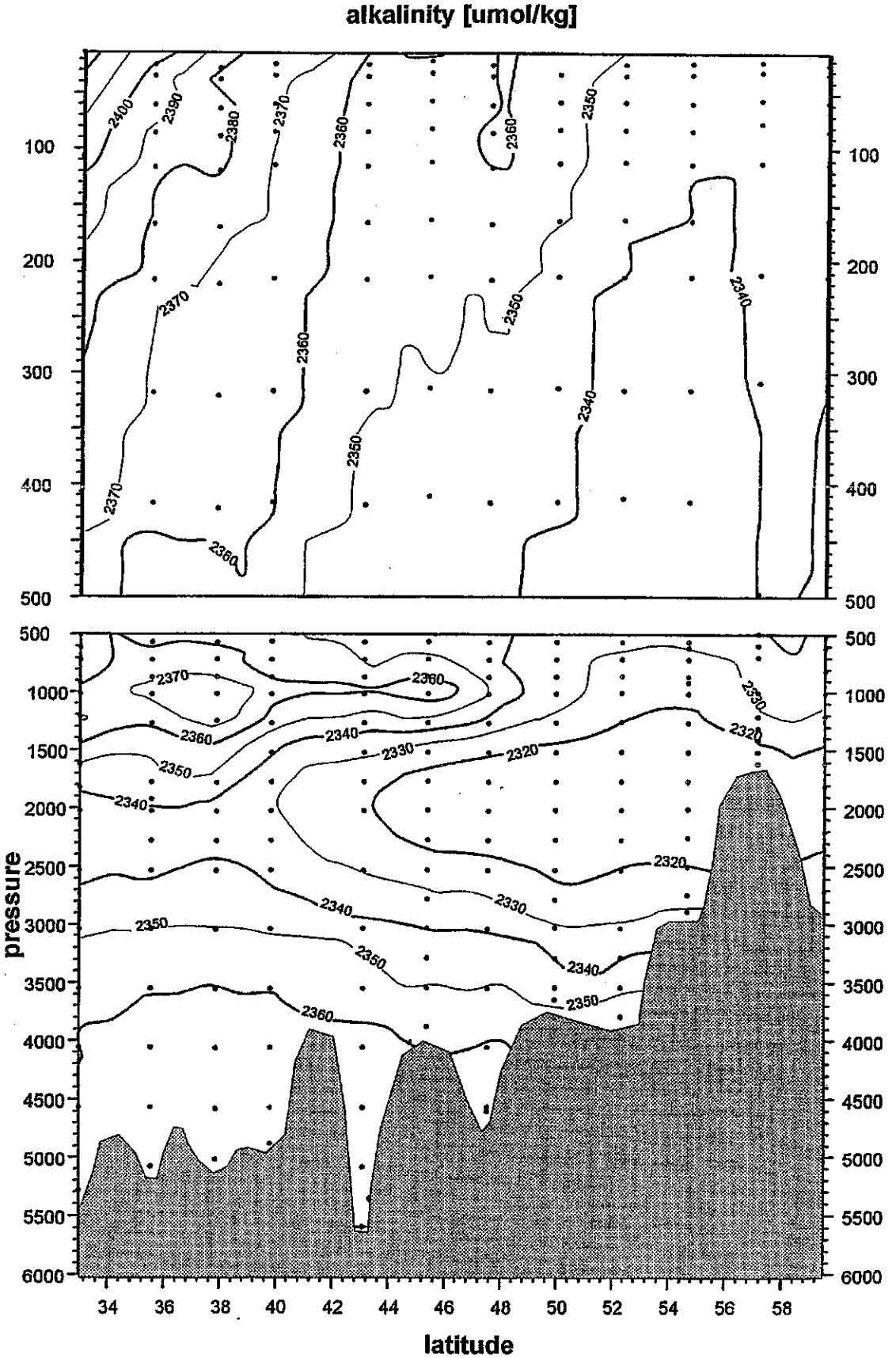

Fig. 12b: Isoplots of the measured parameter total alkalinity (A_T) along the cruise track (nominally 20°W). Values (preliminary) are in µmol/kg. The upper 500 m are enlarged at the upper part of the diagram.

Surface water pCO_2: The pCO_2 of surface water changed from slight oversaturation to pronounced undersaturation in respect to the atmosphere along the track. Values were about 380 ppm (molar fraction of CO_2, µmol/mol) at the beginning of the cruise and reached the atmospheric value of 363 ppm approx. at 38°N. Values decreased to about 340 ppm until about 320 ppm were reached at 47°N. Several negative peaks were recorded on the way further north with values as low as 290 ppm at about 51°N. Further on values stabilised at 320±10 ppm until 56°N and were around 340 ppm up to the northern end of the track. Registration was continued on the further course east towards Bergen, Norway, all the way up onto the shelf (water depth < 200 m). Values with large fluctuations were encountered, mostly around 330 ppm, with occasional dropdowns below 300 ppm; values also measured on the shelf at the end of the registration.

The profiles of pCO_2 vary together with temperature, indicating that water mass characteristics and their short time variability and local patchiness govern the pCO_2. Positive correlation between pCO_2 and temperature would indicate rising pCO_2 when a water mass gets warmer (theoretically about 4% per °C). Since covariation is observed also without positive correlation, it is more likely that temperature indicates different water parcels and their patchy distribution in these cases, which, due to their inherent preformed pCO_2, cause the observed pCO_2 variability. Negative correlation would also be the result of CO_2 uptake after a water parcel had been cooled due to higher solubility of CO_2 in cold water. However, in most cases CO_2 exchange is slow compared to temperature change of surface waters. As an example, Fig. 13 shows profiles of pCO_2 (more exactly, the molar fraction of CO_2 in surface seawater is shown) along the cruise track in the upper part versus time while being stationary in the lower part. Each diagram shows a 24 h registration from 0:00 to 24:00 UTC. The registration in the upper diagram shows the covariation of pCO_2 and temperature, correlated positively in most parts. This might indicate that a single water mass experienced temperature change in a time period too short to allow for CO_2 exchange. The registration at the lower part of the diagram shows large scatter of pCO_2 values without strong temperature variations. Most likely this scatter is caused by short time and small scale variability of photosynthetic and respiration activities of organisms and their patchy distribution. Note that the scale of the x-axis is the same for the upper and lower diagram.

Atmospheric values of pCO_2 (expressed as molar fraction) decrease by 4 ppm from about 363 to 359 ppm along the track. This can be explained by the seasonal cycle of atmospheric CO_2 concentration: Fixation of CO_2 by terrestrial vegetation, mainly in the summer period, will lower the atmospheric concentration. This effect increases from the equator northwards and is most likely responsible for the decrease observed.

The data collected so far represent the molar fraction of CO_2 in moist air. Taking into account the atmospheric pressure from the DVS data file and by calculating the water vapor pressure, the fugacity of CO_2 in dry air will be calculated. The data will be sent to the CO_2 data centre in Oak Ridge, Tennessee, USA, to serve in the development of a seasonal pCO_2 model of the North Atlantic Ocean.

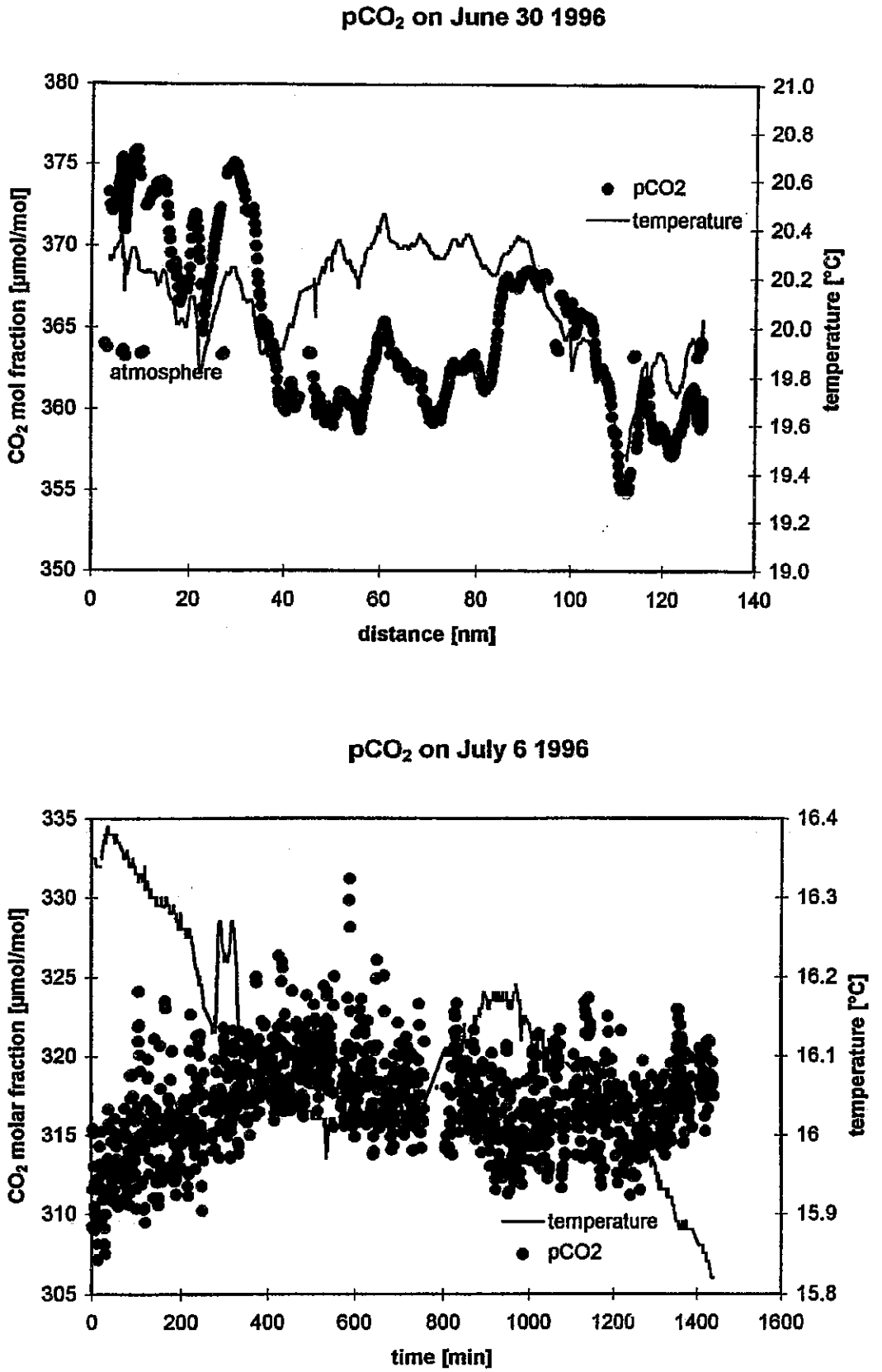

Fig. 13: Examples of 24 hour registration of temperature and molar fraction of CO_2 in surface seawater. Upper diagram shows values versus distance between stations 180 and 181 on June 30, lower diagram shows values versus time while on station 186 on July 6.

Oxygen: Oxygen concentrations at the surface rise in parallel with sinking temperature along the cruise track northbound (see Fig. 14a). Depth profiles clearly show two features: Low oxygen water from the Mediterranean Outflow at 500 to 1500 m depth at the southern end of the track, with width decreasing to 700-800 m, and minimum values increasing from < 4.6 up to > 5 ml/l up to approx. 50°N. The second visible feature is high oxygen NADW, reaching values above 6.4 ml/l from 49°N on northbound, centred at a depth of about 2000 m. Calculation of oxygen saturation and apparent oxygen utilisation (AOU) will be carried out soon to allow for estimation of age and remineralization inventory.

Nutrients: Nutrient concentrations in the upper water column rise along the track, reaching non-zero values at the surface north of 46°N, while values up to 6 µmol/l nitrate were observed at the northern end of the track. A nitrate isoline plot as example is shown in Fig. 14b. Rising isolines are clearly visible in the upper 500 m. The NADW can be identified by a plume of values below 18 µmol/l at about 2000 m depth north of 44°N. Bottom values reach 23 µmol/l and a secondary maximum with values above 19 µmol/l is visible at 50-55°N at 1000 m depth. Phosphate profiles look similar, while nitrite was found at the northern part of the track at depth between 50 and 200 m and values up to 0.5 µmol/l. Detailed investigations of the nutrient data and nutrient-carbon-oxygen relations are to be carried out.

5.2.2.3 Amino Acids: Shipboard Results (U. Lundgreen)

During the legs M 36/1 and M 36/2, suspended particulate matter (SPM) from surface waters (approx. 7 m depth) was sampled with a continuous-flow centrifuge (SCHÜSSLER and KREMLING, 1993), deep-frozen and analysed in the home laboratory. Here we present initial results from the amino acid analysis. Amino acids were analysed from hydrolysates of the particulate matter with a standard chromatographic method using OPA-derivatization and fluorimetric detection. The method is described in detail by LUNDGREEN (1996) and briefly summarised here: Hydrolysis was performed under pure nitrogen in sealed glass ampoules for 70 min at 150°C with 6N hydrochloric acid. After removal of the hydrochloric acid in a vacuum centrifuge, the samples were redissolved in superpure water and injected to the HPLC system. The samples were then pre-column derivatized with orthophthaldialdehyde and mercaptoethanol.
Chromatography was performed on reversed-phase C_{18} columns (spherisorb ODS II, 5 µm), running a two-solvent gradient of sodium acetate buffer (pH 5.2-5.6) and a methanol-acetonitrile mixture. Detection wave length was 450 nm with excitation at 335 nm.

SPM-amino acid concentrations varied between 50 and 1000 µmol/m3 on the two legs; the highest concentrations were found in the coastal waters off Scotland and around 50 °N, near JGOFS station L2, which is depicted in Fig. 15. The spatial distribution of surface amino acid concentration in Fig. 15 closely follows the amount of suspended particles in the water. It depicts the general pattern of productivity of the different biogeochemical regimes throughout the North Atlantic: Clear subtropical waters with low particle load and, therefore, low SPM-amino acid concentration were passed between 30 and 40°N. In temperate regions, the particle

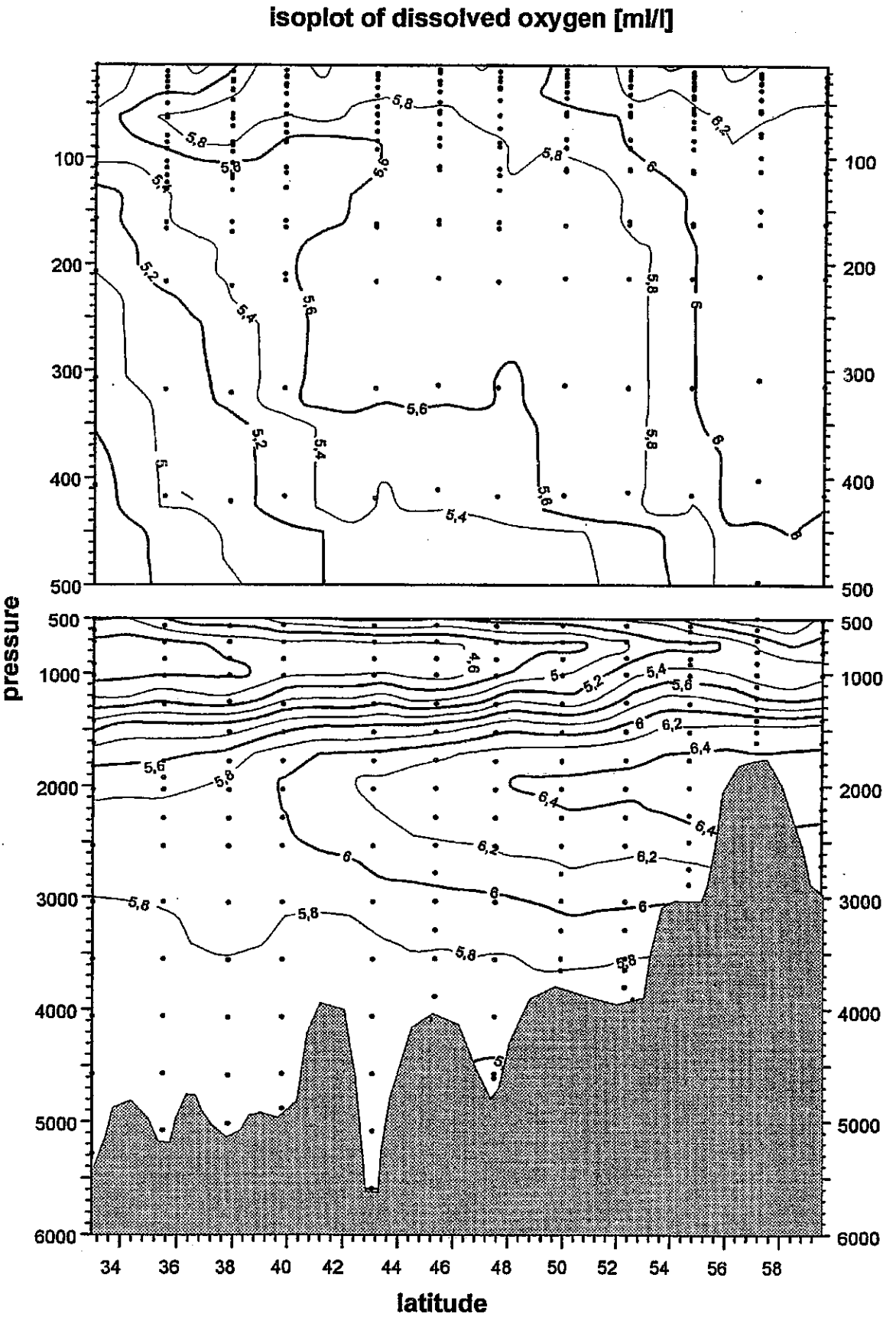

Fig. 14a: Isoplots of dissolved oxygen along the cruise track. Values are in ml/l and µmol/l, respectively.

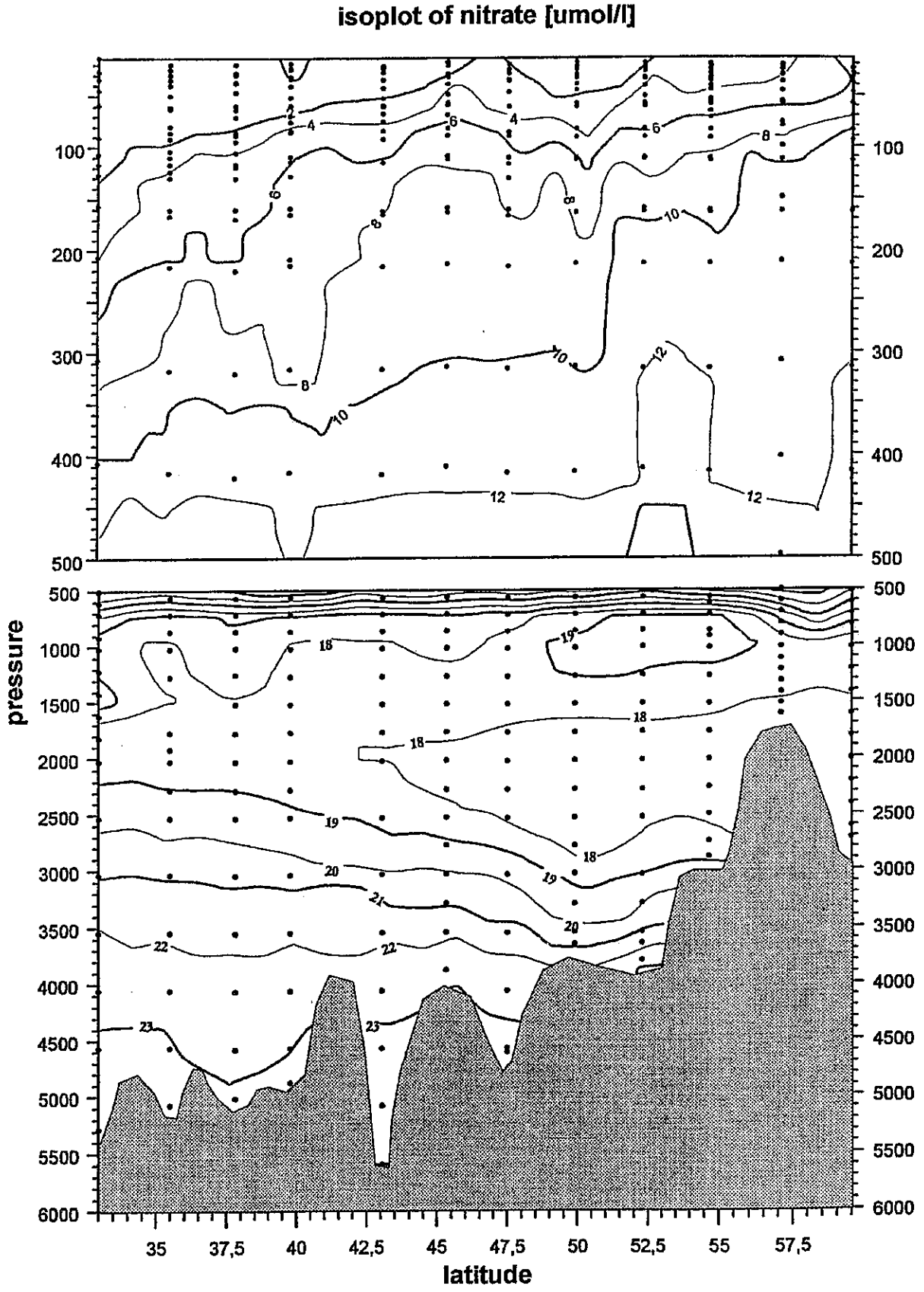

Fig. 14b: Isoplots of nitrate along the cruise track. Values are in ml/l and µmol/l, respectively.

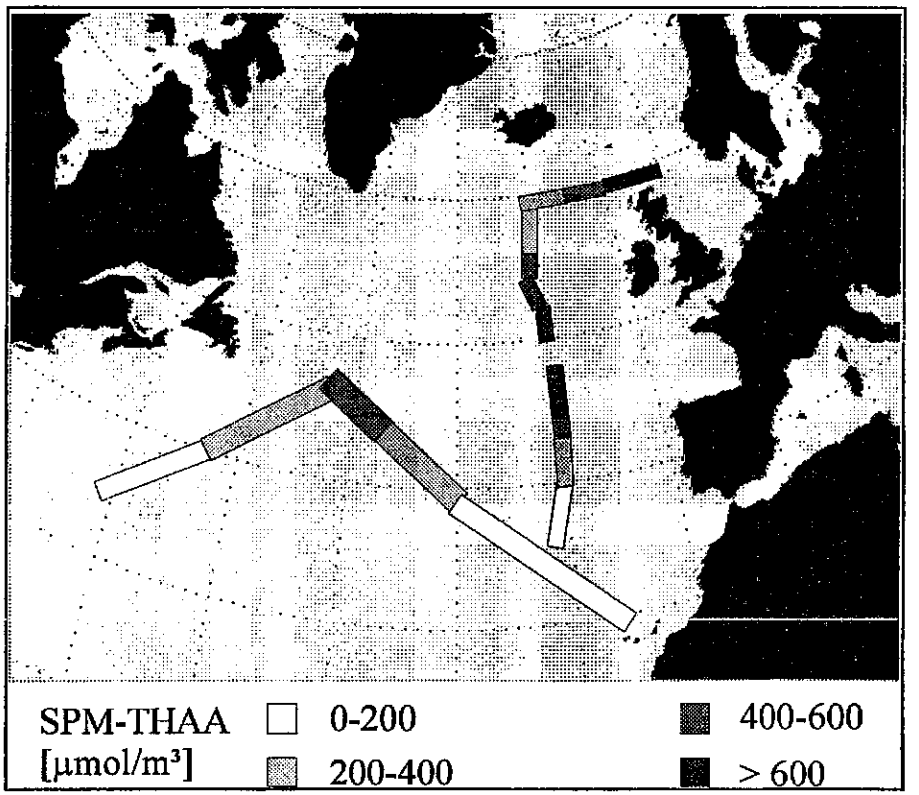

Fig. 15: Amino acid concentrations of suspended particulate matter along the cruise track. Continuous water sampling was performed at approx. 7 m depth on M 36/1 and M 36/2.

load increased towards the north and reached its maximum at approximately 50°N, where METEOR crossed a spring bloom event. Further north, the phytoplankton bloom was not so far developed at that time and SPM concentrations declined again. The final course along the shelf edge led to the coastal waters between the Shetlands and Orkneys, where the highest particle load of the cruise occurred.

Direct microscopical observations (T. Anders, pers. com.) show that different plankton communities were passed during the cruise reaching from almost pure dinoflagellate populations in subtropical waters to a very heterogeneous plankton distribution in the bloom region at about 50°N, which consisted mainly of diatoms, but also of some foraminifers, dinoflagellates and a few crustaceans like copepods. Despite this heterogenity in plankton distribution over the ship's course, the collected SPM only shows small variations regarding its amino acid content, which lie between 1.3 and 2.5 mmol/g on a dry-weight basis.

The amino acid content generally follows the trend of suspended particle concentrations, which means it increases towards the north (Fig. 16). Since zooplankton has a higher amino acid content than phytoplankton (COWIE and HEDGES, 1992), this increase depicts the increasing amount of zooplankton species (foraminifers, crustaceans) caught in net tows during the cruise (T. Anders, pers. com.).

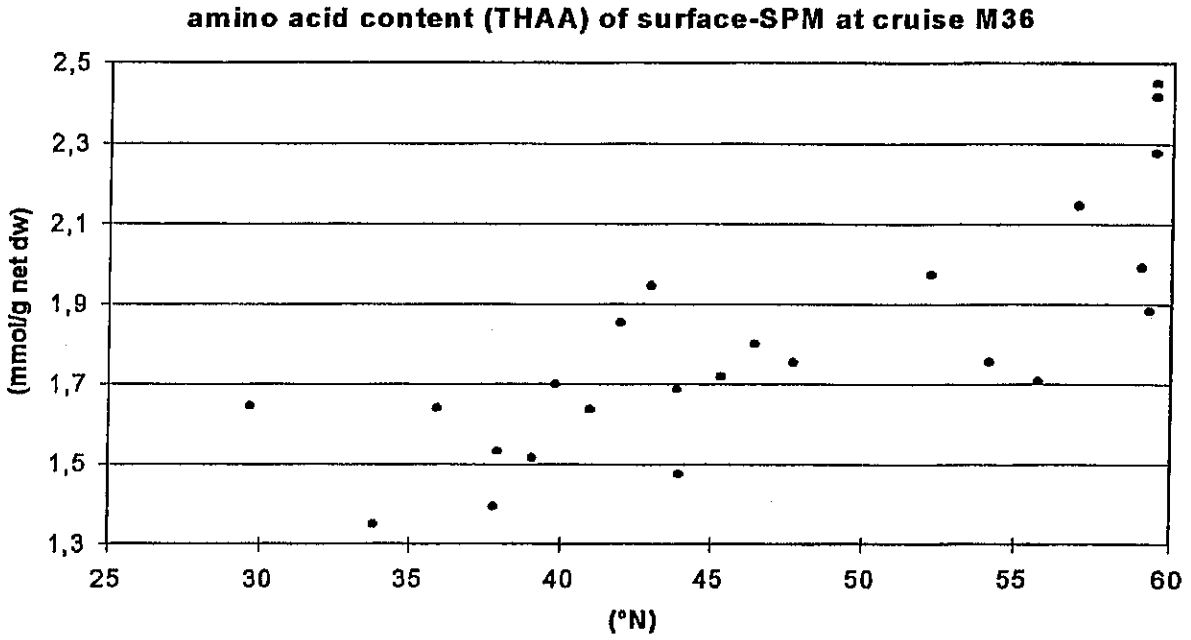

Fig. 16: Amino acid content of surface SPM during our transect.

Less variability is observed in the amino acid composition spectra. Seven amino acids (asp, glu, ala, gly, leu, ser, thr) account for more than 75% of the total amino acid amount and the mean standard deviation for the relative abundance of these amino acids is 5.5 mol% over all SPM samples, which is nevertheless well above the reproducibility of the analytical method (0.4%). Some minor amino acids show higher variability, however. Up until now, a classification of samples according to their amino acid composition was not possible.

So at first sight, the bulk of the surface SPM seems to be remarkably insensible to changes in plankton composition regarding amino acids. Nevertheless, amino acids are biologically produced; they make up 30% of the total organic carbon in the SPM samples and account for 50% of their organic nitrogen. Though they are essential to every form of life, they appear to be ubiquitous and non-specific compounds. Furthermore, amino acids are easily degradable and preferentially remineralized by bacteria (WILLIAMS et al., 1976; KEIL and KIRCHMAN, 1991). Remineralization leads to a reduced amino acid content and a reduced variability in amino acid composition, which was observed in sediment trap samples (LUNDGREEN, 1996). It is not yet quite clear why the variability found in sinking particles is greater than in SPM samples; this could be due to the "freshness" of the particles (which means the degree of remineralization) or a function of particle size, or a combination of both. Further investigations of size-fractioned SPM samples may aid in understanding particle formation and destruction processes.

An interesting comparison of SPM data is shown between the amino acid and trace metal contents in Fig. 17. Therein, a positive correlation is found between biologically produced

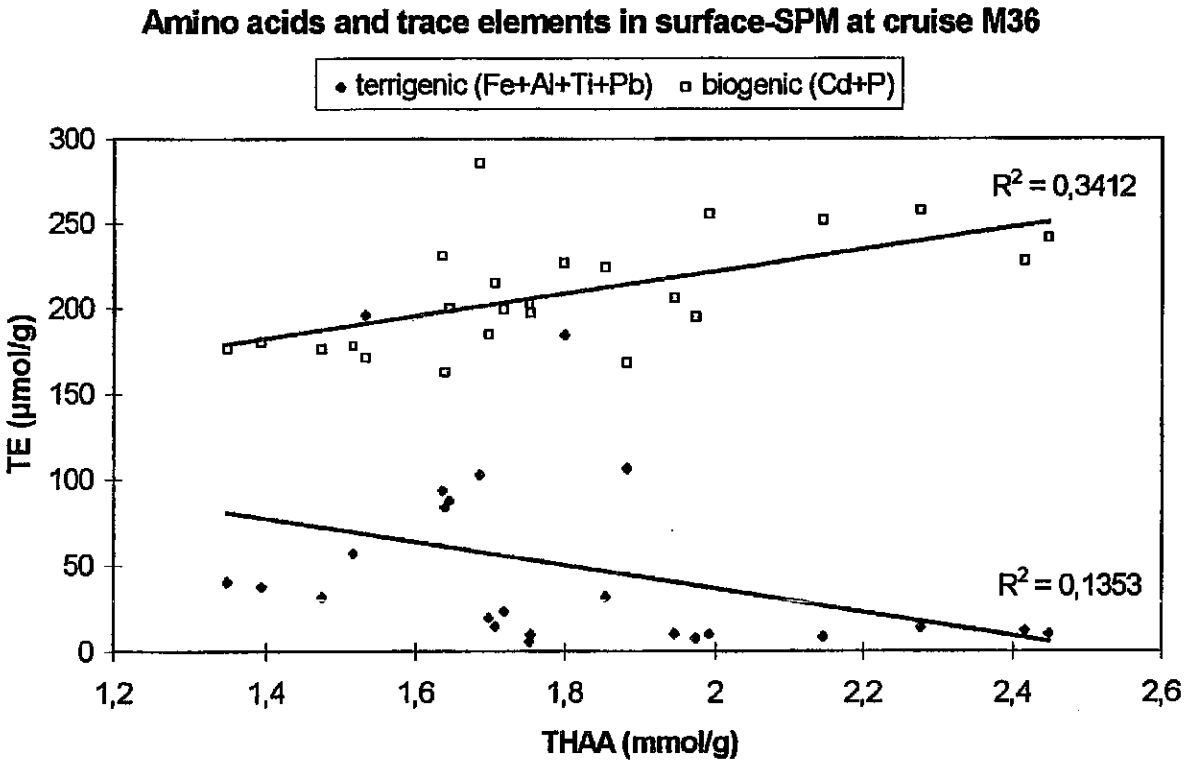

Fig. 17: Amino acid (THAA) content and trace element (TE) content of surface SPM during our transect.

amino acids and the so-called "biogenic" elements cadmium and phosphorus, whereas the "terrigenic" elements are weekly anticorrelated. This reflects the different particle sources of surface SPM sampled on the cruises M 36/1 and M 36/2: dust-derived particles with high content of terrigeneous elements were "diluted" with biologically-produced particles in the more productive regions, which results in a negative correlation between terrigenic elements and indicators of biological activity, such as amino acids.

5.2.2.4 Trace Elements: Shipboard Results

(J. Kuss, P. Streu, A. Prang, K. Kremling)

The main purposes of the trace element studies during the first and second legs are designed to pursue the aims of German contributions to the international JGOFS programme:

- the vertical flux of particulate TE and its short- and long-term variability in relation to biological processes (by means of sediment traps);
- studies on the distribution and chemical composition of suspended particulate material (SPM) in surface and deep Atlantic waters (by means of a surface water pumping system connected to a continuous-flow ultracentrifuge and by in-situ pumps for deep ocean waters, respectively.) In addition, samples for the determination of dissolved TE in surface waters were collected during the transect.

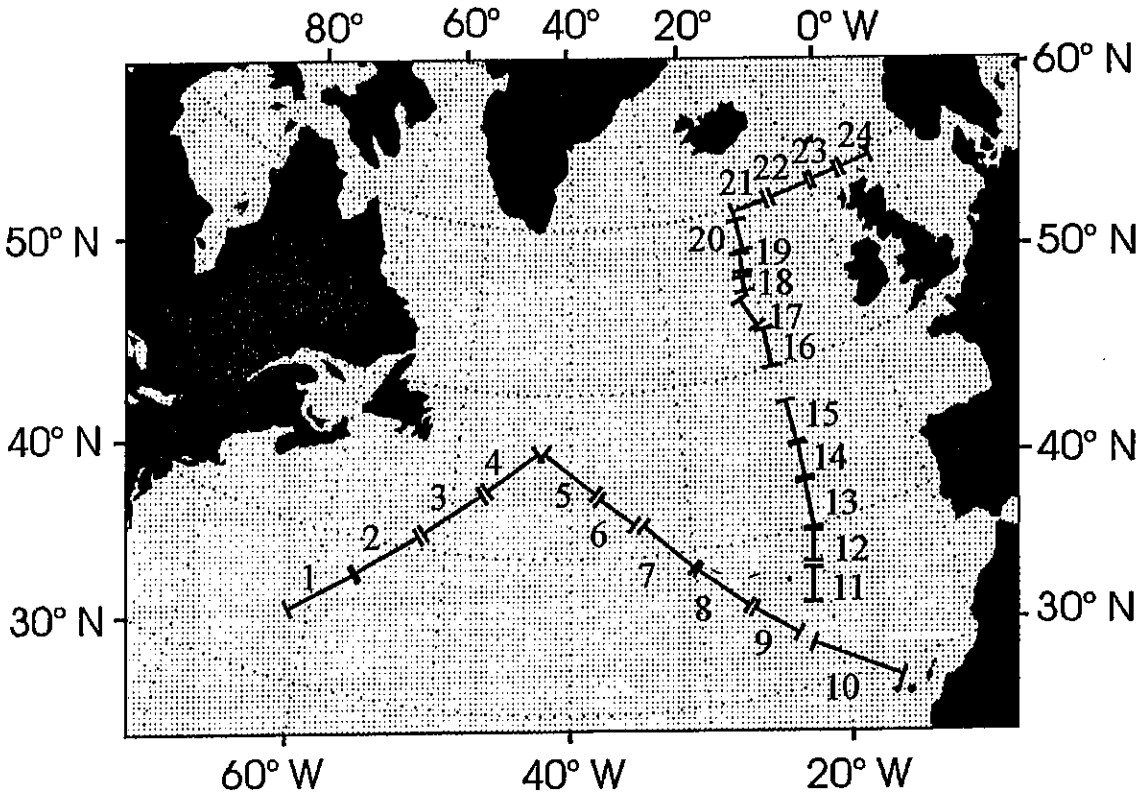

Fig. 18: Study area with 24 sampling intervals.

The following work programme was carried out during our transect and in onshore laboratories:

- The JGOFS long-term moorings at 33°N, 47°N and 54°N on 20°W, fitted with sediment traps and current meters have been recovered and re-deployed. The samples for the analysis of trace chemical substances are worked up (152 samples are 'swimmer' picked, splitted, and freeze dried) for the determination of trace elements (Al, Cd, Co, Cu, Fe, Mn, Ni, P, Pb, Ti, V and Zn) and the bulk composition ($CaCO_3$, POC, PON, and PSi).
- The particulate samples collected underway from Bermuda to the Canary Islands (M 36/2) and further to Bergen (M 36/2) have been freeze-dried, acid digested and measured by emission and absorption spectrometry.
  The analysis of the dissolved TE-fractions still has to be carried out.
- At our main stations (L1, A1, L2, L3 and A2; see Fig. 15, 18), 21 samples of SPM have been collected by means of the in-situ pumps between 25 m to maximum of 4150 m. Here, approximately 0.2 to 0.3 m3 per sample of water were filtered through membrane filters.

Distribution of SPM and the contents of calciumcarbonate, opal, and particulate organic carbon (Fig. 19)

High concentrations of SPM were found in the central North Atlantic, in the mid latitudes (45-55°N) and close to or on the shelf. Relatively low values were observed in the Sargasso Sea and in the south-eastern part of the study area, with values of ca. 50 mg/m3. High $CaCO_3$

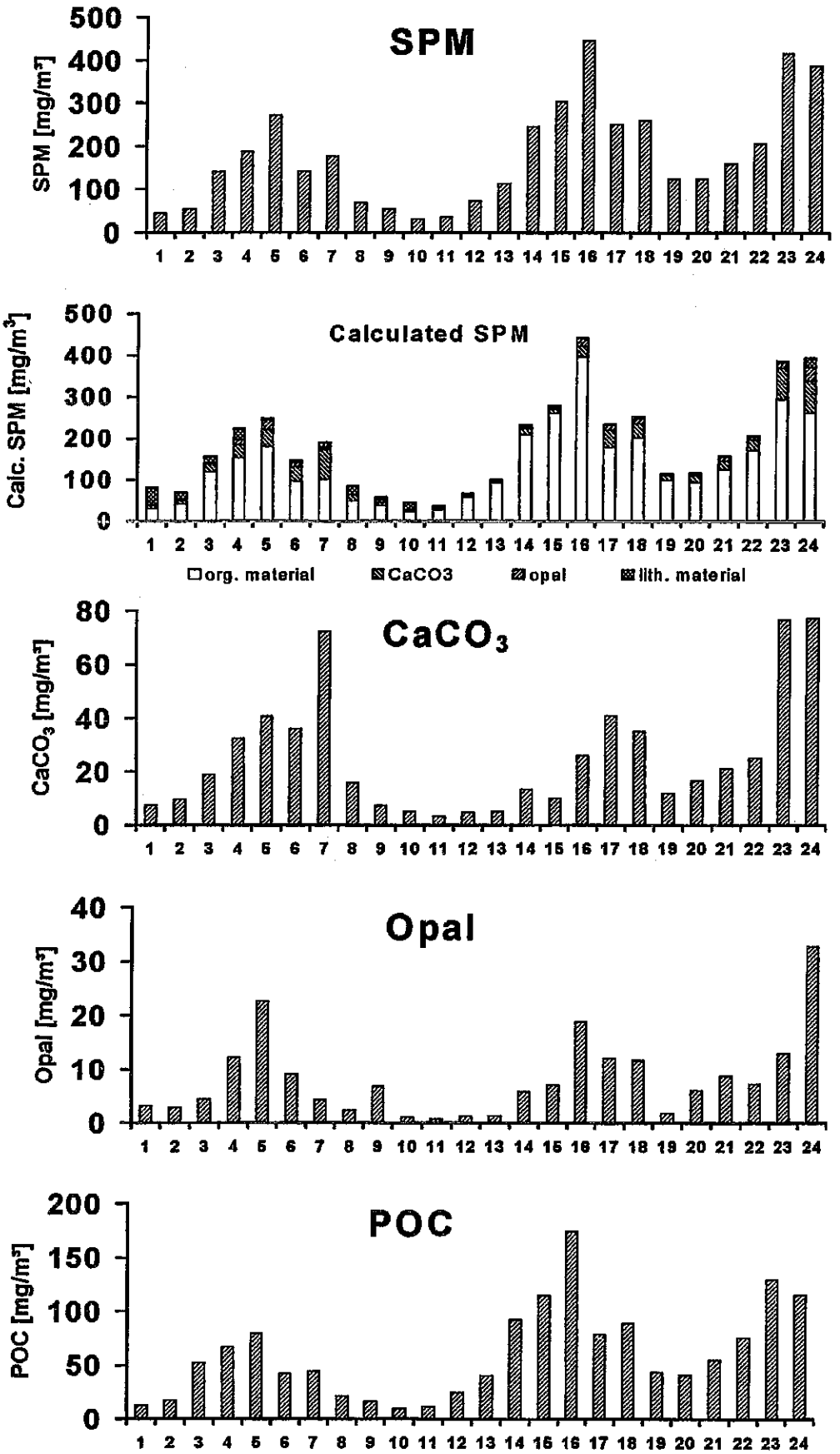

Fig. 19: Distribution of SPM, $CaCO_3$, biogenic opal, POC and the bulk composition of SPM along our transect (samples 1 to 24; see Fig. 18).

contents of 20-40% have been measured in SPM of the eastern part of the central North Atlantic (samples 6-8) and north of 50°N, with a fraction of about 15% $CaCO_3$. Biogenic silica (opal) ranged between 2-8%. The particulate organic carbon (POC) contents of the samples have been found to be relatively constant, with values of 30% (±5%). The concentrations of particulate Al, together with POC, $CaCO_3$ and opal data, were used to calculate the (theoretical) total SPM (e.g., Al and POC represent 10% of the mass of aluminosilicates (SPENCER and SACHS, 1970) or 44% of the organic matter (MARTIN and KNAUER, 1973), respectively. The calculated SPM are in excellent agreement with the measured values.

Distribution of particulate TE-concentration (Fig. 20)
The distributions of Cd, Co, Ni, Mn and Zn exhibit similar concentrations as particulate phosphate and POC. They probably underlie biogenic uptake in plankton material. The concentrations of Cu, Fe, Pb were higher in the central North Atlantic, which is probably caused by entrainment of surface water from the Labrador Sea (from T, S characteristic).

In the area of the subtropical gyre, the particulate TE were significantly depleted, probably due to the spring bloom which had already sedimented out of the surface layer, and also because this oligotrophic area is characterised by minor primary production.

Trace element contents in surface particulate matter (Fig. 21)
The TE contents of Co, Mn, Ni, and P in SPM of the pelagic ocean exhibit a uniform distribution. Close to and on the shelf, distinct increases of several TE contents in SPM were observed, especially for Al, Fe, Mn, Ti, and Zn. The higher Zn concentrations may partly originate from anthropogenic sources (samples 23, 24).

In the northwestern and southeastern part of the study area, higher contents for lithogenic elements (Al, Fe, and Ti) have been measured. This can be explained from input of terrigenic-dominated SPM loads of Labrador Sea water in the north and Sahara dust deposition by southeasterly trade winds (KREMLING and STREU, 1985), near the continent of Africa, respectively.

Residence times (Tab. 4)
Assuming a mixed layer of 100 m depth and an atmospheric flux as reported by CHESTER and MURPHY (1990), the residence times of suspended particulate TE in the surface layer has been calculated. Short residence times (< 1 year) have been determined for refractory elements mainly located in resistant crustal material, whereas residence times up to a few decades for TE involved in biogenic recycling processes were determined (e.g. Cd).

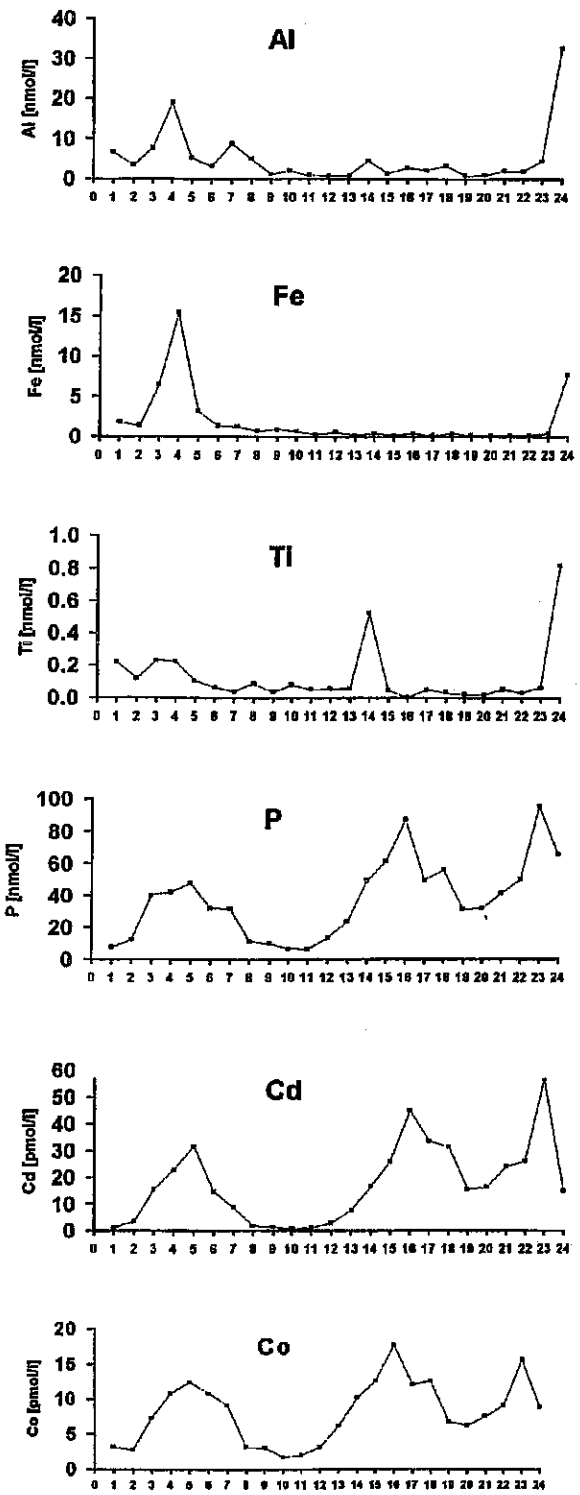

Fig. 20: Distribution of particulate TE along our transect.

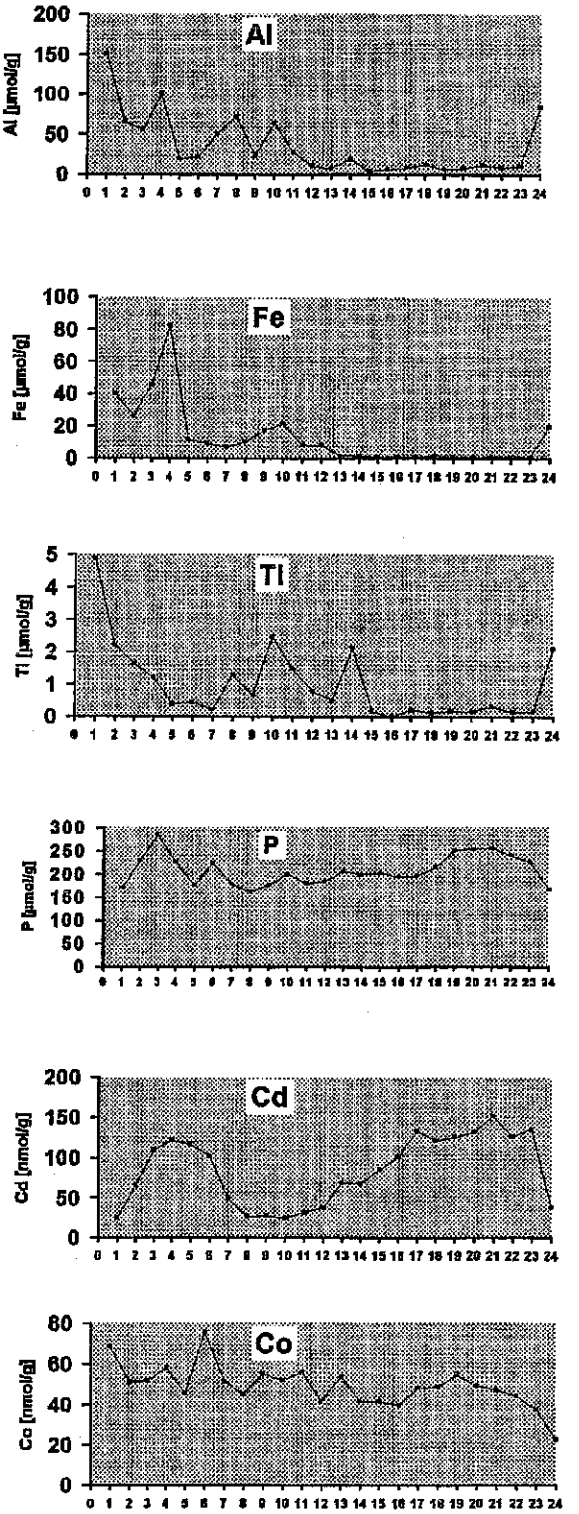

Fig. 21: TE contents in surface particulate matter along our transect.

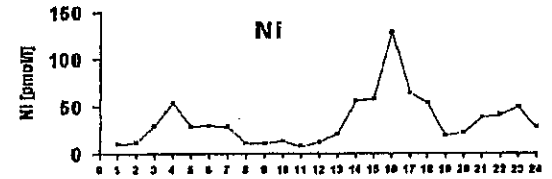

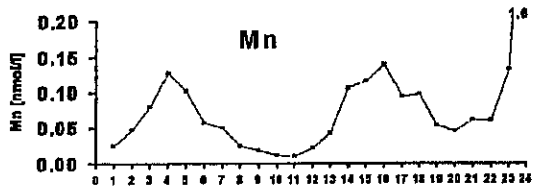

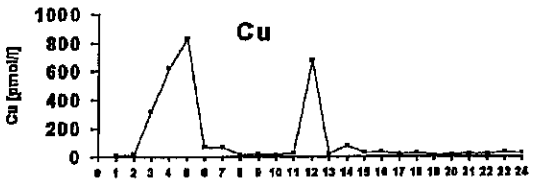

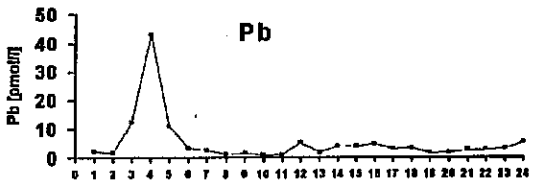

Fig. 20: continued

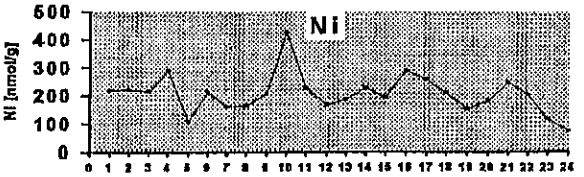

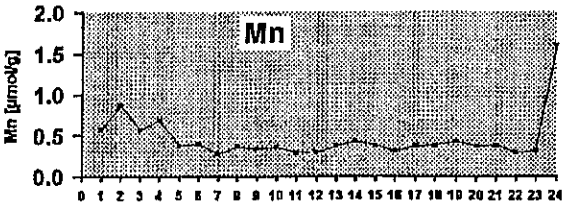

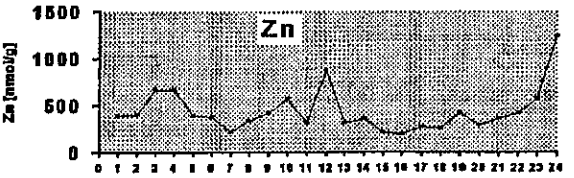

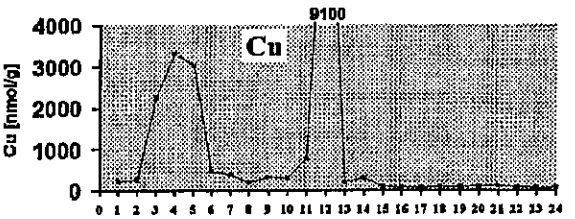

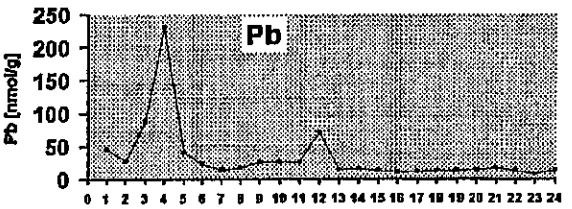

Fig. 21: continued

Tab. 4: Estimated residence times for particulate TE in the North Atlantic in a mixed layer of 100 m, assuming atmospheric input as major source and steady state conditions.

mixed layer (100 m)	SPM standing stock (ca. 7 m)	Atmosph. input (part)*	Residence time
	[mmol/m2]	[mmol/m2yr]	[yr]
Fe	0.17	0.53	0.3
Mn	0.006	0.008	0.8
Al	0.4	1.76	0.2
	[µmol/m2]	[µmol/m2yr]	
Co	0.77	0.35	2.2
Cd	1.53	0.04	43
Cu	14.0	2.75	5
Ni	3.4	2.04	1.7
Zn	5.41	10.9	0.5

5.2.2.5 Distribution of Natural Radionuclides in the Water Column

(J. Scholten, S. Vogler, K. Schmikale)

The project "Radionuclide distribution as tracers for particle dynamics in the water column", which is a part of the German JGOFS III research programme, studies the distribution of natural radionuclides ($^{234, 232, 230, 228}$Th, ^{231}Pa, ^{210}Po, ^{210}Pb) in the water column and the seasonal and spatial variations of radionuclide fluxes in sediment traps.

One aim of the project is to examine the exchange rates of particles in the water column. By means of Th-scavenging models, the exchange rates between dissolved phases and suspended particles (adsorption and desorption) and the exchange rates between suspended and sinking particles (aggregation and disaggregation) shall be determined. In this context the terms of chemical modification of sinking particles is of further interest.

Another objective is to investigate the trapping efficiency of the sediment traps, which is an important factor in determining oceanic fluxes and mass balances. By measuring the distribution of radionuclides in the water column and in sediment traps, the trapping efficiency can be calculated.

The investigations will also include radionuclide measurements in surface sediments and in near-bottom nepheloid layers in order to evaluate the advective sediment supply and to compare fluxes in sediment traps with those in sediments.

Shipboard Results

During M 36/2 water bottles and in-situ filtration pumps were deployed for sampling the water column. The following nuclides (Table 5) were sampled at the sediment trap locations:

Tab. 5: Nuclides sampled at the sediment trap locations

Location	Nuclides	Water depth of samples (m)
L1	^{234,232,230,228}Th; ^{231}Pa, ^{210}Po, ^{210}Pb	450, 1000, 2000, 3000, 4150
L2	^{234,232,230,228}Th; ^{231}Pa, ^{210}Po, ^{210}Pb	500, 1000, 3500, 4200,
L2	^{234}Th, ^{210}Po, ^{210}Pb	above sea floor: 15, 30, 60, 100, 150
L3	^{234,232,230,228}Th; ^{231}Pa, ^{210}Po, ^{210}Pb	500, 1000, 1500, 2200, 2700

By means of filtration, dissolved and particulate phases were sampled. Further chemical purification for radionuclide analyses (Alpha-counting, Thermal Masspectrometry (TIMS)) were conducted on board METEOR. Surface sediments were sampled at the trap locations using a multicorer.

The water column distribution of ^{228}Th ($T_{1/2}$ = 1,91 y) at the trap locations is characterised by low concentrations in the surface waters and a subsurface maximum around 500 m water depth (Fig. 22). From this water depth, concentrations gradually decrease to about 0.002 dpm/l in deep waters. The distribution of ^{234}Th ($T_{1/2}$ = 24 days) at L2 is shown in Fig. 23. ^{234}Th is produced by radioactive decay of ^{238}U. In contrast to ^{234}Th, ^{238}U is a non-particle reactive element. Therefore, the ^{234}Th/^{238}U ratio can be used as a measure of particle fluxes in time scales < 100 days. As shown in Fig. 23, ^{234}Th/^{238}U ratios < 1 can be observed near the sea floor probably due to lateral sediment transport in nepheloid layers. Low ratios are also found in surface waters, suggesting rapid scavenging of ^{234}Th and ^{228}Th on settling particles. Measurements of ^{230}Th and ^{231}Pa by means of TIMS are currently underway.

5.2.3 Biological Oceanography

5.2.3.1 Dissolved Organic Carbon and Nitrogen (DOC and DON) (P. Kähler)

M 36/2 was one of a number of cruises during which we have studied the seasonal dynamics of DOC in the North Atlantic, mainly at the BIOTRANS station at 47°N/20°W. There we observed that DOC in deep water has the constant concentration of 43 µmol and that on top of

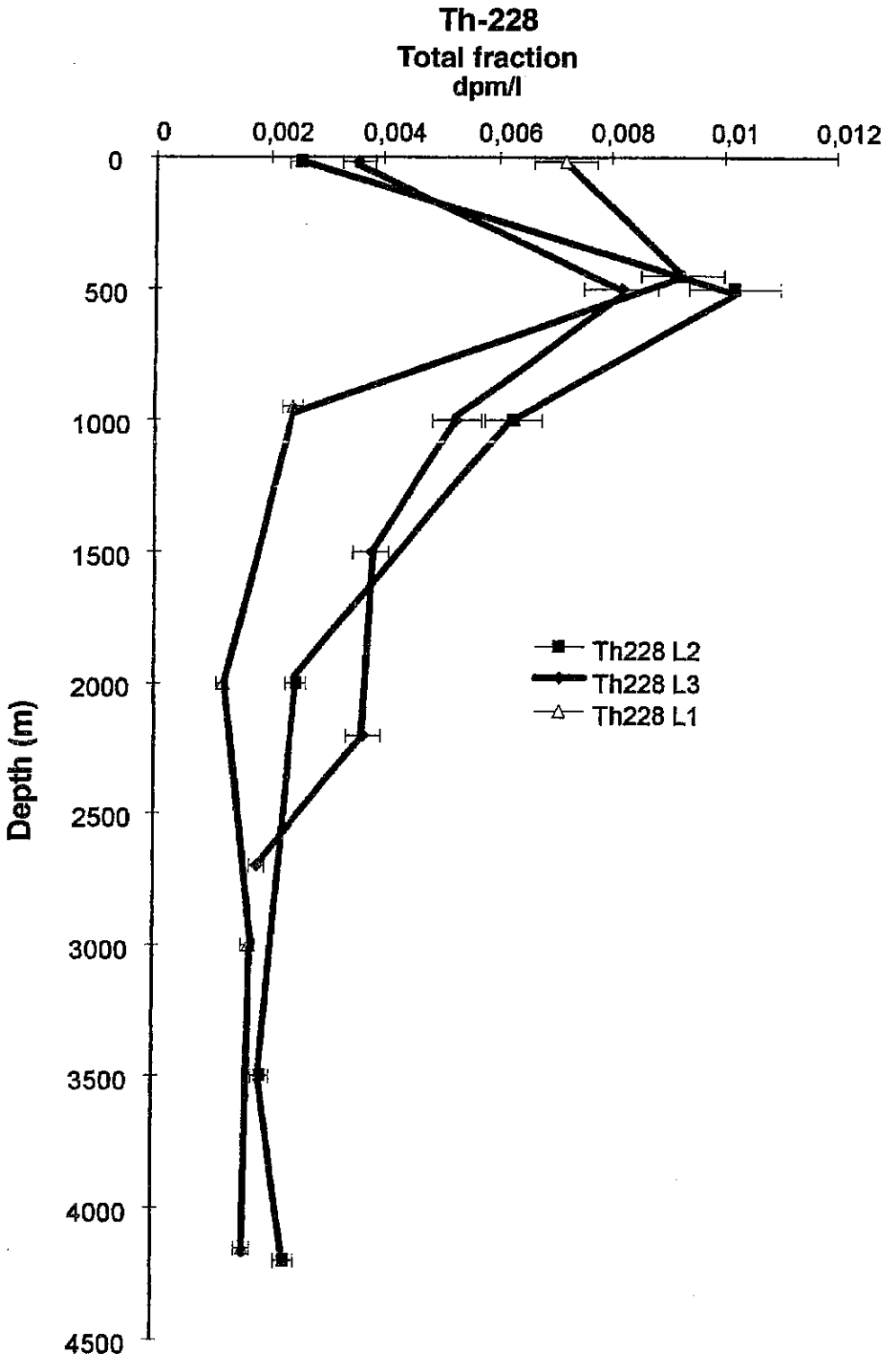

Fig. 22: Distribution of Th-228 (total fraction) in the water column.

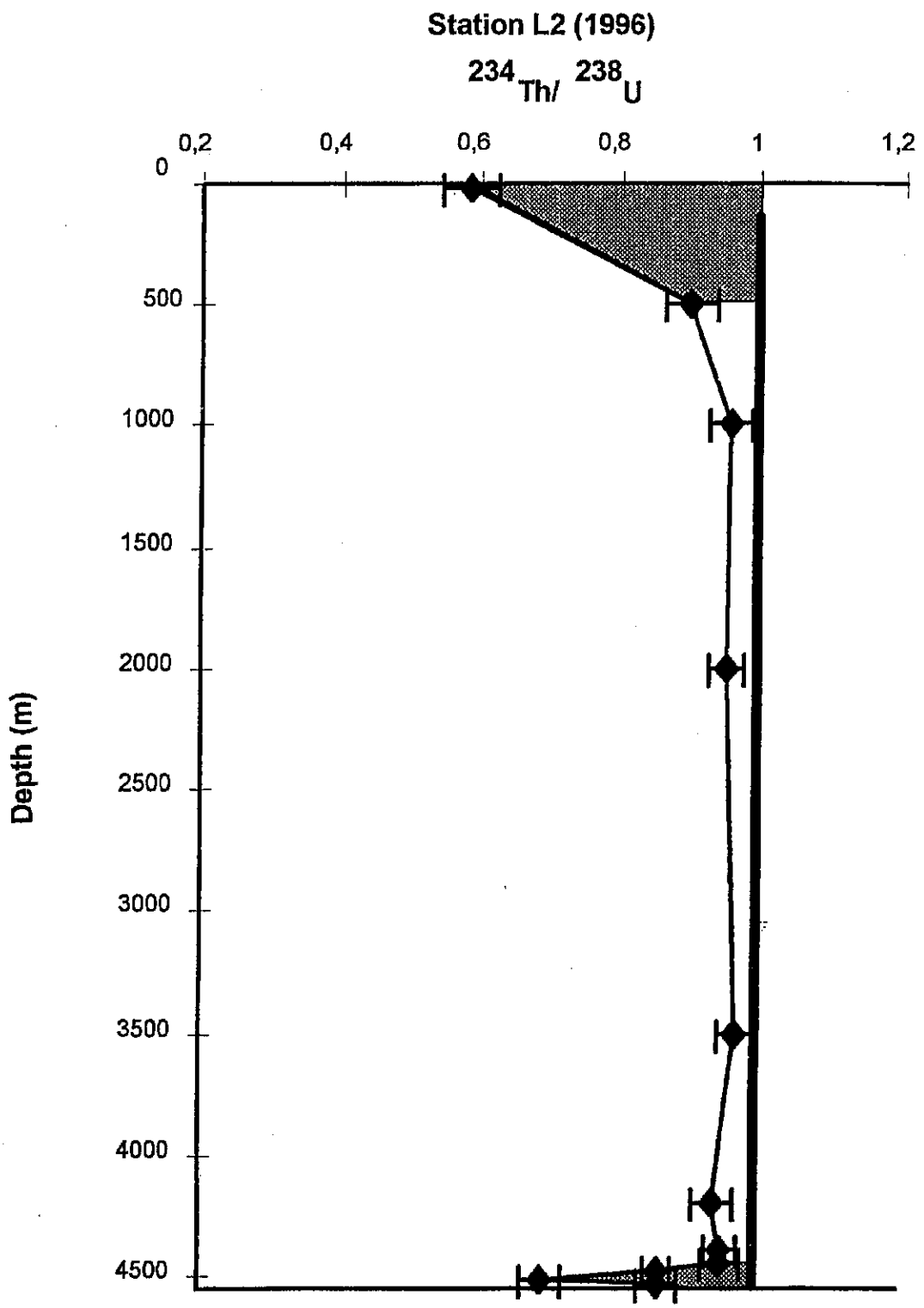

Fig. 23: Th-234/U-238 ratios in the water column; significant depletions of Th-234 are found in surface and near-bottom water.

this material DOC can accumulate by an additional ca. 40 µmol in surface waters. Most of this additional material is biologically labile and its accumulations are transient, i.e. it is broken down soon after its formation. While it constitutes a large momentary sink for CO_2, its long-term effect on the carbon balance of the surface ocean is small, since only a minor fraction of this additional DOC is exported from the surface ocean.

The determination of DOC and DON was carried out as follows: A water sample is acidified to pH < 2 with phosphoric acid thus transforming all carbonate to CO_2, which is removed by bubbling with an O_2/Ar mixture. 100 µl of this CO_2-free water is injected into a quartz tube filled with platinum catalyst (5% Pt on alumina) heated to 850°C. The water evaporates and its organic constituents are burnt; organic carbon to CO_2 and all nitrogen (organic and inorganic) to nitrogen oxide (NO). A constant flow of carrier gas (5% O_2 in Ar) transports the combustion gases to the CO_2 and NO detectors trough a number of traps which remove water and interfering acid vapors and particles. Calibration is against glucose and urea in persulfate treated (C-free) milli-Q water which also serves for blank determination, and deep-ocean water. The high combustion temperature and low oxygen content of the carrier gas are necessary for the complete recovery of nitrogen compounds such as NO. Since, however, this recovery varies with the content of nitrate in the samples, only measurements in samples free of, or poor in, nitrate are trustworthy. This was the case in the surface samples collected during the M 36/2 cruise. After subtraction of particulate C and N and dissolved inorganic N fractions (POC, PON, DIN), the concentrations of DOC and DON are obtained.

Shipboard Results

The transect taken in surface waters between 33°N and 60°N along 20°W during July yields results which are comparable to seasonal observations at given stations. Going north is like going back in the season. While in the south a summer system with surface nutrient depletion and a secondary chlorophyll maximum was well established, at about 52°N the maximum phytoplankton biomass build-up of a "spring" bloom was observed, and north of that the situation of a bloom in progress with nutrients still present in surface waters (Fig. 24).

The accumulation of POC is substantial in the bloom, and a distinct maximum is present. The DOC accumulation is smaller and has a different pattern. It is rather patchy, but the general trend is towards higher concentrations to the south. This is different for DON (Fig. 25). Its concentrations vary between 4.5 and 7.5 µmol, with no north-south trend (stations north of 52°N are not included). Fig. 26 shows the C/N ratios of particular and dissolved organic matter. The C/N of particulates is close to the Redfield ratio, dissolved organic matter (DOM) has a distinctly higher C/N ratio. Note that in Figure 26 the C/N ratios of total DOM are given. If the bulk of the DON present were to be attributed to recalcitrant deep-water DOM, the C/N ratio of the additionally accumulated DOM would be still larger.

The fact that the seasonally accumulating DOM is poor in nitrogen, relative to particular organic matter (which has a close-to-Redfield C/N ratio), may explain an observation by

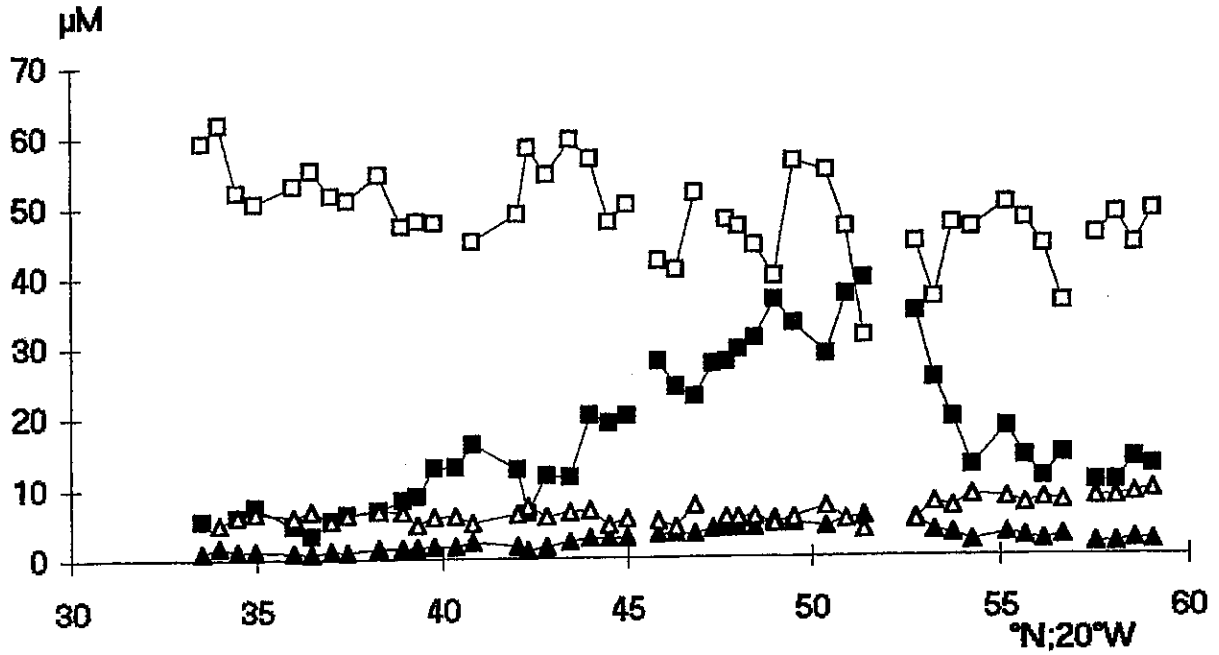

Fig. 24: Dissolved and particular organic carbon and nitrogen along a transect between 30 and 60°N in the North Atlantic in July 1996. North of 52°N, increasing values of NO_3 (3 µmol at 60°N) are included in the DON concentration. Analysis of particulates by W. Koeve and co-workers, preliminary values. Squares: organic carbon, triangles: organic nitrogen; closed symbols: particulate fraction, open symbols: dissolved fraction.

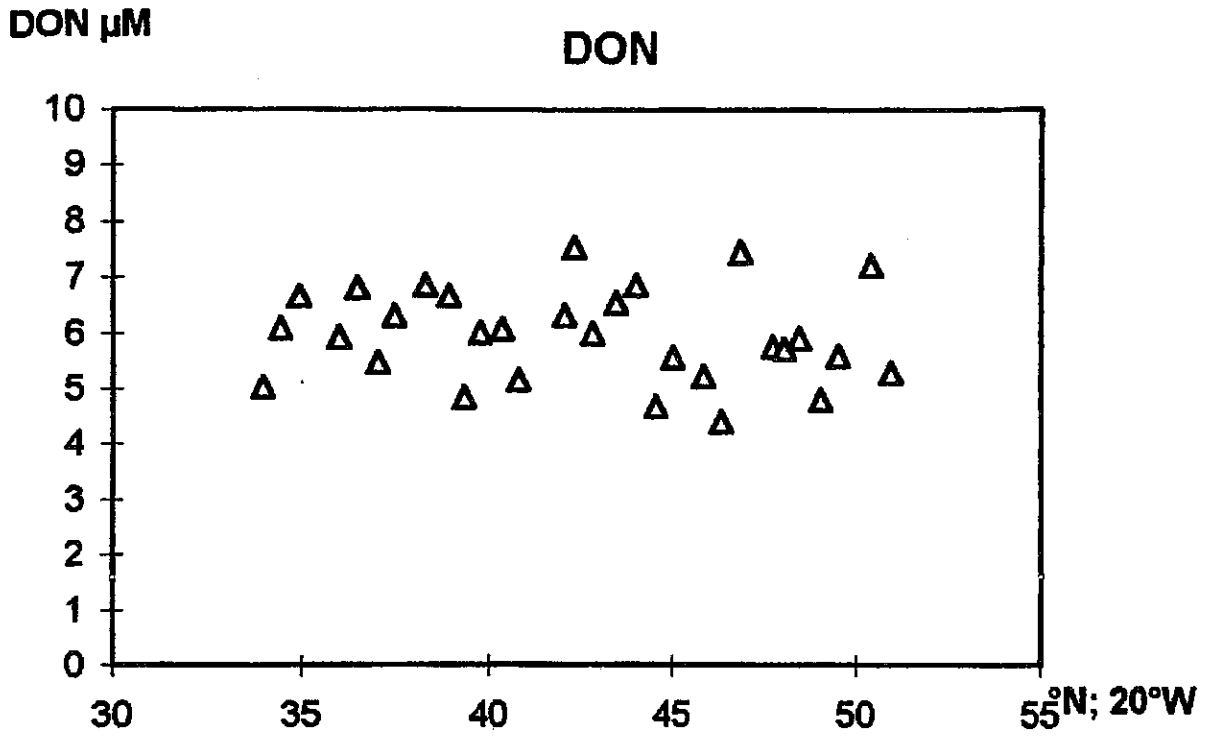

Fig. 25: DON between 30 and 52°N, otherwise as in Figure 24.

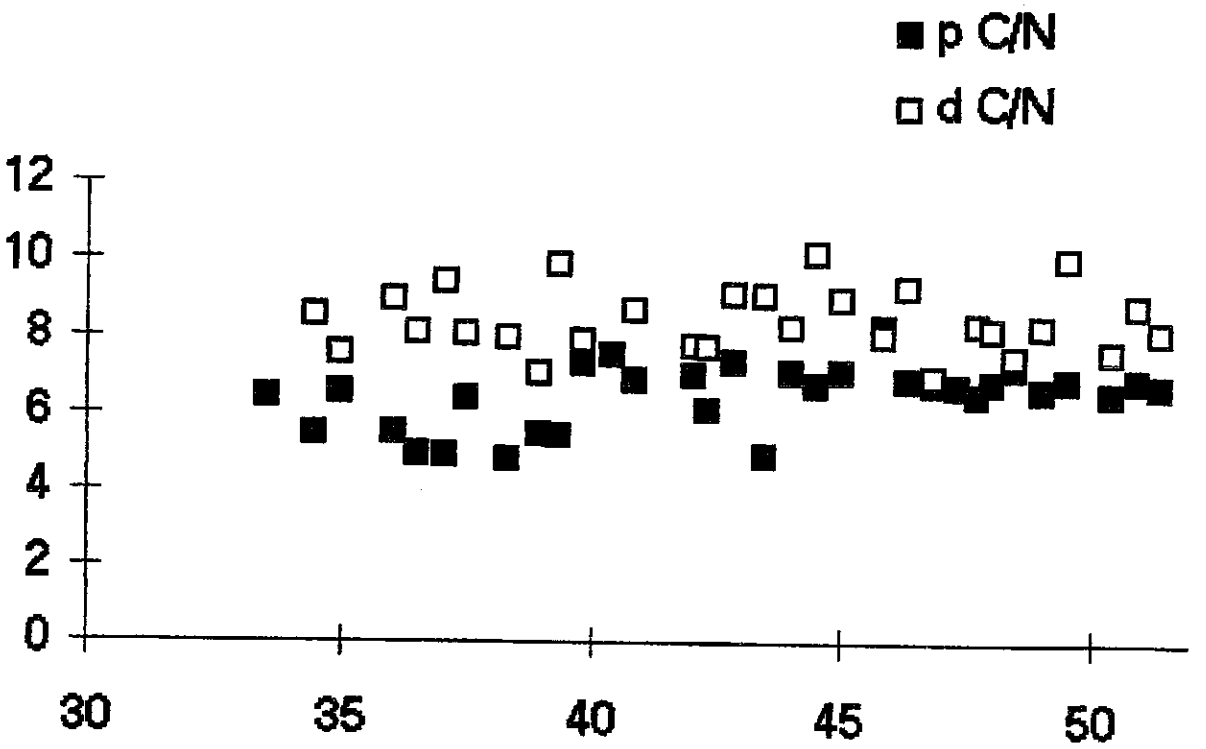

Fig. 26: C/N ratios of particular (closed symbols) and dissolved (open symbols) organic matter between 33 and 52°N (horizontal axis). Analysis of particulates by W. Koeve and co-workers, preliminary values.

SAMBROTTO et al. (1993), who reported that the drawdown of CO_2 relative to NO_3 during phytoplankton development is larger than according to the Redfield ratio. Since the seasonally accumulating DOM is not exported to the deep ocean, its deviating C/N ratio is not imprinted on deep water, or, turning the argument around: The fact that the deep ocean contains the remineralization products of organic matter in the Redfield ratio (delta TCO_2 vs. delta NO_3) is another indication of DOM playing no major role in export from the surface to the deep ocean.

A joint evaluation including the elements of the CO_2 system measured during the same cruise by L. Mintrop (see chapter 5.2.2), and an analysis of the vertical profiles of DOC and DON will shed more light on the issues presented in this report.

5.2.3.2 Upper Ocean Biology along a Transect at 20°W during Summer 1996

(W. Koeve, M. Schroeter, C. Sellmer, C. Reineke, W. Gaul)

During M 36/2 the JGOFS planktological work group from IfM Kiel intended to study characteristic features of optical and biological properties of the epi-pelagic system during the summer in the northeast Atlantic. This study (33°N-60°N along 20°W) was designed to extend the observations carried out during expeditions at the BIOTRANS site (47°N/20°W) in summer 1993 and to a larger area between 46°N and 52°N in summer 1995. The particular focus of the planktological studies was on the relative importance of different size classes of phytoplankton to biomass and production under different production regimes.

The sampling methods applied during the cruise comprised high-frequency near-surface sampling during steaming periods (hourly intervals), continuous sensor-based measurement of surface chlorophyll-fluorescence (sampling interval: one minute) and performances of vertical structures using CTD-mounted Niskin bottles. Here, samples were collected for a varying set of measurements, in particular, including the determination of biomass parameters such as Chl.-a and particulate organic carbon and nitrogen (POC/N) or the measurement of specific variables like biogenic silicium (BSI), particulate inorganic carbon, phytoplankton pigments by HPLC and investigations by means of microscopy. In-situ simulated incubations were carried out to study new production (15N-nitrate uptake) and total primary production ($^{14}CO_2$-uptake). Grazing rates of microzooplankton were measured with the serial dilution approach. Measurements of upper ocean optical properties complemented the planktological studies.

Shipboard Results

Currently not all of the measurements have been carried out; a general description of different epi-pelagic succession states, however, is already possible. This report will mainly present results from surface sampling and, to some extent from the CTD rosette-based sampling of the upper few hundred metres.

Concentrations of Chl.-a at five metres below the surface varied over almost two magnitudes along the transect (Fig. 27a). Very low concentrations of less than 0.1 µg/l Chl.-a were observed in the most southern part of the transect (33°N and 38°N). Up to about 49°N, near-surface concentrations increased steadily up to values of about 1 µg/l Chl.-a. Subsequently, a massive phytoplankton bloom event was observed between about 50°N and 54°N. Maximum Chl.-a values of about 3.4 µg/l Chl.-a found in this region are comparable to or even slightly higher than maximum values observed during the North Atlantic Bloom Experiment (NABE, 1989) both at the BIOTRANS site (47°N/20°W) and the NABEII site at 59°N/20°W. North of the bloom, Chl.-a concentrations dropped rapidly down to values between 0.5 and 1 µg/l Chl.-a. Maximum Chl.-a concentrations were observed at the southernmost stations, with nitrate concentrations being above the detection limit (0.2 µmol; see chapter 5.2.2). North of the peak of the phytoplankton bloom, nitrate concentrations increased rapidly and concentrations as high as 4 to 5 µmol were found between 55°N and 60°N. This is equivalent to about 50% of winter nitrate stocks in this area.

The general trends in the meridional distributions of POC and BSI are very similar to that of Chl.-a. A more detailed look, however, reveals significant and meaningful differences. The ranges of variations for POC and BSI are only about one magnitude (5 to 40 µmol POC; Fig. 27b and 0.1 to 1 µmol; Fig. 27c, respectively). POC highest values are observed in the bloom area, but the shape of the peak is less distinct, and high values extend more to the south into nutrient poor waters than for Chl.-a. For BSI just the opposite is evident. Maximum values are shifted towards the north of the Chl.-a and POC peaks and values north of the peak appear, although with some scatter, higher than south of the peak. Near-surface concentrations of dissolved inorganic silicate (data not shown; see chapter 5.2.2) are low throughout the transect (< 0.4 µmol) and do not support the interpretation of the BSI distribution.

The spring bloom and its northward migration are well-known features of the upper ocean biology in the North Atlantic during the spring/summer seasons. One simple view of the observations along the 20°W transect could be to take it as a quasi time series of observations, having the early spring in the very north and the summer in the south. Much of this view is supported by the vertical distribution of Chl.-a (Fig. 28). The northernmost ''pre bloom peak'' part of this transect (station 190 to 194; 55-60°N) is characterised by intermediate concentrations which, however, reach down to 50 to 80 m. In the small bloom (station 188 and 189; 50° to 52°N) and post bloom (station 183 to 186; 43° to 48°N) areas that follow successively towards the south high Chl.-a concentrations are restricted to the upper about 40 m. All three regions showed surface or very shallow subsurface maxima of Chl.-a. South of 40°N, however, a well established subsurface maximum with small Chl.-a concentrations (0.3 to 0.5 µg/l Chl.-a) has developed. The depths of the maxima varies between 60 and 90 m. This last area has features which are characteristic for typical summer epi-pelagic systems.

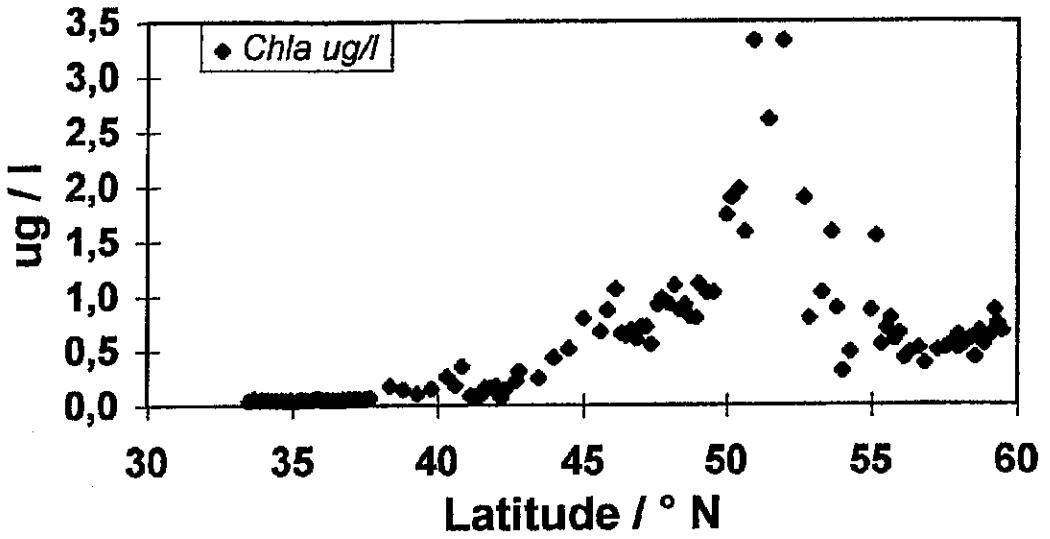

Fig. 27a: Distribution of planktological bulk parameters along 20°W during summer 1996. a) Chl.-a;

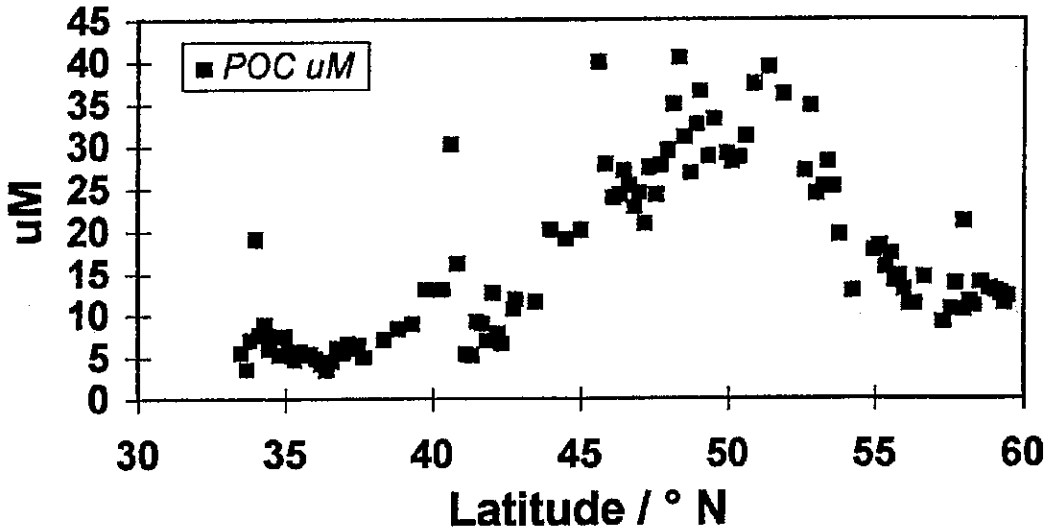

Fig. 27b: Particulate organic carbon (POC);

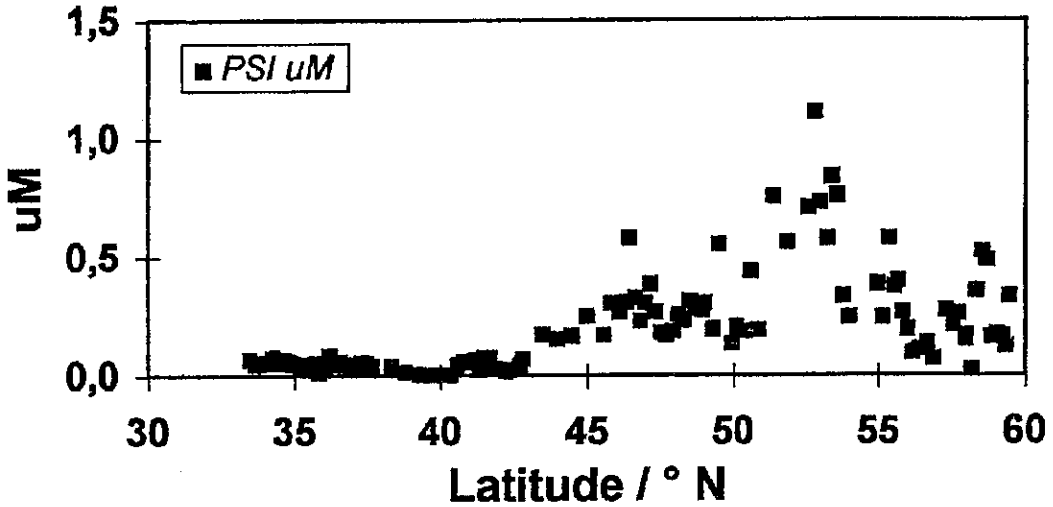

Fig. 27c: Biogenic silicium (BSI).

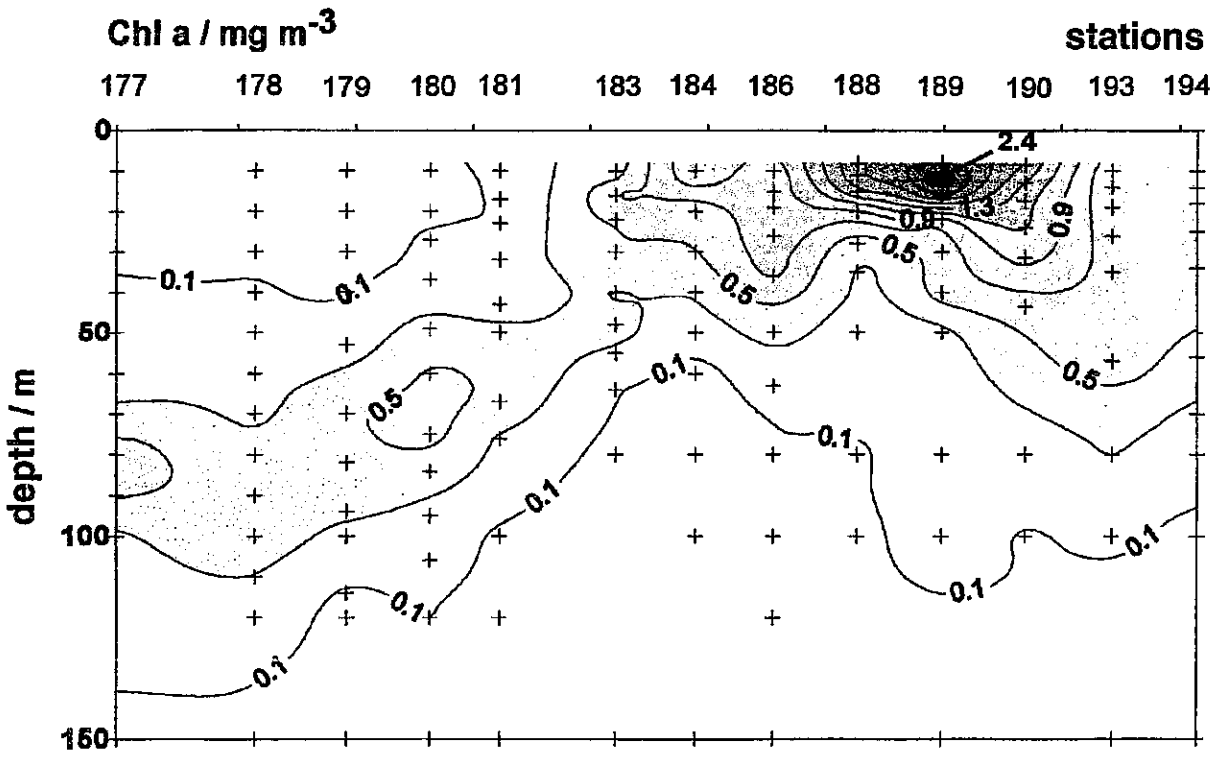

Fig. 28: Vertical distribution of Chl.-a along 20°W during summer 1996.

Furthermore, the meridional distribution of size-fractionated biomass (vertical means) differentiates this view (Fig. 29a-d). Stations south of 40°N are characterised by an absolute dominance of very small phytoplankton (picoplankton, < 2 µm), being well in agreement with what is expected for a summer system. The large importance of nanoplankton on the other stations and in particular the minor importance of large phytoplankton (microplankton, > 20 µm), however, is surprising in view of the above system characterisation, since spring blooms are well known to be characterised by microplankton in general and diatoms in particular. That diatoms do not appear to dominate the phytoplankton community anywhere along the transect is evident from preliminary examination of HPLC phytoplankton pigment data (not shown here), microscopic analysis and very low BSI/PON ratios throughout the whole cruise.

Obviously, the massive phytoplankton bloom observed during summer 1996 was not one of the typical diatom blooms well-known for the North Atlantic. Silicate concentrations in surface waters were always below 0.5 µmol along the transect while nitrate concentrations of up to 50% of winter values where available north of the peak of the bloom. It is therefore suggested that a large diatom bloom took place prior to the cruise and did almost completely sink out of the upper column prior to our observations. A second bloom, consisting of non-siliceous phytoplankton happened to grow on residual nitrate (and phosphate). The size of this bloom is remarkable, keeping in mind that both maximum Chl.-a and POC concentrations observed during M 36/2 compare well to maximum values observed during the NABE diatom bloom.

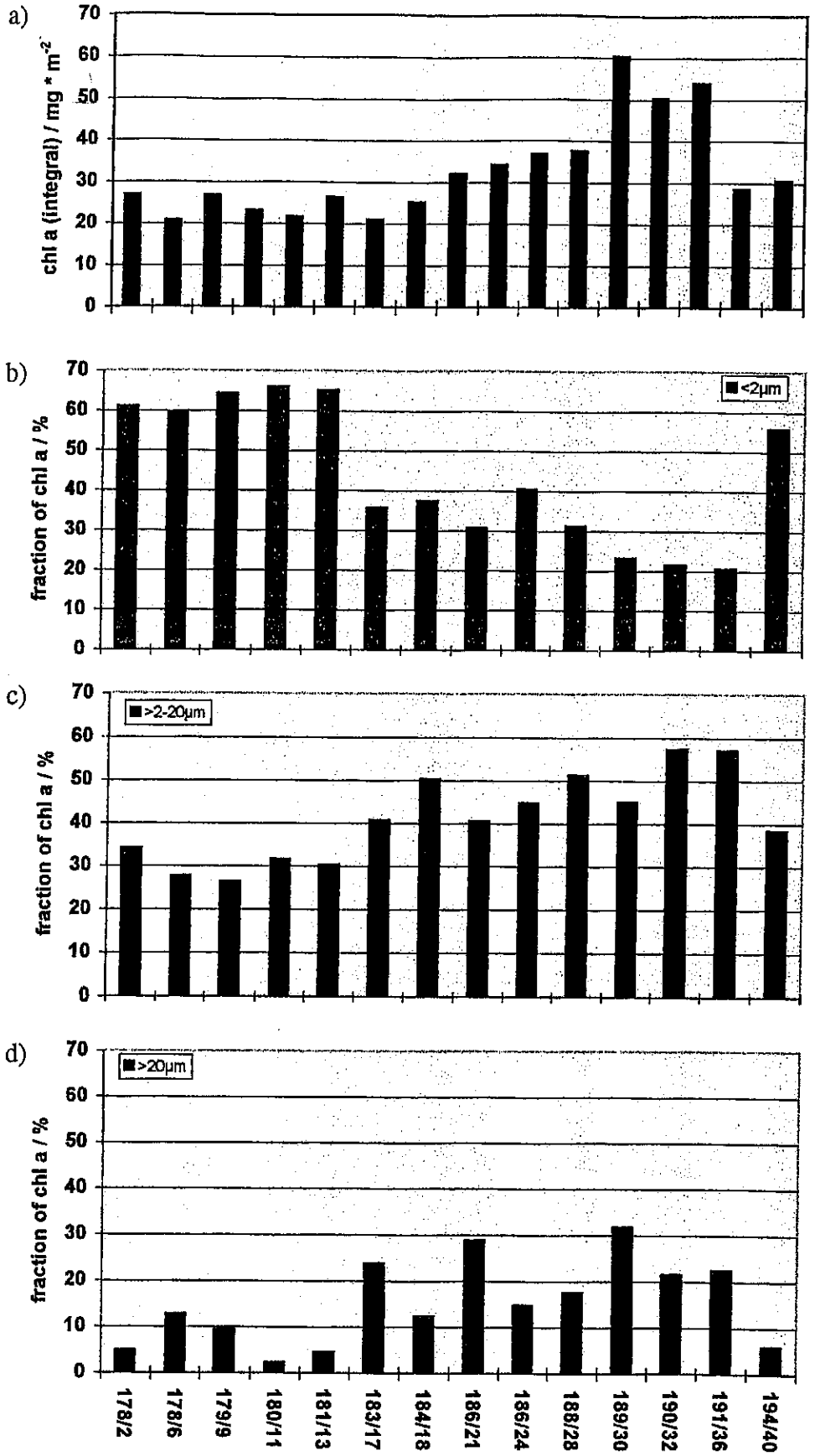

Fig. 29a-d: Vertically integrated stocks of chlorophyll (a) and mean contribution of different size classes to this stock. Picoplankton (b), nanoplankton (c) and microplankton (d).

5.2.3.3 Production and Flux of Biogenous Calcareous Particles in the Eastern North Atlantic (R. Schiebel, A. Zeltner, A.-B. von Gyldenfeldt)

Investigations of planktic foraminifers, pteropods, and coccolithophorids were conducted by means of vertical multinet hauls (mesh size 100 µm) and synchronous water sampling. To study coccolithophorids, water samples were filtered through a 0.45 µm screen (regenerated cellulose, screen diameter = 47 mm) with a pressure of 200 mbar. Coccolithophorid counts were carried out at Tübingen with a scanning electron microscope (SEM). In addition, water samples were collected for stable isotope analyses.

Each of the main JGOFS sites at 20°W, in particular L1 (33°N), L2 (47°N), L3 (57°N), and the sites A1 (40°N) and A2 (59°N) was sampled to a maximum depth of 2500 m, comprising 13 consecutive depth intervals. Multinet samples complement the Tübingen stock of samples from METEOR cruises M 6, M 10, M 11/1, M 12/3, M 17/2, M 21, M 26 and M 27/2. At L3, additional samples were collected to study the bacterial density on calcareous shells. Surface sediment samples were collected with a multicorer device, to investigate the present-day particle flux at the benthic boundary layer and during the late Quaternary.

Shipboard Results

During M 36/2, low numbers of planktic foraminifera were recorded from the upper 100 m of the water column, at 20°W. Small test sizes predominated the fauna. At the southern sites (L1, A1, and L2, at 33°N, 40°N, and 47°N), the fauna consists of tropical and subtropical species like *Globigerinoides sacculifer* and *Globigerinoides ruber*. At 33°N *Globoturborotalita tenella* was the most frequent species (Fig. 30). At this site, high numbers of *Globigerinita glutinata* indicate enhanced primary production, particularly diatoms. In contrast to the planktic foraminiferal fauna recorded at 33°N during M 21/3 (May 1992), *Globorotalia scitula, Globorotalia inflata, Neogloboquadrina incompta*, and *Globigerina bulloides* were rare during June 1996. This points towards the dynamics of the Azores Frontal Zone (AFZ): In 1992, the fauna consisted of a high portion of cold water species; in 1996, warm water species predominated. During both years, an enhanced fertility of the AFZ waters is indicated by relatively high numbers of *G. glutinata*. At L1 (33°N/22°W), the calcareous mesofauna was dominated by pteropods. At 54°N and 59°N (L3 and A2), transitional and subpolar species like *G. scitula, G. bulloides, N. incompta*, and *G. inflata* were frequent. *Globigerinoides conglobatus* and *Orbulina universa* were present in low numbers at most of the sites. Increased numbers of *O. universa* at 47°N and at 54°N, indicate that *O. universa* may not mainly be limited by low water temperatures, but also by the availability of food resources. At 47°N and at 54°N high numbers of copepods occurred. At 54°N many dinoflagellates were recorded.

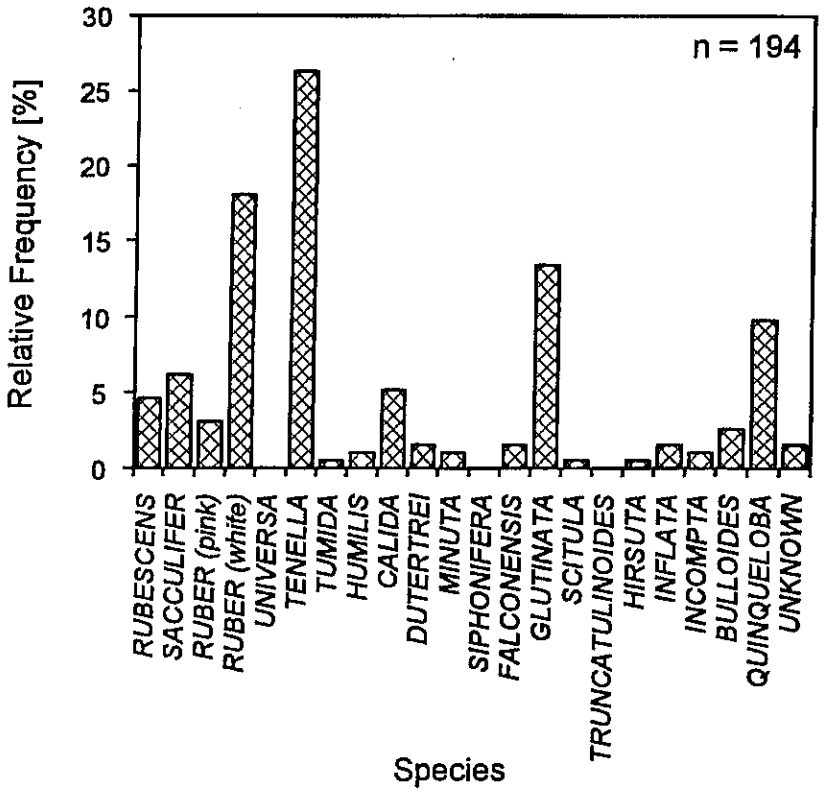

Fig. 30: Planktic foraminiferal species composition at 33°N/20°W, on May 26, 1996. The absolute number of specimens per m^3 was 194. The fauna is dominated by warm water species, which are placed at the left side of the x-axis.

The primary $CaCO_3$ flux of planktic foraminiferal tests in 100 m water depth (F_{100}) at 33°N was about 3.5 times higher in 1992 (35 mg $CaCO_3$ m^{-2} day^{-1}) than in 1996 (10 mg $CaCO_3$ m^{-2} day^{-1}). In contrast, the pteropod (25 mg versus 15 mg $CaCO_3$ m^{-2} day^{-1}) and the (other) gastropod $CaCO_3$ flux (450 mg vs. 47 mg $CaCO_3$ m^{-2} day^{-1}) were higher in 1996.

Three coccolithophorid floral zones (subtropical, transitional, and subarctic) of the Atlantic Ocean (after McINTYRE and BÈ, 1967) were recorded at 20°W. Lowest coccolithophorid cell densities were recorded at station L1 (33°N/22°W: 46 x 10^3 cells l^{-1}), and highest densities at station L2 (47°N/20°W: 237 x 10^3 cells l^{-1}) at 20 m (Fig. 31). A total of 82 taxa has been recorded. Highest species diversity was found in the subtropics (64 coccolithophore species, L1), lowest species numbers (12 coccolithophore species) were recorded at the subarctic station A2 (59.5°N/20°W). Holococcolithophores and *Umbellosphaera tenuis* (Kamptner) Paasche are characteristic species of the subtropic coccolithophorid floral zone. The most frequent species of the transitional floral zone are *Emiliania huxleyi* (Lohmann) Hay et Mohler *var. huxleyi*, *Gephyrocapsa muellerae* (Bréhéret), and various species of the family *Syracosphaeraceae*, in particular *S. marginaporata* (Knappertsbusch), 1993, *orthog. emend.*, *S. pulchra* (Lohmann), *S. dilatata* (Jordan et al.), and *S. halldalii* (Gaarder ex Jordan et Green), *sp. nov.* f. *protrudens*. Species dominating the subarctic floral zone in the upper 60 m and at 100 m respectively were *E. huxleyi* and *Coccolithus pelagicus* (Wallich) Schiller f. *pelagicus*.

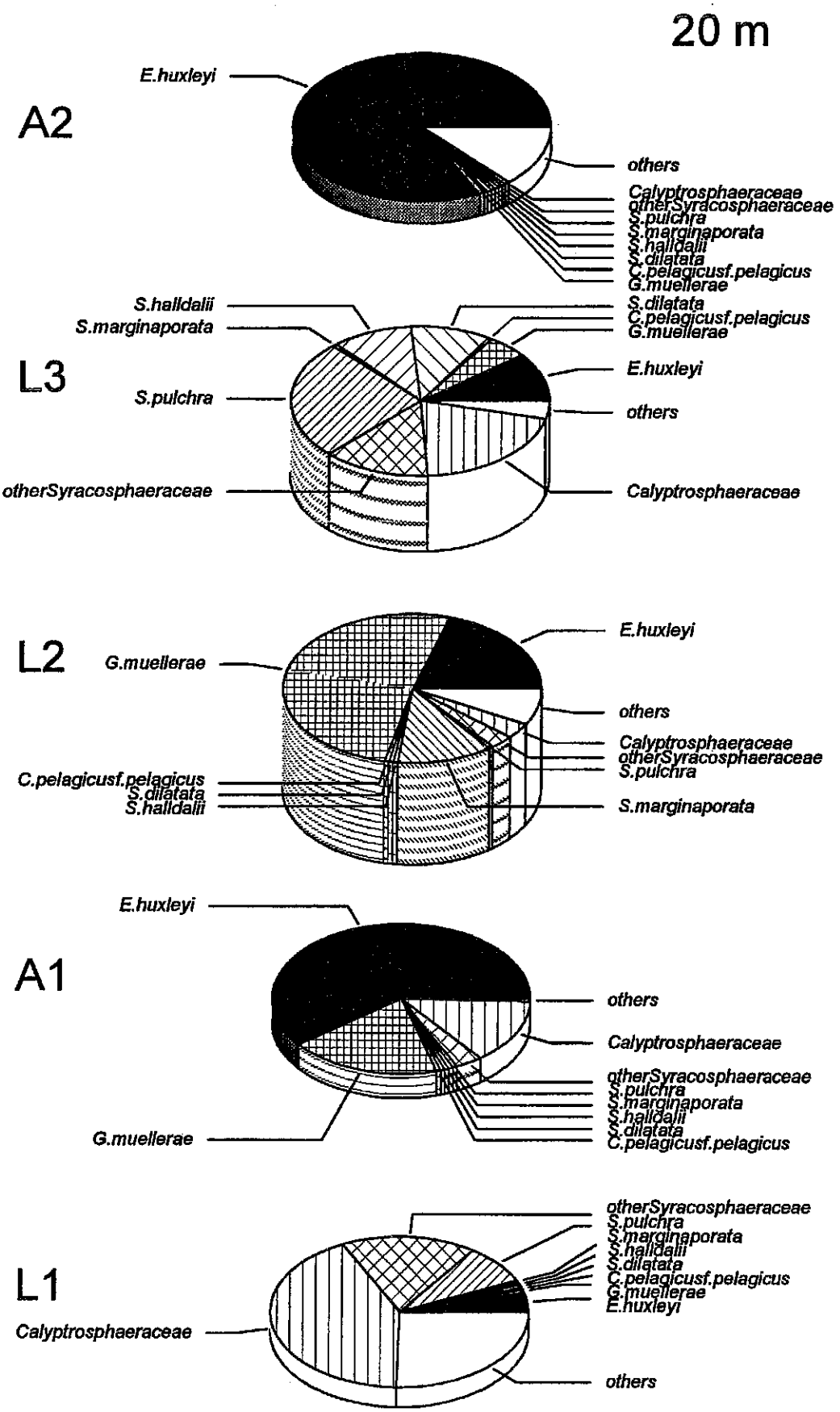

Fig. 31: Coccolithophorid species composition during M 36/2, at 33°N/20°W. The height of the pie charts gives the absolute number of cells per litre (at L2, 237 x 10^3 cells per litre were recorded).

5.3 Leg M 36/3

5.3.1 Geology (O. Costello, D. Dreger, J. Simstich, E. Steen)

5.3.1.1 Faeroe-Shetland Channel

During the first part of the cruise the Faeroe-Shetland Channel, one of the main zones for water mass exchange between the Norwegian-Greenland Sea and the North Atlantic was studied. It is a key area for the reconstruction of Late Pleistocene and Holocene thermohaline circulation patterns and abrupt climatic oscillations.

A total of four coring stations was selected on the basis of parasound profiles (Figs. 32-35). Two of these stations were located in the central part of the channel, and two at its northernmost edge. Both the box corer and the gravity corer were used to obtain the sediment samples (chapter 5.3.1.5). The penetration depth for the former was, on average, 45 cm and for the latter, ranged from 5.90 m to 10.80 m (chapter 7.3.1). No further work was done on the gravity cores during this cruise. The sediment in the upper 10-15 cm of the two centrally-located box cores consists of olive to yellow-brown silty sand, including a very soupy 0-5 cm surface layer. The lower component of these cores is olive-grey to greenish grey moderately compacted sandy silt. Unlike the central channel cores, the yellow-brown silty sand upper layers of the northern cores are confined to the soupy 0-5 cm surface layers. The lower section of the box cores consists of olive-grey silty sand. Box core sampling methods are outlined in the following section.

5.3.1.2 Sampling of Box Cores

The sampling of box cores is intended to provide valuable data for the study of isotopic and faunal variations in foraminifera (planktonic and benthic) and diatoms, general sedimentology, and for the quantification of ketones and organic carbon. Almost all box cores were sampled according to the following procedure. Sediment samples, in addition to samples for benthic foraminiferal studies, were collected from the 0-1 cm surface layer followed by down-core syringe (10 ml) sampling at 5 cm intervals for planktonic foraminferal and sedimentological studies. Depending on sediment availability and the proximity of stations to one another, 1 to 3 subcores were also taken.

For the purpose of benthic foraminiferal studies, one of the subcores was subsequently cut into 1 cm thick slices, with the upper 8 cm immediately placed in a Bengal Rose/methanol solution (10 g/5 l) to stain the protoplasm of any living foraminifera and prevent any subsequent bacterial decay. Benthic foraminifera constitute the majority of life on the ocean floor and, due to their minute tests, are easily sampled in the large numbers required for statistical analysis. Their abundance makes them quite sensitive to both local- and regional-scale environmental changes, and deciphering these environmental changes is our main purpose for collecting sediment samples from the box core stations.

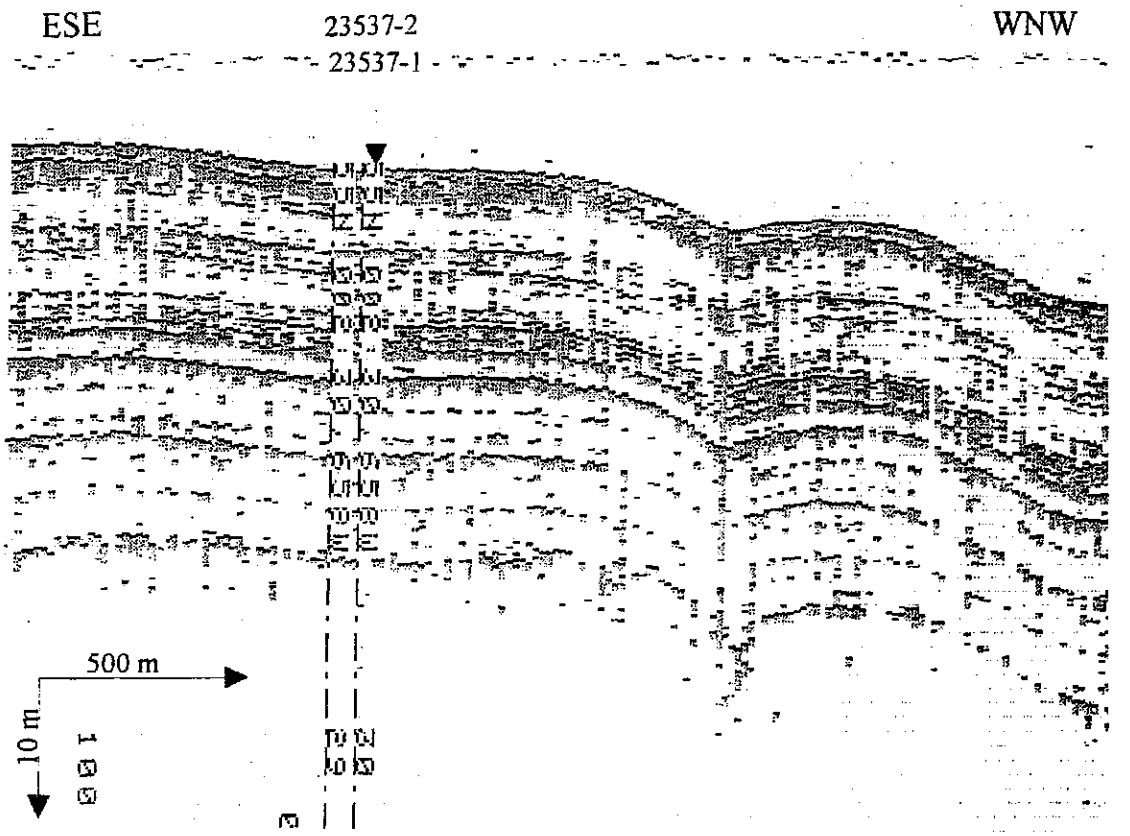

Fig. 32: Station 196: Location of sediment core station 196 (GKG 23537-1 and SL 23537-2) on parasound profile 195. Note the fault structure.

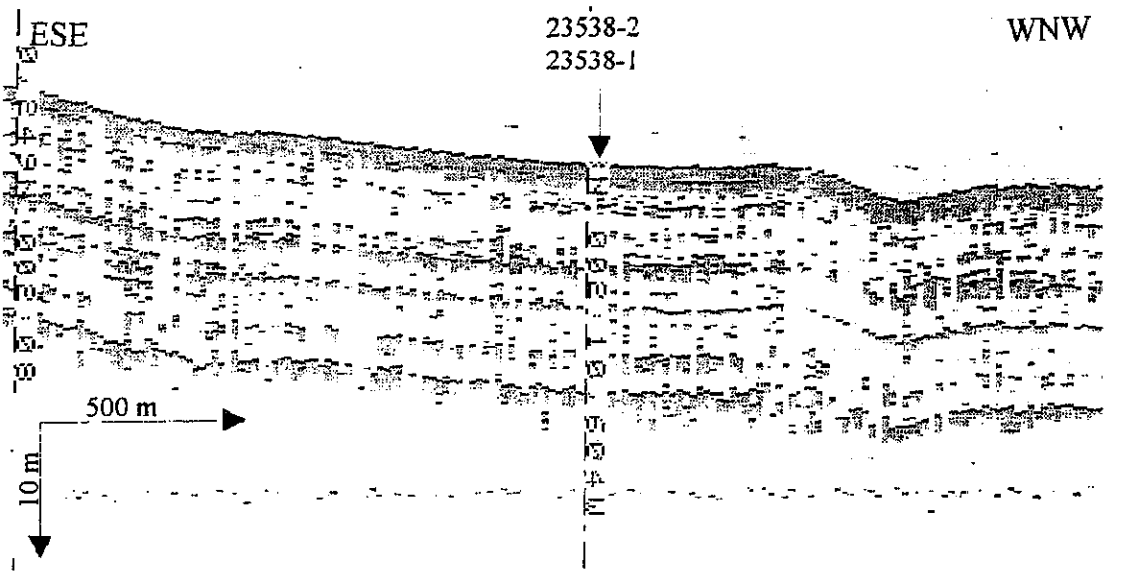

Fig. 33: Station 197: Location of sediment core station 197 (GKG 23538-1 and SL 23538-2) on parasound profile 195. Note the fault structure.

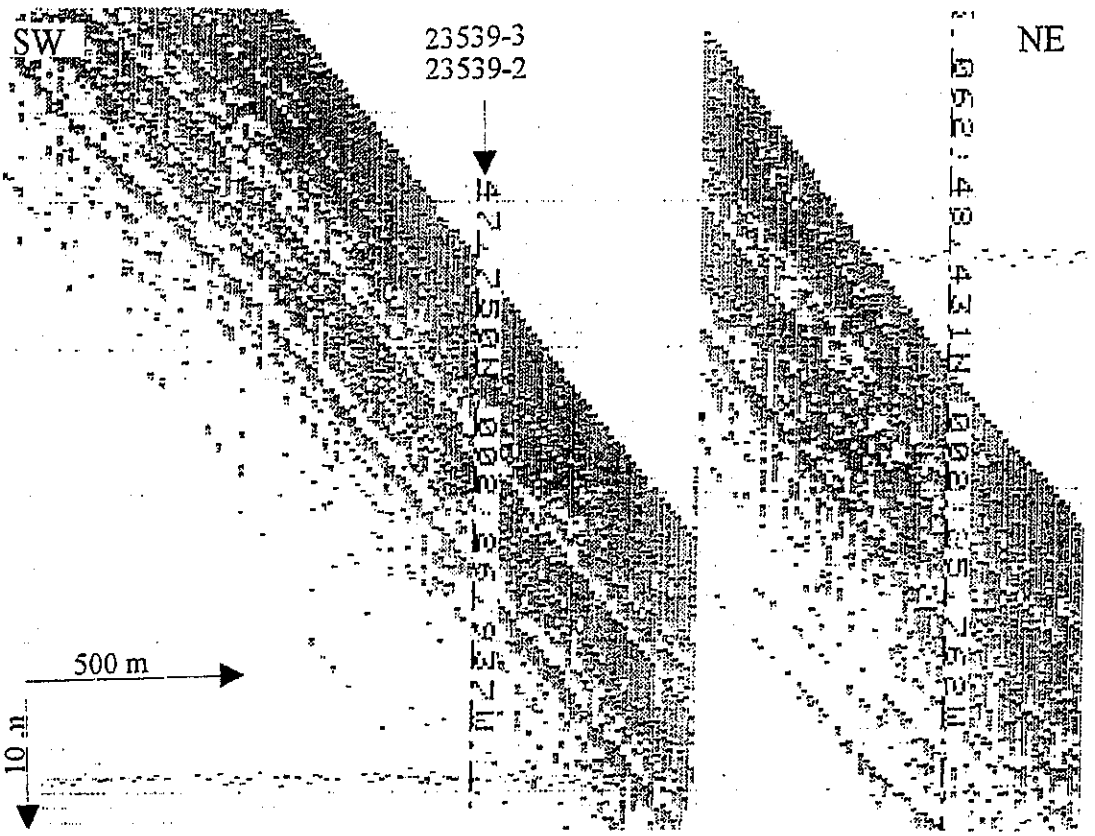

Fig. 34: Station 201: Location of sediment core station 201 (GKG 23539-2 and SL 23539-3) on parasound profile 199.

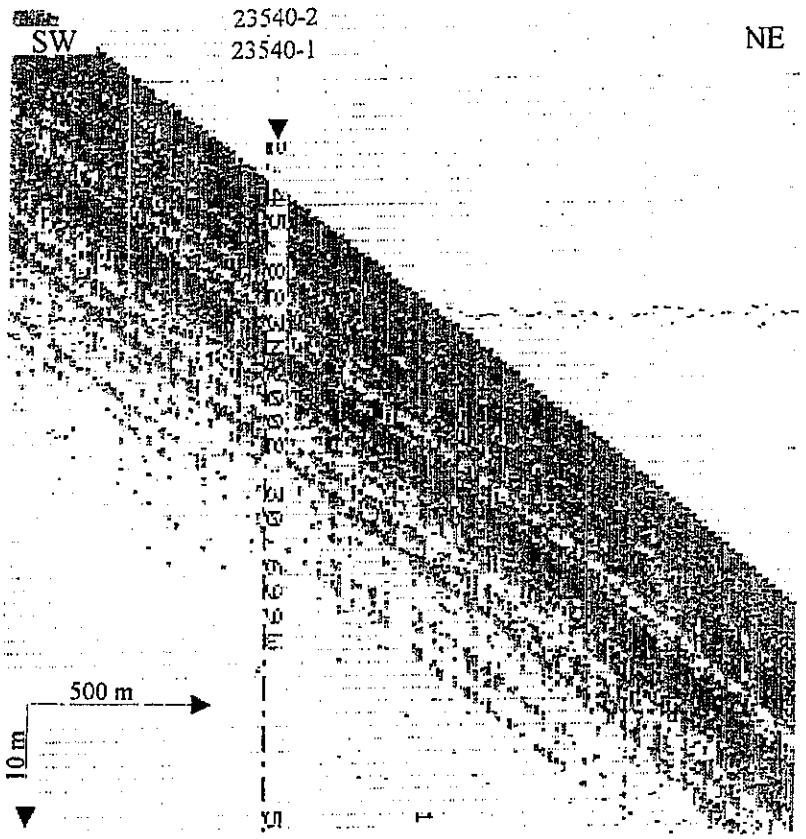

Fig. 35: Station 202: Location of sediment core station 202 (SL 23540-1 and GKG 23540-2) on parasound profile 199.

5.3.1.3 Sampling of Diatoms from Sediments and Surface Water

In order to accurately measure the $\delta^{18}O$ signal of marine diatoms, 10 mg of pure diatomaceous opal (roughly 10^{10} shells) from both surface water and the underlying sediment are required. The purpose of this study is to determine the relationship between the $\delta^{18}O$ signal of the diatoms and the water temperature at the time of growth, as well as the degree to which this signal has been modified in the water column and during subsequent sedimentation.

Diatoms were collected from the upper 50 m of the water column at some stations using a 40 µm plankton net. At the same stations, water from 10 m, 20 m, and 30 m depths was sampled by the CTD, whilst a 0-1 cm sediment sample was recovered by the box corer and, in some instances, the multicorer. The samples will be the subject of further study in Kiel.

5.3.1.4 Sampling of the Water Column for Isotopic Analysis

It is important to establish $\delta^{18}O$ and $\delta^{13}C$ values in the water column for modern oceanographic studies and to improve the calibration of proxy data (e.g. foraminifera). The ages of the water masses, derived from radiocarbon measurements, can be used to calculate rates of water exchange and deep water formation. The water column in the Lofoten Basin, the Greenland Basin and the Denmark Strait was sampled with the CTD. The samples were immediately treated with mercuric chloride and stored at 4°C for future processing at the Leibniz Laboratory for Isotope Research in Kiel.

5.3.1.5 Coring Devices

The collection of surface samples and sediment cores was primarily accomplished using the box corer (GKG) and the gravity corer (SL). The multicorer (MUC) was used for C_{org} studies because its cores can be subsampled in increments up to 1 mm and also because of its capability to retrieve a relatively undisturbed surface. The technical data of the coring devices used on this cruise are as follows:

Multicorer (MUC):
8 subcores, inner diameter 10 cm
Weight assembly up to 250 kg
Manufacturer Fa. Wuttke, Henstedt-Ulzburg

Box Corer (GKG):
Box dimensions 50 x 50 x 60 cm
Weight approximately 1000 kg
Manufacturer Fa.Wuttke, Henstedt-Ulzburg

Gravity Corer (SL)
Weight assembly 2000 kg
Core barrel outer diameter 14 cm
Liner tube inner diameter 12 cm
Length of core barrel segments 5.75 m
Manufacturer Fa. Hydrowerkstätten, Kiel-Hassee

These coring devices are standard tools of marine research and are technically sound. On account of ideal weather conditions, they were deployed with great success. The amount of core recovered after each deployment is noted on the station list (chapter 7.3.1). The following Table 6 presents a summary of the total core recovered:

Tab. 6: Summary of total core recovery

Device	Number of deployments	Successes	Total amount of core recovered (m)
GKG			
SL 6 m	2	2	10.78
SL 12 m	5	5	33.49
SL 18 m	2	2	17.78

The amount recovered by the gravity corer corresponds to the length of the sediment-filled portion of the liner tube (Fig. 36). There is always a difference in penetration depths which can be clearly measured from the sediment smear (A in Fig. 36) on the outside of each core.

The liner tube was removed from the core barrel, cut into 100 cm lengths and labelled from top (0 cm) down. Each core section was labelled with an orientation line, core number, depth, top and bottom.

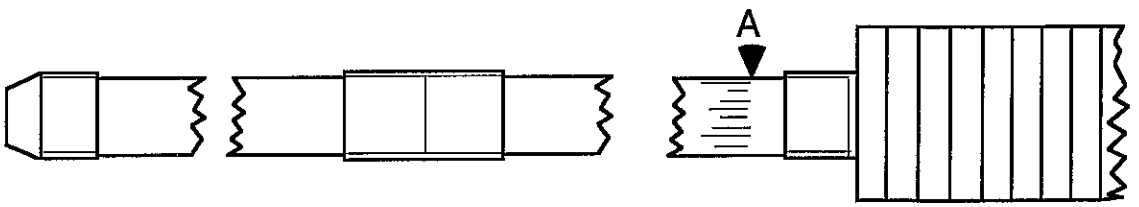

Fig. 36: Schematic drawing of a gravity corer with a core catcher (left), the barrels, and the core weight (right) on the top.

5.3.2 Geophysics: HF-OBH Wide Angle Experiments

(J. Mienert, J. Posewang, M. Baumann, X. Liu)

The High-Frequency Ocean Bottom Hydrophone System (HF-OBH) (Fig. 37) is designed to determine the compressional wave velocity distribution of the uppermost 200 m of deep-ocean sediments. This autonomous recording platform allows us to obtain a high-resolution seismic image. This autonomous recording platform has been successfully applied in the past to determine gas-bearing sediment layers of the Norwegian continental margin (Storegga slide and Svalbard). The HF-OBH has been developed by the Special Research Project 313 of the University of Kiel/Germany.

The presence of gassy and gas-hydrated formations has previously been observed north east of the Voering Plateau and at the edge of the Traendjupet slide on commercial seismic data. During M 36/3, the geophysical investigations aimed at determining the detailed small-scale seismic structure of gassy and gas-hydrated sediments in the Voering Plateau area using the Deep-Towed Boomer System (DTBS) of the British Geological Survey (BGS) as the seismic source. In contrast to the commercial data where only gross velocity information of the large-scale subbottom is derived, our experiments will provide a detailed and high-resolution spatial velocity distribution within a depth range of approximately 200 m below the sea floor (BSF). Furthermore, the high-resolution OBH data contain crucial information about reflection amplitudes which will be analysed in terms of gas concentration within the target gassy and gas-hydrated formations. In addition, the information gained from DSDP site 342 will be used to calibrate the high-resolution seismic structures inferred from the HF-OBH data.

The HF-OBH system consists of the following principal components (Fig. 37):

- three hydrophones receiving acoustic signals transmitted by any seismic source;
- the registration unit containing a programmable logic, a 12 bit A/D converter, a digital audio tape recorder (DAT tape), an internal clock (synchronised with DCF77 time signal) and a 12 V rechargeable power pack. The electronic unit is placed in a cylindrical aluminium pressure housing. The recording unit and the hydrophones are connected to each other by cables and are fixed at the OBH frame.
- two independent release systems ensuring the disconnection of the entire OBH system from the anchor weight (60 kg). The first release system can be acoustically triggered directly from the research vessel. The second is an electro-chemical release which is activated by the programmable internal clock of the registration unit.
- the buoyancy element (synthetic foam) responsible for the upright rising of the OBH system after the release. It is 6000 m pressure-proof.
- a strobe light, a radio transmitter and a signal flag fixed at the upper part of the buoyancy frame facilitating the location of the OBH at the sea surface after the experiment.

The data acquired during this cruise correspond to the first part of a planned series of experiments in 1996 which will be carried out at the same locations along the Norwegian continental margin applying different seismic sources, e.g. airgun (thus providing a larger range of source frequencies).

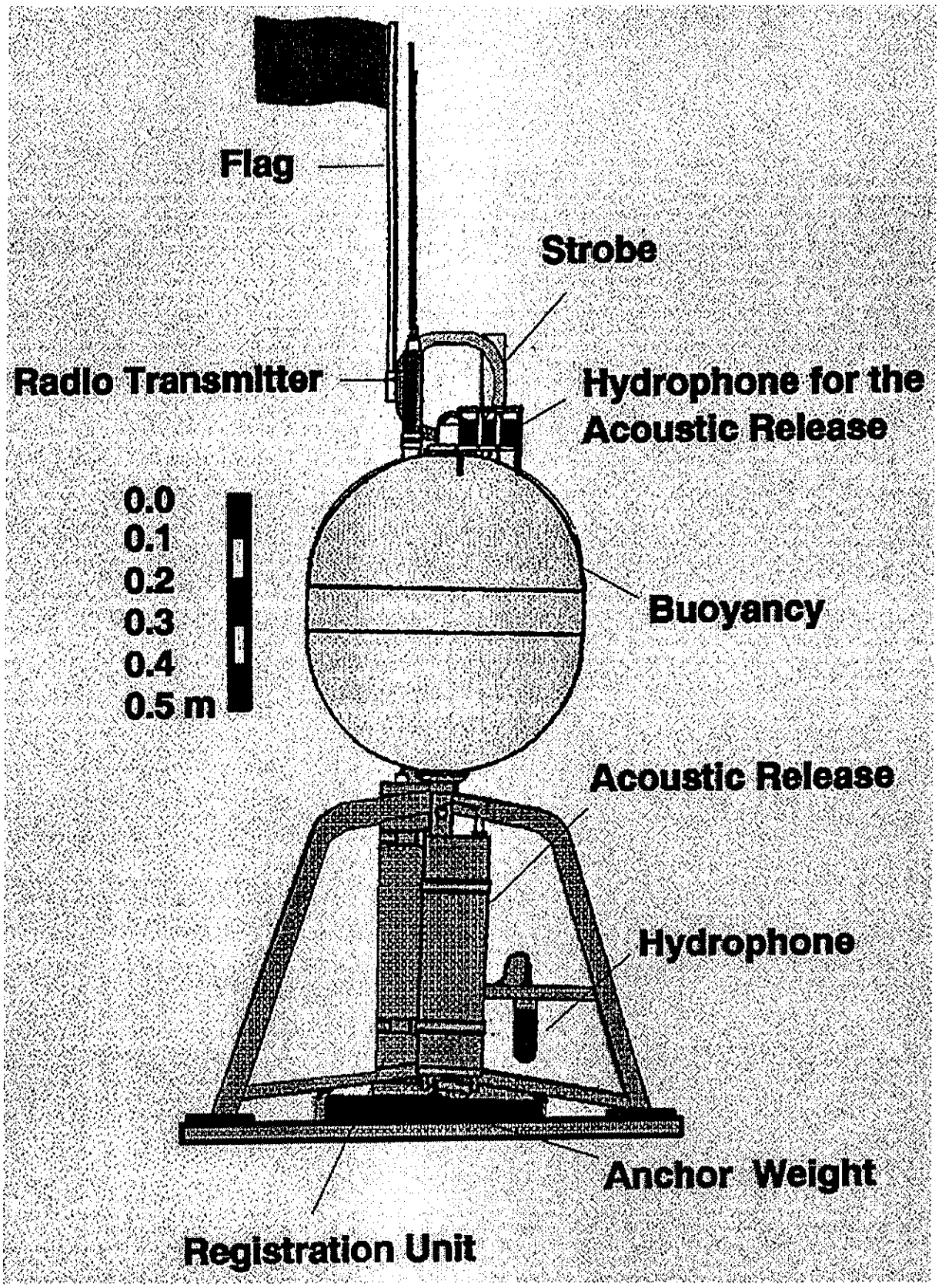

Fig. 37: HF-OBH configuration and the various components of the acoustic system.

5.3.2.1 Seismic Source and OBH Deployments

The deep-towed boomer (DTB) of the British Geological Survey (BGS; see chapter 5.3.4) with a main frequency band between 800 to 2000 Hz was used as a seismic source. A constant shot interval of 2 s guaranteed the maximum required record length necessary for the water depth in which the experiments were carried out. The boomer was winched out along a cable of 1970 m length and reached depths of 600-800 m below sea surface (fish depth). Reflection data were also collected by the DTBS hydrophones (streamers) and stored as digital data on exabyte tapes and as analogue records on the BGS Waverly paper printer.

The choice of the OBH locations was mainly based on the results of the parasound profiling run prior to the seismic experiments. The parasound data provide accurate information about the smoothness of the sea floor and the gross structure of the sediments (see chapter 5.3.3). The complexity of the structure, which can be resolved from data obtained by seismic profiling with only two OBHs, is limited. For this reason, special attention was paid to finding experimental areas characterised by more or less horizontal sediment layering. These requirements allow us to best fulfil one of the aims of the experiments, i.e. acquire high-quality data.
In order to obtain high-resolution data at the sedimentary formations to be imaged, the distance between the two OBHs was set at about 500-700 m. Together with this constraint, the following factors also had to be taken into account for the time planning of the instrumental deployment (see also Fig. 38) and for the programming of the recording units:

- the time needed to set out both OBHs (10-15 min each); and the time taken to carry out depth diagnostics checks, also considering that the OBH unit sinks at a speed of 1 m/s;
- the sailing time between both OBH locations (10 min), and between the last OBH location and the beginning of the seismic profile (30 min at about 10 kn);
- the time used to winch out the DTB source (ca. 20 min) and bring the source in line with the seismic profile, considering that the source was towed 1970 m behind the vessel (about 50 min for 6000 m at 4 kn, including turn at the profile extremity);
- the speed of the vessel during the profiling (ca. 4 kn).

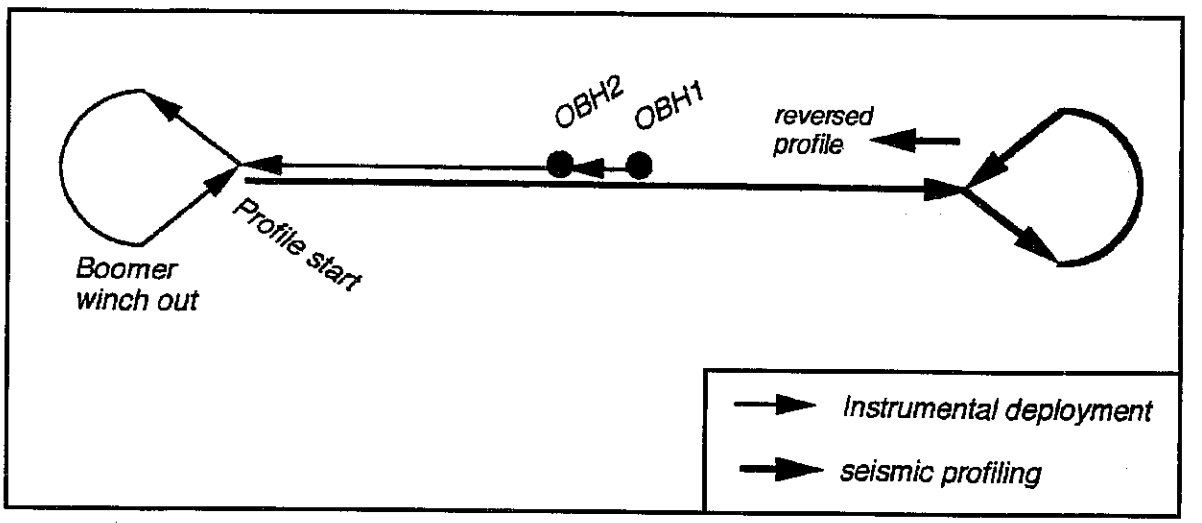

Fig. 38: Graphic showing experimental OBH deployment.

From the point at which the first OBH unit was deployed, about 120 to 150 minutes had to be planned before the OBH units actually started to record. The profile length was chosen to best image the target structure. The profile length was additionally limited by the power of the DTBS source and the maximal recording capacity of the employed DAT tape (2 hours). After the seismic experiments, the OBHs were acoustically released from their anchor weight and recovered.

Time signals of the BGS DTBS (TTL time signal) and the DCF77 time signal with which the OBH units are synchronised were simultaneously recorded on a separate DAT tape. This procedure allows us to exactly correlate the shot numbers with the recorded seismic signals and provide a direct link between the two seismic data sets. During the experiment, the towing depth and corresponding shot numbers of the DTBS were noted in a logbook at one minute intervals.

5.3.2.2 HF-OBH Measurements and Parasound and DTB Profiles at HF-OBH Stations

In the area of the Voering Plateau, four sites were chosen where the seismic experiments were carried out. Three of these sites (218, 225, and 227) were located at the edge of the Traendjupet slide in the northern part of the Voering Plateau. This area is known as a potential site of gas-hydrate bearing formations. The fourth experimental site (244) was located near DSDP site 342. The results of the sonic log data obtained at this borehole will be used for correlating the velocity-depth information gained from our OBH experiment.

Gravity corer and box corer sampling were carried out at sites 218 and 225 to further sample the uppermost sedimentary units. The geological information gained from the core studies will be taken into account during final interpretation of the geophysical data. Additionally, a representative CTD profile was measured at site 203. From the CTD data (Fig. 39), the seismic velocity of the water will be determined and taken into account during the modelling of the OBH data.

At site 203 (July 24) both OBH units were tested in order to check the release systems. The OBH instruments were deployed on the vessel's starboard side using winch W3. First, the instruments were lowered to 500 m water depth, where a depth-diagnostic test was successfully performed. Secondly, the anchor weight, which was fixed at the OBH frame, was released at 1000 m water depth.

The four seismic experiments were carried out successfully between July 27 and 31; this was helped by favourable weather conditions. The co-ordinates of the individual recording sites and water depths can be found in chapter 7.3.1. The total length of the profiles for all the OBH experiments carried out during this cruise was 4000 m. It was hoped that the length of the profile together with the maximal recording time of two hours would have allowed us to record a reversed profile. However, considering the 2000 m cable length of the tow fish, the turn at the

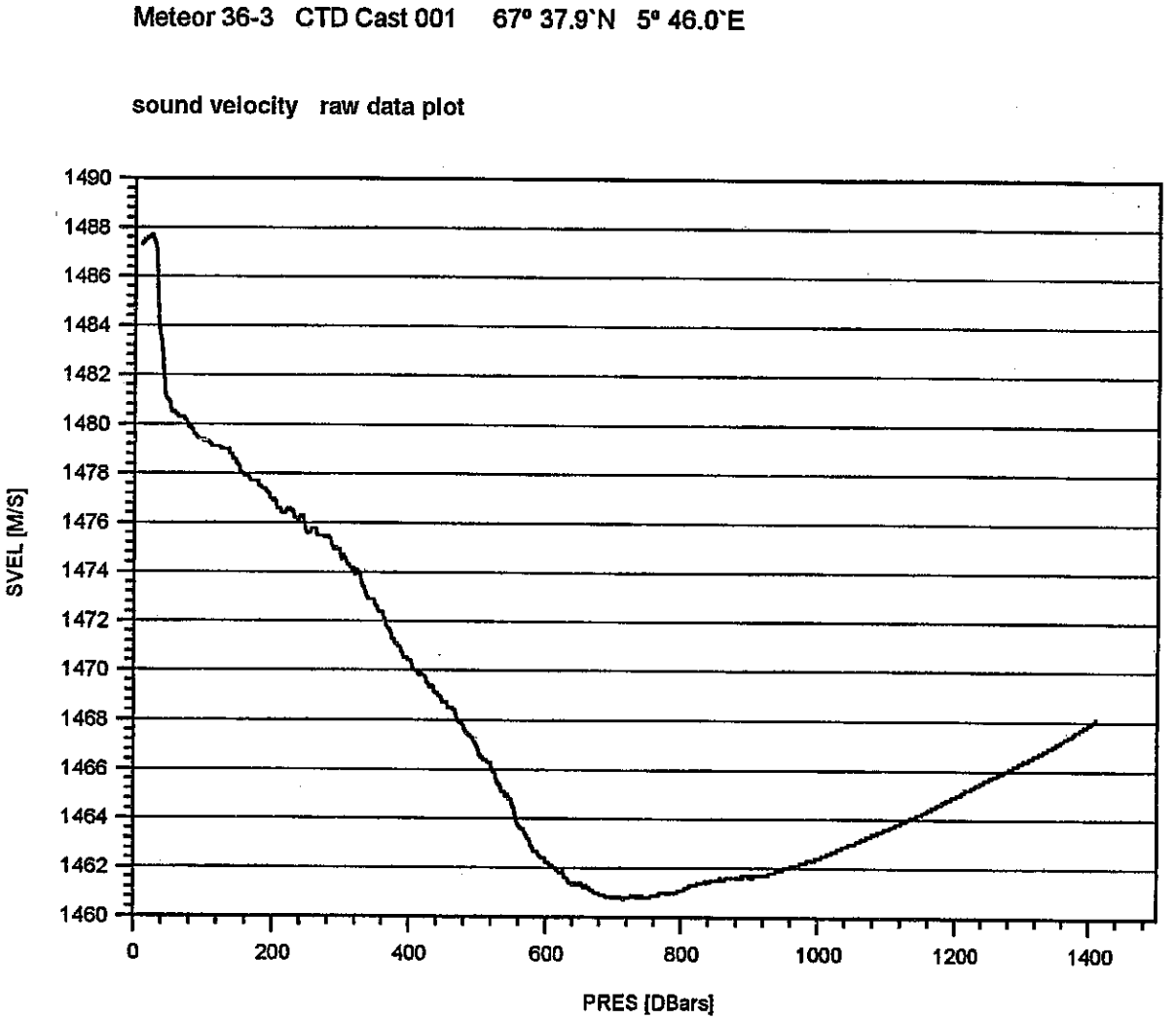

	SVEL [M/S]
arithmetical mean	1467.6172
standard deviation	6.6727
standard error	0.17820832762
median	1465.4
harmonical mean	1467.587
geometrical mean	1467.6021

Fig. 39 Sound velocity raw data plot of the CTD cast 001.

extremity of the profile (start of profile) took considerably longer than expected. The reversed section of the seismic profiling could therefore not be completely recorded.

The data quality was acoustically controlled using a traditional loudspeaker system. As expected, a high signal-to-noise ratio characterises the entire set of data.

During the last experiment near DSDP 342 (site 244), the strong airgun signal of a commercial seismic campaign nearby was also recorded.

Due to an unexpectedly rapid discharging of the battery (station 218, old OBH unit), only the first hour of the profile was recorded on tape. During the subsequent profiles, an extra battery pack guaranteed sufficient power supply. An additional electronic problem (cable failure at tape recorder; station 227 and 244, new OBH unit) implied complete data loss on two tapes. This failure was repaired on board after the completion of the seismic experiments. All the data, including the time signals, were back up on DAT tape after the quality check.

The Parasound and DTB profiles at OBH stations were as follows:
OBH station 218 is located at the northeastern edge of the Traendjupet slide (area 1 on Fig. 62a of chapter 5.3.4). Profile 219 is characterised by a water depth of 1330 m, a smooth ocean bottom (parasound data and DTBS data), and a more or less horizontal undisturbed sedimentary layering running parallel to the ocean bottom (Fig. 40a, b). The penetration of the parasound and DTBS data is about 20 m BSF and 70 ms TWT BSF, respectively.

OBH station 225 is located at the northeastern edge of the Traendjupet slide (area 1 on Fig. 62a of chapter 5.3.4). Profile 225 is characterised by a water depth of 1400 m, and a smooth ocean bottom (parasound data and DTBS data) which is gently dipping in a southwesterly direction. More or less horizontal undisturbed sedimentary layering running parallel to the ocean bottom can be observed (Fig. 41a, b). The penetration of the parasound and DTBS data is about 10-15 m BSF and 40 ms TWT BSF, respectively.

OBH station 227 is located at the northeastern edge of the Traendjupet slide (area 1 on Fig. 62a of chapter 5.3.4). Profile 228 is characterised by a water depth of 1400 m, a smooth and nearly horizontal ocean bottom (parasound data and DTBS data) and horizontal undisturbed sedimentary layering running parallel to the ocean bottom can be observed (Fig. 42a, b). The penetration of the parasound and DTBS data is about 15 m BSF and 60 ms TWT BSF, respectively.

OBH station 244 is located at the northwestern part of the Voering Plateau. Profile 245 is characterised by a water depth of 1305-1320 m, a smooth ocean bottom (parasound data and DTB data) with a wide channel-like feature near the OBH 1 location. A regular layering running parallel to the sea floor is observed (Fig. 43a, b). The penetration of the parasound and DTB data is about 40 m BSF and 100 ms TWT BSF, respectively.

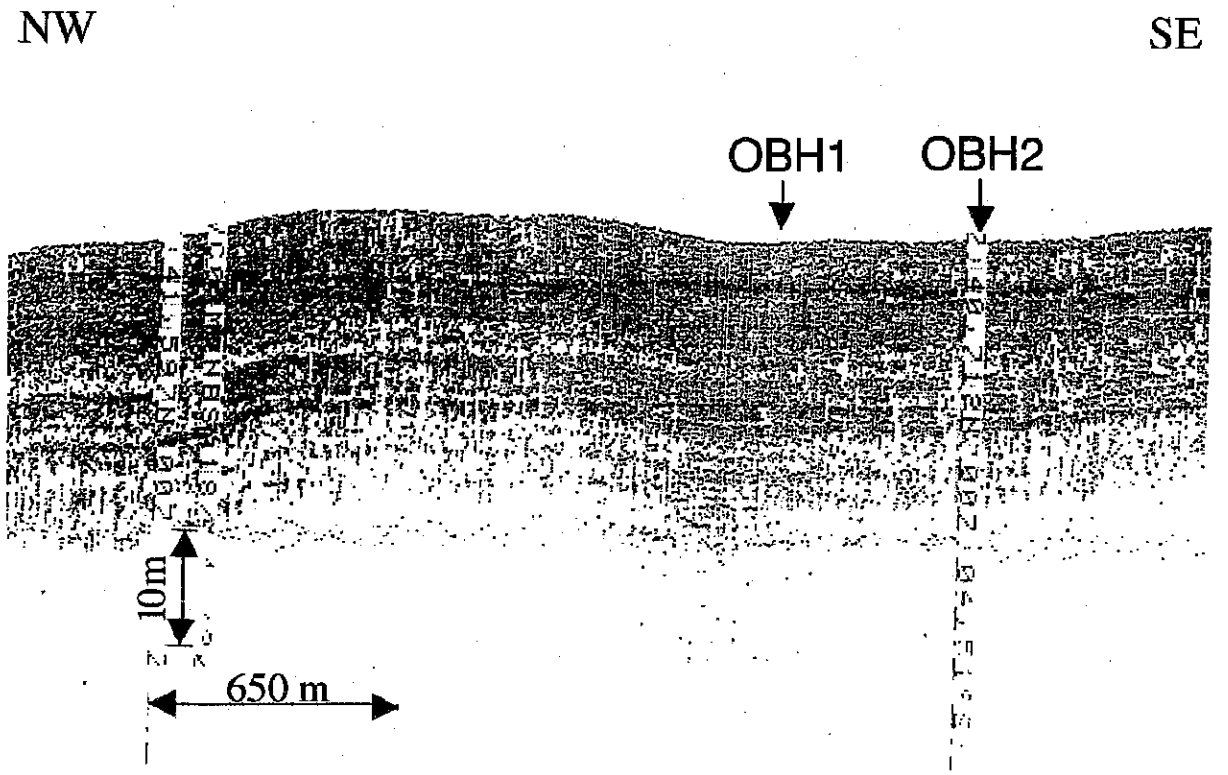

Fig. 40a: Section from parasound profiling at OBH site 218.

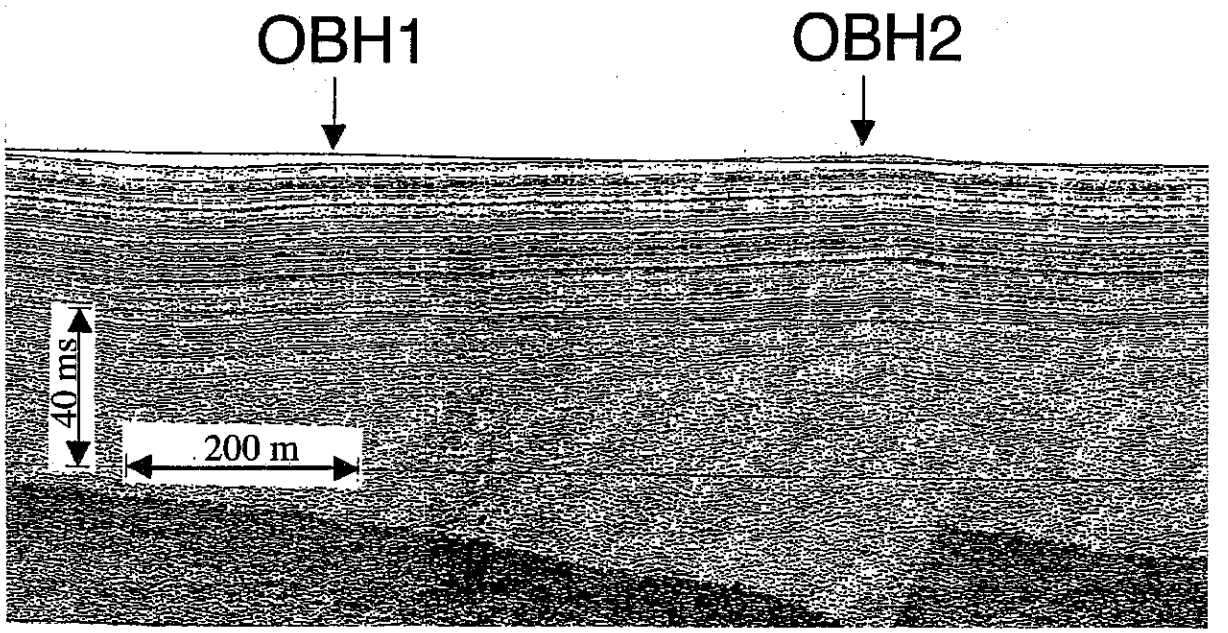

Fig. 40b: BGS DTBS profile 219 with OBH 218 locations.

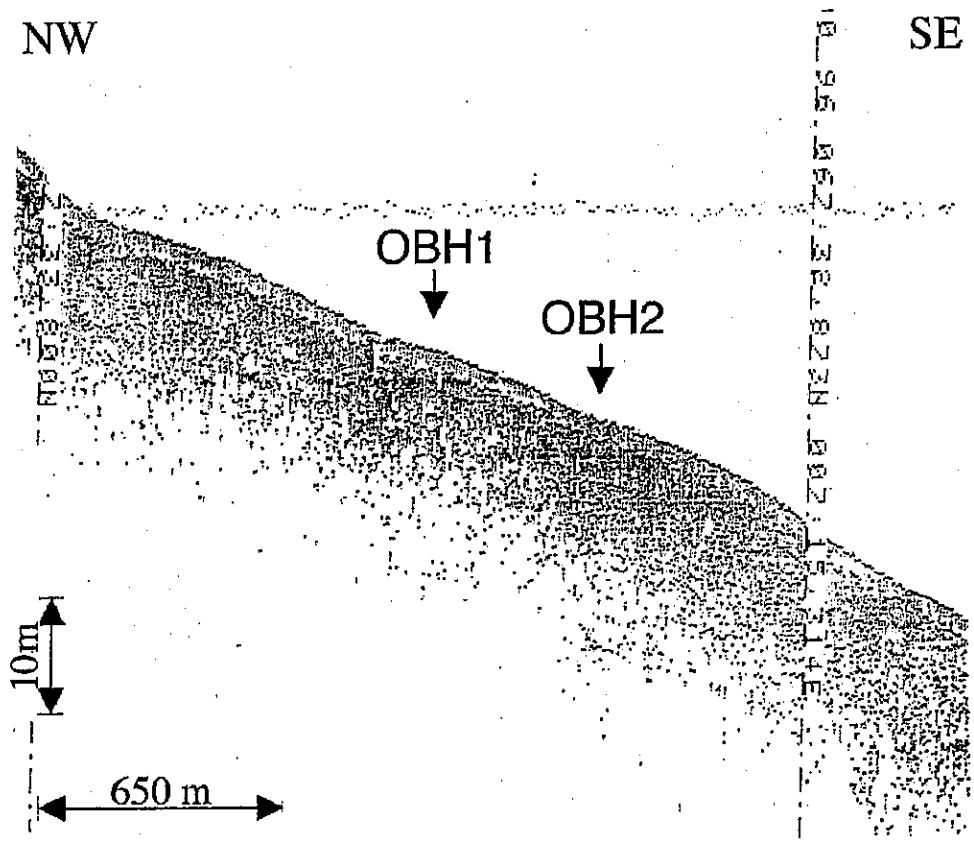

Fig. 41a: Section from parasound profiling at OBH site 225.

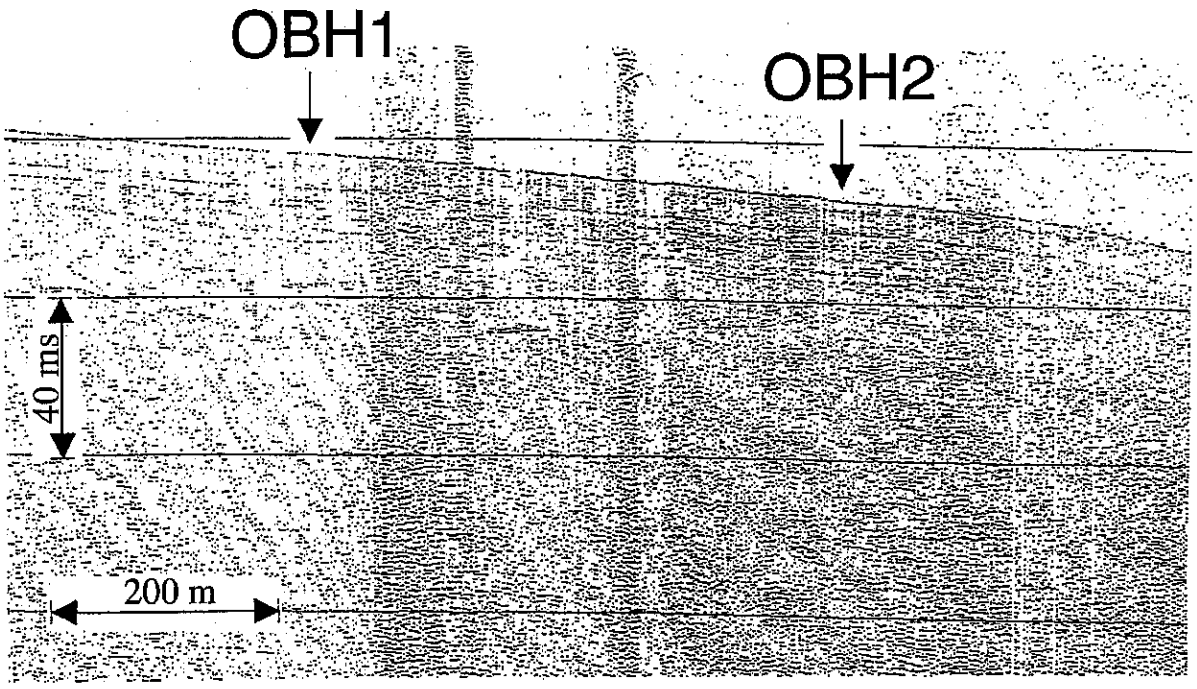

Fig. 41b: BGS DTBS profile 225 with OBH 225 locations.

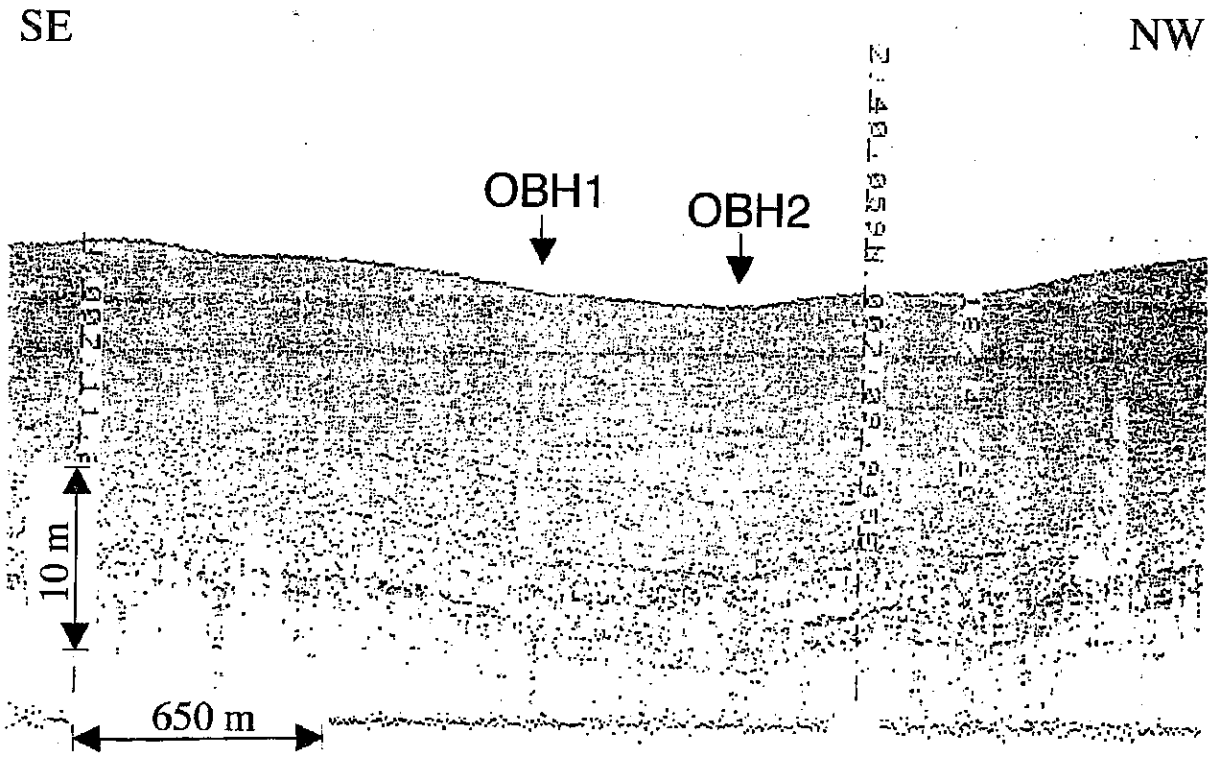

Fig. 42a: Section from parasound profiling at OBH site 227.

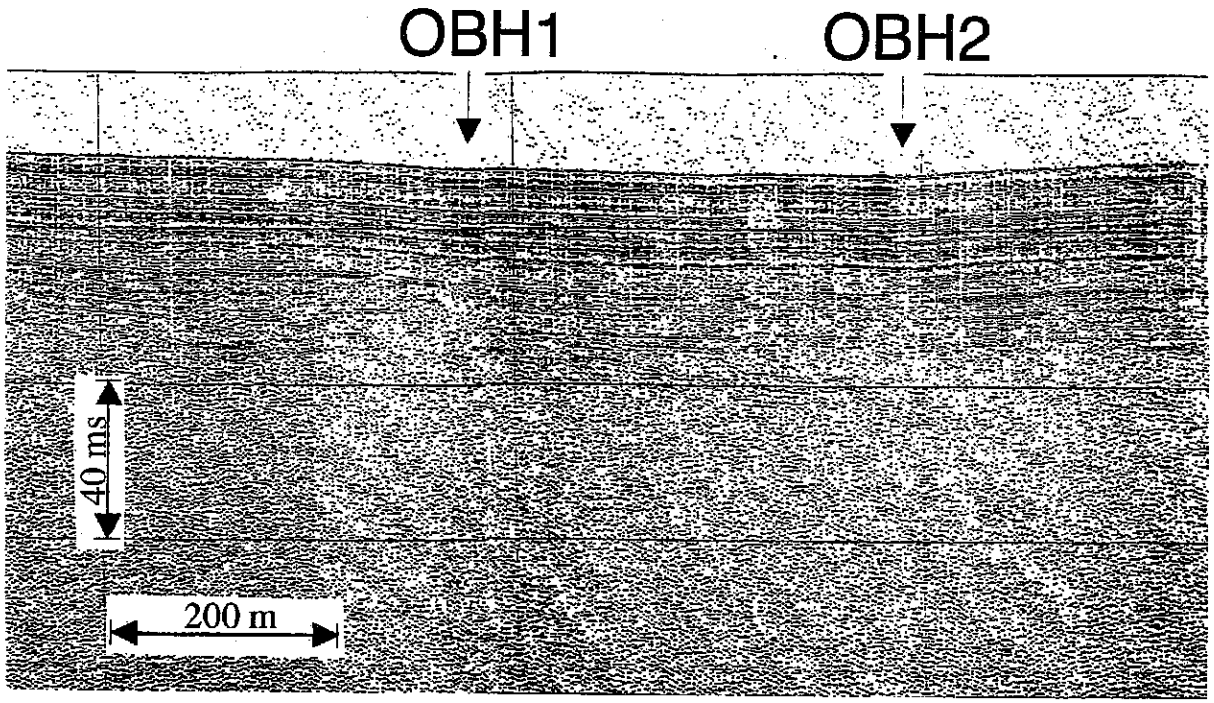

Fig. 42b: BGS DTBS profile 228 with OBH 227 locations.

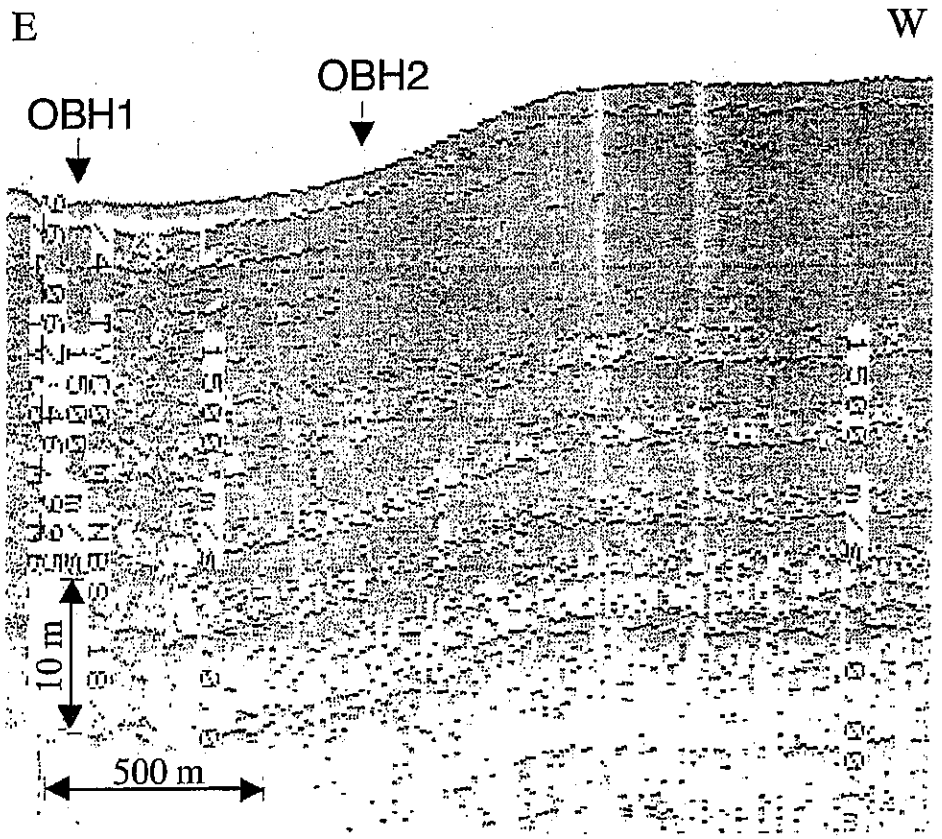

Fig. 43a: Section from parasound profiling at OBH site 244, near DSDP site 342.

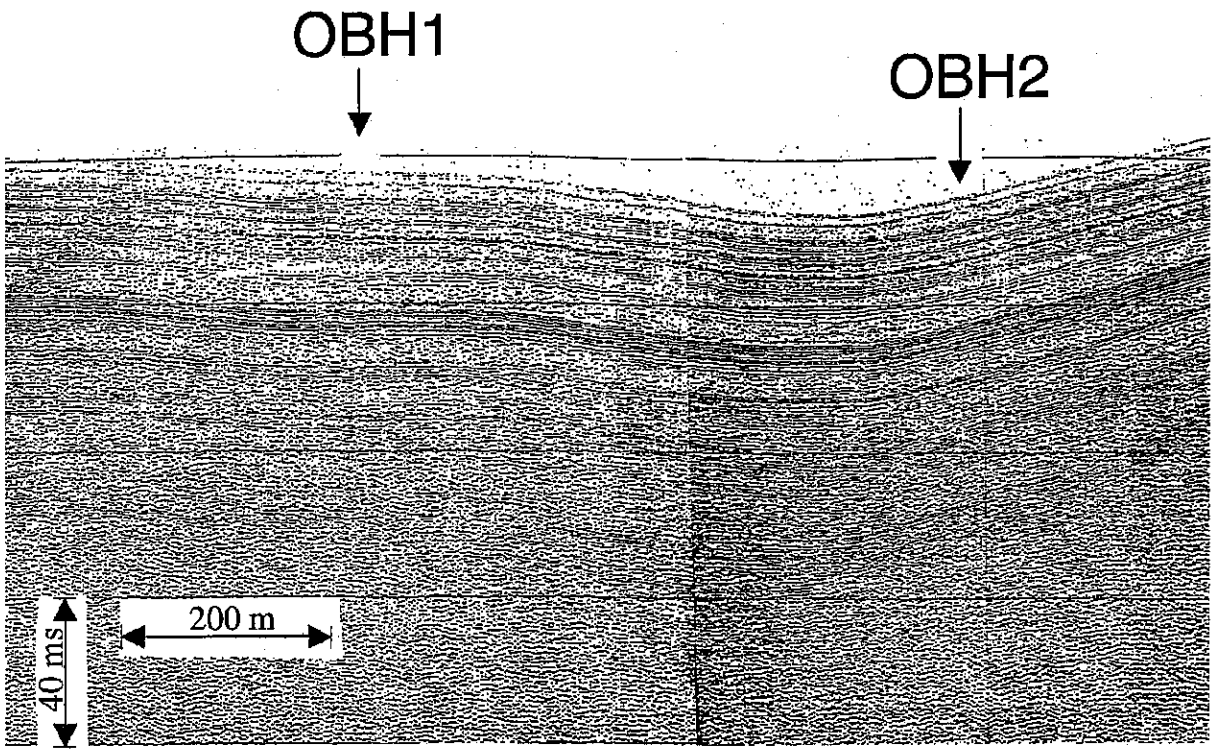

Fig. 43b: BGS DTBS profile 245 with OBH 244 locations, near DSDP site 342.

5.3.3 Geophysics: Parasound and Hydrosweep Profiling (F.-J. Hollender, X. Liu, J. Posewang, O. Bothmann, J. Simstich, D. Dreger, O. Costello)

During M 36/3, parametric echo sounder (parasound) profiling was carried out in four work areas and on the transit between the work areas (Fig. 44). This was done to provide information on recent and currently active sediment mass-wasting processes and on the likelihood of the sediment slope failures. An additional purpose of the survey was to select sediment core stations based on the parasound data.

Parametric echo sounder is a sediment subbottom profiler, which works with two simultaneous primary frequencies (a fixed frequency of 18 kHz and a variable frequency from 18 to 23.5 kHz). Through the parametric effect in water, secondary frequencies are produced in the range from 2.5 to 5.5 kHz. In oceanic sediments, a penetration of up to 100 m is possible. Analogue plots are available for preliminary interpretation on board. In addition, digital data are stored on magnetic tape so that details can be studied with post-processing techniques. The data of the hydrosweep system, a multibeam echo sounder system which operates at a frequency of 50 kHz, were also combined in the interpretation. The combination of the parasound and hydrosweep data provides three-dimensional imaging of superficial structures.

The parasound records are overall of good quality. Preliminary results, presented below, are based on the analogue data. Details will become available after post-processing of the digital data.

5.3.3.1 Faeroe-Shetland Channel and North Sea Fan

Four profiles were recorded in the Faeroe-Shetland Channel (FSC) (profiles 195, 198, 199 and 200) and one profile was run over the North Sea fan (Fig. 44). Profile 195 is oriented ESE-WNW and starts southeast of the Faeroe-Shetland Channel. This profile ends at the FSC. Profile 198 corresponds to the prolongation of profile 195 in a WNW direction and runs almost perpendicular to the FSC. Profile 199 is oriented SW-NE and obliquely crosses the FSC. Profile 200 oriented NW-SE runs perpendicular to the FSC. Based on the data of profiles 195 and 199, four sediment core stations were selected in the FSC where penetration reached over 30 m and very clearly stratified sequences were recorded (Figs. 32-35).

Profiles 195, 198 and 199 show that on both flanks of the FSC, the sea bed is rough, penetration is generally less than 20 m, and there were no stratified sequences. As the water depth increases towards the FSC, the sea bed becomes smooth and penetration of up to 40 m was achieved in stratified sequences. Fault structures, which could be followed to over 30 m below sea bottom, were also recorded in the FSC (Figs. 32-33). The vertical throw of the faults varies between 2 and 4 m.

Very complex features were found in profile 200 in water depth of more than 1700 m. A penetration of over 40 m could be reached and no stratified sequences were recorded. A large

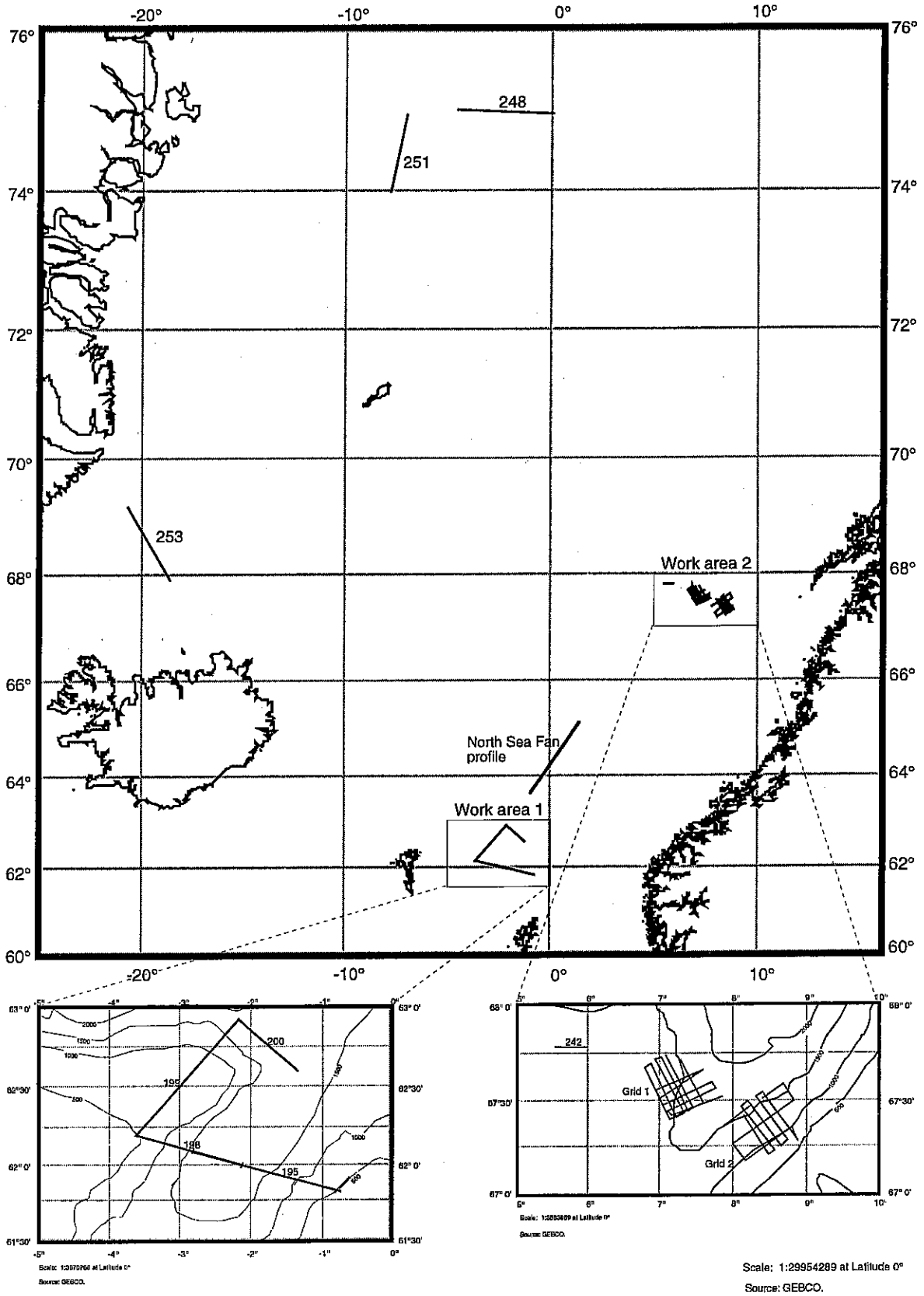

Fig. 44: Work areas of M 36/3 with structural features and the location of the parasound profiles.

transparent lens structure, which is most likely a debris flow, with a thickness of 30 m and a length of over 9000 m was observed (Fig. 45). At seven locations the seismic reflector and sea bed were broken, perhaps due to fluid outflow (Fig. 46 for example).

The North Sea fan profile (Fig. 44) is oriented SW-NE. The structures of this profile are characterised by debris flows of different sizes (for example Fig. 47). At both ends of the profile, the sea bed shows slide-like morphology and features. The penetration only reached approx. 10 m.

5.3.3.2 Northern Voering Plateau

Two grids of parasound profiles were investigated in the northern Voering Plateau (Figs. 44 and 48). Grid 1 is situated northwest of the Traendjupet slide and consists of 17 parasound profiles (profiles 204, 205, 206, 207, 208, 209, 210, 211, 212, 213, 214, 215, 220, 221, 222, 223 and 224) (Fig. 48a). Grid 2 runs through the Traendjupet slide and has 9 profiles (profiles 230, 231, 232, 233, 234, 235, 236, 237 and 241) (Fig. 48b). Profile 229 connects the two parasound grids. The W-E profile 242 is situated northwest of the parasound grids (Fig. 44).

The water depth at grid 1 ranges from 1200-1300 m in the northwest to over 1700 m in the southeast (Fig. 49). Analysis of the parasound data combined with hydrosweep bathymetric data of grid 1 shows following the features:

- In the northwest of the area where the bathymetry is smooth (Fig. 49), the parasound data show a high penetration of up to 40 m. The sea bed is smooth and the seismic records show stratified sequences (Fig. 50a). These results suggest that the north-western region has not been affected by the Traendjupet slide processes.
- In contrast, the southeastern area shows a very rough microtopography and a penetration of less than 20 m. No stratified sequences could be followed in the seismic records. In several locations, possible gas venting structures were observed (Fig. 50b). Debris flows of different sizes were also recorded. The southeastern area may be affected by the Traendjupet slide processes. A slide mass could be observed between profiles 222 and 223 (Fig. 51, see also Fig. 49 for topographic feature of this line).
- A zone with a high sea bed gradient and a varying orientation from SSW-NNE to WSW-ENE (Fig. 49a, b), marks the beginning of the deformed area.

The water depth over grid 2 varies from less than 600 m in the southeast to over 1600 m in the northwest (Fig. 52). The following features have been revealed from the parasound and hydrosweep data:

- In the whole area, no stratified sequences were recorded by the parasound data. The penetration ranges from 10 to 30 m.
- Two different structures are divided by a NW-SE oriented narrow zone, which marks the sharp changes of water depths (Fig. 52). Northeast of this zone, the area is characterised by massive deposits with varied sea bed relief (Fig. 53), whereas

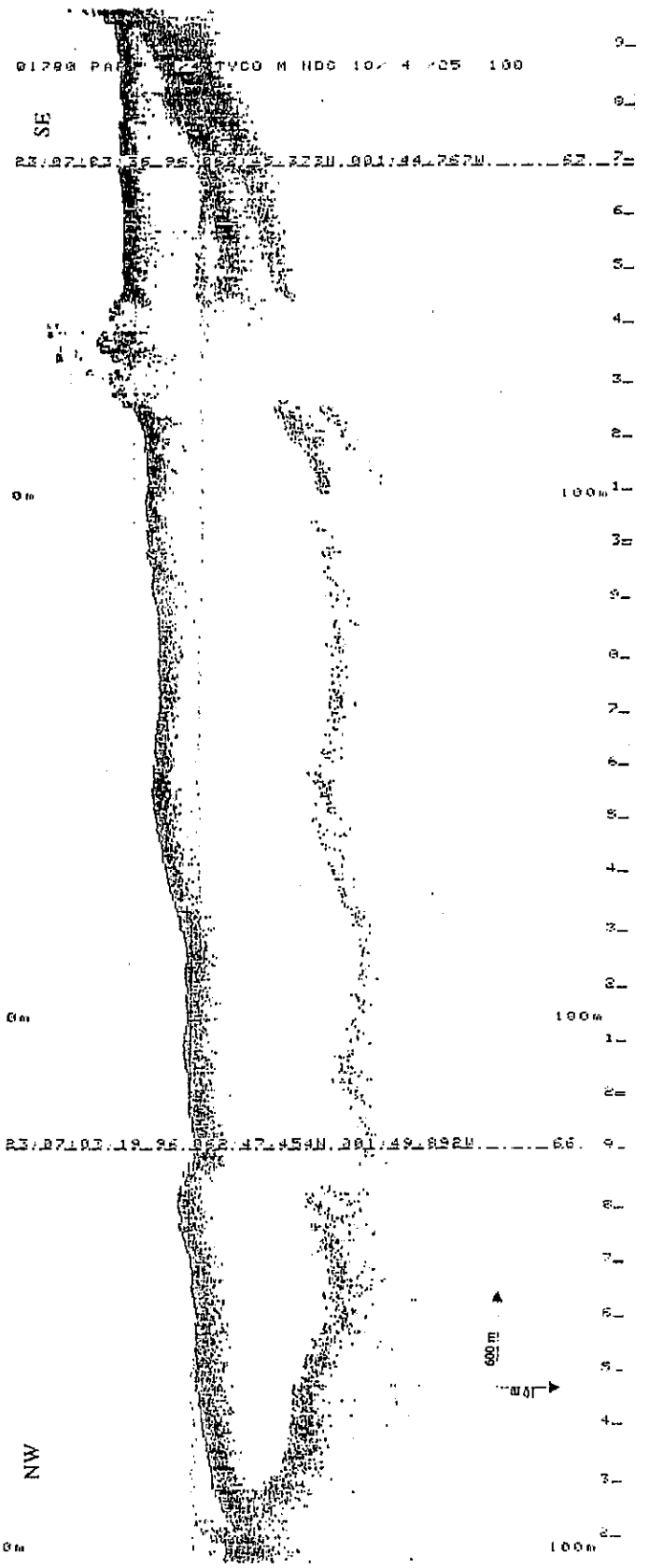

Fig. 45: Debris flow structure with a thickness of 30 m and a length of over 9000 m, parasound profile 200 in Faeroe-Shetland Channel.

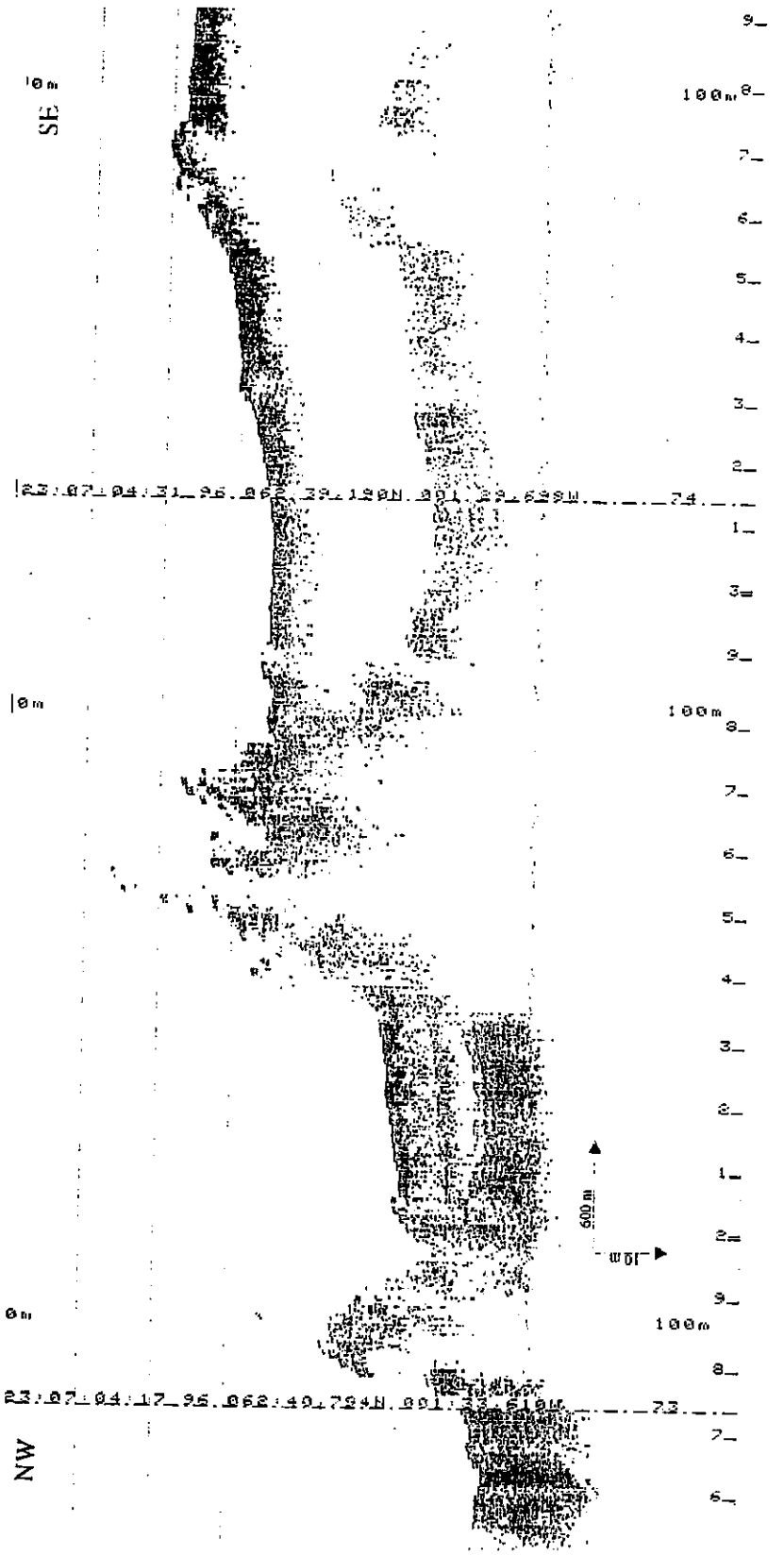

Fig. 46: The seismic reflector and the sea bed probably broken by escaping of fluids, parasound profile 200 in Faeroe-Shetland Channel. Note the upward turning of reflectors at the sea bed.

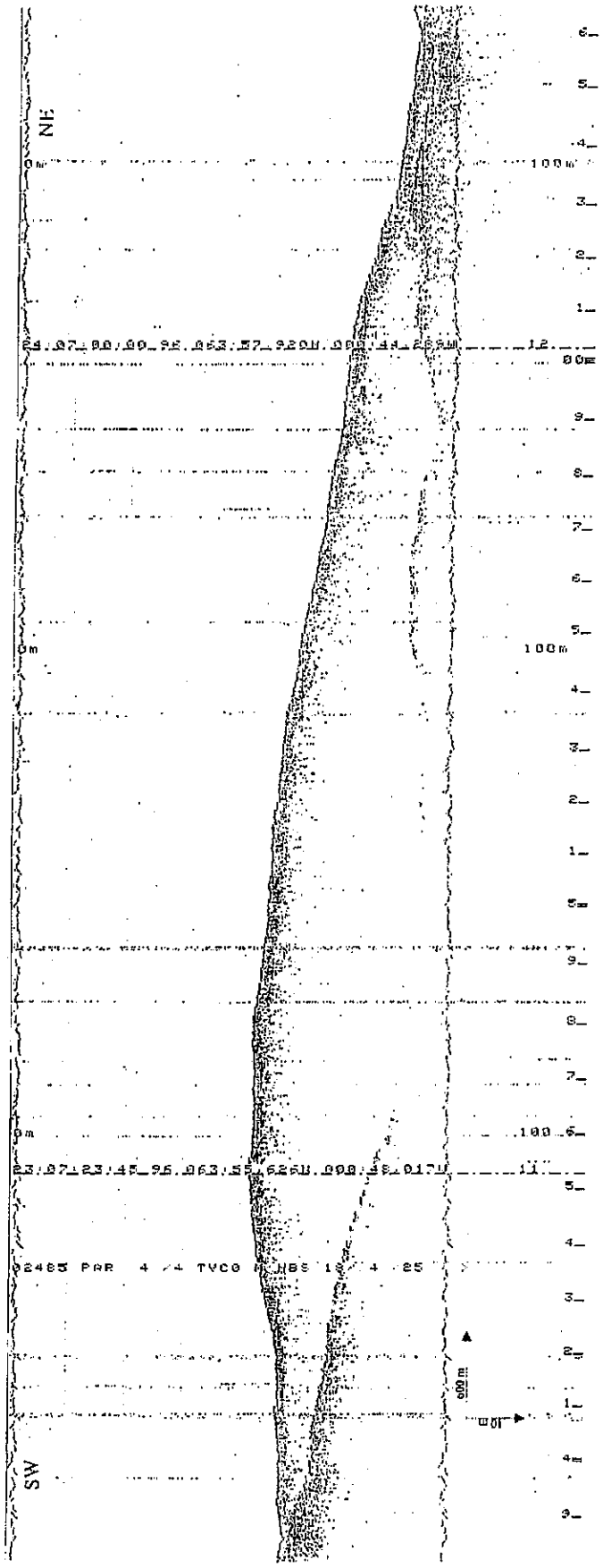

Fig. 47: Debris flows recorded on the North Sea fan parasound profile.

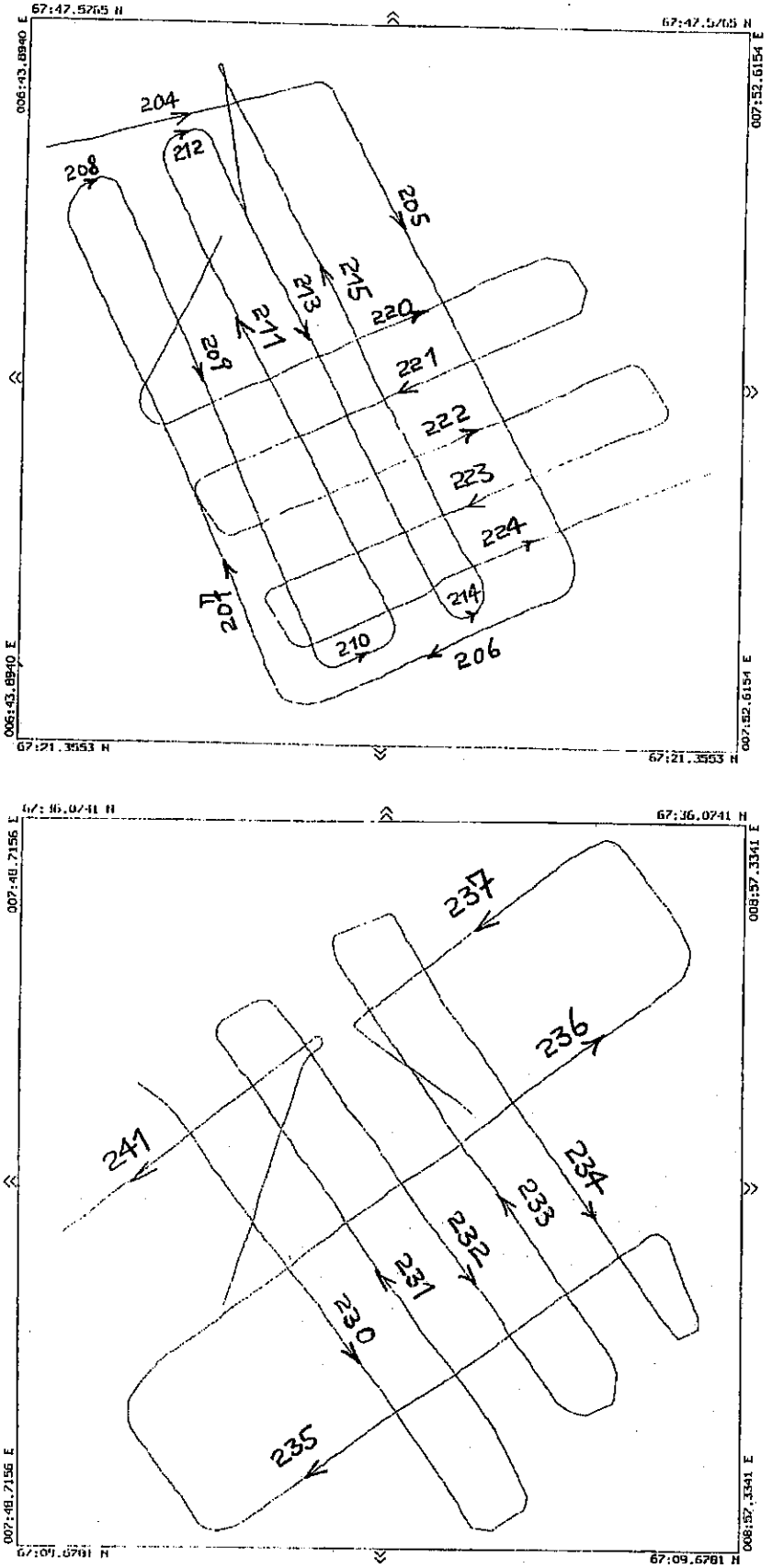

Fig. 48a, b: Location map of the parasound grid profiles in the northern Voering Plateau.

a) Grid 1, northwest of the Traendjupet slide area

b) Grid 2, the Traendjupet slide area

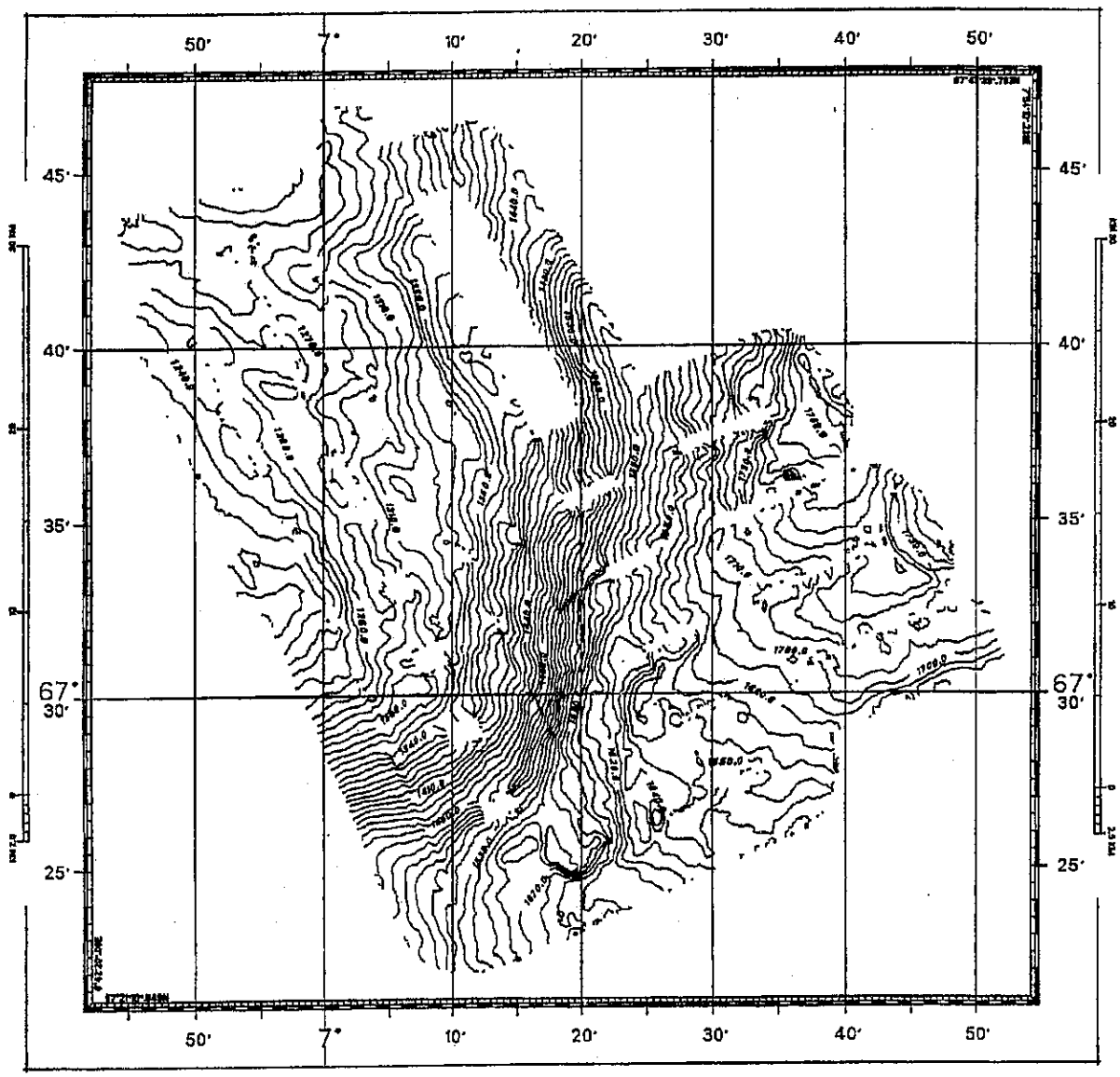

Fig. 49: Hydrosweep bathymetric data of the parasound grid 1 region, northwest of the Traendjupet slide area in the northern Voering Plateau.

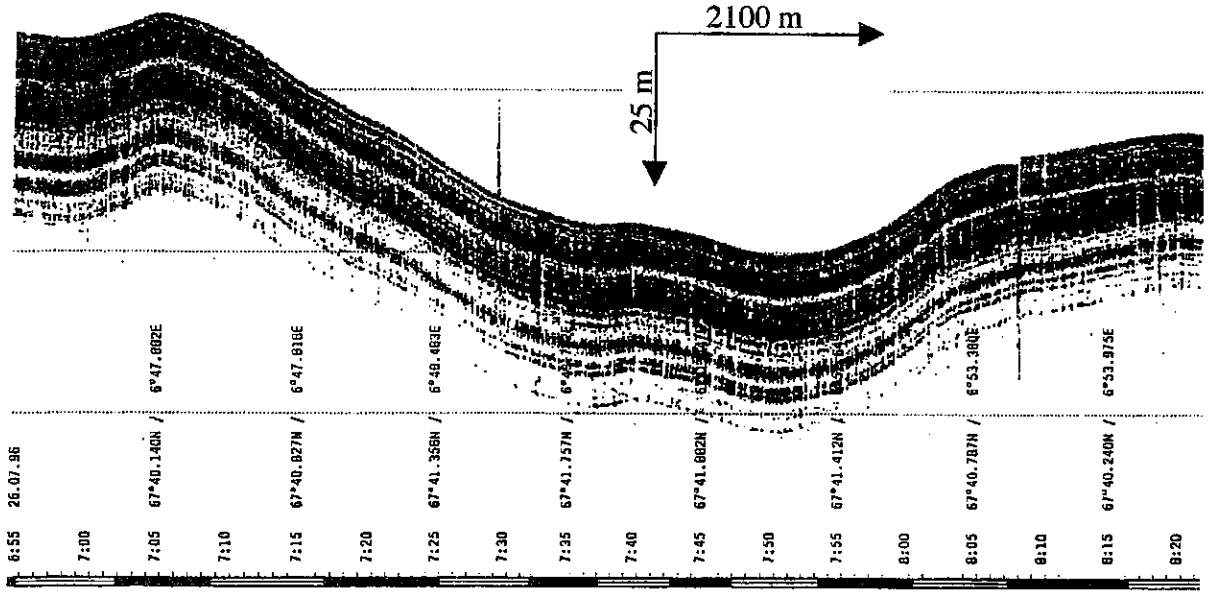

Fig. 50a: Stratified sequences with high penetration, recorded in the northwest of parasound grid 1 northwest of the Traendjupet slide on the northern Voering Plateau.

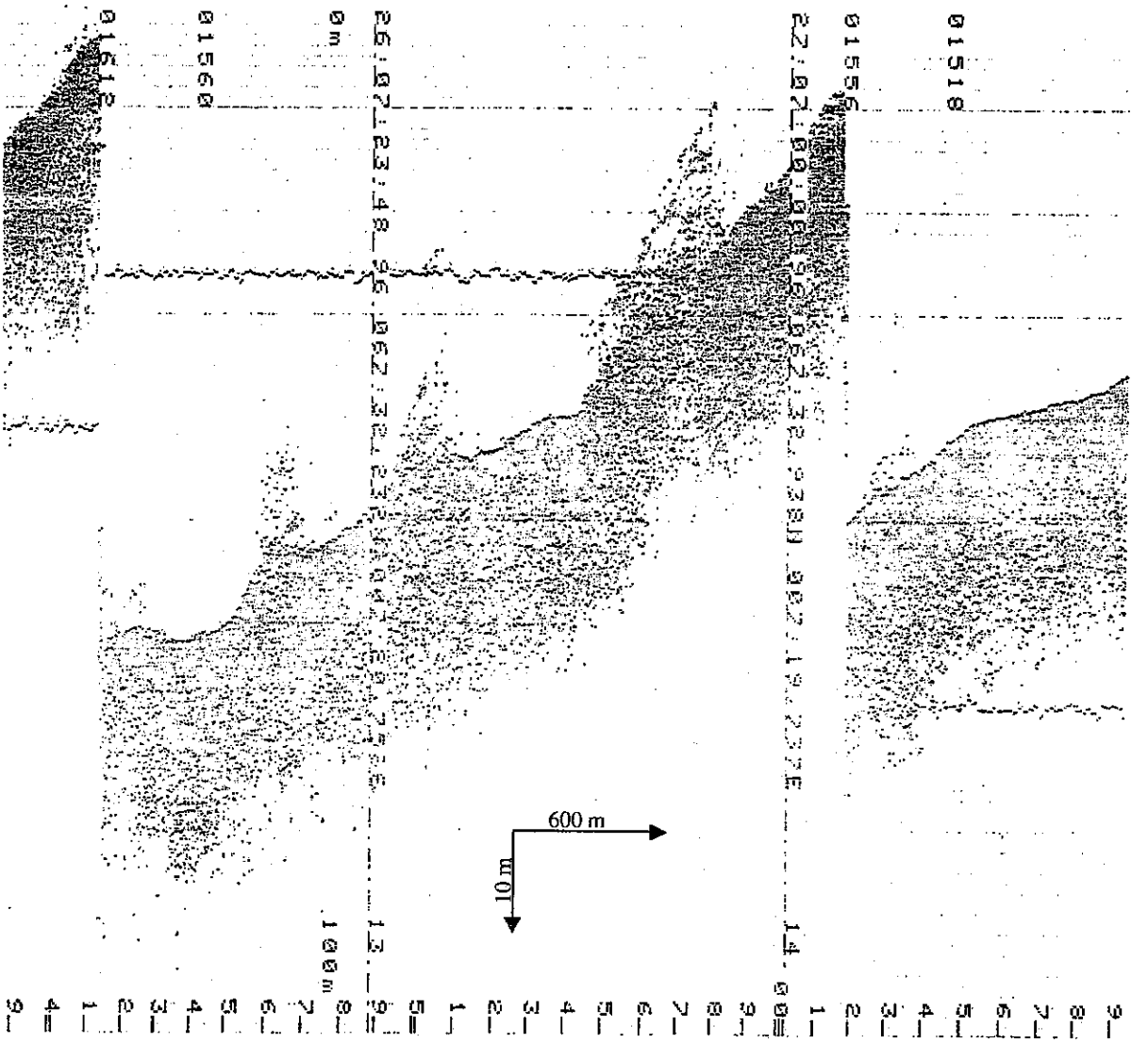

Fig. 50b: Rough sea bed microtopography with possible gas venting structures in the southeast area of the parasound grid 1 northwest of the Traendjupet slide.

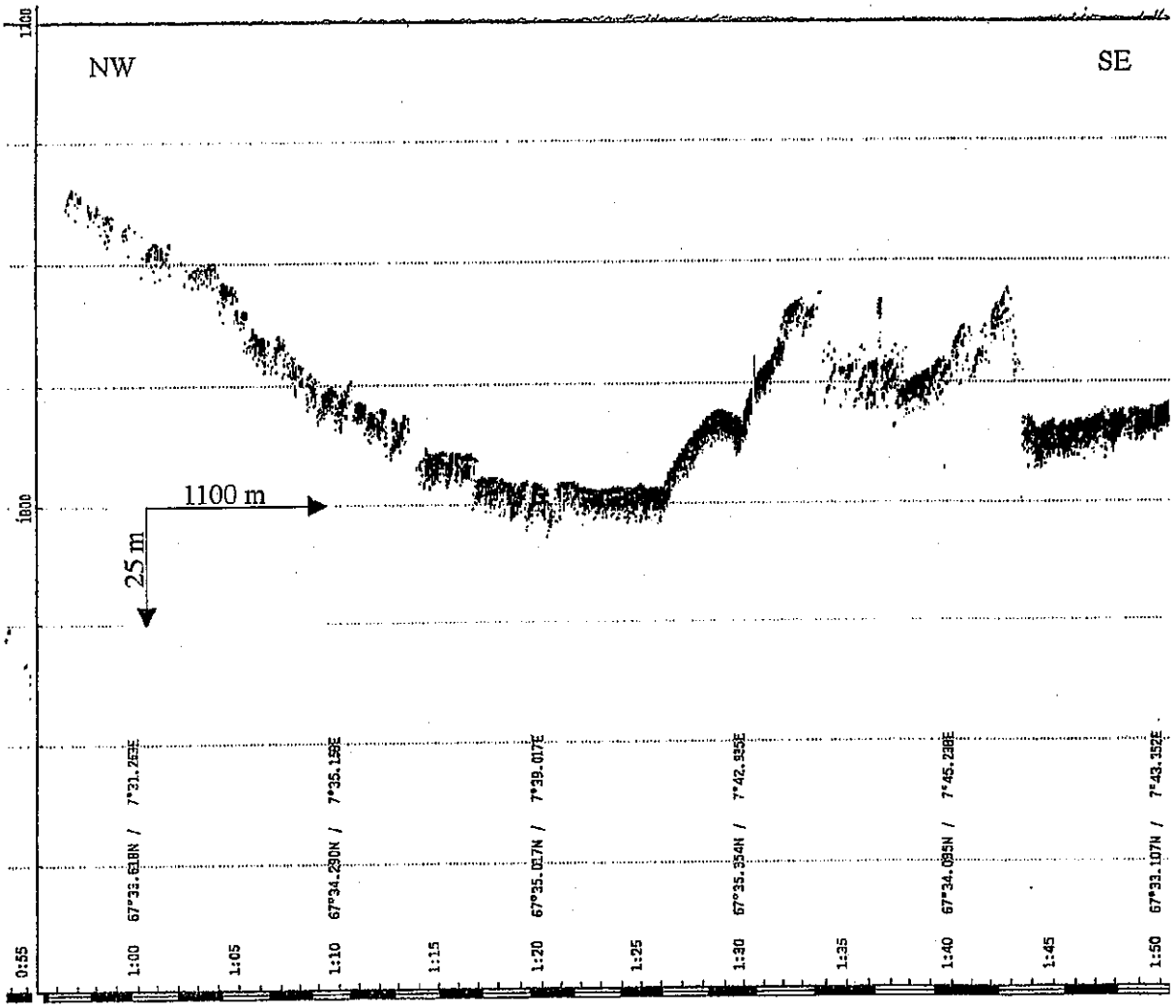

Fig. 51: Slide mass observed by parasound profiling between profiles 222 and 223.

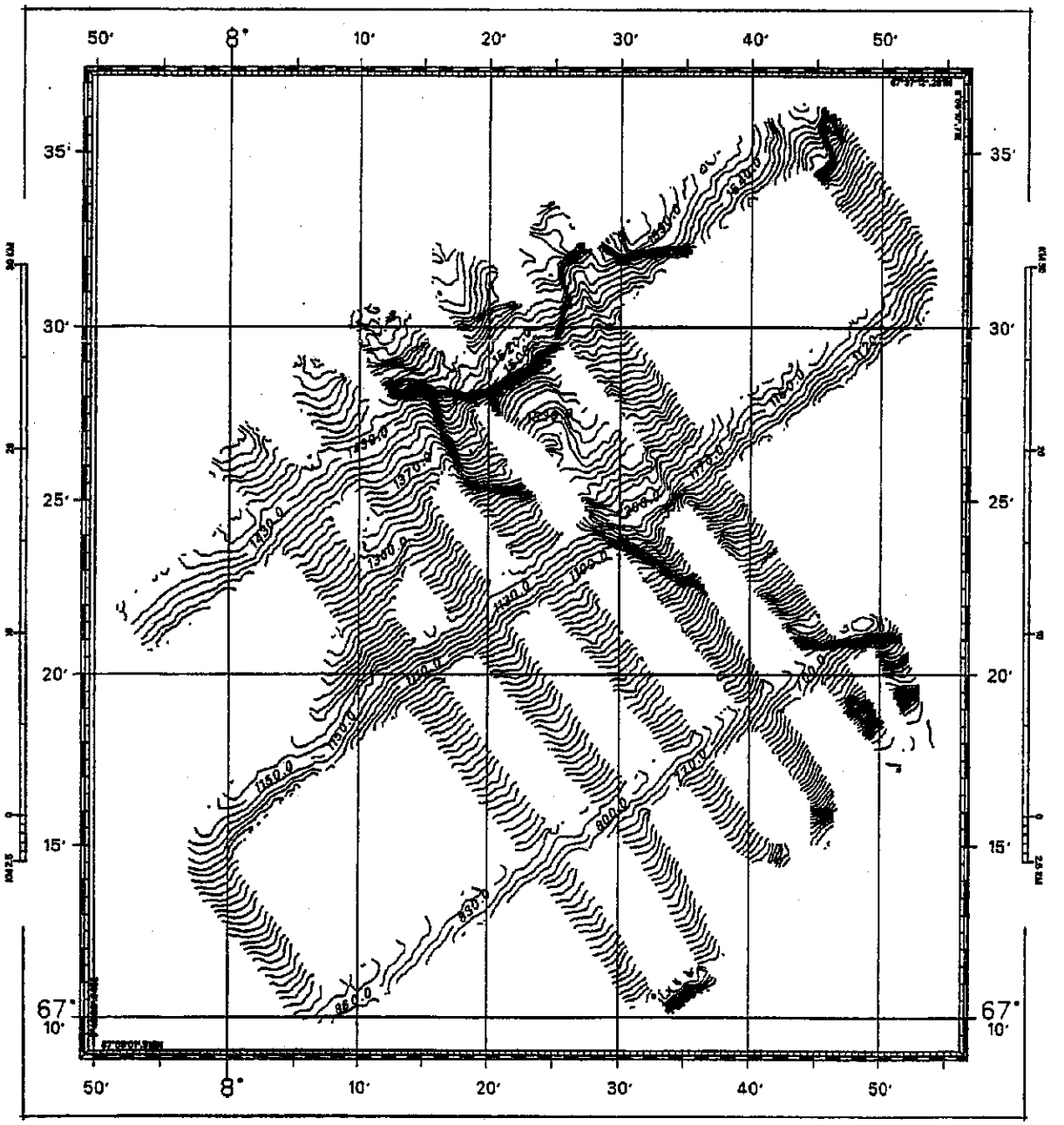

Fig. 52: Hydrosweep bathymetric data for the parasound grid 2 region in the Traendjupet slide area.

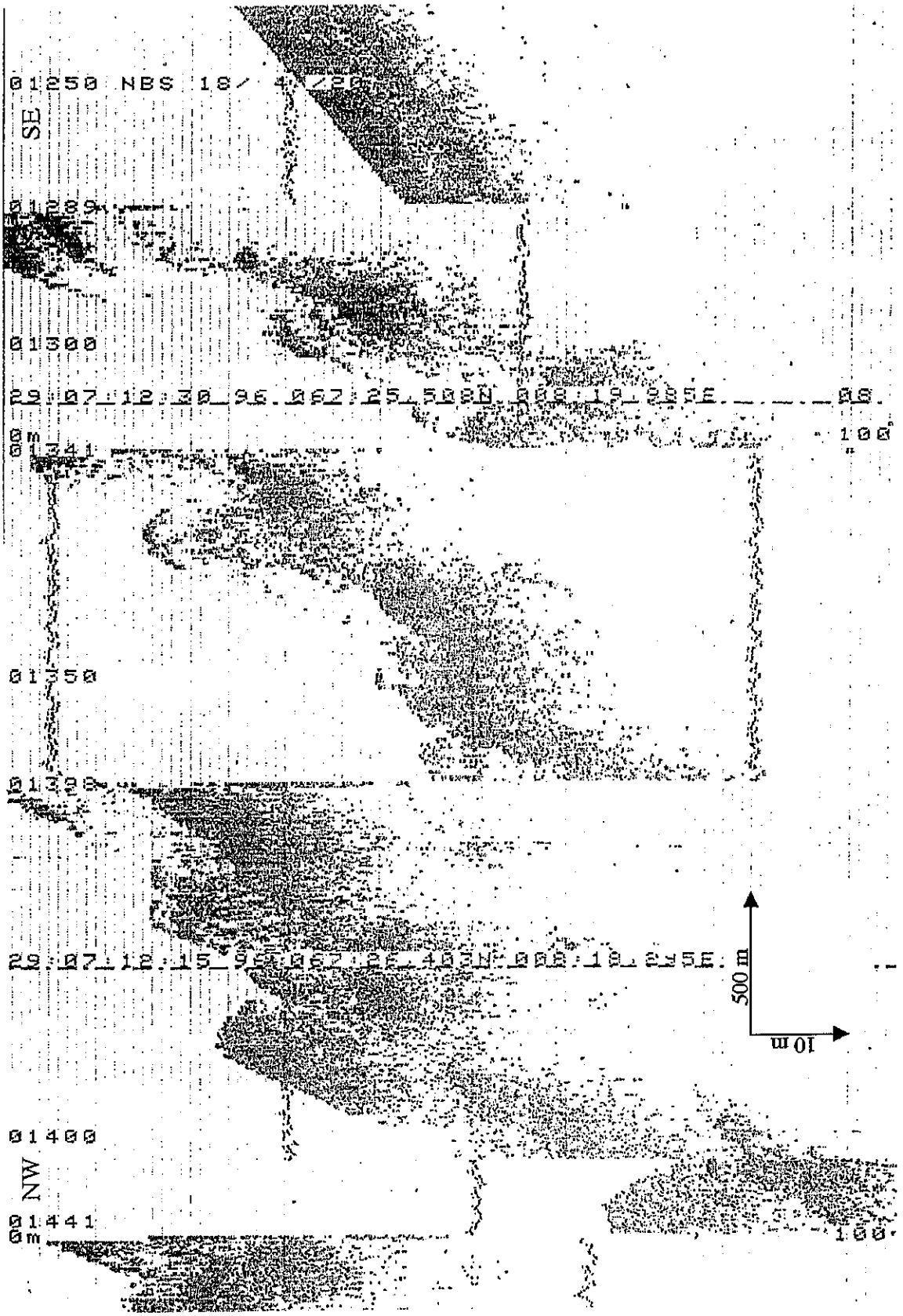

Fig. 53: Massive deposits with varied sea bed relief recorded in the Traendjupet slide area (profile 232).

southwest of this zone, the sea bed is smooth (Fig. 53, far right) and debris flows of different sizes were recorded (Fig. 54).

- Hydrosweep data (Fig. 53) show an additional narrow zone of abrupt changes of water depth in the north of the studied area. This zone may represent the boundary between two slide masses. This boundary is, however, not clear on the parasound records.

The parasound records of profile 242, situated northwest of the two parasound grids, show high penetration of up to 50 m and stratified sequences (up to 20 seismic reflectors).

Three sediment core stations (238, 239 and 240) (Figs. 55-57) were selected in the Traendjupet slide area: one in the region of massive deposits with varied sea bed relief (67°25.1 N/8°32.6 E), and two in the region of smooth sea bed (67°21.2 N/8°18.5 E and 67°17.9 N/8°07.3 E). Studies of these sediment cores may provide detailed information about Traendjupet slide processes.

5.3.3.3 Greenland Basin and Denmark Strait

In 1992, GLORIA, the IOS (now Southampton Oceanographic Centre) long-range side scan sonar, was used on a cruise of the RV LIVONIA to map large-scale changes in sedimentary processes along the East Greenland continental margin. The research area encompassed, from north to south, the Boreas Basin, the Greenland Basin, and a small basin north of Jan Mayen. One of the aims of M 36/3 was to collect detailed information about the surface and subsurface geology of the Greenland Basin. Therefore, parasound and hydrosweep profiles were run. This section presents the preliminary results of the parasound and hydrosweep data, which are of good quality. The preliminary results are based on the analogue data. Details will become available after the post-processing of the digital data (profiles 248, 251).

Most of the profiles show a seismic sequence of regularly stratified reflectors. The penetration into the sequence reached up to 50 m and showed up to 20 bright reflectors. The reflectors tend to occur in bundles, separated by weekly reflective or acoustic transparent zones. A characteristic feature that varies from this pattern are submarine channels believed to be caused by turbidity currents. Channels were observed on the profile 251 and on the transit between station 249 and 250. Most of the channels are V-shaped; their depth varies between 3 and 5 m, their width between 350 and 980 m (Fig. 58). Two channels on the upper continental slope of East Greenland are U-shaped; their depth lies between 22 and 45 m and the width between 1.9 and 3.3 km (Fig. 59). Some of the 8 recorded channels have levees and a characteristic steep slope at the outer bend and more gradual slope at the inner bend. The reason for the levees is the overflow of turbidity currents. All these channels flow northwards from the East Greenland continental margin to the deepest part in the Greenland Basin. At the end of the major channels a depositional lobe has developed. The 6 small channels which are V-shaped occur in the area of the depositional lobe.

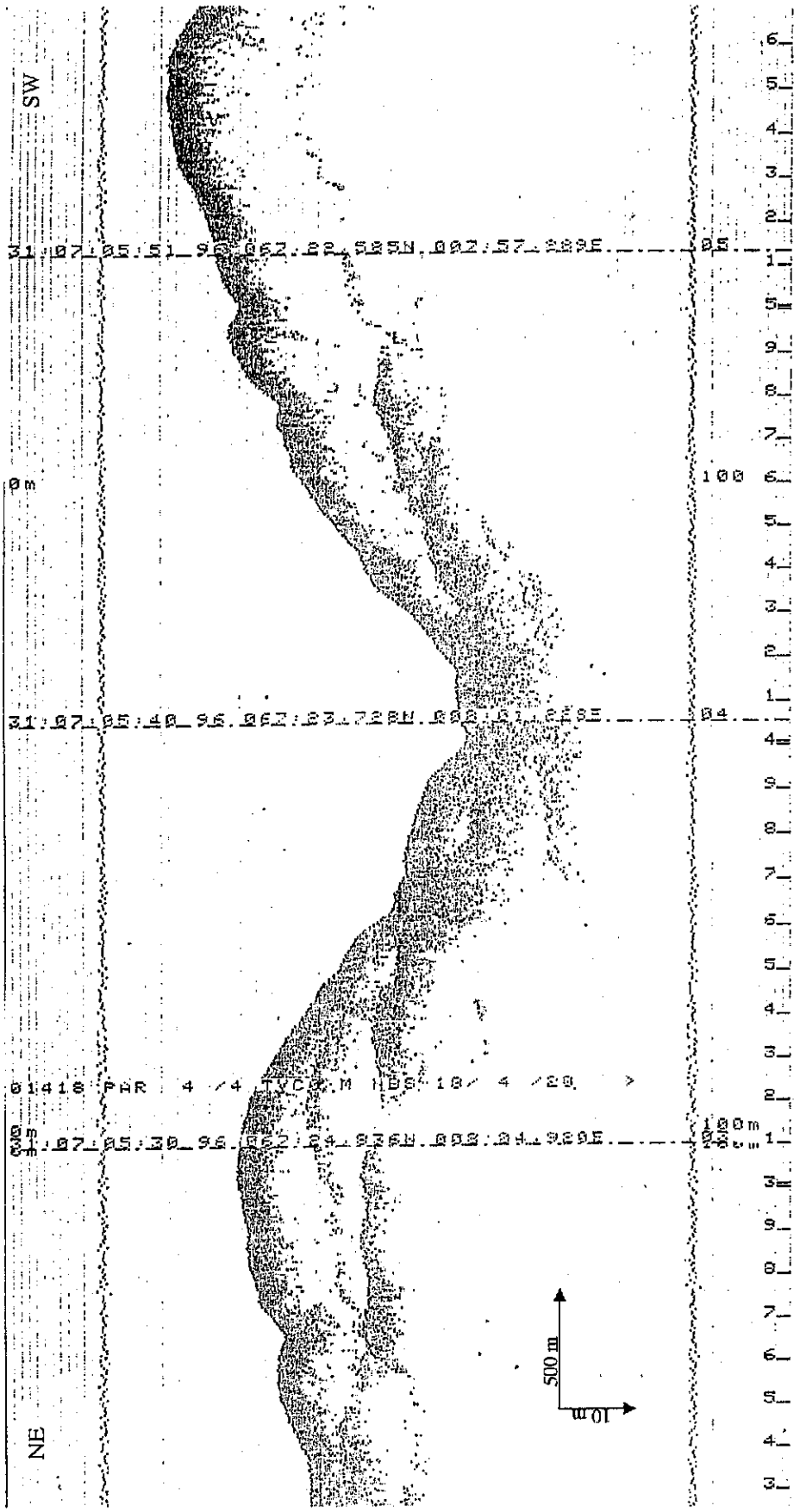

Fig. 54: Debris flows of different sizes recorded in the Traendjupet slide.

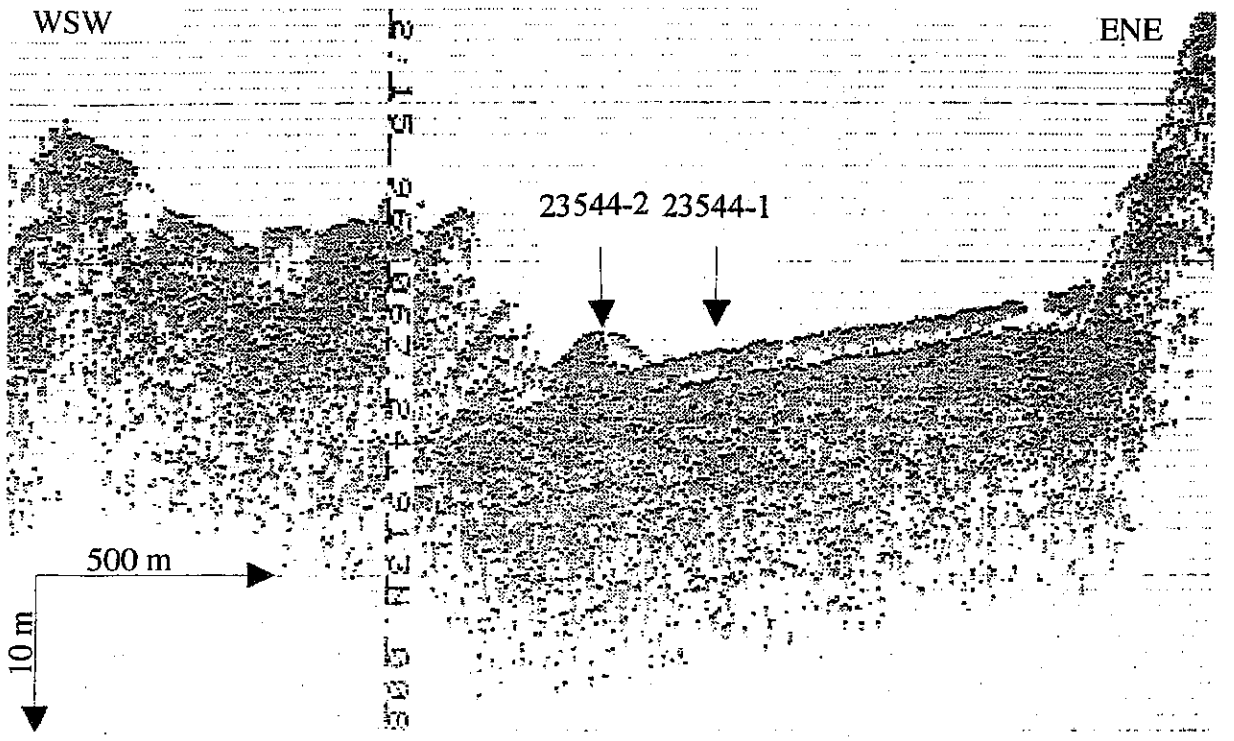

Fig. 55: Parasound profile at Traendjupet slide showing the core stations 23544-1 and 23544-2.

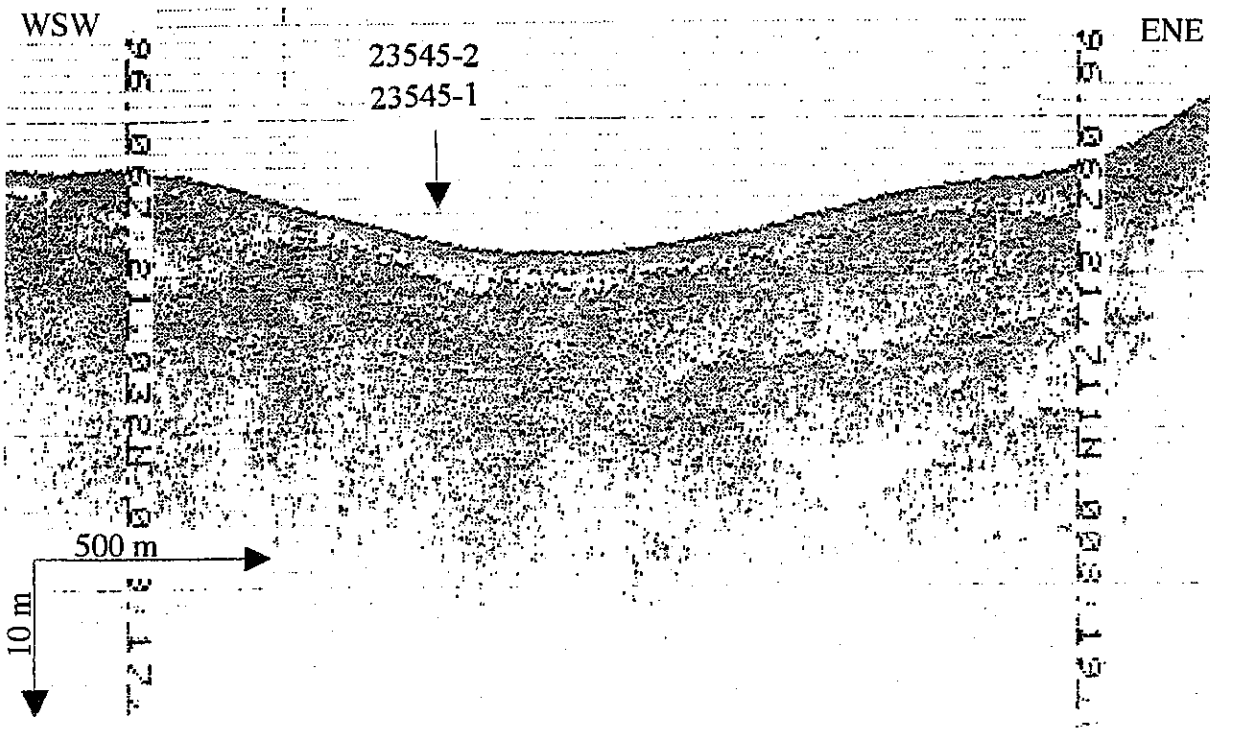

Fig. 56: Parasound profile at Traendjupet slide showing the core stations 23545-1 and 23545-2.

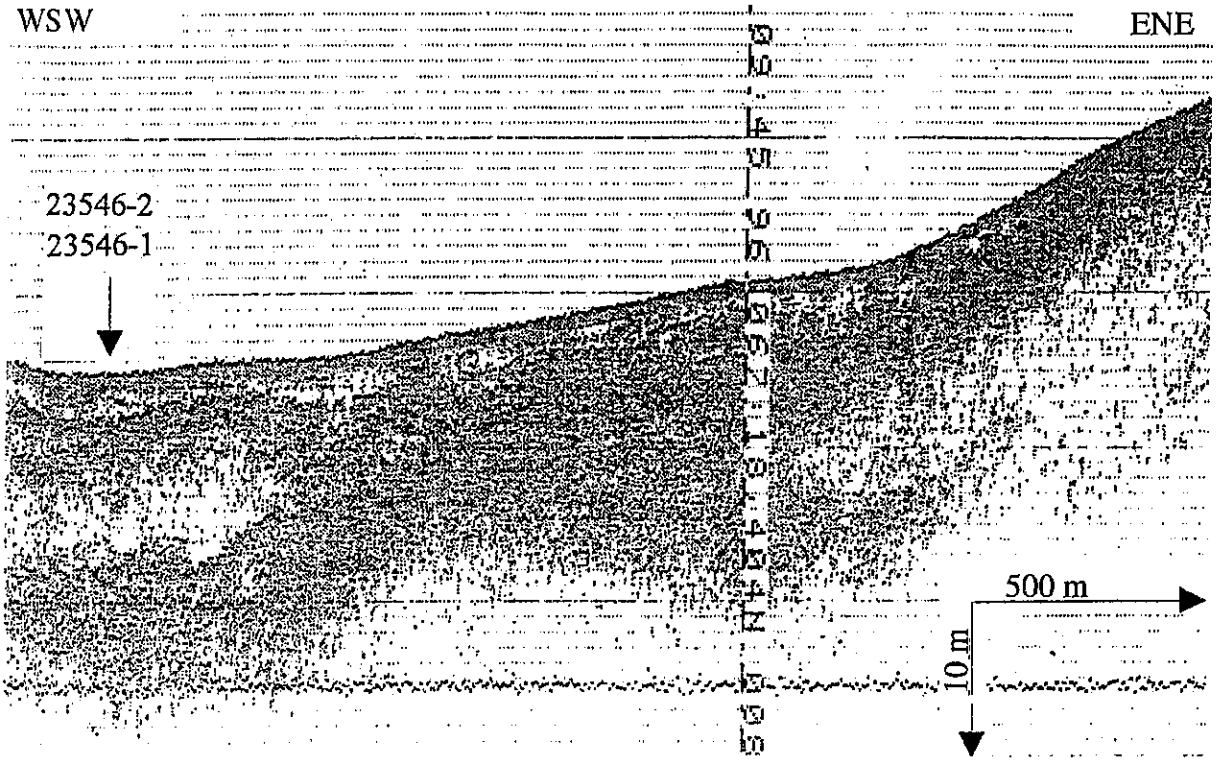

Fig. 57: Parasound profile at Traendjupet slide showing the core stations 23546-1 and 23546-2.

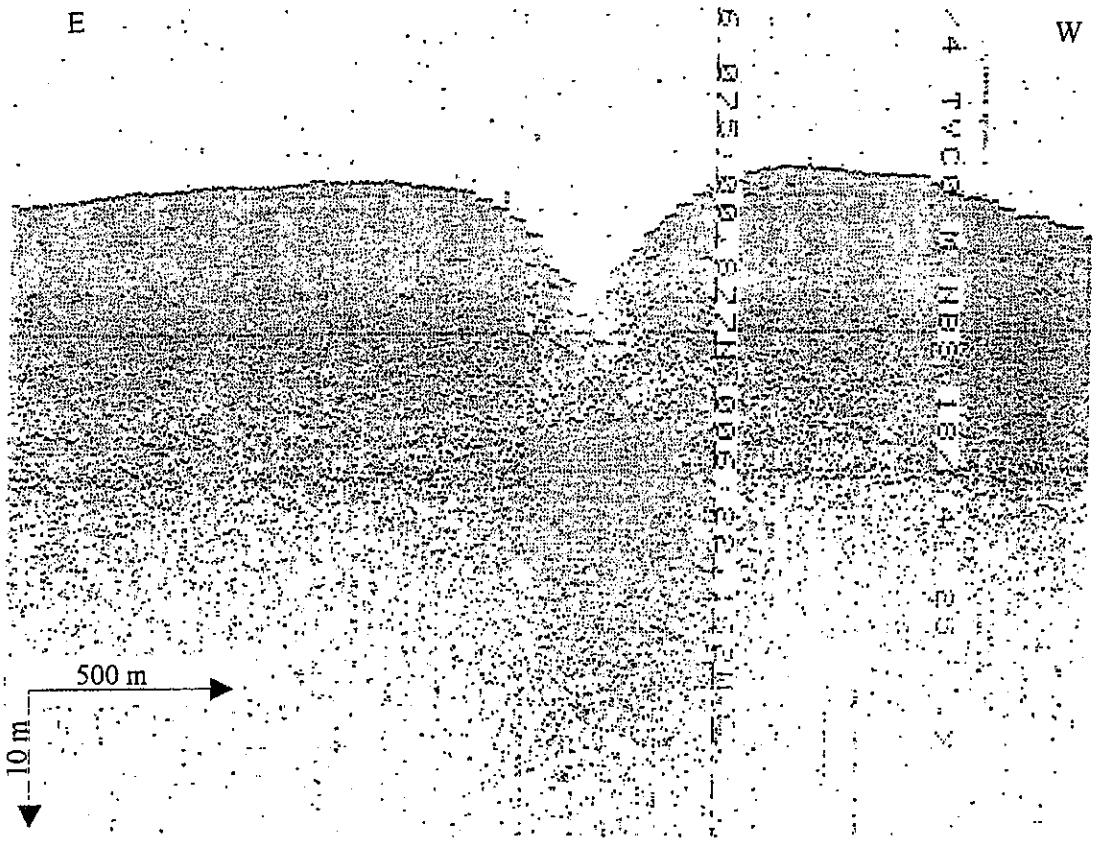

Fig. 58: Submarine channel V-shaped, profile 251, water depth: 3525 m. Location: 75°00 N/6°22 W.

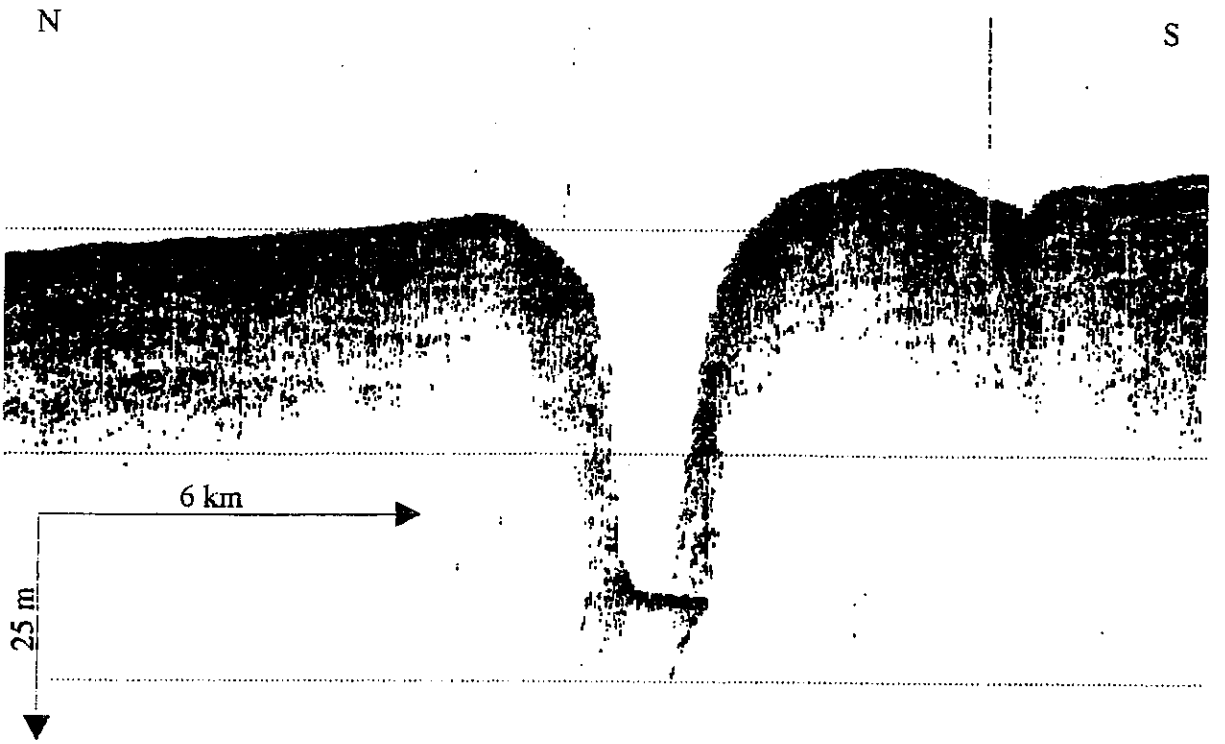

Fig. 59: Submarine channel U-shaped, profile 251, water depth: 3477 m. Location: 74°50 N/7°13 W.

Profile 253 has a SE-NW orientation across part of the Denmark Strait. The Denmark Strait is one of the most important oceanographic gateways for the Arctic Intermediate Water and the North Atlantic Deep Water Flow. The middle part of the profile has a very rough topography. Penetration reached up to 70 m on the eastern side of the strait. The seismic sequence shows up to 25 regularly stratified reflectors. On the west side the penetration was much less, up to 10 m. The deepest part of the profile was at 68°55.42 N and 20°17.797 W with a depth of 1560 m (Fig. 60). Along the East Greenland continental margin, southward-flowing currents such as the East Greenland Current (EGC) are carrying water masses through the Denmark Strait into the North Atlantic. These currents may cause vigorous along-slope transport of sediments across the shelf and the slope as indicated by the parasound profile.

5.3.4 **High-Resolution Deep-Tow Boomer Profiling in the Region of the Traendjupet Slide off Mid-Norway** (D. Evans, D.G. Wallis, N.C. Campbell)

As part of ENAM II (European North Atlantic Margin II: quantification and modelling of large-scale sedimentary processes), D. Evans, D.G. Wallis and N.C. Campbell of the Marine Geology and Operations Group of the British Geological Survey (BGS) participated in M 36/3. The objectives were:

- To collect very high-resolution profiles in the region of the Traendjupet slide off Mid-Norway (Fig. 61) using the BGS deep-tow boomer (DTB), in order to better understand the history of sedimentation and instability. This work would be complementary to

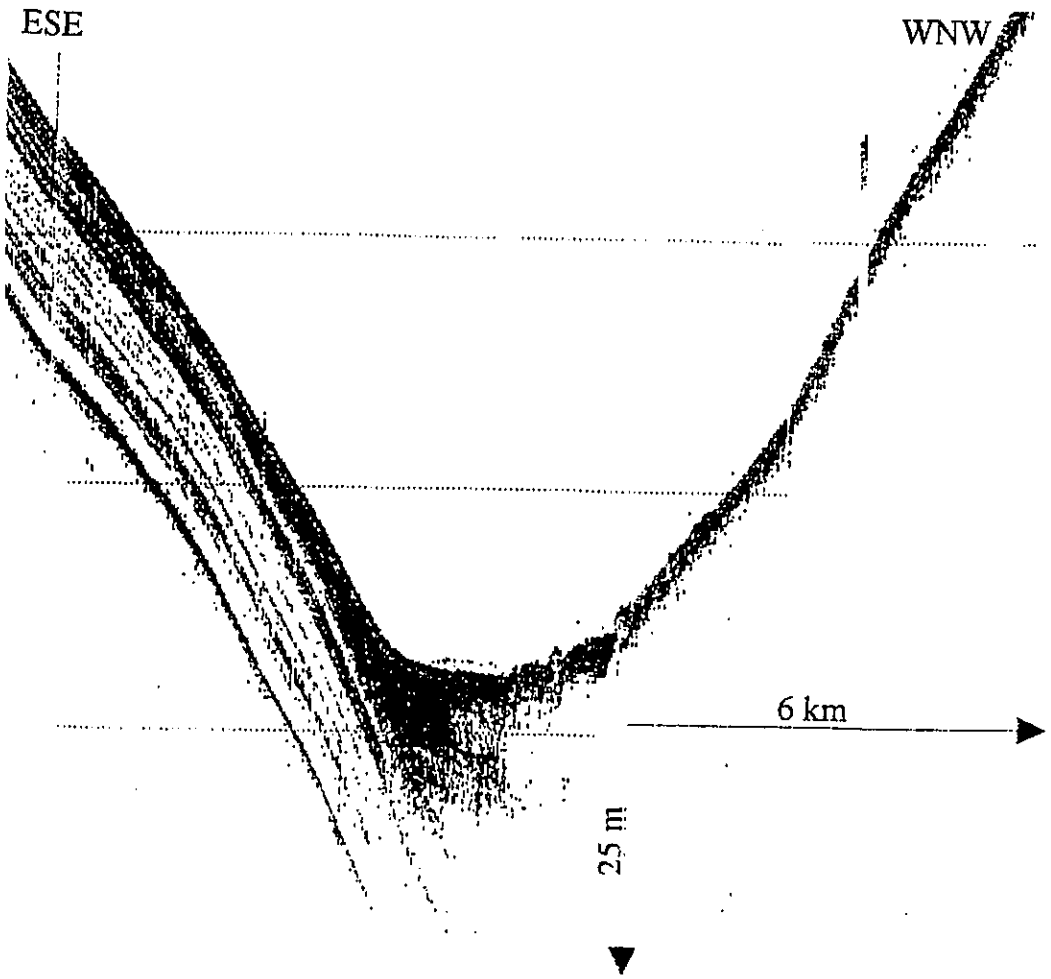

Fig. 60: Deepest part of the Denmark Strait, profile 253, water depth: 1560 m. Location: 68°55 N/20°17 W.

parasound profiling, hydrosweep swath bathymetry and coring carried out by other scientists.

- To use the boomer as a sound source for HF-OBH (Ocean Bottom Hydrophone) experiments being conducted by the GEOMAR group as part of their investigation of gas hydrates.

5.3.4.1 Geological Background

The Traendjupet slide was first identified by BUGGE (1983) and KENYON (1987) as one of the largest slides on the Norwegian margin north of the Voering Plateau. It lies immediately north of a north-west trending cross-shelf trough from which it derives its name, and has its headwall at a water depth of about 400 m (Fig. 61). Beneath the slide, and also on its south-western flank, lies an area of uneven sea bed interpreted by DAMUTH (1978) as the product of mass-flow processes.

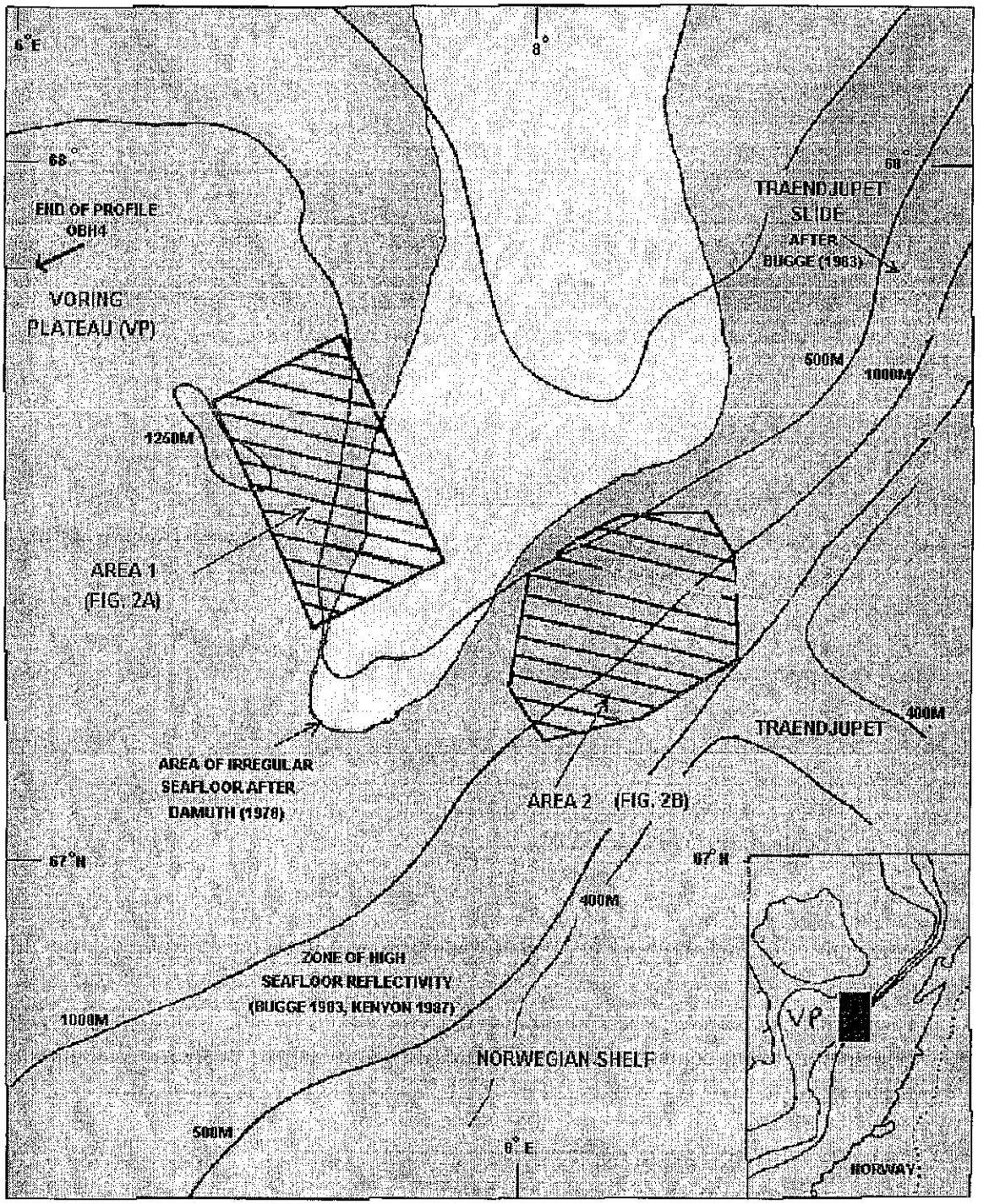

Fig. 61: Sketch map showing the location of the survey area, together with some existing information.

5.3.4.2 Operations

Surveys were carried out in two main areas between latitudes 67 and 68°N, and longitudes 7 and 9°E (Fig. 61):

Area 1: The eastern Voering Plateau (Fig. 62a) in relatively deep water (1250 m and greater) on the projected flank of the Traendjupet slide, an area that includes part of the mass-flow deposits identified by DAMUTH (1978). Three OBH experiments were also carried out in this area.

Area 2: The Norwegian slope (Fig. 62b) along the southeastern flank of the Traendjupet slide, and extending into the slide scar.

In addition, a fourth OBH station was deployed on the Voering Plateau to the northwest of area 1 (Fig. 61).

Together with the deep-tow boomer, parasound profiling and hydrosweep swath bathymetry were carried out simultaneously. In both survey areas some lines were run with parasound and Hydrosweep alone, and another such line joined the two areas; these lines are not shown on Fig. 62a, b.

5.3.4.3 The Deep-Tow Boomer (DTB) System

The BGS deep-tow boomer system has been developed extensively from the Huntec deep-tow boomer, primarily in order to extend its depth capability. The tow fish is rated to a water depth of 1000 m, but with the current cable length, the maximum tow depth achieved is approximately 750 m, giving a maximum operational water depth of about 1500 m.

The system comprises a winch (with 2.1 km long tow cable, slip ring assembly and remote laboratory control), electro-hydraulic power pack, tow fish, towing-sheave assembly, high voltage power supply, boomer onboard electronics including depth compensation, analogue processor/control electronics and output to a Waverley 3710 thermal printer. The tow fish contains the boomer plate, energy storage unit and attitude sensing unit including pre-amplifiers for two seismic channels. Two short (2 m), multi-element hydrophones are towed immediately behind the fish and in normal operation either is selected, the other acting as backup. Pressure compensation for the plate is provided by two large air bags located in the fish side-skins. An electronic system is provided to monitor the winch, which under normal operating conditions is controlled from the laboratory.

The data are also recorded digitally using the BGS, DAMP16, PC-based acquisition system recording to Exabyte tape cartridge in SEGY format.

Throughout this survey, the system was operated with a recorder sweep speed of 320 ms, timing lines at 40 ms and filter passband of 700-2000 Hz. Firing rate was normally 1 second

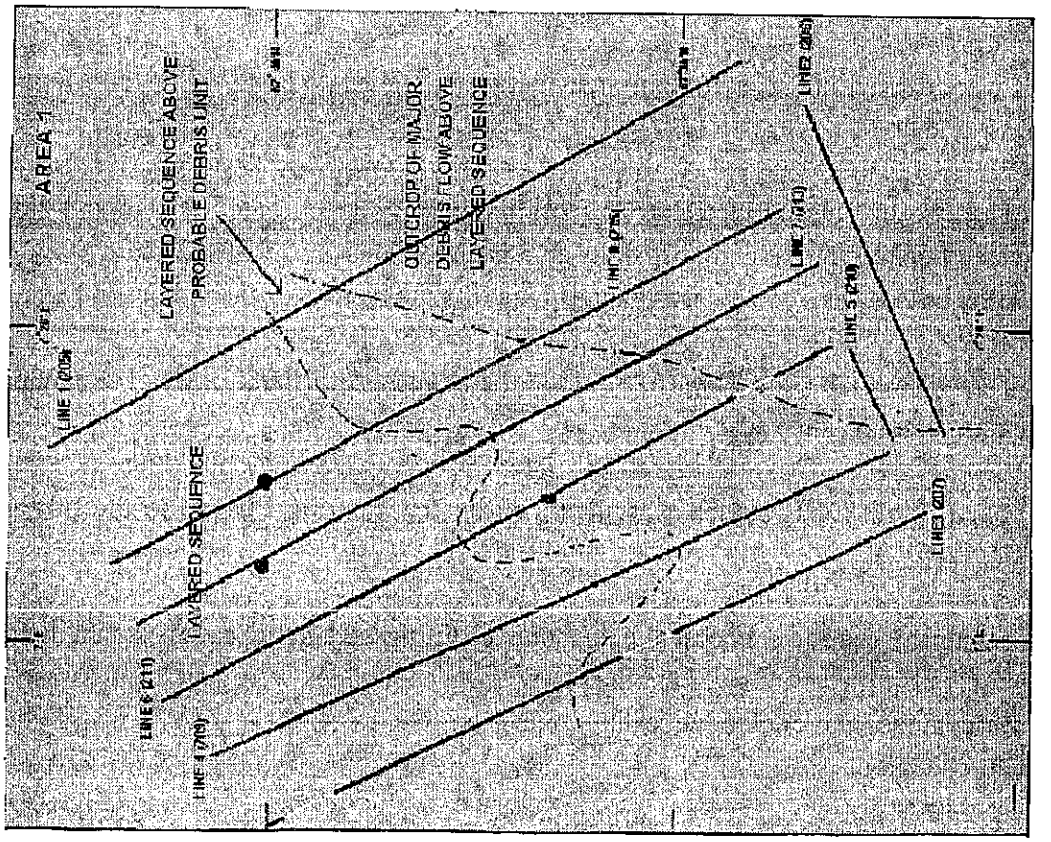

Fig. 62a: Sketch maps with locational information and simplified interpretations for area 1.

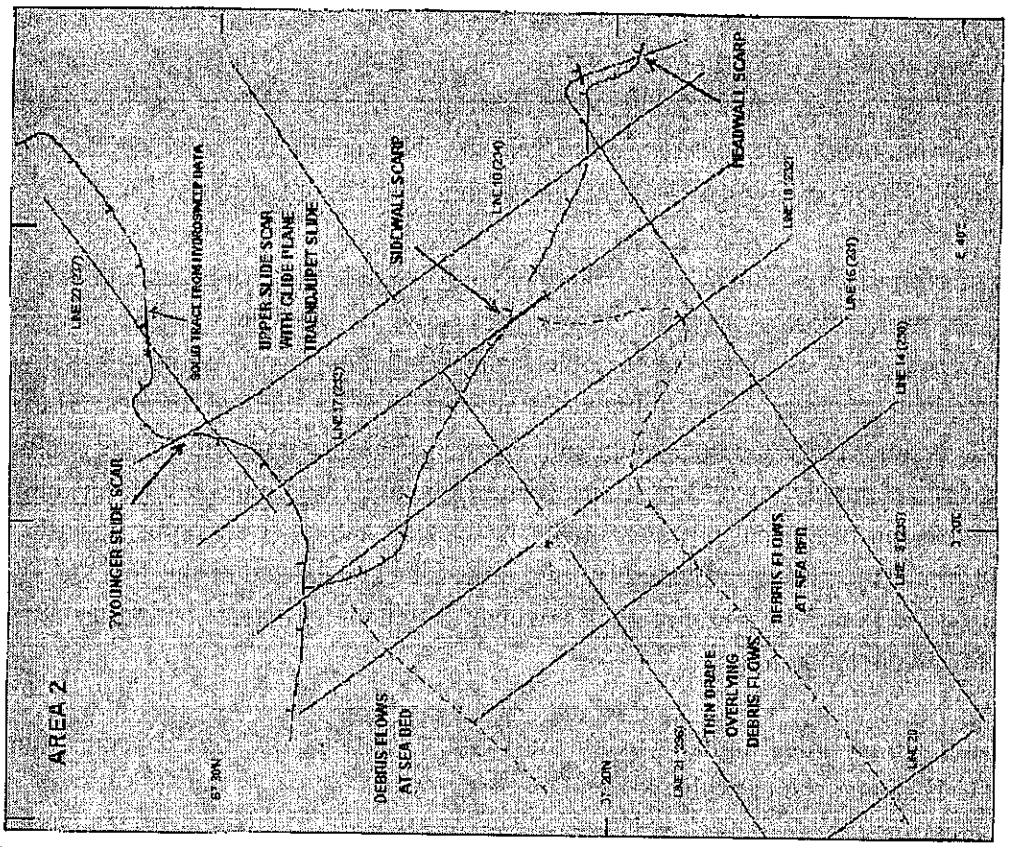

Fig. 62b: Sketch maps with locational information and simplified interpretations for area 2.

except in water depths greater than 850 m when the fish was at maximum tow depth and the firing rate was gradually slowed in increments of 0.1 s as the water depth increased.

5.3.4.4 Mobilisation

The system was mobilised onto METEOR in Bergen on July 19 and 20. The fitting down of the winch and running most of the cabling was completed during the first day. The following day the laboratory equipment installation was completed and the system tested. The hydrophone systems tap tested successfully and the boomer plate was 'popped' successfully on deck at 2 kV. A wet test was felt unnecessary due to the successful operation over the previous two weeks on the Hakon Mosby. The method of deployment was over the BGS block hanging from the stern 'A' frame, similar to previous METEOR cruises M 26/2 and M 26/3. The BGS block was suspended from a centrally located block already in place on the 'A' frame.

5.3.4.5 Deployments

The boomer was first deployed in area 1 at 16:20 UTC on July 25, and BGS Line 1 (METEOR profile 205, see Tab. 7) was started at 17:05. Data quality was very poor from channel 1, and channel 2 failed for reasons unknown (at that point channel 2 was using a spare hydrophone as the one normally used was under repair). The extreme water depth (1600 m) and the irregular nature of the sea bed caused the record to become almost obliterated by 50 Hz mains noise. After some rearranging of the signal earths, some improvement was achieved and survey proceeded satisfactorily.

The boomer was recovered on July 27, at 03:45, at the end of BGS line 8, and the hydrophone on channel 2 replaced with the repaired unit. It was redeployed at 14:00 on the same day and channel 2 now gave excellent results with reduced 50 Hz noise for the first of the OBH experiments (BGS lines 9 and 10). The boomer was recovered at 17:50 on July 27.

A second OBH experiment was conducted on July 28, with the boomer in the water between 09:00 and 20:55 running BGS lines 11 and 12.

The vessel proceeded to area 2 where the boomer was deployed at 01:00 on July 29, when channel 2 failed again for reasons unknown. BGS line 14 was run using channel 1, giving indifferent results. At the end of line 14, the fish was recovered and redeployed following a short repair to the hydrophone on channel 2. BGS lines 15 to 22 were run with channel 2 giving good data, and the boomer was recovered at 18:25 on July 30.

A final OBH experiment was run on July 31; the boomer was deployed at 14:40 and recovered at 17:25. The data were again of good quality.

Tab. 7: Line summary sheet for project 96/04, M 36/3

BGS Line No.	METEOR Profile No.	Start Date/Time	End Day/Time	Kilometres	Equipment	Data Qual
1	205	25/7 1705	25/7 2058	27	DTB	3
2	206	25/7 2140	26/7 0032	22	DTB	3
3	207/208	26/7 0038	26/7 0505	33	DTB	2/3
4	209	26/7 0556	26/7 1043	30	DTB	2/3
5	210	26/7 1055	26/7 1139	4	DTB	2/3
6	211	26/7 1143	26/7 1615	35	DTB	2
7	213	26/7 1659	26/7 2150	33	DTB	2/3
8	215	26/7 2232	27/7 0304	33	DTB	2/3
9	OBH1	27/7 1435	27/7 1525	7	DTB/OBH	2
10	OBH1 rev	27/7	27/7	6	DTB/OBH	2
11	OBH2	28/7	28/7	7	DTB/OBH	2
12	OBH3	28/7	28/7	12	DTB/OBH	1/2
13	OBH3 rev	28/7	28/7	3	DTB /OBH	2/3
14	230	29/7	29/7	32	DTB	2
15	231	29/7	29/7	32	DTB	2
16	232	29/7	29/7	32	DTB	2/3
17	233	29/7	29/7	32	DTB	2/3
18	234	30/7	30/7	33	DTB	2/3
19	235	30/7	30/7	33	DTB	2
20	transit	30/7	30/7	7	DTB	2
21	236	30/7	30/7	44	DTB	2
22	237	30/7	30/7	14	DTB	2/3
23	OBH4	31/7	31/7	7	DTB/OBH	1/2

In general the data were good but some lines suffered from 50 Hz noise. It was found that channel 2 was least susceptible to that noise, and this channel was used whenever possible. Previous experience on the METEOR had demonstrated that the boomer system was particularly vulnerable to 50 Hz interference from the ship, probably due to some idiosyncracy of the layout in use. In general it proved an excellent vessel from which to work, and the deployment/recovery procedure using the 'A' frame was very straight forward. The weather was good throughout the survey, and although line 1 was not of acceptable quality, a total of 484 km of generally good boomer data was acquired.

5.3.4.6 Preliminary Interpretation of Data

Area 1

This area covers the summit and eastern flank of a high on the eastern Voering Plateau (Figs. 61, 62a), and has water depths ranging from 1250 m to over 1700 m in the extreme southeast. Despite the deep water, moderately good data were obtained (except in the deepest water), although penetration was limited to a maximum of 100 m in the shallowest water in the north-west, and was generally between 40 and 60 m. In part this was due to the geology, which comprises three zones (Fig. 62a):

a The northwestern zone shows between 40 and 100 m penetration of a seismically well-layered, blanketing sequence of sediments that is largely sub-horizontal or gently dipping. Fig. 63a shows an example of data in the shallowest water where the penetration was greatest. It is possible that some reflector loss is due to the presence of gas, but no fluid outflow features are evident in this rather featureless sequence. It is not clear what underlies this sequence in this zone.

b The central zone, in deeper water, shows the same layered upper unit underlain by rather poorly imaged but stronger, rather irregular reflectors which are considered to be debris flows (Fig. 63b). The underlying reflectors are not, however, evident in the south at the start of line 3, where possible gas-related features are evident in the layered sequence. In the extreme east on line 1, there are thin, massive units within the layered sequence near the boundary with the major debris flow unit.

c The south eastern zone is characterised by an irregular sea bed with seismically massive deposits at outcrop. The profiles show that this deposit overlies most of the layered sequence and, where most clearly imaged, is apparently equivalent in age to its uppermost 2 to 3 m of the layered sequence (Fig. 63c). The thickness of the unit is unknown as its base is lost as it thickens to some 40 m at its margin; it is hoped that this information will be available after the POSEIDON cruise. The extent of this unit is also apparent from the hydrosweep data, which reveals the irregularity of the sea bed, particularly prior to processing.

The mapped margin compares moderately closely to the edge of the mass-flow deposits as mapped by DAMUTH (1978), and is considered to be an improved definition of the extent of this sediment package. The parasound line joining the two survey areas crosses this mass-flow unit and has been used to define its southeastern margin, which lies to the northwest of area 2 (Fig. 61).

From the distribution of the mass-flow deposit as mapped by DAMUTH (1978), it seems likely that this unit, which extends into the ocean basin (Fig. 61), was largely derived from the Traendjupet slide. However, the portion surveyed in area 1 lies outside the likely path of such a flow, and it appears that the portion surveyed derives from the zone of high sea bed reflectivity identified by BUGGE (1983) on the Norwegian upper slope to the southwest of Traendjupet. It is not known whether the deposit is the product of one or more mass-flow events, but given the

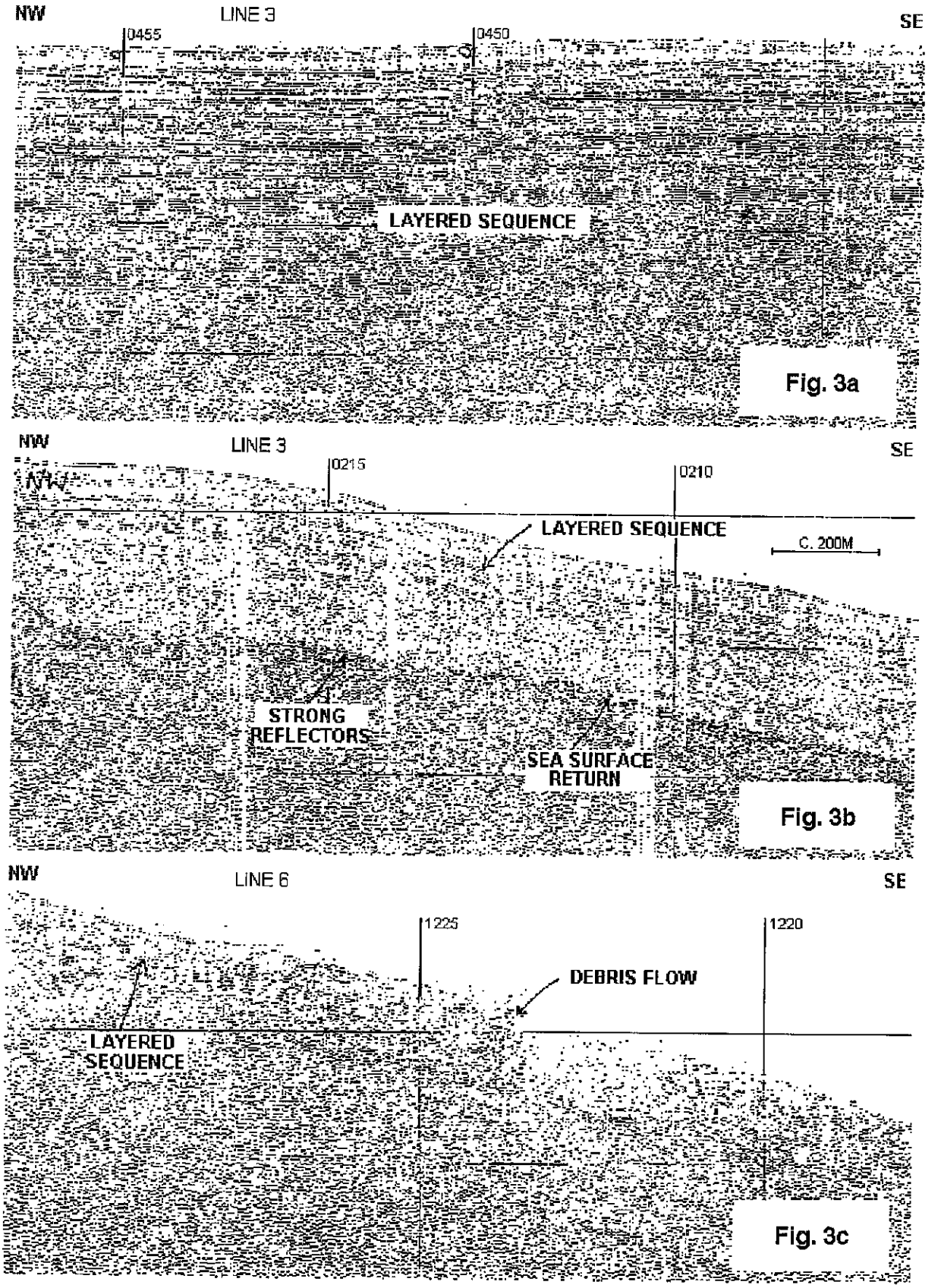

Fig. 63: Examples of deep-tow boomer profiles from area 1.

relationship of the deposits to the layered sequence, it is apparent that the deposits are relatively young. It may be speculated that they are late Weichselian or younger in age, but their age should become constrained by studies of cores taken from the layered sequence during this cruise.

Area 2

This area lies on the upper and mid-slope region of the Norwegian slope (Fig. 62a) and covers the area both within and on the southwestern flank of the Traendjupet slide, in water depths ranging from 300 to over 1600 m. The geology is described in three zones: outside the slide scar, the scarp zone, and within the slide scar.

- Outside the slide scar:
  The data show that the near-surface slope sediments are largely made up of a series of overlapping debris flow lobes which form a gently undulating sea bed. Figs. 64a, b show alongslope and downslope profiles through such lobes. The lobes have a massive internal structure and are commonly up to 10-30 m in thickness, although some appear to be about 40 m thick. Acoustic penetration in this zone is, however, limited to around 60 m at the most, and is negligible on the uppermost slope where there is ringing at the sea bed. It is possible that some gas-related reflectors are imaged on the upper part of line 15.

  Much of the mid-slope is covered by a thin drape of partly-layered sediment that is generally 2-4 m thick with pockets up to 7 m. It is surmised that this is a hemipelagic layer that post-dates glacially-influenced sedimentation in the area, and is thus comparable to the similarly developed MacAuley sequence on the Scottish margin (STOKER et al., 1993). As late Weichselian ice reached the shelfbreak farther south on the North Sea Fan (KING et al, 1996; SEJRUP et al, in press), it is thought likely that this drape was deposited during latest Weichselian and Holocene times. Cores have been taken through the unit to test this interpretation.

- The scarp zone
  The scarp defining the margin of the Traendjupet slide is clear on DTB profiles (eg Fig. 65a), and is particularly well traced on the hydrosweep data, although gaps in the coverage preclude a complete picture (Fig. 66). The nature of the scarp at the south-eastern corner of the survey coverage remains uncertain. At the top of the slope the headwall scarp has a height of some 90 m, but the sidewall height is in the range of 60-80 m. The debris flow lobes of the 'autochthonous' slope appear to be abruptly truncated by the slide, but it is difficult to establish the relationship with the post-glacial drape, which is only 2 m thick at the only recorded location where it is present at the scarp.

c Within the slide scar
  As indicated by the hydrosweep data and illustrated by the many hyperbolic reflectors on the boomer profiles, the sea floor within the scarp is very irregular (Figs. 64c, 65a, 66a).

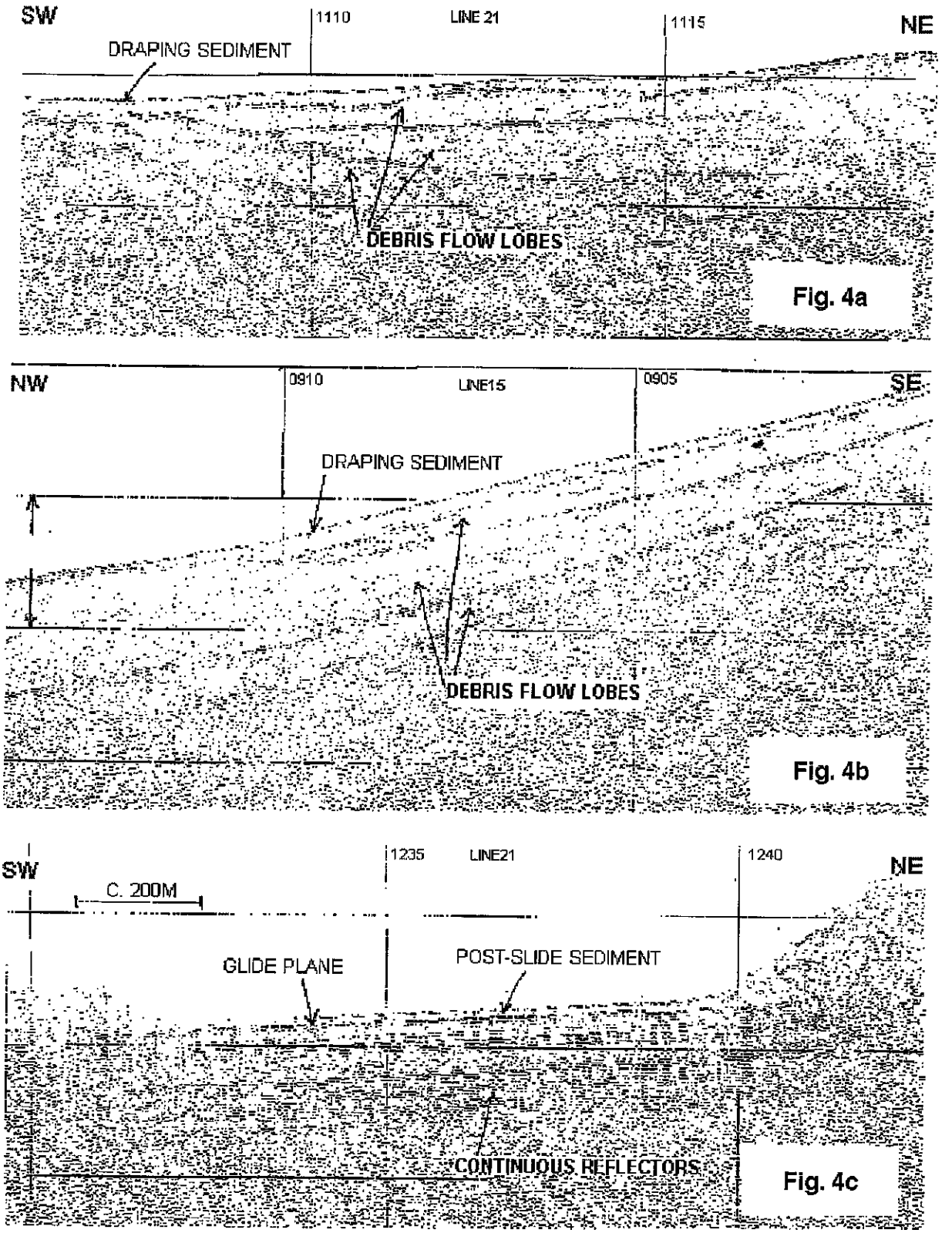

Fig. 64: Examples of deep-tow boomer profiles from area 2.

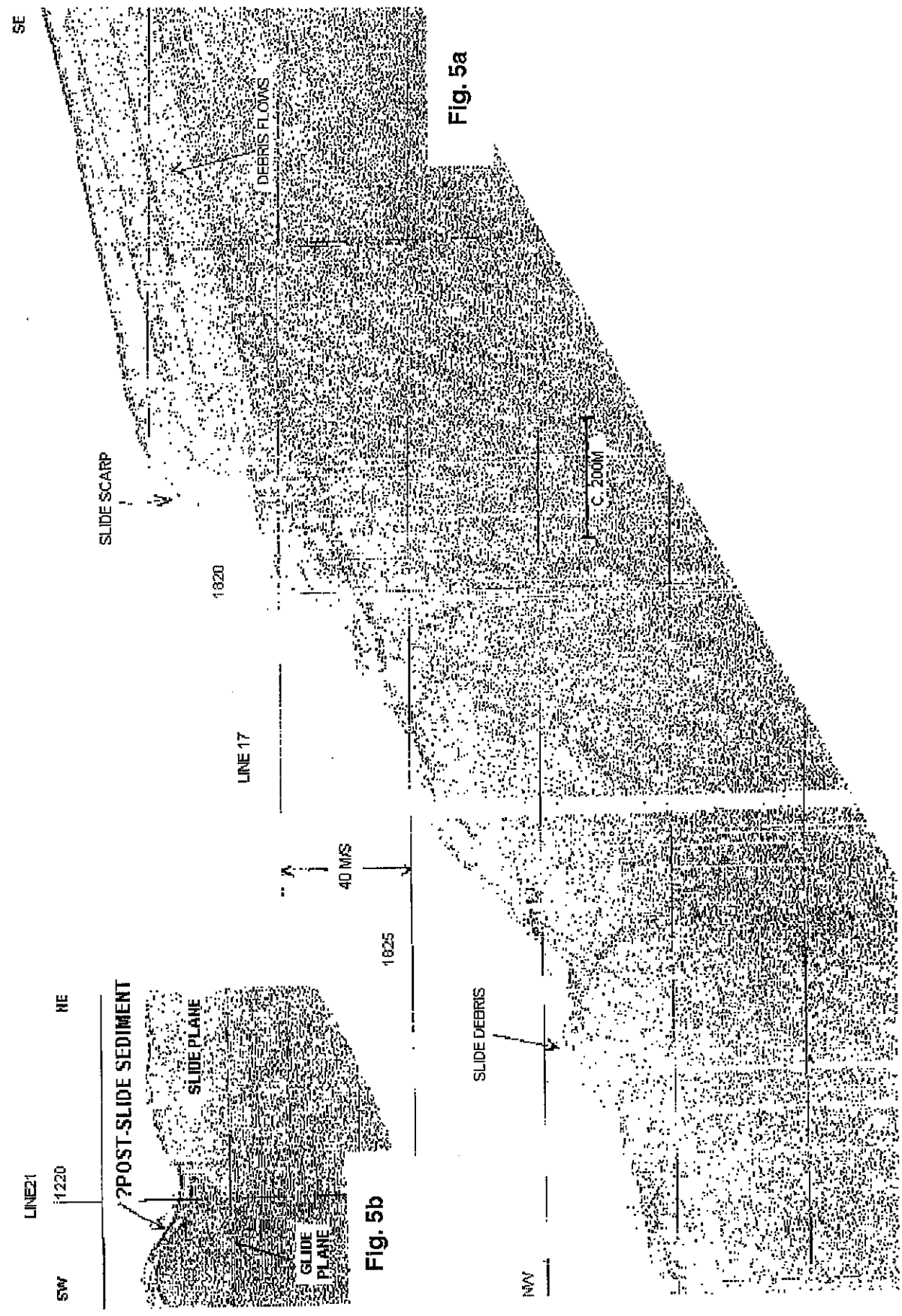

Fig. 65: Examples of deep-tow boomer profiles from area 2.

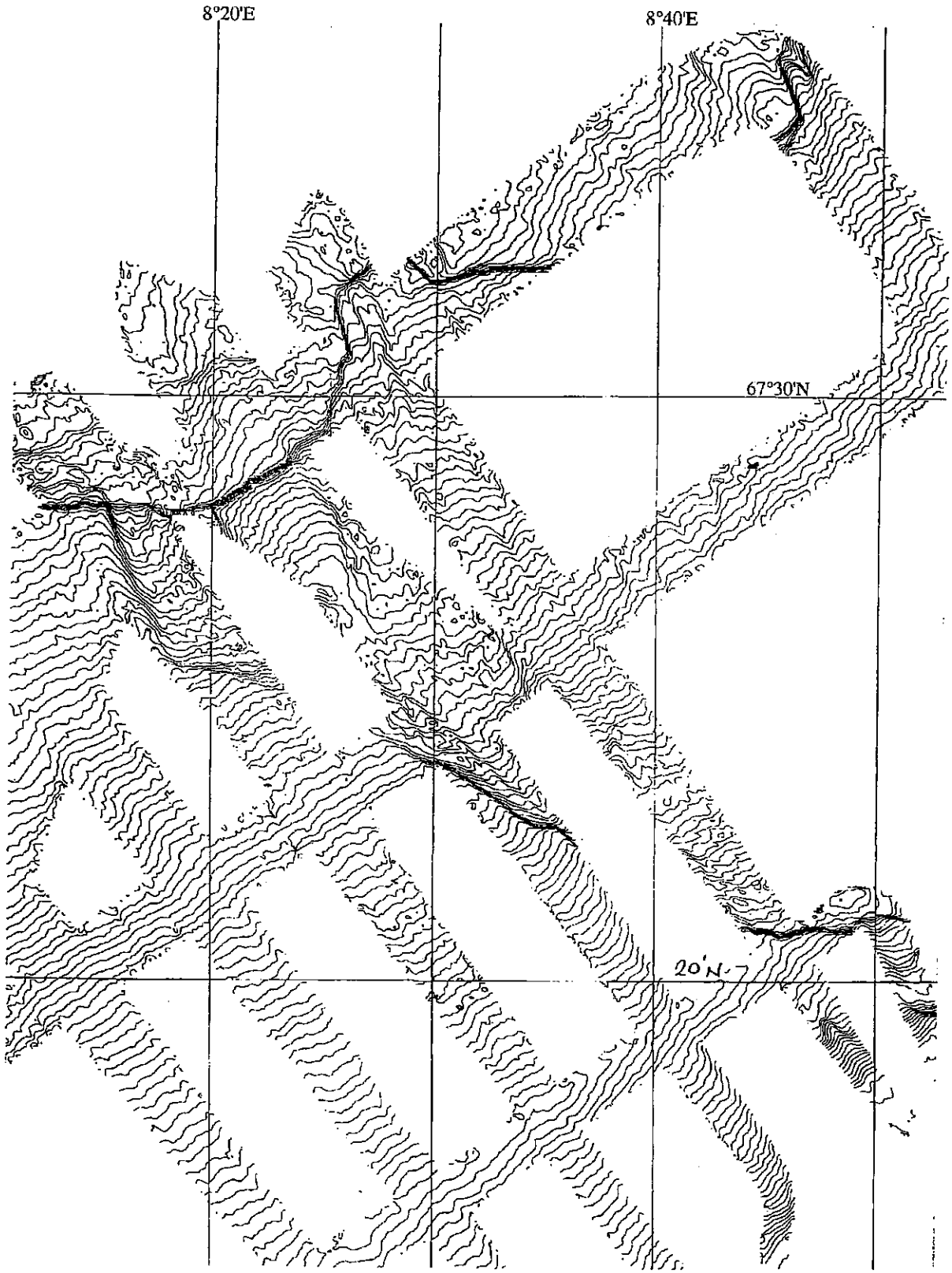

Fig. 66: A portion of hydrosweep data from area 2 (see also Fig. 52).

Beneath the seismically massive debris that appears to form the sea bed, a continuous series of smooth, gently dipping reflectors 20-30 m thick can be mapped over a large area in the upper part of the scar. These reflectors show acoustic pull-up (Figs. 64c, 65b) that is proportional to the thickness of the overlying sediments, which are typically 25-30 m thick, but range up to 45 m. At one location there is a 'window' where these reflectors have no cover of mass-flow debris and the sea bed is smooth over a line distance of 700 m (Fig. 64c). The reflectors are not at outcrop, however, as they are covered by a sediment layer with a constant thickness of 3 m which clearly overlaps the debris at the southeastern margin of this section. This layer is not generally imaged above the mass-flow material, but nearby it is possible that it occurs over a very short distance (Fig. 65b). It is thought likely that this unit is at least partly equivalent to the hemipelagic sequence overlying the debris flows on the 'autochthonous' slope.

The downslope limit of the continuous reflectors is poorly imaged due to the depth of water in the north of the area as well as the irregular nature of the sea bed. It is however closely coincident with a scarp that shows very clearly on the hydrosweep data (Fig. 66). This scarp joins the sidescarp in the north-central portion of area 2, where it appears to cut it at a high angle. On the basis of the angular relationship between the two scarps, the scarp in the lower part of the scar is interpreted as being probably the headwall of a slide movement subsequent to that in the upper part of the slide. An older age however cannot be ruled out without more evidence.

It is believed that the continuous reflectors represent the glide plane for the upper part of the slide. Continuity of these reflectors beneath the uppermost slope and shelf cannot be demonstrated from existing data, but this can be investigated with airgun equipment on RV POSEIDON. If this is so, then the 3 m-thick layer of probably hemipelagic sediment overlying it in the window represent deposition since the time of the slide. A core obtained at this location bottomed in relatively stiff, partly sandy clay; dating of this core will hopefully provide the ages of both the upper part of the slide and the glideplane.

OBH stations

Three of the four stations deployed were located on the eastern Voering Plateau survey area; the fourth was placed on the northern Voering Plateau to the northeast (Fig. 61). At this location (METEOR no. 245), a seismically well-layered sequence was encountered, with over 100 ms penetration despite water that was over 1300 m deep.

5.3.5 **Palaeontology of the Pelagic Realm** (H. Andruleit, S. Jensen)

The goal of project B3 (SYNPAL) of SFB 313 is the synoptic examination of the temporal and spatial development of plankton communities by looking at the five planktic groups: coccolithophores, diatoms, radiolarians, foraminifers and dinoflagellate-cysts.

The remains of these groups in sediments form the scattered evidence of a much higher diversity of planktic life in the upper water column. One goal is to link these remnants with the actual living communities in order to reconstruct the palaeoecology and evolution of planktic life and to use this knowledge to obtain detailed information of the palaeocene-graphic and climatic development. Therefore, we attempt to evaluate the processes which are taking place in the photic zone, the water column and the sediment. The basis for this study is the synoptic examination of samples obtained from plankton nets and water samples, sediment traps and sediments.

On this cruise the focus of research was placed on plankton samples, using plankton nets to collect dinoflagellate cysts, multinet for diatoms, radiolarians and foraminifers, and water samples for coccolithophores:

- For coccolithophore investigations, surface water samples (1 to 2 l) were taken at regular intervals throughout the whole cruise with a water pump. Also, at each CTD station 5 to 9 depth intervals were sampled with a rosette sampler according to temperature and salinity profiles. As soon as the samples were on board, the water was filtered through millepore filters (0.45 µm pore size) by means of a vacuum pump. The filters were then dried at 50°C for some hours and stored, with silica gel, in plastic petri dishes without further washing or conservation.
- To investigate the radiolarian and foraminifer fauna (especially the deep-living radiolarians) and diatom flora, a multinet (61 µm mesh size) was used at five depth intervals from 2000 to 1000 m, 1000 to 500 m, 500 to 150 m, 150 to 50 m, and from 50 m to the surface.
- For dinoflagellate cyst investigations, a ring-net (41 µm mesh size) was used to sample the interval from 50 m depth to the sea surface.

All net samples were treated with formaline and stored under low temperatures.

Additionally, surface sediment samples and some multicorer and short box corer sediment profiles were taken.

5.3.5.1 Shipboard Results

Due to limited possibilities for examination of the samples on board METEOR so far, there are only a few obtainable results. Some observations can however be made:

- There is no direct means available to evaluate the coccolithophore numbers due to their small size (a scanning electron microscope is needed for that). Nevertheless, an indication as to whether there are sufficient specimens is related to the staining of the filter. All filters from the surface samples show a promising staining, whereas the deeper samples often seem to be barren.
- In all net samples, large amounts of copepods, foraminifers and radiolarians were found. The foraminifers are dominated in all samples by *Neogloboquadrina pachyderma* and *Turborotalita quinqueloba*.

- In Atlantic-influenced areas of the Norwegian Current, large amounts of the diatom genus *Rhizosolenia* spp. were found. By contrast, in the Greenland Sea, high cell densities of the cold-adapted genus *Chaetoceros* spp. were seen.
- In the Denmark Strait the plankton densities were generally lower than in the Greenland and the Norwegian Seas.

5.3.6 **Planktology** (O. Haupt, E. Bauerfeind, M. Krumbholz, G. Donner)

The investigations of the plankton group on this cruise aim for better insight into the relationships between the pelagic cycling of primary produced matter and vertical particle export into depth in the Greenland Sea. Data from this cruise in 1996 will be compared with results obtained in the East Greenland Current from the Fram Strait to the Denmark Strait during summer and early winter 1993, 1994 and 1995 to investigate the short-term variability of the different production regimes of the polar water regions, and data will be merged for the calculation of a comprehensive particle flux budget. Another cruise planned for spring 1997 will elucidate the conditions of primary production at the beginning of the growth season. On cruise M 36/3 samples were taken from different regions of the Greenland-Icelandic Sea (Greenland Basin at 75°N and the northern Denmark Strait) to characterise phytoplankton communities, their environments, and living conditions.

5.3.6.1 **Shipboard Results**

Two stations at 75°N and 0 to 4°W were sampled with the CTD to get the vertical distribution of salinity and temperature, and with a water sampler rosette to get water from different depths for the analysis of seston, particulated organic carbon and nitrogen, particulate silica, photosynthetic pigments and nutrients. The light conditions in the water were checked with the Secchi Disk. Initial results show that the 1% light level was located at a depth of about 30 to 35 m. The vertical distributions of chlorophyll show a maximum of 1.5 $\mu g\ l^{-1}$ at a depth of 20 m within the Polar Surface Water (Fig. 67). Microscopic investigations of phytoplankton communities yielded a dominance of diatoms mainly *Chaetoceros* species with a dominance of *Ch. concarvicorne* in the upper 100 m of the water column. Other species observed were: *Ch. atlanticum, Ch. boreale, Ch. sp.* and *Rhizosolenia setigera, Rh. alata* and some dinoflagellates *Ceratium tripos, C. fusus, C. arcticum* and other unidentified small dinoflagellates. Nutrient values from Maaßen et al. (chapter 5.3.8) will be available after data processing in Kiel.

A long-term mooring OG10, deployed at 75°3.4 N/4°35.7 W in October 1995 from RV POLARSTERN, to monitor the vertical particle transport in the seasonally ice-covered area of the Greenland Sea, was successfully recovered. Initial qualitative results of the vertical particle flux in 500 m show a moderate flux in October/November 1995 before the low flux period in winter. In May 1996 vertical particle flux increased and peaked in July 1996 (Fig. 68). A new long-term mooring (OG11) with three sediment traps at 500, 1000 and 2000 m and two current

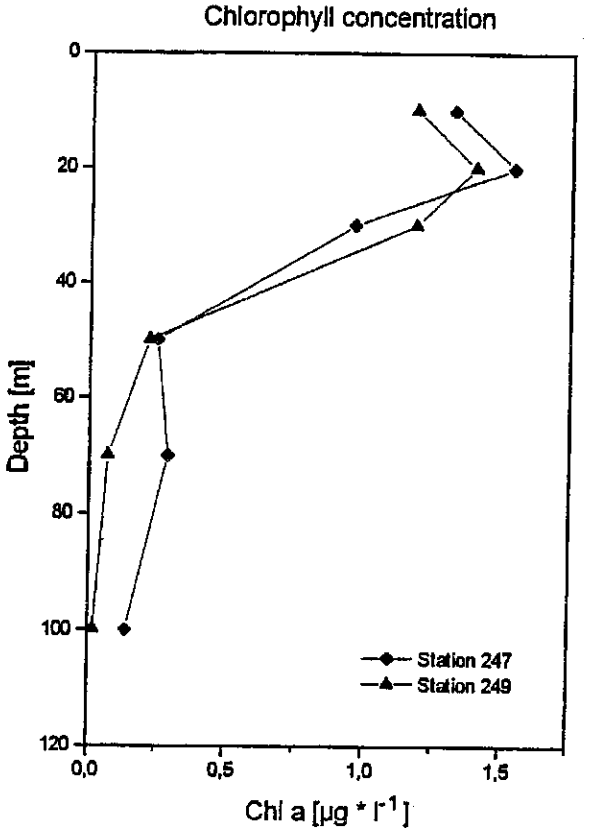

Fig. 67: Vertical chlorophyll distribution of stations 247 and 249 in the Greenland Basin.

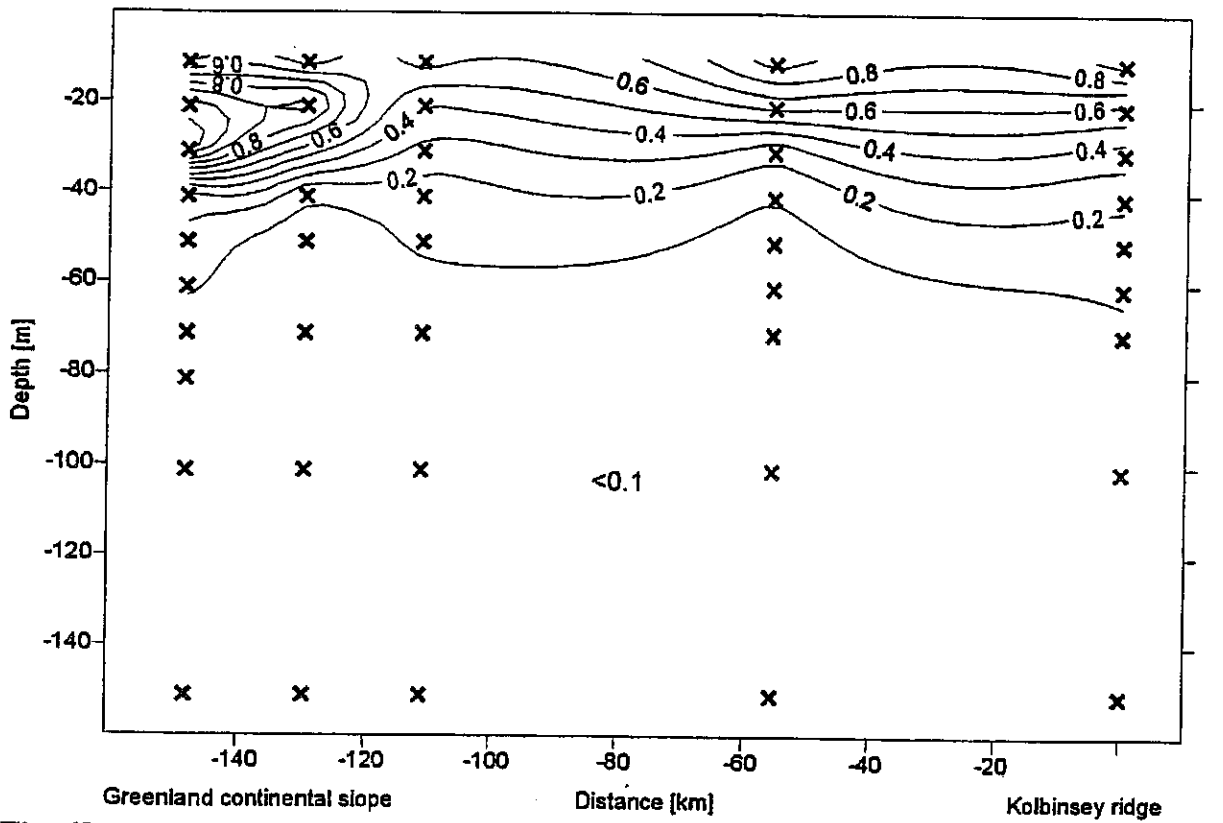

Fig. 68: Vertical chlorophyll distribution along the transect Kolbinsey Ridge to Greenland continental slope (x: samples).

meters within the upper 1000 m was deployed in the Greenland Basin at 74°59.69 N/6°57.39 W.

In the southern investigation area, 6 stations along a transect across the northern Denmark Strait and one more station north of the transect were sampled with the CTD, the water sampler rosette, the Secchi Disk and a plankton net. First results from the CTD show the different characteristics of the Polar Surface Water, Return Atlantic Water and Greenland Sea Deep Water. Chlorophyll yielded maximum concentrations of about 1.1 µg l^{-1} within the Polar Surface Water (upper 50 m). The vertical chlorophyll distribution along the transect is shown in Fig. 69. Microscopic investigations of the phytoplankton community show characteristics similar to the stations in the Greenland Basin. The chlorophyll maximum at a depth of 20 m was dominated by diatoms whereas the layer above shows more heterotrophic plankton species (tintinnids and heterothrophic dinoflagellates). Nutrient data are not available at this time. Further analyses of samples for seston, particulated organic carbon and nitrogen, particulated silica, and pigments will provide knowledge about pelagic processes and vertical particle flux.

5.3.7 Bentho-Pelagic Coupling in the Northern North Atlantic

(J. Berg, O. Bothmann, W. Ritzrau, A. Scheltz, D. Seiler)

The benthos group of the SFB 313 joined M 36/3 to fill in gaps in the existing benthos data set of the northern North Atlantic. During the first half of the cruise previous SFB sampling sites were revisited at the Voering Plateau, at the long-term mooring position in the Norwegian Basin at 70°N/0°E, and a mooring position of Norwegian colleagues of the IMR Bergen at 75°N/0°E. At these three stations the distribution of biogeochemical parameters in the sediment, as well as the sediment oxygen consumption, were studied.

At the station in the Norwegian Basin a fluff layer was observed at the sediment surface, most likely implying an input of recently settled particles. This 1 to 1.5 cm thick layer was rich in phytogenic pigments (Chl.-a equivalents), whereas this "fresh" material has not yet been incorporated in the sediment (Fig. 70). Elevated oxygen consumption rates of the sediment community suggest that either the fluff layer is physiologically very active or the sediment community has already responded to the recent food input. Samples from this station and from the Voering Plateau were incubated on board to elucidate the decay constants material settled to the sea floor.

During the second half of the cruise, special focus was set on the bentho-pelagic coupling in the two main work areas; firstly, at an ice influenced long-term mooring position at 75°N/4°W and secondly, at 7 stations in the northern Denmark Strait (68°-69°N). In close collaboration with the pelagic group, the fate of organic matter will be traced from the zone of primary production to the consumption by benthic communities or final incorporation in the sediment. The transect covered the area from the western Kolbeinsey Ridge (18°43 W, 900 m depth) across the central deeper area (1500 m) onto the East Greenland shelf to a water depth of 400 m (20°43 W). At all stations the composition and the microbial modification (^{14}C-amino acid utilization, ^{3}H-

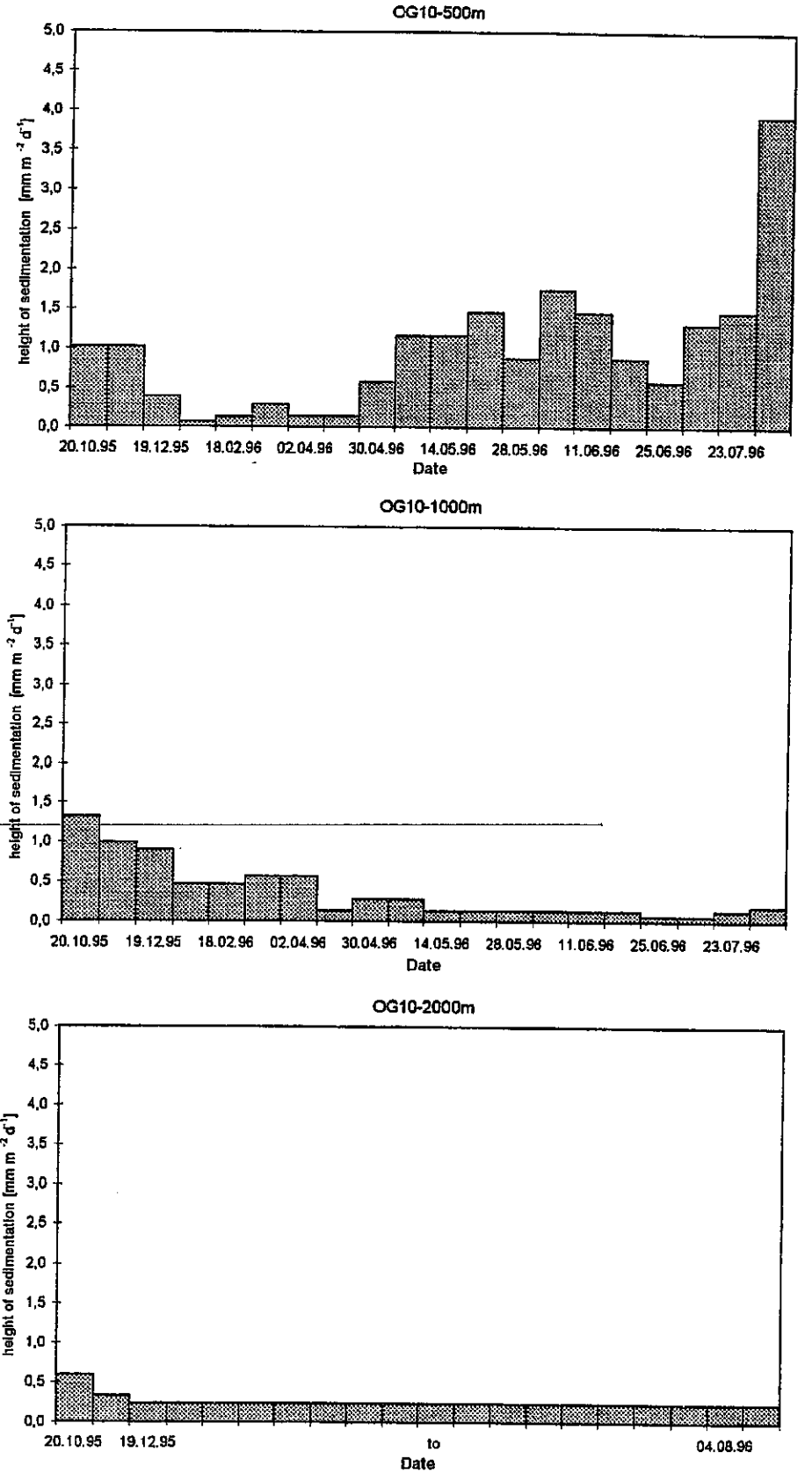

Fig. 69: Vertical particle export to 500 m, 1000 m and 2000 m depth for the sampling period in October 1995 to August 1996. The third sample of the 2000 m trap covers the interval from December 19, 1995, to August 4, 1996. Values are given in millimeters per square meter and day.

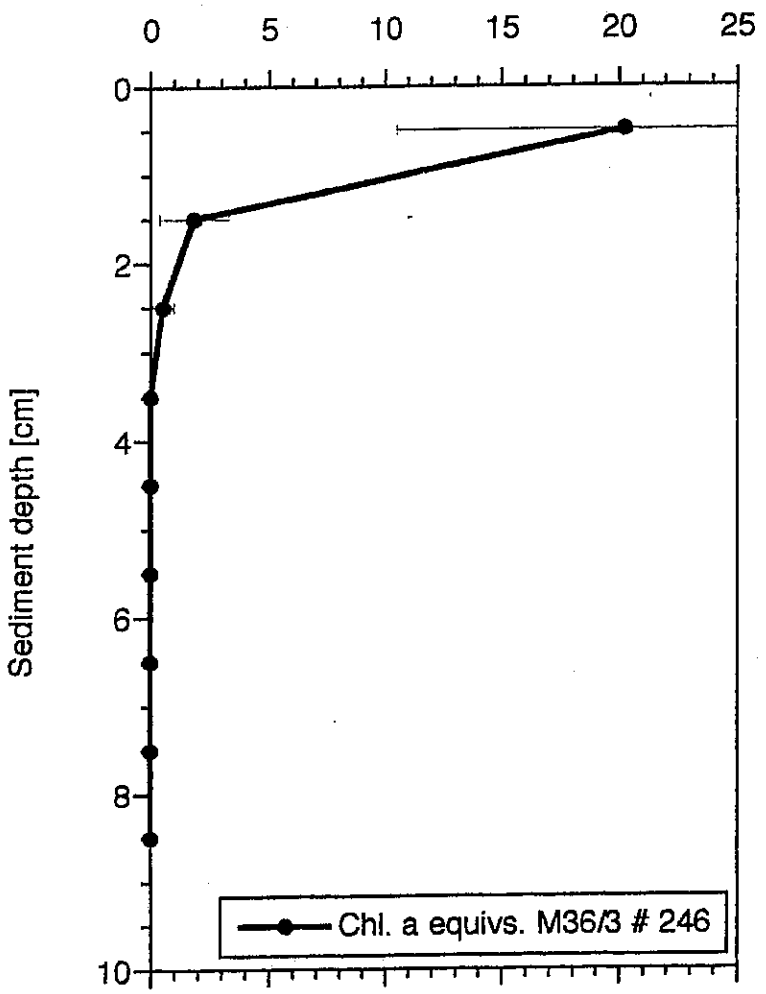

Fig. 70: Sediment depth versus Chl.-a at station 246.

Leucine and ^{3}H-Thymidine incorporation) of near bed particles was investigated using a bottom water sampler. The multicorer provided samples to assess the distribution of phytogenic material and the activity patterns (sediment oxygen demand) of the sediment communities. Samples for the description of community structure of the epi- and endobenthic macrofauna were collected with box corer and the epibenthic sledge. A subset of these samples will be used to establish morphometric characteristics of dominant benthos species on the East Greenland continental slope.

Rate measurements of the microbial activity in the benthic boundary revealed that particle modification is significantly faster near the sea floor than in the intermediate water layer. The sediments at the shallow East Greenland shelf station were dominated by thick mats of sponge spiculae, whereas the sediments of all other stations did not show remnants of these organisms. The analyses of all biogeochemical sediment parameters will be completed at the home institute. The successfully acquired set of samples during the M 36/3 cruise will add to the understanding of benthic processes in the northern North Atlantic.

5.3.8 Marine Geochemistry (J. Maaßen, A. Flügge, A. Lunau, T. Körner)

The main aim of M 36/3 was to sample early diagenesis investigations of organic biomarkers (n-alkanes, isoprenoids, alkenones) and anthropogenic tracers (PAHs and PCBs), as well as primary productivity indicators like opal and barium, within the water column and fluxes through the water/sediment interface. Additional high-resolution (400 µm) in-situ profiles of oxygen in surface sediments were recorded with an in-situ O_2-profiler (FLOORIAN) for the understanding of the decrease of organic carbon in surface sediments (Fig. 71). Measurements of nutrients in the whole water column, and pore water complete the geochemical and organo-chemical studies.

5.3.8.1 Shipboard Results: Organic Chemistry

Particulate organic matter (POM) plays a major role in the biogeochemical cycle of carbon in the oceans. Chemical biomarkers are good tools for monitoring alteration processes within the POM and the influence of bacteria, terrestrial and/or anthropogenic input. As they keep structural information about their possible sources, these markers might be a key to the understanding of the complex system at the water/sediment interface. The understanding of these biomarkers in the contemporary oceans is necessary in order to interpret the composition of sedimentary lipids for palaeoceanographic application. During M 36/3, POM was collected for organic geochemical analysis from surface water and within the water column at the long-term mooring position in the Norwegian Basin and the main SFB work area in the Denmark Strait. In addition, samples at two selected SFB stations around 75°N were collected.

The subsequent analyses will focus on quantification of biological marker compounds, particularly organism-specific biomarkers of *Prymnesiophycea* (C_{37}, C_{38}-alkenones), n-alkanes, isoprenoids and anthropogenic compounds such as PAHs and PCBs. As an additional organic geochemical parameter, the amount of total organic carbon (TOC) will be determined.

At the Norwegian Basin (NB) vertical particle flux of large, fast-sinking particles has been recorded over several years. The mooring consists of 2 traps, deployed at 1000 m and 2500 m depth. The SFB long-term mooring at 70°N/4°E was changed successfully. Mooring NB9, deployed in 1995 on POSEIDON cruise 209/2, was recovered safely on M 36/3. Both traps had performed perfectly and from 1000 m and 2500 m, 18 and 12 samples respectively were safely recovered. After a short overhaul of the releases and floats, and replacement of the trap electronics, the mooring was redeployed for another year's sampling. Mooring NB10 will be recovered in August 1997 with RV POSEIDON.

Surface samples of suspended particulate matter were obtained with a stainless steel Satorius membrane filtration device connected to the Kiel pumping system (KPS), which was attached to the hydrographic dome. This provides continuous clean sampling at an approximate flow rate of 2 l/min during the ship's movement. The distance between two sampling sites was about 60 to 100 nautical miles, depending on hydrographic conditions and on the amount of

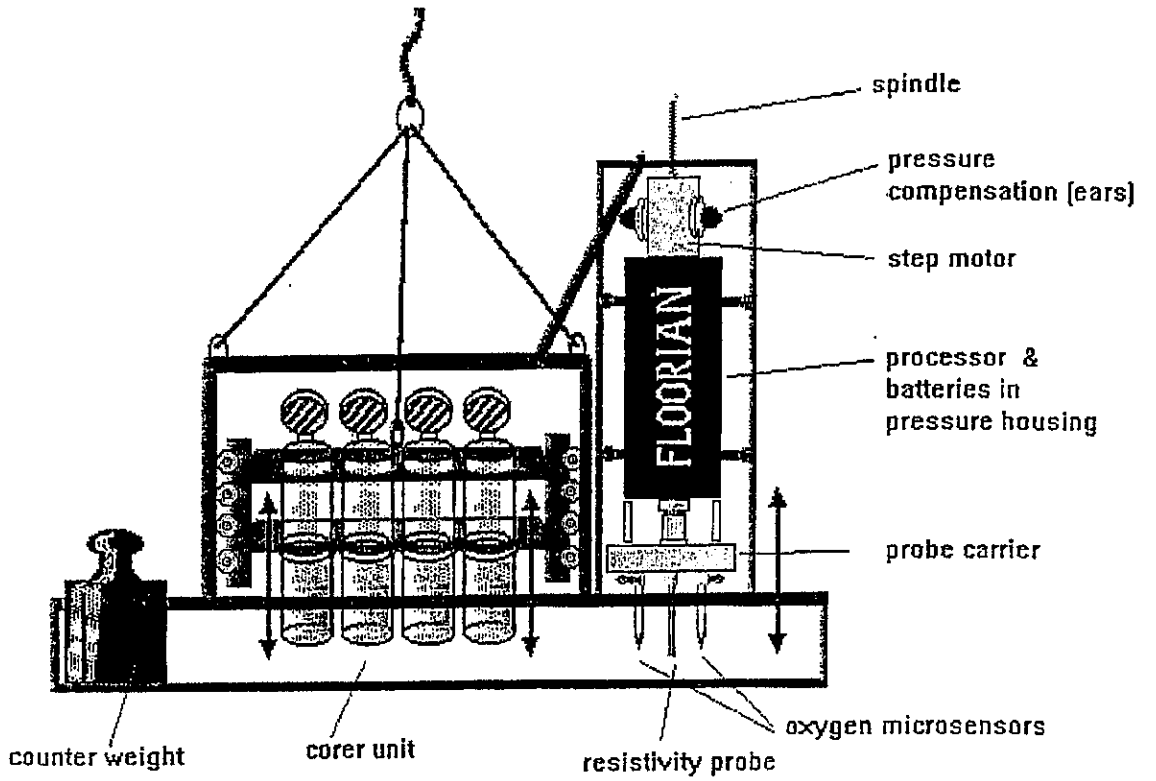

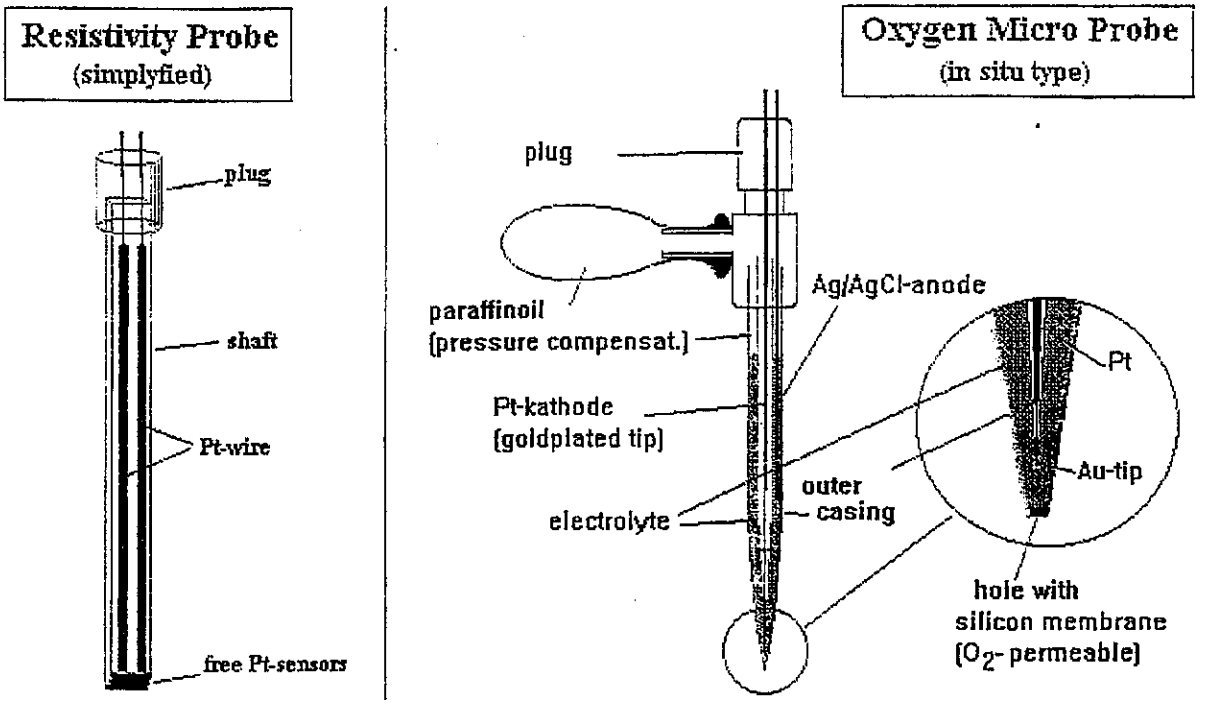

Fig. 71: FLOORIAN device for measuring the O_2-gradients within the upper sediment centimetres of the sea floor on a high-resolution (10-100 µm) scale.

material collected, as visually estimated from the filters afterwards. A total of 48 water samples were taken in this manner.

In addition, the water column was sampled vertically for suspended matter with a series of three deep-sea in-situ pumps and a surface reference taken from the KPS on five locations. POM was obtained by filtering volumes of about 400 l of water through GF/F glass fiber filters (Schleicher & Schuell, 140 mm diameter; pre-combusted at 500°C) in-situ or on board. Table 8 displays the amounts of water filtered by the in-situ pumps at various depths. The filters and sediment samples were deep-freezed at -3°C for further analysis onshore.

A common ultrasonic extraction technique employing methanol/dichloromethane (1:2) will be used as the solvent to completely remove lipids from the filtered material. The crude lipid extract will be separated into compound groups of different polarity by high-performance liquid chromatography. Quantification of biogenic and anthropogenic compounds will be accomplished by capillary gaschromatography. After removal of $CaCO_3$ by acid vapor treatment, TOC will be measured with an HCNO-elemental analyser using an air-dried aliquot of the filter.

Tab. 8: Volume of water filtered in-situ on 5 stations during M 36/3

Station	Position	Water Depth (m)	Sampling Depth (m)	Water Volume (l)	Duration (h:m)
#246	69°59.8 N/004°01.4 E mooring position NB10	3280	100 1000 2500	392.71 423.4 11.7	04:00 04:00 04:00
#249	75°03.4 N/004°35.9 W mooring position OG11	3609	100 1000	354.9 313.2	03:20 02:40
#252	67°52.6 N/018°43.4 W	912	100 500 860(50 m a.b.)	413.7 381.4 419.7	04:00 04:30 04:40
#257	69°31.98 N/003°???	1273	100 500 1220 (50 m a.b.)	394.1 423.9 337.1	03:50 04:40 03:10
#261	68°55.4 N/020°18.1 W	1570	100 500 1520 (50 m a.b.)	332.8 412.5 460.8	03:10 04:40 04:40

5.3.8.2 Shipboard Results: Sea Floor Oxygen in-situ Analyser (FLOORIAN)

During M 36/3, a sea floor oxygen in-situ analyser (FLOORIAN) equipped with resitivity probe, oxygen microsensors and a quatrocorer unit was successfully deployed at three stations (62°47.7 N/2°26.9 W, 69°59.9 N/4°0.5 E, and 75°3.4 N/4°35.7 W). This recently-developed device measures high-resolution profiles (400 µm) of oxygen concentrations and resitivity at the sediment/water interface. At this interface, strong gradients in physical, chemical, and biological properties occur. FLOORIAN thus provides important information about oxygen gradients, as well as resitivity changes within this region that is crucial, especially for diagenetic processes.

Gradients of oxygen in the upper sedimentary layer are directly coupled with the degradation of organic carbon, and the measurements, which will be processed onshore, supply data to model diagenetic degradation processes. Because resistivity of sediments is directly linked to porosity (via form factor), measurements of this physical property provide an elegant method to determine porosity, a factor that also influences diagenetic processes at the sediment/water interface.

In addition to these in-situ measurements, up to four sediment cores were recovered from each deployment. Pore water was extracted by a standard pressure filtration technique at 4°C. The analyses of pore water nutrients (silicate, phosphate, nitrate, and ammonia) were performed onboard, while inorganic compounds (biogenic Ba, Opal), as well as several biomarkers (alkenones, n-alkanes, isoprenoids, etc.) will be quantified at the onshore laboratories in Kiel.

5.3.8.3 Shipboard Results: Nutrients and Dissolved Oxygen

Data were generated utilising an autoanalyser system for the determination of nutrients (nitrate, phosphate, silicate and ammonia) and a computerised Winkler titration system for oxygen analyses. These data, in conjunction with salinity and temperature recordings, provide essential information for the interpretation of organic and inorganic fluxes in the water column and the water/sediment interface, and of environmental parameters for planktic and benthic studies.

During M 36/3 nutrient and oxygen analyses in the water column were performed from CTD casts on the main SFB work areas in the Norwegian Basin at 70°N/4°E, the Jan Mayen Current at 75°N, and the Denmark Strait. Additionally about 50 nutrient samples were taken underway using the KPS.

Initial interpretations of the data reveal a depletion of all nutrients in the surface waters of the central North Atlantic up to a depth of 30 to 40 m. Phosphate and silicate show very low concentrations, while nitrate is almost completely consumed. The concentration of ammonia in the surface waters was up to 0.5 µmol. In deeper water masses, normal gradients of nutrient concentrations occurred. Amounts of 6-10 µmol silicate, 11-14 µmol nitrate and 0.6-0.8 µmol phosphate were measured at all stations. These data correlate well with the oxygen

measurements, which reveal a supersaturation in the first 30 m of the surface waters. Fig. 72 shows a typical example of a vertical profile of nutrients and dissolved oxygen at station OG11 (raw uncorrected data).

5.3.9 CTD Deployments on M 36/3 (H. Beese, O. Haupt)

The CTD system used during the cruise consisted of a Neill Brown Mark III, a water-sampling rosette with twelve Niskinbottles (capacity 12 litres), a EG&G Deck Unit Model 1401 and a General Oceanics RMS MK VI firing module. The data were recorded and stored on an IBM-compatible computer with an attached zip drive. For the purpose of further processing and plotting, the binary raw files were converted into ASCII format. The CTD system was attached to the 11 mm conductive wire (W2) and deployed with 1 m/s, up- and downcasts with the same winch speed. A bottom alarm sensor allowed the CTD to be lowered down to about 15 m above the sea floor.

All planned stations were successfully completed with good data and water recovery.

During the cruise, the vertical distribution of temperature and salinity as well water samples for biological and chemical analyses were collected at eleven stations (Figs. 1d, 73, 74).

During the first half of the cruise, two stations each were located in the Norwegian and Greenland Basins. Initial results of the vertical temperature and salinity profiles of the first four stations are shown in Figs. 75, 76. The surface water in the Norwegian Basin was dominated by warm Atlantic water with salinity values greater than 35 psu. Due to the influence of the melt water from the marginal ice zone, which was about 100 kilometres west of station 249, the surface water in the Greenland Basin was characterised by relatively low salinities.

The second half of the cruise focused on a transect within six stations across the northern Denmark Strait (plus one station a little north of the transect). Preliminary results on the temperature and salinity distribution along this transect display only small variability in the vertical structure of the water masses (Figs. 77, 78). The influence of the close proximity of the marginal ice zone was detected within a very thin surface layer with low salinities, which also showed a seasonal warming. Below this surface layer, the Polar Surface Water of the East Greenland Current with low temperatures (-1.6°C) and salinities of about 34.2 psu was located. The deeper water mass was dominated by the Return Atlantic Water and the Greenland Sea Deep Water with high salinities and low temperatures.

Further analysis of the T/S characteristics will give detailed information of the vertical structure of the different water masses in this area, an important necessity for the sound interpretation of the biological and chemical data.

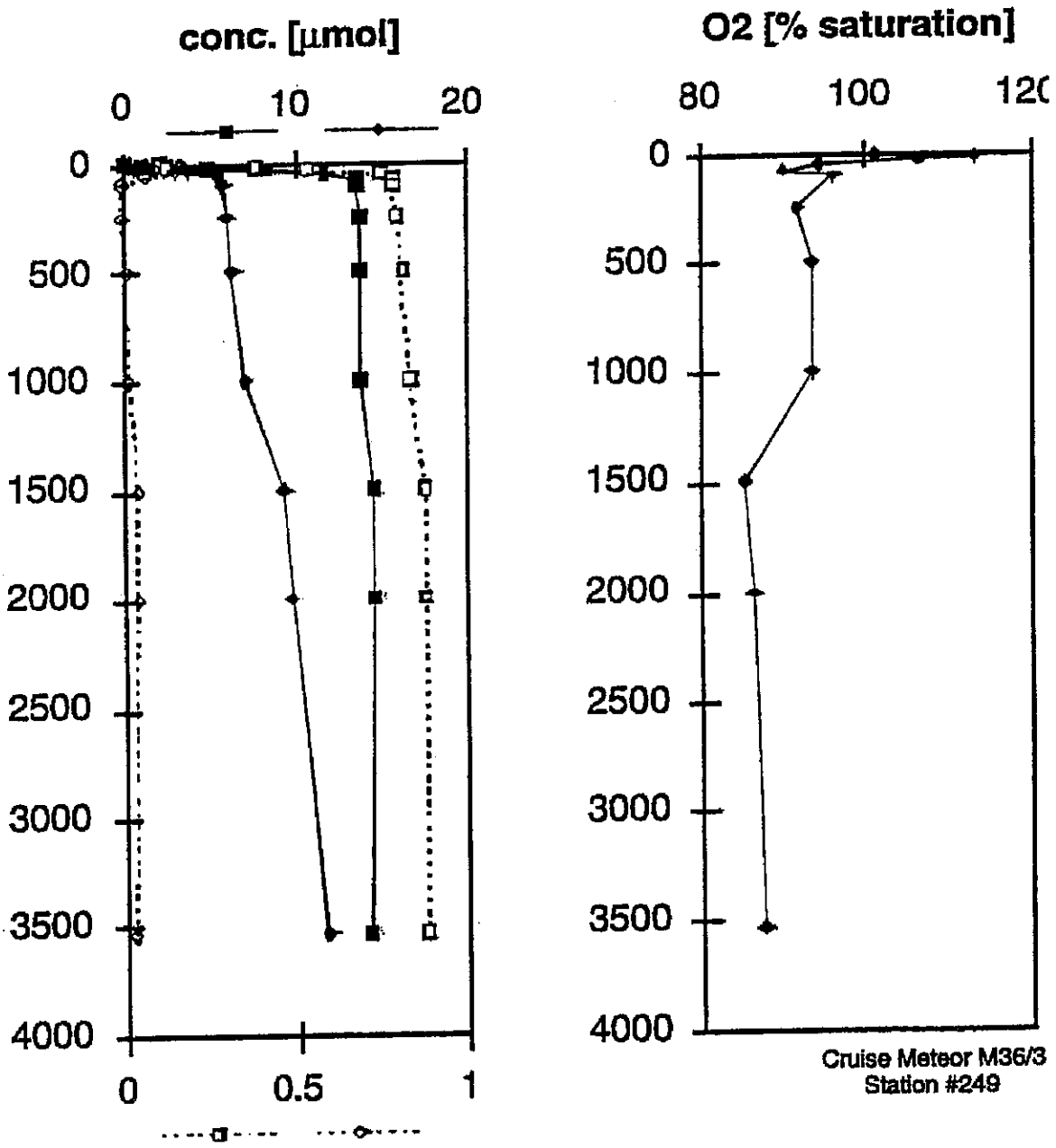

Fig. 72: Vertical profile of nutrients and dissolved oxygen (raw data) at station OG11.

Meteor 36/3

CTD Casts northeast of Norway

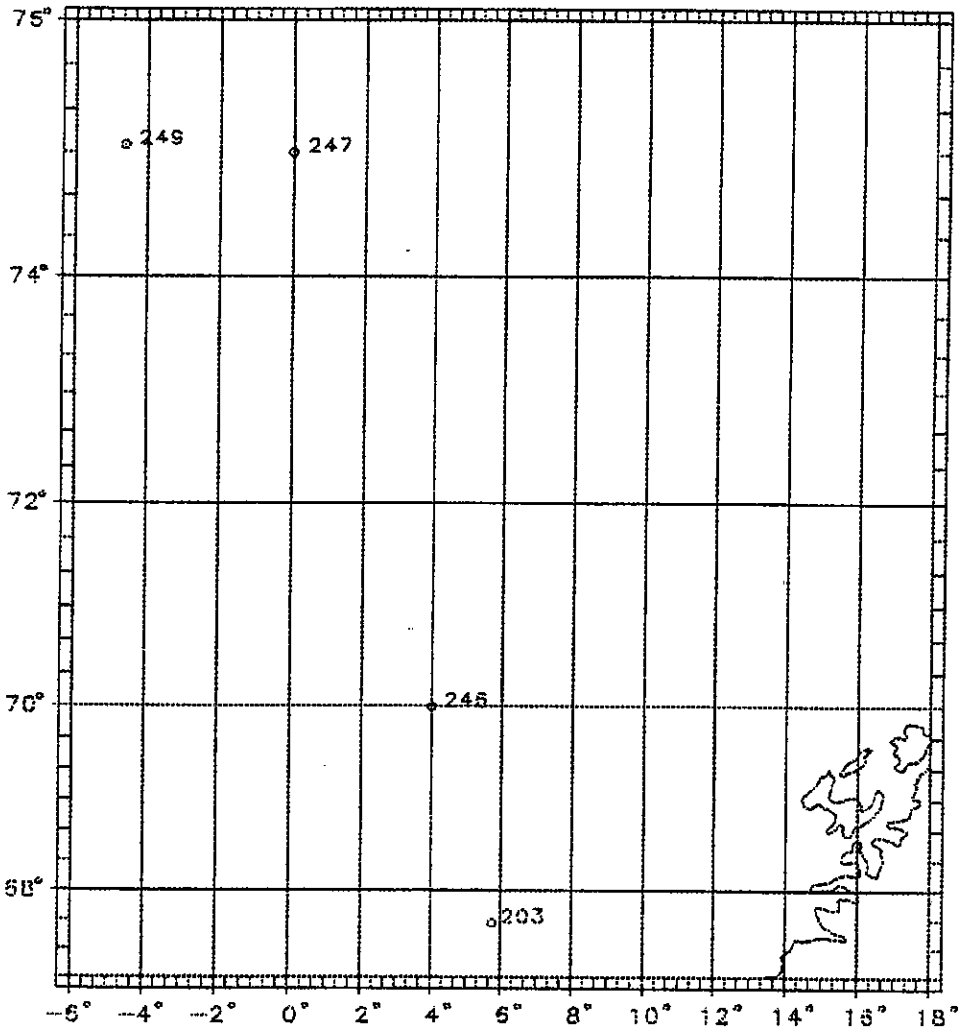

Fig. 73: CTD casts northeast of Norway.

Meteor 36/3

CTD Casts Denmark Strait

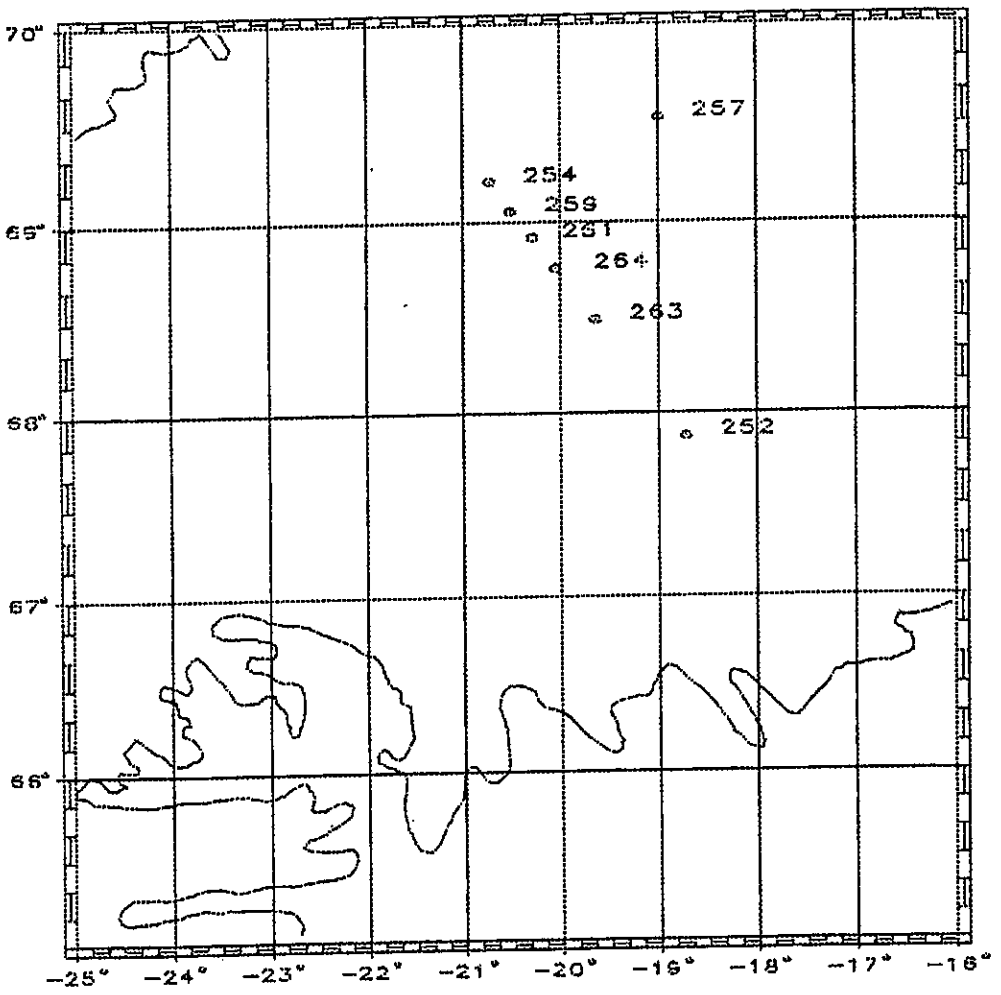

Fig. 74: CTD casts in Denmark Strait.

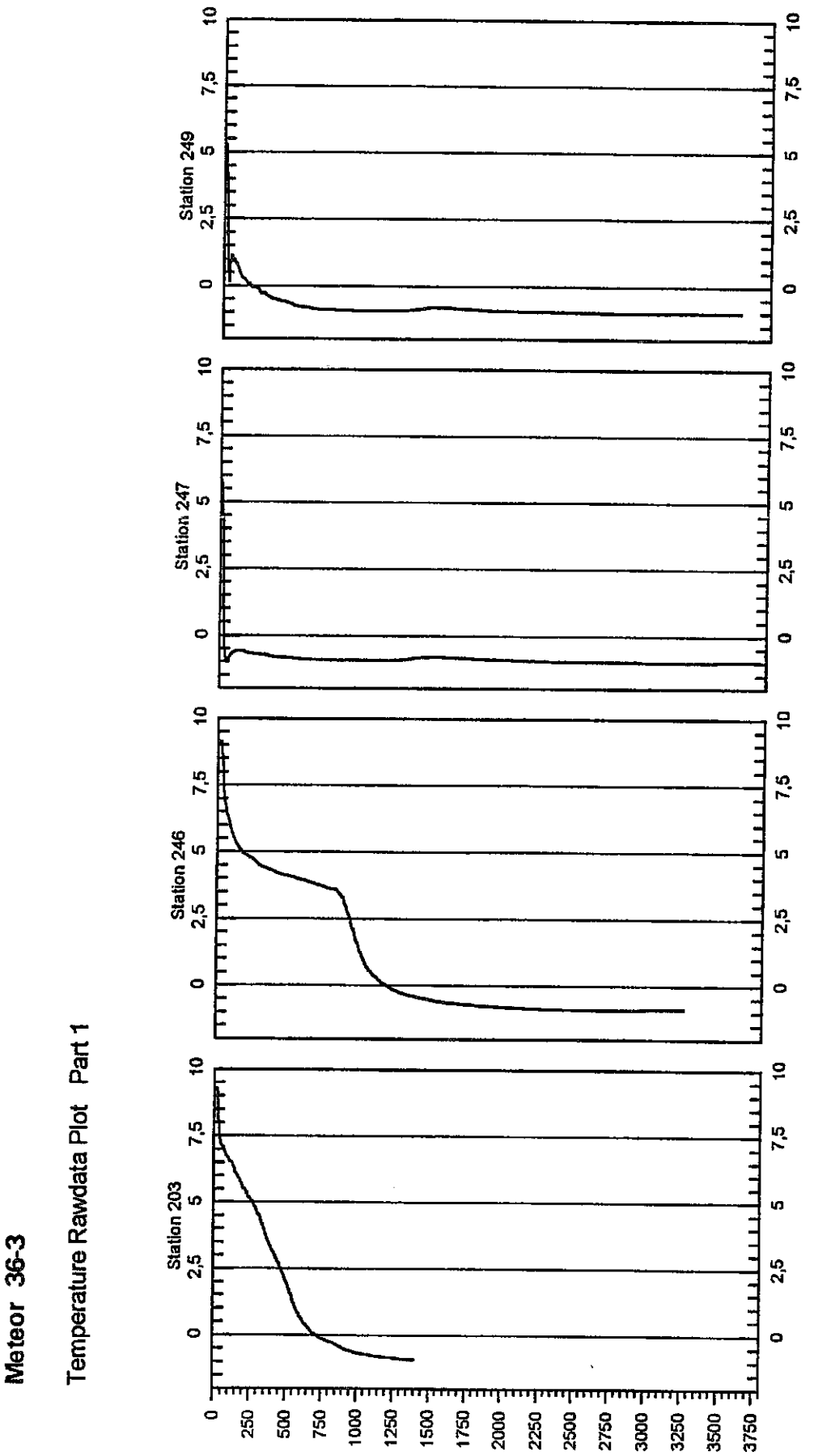

Fig. 75: Temperature rawdata on stations 203, 246, 247, 249.

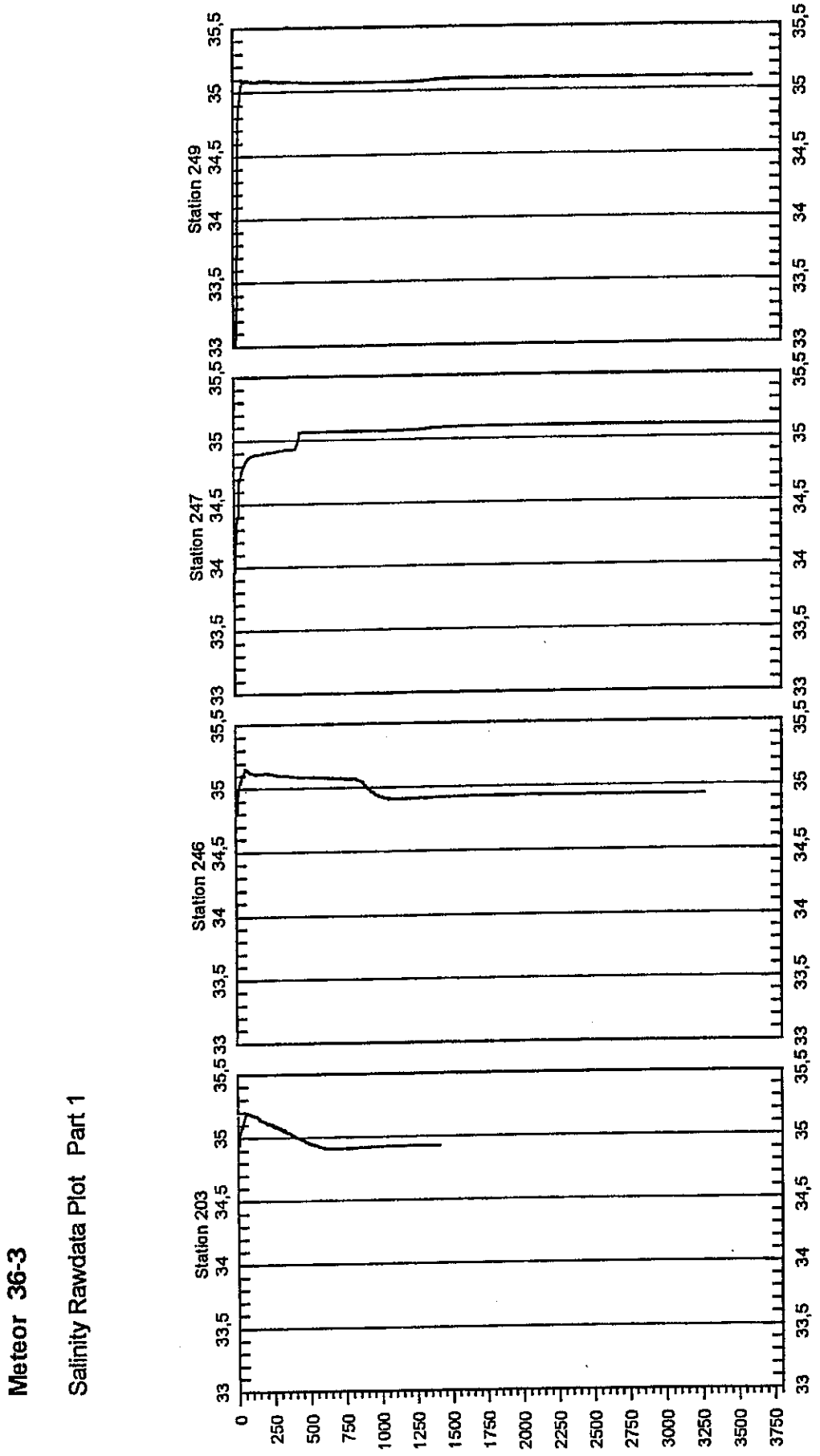

Fig. 76: Salinity rawdata plot part 1.

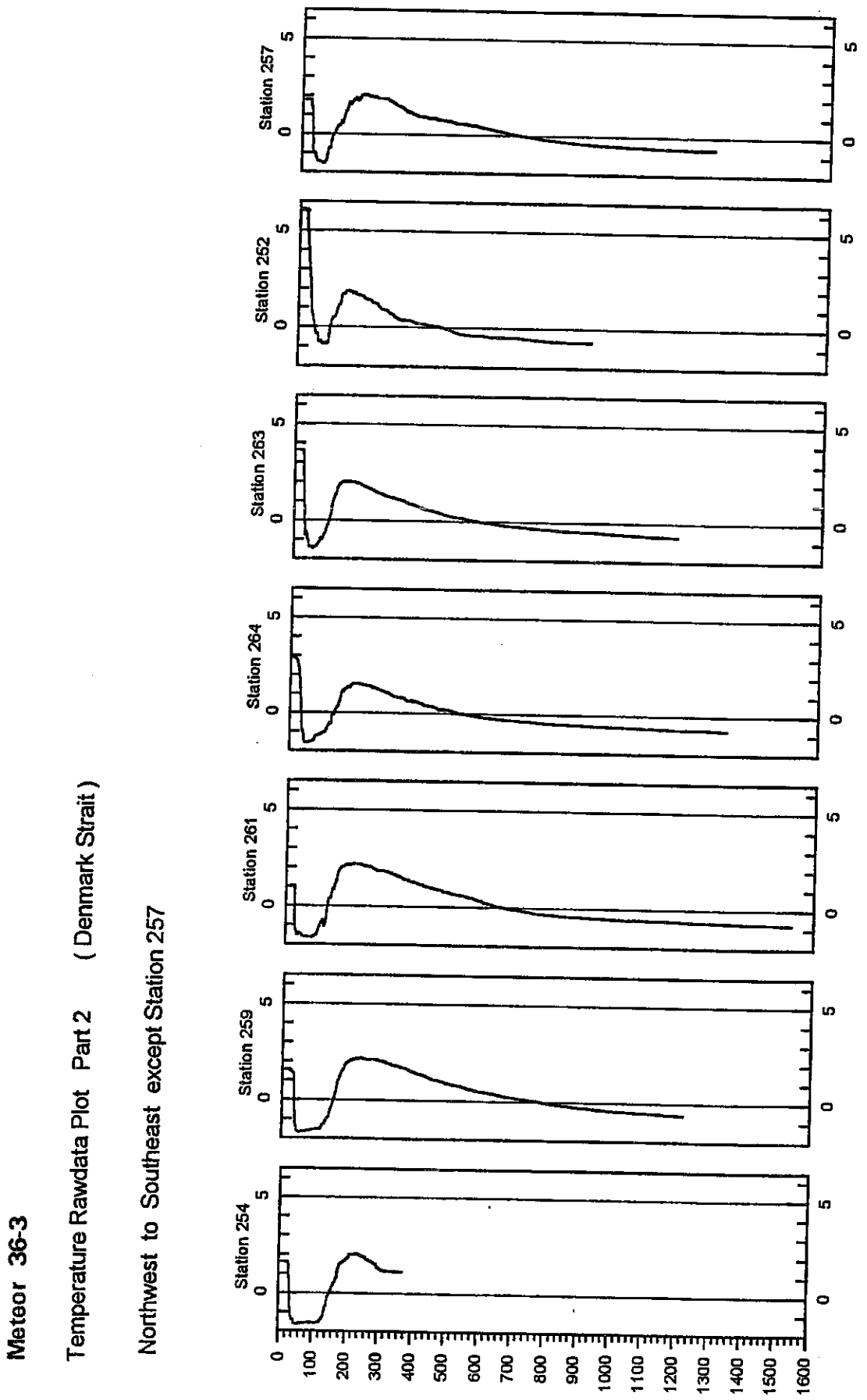

Fig. 77: Temperature rawdata plot part 2 (Denmark Strait).
Northwest to Southeast except station 257.

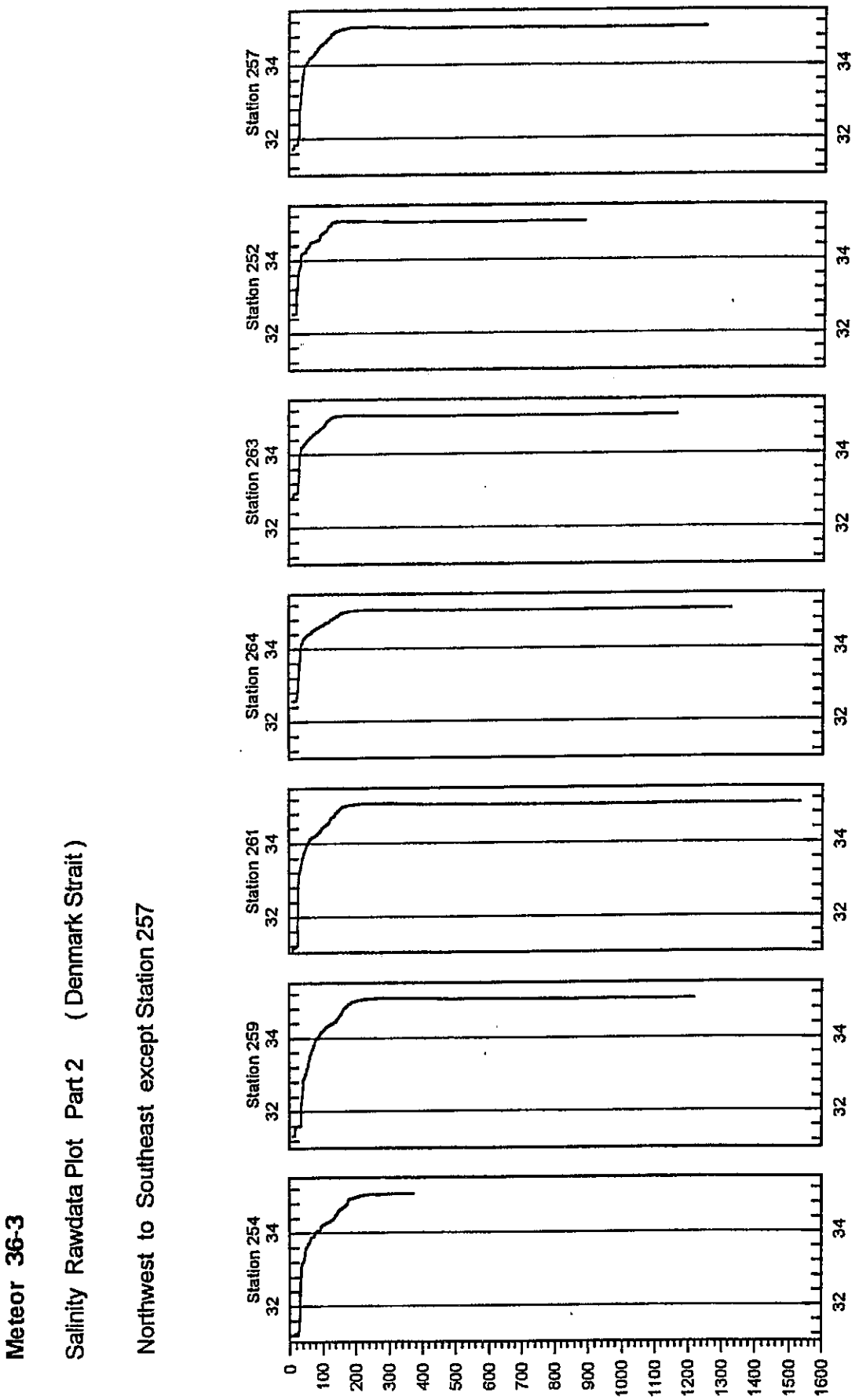

Fig. 78: Salinity rawdata plot part 1 (Denmark Strait).
Northwest to Southeast except station 257.

5.4 Leg M 36/4

5.4.1 CTD Deployments (T.Viergutz)

During M 36/4, a Neil Brown Mark III of the BSH Hamburg equipped with twelve GO niskin bottles (10 litres each) was used. At almost all stations the CTD was used to collect water samples and hydrographic data. Following initial problems, data collection and water samplers were working without any problems from station 281 on. Water samples were taken successfully in water layers relevant for particle dynamics and processed by several work groups aboard the ship. To determine the influence of internal waves in the area of the Whittard Canyon, a grid was sampled with the CTD, which was equipped with a transmissiometer and a turbidity meter.

The priority was to sample the water column for particulate matter. The hydrographic data will be postprocessed later in collaboration with the BSH.
As an example for a deeper station of this cruise, the profile of station 296 is shown (Fig. 79).

5.4.2 Hydrosweep (T. Schillhorn, L. Thomsen)

Onboard METEOR, the bathymetric contours of the ocean floor can be continuously recorded using the swathmapping system hydrosweep (HYDROgraphic multi-beam SWEEPing survey echosounder, made by Atlas Elektronik GmbH, Bremen). The instrument works with a frequency of 15.5 kHz. The input amplifier is situated perpendicular to the longitudinal axis of the ship. With 59 acoustic beams and an opening angle of 90°, a swath about twice as wide as the water depth is surveyed. Precision is about 1% if the ship rolls less than 10° and heaves less than about 5°. The central beam has a range of up to 10,000 m; the outermost ones can range up to at least 7000 m. Postprocessing of hydrosweep data to produce bathymetric maps and coloured 3-D perspective views is done on board with the CARIS system.

Hydrosweep records were acquired during the cruise to get the bathymetry of the Whittard Canyon and, partly, the Austel Spur. On the first day of the cruise, data quality was bad due to a storm. Otherwise, quality was good. For simplicity, an average water velocity of 1485 ms^{-1} was chosen. During the leg, CTD measurements were taken, thus the velocity profile will be available for further processing. In nearly the whole part of Whittard Canyon the topography, comprised of several steep ridges, is clearly imaged.

5.4.3 Parasound (T. Schillhorn, L. Thomsen)

By means of the parametric sediment echosounder parasound (PARAmetric sediment survey echoSOUNDer, Atlas Elektronik GmbH, Bremen), shallow sedimentary layers down to a maximum depth of about 100 m can be imaged.

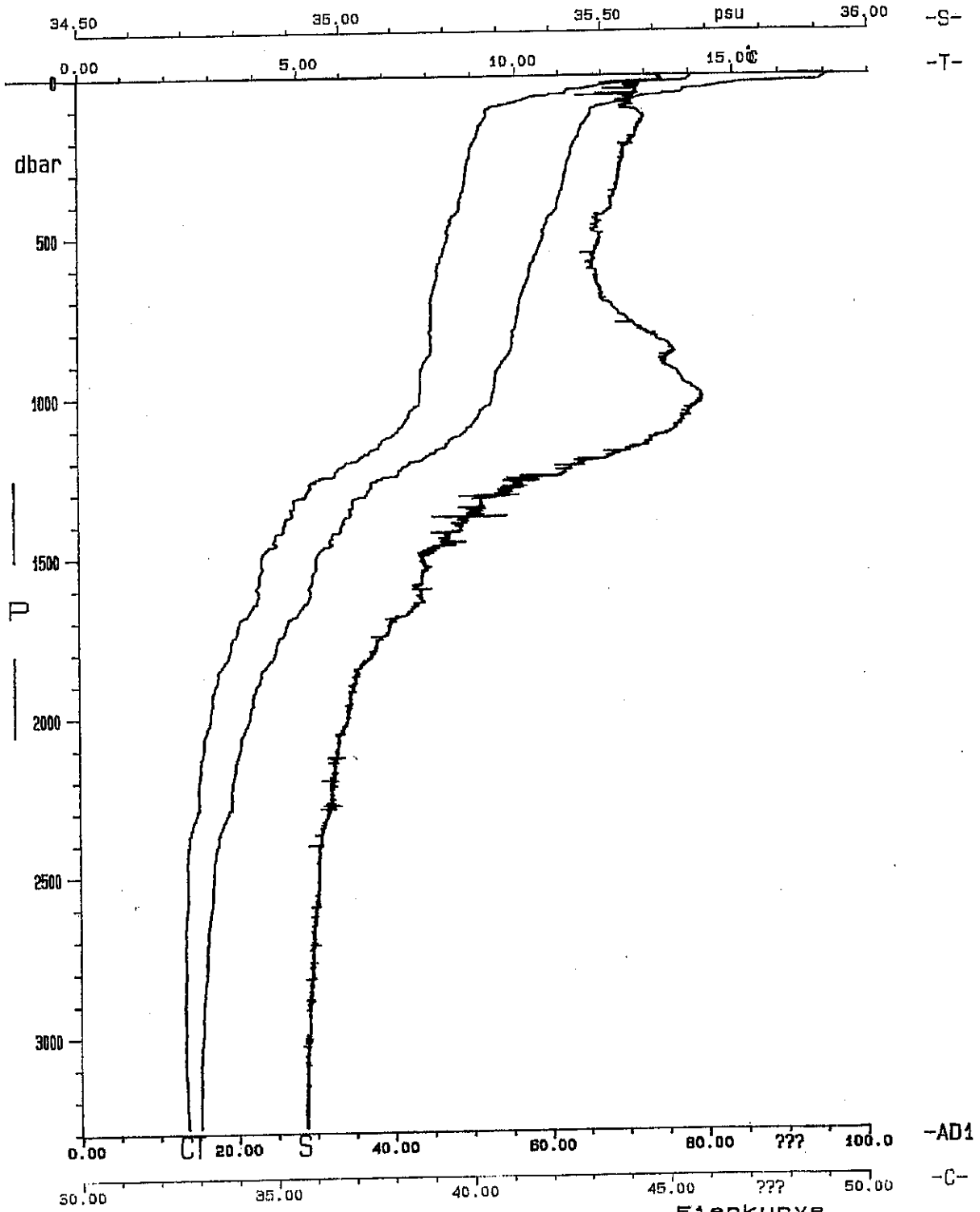

Station	Schiff	Reise	Position	Datum
296/001	METEOR, 13	364	48 21.0 N 10 24.4 W	01.09.1996 02:29

Fig. 79: CTD profile at the Whittard fan site at 3240 m water depth.

Parasound records have been acquired on all hydrosweep profiles for mainly two purposes:

- to get information about the nature of the ocean bottom and shallow subsurface around CTD, GKG (large box corer), and BWS (bottom water sampler) stations;
- to image the shallow sedimentary layers and structures in high resolution.

Many parts of the canyon flanks are too steep to get good parasound records, but if the topography is smooth enough, penetration down to around 50 m and resolution of locally more than 8 layers can be obtained.

At water depths of less than about 300 m in the shelf area, the image of the shallow subsurface completely differs from the seaward part of the Whittard Canyon formed by the ridges with basin-like structures inbetween. Areas where penetration depth is minimal, not exceeding about 10 m, are quite common. The topography in this area is nearly flat. This is interpreted to be caused by coarse, hard sediments which are not penetrated by the parasound signal with a coverage of fine, water-rich mud on top. Further downslope penetration is much better.

In the parasound records, the sediments of the Whittard Canyon fan are clearly expressed. The 3200 m isobath seems to be the seaward border of the fan sediments. It seems to be a change between layered sequences and sequences of more turbiditic character. The NIOZ station shows up to 6 sharp layers typical for hard sediments.

The sediments of the Austel Spur are clearly expressed in the parasound records and penetration down to around 50 m and resolution of locally more than 10 layers can be obtained.

5.4.4 **Microbiology in the Benthic Boundary Layer** (K.-P. Witzel, W. Ritzrau)

During this leg we focused on two major aspects of microbiology in the benthic boundary layer. Firstly, the microbial modification of organic matter in the benthic boundary layer (BBL) and the adjacent water column was assessed by rate measurements, and secondly, the structure of the microbial community will be used to elucidate the origin of particles in the BBL.

Micro-organisms mediate the modification and transformation between particulate and dissolved organic matter. Applying two different rate measurements, bacterial production via ^{3}H-Thymidine incorporation and bacterial protein production (BPP) via ^{3}H-Leucin incorporation, we studied the role of micro-organisms in water samples in BBL and, for comparison, in the intermediate and the euphotic zone of the water column at all stations along the main canyon transect. As described for other areas bacterial production and BPP was significantly higher BBL compared to the intermediate water column. Along the trough axis the highest rates were found on the shelf down to 700 m. The deeper stations displayed a decrease in the measured rates. Further analyses of bacterial abundance and the size distribution, as well as particle composition, will help to explain the activity pattern samples retrieved with bottom water sampler and during CTD casts.

In order to analyse the community structure, water from different depths and the sediment surface were taken at different stations along the canyon axis, and for comparative purposes, also from several other stations during this leg. On board the ship, the bacteria from up to 40 l of water were harvested by tangential flow filtration and subsequent centrifugation. The pellets, as well as the sediment samples, were frozen at -80°C for further transportation to the lab. After extracting DNA in the lab, we will follow two major lines of further research:

1 For analysing and comparing the population structure of general eubacterial communities, we will amplify with PCR (polymerase chain reaction) 16S rDNA of eubacterial origin. Sequence differences of the PCR products will be resolved by denaturing gradient gel electrophoresis (DGGE). Thus, differences in the community structure should be visible by different banding patterns. A more detailed analysis of the nucleotide sequence of the 16S rDNA will provide information about the taxonomic affiliation of the bacterial populations in the different samples. New, previously unknown bacteria have to be expected due to the direct amplification from natural samples.

2 In a more specific approach, we will focus on nitrifying and denitrifying bacteria in these samples. We expect that especially these two groups of bacteria might show differences due to the different availability of oxygen and nitrogen compounds in the water column, the BBL and the sediment. Moreover, their taxonomic composition is less complex, and we have had good experiences from previous studies in freshwater. We will study autotrophic ammonia-oxidizing bacteria in these samples by PCR with group-specific primers for 16S rDNA, and the gene of ammonia-monooxygenase, the key enzyme of ammonia oxidation. Analysis of the nucleotide sequence of the PCR products by restriction enzymes (RFLP), DGGE and sequencing should allow us to identify the dominant nitrifying bacterial populations, and to compare possible differences in the community structure. In a similar manner, we will use sequence differences of the nitrite-reductase gene to describe the composition and activity of the denitrifying bacterial communities. The combination of rate measurements and the genetic analyses of the microbial community will enhance the understanding of the role of micro-organisms for the organic matter dynamics close to the sea floor.

5.4.5 Distribution of Methane and $\delta^{13}C$ of total CO_2 (M. Friedrichs)

A CTD was used to obtain water samples from the water column at different depth intervals and from several stations. Special attention was paid to the canyon area. In this area, samples were taken along a transect following the outline of Whittard Canyon. The purpose of this investigation was to determine the pattern of vertical and horizontal distribution of methane and the $\delta^{13}C$ of total CO_2 in the water column. Therefore, a set of water samples has been taken for the analysis of methane, methane isotope balance and $\delta^{13}C$. In addition, the oxygen and phosphate content of these samples was determined on board.

5.4.6 Processes in the Benthic Boundary Layer at the Whittard Canyon

(L. Thomsen, G. Graf)

The second aim of M 36/4 was to investigate modern continental slope and rise processes. The quantification of fluxes across the ocean margin is a fundamental requirement for the evaluation of the global carbon budget between the continents, the coastal zone and the open ocean. It has been widely recognised today that there is a lack of knowledge and understanding of the processes occurring at the ocean margins, which is critical for the evaluation of global biochemical cycles. The OMEX (Ocean Margin Exchange) programme of the EU concerns the study of ocean margin fluxes and processes along the European shelf break facing the North Atlantic Ocean. Within this interdisciplinary programme, the "benthic processes" subgroup investigates the benthic boundary layer as a possible area of element recycling before final deposition. During the first three years of the programme it became evident that the vertical flux of particles was not sufficient enough to balance the benthic carbon demand, and that lateral advection had to be invoked. However, within the OMEX I box between Porcupine Seabight and La Chapelle bank, the huge "canyon area" was excluded from the investigations due to the expected difficulties in sampling. During M 36/4, a first approach was made to study the processes within the canyon systems between Merriazek Terrace and King Arthur Canyon.

The purpose of the M 36/4 cruise was to briefly examine the bottom topography and morphology of one canyon of the Whittard Canyon site (REID and HAMILTON, 1990), and to combine the data with results from an intense biological survey in both the benthic boundary layer and the surface sediments.

5.4.6.1 Shipboard Results

The survey was carried out over 7 days at the end of August 1996. In water depth of between 170 m (shelf) and 3700 m in one canyon, CTD casts, bottom water samples and sediment samples were taken, underwater video pictures of large particles > 100 micrometer and of the sediment surface were occupied, and bottom currents were measured. Extended hydrosweep and parasound profile work was carried out in order to determine canyon morphology and topography. Additionally, in co-operation with the Technical University of Hamburg-Harburg, (Prof. G. Gust), sediment samples were exposed to increasing shear in order to determine the erosion resistance of the different sediment types.

During a second investigation, nepheloid layers in an area covering King Arthur Canyon, Austel Spur and Whittard Canyon were determined between 800 and 2000 m, the depth where internal waves are supposed to erode the sediment surface.

With the hydrosweep profiles, the canyon topography between 48° to 48°50 N, 10° to 10°40 W was determined. The canyon is slightly S-shaped and approx. 40 nm long before entering the fan system (Fig. 80). At around 2300 m, two other canyons cross the major canyon axis. The upper canyon is characterised by areas of enhanced sediment deposition caused by infilling of blockages of the canyon channel. These blockages form a barrage, behind

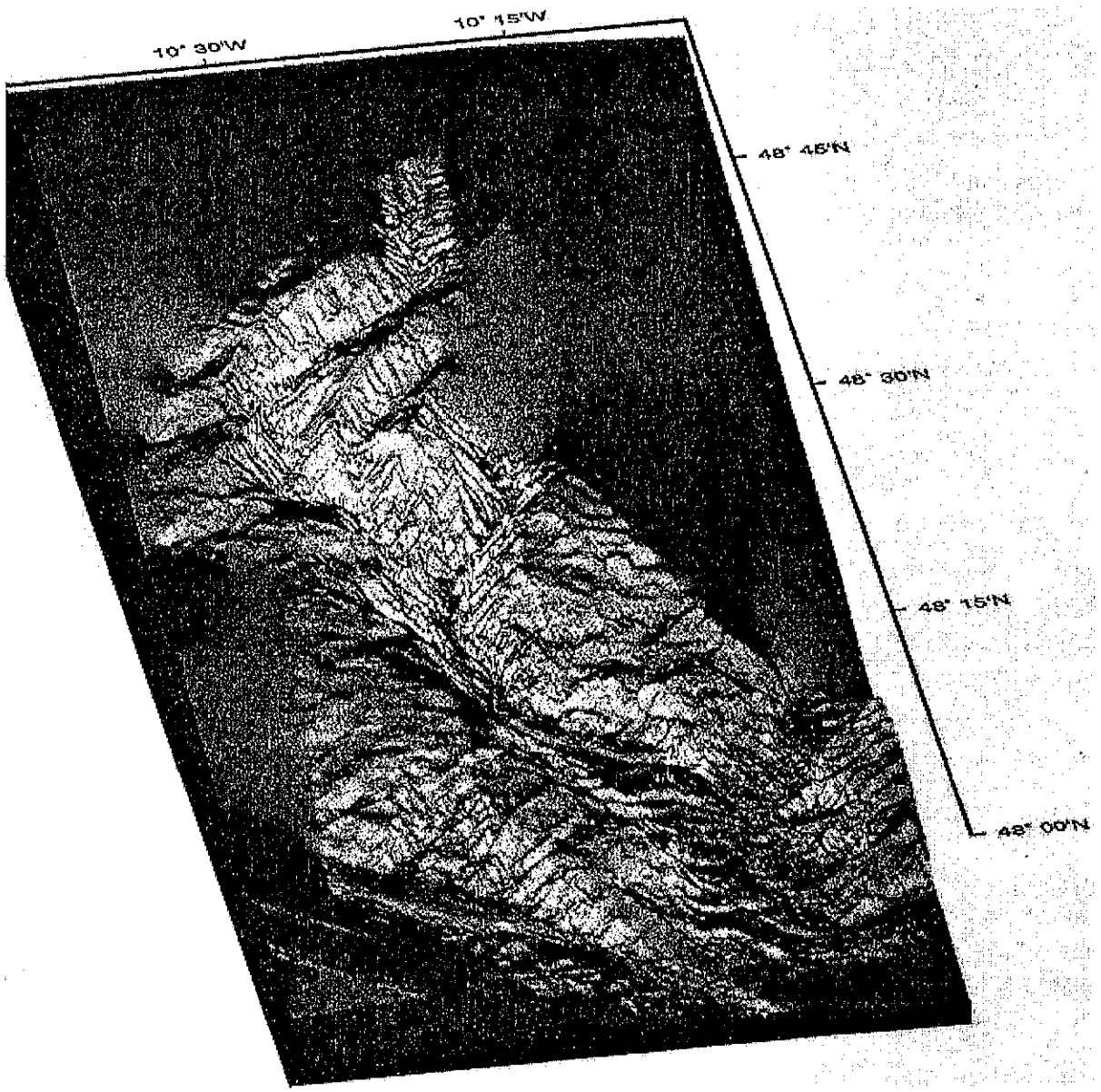

Fig. 80: Plot of the Whittard Canyon site: top=shelf, bottom= fan system around 4000 m.

which deposition from sediment gravity flows would take place. This was found around 700 m, where sediments were of fine sand with a layer of silty sediments at the top and macrofauna seem to be dominated by deposit feeders. Flow velocity was low at that site. Around 1500 m sediments were occupied by interface feeders. Critical bottom shear velocity (u*c) was highest (1.7 cm/s). From 1500 to 3600 m the u*c decreased to 1.2 cm/s. At all stations silty sediments at the sediment surface were easily eroded (u*>0.5 cm/s). The sediment surface seems to increase in carbonate and water contents, thus decreasing sediment stability. Flow velocity decreased again. Large particles measured with a particle camera were found all the way down to the fan system and a settling tube provided initial data for particle settling velocities in the deep sea. At deeper waters macrofauna was again dominated by deposit feeders. Current direction was downslope in the upper part of the canyon and stagnant, perpendicular to the canyon axes in the deeper parts.

Evidence of extreme bottom currents was found in the deeper sediment layers (3-20 cm depth) at stations 2700 m and 3600 m. Here, coarse sand sediments reveal the influence of the Easter boundary contour current or massive canyon downslope transport during times of glaciation. However, not coarse sand, but a 10 cm layer of coarse cold water coral relicts was found between 700 m and 2000 m.

The evidence presented so far suggests that the canyon is presently inactive in terms of major fan development and growth process. Fine sediments may be transported downslope due to their erodebility and accumulate at areas of low flow velocities. Between 200 and 2000 m particle fluxes are supposed to be similar to other sites at the continental margin, although barrages of the canyon form depocenters in areas of expected particle erosion. In deeper waters, coarse sand, superimposed by fine sediment accumulation, reveals high energy events during glacial times.

The other aim of the study was to find intermediate nepheloid layers (INL) between 800 and 2000 m. These water layers of enhanced particle content may act as an additional source for downstream particle accumulation. At all stations within the area studied, huge nepheloid layers were found around 700-1000 m water depth. The intensity of the Intermediate Nepheloid Layer (INL) seems to depend on the size of the canyon which feeds these layers. However, no net increase in particle concentration downstream from the canyon studied could be determined. This raises the question whether the canyons are sources of enhanced particle fluxes downstream.

5.4.7 BENGAL: Benthic Bioturbation and Bioirrigation

(R. Turnewitsch, G. Graf)

In August 1996, sediment was sampled with a multicorer in order to quantify benthic bioturbational and bioirrigational mixing processes at a depth of 4830 m at the BENGAL station (49°N/16°30 W).

Three sediment cores (10 cm diameter) were incubated on board in an incubation chest at in-situ temperature for the quantification of bioirrigational activities. The overlying water was sampled to obtain a value for the natural bromide concentration in the bottom water, reduced to a height of about 10 cm and supplied with a small volume of concentrated sodium bromide solution to increase the bromide concentration to approximately 15 times the natural background. The overlying water was aerated and simultaneously mixed by air bubbled slowly through the water. The cores were covered with lids to reduce evaporation and incubated for 7 days. The overlying water was sampled at least once a day. In order to measure the natural bromide concentrations, the overlying water of three additional sediment cores was sampled, and the cores were cut into slices in which the natural bromide background in the sediment is to be measured. The bromide measurements will be accomplished ionchromatographically at GEOMAR.

In the sediment cores sampled for the measurement of the natural bromide concentrations ^{210}Pb will also be measured alphaspectrometrically at GEOMAR via its granddaughter ^{210}Po. With the help of ^{210}Pb activity profiles, information on sedimentary mixing processes on a time scale of 10-100 years will be obtained.

Another sediment core is analysed for ^{234}Th. The core was cut into slices and subsamples have been leached with 6M HCl. Following coprecipitation, acid dilution and anion exchange steps, the solution containing thorium was electroplated on silver planchets. The activity on these silver planchets is measured in a low level beta counter. The ^{234}Th data will yield information on sedimentary mixing processes on a time scale of 100 days.

5.4.8 Benthic Foraminiferal Habitats and early Diagenetic Processes in Deep-Sea Environments (A. Keller)

Benthic foraminifera react very sensitively to the input of organic carbon and therefore they are a proper proxy for the evaluation of the benthic-pelagic coupling. Variations in the flux of organic particles result in changes of the faunal structure of benthic foraminifera, and influence, on the species and individual level, important changes of the shape of chambers, and of specific behaviour. It may effect migration movements in the sediment and result in the contribution of benthic foraminifera to bioturbation. Culture experiments with living benthic foraminifera of the sediment cores of M 36/4 shall be investigated in the laboratory in Tübingen (feeding experiments with benthic foraminifera under high pressure, observations of mobility, chamber formations, reproduction).

Undisturbed sediment samples were taken from a large box corer (GKG) and the multiple corer (MUC). Samples of the first 10 cm of the sediment for cultures in Tübingen were carefully taken and kept cool under 4°C until on-shore treatment. Sediments of the multicorer were sliced in 0.5 cm intervals in the strata 0-3 cm, and in 1 cm intervals for the rest of the core. The sediment slices were fixed and stained with Rose Bengal down to a depth of 5 cm. All samples of the whole core shall be washed by a 30 µm sieve.

5.4.8.1 Shipboard Results

The following eight stations were sampled: station 269 (BENGAL) and seven stations located in the canyon area of the Celtic Sea, in the Whittard Canyon: stations 270, 271, 275, 278, 281, 286, and 296. These stations on the continental margin were chosen for further studies on the exchange processes between the shelf areas and the adjacent open ocean. In the Whittard area, shelf sediment has been found in the canyon system and presumably provides a significant proportion of the material, which at present passes down the canyon and fan system (REID and HAMILTON, 1990). Today, these authors consider the Whittard fan as being "inactive" because of the present high sea level and the infrequency with which catastrophic events such as turbidity currents occur. The period of activity was associated with lowered sea level during Pleistocene glaciations.

The sediment and benthic microfauna of the stations downslope of the canyon show a decrease of the mean grain size, foraminiferal shell size and sand content downfall, whilst mud content and number of planktic foraminifera and radiolarians increase. The changes reflect the increasing influence of pelagic processes away from the canyon mouth and the head of the fan. First observations of the samples of station 270, (water depth 174 m) display a living foraminiferal assemblage dominated by *Cassidulina laevigata* and by deep infaunal species such as *Bolivina spp.*, *Bulimina costata*, *Globocassidulina subglobosa* and *Trifarina sp.* Planktonic foraminifera represent about 20% of the total foraminiferal fauna.

At station 271 (water depth 804 m), planktonic foraminifera are about 60-70%. The living foraminiferal fauna is characterised by *Bolvina spp.* and *Uvigerina peregrina* but in the dead fauna, *Cassidulina laevigata* clearly dominates. *Cassidulina laevigata* and its typical taphocoenosis of dead infaunal species with overwhelming numbers of empty *C. laevigatus* has been found to be an indicator of very high organic carbon fluxes to the upper slope, although this species is a common constituent on highly productive outer shelf areas around the world.

The fact that, in the stations downslope of the Whittard Canyon, the dead assemblage of foraminifera are sorted by shell size confirms that sediments and faunal associations are reworked by fan and canyon surface processes. However, a complete evaluation of the benthic foraminiferal response can only be carried out after a detailed analysis of the whole data set.

5.4.9 Oxygen and Phytopigment Distribution in the Sediment (J.J.M. Belgers)

During leg M 36/4, X oxygen profiles have been measured at a depth of 4830 m. Sediment samples were therefore taken with a multicorer and from two cores (10 cm) per station, oxygen values in the sediment were measured with a micro-electrode (Diamond 737GC). An automatic micromanipulator was used for the insertion of the probes into the cores with steps of 0.1 millimetre. The measurements were made in the core water from 20 millimetres above the surface and down to a maximum of 70 millimetres in the sediment. Oxygen values (mol/l) were calculated after calibration by means of a Winkler titration and plotted against depth (see Figs. 81, 82).

For the calculation of oxygen fluxes through the sediment, porosity of the sediment samples will be measured. Therefore, small sediment cores were taken from multicore samples and stored (at -20°C) for analyses later. All measurements were done in a coldroom at a temperature of 3°C.

For Phytopigments analyses at 6 stations (269, 271, 272, 275, 278, 281), two sediment cores per station were sliced and stored at -20°C. Phytopigments will be analysed at NIOZ by means of HPLC separation. The levels from which sediment slices have been taken are: 0-1 mm, 2-5 mm, 6-10 mm, 11-20 mm, 21-30 mm, 31-50 mm, 51-70 mm and 71-90 mm.

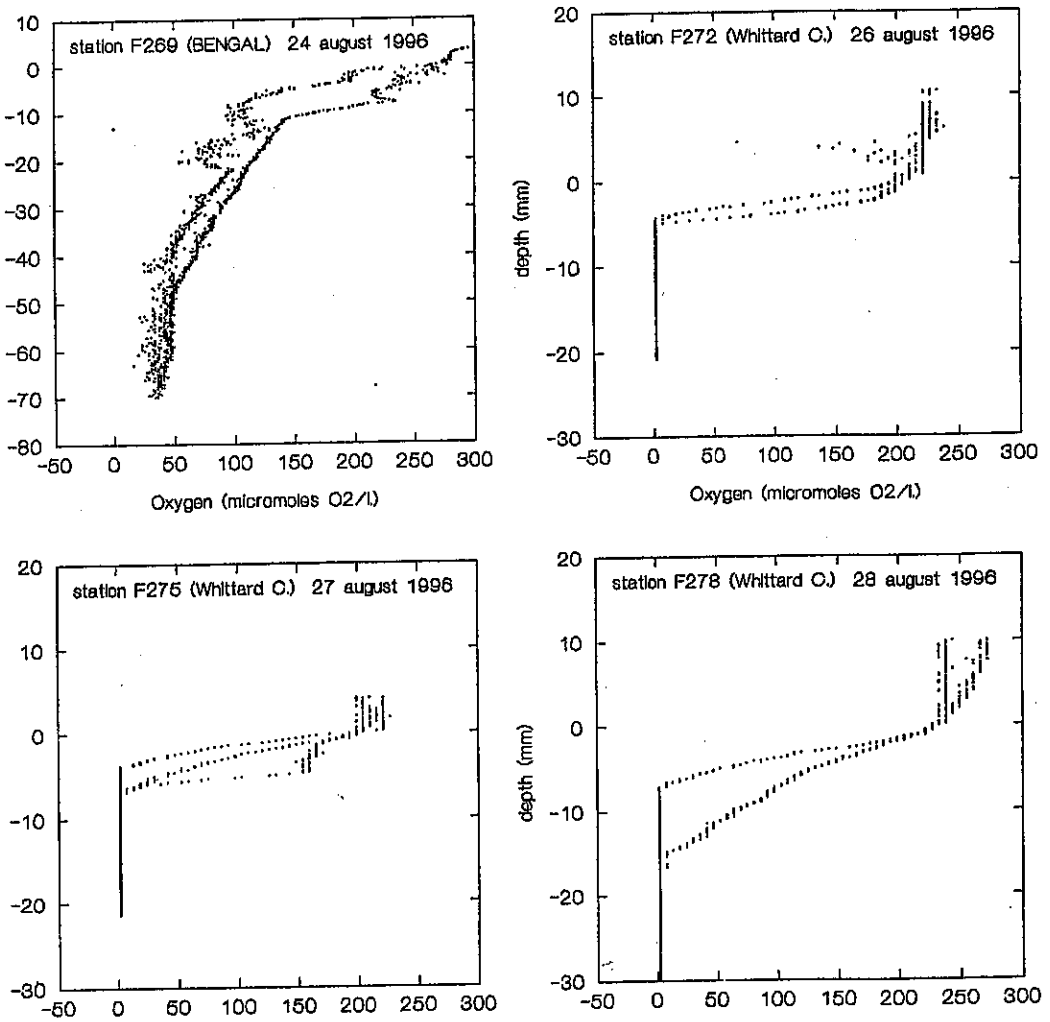

Fig. 81: Sediment oxygen profiles of stations 269-278 (NIOZ).

a

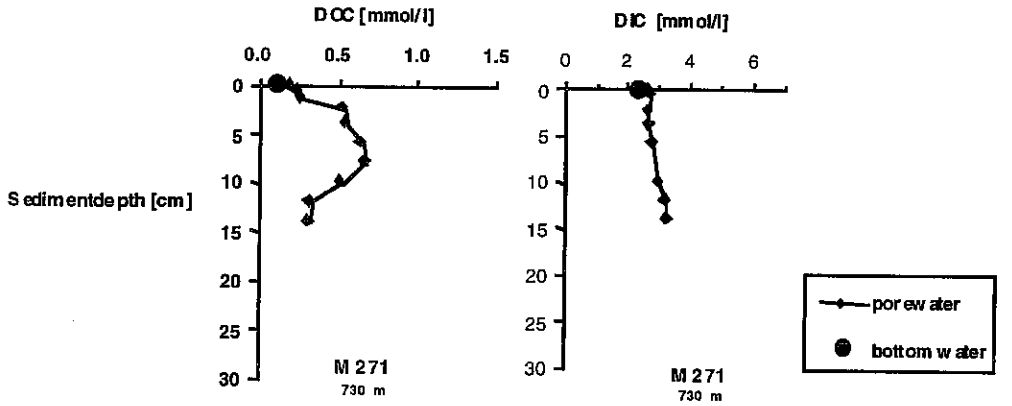

b

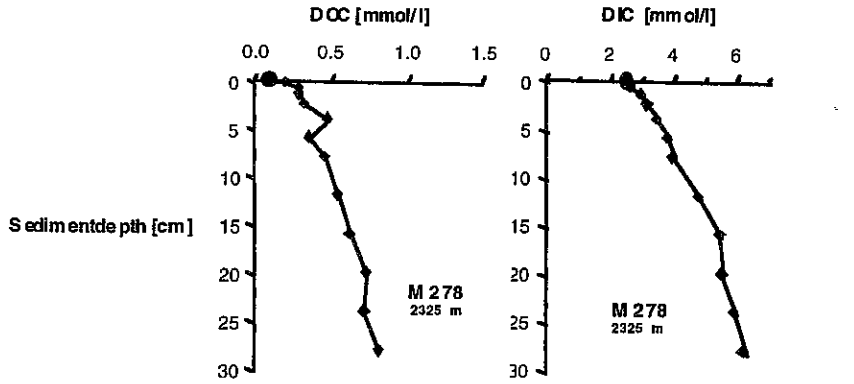

c

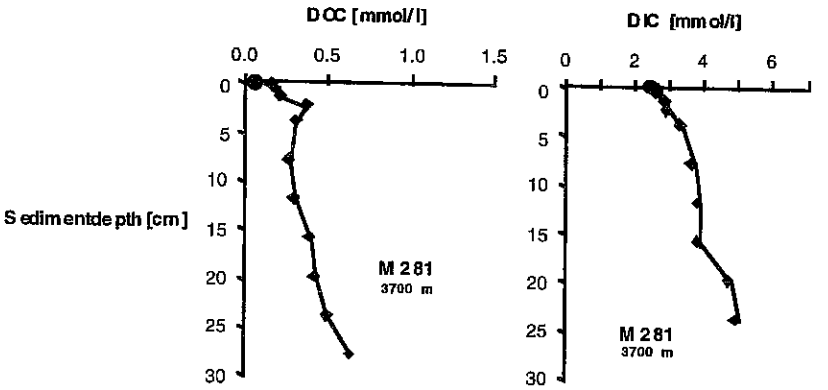

Fig. 82a-e: Selected profiles of pore water species.

d

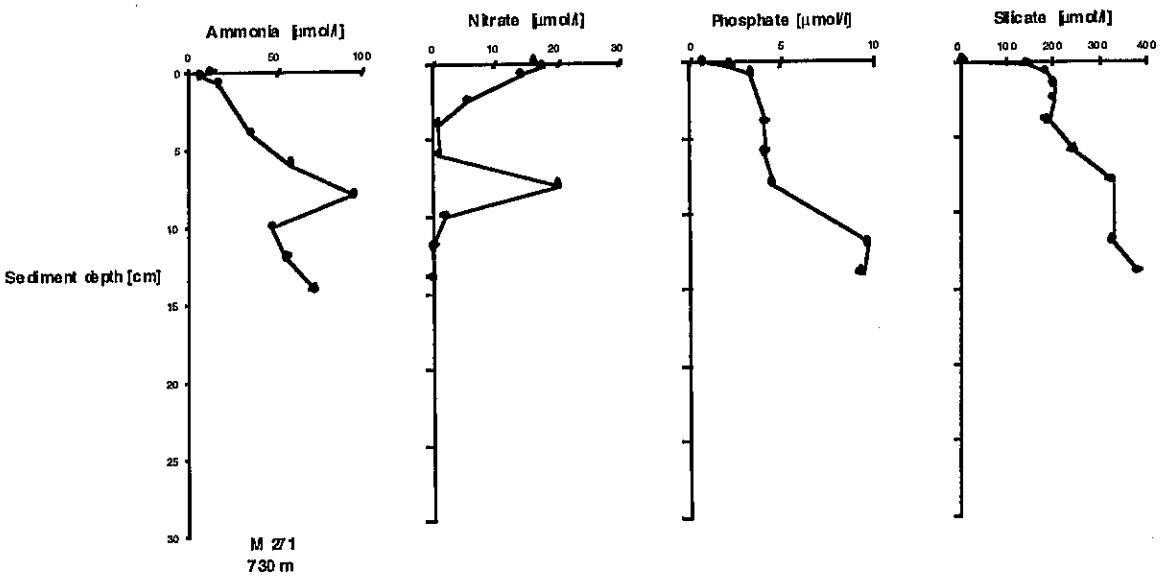

e

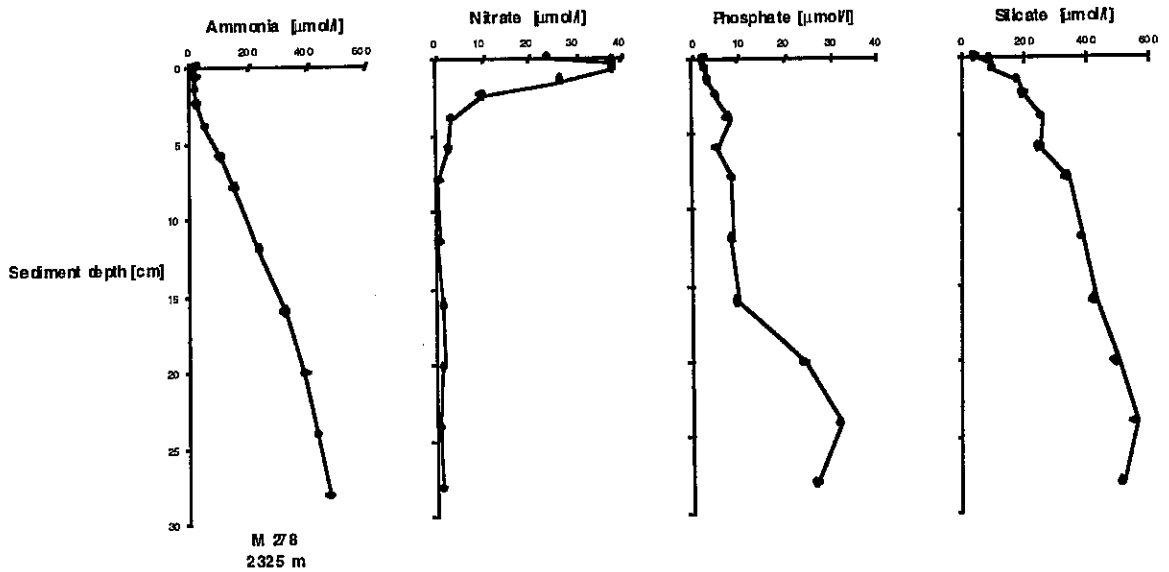

Fig. 82a-e: continued

5.4.10 Organic Matter Degradation, Denitrification and Trace Metal Diagenesis

(S. Otto, T. Stöver, C. Maeß)

At the continental margin, benthic processes are expected to play a significant role for the chemistry of the whole ocean. On one side, the slope sediments may act as a source of trace components for the open ocean, predominately from regions with high intensity of organic matter recycling. On the other hand, the margins may act as a barrier between shelf and open ocean. During benthic remineralization of organic matter the role of dissolved organic carbon (DOC) is poorly understood. Production of DOC during diagenetic processes may result in an underestimation of the amount of remineralized organic matter by modelling pore water profiles of involved solutes as nitrate or oxygen, for example. The role of sediments as a source of deep water DOC and further implications for the organic carbon cycle are also unknown.

A detailed investigation of early diagenetic processes acting within the sediment is necessary for the understanding of the major controls over release fluxes from the boundary sediments. Therefore, samples for the determination of the redox sensitive parameters manganese, iron, nitrate and ammonia were taken from bottom water and pore water along the transect, as well as for phosphate, silicate, trace metals, DOC and dissolved inorganic carbon (DIC).

Sediment samples from the multicorer were taken from all stations along the canyon starting at 167 m water depth to 3770 m. Besides the analysis of the parameters of the interstitial water as indicated above, analysis of the dinitrogenoxid (N_2O) concentration of the sediment and the bottom water were also performed in order to determine denitrification rates. Porosity samples were also taken from each sediment core. DOC samples from the bottom water sampler were taken at the same stations. These water samples were filtrated, acidified, sealed in glass ampoules and stored at 4°C for later determination in Bremen. At some stations, water column samples from the rosette were taken for N_2O.

The sediment cores from the multicorer were sliced in a cool lab at about 2°C. The samples for trace elements were handled in an argon box. The sediment was centrifuged and the pore water filtered through 0.4 µm filters and, together with the overlying water, analysed on board for ammonia, nitrate/nitre, silicate and phosphate within 12 hours. Analysis followed standard colourimetric procedures.

DOC of pore water and bottom water (from the MUC) was determined by high-temperature combustion (HTC) on board. DIC was analysed by injecting the sample on an acidified silica support (160°C) and measuring the amount of CO_2 by IR-detection.
Sediment samples, bottom water and selected probes from the water column were analysed by gas chromatograph (GC) for N_2O within 6 hours after sampling. Because porosity is needed for calculation of N_2O concentration, these results are not yet available.
Porosity will be calculated from weight loss after drying at the home laboratory in Bremen.
Sediment and acidified pore water samples will be analysed on shore by atomic absorption technique for selected trace metals and some major components. Mn and Fe will be analysed

directly from the pore water, other trace metals after pre-concentration and separation from the salt matrix will be analysed by chelation and solvent extraction procedures.

5.4.10.1 Shipboard Results

At all stations in the Whittard Canyon, nitrate/nitrite is depleted by denitrification within the upper 8 cm. Ammonia, as the end product of mineralization of organic N under anoxic conditions, increases with depth in the pore water profiles of all stations, indicating mineralization of organic matter due to (mainly) sulphate reduction.

Compared with the Goban Spur where strong increasing ammonia concentrations could only be detected at shallower sites, the Whittard Canyon seems to be an area of much higher intensity of organic matter recycling with maximum concentrations for ammonia, phosphate and silicate at station M 278.

The DOC pore water concentration increases from bottom water values (MUC overlying water) of 60-120 (mol/l to ~ 0.2 mmol/l in the upper most centimetre) to approximately 0.8 mmol/l in greater sediment depth. While at the shallower stations (M 286 and M 271) the DOC profile shows a maximum; the DOC concentration of the deeper stations increases relatively continuously with sediment depth (see M 278 and 281). The increase in the DIC profile from 2.5 mmol/l to about 6 mmol/l (M 278) and 5 mmol/l (M 281) indicates intensive organic matter remineralization in this part of the canyon, as already recognised from the nutrient results (see Fig. 82a-e).

5.5 Leg M 36/5

5.5.1 Hydrographical Studies (T.P. Zeitzschel, J. Waniek, K. Bülow, P. Schröder)

One of the goals of JGOFS is to determine the processes controlling the carbon fluxes between atmosphere, ocean and sea floor and to quantify marine sinks and sources of CO_2. The aim of the pelagic studies of the planktological JGOFS project at IfM Kiel is to improve the understanding of the processes of particle formation, modification and primary particle export. For the geographical focus of this work, the German JGOFS depicted the BIOTRANS (47°N/20°W) site.

Pre-study: METEOR left Lisbon (Portugal) in very good weather on September 7, 1996, heading for the BIOTRANS station (47°N/20°W). 100 nm southeast of the BIOTRANS station we started our investigations by dropping XBTs (Expendable Bathythermographs, every 30 nm) and taking samples for JGOFS level one parameter from a surface pump system (every 15 nm) and some CTD casts at several positions down to 700 m depth. The pre-study was carried out to get a minimum characterisation of the vertical structure of the hydrographic and

biological field and the spacial variability in the upper 700 m depth and delivered an overview of the general situation in the research area.

The standard sampling device was a combined CTD water sampler with additional sensors for oxygen and Chl.-a fluorescence. On the cruise track between the stations, a surface pump system was used, which delivered samples for the filtration of Chl.-a, particulate organic nitrogen (PON)/particulate organic carbon (POC), PSi, particular $CaCO_3$, HPLC and determination of nutrient concentrations, salinity and the description of the large-scale distribution of phytoplankton biomass.

Detailed study: Based on the findings of the pre-study, a grid 180 x 180 nm around the BIOTRANS station was developed (Fig. 83), which is a combination of CTD casts (700 m), XBT drops (760 or 1800 m) and mainstations: CTD (200 m and down to the bottom), Multi-Closingnets (100, 500, 700, 2500 m and Jojo), Ringnets, Apsteinnets and optical measurements. The resolution of the described grid was also supported by continuous Chl.-a fluorescence measurements, continuous CTD measurements as continuous acoustical current measurements (ADCP, Acoustical Current Doppler Profiler) along the cruise track in the upper 300 m of the water column.

Additional optical measurements were carried out with a bio-optical sensor system at the main stations. This device measures the photosynthetic available radiation (4 pi, 2 pi-downwelling and 2 pi-upwelling), Chl.-a and phycoerithrin fluorescence. In addition, the spectral composition of light and the oxygen concentration are measured down to 100 m depth. Continuous reference measurements of incident PAR radiation on deck complete the optics programme.

After finishing the station work at the BIOTRANS site, we left for BENGAL station 49°N/16°30 W), where only some net samples and one CTD cast down to 3000 m depth were carried out. Because of the good weather conditions at BENGAL station, there was a lot of spare time left, which gave us the possibility to return to the BIOTRANS area and repeat the section (Stat. 307-Stat. 310) east of the central position. This gave us a opportunity to compare the observations along the section with a time interval of 19 days despite a storm (Fig. 83).

5.5.1.1 Shipboard Results

The pre-study showed that the research area is dominated by a summer system: the surface temperatures are relatively high and range between 19-17°C, the measured Chl.-a concentrations have values between 0.2-0.4 µg/l and the nutrient concentrations range around zero (Fig. 84, underway stations 1-20). The Chl.-a concentration measured at the sea surface is correlates well with the sea surface temperature: high Chl.-a content is observed in areas with lower sea surface temperatures and high nutrient content.

The same features are observed in the water column. The vertical temperature distribution in the upper 200 m during leg 5 of the M 36 showed a very shallow mixed layer with a mean depth of

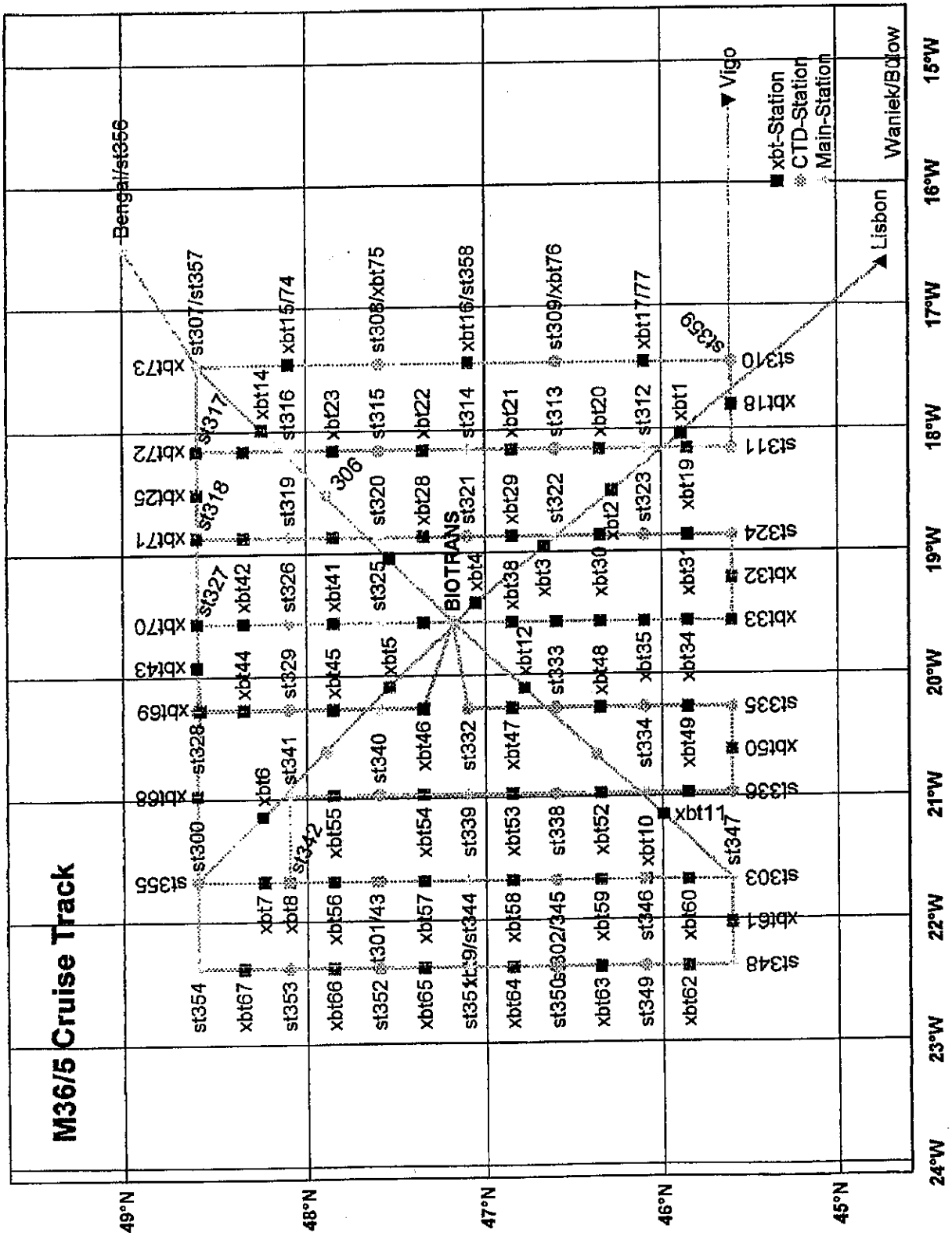

Fig. 83: Cruise track and the research area during M 36/5.

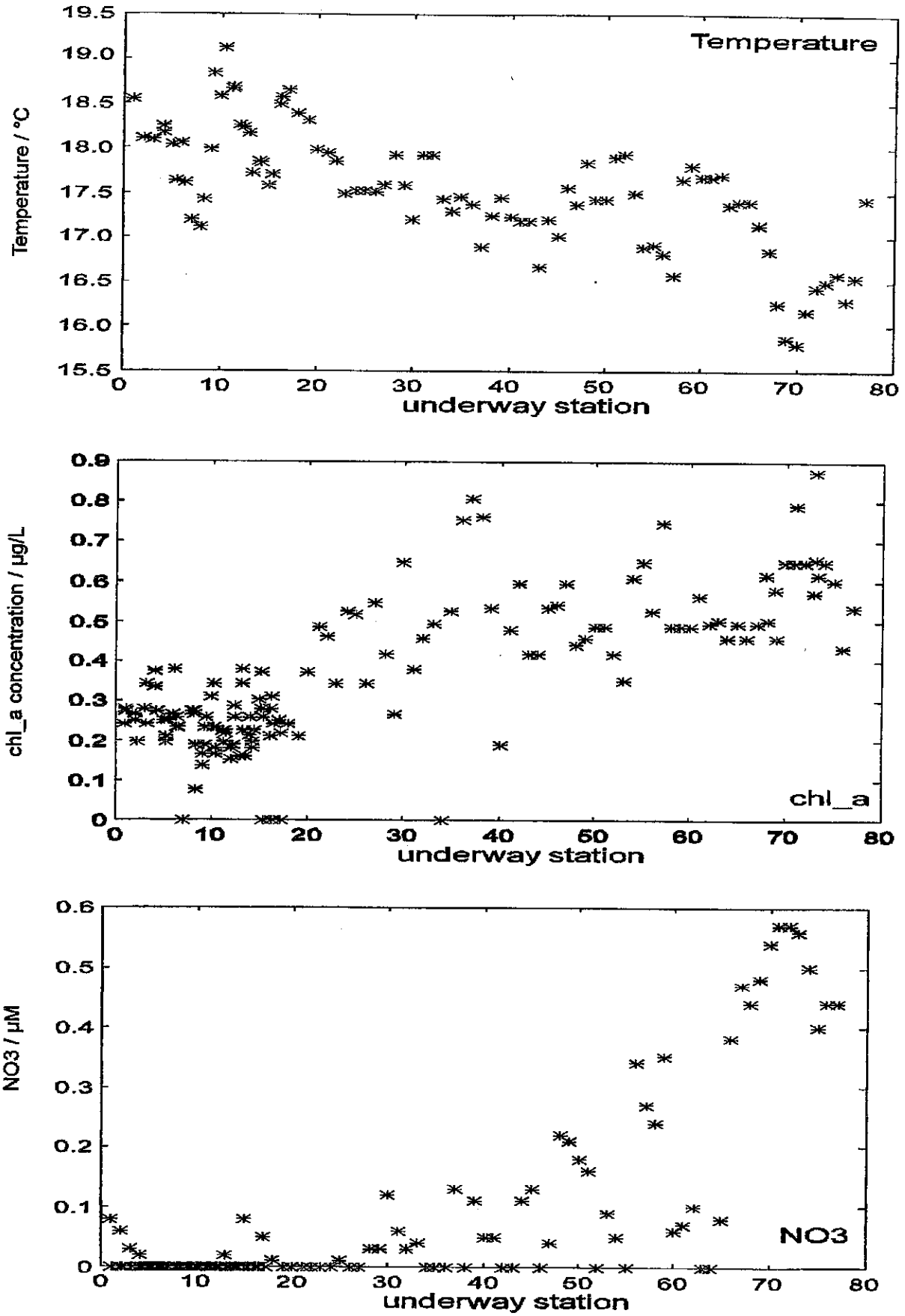

Fig. 84: Temperature (a), Chl.-a (b) and NO_3 concentration (c) at sea surface versus underway station number.

40 m at the beginning of the cruise (Fig. 85). Below the mixed layer was a very stable stratified water column. The main gradient between the mixed layer and the deeper water column was at least 3°C (seasonal thermocline). The dominating conditions are typical for a late summer situation in the open North Atlantic. Nutrients are depleted in this shallow, but very stable surface layer and a subsurface Chl.-a maximum is mainly observed at the depth of the nitracline between 30-50 m depth (Fig. 86).

The vertical distribution changed drastically after the storm events. The surface temperature decreased (Fig. 84, underway stations 25-77), the observed temperature difference reached 1.5°C in the upper 60 m of the water column and the strong vertical gradient in the temperature distribution is more dispersed (Fig. 85). The mixed layer now reached down to 50 m, caused by the turbulent mixing induced by the storm (9 Bft with maxima of 11 Bft). The nutrient concentration at sea surface increased (NO_3: 0.12 µmol; NO_2: 0.03 µmol; SiO_4: 0.38 µmol; PO_4: 0.08 µmol) caused by the transport of nutrients to the euphotic zone from below and the nitracline rose up to depths of 10-20 m. The Chl.-a distribution in the upper water column changed as well, from a subsurface maximum at the beginning of the cruise (summer situation) to a widely-spread area down to 50 m depth with uniform values (Fig. 86).

The summer situation, which is dominating at the beginning of the cruise, changed into a autumn situation.

5.5.2 Dissolved Inorganic Carbon Measurements (C.C. Neill)

On German JGOFS cruise M 36/5, total inorganic carbon measurements were performed on 630 water samples. These data will be used by other groups who participated in the cruise in order to calculate primary production in the area of the BIOTRANS station. The data will also be combined with data from total alkalinity measurements that were done on the cruise in order to calculate a pCO_2 data set.

Samples were collected in 300 ml BOD bottles using the standard technique for sampling for dissolved gases - using a short piece of tubing, avoiding bubbles and overflowing the sample by two volumes. Samples were stored in the dark at 11°C until being analysed. Most (95%) samples were analysed within 24 hours of being collected and all samples were analysed within 36 hours.

The analyses were made by the coulometric titration method using a SOMMA (single operator multi-parameter metabolic analyser) system. The SOMMA collects and dispenses an accurately known volume of seawater to a stripping chamber, acidifies it, sparges the CO_2 from the solution, dries the gas, and delivers it to a coulometer cell. The coulometer cell is filled with a partially aqueous solution containing monoethanolamine and a colorimetric indicator. A platinum cathode and a silver anode are positioned in the cell and the assembly is positioned between a light source and a photodetector in the coulometer. When the gas stream from the SOMMA stripping chamber passes through the solution, CO_2 is quantitatively absorbed,

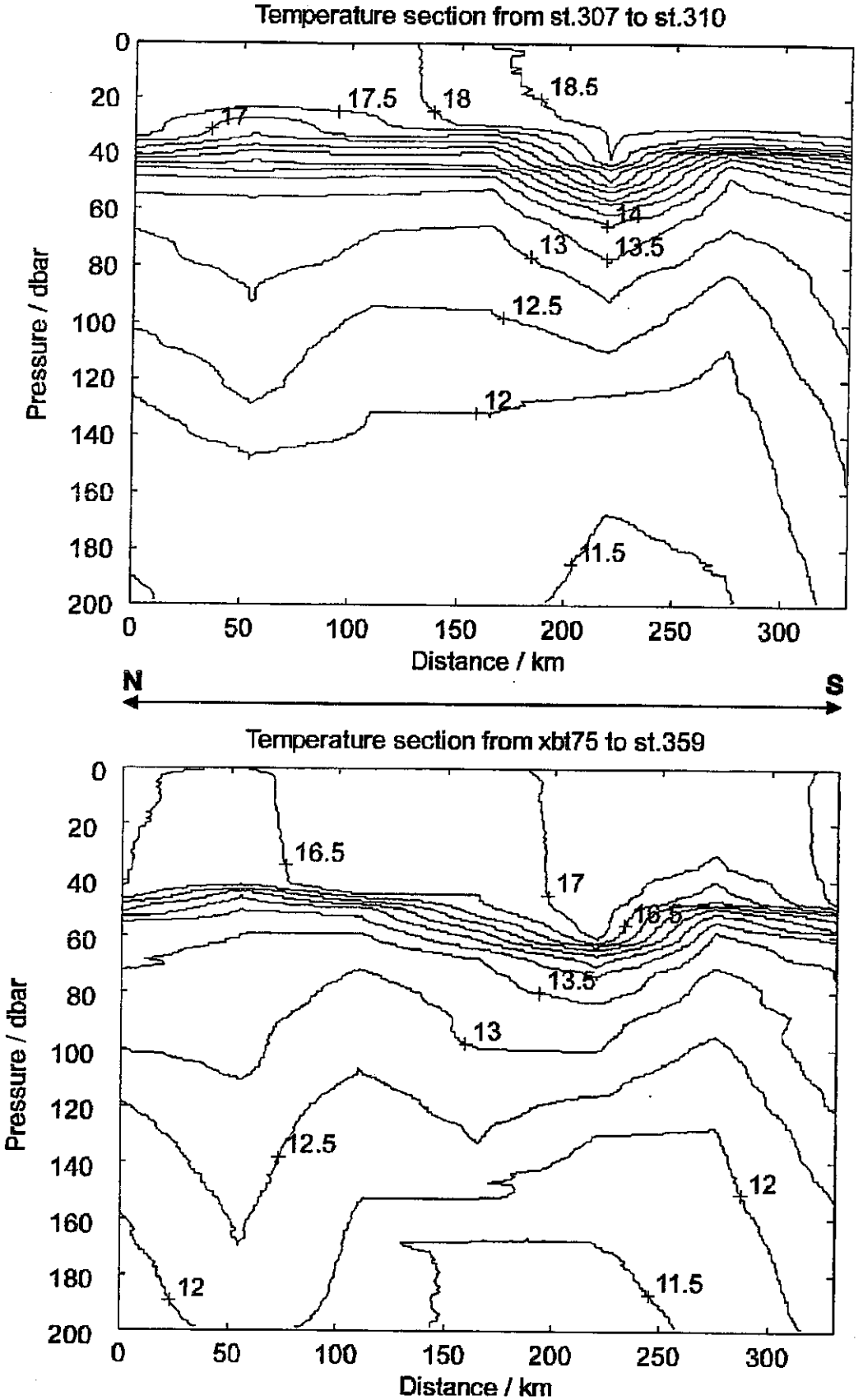

Fig. 85: Temperature distribution in the upper 200 m of the water column: upper panel section (Stat. 307-310), lower panel section (XBT 75-Stat. 359); incl.: delta T=0.5°C, the distance is calculated relative to Stat. 307 and XBT 75 respectively.

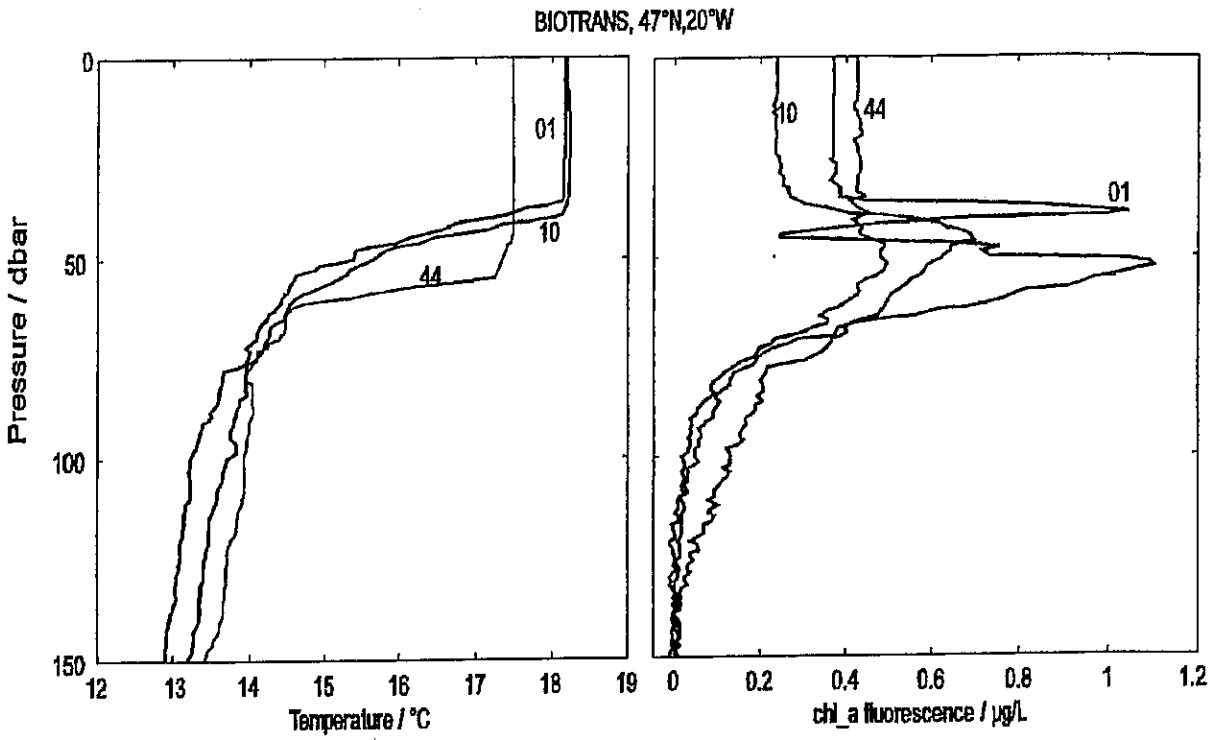

Fig. 86: BIOTRANS station: comparison of vertical temperature and Chl.-a fluorescence distribution for three CTD profiles taken before (profiles 1 and 10) and after a storm event (profile 44) at the central position (47°N/20°W). The continuous Chl.-a fluorescence profiles are calibrated with measured Chl.-a data.

reacting with the ethanolamine to form a titratable acid. This acid causes the colour indicator to fade. When the photodetector sees the colour fade, the coulometer activates a titration current to generate base until the solution reaches its original colour. The titration current is integrated over the time of the analysis, which provides a determination of CO_2 in the sample. Each sample is sparged and titrated until the amount of CO_2 coming from the stripping chamber is at blank level for 4 minutes - this is usually between 10 and 16 minutes per sample.

Calibration: An integral part of the SOMMA is a gas calibration system that is used to calibrate the coulometer. In the gas calibration procedure, each of two gas sample loops are filled with pure CO_2 gas; the temperature of the loop and the atmospheric pressure are automatically measured so that the mass of CO_2 in the loop can be calculated. The contents of the loop are then injected into the SOMMA gas stream - following the same path through the stripping chamber and to the coulometer cell that is used by water sample sparge gas. Each time a new coulometer cells prepared (once per day minimum) three gas calibrations are run.
After the instrument is calibrated, as an additional reference, a bottle of certified reference material (CRM) is analysed. The CRM bottles are prepared by Dr. Andrew Dicksons laboratory at the Scripps Institute of Oceanography. The CO_2 content of each batch of CRMs is analysed by the vacuum extraction - manometric method by Dr. C. D. Keeling, also at Scripps. Normally the CO_2 content measured by the SOMMA should be within 2 µmol/kg (about 0.1%) of the certified value.

5.5.2.1 Shipboard Results

Samples were taken at all hydrographic stations (see chapter 7.5.2, Fig. 87) at a minimum of two depths: surface (10 - 20 m) and the Chl.-a maximum. Full profiles (samples from bottom to surface) of approximately 20 depths were taken on all (11) stations where there were deep CTD casts: numbers 305, 312, 314, 322, 326, 330, 333, 337, 339, 341 and 356. All stations to 700 m were sampled with the number of samples varying from 2 to 12. Once daily a biology station was taken, with 8 depths all in the top 100 metres. Often these were at the same location as a full profile or 700 metre station - giving some stations with a total of up to 30 measured depths.

The precision and accuracy of the measurements were monitored in two ways: by analysing duplicate samples and by analysing the certified reference material mentioned above in the methods section. 50 pairs of duplicated samples were taken and analysed during the cruise (2 or 3 pairs per day). For the 50 pairs of samples, the mean difference in measured dissolved inorganic carbon (DIC) was 0.65 µmol/kg, or about 0.03%. 30 bottles of certified reference material were analysed during the cruise - at least one and usually two for each coulometer cell that was used. The mean measured value of the CRMs was 1875.99 (0.84) µmol/kg. The certified value of the material is 1876.57 (1.27) µmol/kg. The values in parentheses represent one standard deviation.

5.5.3 Alkalinity and pH Measurements (J.M.G. Pineiro)

The carbonate system in seawater has four parameters, these are: pH, total inorganic carbon (TIC), alkalinity and partial pressure of carbon dioxide. With two of these parameters and the appropriate thermodynamic relationships, we can calculate the other two. We use the potentiometric method to determine the pH and alkalinity of seawater. With the in-situ temperature and salinity we will evaluate the values of the total inorganic carbon and the partial pressure of carbon dioxide. The values of the partial pressure of carbon dioxide will serve to determine the transfer of carbon dioxide from the atmosphere to the ocean or vice versa.

The following analytical equipment and methods were used:
pH: The determination is made with a combined electrode Metrohm 6.023.100 connected to a Metrohm 654 pH meter. A Pt-100 temperature probe connected to the pH meter is used to correct the nerstian behaviour of the electrode to the temperature of the sample.

Alkalinity: The analytical system is composed of a combined electrode Metrohm 6.023.100 and a Pt-100 temperature probe which is also connected to an automated Metrohm 716 DMS titrator.

pH measurements: The samples (see chapter 7.5.3) were analysed within one hour after the sampling was finished. The pH meter was calibrated once a day with NBS buffers and then

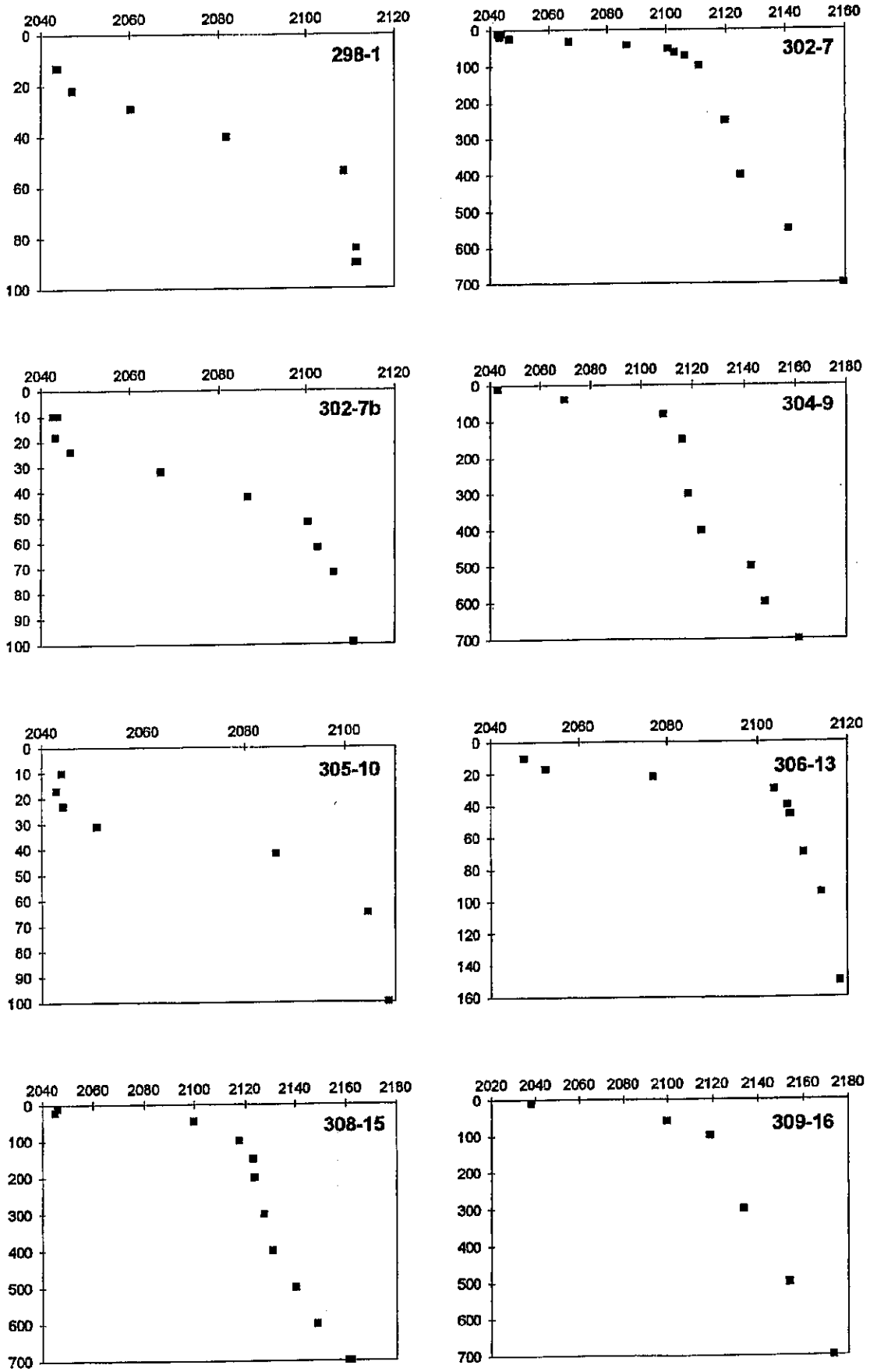

Fig. 87: Hydrographic stations showing water depth versus CRM values (µmol/kg).

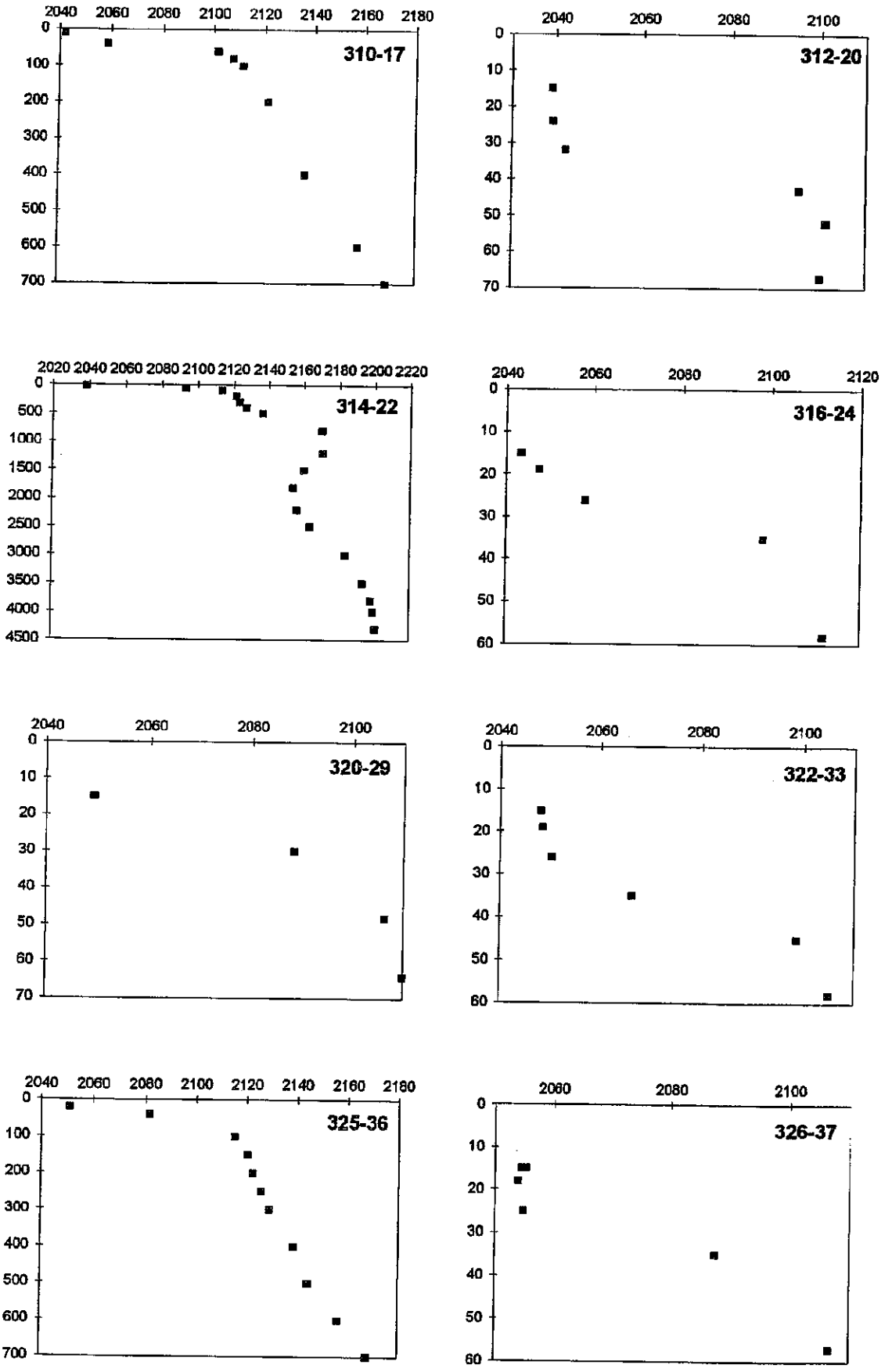

Fig. 87: continued

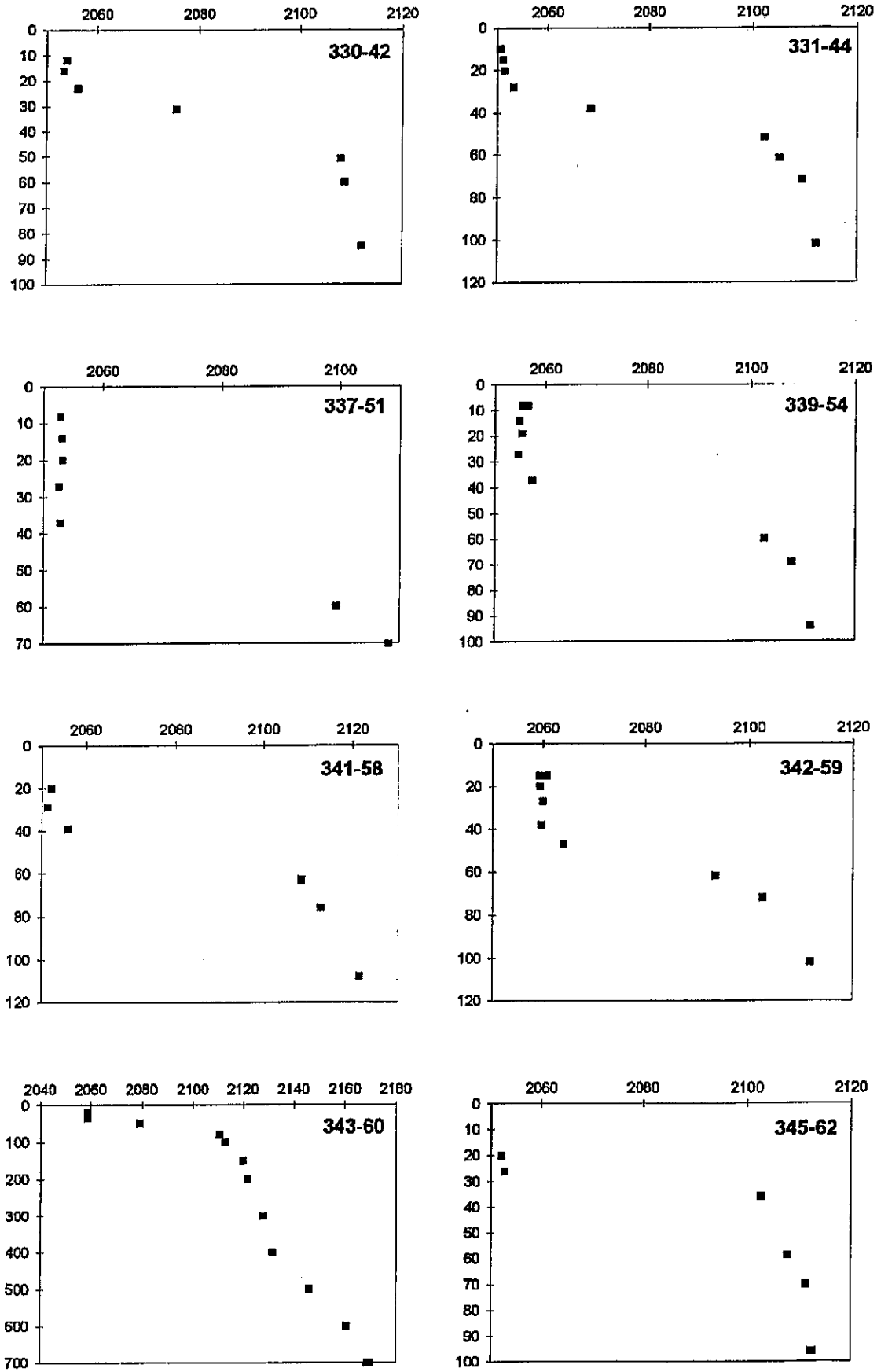

Fig. 87: continued

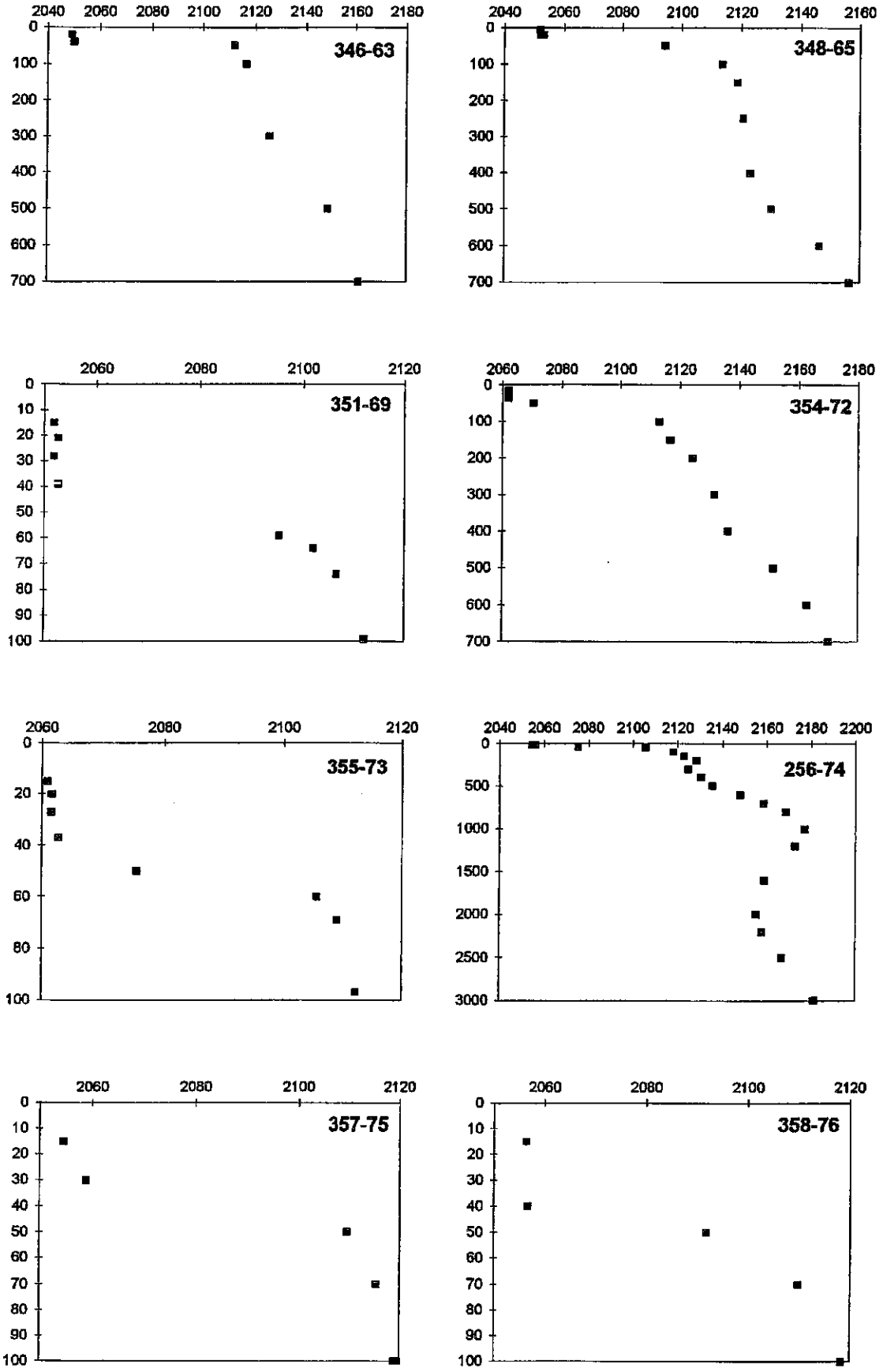

Fig. 87: continued

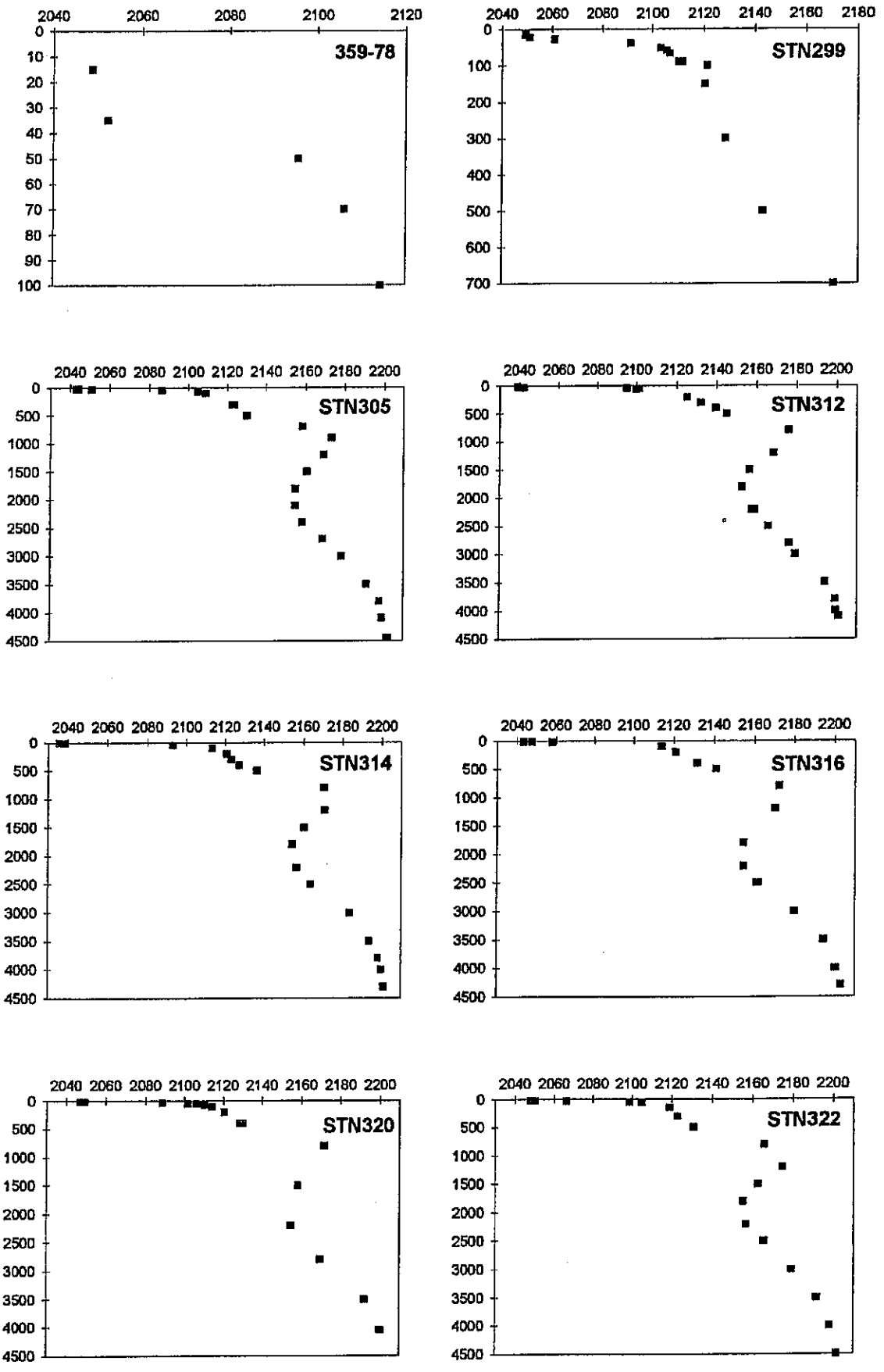

Fig. 87: continued

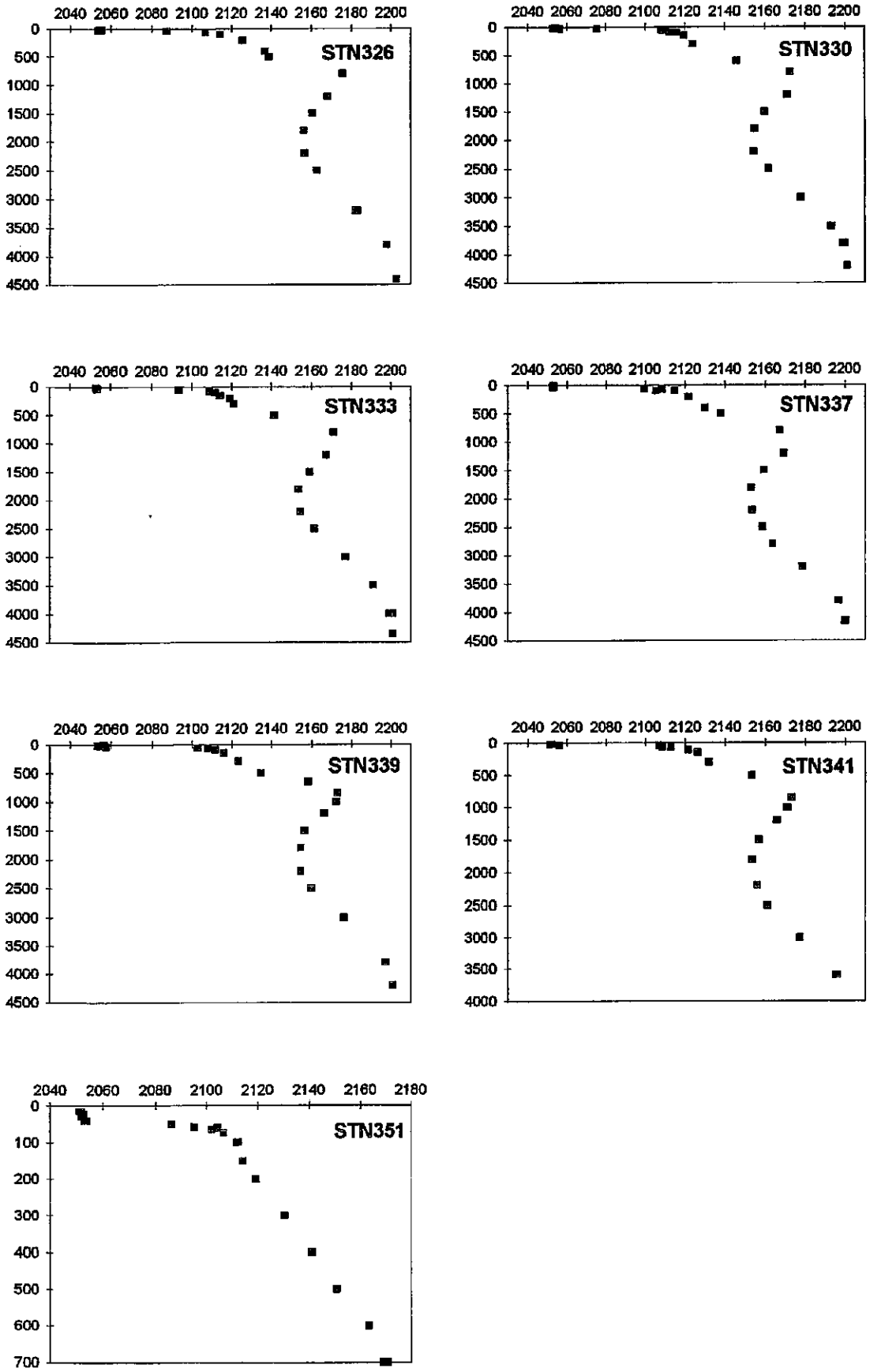

Fig. 87: continued

adapted to the ionic strength of seawater with a pH 4.4 buffer prepared in seawater. The drift of the electrode was controlled with a substandard (surface seawater filtered and stored).

Alkalinity measurements: The pH method was used which is essentially a single point potentiometric titration. The calibration is as described for pH measurements. 250 ml of sample is acidified to pH 4.4. The alkalinity can then be calculated from the difference between the amount of acid added and the excess acid present. The samples were stored in the dark in a cool room (about 10°). As a reference, CRM (Certified Reference Material) supplied by Dr. Andrew G. Dickson from the University of California were used. Also, a substandard was used to control the drift of the electrode (see chapter 7.5.3).

5.5.4 Bacterial Degradation of Organic Matter (C. Petry, D. Setzkorn)

In addition to the investigations in the water column conducted by the planktological-hydrographical team from Kiel, the microbiology group from the IOW provided measurements of bacterial parameters to get an idea of bacterial degradation rates in the planktonic system of late summer/early autumn. Sampling was closely linked to phytoplankton and primary production studies to measure bacterial production (via ^{3}H-thymidine incorporation), bacterial growth (via ^{3}H-leucine incorporation) and to take samples for the quantification of bacterial cell numbers (JGOFS level 1 parameters). Measured rates are supposed to contribute to the parametrisation of carbon cycling models. To complete our understanding of bacterial degradation processes in the water column, experiments were conducted where the influence of temperature on these processes was examined.

5.5.4.1 Shipboard Results

Particular organic material (POM, > 0.16 µm) from different depths (42 m , 100 m, 850 m and 4500 m) was enriched in a ratio of 1:2 via 'tangential flow' and incubated in the dark under simulated in-situ temperature conditions. Additionally, POM from 850 m (8°C) and 4500 m (2°C) depth was incubated at 15°C. During the 3 week incubation time, different bacterial parameters (extracellular exoenzymatic activity and bacterial production) and the O_2-consumption rate were measured. Samples were also taken for the determination of bacterial cell numbers, POC/PON, DOC/DON, dissolved and particulate amino acids and carbohydrates, as well as for the determination of the concentration of nitrate and ammonia. Among the above mentioned parameters, extracellular exoenzymatic activity, O_2 concentration and nutrient measurements were conducted and partly analysed on board.

The determination of exoenzymatic activity in the beginning of the experiments was problematic. In the oligotrophic late summer system, activities of most of the enzymes are probably too low and cannot be determined via fluorigenic model substrates. Among the investigated enzymes a- and b-glucosidase, chitobiase, esterase and aminopeptidase in fresh seawater, only the determination of esterase activity gave reliable results. Later, during the

experiments, i.e. with increasing age of the POM in the water, hydrolysis rates increased at 15°C incubation temperature, so that exoenzymatic activities were measurable. In seawater samples from 850 and 4500 m depth that were incubated at 8 and 2°C, respectively, measurements were questionable.

Esterase activity decreased with increasing depth and decreasing temperature (Tab. 9). The temperature rise from 8 to 15°C in 850 m water and from 2 to 15°C in 4500 m water revealed an effect only in the former case. Activity increased in 850 m water and was then as high as in 100 m water at 15°C. In 4500 m water the temperature rise did not cause an increase in activity during the first 10 days.

Tab. 9: Overview of the extracellular esterase activity. Hydrolysis rates during incubation are given as minimal and maximal values.

Incubation temperature	Water depth	Hydrolysis rates (pM/h)
15°C	42 m	1300-4500
	100 m	1200-3900
	850 m	1000-3800
	4500 m	500-900; 3000*
8°C	850 m	800-1600
2°C	4500 m	500-900

*) This value was measured on the last day of the incubation, after 19 days.

O_2 consumption rates decreased strongly at 15°C in water from 42 m and 100 m depths. At 2°C, O_2 concentrations did not change at all. In 850 m and 4500 m water, the temperature rise caused an increase in the O_2 consumption rate.

At the same time, ammonia concentrations increased in all incubations. Both in 42 m and 100 m water at 15°C, and in 850 m water at 8°C, an increase from 0.1 to 1.0 µmol/l NH_4^+ was observed. In 850 m water at 15°C, the increase was smaller with 0.1 to 0.6 µmol/l NH_4^+. In 4500 m water, ammonia concentration rose from 0.1 to 0.4 µmol/l NH_4^+ at 2°C. Here, NH_4^+-concentrations were also lower at the end of the 15°C incubation.

In all treatments nitrate concentrations increased slightly. During the incubation nitrate concentrations rose from 2.25 to 5.43 µmol/l NO_3^- at 42 m and 15°C, from 6.83 to 7.63 µmol/l NO_3^- at 100 m and 15°C, from 18.74 to 18.98 µmol/l NO_3^- at 850 m and 8°C and from 22.21 to 22.45 µmol/l NO_3^- at 4500 m and 2°C. The temperature rise in 850 m water caused a slightly higher nitrate value at the end of the incubation at 15°C (19.20 µmol/l NO_3) and in 4500 m water a slightly lower value (22.39 µmol/l NO_3^-).

In addition to this experiment "untreated" seawater from 42 m, 100 m, 850 m and 4500 m depth was incubated at 15°C, 8°C and 2°C, respectively. Over 2 weeks, extracellular

exoenzymatic activity, bacterial production, growth and bacterial cell numbers were measured to check for temperature dependence of bacterial activity and for the influence of enrichment. In a second experiment, seawater from the Chl.-a maximum and seawater enriched with POM was incubated in the dark at 15°C. The POM for this experiment was taken with a plankton net with 55 µm mesh size from the water column from 60 m to the surface. This kind of experiment was set up for comparison with similar experiments conducted in the Arabian and in the Gotland Sea.

All experiments showed that changes of measured parameters were minor. A comprehensive interpretation of the results will be possible when the analyses of bacterial production, growth and cell numbers, POC/PON, DOC/DON, dissolved and particular amino acids and carbohydrates in the experiments and in the water column are completed.

5.5.5 **Planktological Studies** (C. Sellmer, U. Fehner, K. Nachtigall, C. Reineke, P. Fritsche, K. Lisok, B. Obermüller, D. Adam)

The aim of the pelagic studies of the planktological JGOFS project at IfM Kiel is to improve the understanding of the processes of particle formation, modification and primary particle export. For the geographical focus of this work, the German JGOFS depicted the BIOTRANS site (47°N/20°W). M 36/5 is planned to study the autumn/late summer system; hereby it will add to a number of cruises carried out during other seasons. At the end of summer, oligotrophic conditions are expected to dominate the planktonic system. Nutrients will be depleted in a shallow but stable surface layer and a subsurface chlorophyll maximum is expected at the nutricline (30-50 m). During autumn, cooling starts and the mixed layer deepens; a process that will be forced by storms. This has two concurrent effects on phytoplankton: a stimulated input of nutrients and a decrease of light. In coastal regions, the positive effect dominates: autumn blooms can be detected. There is a lack of observation on this topic for the open ocean.
The aim of this work is first to describe the typical composition and vertical distribution of the main phytoplankton species during autumn, and second, to study the response of phytoplankton community to storm events.

The planktological-hydrographical work group took care of measurements concerned with hydrography, optics, nutrient chemistry, phytoplankton biomass and composition, zooplankton biomass and distribution (including grazing experiments) and planktological bulk variables (POC/N, BSI, $CaCO_3$), as well as rate measurements like those for new and primary production and calcificationrates. To reveal insight into the relative importance of different phytoplankton groups of the measurements - like those for Chl.-a primary and new production - were carried out on different size classes. The group also took care of a significant part of the JGOFS core measurements.
The standard sampling device was the combined CTD water bottle rosette with additional sensors for oxygen and fluorescence. Water sampling for the filtration parameters was concentrated on the upper 200 to 700 m. On the cruise track inbetween the CTD stations the surface pumping system was used to sample the large-scale distribution of nutrients, Chl.-a and

planktological bulk parameters. The sampling was carried out every 15 nm, where XBTs were dropped at a distance of about 30 nm to get a minimum characterisation of the vertical structures in the upper 700 to 1800 m. (For details see chapter 5.5.1)

5.5.5.1 Shipboard Results

Distribution and composition of phytoplankton
For analysing the qualitative composition of the phytoplankton Apstein nets (55 µm and 20 µm mash size) were used. Sampling took place to a depth of ca. 10 m below the Chl.-a maximum. After running the net, part of the sample was studied under the microscope on board and the rest was fixed with formol (endconcentration: 1%) for further studies in the laboratory. Nets ran at 20 stations.

For analysing the quantitative composition and the vertical distribution of the phytoplankton, water samples were taken and fixed with formol (endconcentration: 1%) for Utermöhl-microscopy at CTD and XBT stations. At the CTD stations, samples were taken from the whole euphotic zone (up to 0.1% light depth) and from the Chl.-a maximum layer and the pre-study and the main survey. At the pre-study, six sampling stations were taken each for the whole euphotic zone and from the Chl.-a maximum layer. At the main survey 30 (32) stations were sampled.

5.5.5.2 Shipboard Results from Microscopic Studies of the Net Samples

At every station autrophic dinoflagellates dominated the phytoplankton community. The main species were two Gonyaulax subspecies. They dominated the phytoplankton at every station. In the northeast (Stat. 306, 307), these species represented nearly 90% of the phytoplankton standing stock. The whole phytoplankton biomass was the highest at these two stations. Parallel to the Gonyaulax group, some Ceratium species were important and heterotrophic dinoflageflagellates (e.g. *Protoperidinium depressum*) were present, too. Diatoms (main groups: *Rhizosolenia spec., Bakteriastrum spec.*) were rare. There were only present in high numbers at stations 302 and 303. Small flagellates (< 20 µm), both heterotrophic and autotrophic, were present at all stations. Details about their abundance require further investigations in the laboratory. But the measurement of chlorophyll in different size classes showed that these groups (< 20 µm) are the main fraction of the phytoplankton.

During the main survey, the phytoplankton community showed the same composition as in the pre-study at most stations. The main species were *Gonyaulax spec.* accompanied by Ceratium species and a small number of diatoms. Small flagellates were present, too. In two areas there was a remarkable change in the phytoplankton composition. Firstly, at stations 344 and 351, the abundance of phytoplankton > 20 µm was very low. *Ceratium spec.* were the only present group. Gonyaulax species and diatoms were nearly absent. Therefore, there was a high number of flagellates (< 20 µm) and heterotrophic protozooplankton (tintinnids, radiolarians etc.).

Secondly, at stations 357, 358 and 359, the composition of the phytoplankton changed, too. Here Gonyaulax and Ceratium species dominated the population in the same ranges. Diatoms (mostly *Rhizosolenia spec.*) were present in higher numbers than elsewhere observed.

5.5.5.3 Shipboard Results from Experimental Work for Production Measurements (^{14}C and ^{15}N uptake)

Incubation experiments for primary and new production and calcification rates were carried out on 14 and 7 main stations on the cruise track (Fig. 83). In-situ incubation of the samples was simulated at surface temperature on deck for 12 h (a whole light day). Eight light depths were taken through the euphotic zone: from 100% light (surface) to the 1% light depth (bottom of the euphotic zone). Three light depths for primary and new production were fractionated in the same size fractions as fractionated Chl.-a (total, < 20 µm,< 5 µm, < 2 µm).
The primary production and the calcification rates could be measured directly on board in a liquid scintilation counter. The ^{15}N uptake has to be analysed at home. The calcification rates as well will have to be calibrated at home and thus cannot be represented here.

Like we have seen after the pre-study in the hydrographical data (Fig. 84), the very first phytoplankton observations, and the primary production, the research area was dominated by a summer system. The fractionated primary production rates showed the highest amount in the fraction < 20 µm. This correlates conform with the values for fractionated Chl.-a and the observations we could make for the phytoplankton composition (see above).

The research area showed differences in the SW and the NE region around the BIOTRANS station. The production rates were lowest in the SW with 11 to 22 µmol C/m^2 d, and highest NE of the BIOTRANS site with values around 38 µmol C/m^3 d (integrated from the sea surface to the 1% light depth).

During the surveys there were a few little storm events with 9 to 11 Bft. This caused changes in the vertical distribution (see above). The Chl.-a distribution in the upper water column changed from a subsurface maximum to a widely spread area with uniform values down to 50-60 m depth.
The BIOTRANS station could be sampled before and after a storm event (Fig. 88). The primary productivity values after the storm (14.67 µmol C/m^2 d) were only half as high as before the storm event (28.62 µmol C/m^2 d) caused by the turbulent mixing induced by the strong winds.
Together with the hydrographical observations these preliminary data showed that the summer/late summer situation we found at the beginning of the cruise later changed into an autumn situation.

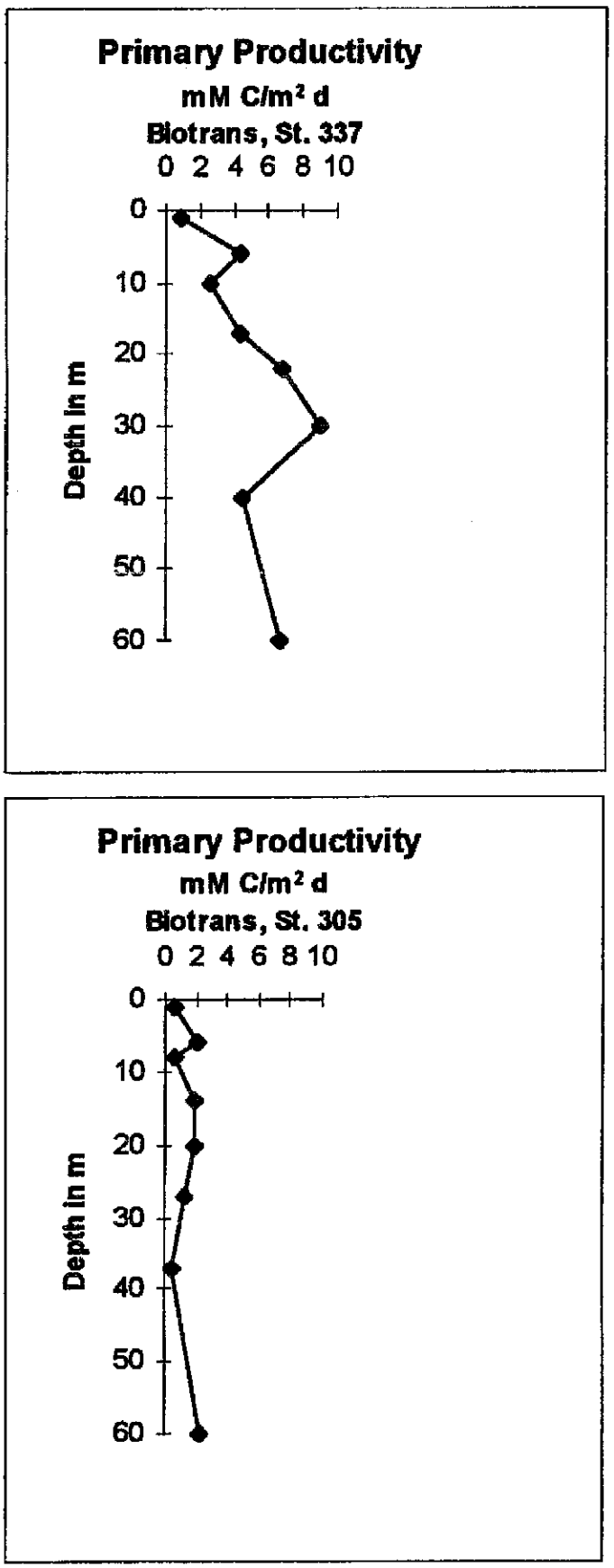

Fig. 88: Primary productivity at the BIOTRANS station before (Stat. 305) and after (Stat. 337) the storm.

5.5.6 Primary Production - P vs I Experiments (B. Irwin)

Water samples were collected with the rosette sampler from the euphotic zone of the water column. The depths selected were 10 metres and the deep chlorophyll maximum. Aliquots of these samples were spiked with ^{14}C sodium bicarbonate and then incubated in a light gradient for three hours. At the end of the experiment the phytoplankton cells were harvested onto glass fibre filters. The dried filters will be taken back to the Bedford Institute for analysis.
Additional samples were filtered for chlorophyll analysis, absorption spectrum and total pigments by High Pressure Liquid Chromatography. The latter analysis will identify the principal phytoplankton groups present.

5.5.7 Zooplankton (U. Zeller)

The vertical structure of communities in the marine environment is of interest from several viewpoints. It gives information on vertical partitioning of the environment especially by congeneric species, vertical migration of species and flux of organic mater.

Zooplankton samples were taken in vertical hauls covering discrete depth layers of about 300, 100 and 25 m thickness, respectively, over a depth ranging from 0-500 metres, on a day-night basis according to JGOFS level-one protocols. The samples were collected from 18 stations along the sampling strategy on and around the BIOTRANS (47°N/20°W) site using a multiple opening and closing net (five vertically-stratified samples per tow with a 200 µm mesh size and a mouth area of 0.25 m^2). These samples will be splitted for biomass measurements (dry weight, POC/PON) and studies on the species composition in comparation to samples carried out during the summer.
The samples for grazing experiments and faecal pellet sampling were taken using a ringnet (200 µm mesh size and a mouth area of 1 m^2) for the water column down to 60 m which covers the depth of chlorophyll maximum. The net was equipped with a non-filtering cod-end made of PVC to prevent damage to specimens. Food uptake was measured by incubating the copepods in the dark in 1 litre bottles on a rotating wheel, in seawater from the chlorophyll maximum depth with phytoplankton of natural concentration. Incubation time was 12-24 hours. The grazing experiments were conducted by the disappearance of chlorophyll (by fluorometra and HPLC) technique. For faecal pellet material, the animals were placed in natural seawater or enrichments (using a 55 µm net) of natural phytoplankton, in specially-designed faecal pellet collectors (fitting with a 200 µm gauze) for at least one day. Faecal material was collected from faecal pellet collectors by opening the top.

5.5.7.1 Shipboard Results

Zooplankton composition was quite constant during the whole investigation time, with a subtropical assemblage of mesozooplankton of high diversity of the different groups (Tab. 10). The highest biomass concentration was found in the upper 50 m. This was found to

Tab. 10: Zooplankton diversity.

Radiolaria	Spumellaria				
	Nasellaria				
	Sarcodina				
Cnidaria	Hydromedusae				
	Siphonophora				
Annelida	Polychaeta			*Tomopteris* spp.	
Chaetognatha					*Sagitta* spp.
Mollusca	Thecosomata				
Crustacea	Cladocera			*Evadne* spp.	
	Copepoda	Calanidae	Calanidae	*Calanus* spp.	
			Eucalanidae	*Eucalanus* spp.	
			Paracalanidae	*Paracalanus parvus*	
			Calocalanus spp.		
			Pseudocalanidae		
	Clausocalanus spp.				
			Euchaetidae	*Euchaeta* spp.	
			Metridiidae	*Metridia* spp.	
				Pleuromamma spp.	
			Centropagidae	*Centropages* spp.	
			Temoridae	*Temora* spp.	
			Acartiidae	*Acartia* spp.	
			Pontellidae	*Pontella* spp.	
		Harpacticoida		Macrosetellidae	*Macrosetella* spp.
			Clytemnestridae		
	Clytemnestra spp.				
		Cyclopoida	Oithonidae	*Oithona* spp.	
			Oncaeidae	*Oncaea* spp.	
	Ostracoda			*Conchoecia* spp.	
	Amphipoda			*Parathemisto* spp.	
	Mysidacea				
	Euphausiacea				
Tunicata	Appendicularia			*Oikopleura* spp.	

be independent of the time of day during the investigation time. The mesozooplankton community was dominated by large calanoid copepods such as *Centropages spp.* and *Acartia* spp., as well as by small calanoid copepods such as *Paracalanus* spp., *Ctenocalanus* spp *Clausocalanus* spp. and *Calocalanus* spp. Together they comprised ca. 80% of the total population. Although some mesozooplankton (Copepoda like *Pleuromamma* spp., *Metrdia* spp.; Chaetognatha; Euphausiacea and Amphipoda), which exhibited diurnal vertical migration, were present in the samples, no conclusive answer can be given at this stage to the

value of diel vertical migration because of the lesser number of these animals in the samples.

A total of 10 grazing experiments were conducted during the investigation time. In the preliminary experiments there was a high decrease in chlorophyll concentration in the bottles without animals (control bottles), which indicated that microzooplankton were present as a active grazer from phytoplankton. To mind this effect, the seawater used for the feeding experiments were preliminarily filtered through a 64 µm mesh size for retention of microzooplankton.
Moderate to low disappearance of chlorophyll (by fluorometra technique) was measured (Fig. 89). In terms of food chain relationships, this means that the transfer of organic carbon to higher trophic levels in this area is influenced not only by the feeding behaviour of herbivorous copepods, but also by microzooplankton. The trophic fate of phytoplankton depends on its size structure, in this case, small cells, which are mostly grazed by microzooplankton protists, and micrometazoans support a „microbial-type" food web. Whereas large cells are ingested by large particle feeders and support a classical food chain. These large grazers probably complete their diet with other available food sources, such as micrometazoans and microzooplanton.

The faecal material collected from the faecal pellet collectors were main copepod faecal pellets approximately 50 - 70 µm in length. The preliminary investigation of the particulate content of the faecal material was conducted on board using a microscope and shows mostly fluffy, amorphous material. In our investigation the faecal material did not contain intact cells or fragments of large diatoms, only certain, and very few, representatives of dinoflagelates were found in the pellets. For more details about the pellet content, scanning electon microscopy will be done in the laboratory at home.

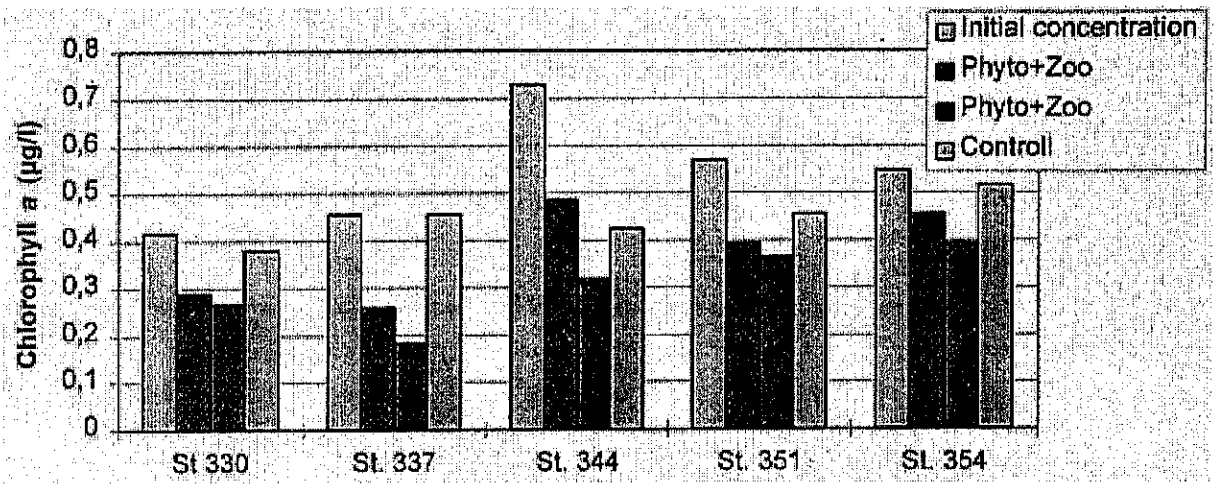

Fig. 89: Disappearance of chlorophyll (by fluorometra technique) on example of 5 station over the investigation time.

5.5.8 Calcareous Zoo- and Phytoplankton (C. Hemleben, R. Schiebel)

Planktic Foraminifera, Pteropods and Coccolithophorids: The objectives of this subprogramme of M 36/5 were to quantitatively describe the temporal and spatial distribution of the planktic calcareous flora and fauna in the BIOTRANS area and to trace the fate of calcareous particles. The sample grid has been adjusted to the hydrographical grid displayed in Fig. 90. To cover the area of 180 x 180 nm, 318 hauls were taken with a multiple opening/closing net (mouth 50 x 50 cm). Three main intervals were chosen: 2500-0 m in steps of 2500-2000-1500-1000-700-0 m, 700-0 m (700-500-300-200-100-0 m), and 100-0 m (100-80-60-40-20-0 m). These intervals were chosen in order to get high resolution within the photic zone and a medium resolution for the upper export zone as well as for deeper parts of the water column. Some stations were sampled two or three times in order to trace the changing water body. This study is part of our long-term survey in this area to characterise the population dynamics of the calcareous flora and fauna, and their fate in relationship to the carbon and calcium cycle.

5.5.8.1 Shipboard Results

Several times during the cruise we sampled water bodies north and south of frontal zone systems belonging either to northerly-derived eddies, filaments or northward-drifting warm water bodies. The following two graphs display the planktic foraminiferal faunal composition north and south of such a frontal system (Figs. 91, 92). South of the frontal zone, we observed a subtropical/tropical fauna in the upper 100 m of the water column (Fig. 92), whereas the north displays (Fig. 91) a cold water fauna dominated by *G. bulloides* and *T. quinqueloba*. *Globigerinita glutinata* is also a prominent species within this fauna, but *N.* incompta is totally missing. Furthermore, the southern sample shows many more specimens per m^3 with a maximum 60-80 m. North of the frontal system, the fauna has its maximum between 20 and 40 m and displays only a rather poor assemblage in numbers (> 80 specimens/m^3). This is typical of the summer which changes into an autumn/winter situation.
During the summer, the pteropod fauna showed a much higher diversity compared to the fauna north of the front.
Preliminary results on the coccolithophorids support our observations. When we arrived at the BIOTRANS station we still had a summer situation. Coccolithophors collected at this station displayed the same species and numbers per litre compared to station A1 samples collected earlier on METEOR cruise M 35/2.

5.5.9 Molecular Genetic Differentiation among Planktic Foraminifera as Indicators of Water Masses (M. Langer, C. Hemleben)

During M 36/5, we collected various species of planktic foraminifera to decipher molecular phylogenetic relationships and evolutionary lineages by an approach independent of the conventional method of comparing phenotype morphologies. Planktic species were collected

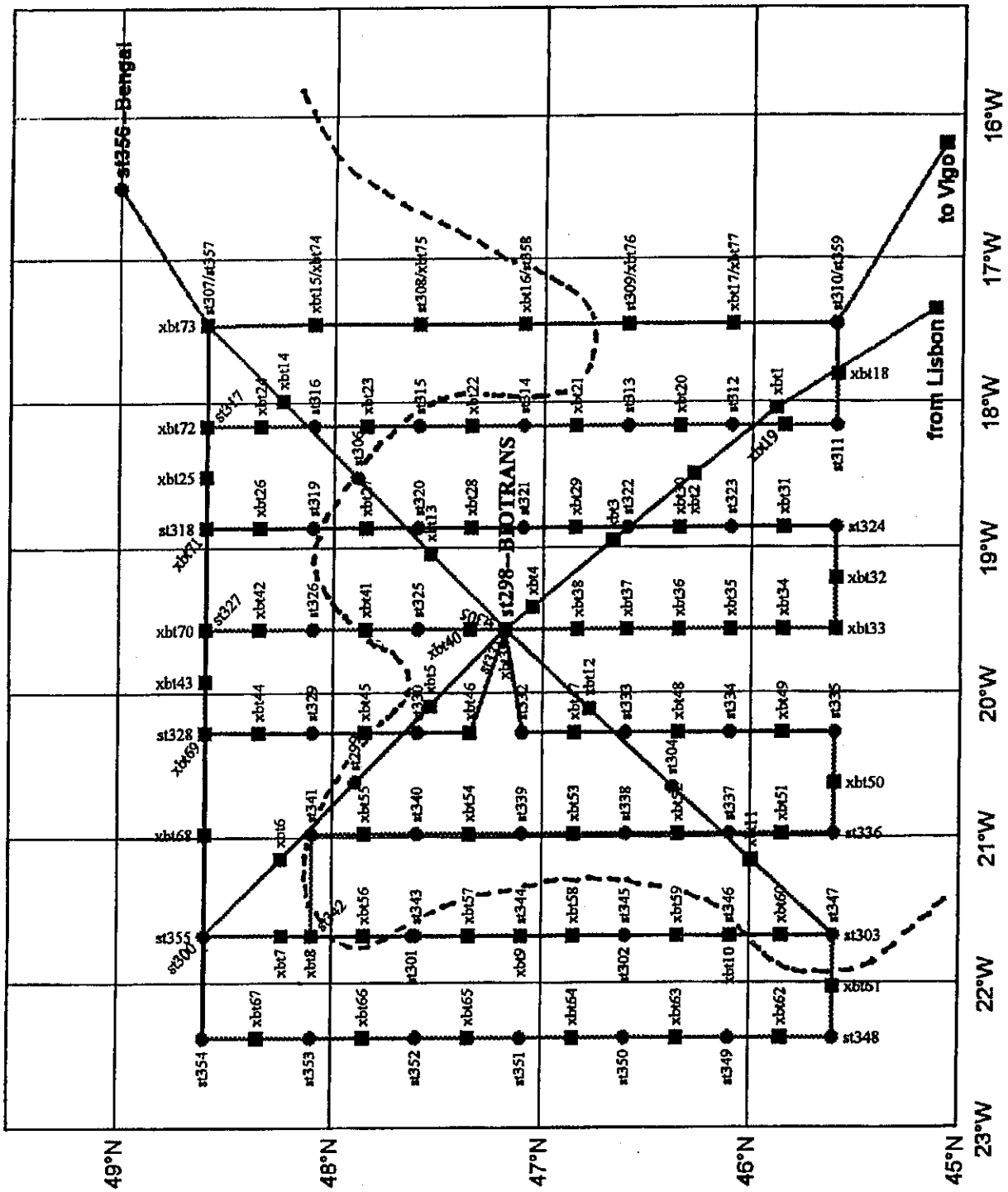

Fig. 90: Cruise track and frontal system boundary according to planktic foraminifera fauna.

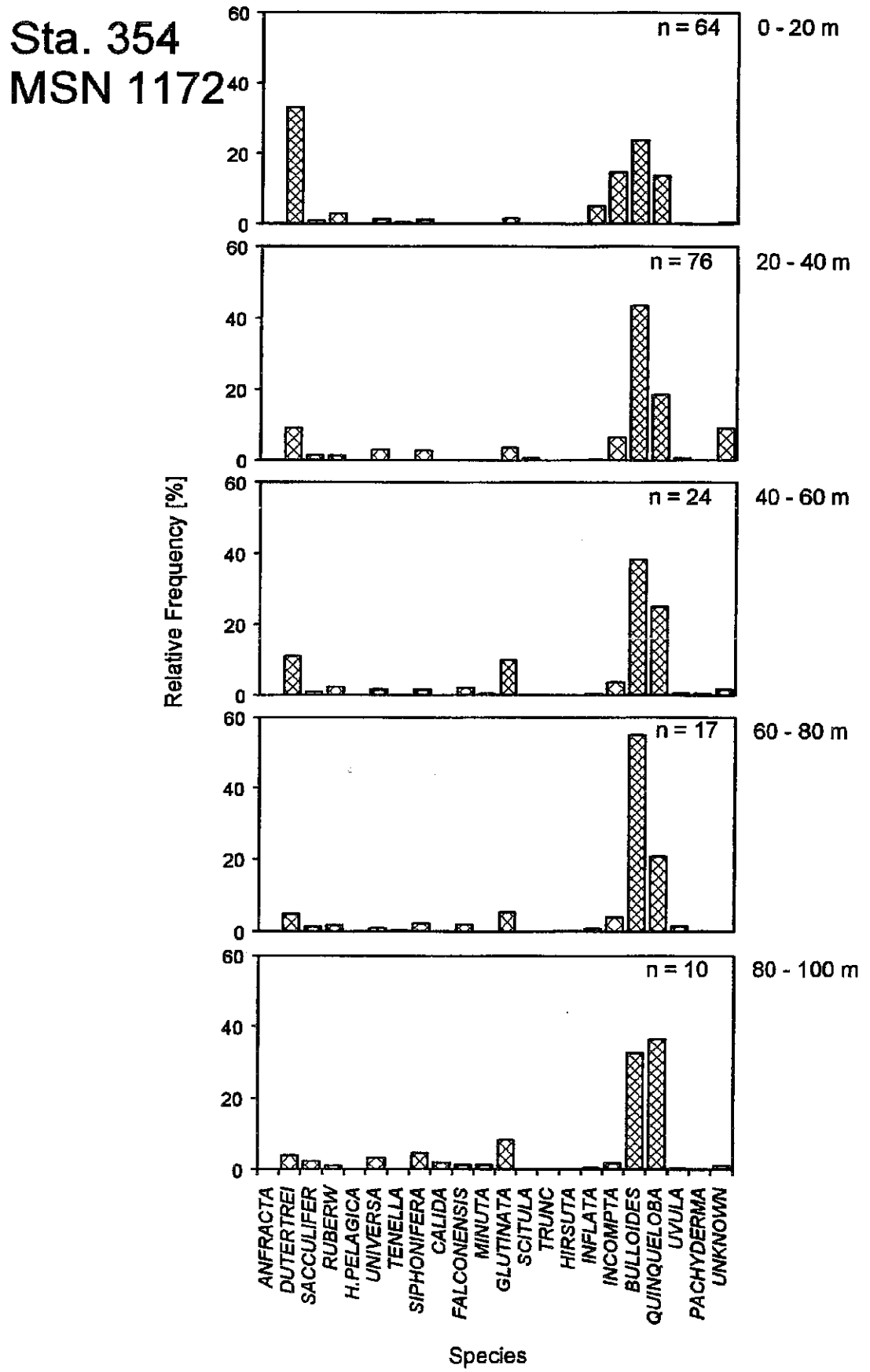

Fig. 91: Shows the faunal composition north of the frontal system, dominated G. bulloides and T. quinqueloba. It is a fauna of rather low abundance.

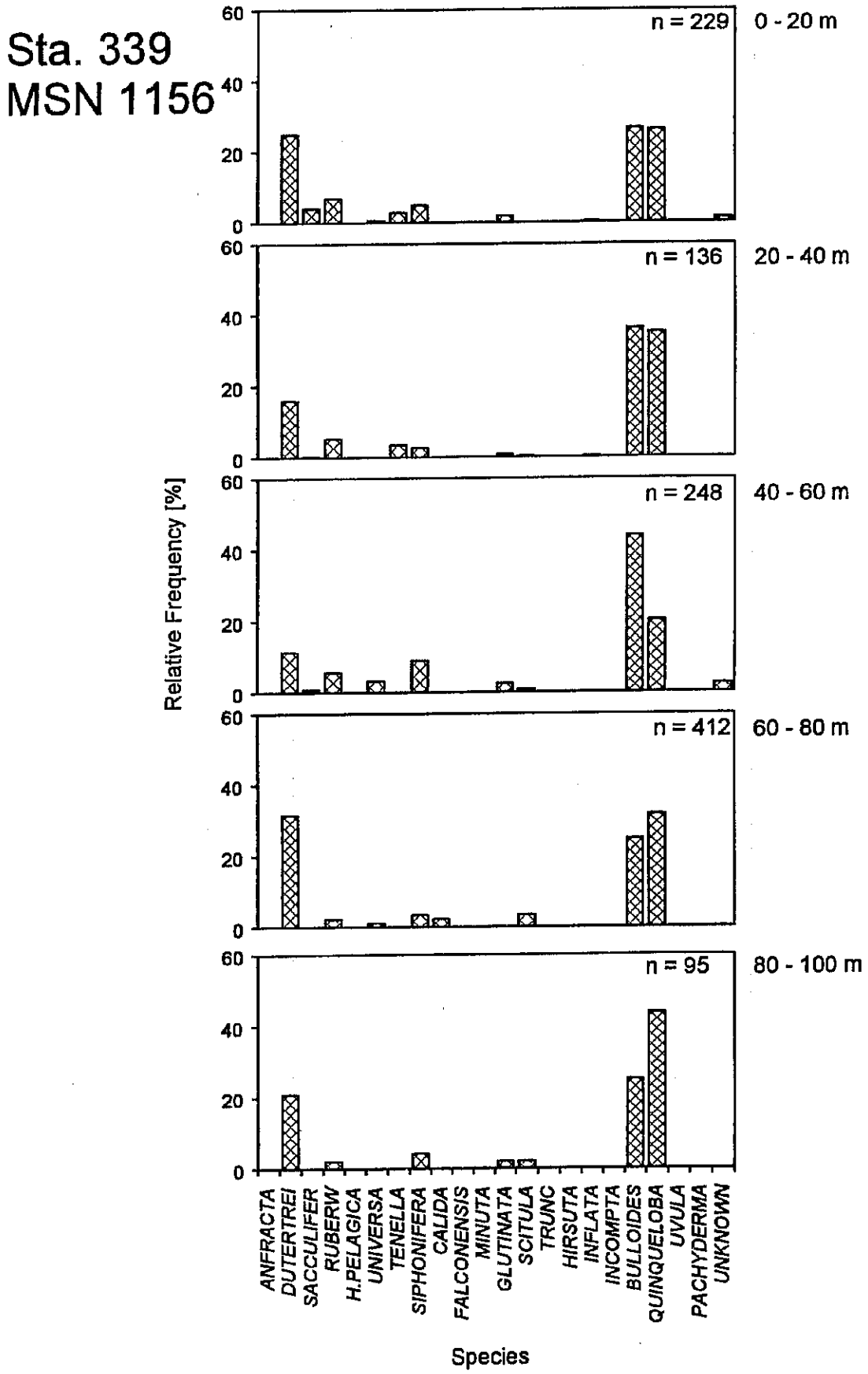

Fig. 92: Displays the southern fauna with a high abundance of species.

by multiple net hauls and DNA was successfully extracted using the standard cetyl trimethyl ammonium bromide (CTAB)-based extraction protocol.
The polymerase chain reaction was used for the in vitro amplification of ribosomal DNA (18S small subunit), utilising primers complementary to conserved regions. PCR reactions were performed in a DNA Thermal Cycler and the amplified products were ligated and cloned. Seven to twelve clones were sequenced for each species using an automated sequencing system. The foraminiferal sequences obtained were aligned to homologous sequences of previously published sequences and sequences were then analysed using the neighbour joining and maximum parsimony methods.

5.5.9.1 Shipboard Results

Results obtained to date suggest that planktic foraminifera may have originated much earlier than indicated by their fossil record. Ribosomal DNA sequence analyses also provide evidence that genetic variation among the taxa analysed may exhibit patterns that are particularly useful to decipher biogeographic provinces and water masses. The molecular phylogeny of foraminifera also exhibits congruence with some of the traditional morphological and biological hypotheses.

For samples collected at stations see chapter 7.5.4.

5.6 Leg M 36/6

5.6.1 Benthic Standing Stock and Activity in the Benthic Boundary Layer at the BIOTRANS and BENGAL Sites (O. Pfannkuche, B. Springer, R. Turnewitsch, A. Cremer, A. Kähler, T. Viergutz)

Previous investigations at the BIOTRANS site in 47°N/20°W showed distinctive seasonal changes of benthic activity and small size scale biomass that were closely coupled with primary production in the mixed oceanic surface layer. Maximum sedimentation rates in early summer, resulting in the deposition of a pytodetrital carpet on the sea floor, led to a 3-5 times increase of benthic metabolic activity (in comparison to early spring values) (PFANNKUCHE, 1992) and to a doubling of bacterial biomass (LOCHTE, 1992).

5.6.1.1 Shipboard Results: Standing Stock and Activity of Small Benthic Size Classes

The research objective was an evaluation of the biomass and metabolic activity of small benthic size classes ranging from 2 - 500 µm in cross diameter, namely bacteria, nano- and meiofauna. These groups represent the main decomposers in deep-sea sediments. About 80% of deep-sea biological benthic carbon consumption is channelled through these benthic size classes (PFANNKUCHE, 1993), with bacteria clearly dominating (LOCHTE, 1993).

Sediment samples with a multiple corer (BARNETT et al., 1984) were taken at BENGAL during legs M 36/4, M 36/5 and M 36/6, and at BIOTRANS during legs M 36/5 and M 36/6. Randomly selected multiple corer tubes were subsampled with small piston corers of 1.1 cm or 3.46 cm cross diameter. Three replicates for each parameter were taken from one multiple corer cast. Sediment samples were analysed in 1 cm intervals down to 10 cm depth and in 2 cm intervals to a maximum of 30 cm depth. Samples for the following benthic groups and biochemical sediment analysis were taken (measurements marked with an asterisk were carried out in the ship's laboratory) all other determination will be carried out at GEOMAR:

Biochemical sediment analysis

Measurements of biomass
- Adenylates (ATP+ADP+AMP)
- DNA

Measurements of metabolic activity
- electron transport system activity (ETA, respirative potential)*
- ATP
- hydrolysis rates of fluorescein diacetate (activity of bacterial exoenzymes)*

Measurements of plant pigments
- chlorophyll-a and pheopigments (fluorimetric)*
- Pigments (HPLC)

Other measurements
- proteins*
- C_{org}, N_{org}
- water content

Sediment chloroplastic pigments (CPE: chloroplastic pigment equivalents) at both stations were slightly higher in autumn in comparison to summer values at BIOTRANS (Fig. 93). The increase of CPE (10-20%) between September and October was found in all depth horizons. At BENGAL a continuous increase of CPE contents was registered between August and October (Fig. 94). CPE contents at BENGAL were slightly higher than at BIOTRANS. Although sediment samples were taken at the same locality during the different months spatial inhomogeneity of CPE values must be considered for the evaluation of any seasonal changes. Under this aspect a seasonal increase of CPE in autumn is only small.

Electron transport activity (ETA) showed higher values in September at BIOTRANS whereas in October, ETA was already clearly reduced (Fig. 95). At BENGAL a continuous increase in ETA was observed from August to October (Fig. 96). In comparison between the two sites ETA was always higher at BIOTRANS than at BENGAL.

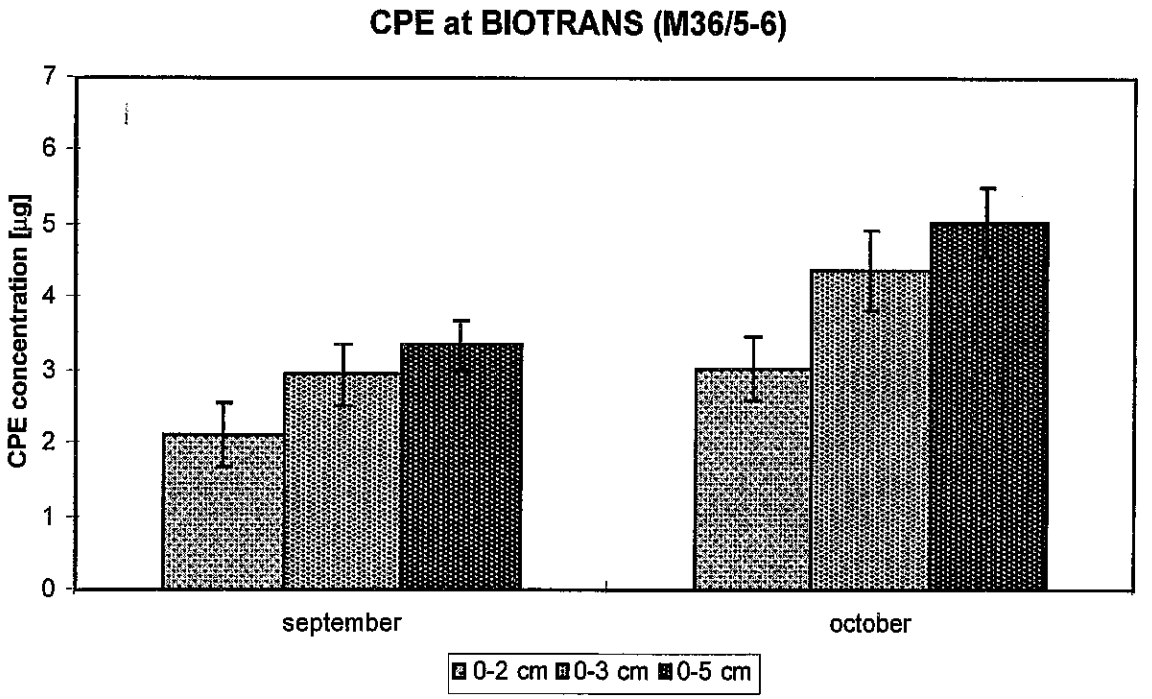

Fig. 93: Sediment bound chloroplastic pigments (CPE) at the BIOTRANS station (values from legs M 36/5, M 36/6).

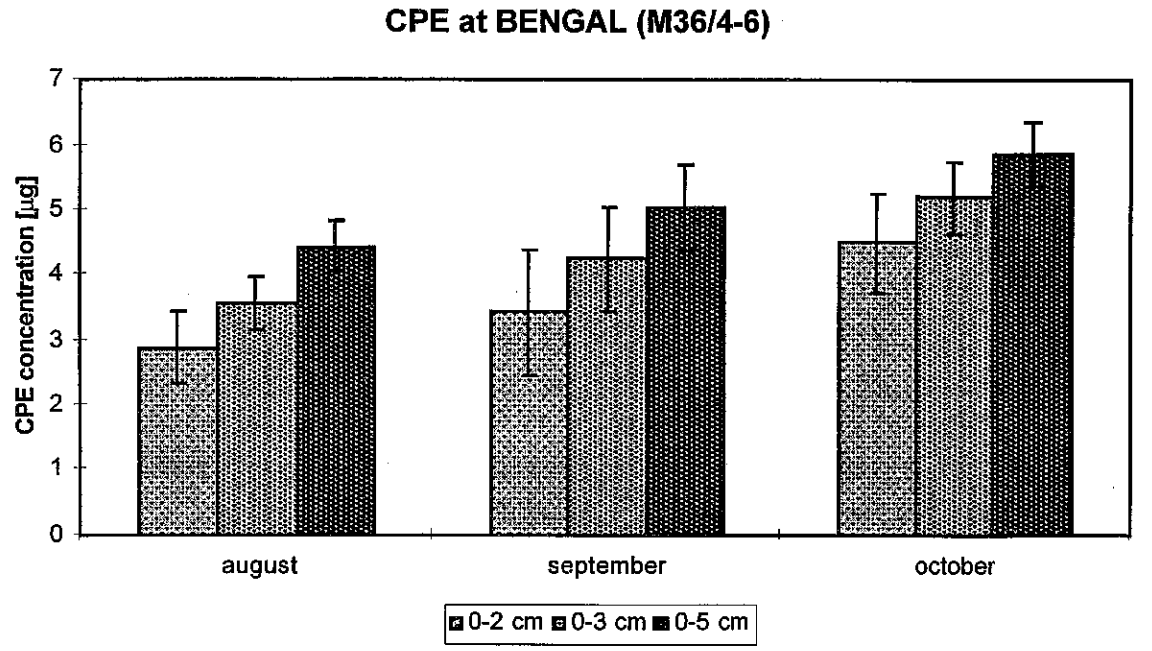

Fig. 94: Sediment bound chloroplastic pigments (CPE) at the BENGAL station (values from legs M 36/4, M 36/5, M 36/6).

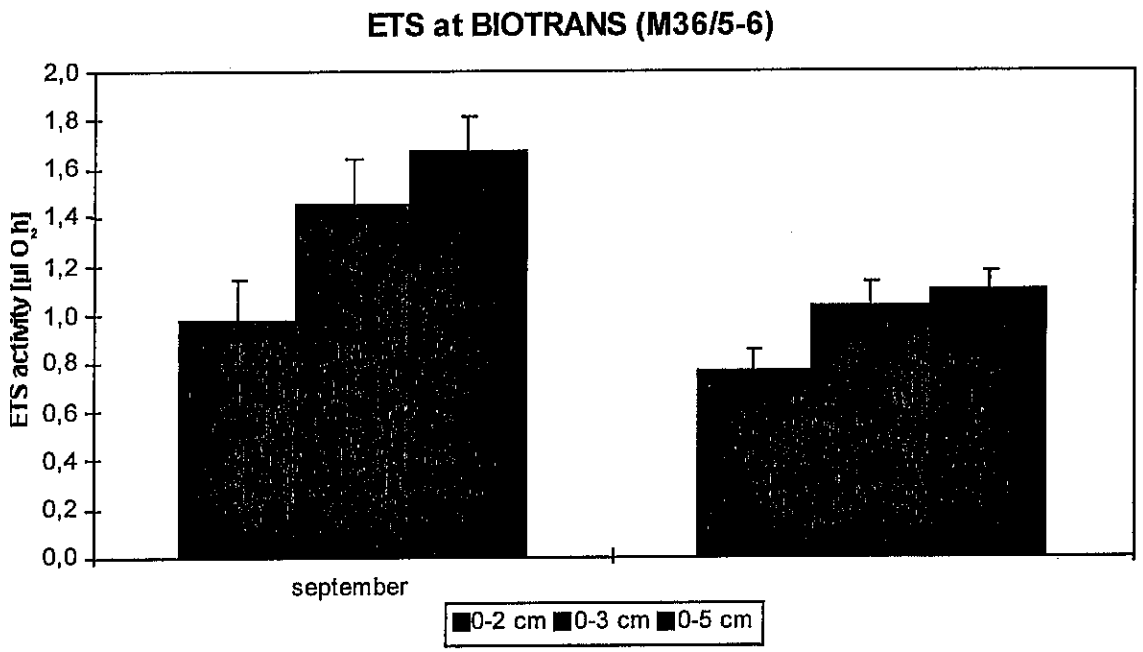

Fig. 95: Electron transport activity (ETA) at the BIOTRANS station (values from legs M 36/5, M 36/6).

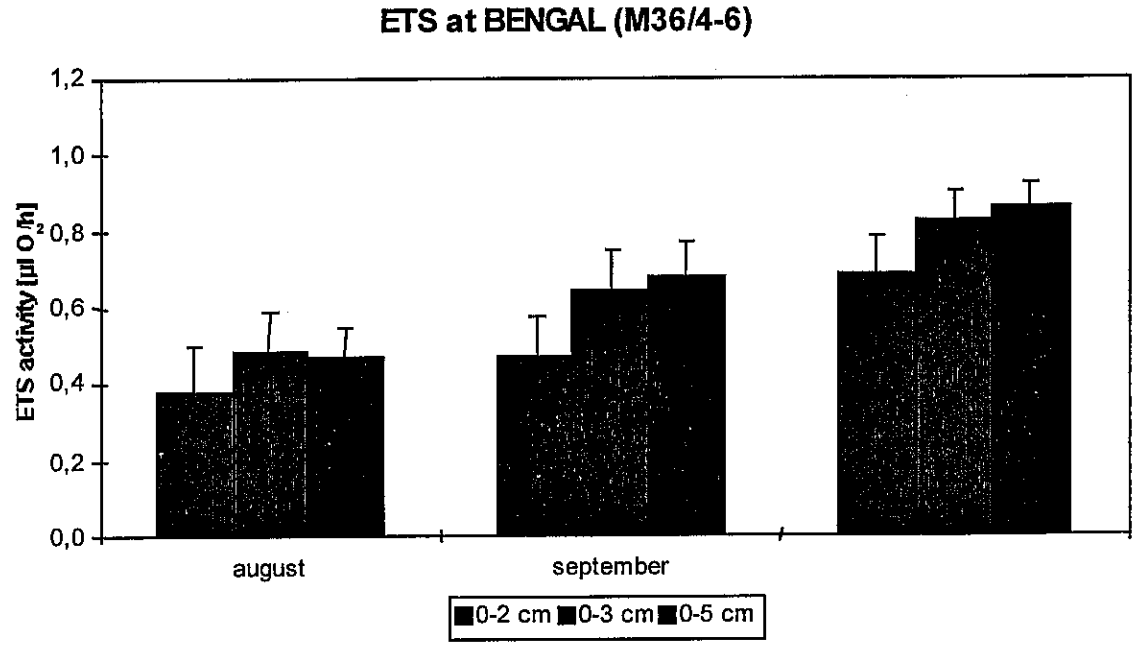

Fig. 96: Electron transport activity (ETA) at the BENGAL station (values from legs M 36/4, M 36/5, M 36/6).

Bacterial exoenzymatic activity determined by the reduction of fluorescein-diacetate (esterase activity) was found to be on the same level at BIOTRANS both in September and October (Fig. 97). At BENGAL FDA values increased significantly between August and September, when the maximum was reached (Fig. 98).
In October, FDA values were already reduced but still significantly higher than in August. Like in ETA esterase activity was generally higher at BIOTRANS than at BENGAL.

August observations at BIOTRANS during a MAST III cruise reported the occurrence (KEEGAN et al., pers. com.) of phytodetritus on the sea floor which was not found at BENGAL during this expedition. The relatively high activity values at BIOTRANS in comparison to BENGAL point toward a slow decrease of maximum activities which occurred prior to this investigation.

The situation at BENGAL points to the deposition of a smaller food pulse in September which led to an increase in activity. However, this seasonal maximum could only be maintained for a short period as October values were already smaller.

5.6.1.2 Shipboard Results: Benthic Respiratory Activity

The GEOMAR benthic chamber lander system (BIO-C-FLUX Lander, TENGBERG et al., 19895) for in-situ determination of benthic oxygen consumption could be deployed successfully at both BIOTRANS and BENGAL sites, despite unfavourable weather conditions. The in-situ remineralisation rates showed relatively low benthic activity at both sites. With 0.3 mmol O_2 m^{-2} d^{-1} (uncorrected) activity was slightly higher at BENGAL compared to BIOTRANS with 0.22 mmol O_2 m^{-2} d^{-1}, uncorrected.

For direct comparison of benthic standing stock and activity, sediment samples were taken from the incubation chambers in order to analyse FDA, CPE and phospholipids. The flux of silicate and nitrate across the sediment/water interface will be determined from water samples collected from the incubation chamber during deployment.

5.6.1.3 Shipboard Results: Bioturbation and Bioirrigation

In order to quantify benthic bioturbational and bioirrigational mixing processes at the BENGAL station, sediment was sampled in August 1996 (M 36/4) at a depth of 4830 m, and in October 1996 (M 36/6) at a depth of 4805 m with a multiple corer.

For the quantification of bioirrigational activities on cruise M 36/4 three sediment cores (10 cm diameter) were incubated on board in an incubation chest at in-situ temperature. The overlying water was sampled to obtain a value for the natural bromide concentration in the bottom water, reduced to a height of about 10 cm and supplied with a small volume of concentrated sodium bromide solution to increase the bromide concentration to approximately

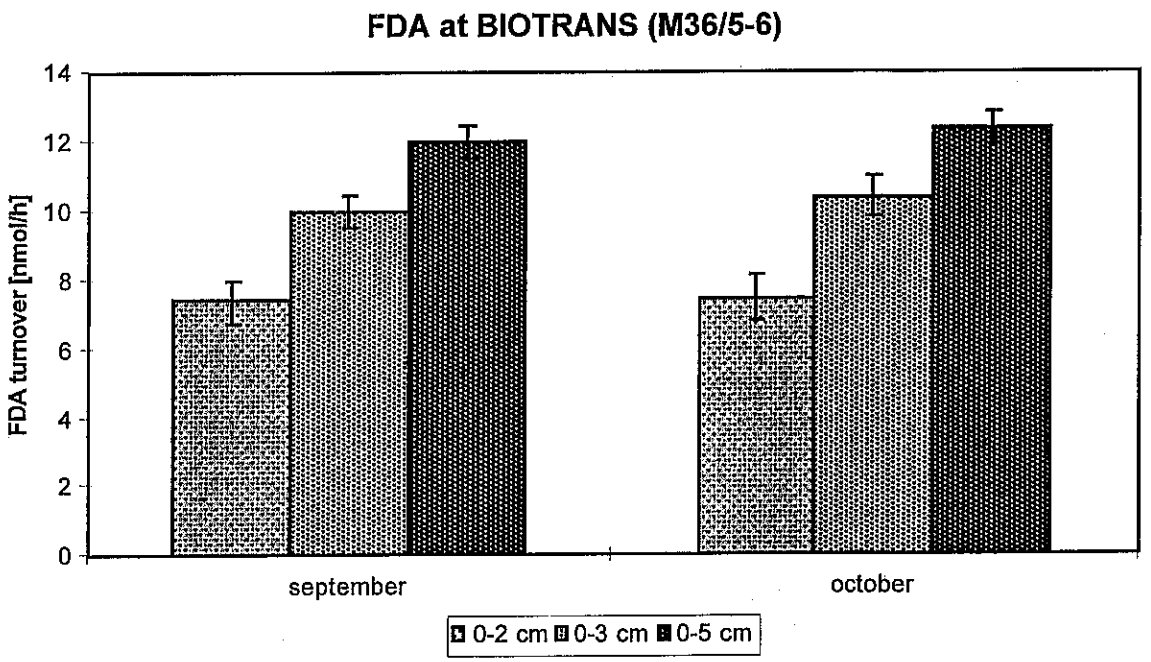

Fig. 97: Activity of esterases in sediment profiles at the BIOTRANS station (values from legs M 36/5 and M 36/6).

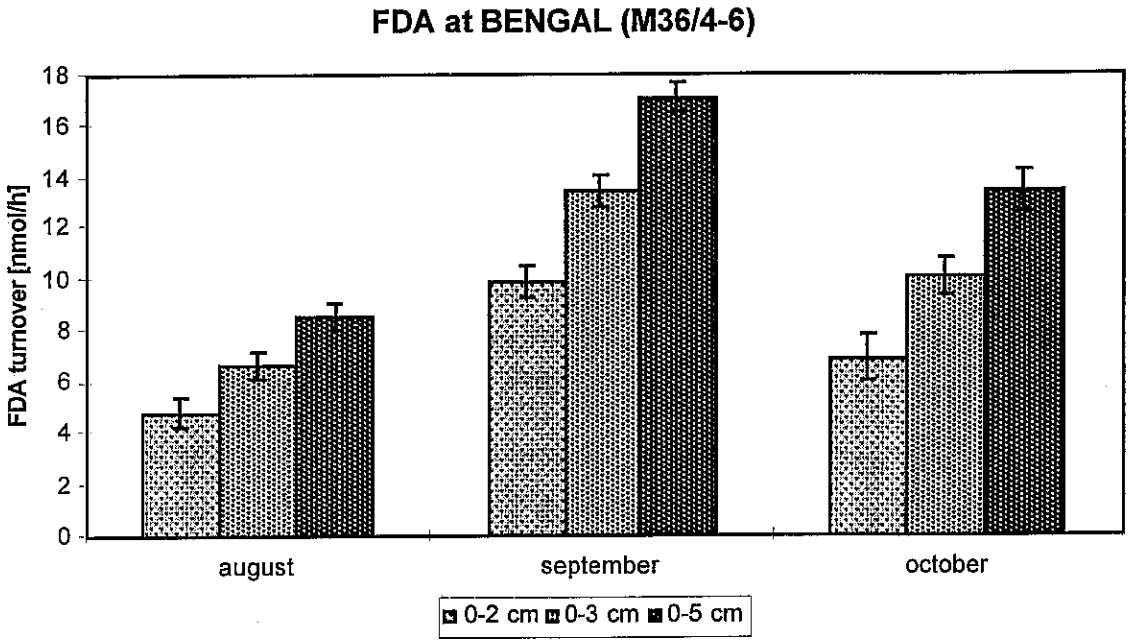

Fig. 98: Activity of esterases in sediment profiles at the BENGAL station (values from legs M 36/4, M 36/5 and M 36/6).

15 times the natural background. The overlying water was aerated and simultaneously mixed by air bubbled slowly through the water. The cores were covered with lids to reduce evaporation and incubated for 7 days. The overlying water was sampled at least once a day. In order to measure the natural bromide concentrations the overlying water of three additional sediment cores was sampled, and the cores were cut into slices in which the natural bromide background in the sediment is to be measured.

On M 36/6 a similar experiment was conducted in a cool room on a platform that compensates for the ship's movements. Natural bromide concentrations will be determined through the chloride-bromide ratio in the pore water. The bromide and chloride measurements will be accomplished ionchromatographically at GEOMAR.

^{210}Pb activity profiles yield information on sedimentary mixing processes on a time scale of 10-100 years. In the sediment cores sampled on leg M 36/4 for the measurement of the natural bromide concentrations ^{210}Pb will also be measured alpha-spectrometrically at GEOMAR via its granddaughter ^{210}Po. On leg M 36/6, three cores for the measurement of ^{210}Pb were taken at the BENGAL station and an additional three cores on the BIOTRANS station. ^{234}Th data will yield information on sedimentary mixing processes on a time scale of 100 days. On both cruises one sediment core was analysed for ^{234}Th at the BENGAL station. The core was cut into slices and subsamples have been leached with 6 M HCl. Following coprecipitation, acid dilution and anion exchange steps the solution containing thorium was electroplated on silver planchets. The activity on these silver planchets is measured in a low level beta counter and will be corrected for chemical yield and ^{238}U (supported ^{234}Th) at GEOMAR.

5.6.1.4 Shipboard Results: Benthic Boundary Layer Activity

In order to quantify fluxes of particulate and dissolved substances in the bottom near water body at the BENGAL and BIOTRANS stations bottom water was sampled with the bottom water sampler (21, 31, 41 and 66 cm above bottom) and with near bottom CTD cast (13 m above bottom) twice at each station.

Observation of particles and in-situ and bottom current measurements failed after the implosion of the particle camera housing at its first use at the BENGAL station.

Bottom water (1-3 litres) was filtered on GF/F filters and 150 ml of each horizon were preserved in formalin. The filters were stored at -20°C. The following determinations will be carried out in the laboratory at GEOMAR:

- Numerical abundance and biomass of bacteria;
- Chlorophyll-a and pheopigments (fluorometric);
- Pigments (HPLC in co-operation with TP 4);
- C_{org}, N_{org};
- TPM.

The oxygen content was determined directly on board. The microbial activity will be measured by our partners from IO-Warnemünde. Phosphate, nitrate, silicate content and alkalinity will be determined by the GEOMAR geochemists.

5.6.2 Meiofauna Sampling at the BENGAL and BIOTRANS Stations
(T. Mutch)

Metazoan meiofauna sampling at the BENGAL station on behalf of Ann Vanreusel was carried out on board. Metazoan meiofauna, as defined by all benthic metazoan smaller than 1 mm but retained on a 32 µm sieve, were sampled at the Porcupine Abyssal Plain (BENGAL).
Initially it was hoped to obtain two cores from each of between four to six multicorer (MC) deployments. One core was to be sampled for meiofaunal analysis, the other for chemical analysis (organic C and pigment analysis).
Under the circumstances, only one MC deployment (station 362) yielded the required sediment cores.

From the first core, samples of overlying water and 1 cm slices from 0-5 cm down core were taken for meiofauna analysis. The whole section of sediment from 5-10 cm was also stored. All samples have been fixed with 4% formalin and are awaiting shipment back to Germany.

For chemical analysis, the second core was also sliced at 1 cm intervals from 0-5 cm down core but no other samples were taken from this core. Samples are stored in the -20°C room and will be brought back to England in a dry ice package.

Sampling of foraminifera from the BENGAL station on behalf of Andy Gooday was carried out on one core. One core was sampled from station 362 instead of the proposed three. From this core, the following samples were taken: 3 cm bottom water, every 0.5 cm down to 2 cm, then every 1 cm down to 10 cm, and finally every 2.5 cm down to 15 cm. The samples have been fixed with 4% formalin.

Sampling of foraminifera from the BIOTRANS site on behalf of Tom Mutch was carried out on cores from stations 398 and 405. The objective here was originally to take samples from several different bathymetric settings and examine how the planktonic foraminiferal record of the last 10,000 years changes with water depth. Samples from the Abyssal Plain (4500 m), and from the flanks and summit of the Great Trident (Großer Dreizack) were proposed to be taken. Where possible, two cores from any MC deployment would be kept. One would be sliced every 1 cm to the base of the sediment. The other would be frozen and returned to England intact for analysis through the S.O.C. multi-sensor logger. This measures p-wave velocity, gamma ray attenuation and magnetic susceptibility. In turn, this can lead to stratigraphic correlation, and the measurement of sediment bulk density and porosity. Unfortunately, it was only possible to acquire four cores (two MC deployments), all from the Abyssal Plain (stations 398, 405) with two cores acquired at station 398. One sliced every

1 cm to a depth of 14.75 cm, the other frozen. Also two cores were acquired at station 405. One sliced every 1 cm to a depth of 22 cm, the other frozen.

5.6.3 Benthic and Planktic Foraminifera Sampling at the BENGAL and BIOTRANS Station (P. Heinz, F. Kurbjeweit)

The main objectives were to study deep-sea benthic foraminifera at the BENGAL and BIOTRANS stations (northeast Atlantic) in order to get more detailed information on ecology and biotic processes with respect to the environmental constraints (biogeochemistry and related processes). In addition, the planktic foraminiferal fauna was investigated to continue our long-term survey in the area. Therefore, our studies focused on species composition and distribution, food web, habitat preferences, pore water chemistry, bioturbation, growth, reproduction and benthic-pelagic coupling. This will help us to understand the role of deep-sea benthic foraminifera within the deep-sea communities and their environment.

For the sampling within the water column the multinets (planktic foraminifera) and CTD casts (coccolithophores) were used. Generally, the multinet used was equipped with five nets (100 µm mesh size) and three water bottles. We sampled the intervals 100-80-60-40-20-0 m to record the productive zone, the intervals 700-500-300-200-100-0 m were used to create a record to characterise upper export zone and the deep-tow (2500-2000-1500-1000-500-0 m) to sample the deep export levels. Parallel, water samples were taken from 2500, 1500, 700, 500, 300, 200, 100, 60 and 20 m to investigate the nannoflora. This was done also in combination with CTD casts running directly before the multinet. The plankton samples were immediately examined for species composition and subsequently fixed in 4% hexamin-buffered formaldehyde. The water samples were filtered through 0.45 µm regenerated cellulose filters. The filters were dried overnight and stored in plastic petri dishes for further scanning electron microscopy (SEM) examination and countings at home in the laboratory.

Multicorers and box corers were used at both BENGAL and BIOTRANS stations, multicorer samples were taken for species composition and experimental work. Immediately after arriving on deck, the cores were transferred to the cool room (4°C). First, the cores were photographed to document the original fabrics. After that, the upper 1 or 2 cm of sediment as well as the bottom water were transferred into DURAN flasks. These were kept under semi in-situ conditions (4°C and darkness). The samples were regularly inspected every 3-4 days for foraminifera and their tracks in the sediment.

A second core was sliced in half-centimetre intervals for the top two centimetres and thereafter in one centimetre slices. The slices of the upper 10 cm were stained with Rose Bengal for identifying living and dead specimens.

To record microhabitat preferences of deep-sea benthic foraminifera pore water and BNL water samples were taken for ^{13}C and ^{18}O analysis. The pore water was obtained by pressing the sediment with N_2 for twenty minutes. Both samples were poisoned with $HgCl_2$. The

remaining sediment („press cake") was transferred into plastic foil and sealed for determination of species and their ^{13}C and ^{18}O composition. Special attention was paid to keep transfer times as short as possible and to avoid contamination by atmospheric CO_2 during compression.

At station 388 samples were taken to determine the concentration of bacteria within the sediment and in the BNL. The bacterial development under laboratory conditions will be followed during the forthcoming weeks. Furthermore, samples were taken after 1, 3 and 8 days for counting.

5.6.3.1 Experiments

For experiment 1 at station 372, three small cores were taken to obtain 15 subcores 1.8 cm in diameter which were incubated with *Chlorella* in a time series (2, 5, 7, 11, 14 days) with defined numbers of microbeads of 1, 3, 6 and 10 µm in size in order to estimate incorporation of *Chlorella* as food particles and transfer into deeper sediment layers (bioturbation).

For experiment 2 at station 388 (BIOTRANS), the upper 3 cm of one core was used for an incubation experiment under in-situ conditions with microbeads and *Chlorella* as mentioned above. The sediment was filled in small plastic bags with overlying water and sealed. Subsequently they were incubated at 4°C under 450 atmospheres and darkness for 8 days. Consequently, the samples were decompressed and sorted under a dissecting microscope for greenish to brownish foramaminifers after sieving over 63 and 125 µm. Furthermore, up to twelve specimens of the six subsamples were fixed for transmission electron microscopy (TEM) to see if and how many microbeads and *Chlorella* have been ingested.

For experiment 3 seawater from 4000 m was enriched with 5% Bacto peptone and 1% Bacto yeast extract and incubated at room temperature for at least 9 days to generate high concentrations of bacteria. Planktic foraminifera from three multinets was selected and incubated in the bacteria culture for different periods of time.

In each case 50% of the specimen was directly fixed in 2% buffered formaldehyde; the remaining portion was washed twice with 0.2 µm filtered seawater and then fixed with 2% formaldehyde. In addition, a subsample of the bacteria suspension was taken to determine the concentration. In addition the pH of the culture was measured.

5.6.3.2 Shipboard Results

During the cruise, 15 tows (100, 700 and 2500 m each including five intervals), and 11 samples from multicorers and two box corers were collected at BENGAL (48°58 N/16°28 W) and BIOTRANS (47°11 N/19°34 W). In addition, water from seven CTD casts were filtered for coccolithophore studies.

Regular observations of all cultures in the DURAN flasks and the aquarium in the laboratory every 3-4 days showed that unfortunately no foraminifera survived the decompression from 4400 m depth or deeper.

Results of the experiments are not available at this point in time. They will be published.

5.6.4 Microbial Enzyme Activities in the NE Atlantic Deep Sea

(A. Boetius, C. Chwieralski)

In deep-sea sediments, bacterial enzymes are the primary agents of the early diagenesis of organic matter (OM). Most extracellular enzymes are produced when respective substrates become available (substrate induction), others are constantly produced but repressed in the presence of readily available nutrients. An experiment was performed to test whether the amount of enzymes produced by the natural microbial assemblages is relative to the supply with specific organic compounds. Three different concentrations of chitin and cellulose were added to subsamples from one sediment slurry, which were incubated under in-situ temperature and pressure. After several days, activity of b-glucosidase and chitobiase in the enriched samples increased substantially, depending on the amount of substrate added (Fig. 99). Thus, the distribution of both enzymes in deep-sea sediments most likely indicates differences in the availability of their respective substrates.

5.6.4.1 Shipboard Results

Samples for the determination of extracellular enzyme activities (EEA), microbial biomass, bacterial production and availability of specific organic compounds were collected at the BENGAL and BIOTRANS stations (Tab. 11). Bacterial production is estimated by measuring the incorporation of H_3-Thymidine and leucine into DNA and bacterial protein, respectively. For the determination of microbial biomass, bacterial numbers, cell volumes as well as phopholipid concentrations are measured in the home laboratory. Hydrolytic activities of a-, b-glucosidase, chitobiase, esterase, lipase, peptidase, phosphatase, sulphatase were measured on board using fluorescence-labelled Methylumbelliferyl (MUF)-substrates. Most enzymes displayed highest activities in the first centimetre, indicating that most of the OM is degraded at sediment surface (Fig. 100). At station BIOTRANS, extracellular hydrolytic activity of the micro-organisms was about twice as high as in October 1996 compared to August 1992. This could be related to a seasonal rise in the supply with organic matter due to sedimentation of the autumn bloom.

Potential activities of hydrolytic enzymes were also measured in water samples from the benthic boundary layer, collected from 5-50 m above bottom with the CTD/rosette or with the bottom water sampler. Enzyme activities in the benthic boundary layer were 100-10,000-fold lower than at the sediment surface (0-0.5 cm), and no depth-related trend was detected (Fig. 101).

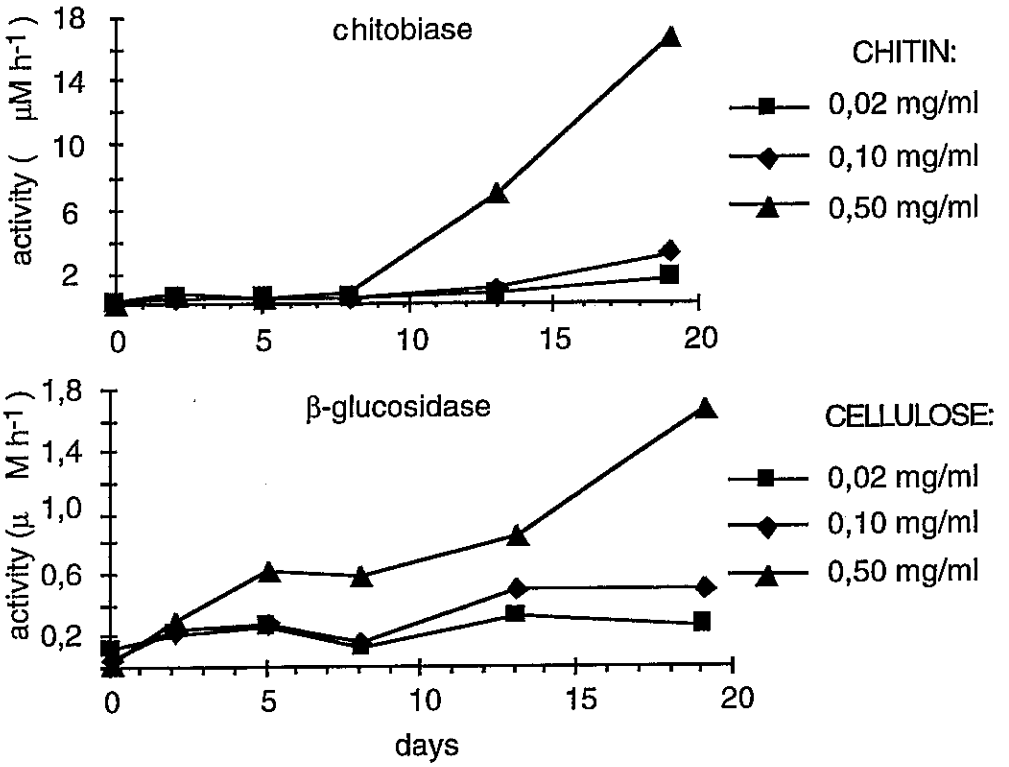

Fig. 99: Enrichment experiment.

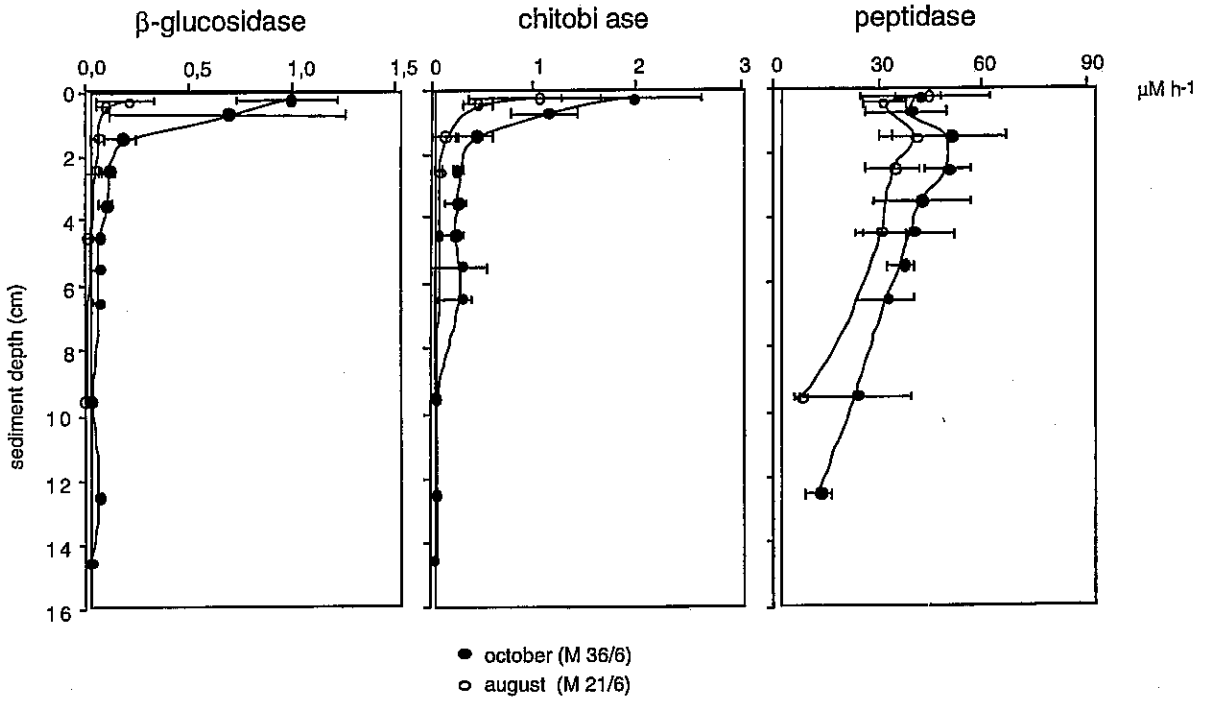

Fig. 100: Profiles of enzyme activity at BIOTRANS. Error bars indicate 95% confidence levels (October: n=7; August: n=7).

Table 11: List of samples. Enzyme activities were measured on board, the other samples will be analysed in the home laboratory.

Gear	Station			Methods		
		Enzymes	Phospho-lipids	Bacterial Biomass	Bacterial Production	Organic Compounds
MC No	30/31 (Experiment)	x	x	x	x	x
	33	x	x	x		
	38	x	x			
	39					x
FFG No	1	x		x	x	
CTD No	4	x				
	5	x				
	6	x				
BWS No	19	x				
	20	x				
MC No	41		x	x		
	42/43/44 (Mix)	x		x	x	
	47	x				
	49		x			
	50	x				
	52					x
	53	x				x
	54		x	x		
	56	x				
	57	x		x	x	
	58	x	x	x		
	59	x				
	60		x			
CTD No	12	x				
BWS No	21	x				
	22	x				

5.6.5 **Bacterial Biomass and Community Structure** (D. Eardly)

The aims of this cruise were to obtain sediment samples and large volume near-bottom water samples to determine bacterial biomass and community structure via DNA analysis.
Three sediment cores were collected: 1 from BENGAL and 2 from BIOTRANS.

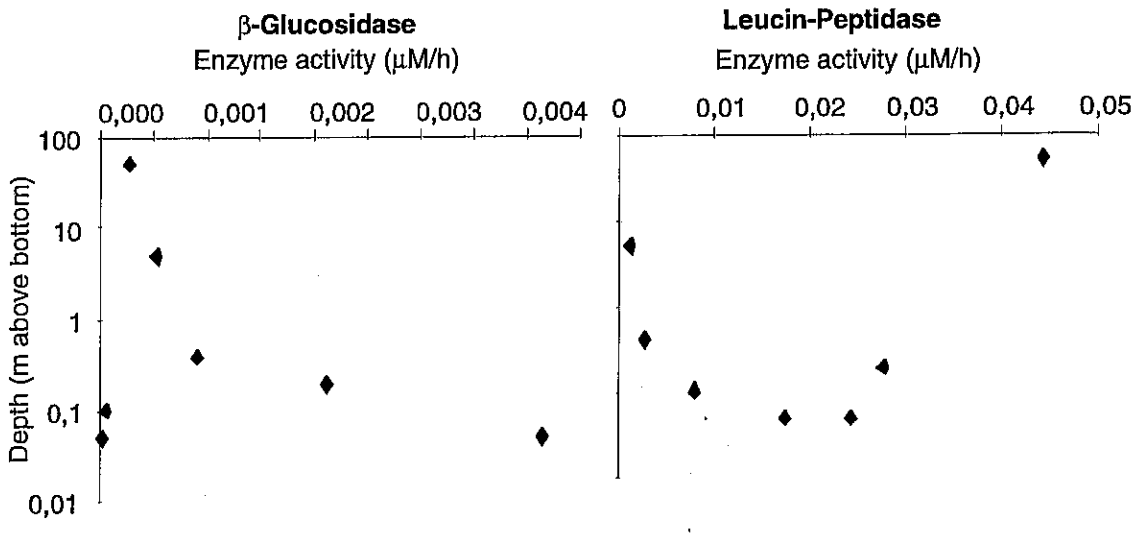

Fig. 101: Enzyme activity in the benthic boundary layer.

Sediment samples

Site: BENGAL Station no. 362

The core was sectioned at 1 cm intervals down to 10 cm depth and frozen. 1 ml subsamples were fixed in formaldehyde for bacterial biomass analysis.

Site: BIOTRANS Station no. 395

The core was sectioned at 1 cm intervals down to 10 cm depth and frozen. 1 ml subsamples were fixed in formaldehyde for bacterial biomass analysis.

Site: BIOTRANS Station no. 398

The core was sectioned at 1 cm intervals down to 3 cm depth and frozen. 1 ml subsamples were fixed in formaldehyde for bacterial biomass analysis.

Water samples

Bacteria in 30 litre water samples from a CTD cast were concentrated by Tangential Flow Filtration down to a 200 ml volume. 50 ml of 40% glycerol was added and the samples frozen at -70°C.

Site: BENGAL Station no. 375

Sample Depth: 4765 m (45 m over bottom)

Site: BENGAL Station no. 380

Sample Depth: 4794 m (10 m over bottom).

5.6.6 **Benthopelagic Fauna** (B. Christiansen)

The benthopelagic fauna *sensu latu* comprises a wide variety of organisms, from minute plankton to large fish as well as epibenthic megafauna. The investigations on the benthopelagic fauna, which were conducted within the framework of the MAST III project BENGAL, focused on the near-bottom zooplankton and on necrophagous amphipods. Different methods have to be employed to sample these faunal components. A 1 m^2-MOCNESS (WIEBE et al., 1985) allowed to sample benthopelagic zooplankton from a minimum distance of 10 m off the bottom. A video-controlled epibenthic sledge (fototrawl) (CHRISTIANSEN et al., in press) was used to sample near-bottom plankton and epibenthic megafauna. The new version of the fototrawl is equipped with 5 plankton nets (mouth opening 0.8 m^2, mesh size 333 µm) which fish at a distance from 0.5 to 1.5 m off the bottom and can be opened and closed sequentially. An epibenthic net at the rear end of the sledge samples epibenthic megafauna. A still camera with a capacity of 800 frames photographs the bottom in front of the sledge and is used for quantitative estimates of megafaunal density. The sledge is controlled by a TV camera with on-line transmission to the ship.

Large necrophagous deep-sea amphipods are rarely caught with nets, but can be captured in baited traps, often in vast numbers. We used a free-vehicle baited trap set (CHRISTIANSEN, 1996) which was moored at the bottom. Ten traps were fastened to the mooring line from 0 to 500 m above bottom.

At the BENGAL station, the fototrawl was employed once and the trap set was employed twice. Two MOCNESS hauls were conducted, with two samples each in the layers 15 m above bottom, 50 m above bottom and 100 m above bottom. A third MOCNESS haul had to be terminated after one hour because of rapidly worsening weather conditions. At the BIOTRANS station, one haul was conducted for the MOCNESS, which was fished at 15, 50 and 100 m above bottom, and the trap set was also deployed once.

Because the samples have to be analysed in the laboratory, only a first impression can be presented. The fototrawl haul at the BENGAL station had to be terminated after 40 min at the bottom because of a short circuit in the conducting cable. However, a total of more than 300 frames could be shot. The epibenthic net caught only a few megafaunal organisms, mainly small holothurians. In particular, some very small specimens of *Psychropotes longicauda* were caught. Only the first of the plankton nets could be opened and closed properly before terminating the haul. However, the catch was useless, since all plankton nets were damaged, probably due to turbulence during lowering.

Two amphipod trap deployments, one at BENGAL and one at BIOTRANS, could be recovered only after 5 days due to stormy weather conditions. This long exposure, compared with the usual bottom time of about one day, resulted in cannibalism in the traps so that only the exoskeletons of a great part of the amphipods captured were left, at least in the near-bottom traps. Total catch numbers were relatively high in all deployments, particularly in the traps up to 30 m above bottom. All amphipods captured in traps from 7 to 500 m above

bottom belonged to the species *Eurythenes gryllus*, some specimens reaching a total length of ca. 13 cm. In the bottom traps large numbers of mostly small amphipods were captured; besides juveniles of *Eurythenes gryllus* several other lysianassoid species were found. The catch numbers and the distributions of the amphipods appeared to be similar at both stations.

5.6.7 **Geochemistry** (D. Rickert, H. Schale, S. Grandel, A. Bleyer)

Pore waters were sampled from cores taken at the BENGAL (49°N/16°30 W) and BIOTRANS (47°10 N/19°35 W) station in order to investigate the complex interplay of aerobic and anaerobic degradation and local and non-local transport processes.

The main aim of the work is to get data sets which would allow to model transport and degradation as well as redox and dissolution reactions in sediments with high C_{org} inputs in order to contribute to data sets which facilitate a comprehensive modelling of benthic turnover rate and fluxes. With samples taken from multicorer (MC), box corer (KG), CTD water sampler and bottom water sampler (BWS) the vertical distribution of nitrate, phosphate, silicate, and ammonia in the sediments and in the water column was determined. Moreover a stirred flow-through reactor technique was used on board to determine silica solubilities in different kinds of sediment. The benthic regeneration of silica depends on a number of processes, including sediment burial and mixing, dissolution of the silica tests, transport of silic acid through the porous medium, and precipitation of authigenic silicate minerals. The goal of the present studies is to develop a mechanistically correct model for the dissolution kinetics of biogenic opal in order to interpret dissolved silica profiles measured in sediments.

In co-operation with the investigations of pore water chemistry high-resolution analysis of the composition of solid matter will be carried out in order to investigate the interaction of seasonally variable benthic turnover rates and distribution of trace elements in deep-sea sediments.

Surface sediments taken with a multicorer or a box corer subsampled on board with multicorer tubes were brought into the cold room of METEOR immediately after recovery. They were sampled and processed within 3-4 hours at in-situ temperature. Pore water of wet sediment segments was extracted using a squeezer pressurised by nitrogen and samples were filtered on line through 0.4 µm cellulose acetate filters. The following depths intervals were taken and analysed (cm): 0-0.5, 0.5-1, 1-2, 2-3, 3-4, 4-5, 5-6, 6-7, 7-8, 8-9, 9-10, 10-13, 13-16, 16-19, 19-22, 22-25, 25-28, 28-31. The remaining sample volumes were also stored frozen at -20°C in the dark in order to inhibit microbial degradation and assimilation activity. HCl acidification was avoided to prevent a decrease in silica concentrations which may be caused by precipitation reactions during sample storage.

Samples were also taken for laboratory studies of trace element distribution in the system pore water/solid phase. At BENGAL station 369 (station 369, MC-36, station 369, MC-37) two cores of 10 cm diameter and 30 cm length were recovered from multicorer runs #36 and

#37. One core was stored frozen at -20°C, the other was cut into slices for pore water squeezing. Depth intervals taken were: 0.5 cm for the first 5 cm, 1 cm from 6-10 cm, and 2 cm for the remaining core. Squeezed sediment samples (see chapter 7.6.1) were stored in plastic bags whereas the pore water was immediately frozen at -20°C. A 15% solution of $BaCl_2$ was added to 1 ml pore water subsamples of each depth interval for SO_4 precipation. These samples were also stored frozen. The overlying bottom water of one of the cores (1 l) was filtered through 0.45 µm Nalgene SFCA filters and acidified with 2% HNO_3. This sample was kept in a refrigerator. At BIOTRANS station 388 one core (MC-46#388) of 8 cm diameter and 11.5 cm length was sliced and squeezed with a depth resolution of 0.5 cm. The samples were treated like those above; SO_4 was not precipitated due to lack of sample volume. The bottom water sample was treated as described above. At station 398 that is located slightly northward of BIOTRANS, a core (MC-52#398) of 6 cm diameter and 16 cm length was recovered. Because of the small diameter, it could only be subsampled with a resolution of 0.5 cm for the first centimetres, the resolution was 1 cm from 1-10 cm and 2 cm for the remaining core. After squeezing, the pore water samples were treated like those from station 388. The sediment of box corer KG-10#405 looked relatively undisturbed and suitable for further investigations. For this reason, 3 multicorer tubes of 10 cm inner diameter were slowly pushed into the sediment down to a length of 40 cm and two of them were sliced in a depth resolution comparable to the BENGAL samples. Pore waters and bottom water were handled like those from BENGAL station. The third tube was kept frozen. Finally, two cores of 8 cm diameter and 14 cm length from MC-59#405 were recovered. While one of the cores was frozen the other was subsampled in a depth resolution like the core from station 398. From 20 ml of each water sample taken from CTD#386 and #392/8 SO_4 was precipitated with $BaCl_2$, 2 ml were frozen, and 20 ml were acidified with 2% HNO_3 for storing.

5.6.7.1 Shipboard Results: Sediment Geochemistry and Nutrients in the Water Column

Cores analysed for pore water chemistry, samples taken for trace element analysis and parameters measured on board are listed in Table 12.

Analysis

Subsamples with a volume of 1 ml were taken from fresh pore water samples for determination of pH and alkalinity at 2-6°C in the cold room. In addition a set of subsamples from the sediment were taken for determination of pH in the sediment. pH electrodes were calibrated using buffers prepared in artificial seawater (DICKSON, 1993). BIS and 2-Aminopyridine were used as buffers in the neutral pH range (pH 7 to 9). Both, electrode potential and solution temperature were independently recorded using a pH meter and a thermometer. Total alkalinity (TA) was determined from the pH value measured after one-step HCl addition. A volume of 0.3 to 0.5 ml of 0.01 mol HCl was added to 1 ml pore water sample to produce a pH value of 3.0 to 4.0. The electrode was calibrated with pH 3.00 and pH 3.52 buffers prepared from 10.637 ml 0.01 mol HCl + 19.363 ml purified water + 70 ml artificial seawater. The alkalinity of the artificial seawater resulting from salt impurities was

determined by a GRAN titration and considered in the buffer preparation. Artificial seawater was prepared by adding the following:
0.42764 mol NaCl (suprapur);
0.01058 mol KCl (p. a.);
0.05474 mol $MgCl_2$ (p. a.);
0.01075 mol $CaCl_2$ (p. a.);
0.2927 mol Na_2SO_4 (p. a.) to 1 litre of MilliQ® purified water.

A mean TA of 2.29 mmol/kg with a standard deviation of 0.05 mmol/kg results from repeated (n = 10) one-step titration of IAPSO seawater standard.

Concentration of dissolved nitrate, phosphate, silicate and ammonia was determined using standard photometric procedures (GRASSHOF et al., 1983) on a convential two beam photometer in fresh pore water subsamples and water samples taken with the BWS or CTD water samplers.

Results of multicorer (MC) and box corer analysis (KG) are listed in chapter 7.6.1 and depth profiles of chemical constituents of the pore water analysis are illustrated in Fig. 102. Quantification of aerobic and anaerobic organic matter degradation as well as transport processes and dissolution reactions in sediments were the main scientific goals of the geochemical work group.

Tab. 12: Cores analysed for pore water chemistry and samples taken for trace elements:
+ measured on board
- not determined on board
Σ samples taken

Station	nutrients	pH	alkalinity	aluminium	trace elements
BENGAL					
MC-33#362	+	+	+	•	-
MC-34#362	+	+	+	-	-
MC-36#369	+ (silica)	-	-	-	•
MC-37#369	-	-	-	-	•
BIOTRANS					
MC-46#388	+	+	-	-	•
MC-50#395	+	+	-	-	-
MC-52#398	-	-	-	-	•
MC-56#399	+	+	-	-	-
MC-59#405	+	+	+	•	•
KG-10#405	+	+	+	•	-

All multicorer show silica concentrations increasing as a consequence of different dissolution behaviour of diagenetically altered biogenic opal from bottom water values of about 40 µmol to constant values of just between 180 and 250 µmol. The different saturation concentrations and depths where saturation is reached is affected by a great variety of the amount of dissolvable particulate biogenic silica. Moreover, the release of silica in the pore water is the result of dissolution kinetics of biogenic opal which vary widely because of diagenetic alteration, different sediment matrix effects and involved adsorption-desorption reactions. Biological mixing, by affecting the depth at which recently deposited solid silicate materials dissolve, also plays a critical role in determining interstitial concentrations.

Nitrate pore water profiles measured at BENGAL or BIOTRANS show almost the same behaviour: they increase from bottom water values of about 20 µmol to reach a maximum of 35 µmol at 4-5 cm (BENGAL) or 6-7 cm (BIOTRANS) and decrease below it. The ammonia profiles, on the other hand, show almost constant values (6-8 µmol), but a significant maximum at the first centimetre in samples taken at BIOTRANS station is observed. This indicates great communities of microbial decomposer organisms. Their excretions probably cause the high ammonia values measured in the first centimetre. Especially high values for ammonia coupled with phosphate concentrations of almost 7 µmol are observed in the first centimetre of MC-46#388. The increase in nitrate concentrations indicates the release of nitrate from organic matter mineralisation during nitrification in the top oxic sediment layers. Below the maximum the decrease shows the beginning of consumption of nitrate caused by denitrification in deeper suboxic layers. Zero nitrate and increasing ammonia concentrations, indicating anoxic conditions, were not observed. The somewhat noisy nitrate profile in the oxic layers was possibly caused by bioturbation. Phosphate profiles show a slight increase with depth. The metabolite stoichiometry seen in the pore water profiles is also of interest. In the oxic sediment layers, the N/P ratio of about 20 in the first centimetre is somewhat too high for marine organic matter, but can be explained by the high ammonia values. Below the first centimetre in all cores the N/P ratio of about 15 is typical for marine organic matter, but slightly decreases with depth as a result of denitrification in deeper suboxic layers. A minimum of about 5 is observed in KG-10#405 at about 27 cm depth.

The pH in all sediments is about 7.6 and a mean alkalinity of 2.3 is observed. Other pore water data are available and may be requested from the authors.
Further investigations are needed to evaluate first results of the dissolution kinetics of biogenic opal. Trace element analysis will be performed in home laboratories.

Results from CTD samplers /bottom water samplers (BWS) are as follows:
A whole profile of all nutrients was taken at each station by combination of 3 CTD deployments. All nutrients are almost totally depleted in surface waters. Remineralisation of organic matter sinking from surface waters return the nutrients to solution. The profiles for nitrate (21 µmol) and phosphate (1.6 µmol) reach maxima at about 3000 m depth, while the maximum for silicate (46 µmol) is reached deeper at 4500 m. The skeletal remains of siliceous organisms (biogenic opal) are much more resistant to solution than soft organic tissue, and it therefore sinks deeper before significant solution occurs. Water samples from bottom water

Fig. 1 Pore water profiles (BIOTRANS)

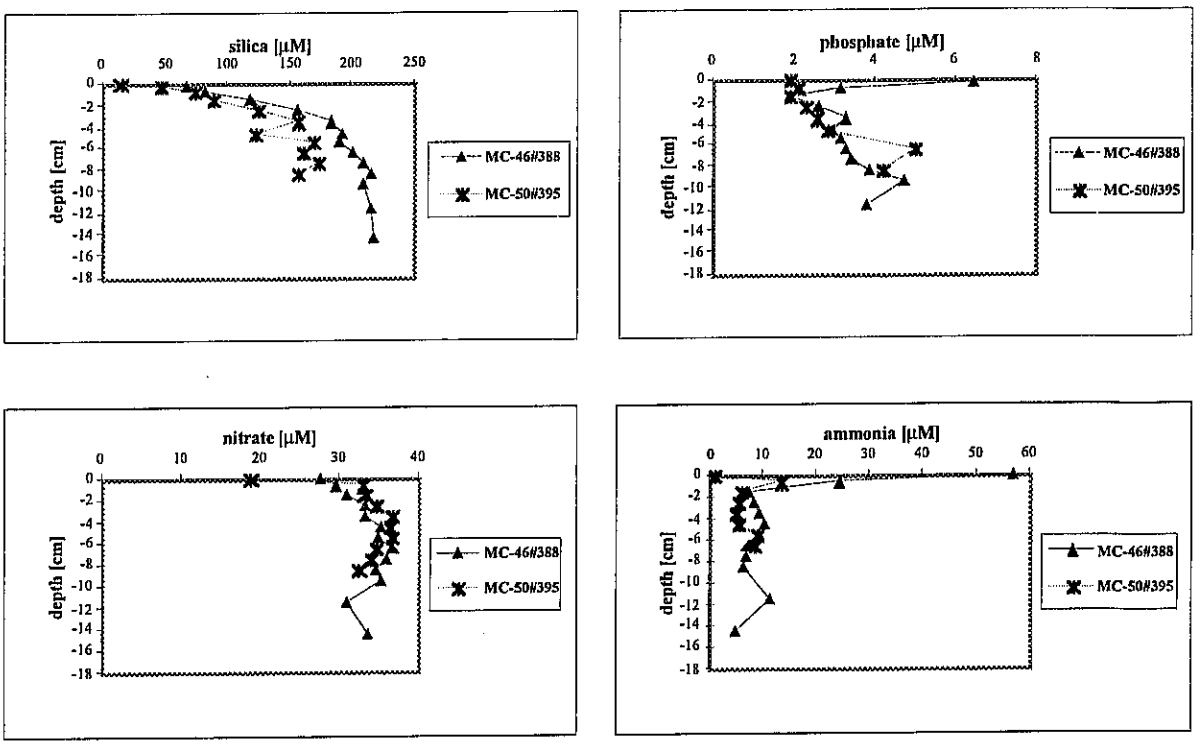

Fig. 102a: Pore water profiles (BIOTRANS).

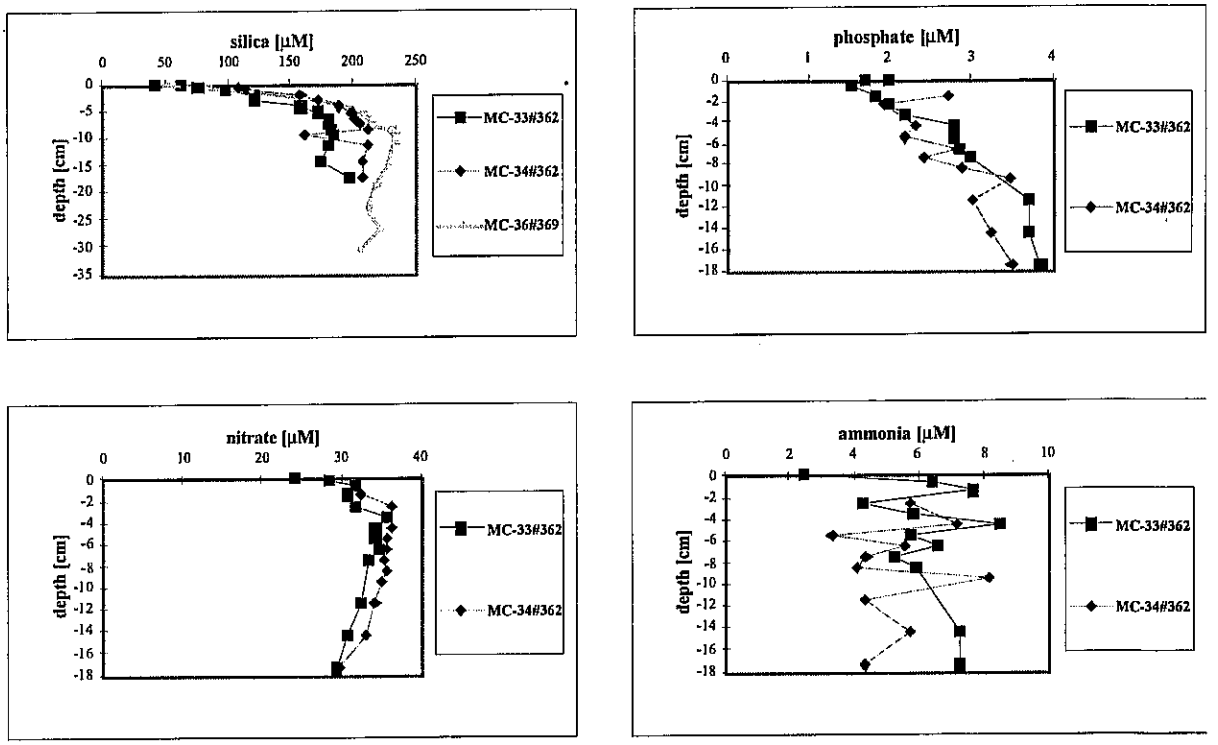

Fig. 102b: Pore water profiles (BENGAL).

samplers were also analysed for nutrients. A small-scale resolution of gradients close to the bottom (0-1 m) are obtained for all nutrients. Data can be requested from the authors.

5.6.8 Biogeochemistry of Sediments and Megafauna of the Porcupine Abyssal Plain (I. Horsfall)

It was intended that experiments would be carried out on this cruise to compliment those completed on DISCOVERY cruise 222 leg 2 in August 1996. Briefly, holothurian gut content samples were to be incubated with fluorogenic substrates in order to calculate maximum digestive enzyme activity. This data would have been combined with information on natural substrate concentrations, determined on samples taken back to the lab, and used to calculate the feeding rate of abyssal holothurians. A minimum of 2-3 large specimens (depending on species and gut volume) were required to complete these experiments. Unfortunately, the one and only trawl carried out did not produce enough animals.

More successfully, sediment cores were taken from the multiple corer in order to compare the methods used by the research group in Liverpool with those used at GEOMAR. To this end, two 6 cm diameter cores, one from BENGAL and one from BIOTRANS (station 362 MC-33 and station 395 MC-49 respectively) were taken from the same multicorer deployments as the GEOMAR group (Benthic biology). Cores were sliced down to 5 cm using the same depth horizons as the GEOMAR group. The sediments obtained will be analysed for a number of organic fractions including individual amino acids and lipids.

5.6.9 Geochemical Analysis of Near Bottom Water and Sediments (D. Panagiotaras)

Near bottom water from CTD casts and water from multiple corer tubes stations 367, 373, 375, 383, 388, 393 was sampled for the analysis of Ca, Mg, P, Mn, Fe. The water samples were filtered under a vacuum pump system on 0.45 μm pore size millipore filters and acidified with Hcl 6 M until pH 2.

The sediments from BENGAL and BIOTRANS stations were collected from a multiple corer and a box corer (stations 372, 373, 388, 398, 405) for the analysis of silicate, barite, Fe, Mn, Ca, Mg, and P. At BENGAL station a multiple corer tube was sliced in 3 cm intervals up to 12 cm and 15 cm depth respectively. Pore water was collected for each layer by centrifugation for 20 minutes.

At BIOTRANS an 8 cm core was sectioned into 2 cm intervals for pore water. This core was sliced into 2 cm layers. A box core sample of 30 cm total length (station 405) was cut in 2 cm intervals up to 12 cm depth and in 5 cm intervals up to 30 cm depth for pore water analysis.

5.6.10 Particle Flux and Organic Geochemistry of Sediments and Pore Waters

(P. Schäfer, N. Lahajnar)

Mooring with sediment trap and water transfer systems were used. Details of the moorings are given in Table 13. At the BENGAL station one sample of sinking particles was collected in a water depth of 4266 m (566 m above the sea floor). At the BIOTRANS station the sediment trap has been moored in a water depth of 3986 m (564 m above the sea floor).

Tab. 13: Details of short-term moorings NE Atlantic Ocean, BIGSET

Region	**BENGAL**	**BIOTRANS**
Mooring name	ENAT-01	WNAT-01
Mooring position	48°55.6' N/16°35.1 W	47°07.8' N/19°40.4 W
Deployment	12.10.96, 07:20-08:10 (UTC)	24.10.96, 15:15-16:00 (UTC)
Deployment station	361	387
Recovery	20.10.96, 08:20-11:00 (UTC)	29.10.96, 11:10-12:50 (UTC)
Recovery station	377	401
Water depth (m)	4832	4550
Trap depth (m)	4266	3986
Distance to sea floor (m)	566	564
Sampling start	12.10.96, 13:00 (UTC)	24.10.96, 00:00 (UTC)
Sampling end	20.10.96, 05:00 (UTC)	29.10.96, 05:00 (UTC)
Sampling duration (h)	184	125
Pump depth (m)	4295	4495
Distance to sea floor (m)	537	55
Sampling start	12.10.96, 13:00 (UTC)	24.10.96, 00:00 (UTC)
Sampling end	20.10.96, 03:30 (UTC)	29.10.96, 02:00 (UTC)
Sampling volume	24 x 10 l	6 x 10 l

5.6.10.1 Shipboard Results of Sediment Trap Analysis

The particle colour of the sediment trap sample at the BENGAL station (ENAT-01) was brown-green. The major constituents were large amorphous aggregates whereas the abundance of fine-grained material and faecal pellets was less. One pteropod with a length of 2.5 cm was removed as a subsample. A faecal pellet (0.5 x 0.7 cm), some smaller pteropods and foraminifers were also visable. The sample was wet sieved (1 mm) and split. Three quarters of the < 1 mm-sample were filtered on a preweighed polycarbonate filter and dried (40°C). The rest was fixed with formalin for microscopic analysis in the home laboratory. A preliminary microscopic analysis on board showed that the main constituents of the sample were

fragments of diatoms. The other remaining identified plankton belonged to foraminifers, radiolaria, silicoflagellates and dinoflagellates.

At the BIOTRANS station (WNAT-01) the particle colour was greenish-brown. The major constituents were large amorphous aggregates (70%) whereas fine and coarse grained material and faecal pellets were less abundant. Pteropods and foraminifers were present as trace amounts. One per cent of the total suspended sample was used for preliminary microscopic analysis on board. The rest was filtered on a preweighed polycarbonate filter and dried (40°C). The microscopic analysis on board showed that the main constituents of the sample were small fragments of phytodetritus. The remaining identified plankton belonged to coccolithophorids, diatoms, pteropods, foraminifers, silicoflagellates and dinoflagellates.

The sample at the BIOTRANS station was more greenish, contained smaller phytodetritus and less remains of foraminifers and radiolarians than at the BENGAL station.

With the weight of the dry sample material from the filter the total flux was calculated (Fig. 103). Analysis of C_{org}, nitrogen and carbonate have been completed. The content of biogenic opal, lithogenic material, amino acids, hexosamines and carbohydrates will be measured. Analysis of stable carbon and nitrogen isotopes will be performed.

The total flux at the BENGAL station is higher than at the Biotrans station (Fig. 103). The contents of C_{org} and N in sinking particles as well as the fluxes of C_{org}- and N at the BENGAL station are higher than at the BIOTRANS station (Figs. 103 and 104). The fluxes of carbonate are similar at both stations.

The fluxes for the period July-October 1989 reported by HONJO and MANGANINI (1993) are higher than the fluxes measured in October 1996. Reasons for this may be the higher fluxes in summer 1989 and interannual variability.

For sediment and pore water studies, cores from three multiple corer hauls and one box core were subsampled for sediment, centrifuged sediment and pore water. At BENGAL station, cores from one multiple corer haul were subsampled (MC-39). At BIOTRANS station, one multiple corer (MC-53) and a box corer (KG-10), and near the BIOTRANS station, one multiple corer (MC-52) were subsampled.

Sediment was subsampled at selected intervals (Table 14). Pore water for the analysis of dissolved organic compounds was centrifuged from the sediment subsamples at a temperature of 2°C at 2000 rpm for 20 minutes. Subsequently, the supernatant pore water was removed with syringes and filtered through glass microfibre filters (GF/F, 0.7 µm, pre-combusted at 450°C, 4.5 h). The pore waters were filled in 10 ml glass ampoules (pre-combusted at 500°C, 12 h), the ampoules were sealed under nitrogen and deep freezed. The sediment residue as well as the untreated sediment were dried at 40°C and stored in glass vials.

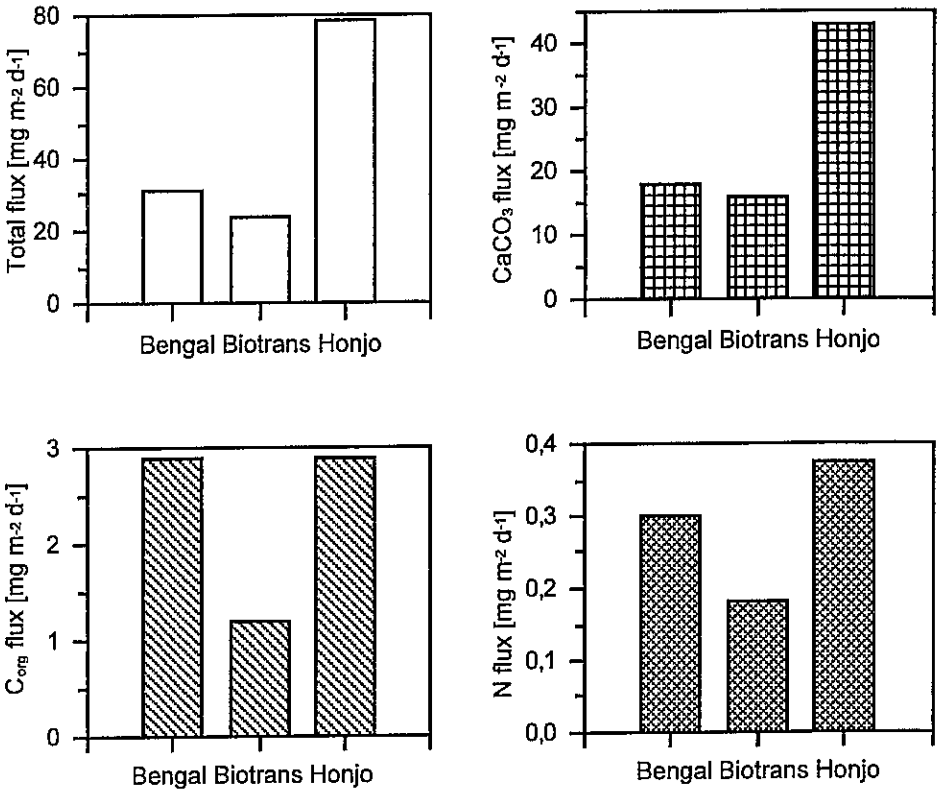

Fig. 103: Total flux, carbonate flux, C_{org} flux and nitrogen flux in the NE Atlantic Ocean. Station description for BENGAL and BIOTRANS (see Table 13). For comparison flux data for a station near by the BIOTRANS station (= Honjo, 48°N/21°W) are also given (trap depth = 3700 m, post-bloom period: 18.7.-30.10.1989, HONJO and MANGANINI. 1993).

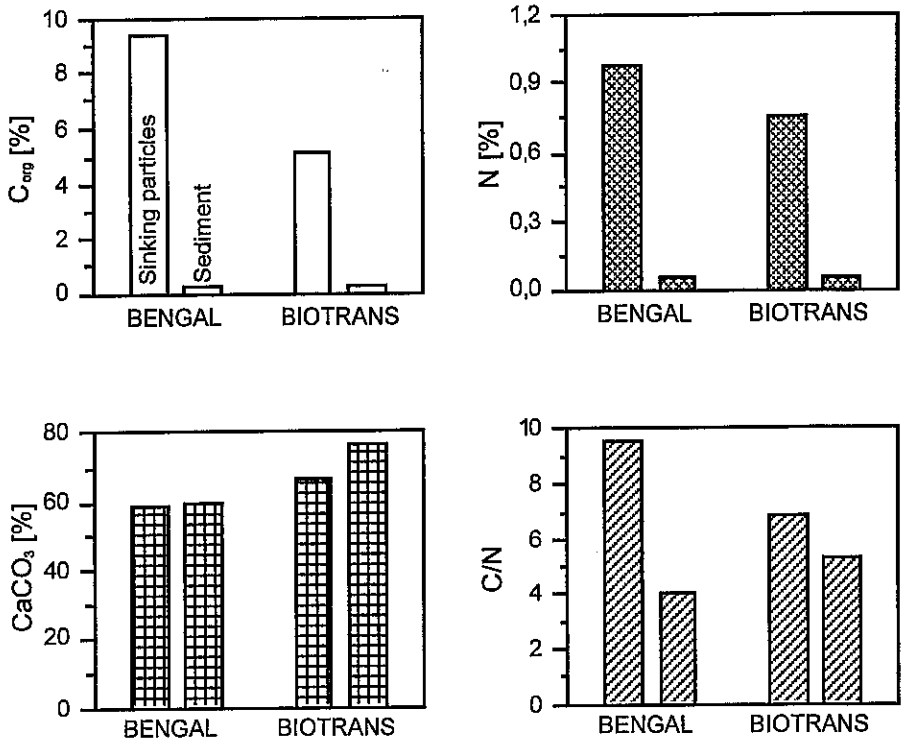

Fig. 104: Concentration of C_{org}, nitrogen and carbonate as well as C/N (weight) values of sinking particles in comparison to underlying sediment.

Tab. 14: Sediment and pore water sampling

Sample	**MC-39**	**MC-52**	**MC-53**	**KG-10**
Date	18.10.1996	28.10.96	28.10.1996	28.10.1996
Region	BENGAL	near BIOTRANS	BIOTRANS	BIOTRANS
Latitude	48°58 N	47°28,3 N	47°11,7 N	47°11,1 N
Longitude	16°28 W	19°40,5 W	19°34,1 W	19°33,9 W
Station	372	398	399	405
Lot-depth (m)	4805	4530	4565	4564
Cable length (m)	4850	4570	4595	4598
Sample intervals (cm)	0-0.5 0.5-1 1-1.5 1.5-2 2-2.5 2.5-3 3-4 4-5 6-7 9-10 14-15 19-20 24-25 29-30	0-0.5 0.5-1 1-1.5 1.5-2 2-2.5 2.5-3 3-4 4-5 7-8 9-10 14-15 18-19	0-0.5 0.5-1 1-1.5 1.5-2 2-2.5 2.5-3 3-4 4-5 6-7 9-10 12-13	0-0.5 0.5-1 1-1.5 1.5-2 2-2.5 2.5-3 3-4 4-5 6-7 9-10 14-15 19-20 24-25 29-30 34-37

Sediment will be analysed for C_{org}, nitrogen, carbonate, biogenic opal, lithogenic material, amino acids, hexosamines, carbohydrates and stable carbon and nitrogen isotopes. Pore water will be analysed for dissolved organic carbon, dissolved combined and dissolved free amino acids, hexosamines and carbohydrates.

The concentration of C_{org} and nitrogen is higher in sinking particles than in sediment. The concentration of carbonate is similar. C/N ratios are lower in the sediment. In sediments with very low C_{org} contents the inorganic nitrogen that is included in the total nitrogen measurements becomes more important in influencing the C/N ratio towards lower values (MÜLLER, 1977).

For suspended matter studies, water samples (Table 15) were taken with a rosette water sampler equipped with 10 l Niskin bottles from selected depths for filtration of suspended matter and for the measurement of the grain-size distribution of suspended particles. For sampling of suspended matter seawater was filtered using preweighed glass microfibre filters (GF/F, 0.7 µm, pre-combusted at 450°C, 4.5 h). Some of the filters were rinsed with double

deionized water (Tab. 15). The filters were dried at 40°C. For grain-size analysis water samples were stored in polyethylene bottles. Mercuric chloride was added to some of the water samples (Tab. 15, 0.5 ml saturated $HgCl_2$ solution/l).

Tab. 15: Water sampling

Station	Depth (m)	Filtered volume for sampling of suspended matter (ml)	Sample for grain size (ml)
14.10.1996 - BENGAL	15	8800*	100
48°58,1 N - 16°27,8 W	30	5950*	100
Station 365 - Profile 3	50	9400*	100
	60	9400*	100
	70	9100*	100
	80	9000*	100
	100	9300*	100
	150	9000*	100
	200	9400	100
	250	8000	100
	300	9000	100
16.10.1996 - BENGAL	4300	28400	100
48°58,0 N - 16°28,0 W			
Station 367 - Profile 4			
23.10.1996 - BIOTRANS	20	4850	100
47°10,9 N - 19°33,8 W	50	18000	100
Station 386 - Profile 5/7	100	9300	100
	200	17600	100
30.10.1996 - BIOTRANS	4000	18800*	100
47°11,1 N - 19°34,0 W	4500	35400*	100
Station 404 - Profile 12			
31.10.1996 - BIOTRANS	20		1 l**
46°35,2 N - 18°52,6 W	40		1 l**
Station 409 - Profile 14	60		1 l**
	80		1 l**
	100		1 l**
	300		1 l**
	500		1 l**
	700		1 l**

6 Ship's Meteorological Station

6.1 Weather and Meteorological Conditions during Leg M 36/1 (C. Joppich)

The weather in the first two days of the cruise was dominated by the subtropical high. Its centre was nearly stationary near 33°N/44°W. METEOR sailed northeastward in a light, moderate southerly, later southwesterly breeze. On June 9, a low over the Gulf of St. Lorenz moved southeastward, later eastward, affecting the investigation area for the next two days. In front of the low a strong westerly wind was observed, while the northwest wind at the rearside calmed down soon. Due to a high moving southeast from Newfoundland, the cold polar air was under high pressure influence. On June 11, a new low moved eastward from Labrador and passed far north of METEOR on June 12. In front of this low, southwesterlies increased near gale force, but METEOR sailed southeastward and enlarged the distance from the centre of the low. Over the next three days the ship's speed was nearly equal to the easterly drift of the front. Therefore foul frontal weather conditions with temporary rain accompanied METEOR on its southeasterly course until June 16. During the last two days of the cruise, high pressure influence dominated again, and moderate northerly to northeasterly trade wind were blowing as METEOR reached the harbour of Las Palmas.

6.2 Weather and Meteorological Conditions during Leg M 36/2 (G. Kahl, H.-P. Lambert)

When METEOR left Las Palmas, Gran Canaria on June 22, 1996, there were normal Trade Winds, which means northeasterly winds of 5 to 6 Bft. These resulted from the North Atlantic Subtropical Anticyclone, shortly the Azores High, being at its early summer position in the vicinity of that archipelago facing a low over Morocco. During the last days of the month of June, the Azores High's central pressure exceeded barely 1030 hPa whereas the intensity of the Moroccan low varied from 1012 hPa at the onset of the cruise to 1003 hPa a few days later. Ships in the vicinity of that country reported northerly winds up to 8 Bft, but METEOR, having proceeded on a northwesterly course, was not affected that severely. When METEOR worked on its station A1, there were still northerly winds 4 to 5. The Moroccan low, though present, was no longer responsible for that at a latitude of 40°N, but a low resulting from intense heating of the Iberian peninsula had developed there. From this, it may be said that the roots of the Trade Winds had extended to 40°N.

As soon as METEOR started to go on further north it entered the realm of the westerly winds where METEOR stayed until berthing at the port of Bergen. There was a gale centre pf 983 hPa in northern Ireland moving slowly away northeastward. A cold front passed the ship causing a maximum of northwest 7 Bft for a few hours on July 7, 1996. Thereafter, an extraordinary development took place. A wave developed at this cold front east of Newfoundland, and when it was of a low of 1010 hPa, it passed METEOR rather quickly moving on to the Bay of Biscay on July 6, 1996. Northeasterly winds 6 to 7 Bft were recorded by METEOR's wind speed meters because the surface air pressure rose sharply after passage of the low which was

developing into a gale centre at the time. During July 8, this low further developed into a storm low over the Alps and later it was responsible for gales in the eastern and northern parts of the Baltic Sea. Meanwhile, the Azores High had been strengthened to a central pressure of 1037 hPa and drifted north to the area west of the Bay of Biscay. A low coming from Labrador passing Greenland moved on to Iceland and developed on its way during July 9. Its cold front, however, did not pass the ship approaching its station L3 due to a wave deployment. The wave and the Azores High being displaces northward resulted in southwesterly winds of 7 Bft combined with fog. The fog was the only weather element that hampered METEOR's operations because it lifted only after the wave had passed the ship in the afternoon of July 10. The next day offered light, westerly winds. A new gale centre developing southwest of Greenland was lurking already, however, and during July 13, when it had developed to a minimum central pressure of under 985 hPa southeast of Iceland, westerly gales 7 to 8 Bft, the maximum winds during M 36/2, were felt on board. METEOR proceeded on its way and when station A2, the most northerly one, was reached, the Azores High moved to Scotland, this meaning light westerly winds for our ship.

6.3 Weather and Meteorological Conditions during Leg M 36/3

(G. Kahl, H.-P. Lampert)

When METEOR left Bergen in the morning of July 21, 1996, the synoptic situation was that of a migrating high that moved northeastward along the Norwegian coast resulting in light, southerly winds. A low following that high had reached the Faeroe Islands, approaching the first work area at the same time as the research vessel. When sampling was being done north of the Shetland-Faeroe Ridge, the low of 1004 passed on northward, and southeasterly winds 4 to 5 Bft veered to the northwest. The low then moved away northward faster than the ship on its way to the Voering Plateau being visited on July 25. The synoptic situation comprised of a gale centre 995 at the western entrance of the Denmark Strait, its occluded front extending from Jan Mayen to the Shetlands and the ridge of high pressure ahead of it just over our position. Winds were light and variable.

METEOR spent the last days of July moving up and down the Norwegian continental slope. The gale centre passed Iceland and then filled. Instead, a high 1017 developed east of Greenland so that northeasterly winds about 4 Bft were observed. Meanwhile, another gale centre had reached the waters off Eastern Greenland only to be dissipated, but a secondary low moving further south had reached a central pressure of about 980 before filling to 995 near the Orkneys on August 1. The high in the Norwegian Sea was still there though its central pressure had weakened to a mere 1013. As a result, winds were much the same as before when a mooring at 70°N/4°E was recovered and deployed again.

The ship called at its next work area: East Greenland, extending from 0° to 7°N from August 3 to August 5, 1996. Another Icelandic gale centre of 985 central pressure had developed, but METEOR being that far north was not affected. As before, light easterly winds were felt.

The next scheduled work area was the seamount Vesteris Banken, rising steeply from surroundings of more than 3000 m depth to a minimum depth of 123 m. The ship proceeded into the ice as far as it could go avoiding direct contact with the floes. In this manner, Vesteris Banken proved to be unaccessible, so METEOR had to turn around to find the way back into open waters while there were still light easterly winds. Mist, however, had turned into thick fog. The Icelandic gale centre had started to fill and to move northward, and the advection of warm air north of the centre of the low caused the plight of arctic shipping to occur.

The ship turned south to Jan Mayen Island. The waters there proved ice-free on August 8, 1996, so the island could be passed on its western side while southeasterly winds Bft 5 were blowing. These prompted a foehn effect so that nearly all the island was to be seen, just a few lenticularis clouds in the sky on its leeward side. When this rare sight had been fully appreciated by everyone interested, METEOR indulged in fog again, heading for the Denmark Strait.

The eastern entrance of the Denmark Strait was reached on August 9. Easterly winds of about 5 Bft were prevailing. West of Ireland, however, there was a gale centre of 985 extending into higher levels of the atmosphere. In mid-tropospheric levels, an area of divergence pointed towards the Denmark Strait, and so, northeasterly gales of 8 Bft were observed on August 10. At 09:00 UTC, the maximum wind velocity of 41 kn was recorded. This one hour may be called Bft 9. Wind velocity lessened thereafter, but in the evening it was still Bft 6. To bring about these gales, some effects are responsible:

- the aforementioned mid-tropospheric divergence area;
- rising atmospheric pressure in Scoresbysund at the same time, thereby enhancing pressure differences;
- air masses approaching the Greenland mountain barrier do not climb it, but they are pressed southward, and so the ensuing gale was observed by scientists and crew alike. This effect is better known in the area east of Cape Farvel, where it produces storm force northerlies in winter.

The low was then being taken up by the changing upper air flow and it moved away northeastward. So winds abated further, and at midnight, August 11/12, they were light and variable. Meanwhile, a low 1000 had passed Cape Farvel and headed for northwestern Iceland. It passed Iceland during the night of August 12/13, thereby filling somewhat. This synoptic situation resulted in northeasterly winds 6 to 7 Beaufort on August 13. In contrast to the synoptic situation on August 10, the effect listed as second point, rising pressure on the east coast of Greenland, was missing, and so no gales occurred.

During the last days of M 36/3, a gale centre approached the Icelandic south coast and went on northeastward, so that northeasterly winds of medium strength were maintained, backing north and abating somewhat when METEOR rounded northwestern Iceland.

6.4 Weather and Meteorological Conditions during Leg M 36/4

(G. Kahl, W.-T. Ochsenhirt)

When METEOR left Reykjavik during the afternoon of August 19, the sun shone over the city, and winds were light and variable. These favourable conditions resulted from a gale centre near Cape Farvel building a wedge of high pressure over western Iceland. As the vessel pursued its southeasterly course, the gale centre of 1000 remained nearly stationary, but a secondary low was formed, and on August 8, its central pressure was also about 1000, at 53°N/25°W. METEOR was east of that position, experiencing southeasterly winds 6 to 7 Bft. The gale centre deepened further to 995 when the ship passed it on August 22. Meanwhile, another low had migrated to 44°N/40°W, and as it tried to build up high pressure northeast of its position, the pressure gradient west of the gale centre, which METEOR had just passed, tightened. The ensuing winds reached a peak force of northwest 7 to 8 Bft during the early morning hours of August 23, and slowly lessened thereafter, northwest 5 being recorded on August 24. These were the days of the ship's first station at 49°N/16°5 W.

The winds prevailing up to August 30 were northwest to north 3 to 5 Bft. These winds resulted from the building and subsequent strengthening of a high 1022 at 55°N/32°W on August 25 and 1032 at 44°N/20°W on August 8. Thereafter, the high elongated northeast to the Celtic Sea, the ensuing light winds over the Whittard Canyon veering northeast. So it may be said that the outer Bay of Biscay did nothing to justify its bad reputation for ill weather when METEOR did research there.

During the last few days of leg M 36/4 there was a low west of Gibraltar. It caused the formation of a secondary low near Porto, which intensified as METEOR passed it. So there were northeasterly gales of 8 Bft in the vicinity of Cape Finisterre, abating quickly to northerlies about 3 Bft along the coast until Lisbon was reached on September 4.

6.5 Weather and Meteorological Conditions during Leg M 36/5 (H. Weiland)

In the first week from September 7 to September 14, the weather situation was dominated by high pressure over the northeastern part of the North Atlantic, so the winds in the work area of METEOR came from easterly directions and did not increase above Bft 6. On the weekend, a second low split from a large low pressure system south of Greenland and went eastward towards Spain. So the situation changed to a westerly stream over the Atlantic. On Monday, September 16, the ex-hurricane "Hortence" crossed the North Atlantic from west to east and affected the work area on Tuesday with a storm up to Bft 11 for few hours, but there was not enough time to build up a high swell. Another low of only small extension but of extratropical origin crossed the Atlantic two days later with Bft 9. As the storm did not last long, not much time was lost for the scientific activities. On Friday, September 20, the pressure distribution expected for this season became predominant: a nearly stationary low between Iceland and Greenland which regenerated every few days due to a new low arriving from Newfoundland. The intensity of these lows increased, and on September 26, an intense low with a stormfield

extending from Labrador to Ireland had been developed. Due to this situation a persisting swell built up which made the works on board difficult for the next days. For many hours it was impossible to run any scientific equipment. On September 29, the situation improved so that there were no more problems. The last days of this expedition were dominated by high pressure over the mid-North Atlantic.

6.6 Weather and Meteorological Conditions during Leg M 36/6

(D. Bassek, H. Weiland)

METEOR cruise M 36/6 to the BENGAL and BIOTRANS areas began on October 9, leaving the port of Vigo. On the first two days there was high pressure in the area between Ireland and Spain, so the trip began with light winds from easterly directions. But when the ship arrived in the BENGAL area, the weather situation developed as it is expected for the season. A low was moving from Newfoundland to the areas west of the Hebrides. Soon the wind force increased to Bft 8, so the scientific activities became difficult already on the first days. Due to a long fetch, a high swell was building up, which persisted for several days and decreased only slowly. On October 16, the situation became better, but on the next day, another low went from Newfoundland to southern Iceland with increasing wind force. On October 20, a very strong northerly flow of cold air over the western North Atlantic was responsible for intense cyclonic activity in the area northwest of the Azores after which only a new storm depression had been established, which became a depression centre for the next days and caused problems for the activities on board again due to storm forces and high swells. On October 25, the hurricane „Lili", which had stayed near the Bermuda Islands for several days, began to move east and reached the BIOTRANS area on October 27. Lili crossed the area about 150 miles north of METEOR. The ship first got the forward-side with southerly storm force 11, then the trough with force near Bft 12 and the rear-side with northwesterly storm force 11. For about 7 hours the gusts went up to Bft 12 with a maximum of 81 knots and wave highs up to 14 meters. On October 28, the scientific activities could be continued; on the following days there were wind forces between Bft 5 and 7. The ship arrived in Viana do Castelo on Sunday, November 3, with light winds under the influence of a stationary high over Spain.

7 Lists

7.1 Leg M 36/1

7.1.1 List of Stations

Station	Time UTC	Device	Date	Geographical position Latitude	Longitude	Water depth (m)
172	13:20	CTD	11.06	46°39.2	41°54.3	4185
173	13:28	CTD	13.06	41°55.1	34°04.9	3928
174	10:51	CTD	16.06	33°27.2	22°10.0	5272
175	12:02	CTD	17.06	31°16.4	19°04.1	4694

7.2 Leg M 36/2

7.2.1 List of Stations

Station	Number	Time UTC	Device	Date	Geographical position Latitude	Longitude	Water depth uncorrected (m)	Wire length (m)	Comments
177	1	07.07 09.35	CTD	23.06	30°34.0'N 30°33.9'N	18°35.0'W 18°35.5'W	4635	3000	Teststation
178		12.50 16.17		24.06	32°59.4'N 33°00.4'N	21°58.2'W 22°00.4'W			recovering L1
		17.42 19.00	Go-Flo		33°00.5'N	22°00.7'W	5220	1000	Test
		19.23 00.18	Go-Flo		33°00.5'N 33°00.6'N	22°00.7'W 22°00.8'W	5220	4200	
	2	00.27 01.27	CTD	25.06	33°00.7'N 33°00.7'N	22°01.1'W 22°01.2'W	5219	500	
		01.35 01.42	APN		33°00.7'N	22°01.2'W	5220	50	
	3	02.37 06.30	CTD		33°00.5'N 33°00.6'N	22°01.0'W 22°01.0'W	5200	5243	
		08.54 09.08	Secchi		33°00.1'N 33°00.2'N	21°59.9'W 22°00.0'W	5218	24.5	
	4	09.14 12.06	CTD		33°00.5'N 33°00.6'N	22°00.2'W 22°00.1'W	5218	4200	
	5	13.17 14.51	CTD		33°00.2'N 33°00.2'N	22°00.3'W 22°00.3'W	5241	2010	
		15.09 22.35	IPS		33°00.0'N 33°00.2'N	22°00.0'W 22°00.0'W	5237	4205	
		23.03 23.16	MSN		33°00.2'N	22°00.0'W	5237	100	
		23.38 00.27	MSN	26.06	33°00.2'N	22°00.1'W	5240	700	
		02.09 08.20	IPS		33°00.0'N 33°00.0'N	22°00.2'W 22°00.0'W	5219	2505	
	6	08.53 9.56	CTD		33°00.4'N 33°00.4'N	22°00.0'W 22°00.1'W	5242	150	
		10.55 11.26	OS		33°00.3'N	21°59.9'W	5242	150	
	7	11.38 12.02	CTD		33°00.4'N 33°00.5'N	21°59.9'W 21°59.8'W	5244	120	
		12.55 19.39	IPS		33°00.1'N 33°00.1'N	21°59.9'W 21°59.9'W	5218	4155	

Station	Number	Time UTC	Device	Date	Geographical position Latitude	Longitude	Water depth uncorrected (m)	Wire length (m)	Comments
		21.05	MSN		32°59.9'N	22°00.0'W			defective
		21.07							
	8	22.12	CTD		33°00.5'N	22°00.5'W	5219	5000	
		01.40		27.06	33°00.5'N	22°00.9'W			
		07.22			33°00.4'N	21°57.9'W	5239	5239	deployment
		10.23			32°58.4'N	21°58.0'W			L1, line break
		11.18			32°59.7'N	21°58.3'W			recovering L1
		15.00			32°59.1'N	21°58.3'W			
		16.09	MUC		32°59.8'N	21°59.5'W	5233	5287	
		19.48							
		07.29		28.06	33°00.1'N	21°57.9'W	5244		deployment
		12.17			33°00.0'N	22°00.0'W			L1/267-17
	1	15.14	XBT		33°29.3'N	21°52.1'W	5280	760	
	2	18.20	XBT		33°58.4'N	21°44.3'W	5283	760	
	3	21.14	XBT		34°27.7'N	21°36.3'W	5200	760	
	4	00.09	XBT	29.06	34°57.1'N	21°28.5'W	5246	760	
179	9	03.30	CTD		35°30.1'N	21°19.9'W	5194	500	
		04.33			35°30.1'N	21°20.0'W			
	10	05.21	CTD		35°30.2'N	21°20.1'W	5192	5000	
		11.05			35°30.3'N	21°20.1'W			
		11.22	MSN		35°30.3'N	21°20.2'W	5192	20	test
		11.27							
	5	14.15	XBT		35°59.2'N	21°11.7'W	4966	760	
	6	17.00	XBT		36°28.5'N	21°03.4'W	4833	760	
	7	19.44	XBT		36°57.8'N	20°05.1'W	3866	760	
	8	22.26	XBT		37°27.2'N	20°46.7'W	4091	715	
180	11	00.42	CTD	30.06	37°50.0'N	20°40.0'W	4935	500	
		01.38			37°50.0'N	20°40.1'W			
	12	02.20	CTD		37°49.9'N	20°40.0'W	4936	4930	
		06.26			37°50.0'N	20°40.0'W			
	9	09.28	XBT		38°19.3'N	20°31.1'W	4562	760	
	10	12.19	XBT		38°48.3'N	20°22.1'W	4329	737	
	11	15.13	XBT		39°07.5'N	20°13.1'W	5006	760	
	12	18.06	XBT		39°09.0'N	20°03.9'W	4898	742	
181		18.18	IPS		39°47.8'N	20°03.6'W	4994	4055	
		01.42		01.07					
	13	01.51	CTD		39°47.5'N	20°03.7'W	4982	500	
		02.45			39°47.5'N	20°03.7'W			

Station	Number	Time UTC	Device	Date	Geographical position Latitude	Longitude	Water depth uncorrected (m)	Wire length (m)	Comments
	14	03.36 07.22	CTD		39°47.7'N 39°47.6'N	20°03.6'W 20°03.6'W	4991	4800	
		07.30 08.05	OS		39°47.7'N	20°03.8'W	4982	100	
		08.22 08.56	OS		39°47.7'N	20°03.7'W	4889	100	
		10.56 13.01	MSN		39°47.8'N 39°47.8'N	20°03.6'W 20°03.7'W	4980 4998	100, 100, 700	
		13.27 16.33	MUC		39°47.9'N	20°03.3'W	4990	5033	
182		19.56 20.30	APN		40°20.0'N	19°59.9'W	5096	80	
		20.35 20.38	Secchi		40°20.0'N	19°59.9'W			
	15	20.46	CTD		40°20.0'N	20°00.0'W	5094	200	
	15	21.22	CTD		40°19.9'N	20°00.1'W	5049	200	
	13	00.18	XBT	02.07	40°50.0'N	19°58.1'W	4435	754	
	14	03.07	XBT		41°20.2'N	19°56.3'W	3296	760	
	15	05.57	XBT		41°49.9'N	19°54.4'W	3627	760	
	16	08.44	XBT		42°19.8'N	19°52.4'W	3246	760	
	17	11.36	XBT		42°49.8'N	19°50.6'W	2943	760	
183	16	13.07 17.46	CTD		43°04.0'N 43°04.0'N	19°49.9'W 19°50.1'W	5904	5600	Nr. prüfen
		17.54 18.00	Secchi		43°04.0'N	19°50.2'W		14.5	
	17	18.32 19.24	CTD		43°04.0'N 43°03.9'N	19°50.2'W 19°50.1'W	5991	500	
	18	22.08	XBT		43°30.1'N	19°50.0'W	4150	760	
	19	02.07	XBT	03.07	44°00.0'N	19°50.0'W	3990	760	
	20	04.55	XBT		44°30.0'N	19°50.0'W	4420	760	
	21	08.46	XBT		45°00.1'N	19°50.1'W	3997	760	
184	18	11.15 11.55	CTD		45°20.0'N 45°20.1'N	19°49.9'W 19°50.0'W	3830	500	
		11.31 13.20	APN		45°20.0'N	19°49.9'W	3830	80	
		12.02 12.06	Secchi		45°20.0'N	19°49.9'W		11	
	19	13.51 15.52	CTD		45°20.1'N 45°19.8'N	19°49.8'W 19°49.6'W	3836	3847	Releaser test

Station	Number	Time UTC	Device	Date	Geographical position Latitude	Longitude	Water depth uncorrected (m)	Wire length (m)	Comments
	22	19.00	XBT		45°50.0'N	19°49.9'W	4749	760	
	23	21.45	XBT		46°20.0'N	19°49.8'W	4748	760	
	24	00.35	XBT	04.07	46°50.0'N	19°49.8'W	4255	760	
	25	03.21	XBT		47°20.0'N	19°49.7'W	4512	383	
	26	05.28	XBT		47°42.3'N	19°49.6'W	4537	760	
185		05.30			47°43.0'N	19°49.7'W	4440		recovering
		09.35			47°44.7'N	19°47.6'W			L2o
186		11.24			47°31.9'N	19°47.8'W	4535		recovering
		13.28			47°30.6'N	19°47.0'W			L2u
		14.29	APN		47°30.5'N	19°46.9'W	4535	50	
		16.30							
		14.40	Go.Flo		47°30.5'N	19°46.9'W	4535	1205	
		15.55							
		16.13	Go-Flo		47°30.7'N	19°46.9'W	4535	3705	
		20.00							
	20	20.27	CTD		47°30.6'N	19°46.8'W	4537	4537	Releasertest
		00.18		05.07	47°30.6'N	19°47.3'W			
	21	01.00	CTD		47°30.7'N	19°47.0'W	4553	500	
		01.50			47°30.7'N	19°47.1'W			
		02.25	MSN		47°30.8'N	19°46.8'W	4552	100, 700,	
		06.49			47°30.9'N	19°47.1'W	4651	2500	
	22	09.09	CTD		47°31.5'N	19°48.4'W	4544	2000	
		10.53			47°31.5'N	19°48.7'W			
		11.01	OS		47°31.4'N	19°48.7'W	4547	150	
		11.28							
		11.48	OS		47°31.4'N	19°48.5'W	4547	80	
		11.56							
	23	12.00	CTD		47°31.5'N	19°49.0'W	4544	4500	
		15.32			47°31.5'N	19°48.2'W			
		16.27	IPS		47°31.1'N	19°48.6'W	4547	3555	
		03.46		06.07					
	24	03.44	CTD		47°31.2'N	19°48.4'W	4548	200	
		04.27			47°31.2'N	19°48.6'W			
		05.44	IPS		47°31.2'N	19°48.4'W	4532	3555	
		12.34			47°31.2'N	19°48.4'W			
	25	12.48	CTD		47°32.0'N	19°49.0'W	4544	4583	
		16.27			47°33.4'N	19°48.8'W			
		16.24	Secchi		47°33.5'N	19°48.8'W			
		16.37							

Station	Number	Time UTC	Device	Date	Geographical position Latitude	Longitude	Water depth uncorrected (m)	Wire length (m)	Comments
		16.41 17.25	OS		47°33.8'N	19°48.6'W	4548	50	
	26	18.00 18.52	CTD		47°31.3'N 47°31.6'N	19°48.3'W 19°48.2'W	4547	100	4x jojo
		19.18 03.32	IPS	07.07	47°31.9'N 47°31.7'N	19°48.3'W 19°48.7'W	4533	3555	
		09.36 10.24			47°29.4'N 47°30.0'N	19°40.8'W 19°41.6'W	4536		deployment L2u
187		12.00 14.24			47°43.8'N 47°44.0'N	19°46.5'W 19°48.0'W	4517		deployment L2o
		15.17 18.07	MUC		47°48.5'N	19°50.8'W	4452	4474	
	27	19.30	XBT		48°02.5'N	19°54.0'W	4336		defective
	28	21.59	XBT		48°31.0'N	19°59.2'W	4043	760	
	29	00.35	XBT	08.07	49°00.6'N	20°04.6'W	4396	600	
	30	03.19	XBT		49°30.4'N	20°10.1'W	4113	760	
188	28	05.47 06.35	CTD		49°54.1'N 49°54.3'N	20°14.5'W 20°14.5'W	3628	500	
	29	07.27 10.36	CTD		49°54.1'N 49°53.8'N	20°14.5'W 20°14.4'W	3616	3600	
		10.42 10.45	Secchi		49°53.8'N	20°14.4'W		10	
		10.55 11.01	OS		49°53.8'N	20°14.3'W		50	
		11.27 11.59	APN		49°53.6'N	20°14.3'W		30	3x
	31	14.52	XBT		50°24.0'N	20°19.0'W	4365	760	
	32	17.34	XBT		50°53.8'N	20°25.5'W	4126	760	
	33	20.19	XBT		51°23.7'N	20°31.3'W	4210	760	
	34	22.58	XBT		51°53.5'N	20°37.0'W	3896	760	
189	30	01.08	CTD	09.07	52°17.3'N	20°41.5'W	3831	500	
189	30	02.01	CTD	09.07	52°17.3'N	20°41.5'W	3831	500	
		02.03 02.47	APN		52°17.2'N	20°41.3'W		30	5x
	31	02.50 06.02	CTD		52°17.1'N	20°41.3'W	3831	3750	GPS error
	35	08.46	XBT		52°47.1'N	20°47.4'W	3660	760	
	36	11.21	XBT		53°16.8'N	20°53.3'W	2913	760	
	37	13.53	XBT		53°46.6'N	20°59.3'W	2572	760	

Station	Number	Time UTC	Device	Date	Geographical position Latitude Longitude	Water depth uncorrected (m)	Wire length (m)	Comments
	38	16.32	XBT		54°16.4'N 21°05.4'W	2997	760	
190		19.00	Go-Flo		54°37.9'N 21°09.0'W	3047	2405	
		22.15						
		23.02	IPS		54°38.1'N 21°09.8'W	3058	2255	
		04.57		10.07				
	32	05.11	CTD		54°37.8'N 21°09.7'W	3033	500	
		05.58			54°37.3'N 21°09.9'W			
		06.11	APN		54°37.0'N 21°09.7'W		30	2x
		06.43						
	33	07.09	CTD		54°38.5'N 21°09.7'W	3045	3045	
		09.42			54°37.7'N 21°09.5'W			
		10.15			54°39.9'N 21°09.5'W			recovering L3
		13.00			54°38.3'N 21°07.7'W			
		13.32	OS		54°40.2'N 21°10.0'W	3046	40	
		13.59						
		14.03	Secchi		54°40.0'N 21°09.9'W		12	
		14.07						
	34	14.10	CTD		54°39.6'N 21°09.5'W	3050	2700	
		16.12			54°39.1'N 21°09.0'W			
		16.35	APN		54°40.3'N 21°10.1'W		30	2x
		17.00						
	35	17.04	CTD		54°40.0'N 21°09.8'W	3050	1500	
		18.23			54°39.6'N 21°09.5'W			
		18.27	APN		54°39.1'N 21°09.3'W		30	4x
		19.49						
		20.19	MSN		54°40.1'N 21°09.8'W	3057	100, 700,	
		00.55		11.07	54°39.2'N 21°09.6'W	3037	2500	
		01.17	IPS		54°40.2'N 21°09.7'W	3048	2255	
		10.26			54°39.6'N 21°09.2'W			
		10.43	MSN		54°39.2'N 21°09.2'W	3047	100, 700	
		11.57			54°38.8'N 21°09.1'W	3048		
		12.02	Secchi		54°38.2'N 21°09.1'W			
		12.10						
		12.16	OS		54°38.2'N 21° 09.1'W	3038	50	
		12.45						
		13.00	APN		54°35.9'N 21°09.6'W		10	10x
		13.40						
191		17.00			54°40.8'N 21°12.6'W	3060		deployment
		18.45			54°40.8'N 21°10.3'W	3048		L3

Station	Number	Time UTC	Device	Date	Geographical position Latitude	Longitude	Water depth uncorrected (m)	Wire length (m)	Comments
		19.32	IPS		54°38.9'N	21°09.8'W	3043	2255	
		03.29		12.07	54°38.4'N	21°09.5'W			
	36	03.40	CTD		54°38.1'N	21°09.2'W	3043	500	
		04.33			54°37.7'N	21°09.1'W			
		04.43	APN		54°37.4'N	21°09.0'W		30	4x
		05.23							
	37	05.51	CTD		54°38.4'N	21°09.7'W	3053	3000	
		08.35			54°37.1'N	21°08.9'W			
192		08.52	MUC		54°36.7'N	21°09.0'W	3014		
		11.00							
		11.27	APN		54°38.3'N	21°08.0'W		30	6x
		12.30							
	39	15.35	XBT		55°11.0'N	21°03.6'W	2712	760	
	40	18.11	XBT		55°40.8'N	20°56.7'W	1836	760	
	41	20.57	XBT		56°10.5'N	20°49.6'W	1359	760	
	42	23.54	XBT		56°40.3'N	20°42.6'W	1501	760	
193	38	02.46	CTD	13.07	57°05.3'N	20°36.7'W	1642	500	
		03.44			57°05.3'N	20°37.0'W			
	39	04.26	CTD		57°05.1'N	20°36.9'W	1642	1600	
		05.58			57°49.2'N	20°37.2'W			
	43	09.06	XBT		57°34.7'N	20°29.1'W	2041	760	
	44	11.52	XBT		58°04.6'N	20°22.0'W	2406	760	
	45	14.39	XBT		58°34.3'N	20°14.5'W	2891	760	
	46	17.36	XBT		59°04.1'N	20°07.0'W	2784	760	
194		21.32	IPS		59°29.1'N	20°00.6'W	2773	2455	
		03.37			59°27.5'N	19°59.4'W			
	40	04.26	CTD		59°29.8'N	20°00.0'W	2775	500	
		05.16			59°29.3'N	20°00.5'W			
	41	06.00	CTD		59°28.9'N	20°00.9'W	2775	2700	
		08.16			59°27.7'N	20°01.8'W			
	42	09.04	CTD		59°29.1'N	20°00.5'W	2773	60	
		09.28			59°28.8'N	20°00.9'W			
		10.04	MSN		59°29.1'N	20°00.5'W	2776	100, 700,	
		14.44			59°28.7'N	20°00.3'W	2773	2500	
		14.53	MUC		59°27.7'N	20°01.5'W	2776	2794	
		16.44							
		17.40	APN		59°28.6'N	19°58.1'W	2775	30	44x
		03.00			59°22.2'N	19°59.7'W			

Abbreviations:

CTD	CTD sensor with rosette system
Go-Flo	Go-Flo-water sampling bottles
IPS	In situ pumps
MUC	Multicorer
MSN	Multinet
OS	Optic sensor
APN	Apstein net
Secchi	Secchi disc
XBT	Expandable Bathythermographs

7.3 Leg M 36/3

7.3.1 List of Stations

Station	Number GPI	Time (UTC)	Device	Date	Geographical Postition Latitude Longitude	Water depth uncorrected (m)	Wire length (m)	Comments
195		00.52	PS	22.07	61°50.0´N 000°45.0´W			Profile start 195
		06.50			62°05.5´N 002°49.4´W			Profile end 195
196	23537-1	08.48	GKG		62°03.0´N 002°30.1´W	1696	1674	Core recovery 0.46 m
	23537-2	10.23	SL(12)		62°03.0´N 002°30.7´W	1699	1660	Core recovery 9.53 m
197	23638-1	13.01	GKG		62°00.6´N 002°10.5´W	1665	1632	Core recovery 0.45 m
	23538-2	14.00	SL(12)		62°00.7´N 002°10.1´W	1667	1635	Core recovery 9.70 m
198		15.24	PS		62°00.7´N 002°10.1´W			Profile start 198
		20.07			62°11.7´N 003°37.0´W			Profile end 198
199		20.07	PS		62°11.7´N 003°37.0´W			Profile start 199
		02.00		23.07	62°56.0´N 002°11.0´W			Profile end 199
~~200~~		~~02.00~~	~~PS~~		~~62°56.0´N 002°11.0´W~~			~~Profile start 200~~
		04.56			62°36.3´N 001°22.5´W			Profile end 200
201	23539-1	9.26	FLO		62°47.7´N 002°26.9´W	1249	1337	Core recovery 0.15 m
	23539-2	11.09	GKG		62°47.7´N 002°26.9´W	1256	1218	Core recovery 0.45 m
	23539-3	12.39	SL(12)		62°47.7´N 002°26.8´W	1251	1218	Core recovery 5.86 m
202	23540-1	14.19	SL(18)		62°46.0´N 002°30.3´W	1138	1103	Core recovery 10.78 m
	23540-2	15.35	GKG		62°46.0´N 002°30.2´W	1130	1110	Core recovery 0.44 m
203	23541-1	00.54	FLO	25.07	67°37.0´N 005°46.1´E	1445	1438	Core recovery 0.10 m
		02.50	CTD		67°38.0´N 005°46.3´E	1444	1393	
	23541-3	04.16	MUC		67°37.1´N 005°45.9´E	1447	1413	Core recovery 0.30 m
	23541-4	05.29	MUC		67°37.2´N 005°46.1´E	1446	1411	Core recovery 0.35 m
	23541-5	06.39	MUC		67°37.0´N 005°46.0´E	1447	1411	Core recovery 0.30 m
	23541-6	07.52	MUC		67°37.0´N 005°46.1´E	1448	1411	Core recovery 0.30 m
	23541-7	09.10	GKG		67°37.0´N 005°45.9´E	1445	1408	Core recovery 0.42 m
		11.06	OBH1		67°37.0´N 005°46.3´E	1442	1000	Release control
		12.15	OBH2		67°37.0´N 005°46.3´E	1444	1000	Release control
205		17.00	DTPS+		67°42.7´N 007°16.3´E	1710	1950	Profile start 205
		21.00			67°28.9´N 007°36.0´E			Profile end 205
206		21.00	DTPS+		67°28.9´N 007°36.0´E			Profile start 206
		00.32		26.07	67°23.8´N 007°07.9´E			Profile end 206
207		00.32	DTPS+		67°23.8´N 007°07.9´E		1970	Profile start 207
		05.05			67°40.1´N 006°47.9´E			Profile end 207
208		05.05	DTPS+		67°40.1´N 006°47.9´E			Profile start 208

Station	Number GPI	Time (UTC)	Device	Date	Geographical Postition Latitude Longitude	Water depth uncorrected (m)	Wire length (m)	Comments
		05.57			67°41.3´N 006°52.7´E			Profile end 208
209		05.57	DTPS+		67°41.3´N 006°52.7´E		1970	Profile start 209
		10.41			67°24.6´N 007°12.0´E			Profile end 209
210		10.41	DTPS+		67°24.6´N 007°12.0´E			Profile start 210
		11.39			67°25.8´N 007°19.2´E			Profile end 210
211		11.39	DTPS+		67°25.8´N 007°19.2´E		1972	Profile start 211
		16.18			67°42.6´N 006°56.4´E			Profile end 211
212		16.18	DTPS+		67°42.6´N 006°56.4´E			Profile start 212
		17.03			67°43.3´N 007°01.2´E			Profile end 212
213		17.03	DTPS+		67°43.3´N 007°01.2´E		1975	Profile start 213
		21.50			67°26.4´N 007°24.0´E			Profile end 213
214		21.50	DTPS+		67°26.4´N 007°24.0´E			Profile start 214
		22.32			67°27.6´N 007°27.0´E			Profile end 214
215		22.32	DTPS+		67°27.6´N 007°27.0´E		1900	Profile start 215
		03.04		27.07	67°44.0´N 007°04.5´E			Profile end 215
216	23542-1	05.05	GKG		67°40.7´N 007°04.2´E	1337	1307	Core recovery 0.42 m
	23542-2	06.30	SL(18)		67°40.9´N 007°04.1´E	1339	1304	Core recovery 5.31 m
217	23543-1	09.17	GKG		67°34.7´N 007°12.9´E	1409	1380	Core recovery 0.44 m
	23543-2	10.50	SL(12)		67°34.8´N 007°13.1´E	1416	1379	Core recovery 5.59 m
218		12.44	OBH2		67°40.8´N 007°04.4´E	1334		
		13.08	OBH1		67°40.5´N 007°04.7´E	1330		
		14.30	DTPS+		67°41.5´N 007°10.1´E	1358	1950	Profile start 218
		15.45			67°42.6´N 007°01.7´E			Profile end 218
219		17.00	DTPS+		67°41.1´N 007°04.0´E			Profile start 219
		17.19			67°40.2´N 007°05.3´E			Profile end 219
220		20.03	PS		67°32.8´N 006°56.0´E			Profile start 220
		21.38			67°39.6´N 007°35.0´E			Profile end 220
221		21.38	PS		67°39.6´N 007°35.0´E			Profile start 221
		23.34			67°30.8´N 006°59.5´E			Profile end 221
222		23.48	PS		67°28.8´N 007°03.0´E			Profile start 222
	28.07	01.28			67°35.6´N 007°42.5´E			Profile end 222
223		01.45	PS		67°33.6´N 007°46.0´E			Profile start 223
		03.22			67°26.9´N 007°07.3´E			Profile end 223
224		03.34	PS		67°25.2´N 007°09.4´E			Profile start 224
		05.20			67°31.6´N 007°49.5´E			Profile end 224
225		07.34	OBH2		67°33.0´N 007°15.0´E	1400		
		08.10	OBH1		67°33.2´N 007°14.7´E	1402		
		09.00	DTPS+		67°36.7´N 007°10.0´E			Profile start 225

Station	Number GPI	Time (UTC)	Device	Date	Geographical Postition Latitude Longitude	Water depth uncorrected (m)	Wire lenght (m)	Comments
		10.37			67°32.2´N 007°16.3´E			Profile end 225
226			DTPS+					Cancelled
227		15.47	OBH2		67°39.8´N 007°10.2´E	1401		
		16.04	OBH1		67°39.5´N 007°10.7´E	1397		
		17.27	DTPS+		67°39.5´N 007°14.8´E			Profile start 227
		19.00			67°42.7´N 007°06.4´E			Profile end 227
228		19.55	DTPS+		67°42.3´N 007°07.6´E			Profile start 228
		20.20			67°40.8´N 007°08.8´E			Profile end 228
229		22.25	PS		67°33.6´N 007°10.7´E			Profile start 229
		00.55		29.07	67°25.8´N 008°02.4´E			Profile end 229
230		01.00	DTPS+		67°25.4´N 008°08.5´E			Profile start 230
		04.49			67°12.5´N 008°28.5´E			Profile end 230
231		06.41	DTPS+		67°14.2´N 008°33.6´E		1950	Profile start 231
		10.43			67°28.2´N 008°07.2´E			Profile end 231
232		11.25	DTPS+		67°29.4´N 008°12.6´E		1950	Profile start 232
		15.28			67°15.3´N 008°39.6´E			Profile end 232
233		16.24	DTPS+		67°16.9´N 008°44.9´E		1900	Profile start 233
		20.28			67°30.8´N 008°18.7´E			Profile end 233
234		21.27	DTPS+		67°32.3´N 008°24.4´E		1950	Profile start 234
		01.35		30.07	67°17.7´N 008°51.1´E			Profile end 234
235		02.46	DTPS+		67°21.0´N 008°48.0´E			Profile start 235
		07.00			67°10.8´N 008°10.1´E			Profile end 235
236		08.50	DTPS+		67°15.9´N 008°00.4´E			Profile start 236
		14.10			67°30.0´N 008°50.0´E			Profile end 236
237		16.00	DTPS+		67°35.0´N 008°41.5´E	1519		Profile start 237
		18.00			67°30.1´N 008°24.1´E			Profile end 237
238	23544-1	20.06	GKG		67°25.1´N 008°32.6´E	1235	1216	Core recovery 0.60 m
	23544-2	21.25	SL(12)		67°25.0´N 008°32.8´E	1223	1200	Core recovery 2.81 m
239	23545-1	23.16	SL(6)		67°21.2´N 008°18.5´E	1158	1137	Core recovery 5.04 m
	23545-2	00.21	GKG	31.07	67°21.2´N 008°18.4´E	1160	1138	Core recovery0.50 m
240	23546-1	02.00	GKG		67°17.9´N 008°07.3´E	1187	1164	Core recovery 0.48 m
	23546-2	03.17	SL(6)		67°17.9´N 008°06.9´E	1189	1166	Core recovery 5.74 m
241		05.00	PS		67°28.0´N 008°16.0´E			Profile start 241
		06.03			67°21.1´N 007°52.7´E			Profile end 241
242		11.17	PS		67°47.0´N 005°31.0´E			Profile start 242
		12.45			67°47.0´N 006°00.0´E			Profile end 242
243		13.29	OBH2		67°47.0´N 005°51.5´E	1304		
244		13.55	OBH1		67°47.0´N 005°50.6´E	1320		

Station	Number GPI	Time (UTC)	Device	Date	Geographical Postition Latitude Longitude	Water depth uncorrected (m)	Wire length (m)	Comments
245		15.15	DTPS+		67°47.0´N 005°45.7´E	1314	1950	Profile start 245
		16.50			67°47.0´N 006°03.2´E			Profile end 245
246		08.15	NB9	01.08	69°58.7´N 004°03.8´E	3238		Rcovery of mooring
		10.03	CTD		69°59.8´N 004°00.2´E	3282	3264	
		12.33	MN		70°00.1´N 004°01.1´E	3280	2000	
		15.37	ISP		69°59.8´N 004°01.4´E	3280	2520	
	23547-4	22:40	FLO		69°59.9´N 004°01.5´E	3278	3333	Core recovery 0.25 m
02.08	23547-5	01.38	MUC		69°59.5´N 004°00.1´E	3280	3265	Core recovery 0.45 m
		03.36	NB10		69°59.35´N 003°59.90´E	3264		Deployment of mooring
247		07.40	CTD	03.08	75°00.1´N 000°00.2´E	3763	3708	
		13.30	MN		75°00.1´N 000°00.3´E	3782	2000	
		13.38	CTD		75°00.0´N 000°00.5´W	3789	380	
		14.26	PN		75°00.0´N 000°00.7´W	3789	100	
		14.54	CTD		75°00.0´N 000°00.8´W	3764	1000	
		16.53	PN		75°00.0´N 000°00.0´W	3764	100	
		16.12	PN		75°00.0´N 000°00.0´W	3764	100	
	23548-8	18.14	MUC		75°00.0´N 000°00.4´E	3764	3716	Core recovery 0.30 m
248		19.25	PS		75°00.0´N 000°00.4´E			Profile start 248
		03.06		04.08	75°03.6´N 004°34.8´W			Profile end 248
249		04.10	OG10		75°03.4´N 004°35.2´W	3609		Rcovery of mooring
		06.53	CTD		75°03.4´N 004°35.7´W	3608	3549	
		09.29	PN		75°03.3´N 004°35.6´W		40	
		10.15	CTD		75°03.5´N 004°35.4´W	3608	100	
		10.41	MN		75°03.6´N 004°35.9´W	3526	2000	
		13.48	CTD		75°03.5´N 004°35.6´W	3608	3550	
		17.51	BWS		75°03.3´N 004°35.8´W	3627	3580	Bottom contact
		19.35	ISP		75°03.4´N 004°35.9´W	3608	1015	
	23549-9	02.10	FLO	05.08	75°03.4´N 004°35.6´W	3627	3573	Core recovery 0.25 m
	23549-10	05.09	MUC		75°03.4´N 004°35.9´W	3629	3559	Core recovery 0.30 m
	23549-11	07.35	GKG		75°03.5´N 004°35.7´W	3608	3556	Core recovery 0.30 m
	23549-12	10.11	GKG		75°03.5´N 004°36.0´W	3624	3556	Core recovery 0.26 m
	23549-13	12.39	GKG		75°03.5´N 004°35.8´W	3636	3558	Core recovery 0.35 m
250		17.43	OG11		74°59.69´N 006°57.39´W	3466		Deployment of mooring

Station	Number GPI	Time (UTC)	Device	Date	Geographical Postition Latitude Longitude	Water depth uncorrected (m)	Wire length (m)	Comments
251		20.40	PS		74°59.0´N 007°00.9´W			Profile start 251
		11.00		06.08	74°00.1´N 007°44.3´W			Profile end 251
252		10.20	CTD	09.08	67°52.5´N 018°43.3´W	912	875	
		11.21	MN		67°52.6´N 018°43.5´W	902	800	
		12.55	PN		67°52.6´N 018°43.6´W	898	50	
		13.38	ISP		67°52.6´N 018°43.4´W	908	860	
		19.02	CTD		67°52.6´N 018°43.3´W	905	60	
		19.22	MN		67°52.6´N 018°43.2´W	889	500	
		20.22	CTD		67°52.7´N 018°43.2´W	894	880	
		21.54	BWS		67°52.5´N 018°43.6´W	893	870	Bottom contact
	23550-9	23.00	MUC		67°52.4´N 018°43.6´W	895	872	Core recovery 0.10 m
	23550-10	23.49	GKG		67°52.5´N 018°43.5´W	900	882	Core recovery 0.46 m
	23550-11	00.32	GKG	10.08	67°52.6´N 018°43.7´W	899	880	Core recovery 0.43 m
	23550-12	01.18	GKG		67°52.6´N 018°43.7´W	901	880	Core recovery 0.45 m
253		01.45	PS		67°52.8´N 018°43.2´W			Profile start 253
		10.45			69°12.6´N 020°43.7´W			Profile end 253
254		11.15	CTD		69°12.6´N 020°43.6´W	383	360	
		12.11	CTD		69°12.5´N 020°43.7´W	383	50	
		12.46	GKG		69°12.5´N 020°43.8´W	382	384	Failure
	23551-3	13.15	GKG		69°12.6´N 020°43.8´W	383	386	Core recovery 0.46 m
	23551-4	13.45	GKG		69°12.5´N 020°43.9´W	385	385	Core recovery 0.45 m
	23551-5	14.15	GKG		69°12.7´N 020°43.4´W	384	383	Core recovery 0.45 m
	23551-6	15.10	MUC		69°12.7´N 020°43.8´W	383	382	Core recovery 0.20 m
255		16.36	PS		69°15.7´N 020°53.1´W			Profile start 255
		19.32			68°47.9´N 021°48.4´W			Profile end 255
256		19.39	PS		68°47.2´N 021°48.4´W			Profile start 263
		07.18		11.08	69°32.0´N 019°19.0´W			Profile end 256
257		07.30	CTD		69°32.0´N 019°19.0´W	1277	1240	
		08.39	MN		69°32.0´N 018°59.8´W	1276	1000	
		10.20	CTD		69°31.9´N 019°19.1´W	1274	70	
		10.42	PN		69°31.9´N 018°59.9´W	1276	50	
		11.06	CTD		69°31.9´N 019°19.1´W	1274	1240	
		12.45	BWS		69°31.9´N 019°19.2´W	1276	1259	Bottom contact
		13.42	ISP		69°32.0´N 019°19.3´W	1275	1220	
	23552-8	20.33	GKG		69°32.2´N 018°59.8´W	1261	1242	Core recovery 0.45 m

Station	Number GPI	Time (UTC)	Device	Date	Geographical Postition Latitude Longitude	Water depth uncorrected (m)	Wire lenght (m)	Comments
	23552-9	21.35	GKG		69°32.1´N 018°59.9´W	1269	1252	Core recovery 0.46 m
	23552-10	22.13	GKG		69°32.0´N 019°19.2´W	1268	1249	Core recovery 0.45 m
	23552-11	23.30	MUC		69°32.0´N 019°19.3´W	1268	1244	Core recovery 0.35 m
258		00.00	PS	12.08	69°32.0´N 019°19.0´W			Profile start 258
		07.27			69°03.6´N 020°30.5´W			Profile end 258
259		07.34	CTD		69°03.6´N 020°30.4´W	1246	1205	
		08.53	MN		69°03.6´N 020°30.4´W	1252	1000	
		10.36	CTD		69°03.6´N 020°30.3´W	1252	70	
		10.55	PN		69°03.6´N 020°30.5´W	1251	50	
		11.22	CTD		69°03.6´N 020°30.9´W	1242	1222	
		13.06	BWS		69°03.6´N 020°30.9´W	1241	1219	Bottom contact
	23553-7	14.34	GKG		69°03.6´N 020°31.0´W	1253	1220	Core recovery 0.42 m
	23553-8	15.28	GKG		69°03.6´N 020°30.6´W	1255	1221	Core recovery 0.40 m
	23553-9	16.21	GKG		69°03.6´N 020°30.8´W	1252	1219	Core recovery 0.45 m
	23553-10	17.25	MUC		69°03.6´N 020°30.7´W	1251	1217	Core recovery 0.35 m
		19.16	EBS		69°04.4´N 020°30.0´W	1252	1225	Bottom contact
260		21.20	PS		69°03.7´N 020°30.7´W			Profile start 260
		00.10		13.08	68°55.4´N 020°17.8´W			Profile end 260
261		01.01	IPS		68°55.6´N 020°18.1´W	1574	1530	
		07.35	CTD		68°55.8´N 020°18.5´W	1564	1530	
		09.25	MN		68°55.5´N 020°18.2´W	1565	1000	
		11.14	CTD		68°55.7´N 020°18.8´W	1564	70	
		11.31	PN		68°55.8´N 020°19.1´W	1565	50	
		11.48	PN		68°55.8´N 020°19.5´W	1565	20	
		12.16	CTD		68°55.5´N 020°17.7´W	1572	1514	
		14.00	BWS		68°55.5´N 020°18.4´W	1574	1531	Bottom contact
	23554-8	15.33	GKG		68°55.3´N 020°17.9´W	1573	1531	Core recovery 0.41 m
	23554-9	16.45	GKG		68°55.4´N 020°18.2´W	1569	1529	Core recovery 0.42 m
	23554-10	18.00	GKG		68°55.4´N 020°18.1´W	1565	1529	Core recovery 0.45 m
	23554-11	18.46	MUC		68°55.5´N 020°18.2´W	1571	1519	Core recovery 0.30 m
262		20.00	PS		68°55.1´N 020°17.4´W			Profile start 262
		02.25		14.08	68°30.0´N 019°38.5´W			Profile end 262
263		02.35	CTD		68°29.9´N 019°38.2´W	1184	1146	
		03.38	MN		68°30.1´N 019°38.8´W	1187	1000	

Station	Number GPI	Time (UTC)	Device	Date	Geographical Postition Latitude Longitude	Water depth uncorrected (m)	Wire length (m)	Comments
		05.27	CTD		68°30.0´N 019°38.9´W	1187	60	
		05.46	PN		68°29.9´N 019°39.1´W	1185	50	
		06.21	CTD		68°29.9´N 019°38.9´W	1185	1130	
		07.51	BWS		68°30.0´N 019°38.8´W	1178	1156	Bottom contact
	23555-7	09.10	GKG		68°30.0´N 019°38.9´W	1179	1154	Core recovery 0.42 m
	23555-8	10.20	GKG		68°30.0´N 019°39.1´W	1178	1153	Core recovery 0.46 m
	23555-9	11.14	GKG		68°29.9´N 019°39.0´W	1178	1153	Core recovery 0.45 m
	23555-10	12.05	MUC		68°30.0´N 019°38.9´W	1186	1152	Core recovery 0.30 m
264		15.34	CTD		68°45.9´N 020°02.9´W	1355	1346	
		16.48	MN		68°45.9´N 020°02.8´W	1364	1000	
		18.32	CTD		68°45.3´N 020°02.8´W	1364	70	
		18.48	PN		68°45.9´N 020°02.8´W	1364	50	
264		19.12	CTD		68°45.9´N 020°03.1´W	1365	1308	
		21.05	BWS		68°45.9´N 020°02.8´W	1356	1330	Bottom contact
	23556-7	22.26	GKG		68°45.9´N 020°03.4´W	1356	1325	Core recovery 0.42 m
	23556-8	23.19	GKG		68°45.9´N 020°03.4´W	1355	1326	Core recovery 0.42 m
	23556-9	00.14	GKG	15.08	68°45.9´N 020°03.7´W	1364	1328	Core recovery 0.42 m
	23556-10	01.13	MUC		68°45.9´N 020°03.5´W	1364	1324	Core recovery 0.30 m
		03.13	EBS		68°47.5´N 020°03.1´W	1397	1590	Bottom contact
265		07.13	EBS		68°55.6´N 020°17.7´W	1570	1655	Bottom contact
266		10.57	EBS		69°03.8´N 020°30.5´W	1241	1360	Bottom contact
267		12.30	PS		69°04.9´N 020°25.2´W			Profile start 267
								Profile end 267

Abbreviations:

BWS:	Bottom Water Sampler
CTD:	Salinity-Temperature-Water Sampling Device
DTPS7:	Deep Tow Boomer
EBS:	EP: Benthos Sledge
FLO:	FLOORIAN (in-situ O_2 grab)
GKG:	Box Corer
ISP:	
MN:	Multinet
MUC:	Multicorer
NB10:	Norwegian Basin Mooring 10
NB9:	Norwegian Basin Mooring 9
OBH 1/2:	Ocean Bottom Hydrophone
OG10:	East Greenland Basin Mooring 10
OG11:	East Greenland Basin Mooring 11
PN:	Plankton Net
PS:	Parasound
SL (12):	Gravity Corer (12 m)
SL (18):	Gravity Corer (18 m)

7.4 Leg M 36/4

7.4.1 List of Stations

Station	Time (UTC)	Device	Date	Geographical Position Latitude Longitude	Water-depth uncorrected (m)	Wire-length (m)	Comments
Test	15.40	CTD/Ro	20.08.	60°09,1 N 20°54,5 W	2752	100	
268	01.35	CTD/Ro	21.08.	58°37,9 N 20°10,5 W	2882	2878	
269	12.37	CTD/Ro	23.08.	49°00,7 N 16°29,8 W	4809	4851	
	15.21	BWS		49°00,5 N 16°29,6 W	4831	200	Test
	17.33	BWS		49°00,4 N 16°29,8 W	4831	4450	
	20.43	GKG		49°00,5 N 16°30,2 W		4833	Bottom contact
	23.02	MUC		49°00,6 N 16°30,1 W	4808	50	
	00.32	MUC	24.08.	49°00,7 N 16°29,7 W		4849	Bottom contact
	03.59	MUC		49°00,7 N 16°29,8 W		4844	Bottom contact
	07.15	MUC		49°0 ,4 N 16°29,7 W	4825	4847	Bottom contact
	11.05	MUC		49° 0,3 N 16°30,1 W	4832	4843	Bottom contact
	15.11	MUC		49 00,6 N 016°30,1 W	4806	4843	Bottom contact
	23.05	CTD/Ro		4 °00,5 N 16°9,8 W	4807	4854	
			25.08.				
270	08.00	CTD/Ro	26.08.	48°50,0 N 10°20,0 W	166	145	
	08.49	BWS		48°50,0 N 10°20,1 W	169	171	Bottom contact
	09.34	BWS		48°50,1 N 10°20,1 W	170	166	Bottom contact
	10.07	CTD/Ro		48°50,1 N 10°20,1 W	172	20	
	10.57	GKG		48°50,1 N 10°20,0 W	170	170	
	11.18	GKG		48°50,1 N 10°20,1 W	174	173	Bottom contact
	11.47	MUC		48°50,0 N 10°20,1 W	175	179	Bottom contact
	12.23	MUC		48°50,0 N 10°20,1 W	172	178	Bottom contact
	12.52	MUC		48°50,0 N 10°20,1 W	171	177	Bottom contact

Station	Time (UTC)	Device	Date	Geographical Position Latitude	Longitude	Water-depth uncorrected (m)	Wire-length (m)	Comments
271	14.18	CTD/Ro		48°43,0 N	10°22,7 W	783	730	
	15.38	BWS		48°42,9 N	10°23,0 W	714	727	Bottom contact
	16.50	GKG		48°43,0 N	10°22,8 W	762	760	Bottom contact
	17.40	GKG		48°43,1 N	10°22,6 W	774	777	Bottom contact
	18.38	MUC		48°42,9 N	10°22,7 W	804	811	Bottom contact
	19.36	MUC		48°42,9 N	10°22,7 W	806	811	Bottom contact
272	21.05	BWS		48°43,9 N	10°25,9 W	193	430	
273	22.48	BWS		48°38,9 N	10°33,1 W	558	568/578	Bottom contact
274	00.21	BWS	27.08.	48°37,0 N	10°35,0 W	993	978	Bottom contact
275	07.35	CTD/Ro		48°37,9 N	10°29,6 W	1515	1466	
	9.36	BWS		48°37,9 N	10°29,5 W	1516	1531	Bottom contact
	11.46	BWS		48°38,0 N	10°29,5 W	1514	1524	Bottom contact
	13.29	GKG		48°34,0 N	10°29,4 W	1490	1499	Bottom contact
	14.52	MUC		48°37,9 N	10°29,4 W	1506	1509	Bottom contact
	16.10	MUC		48°38,0 N	10°29,4 W	1510	1519	Bottom contact
	17.23	MUC		48°37,9 N	10°29,5 W	1515	1518	Bottom contact
276	20.04	BWS		48°32,0 N	10°38,2 W	1288	1289	Bottom contact
277	22.44	BWS		48°31,1 N	10°26,1 W	1324	1335/1350	Bottom contact
278	05.27	CTD/Ro	28.08.	48°31,0 N	10°30,0 W	2312	2313	
	08.46	BWS		48°30,9 N	10°30,2 W	2323	2331	Bottom contact
	11.03	GKG		48°30,9 N	10°30,1 W	2298	2285	Bottom contact

Station	Time (UTC)	Device	Date	Geographical Position Latitude	Longitude	Water-depth uncorrected (m)	Wire-length (m)	Comments
	12.56	MUC		48°31,0 N	10°30,1 W	2317	2310	Bottom contact
	14.42	MUC		48°30,9 N	10°30,1 W	2326	2323	Bottom contact
	16.24	MUC		48°31,0 N	10°30,1 W	2330	2334	Bottom contact
279	18.55	BWS		48°29,0 N	10°26,0 W	2149	2191/2201	Bottom contact
280	19.43	BWS		48°26,9 N	10°28,1 W	1753	1809	Bottom contact
281	05.03	CTD/Ro	29.08.	48°09,0 N	10°15,0 W	3694	3701	
	06.39	CTD/Ro		48°09,0 N	10°15,1 W	3643	100	
	08.59	BWS		48°09,1 N	10°15,1 W	3651	3726	Bottom contact
	13.54	GKG		48°09,3 N	10°14,9 W	3710	3708	Bottom contact
	16.24	MUC		48°09,2 N	10°14,9 W	3712	3721	Bottom contact
	18.51	MUC		48°09,2 N	10°15,0 W	3677	3692	Bottom contact
	22.11	BWS		48°09,2 N	10°14,9 W	3697	3718-3734	Bottom contact
282	02.00	GKG	30.08.	48°05,0 N	10°25,8 W	3797	3826	Bottom contact
283	10.16	CTD/Ro		48°36,0 N	11°16,9 W	2003	2009	
284	12.39	CTD/Ro		48°45,2 N	11°16,9 W	1384	1384	
285	14.36	CTD/Ro		48°52,9 N	11°17,0 W	982	980	
286	17.00	MUC		48°57,1 N	10°50,0 W	177	180	Bottom contact
287	18.31	CTD/Ro		48°51,2 N	10°50,0 W	756	771	
288	20.48	CTD/Ro		48°39,9 N	10°50,5 W	1188	1180	
289	22.56	CTD/Ro		48°33,9 N	10°50,3 W	2147	2158	
290	01.32	CTD/Ro	31.08.	48°37,0 N	10°35,0 W	997	984	
	02.24	CTD/Ro		48°37,0 N	10°50,0 W	1001	1009	
291	03.58	CTD/Ro		48°32,0 N	10°38,1 W	1295	1287	
292	05.51	CTD/Ro		48°28,0 N	10°38,0 W	1868	1836	
	07.49	CTD/Ro		48°28,1 N	10°38,0 W	1878	1000 max.	

Station	Time (UTC)	Device	Date	Geographical Position Latitude Longitude	Water-depth uncorrected (m)	Wire-length (m)	Comments
293	11.05	CTD/Ro		48°43,0 N 10°18,1 W	167	160	
294	12.50	CTD/Ro		48°34,1 N 10°29,3 W	1067	1046	
295	14.12	CTD/Ro		48°32,8 N 10°30,4 W	1372	1389	
296	03.26	CTD/Ro	01.09.	48°21,0 N 010°24,4 W	3242	3247	
	04.52	BWS		keine Datenüber-tragung	3242	316	
	06.32	MUC		48°21,2 N 10°24,3 W	3223	3235	Bottom contact
	09.35	BWS		48°21,1 N 010°24,0 W	3228	3265-3276	Bottom contact
	12.31	MUC		48°21,3 N 10°4,0 W	3242	3266	Bottom contact
297	02.03	GKG	02.09.	48°06,0 N 10°25,9 W	3799	3824	Bottom contact

07:30 End of work

7.4.2 HS and PS Profiles

Date	Profile No.	Geographical Position Start		Geographical Position End		Profile Distance	Duration
26.08.	P 1	48°48.9'N	10°20.9'W	48°50.0'N	10°20.0'W	46 sm	6.2 h
27.08.	P 2	48°37.0'N	10°35.0'W	48°34.0'N	10°29.0'W	45 sm	5.0 h
28.08.	P 3	48°31.0'N	10°26.0'W	48°29.0'N	10°21.0'W	40 sm	4.4 h
29.08.	P 4	48°24.0'N	10°27.0'W	48°09.0'N	10°15.0'W	41 sm	3.7 h
30.08.	P 5	48°00.0'N	10°30.0'W	48°25.0'N	11°12.0'W	50 sm	5.2 h
30.08.	P 6	48°36.0'N	11°17.0'W	48°45.0'N	11°17.0'W	9 sm	1.0 h
30.08.	P 7	48°45.5'N	11°17.0'W	48°53.0'N	11°17.0'W	8 sm	0.9 h
31.08.	P 8	48°28.0'N	10°37.0'W	48°43.0'N	10°18.0'W	20 sm	2.1 h
31.08.	P 9	48°34.0'N	10°25.0'W	48°21.0'N	10°24.4'W	85 sm	11.0 h
01.09.	P 10	48°21.0'N	10°24.4'W	48°06.0'N	10°25.9'W	105 sm	11.1 h

7.5 Leg M 36/5

7.5.1 List of Stations

Date	Station	Time [UTC]	Device	Depth of device (m)	Water depth (m)	Geographical Position Latitude	Longitude	Remarks
07.09.1996		7:54	Departure from Lisboa					
09.09.1996		18:46	Start of programme, XBT-profile					
		18:46	XBT-01 drop		3953 m	45°53,4 N	018°02,6 W	
		21:25	XBT-02 drop		3809 m	46°16,6 N	018°29,7 W	
10.09.1996		0:00	XBT-03 drop		4623 m	46°40,0 N	018°57,1 W	
		2:38	XBT-04 drop		4367 m	47°03,2 N	019°24,6 W	
	298	4:45	CTD	3000 m		47°11,0 N	019°34,0 W	
		6:57	MSN	500 m	4570 m	47°11,0 N	019°34,0 W	
		7:46	MSN	100 m	4567 m	47°11,1 N	019°34,0 W	
		8:29	MSN	700 m	4567 m	47°11,1 N	019°34,1 W	
		10:32	MSN	2500 m	4568 m	47°11,1 N	019°33,9 W	
		12:13 - 12:22	MSN	5 x 30 m	4569 m	47°11,1 N	019°34,0 W	JoJo
		12:44	OS	150 m	4569 m	47°11,2 N	019°34,0 W	
		13:10	APN	60 m	4569 m	47°11,2 N	019°34,0 W	
		13:44	APN	60 m	4569 m	47°11,1 N	019°34,0 W	
		14:10	RM	60 m	4569 m	47°11,1 N	019°33,9 W	
		14:34	RN	60 m	4569 m	47°11,1 N	019°33,9 W	
		16:12	CTD	4520 m	4569 m	47°11,0 N	019°34,0 W	
		19:34	MUC	4596 m	4566 m	47°11,0 N	019°34,0 W	
		22:46	MUC	4596 m	4567 m	47°11,1 N	019°33,9 W	
11.09.1996		3:00	XBT-05 drop		4422 m	47°32,2 N	020°05,3 W	
	299	6:00	CTD	700 m	4414 m	47°53,4 N	020°36,9 W	
		7:18	MSN	500 m	4397 m	47°53,3 N	020°36,9 W	
		8:12	CTD	700 m	4397 m	47°53,6 N	020°36,9 W	
		9:02	MSN	100 m	4397 m	47°53,7 N	020°36,8 W	
		9:22	RN	60 m	4396 m	47°53,7 N	020°36,8 W	
		12:20	XBT-06 drop		4276 m	48°14,6 N	021°08,6 W	
	300	15:16	CTD	700 m		48°36,1 N	021°40,3 W	
		17:58	XBT-07 drop		4412 m	48°14,3 N	021°40,5 W	
		18:40	XBT-08 drop		4422 m	48°05,9 N	021°40,6 W	
	301	21:44	CTD	700 m	4340 m	47°35,9 N	021°40,3 W	
12.09.1996		1:11	XBT-09 drop		4567 m	47°05,9 N	021°40,6 W	
	302	4:15	CTD	700 m	44 45 m	46°35,9 N	021°40,5 W	
		8:01	XBT-10 drop		4166 m	46°05,6 N	021°40,6 W	
	303	10:55	OS	150 m	3822 m	45°35,9 N	021°40,6 W	

Date	Station	Time [UTC]	Device	Depth of device (m)	Water depth (m)	Geographical Position Latitude	Longitude	Remarks
		11:17	RM	60 m	3821 m	45°35,9 N	021°40,6 W	
		11:37	APN	70 m	3819 m	45°35,9 N	021.40,6 W	
		12:04	CTD	700 m	3817 m	45°36,0 N	021°40,5 W	
		12:52	MSN	100 m	3813 m	45°36,0 N	021°40,5 W	
		13:34	MSN	700 m	3811 m	45°36,0 N	021°40,4 W	
		14:08 - 14:19	MSN	5 x 30 m	3812 m	45°35,9 N	021°40,4 W	JoJo
		17:17	XBT-11 drop		4620 m	45°59,5 N	021°09,5 W	
	304	20:32	CTD	700 m	4784 m	46°22,9 N	020°38,1 W	
		23:59	XBT-12 drop		4406 m	46°46,6 N	020°06,7 W	
13.09.1996	305	3:06	CTD	700 m	4568 m	47°11,0 N	019°33,8 W	
		4:17	MSN	508 m	4570 m	47°11,0 N	019°33,9 W	
		5:02	CTD	700 m	4569 m	47°11,0 N	019°33,9 W	
		5:51	MSN	100 m	4569 m	47°11,0 N	019°33,9 W	
		6:34	MSN	700 m	4569 m	47°11,0 N	019°34,0 W	
		7:43	OS	100 m	4569 m	47°11,0 N	019°34,0 W	
		8:03	RM	60 m	4568 m	47°10,9 N	019°34,0 W	
		8:24	PN	60 m	4567 m	47°11,0 N	019°33,8 W	
		8:38	APN	60 m	4567 m	47°11,0 N	019°33,8 W	
		8:52	RN	60 m	4567 m	47°11,1 N	019°33,7 W	
		9:04	RN	60 m	4567 m	47°11,2 N	019°33,5 W	
		10:52	MSN	2500 m	4567 m	47°11,1 N	019°33,7 W	
		12:42 - 12:52	MSN	5 x 30 m	4568 m	47°11,2 N	019°33,7 W	JoJo
		14:26	CTD	4 450 m	4569 m	47°11,0 N	019°33,8 W	
		17:48	MUC	4600 m	4569 m	47°11,0 N	019°34,1 W	
		21:03	MUC	4600 m	4568 m	47°11,0 N	019°34,0 W	
14.09.1996		0:59	XBT-13 drop		4314 m	47°32,2 N	019°02,7 W	
	306	3:49	CTD	700 m	4568 m	47°53,4 N	018°31,2 W	
		4:44	APN	60 m	4568 m	47°53,4 N	018°31,2 W	
		7:28	XBT-14 drop		4359 m	48°14,7 N	017°59,2 W	
	307	10:27	CTD	700 m	4315 m	48°35,9 N	017°27,5 W	
		11:17	MSN	100 m	4314 m	48°35,9 N	017°27,5 W	
		11:50	OS	150 m	4312 m	48°35,9 N	017°27,6 W	
		12:07	APN	60 m	4309 m	48°35,9 N	017°27,7 W	
		15:06	XBT-15 drop	4412 m		48°05,9 N	017°27,4 W	
	308	18:14	CTD	700 m	4151 m	47°35,8 N	017°27,4 W	
		21:50	XBT-16 drop		4350 m	47°05,8 N	017°27,4 W	
15.09.1996	309	1:05	CTD	700 m	4890 m	46°35,9 N	017°27,4 W	
		4:45	XBT-17 drop		4529 m	46°05,9 N	017°27,4 W	
	310	8:05	CTD	700 m	4669 m	45°35,9 N	017°27,1 W	
		8:56	MSN	100 m	4680 m	45°36,1 N	017°26,7 W	
		10:44	XBT-18 drop		4 451 m	45°35,9 N	017°48,5 W	

Date	Station	Time [UTC]	Device	Depth of device (m)	Water depth (m)	Geographical Position Latitude	Longitude	Remarks
	311	12:44	CTD	700 m	4394 m	45°35,9 N	018°09,5 W	
		14:36	XBT-19 drop		4009 m	45°50,9 N	018°09,6 W	
	312	16:18	MSN	500 m	4126 m	46°05,9 N	018°09,5 W	
		16:52	MSN	100 m	4126 m	46°05,8 N	018°09,5 W	
		17:33	MSN	700 m	4126 m	46°05,7 N	018°09,5 W	
		19:05	XBT-20 drop		4170 m	46°05,5 N	018°09,0 W	
16.09.1996		1:05	CTD	4100 m	4139 m	46°05,9 N	018°09,8 W	
		4:07	CTD	200 m	no display	46°05,9 N	018°09,6 W	
		6:40	XBT -20		4047 m	46°20,9 N	018°03,6 W	
	313	8:42	CTD	700 m	4141 m	46°35,9 N	018°09,6 W	
		11:21	XBT-21 drop		4429 m	46°50,9 N	018°09,6 W	
	314	14:31	CTD	4300 m	4435 m	47°05,8 N	018°09,5 W	
		16:45	MSN	100 m	4407 m	47°05,6 N	018°09,9 W	
		17:26	MSN	700 m	4390 m	47°05,4 N	018°10,2 W	
		19:42	XBT-22 drop	4618 m		47°20,9 N	018°09,6 W	
	315	21:34	CTD	700 m	4 462 m	47°35,8 N	018°09,6 W	
		23:46	XBT drop		4473 m	47°50,0 N	018°09,6 W	
17.09.1996	316	1:29	CTD	200 m	4443 m	48°05,9 N	018°09,6 W	
		2:41	MSN	500 m	4441 m	48°05,9 N	018°09,7 W	
		3:17	MSN	100 m	4442 m	48°05,7 N	018°09,6 W	
		4:00	MSN	700 m	4442 m	48°05,7 N	018°09,3 W	
		6:10	MSN	2500 m	4442 m	48°05,8 N	018°09,5 W	
		07:53 to 08:05	MSN	4x50 m	44 46 m	48°05 8 N	018°09,5 W	JoJo
		8:23	APN	60 m	4443 m	48°05,9 N	018°09,4 W	
		8:34	APN	60 m	4442 m	48°05,9 N	018°09,4 W	
		8:51	RN	60 m	4441 m	48°05,9 N	018°09,4 W	
		9:09	RN	60 m	4436 m	48°06,0 N	018°09,3 W	
		10:50	CTD	4300 m	4433 m	48°06,2 N	018°09,3 W	
		16:19	XBT-24 drop	4530 m		48°20,9 N	018°08,3 W	
	317	19:13	CTD	700 m	4704 m	48°35,9 N	018°09,7 W	
		21:40	XBT-25 drop		4184 m	48°35,9 N	018°30,7 W	
	318	23:32	CTD	700 m	4359 m	48°35,9 N	018°51,8 W	
18.09.1996		1:39	XBT-26 drop		4201 m	48°20,9 N	018°51,8 W	
	319	3:22	CTD	700 m	4436 m	48°05,9 N	018°51,8 W	
		7:34	XBT-27 drop		4591 m	47°50,9 N	018°51,8 W	
	320	7:23	MSN	500 m	4169 m	47°35,9 N	018°51,8 W	
		07:55 - 08:08	MSN	5 x 50 m	4171 m	47°35,8 N	018°52,1 W	

Date	Station	Time [UTC]	Device	Depth of device (m)	Water depth (m)	Geographical Position Latitude	Longitude	Remarks
		8:19	MSN	100 m	4170 m	47°35,8 N	018°52,2 W	
		8:55	MSN	700 m	4177 m	47°35,8 N	018°52,4 W	
		9:39	OS	150 m	4174 m	47°35,9 N	018°52,8 W	
		10:16	CTD	200 m	4174 m	47°35,9 N	018°52,0 W	
		11:02	RM	60 m	4182 m	47°36,1 N	018°52,2 W	
		11:24	APN	60 m	4176 m	47°36,1 N	018°52,5 W	
		11:33	APN	60 m	4174 m	47°36,0 N	018°52,6 W	
		11:43	RN	60 m	4172 m	47°36,0 N	018°52,7 W	
		13:33	CTD	4050 m	4173 m	47°35,9 N	018°52,1 W	
		16:58	XBT-28 drop		4590 m	47°20,9 N	018°51,8 W	
	321	18:42	CTD	700 m	4596 m	47°05,9 N	018°51,8 W	
		20:53	XBT-29 drop		4387 m	46°50,9 N	018°51,8 W	
	322	23:52	CTD	4500 m	4613 m	46°35,1 N	018°51,3 W	
19.09.1996		2:37	MSN	500 m	4615 m	46°35,7 N	018°51,7 W	
		3:08	APN	60 m	4614 m	46°35,6 N	018°51,8 W	
		3:20	APN	60 m	4614 m	46°35,5 N	018°51,9 W	
		3:34	RN	60 m	4614 m	46°35,5 N	018°52,2 W	
		4:20	CTD	200 m	4613 m	46°35,2 N	018°52,7 W	
		6:48	XBT-30 drop		4612 m	46°20,9 N	018°51,8 W	
	323	10:36	MSN	2500 m	4275 m	46°06,1 N	018°52,1 W	
		12:32	MSN	700 m	4276 m	46°05,9 N	018°51,7 W	
		13:09	MSN	100 m	4268 m	46°05,7 N	018°51,6 W	
		13:57	CTD	700 m	4257 m	46°05,6 N	018°51,6 W	
		16:17	XBT-31 drop		4412 m	45°50,9 N	018°51,8 W	
	324	18:09	CTD	700 m	4621 m	45°35,8 N	018°51,8 W	
		21:09	XBT-32 drop		4557 m	45°35,9 N	019°20,1 W	
		23:42	XBT-33 drop		4371 m	45°35,9 N	019°34,0 W	
20.09.1996		2:35	XBT-34 drop		4857 m	45°50,9 N	019°34,0 W	
		5:37	XBT-35 drop		4783 m	46°05,9 N	019°34,0 W	
		8:35	XBT-36 drop		4365 m	46°21,0 N	019°34,0 W	
		13:23	XBT-37 drop		4315 m	46°35,9 N	019°34,0 W	
		15:51	XBT-38 drop		4306 m	46°50,9 N	019°34,0 W	
		18:42	XBT-39 drop		4564 m	47°11,0 N	019°34,0 W	
		20:05	XBT-40 drop		4502 m	47°20,9 N	019°34,0 W	
	325	22:42	CTD	700 m	4540 m	47°35,9 N	019°34,0 W	
21.09.1996		1:21	XBT-41 drop		4543 m	47°50,9 N	019°34,0 W	
	326	3:21	CTD	200 m	4524 m	48°05,8 N	019°34,0 W	
		4:20	MSN	500 m	4527 m	48°05,9 N	019°34,0 W	
		6:10	CTD	4400 m	4528 m	48°05,9 N	019°34,0 W	
		8:18	MSN	100 m	4528 m	48°06,0 N	019°34,1 W	
		8:55	MSN	700 m	4529 m	48°06,0 N	019°34,4 W	
		10:50	MSN	2500 m	4523 m	48°06,2 N	019°34,9 W	

Date	Station	Time [UTC]	Device	Depth of device (m)	Water depth (m)	Geographical Position Latitude	Longitude	Remarks
		12:37	RN	60 m	4519 m	48°06,2 N	019°33,5 W	
		14:20	XBT-42 drop		4537 m	48°20,9 N	019°34,0 W	
	327	15:59	CTD	700 m	4339 m	48°35,8 N	019°33,7 W	
		14:44 - 16:55	MSN	5 x 40 m	4344 m	48°35,6 N	019°33,3 W	JoJo
		18:30	XBT-43 drop		4078 m	48°35,9 N	019°55,1 W	
	328	20:14	CTD	700 m	4395 m	48°35,9 N	020°16,1 W	
		22:35	XBT-44 drop		4399 m	48°20,9 N	020°16,2 W	
22.09.1996	329	0:29	CTD	700 m	4153 m	48°06,0 N	020°16,2 W	
		2:53	XBT- 45 drop		4 454 m	47°50,9 N	020°16,2 W	
	330	4:37	CTD	200 m	4375 m	47°35,9 N	020°16,2 W	
		5:37	MSN	500 m	4375 m	47°35,9 N	020°16,2 W	
		6:11	MSN	100 m	4376 m	47°35,9 N	020°16,2 W	
		6:52	MSN	700 m	4376 m	47°35,9 N	020°16,3 W	
		8:52	CTD	4200 m	4373 m	47°35,9 N	020°16,4 W	
		11:06	OS	150 m	4374 m	47°36,0 N	020°16,4 W	
		11:25	RM	70 m	4374 m	47°36,0 N	020°16,4 W	
		11:48	APN	60 m	4375 m	47°35,9 N	020°16,4 W	
		11:58	APN	60 m	4375 m	47°35,9 N	020°16,4 W	
		12:08	RN	60 m	4376 m	47°35,9 N	020°16,4 W	
		12:38	MSN	500 m	4377 m	47°35,5 N	020°16,5 W	
		14:25	XBT- 46 drop		4504 m	47°20,9 N	020°16,2 W	
	131	18:05	MSN	100 m	4564 m	47°11,0 N	019°34,0 W	
		18:43	MSN	700 m	4564 m	47°11,0 N	019°34,0 W	
		20:54	MSN	2500 m	4564 m	47°11,0 N	019°33,9 W	
		22:25 - 22:34	MSN	5 x 30 m	4564 m	47°11,0 N	019°33,9 W	
		22:50	CTD	200 m	4564 m	47°11,0 N	019°33,9 W	
23.09.1996		0:01	MSN	500 m	4564 m	47°11,0 N	019°34,0 W	
		0:34	CTD	200 m	4565 m	47°11,0 N	019°34,0 W	
		1:11	APN	60 m	4564 m	47°11,0 N	019°34,0 W	
		1:19	APN	60 m	4564 m	47°11,0 N	019°34,0 W	
		1:29	RN	60 m	4565 m	47°10,9 N	019°33,9 W	
		3:18	MUC	4601 m	4564 m	47°11,0 N	019°34,0 W	
	332	8:39	CTD	700 m	4282 m	47°05,8 N	020°16,3 W	
		10:52	XBT-47 drop		4060 m	46°50,8 N	020°16,2 W	
	333	13:43	CTD	4350 m	4471 m	46°35,9 N	020°16,2 W	
		15:45	MSN	100 m	4582 m	46°35,9 N	020°16,1 W	
		17:20	XBT-48 drop		4782 m	46°20,9 N	020°16,2 W	
	334	19:02	CTD	700 m	4307 m	46°05,9 N	020°16,2 W	

Date	Station	Time [UTC]	Device	Depth of device (m)	Water depth (m)	Geographical Position Latitude	Longitude	Remarks
		21:10	XBT-49 drop		4609 m	45°50,9 N	020°16,2 W	
	335	22:56	CTD	700 m	4249 m	45°35,9 N	020°16,4 W	
24.09.1996		1:09	XBT-50 drop		4686 m	45°35,9 N	020°37,3 W	
	336	2:56	CTD	700 m	4241 m	45°35,9 N	020°58,4 W	
		5:05	XBT-51 drop		4612 m	45°50,9 N	020°58,4 W	
	337							
		6:44	CTD	200 m	4967 m	46°05,8 N	020°58,0 W	
		7:42	MSN	500 m	4203 m	46°05,4 N	020°57,5 W	
		8:30	MSN	100 m	4268 m	46°05,8 N	020°58,3 W	
		9:08	MSN	700	4268 m	46°05,6 N	020°57,9 W	
		11:33	MSN	2500 m	4280 m	46°05,3 N	020°57,8 W	
		13:29	OS	150 m	4290 m	46°05,7 N	020°58,4 W	
		13:46	RM	100 m	4281 m	46°05,6 N	020°58,3 W	
		14:12	APN	60 m	4285 m	46°05,3 N	020°58,0 W	
		14:20	APN	60 m	4277 m	46°05,2 N	020°57,9 W	
		16:13	CTD	4150 m	4289 m	46°05,7 N	020°58,3 W	
		18:20	RN	60 m	4289 m	46°05,4 N	020°58,7 W	
		20:08	XBT-drop		4791 m	46°20,9 N	020°58,4 W	
	338	21:56	CTD	700 m	4793 m	46°35,8 N	020°58,4 W	
25.09.1996		0:08	XBT-53 drop		4689 m	46°50,9 N	020°58,4 W	
	339	1:57	MSN	500 m	4356 m	47°05,9 N	020°58,4 W	
		2:28	APN	60 m	4278 m	47°05,8 N	020°58,2 W	
		2:37	APN	60 m	4288 m	47°05,8 N	020°58,1 W	
		2:58	CTD	200 m	4341 m	47°05,9 N	020°58,3 W	
		3:49	MSN	100 m	4340 m	47°05,9 N	020°58,4 W	
		4:27	MSN	700 m	4340 m	47°05,8 N	020°58,3 W	
		6:30	MSN	2500 m	4386 m	47°05,7 N	020°58,3 W	
		9:41	CTD	4200 m	4267 m	47°05,7 N	020°58,2 W	
		11:46	RN	60 m	4282 m	47°05,8 N	020°58,2 W	
		12:00	RN	60 m	4307 m	47°05,8 N	020°58,1 W	
		12:13	RM	100 m	4318 m	47°05,7 N	020°58,1 W	
		14:10	XBT-54 drop		4478 m	47°20,9 N	020°58,4 W	
	340	15:54	CTD	700 m	4210 m	47°35,9 N	020°58,3 W	
		18:00	XBT-55 drop		no display	47°50,9 N	020°58,4 W	
	341	21:03	MSN	2500 m	3721 m	48°05,9 N	020°58,4 W	
		23:50	CTD	3600 m	3718 m	48°05,9 N	020°58,4 W	
26.09.1996		1:58	MSN	500 m	3717 m	48°05,8 N	020°58,4 W	
		2:33	CTD	200 m	3717 m	48°05,8 N	020°58,3 W	
27.09.1996	342	6:29	CTD	700 m	no display	48°05,4 N	021°41,1 W	
		8:46	MSN	100	4418 m	48°05,9 N	021°40,3 W	
		9:23	MSN	700 m	4419 m	48°05,9 N	021°40,8 W	

Date	Station	Time [UTC]	Device	Depth of device (m)	Water depth (m)	Geographical Position Latitude	Longitude	Remarks
		11:32	XBT-56 drop		4012 m	47°50,9 N	021°40,6 W	
	343	13:15	OS	150 m	4351 m	47°35,8 N	021°40,5 W	
		13:31	RM	100 m	4351 m	47°35,7 N	021°40,5 W	
		14:15	CTD	700 m	4366 m	47°35,6 N	021°40,6 W	
		15:00	MSN	100 m	4367 m	47°35,5 N	021°40,6 W	
		17:41	XBT-57 drop		4391 m	47°20,9 N	021°40,6 W	
	344	18:34	CTD	700 m	4562 m	47°05,6 N	021°40,6 W	
		19:39	MSN	500 m	4565 m	47°04,9 N	021°40,6 W	
		20:11	MSN	100 m	4564 m	47°04,7 N	021°40,6 W	
		20:49	MSN	700 m	4564 m	47°04,6 N	021°40,6 W	
		21:31	APN	60 m	4566 m	47°04,1 N	021°40,7 W	
		21:44	RN	60 m	4565 m	47°04,0 N	021°40,7 W	
		23:16	XBT-58 drop		4556 m	46°50,9 N	021°40,6 W	
28.09.1996	3 45	1:16	CTD	700 m	4437 m	46°35,9 N	021°40,6 W	
		2:15	MSN	100 m	4439 m	46°35,9 N	021°40,6 W	
		4:16	XBT-59 drop		4 460 m	46°20,9 N	021°40,6 W	
	3 46	6:30	CTD	700 m	4171 m	46°05,9 N	021°40,5 W	
		9:26	XBT-60 drop		3635 m	45°50,9 N	021°40,6 W	
	347	11:45	CTD	700 m		45°35,9 N	021°40,5 W	
		12:28	MSN	100 m	3812 m	45°35,9 N	021°40,5 W	
		13:07	MSN	700 m	3811 m	45°35,9 N	021°40,5 W	
					3809 m			
		15:37	XBT-61 drop		3727 m	45°35,9 N	022°01,7 W	
	348	17:56	CTD	700 m	3650 m	45°35,9 N	022°22,7 W	
29.09.1996		7:01	XBT-62 drop		3879 m	45°50,9 N	022°22,8 W	
	349	8:52	CTD	700 m	4057 m	46°05,9 N	022°22,9 W	
		9:44	MSN	100 m	4052 m	46°05,9 N	022°22,8 W	
		11:32	XBT-63 drop		3975 m	46°20,9 N	022°22,8 W	
	350	13:17	CTD	700 m		46°35,9 N	022°22,8 W	
					4140 m			
		15:24	XBT-64 drop		4065 m	46°50,9 N	022°22,8 W	
	351	17:10	CTD	700 m	4353 m	47°05,9 N	022°22,9 W	
		18:00	MSN	100 m	4353 m	47°06,0 N	022°22,8 W	
		18:36	MSN	700 m	4348 m	47°05,9 N	022°22,9 W	
		20:42	MSN	2500 m	43 45 m	47°06,0 N	022°22,9 W	
		22:42	MSN	500 m	4344 m	47°05,9 N	022°23,0 W	
		23:12	APN	60 m	4341 m	47°05,9 N	022°23,0 W	
		23:23	RN	60 m	4341 m	47°05,9 N	022°23,0 W	
		23:40	CTD	200 m	4340 m	47°05,9 N	022°23,1 W	
30.09.1996		1:51	MUC	4385 m	43 45 m	47°05,9 N	022°22,8 W	

Date	Station	Time [UTC]	Device	Depth of device (m)	Water depth (m)	Geographical Position Latitude	Longitude	Remarks
		7:06	XBT-65 drop		4295 m	47°20,3 N	022°22,8 W	
	352	7:03	CTD	700 m	4 458 m	47°35,9 N	022°22,8 W	
		9:43	XBT-66 drop		4442 m	47°50,9 N	022°22,8 W	
	353	11:58	CTD	700 m	3994 m	48°05,8 N	022°22,8 W	
		14:27	XBT-67 drop		4222 m	48°20,9 N	022°22,8 W	
	354	16:17	CTD	700 m	4140 m	48°35,8 N	022°22,9 W	
		17:12	MSN	100 m	4143 m	48°35,7 N	022°23,0 W	
		17:50	MSN	700 m	4144 m	48°35,8 N	022°23,3 W	
		19:51	MSN	2500 m	4121 m	48°35,6 N	022°23,4 W	
		21:53	MSN	500 m	4155 m	48°35,8 N	022°22,6 W	
		22:21	APN	60 m	4163 m	48°35,7 N	022°22,6 W	
		22:33	RN	60 m	4167 m	48°35,8 N	022°22,4 W	
01.10.1996		0:00	MUC	4183 m	4143 m	48°35,9 N	022°22,8 W	
	355	4:21	CTD	200 m	3918 m	48°35,9 N	021°40,6 W	
		7:27	XBT-68 drop		4395 m	48°35,9 N	020°58,3 W	
		10:03	XBT-69 drop		4396 m	48°35,9 N	020°16,2 W	
		12:30	XBT-70 drop		4337 m	48°35,9 N	019°34,0 W	
		14:57	XBT-71 drop		4352 m	48°35,9 N	018°51,8 W	
		17:31	XBT-72 drop		4696 m	48°35,9 N	018°09,6 W	
		20:02	XBT-73 drop		4318 m	48°35,9 N	017°27,5 W	
02.10.1996	356 - Bengal	1:27	MUC	4854 m	4802 m	49°00,0 N	016°30,0 W	
		4:12	MUC	4835 m	4803 m	48°59,9 N	016°29,8 W	
		7:19	MUC	4852 m	4804 m	49°00,0 N	016°29,9 W	
		10:37	CTD	3000 m	4805 m	49°03,5 N	016°35,3 W	
		12:14	MSN	100 m	4804 m	49°03,5 N	016°35,2 W	
		12:53	MSN	700 m	4084 m	49°03,6 N	016°35,3 W	
	357	18:42 - 19:22	CTD	3x200 m, 1x700 m	4313 m	48°35,7 N	017°27,4 W	JoJo
		20:08	MSN	100 m	4309 m	48°35,7 N	017°27,4 W	
		20:43	MSN	700 m	4298 m	48°35,7 N	017°27,6 W	
		21:39	MSN	500 m	4285 m	48°35,7 N	017°27,6 W	
		22:08	APN	60 m	4274 m	48°35,8 N	017°27,7 W	
03.10.1996		1:25	XBT-74 drop		4407 m	48°05,9 N	017°27,4 W	
		4:29	XBT-75 drop		4150 m	47°35,9 N	017°27,4 W	
	358	07:37 - 08:12	CTD	3 x 200 m, 1 x 700 m	4291 m	47°05,7 N	017°27,0 W	JoJo
		9:03	MSN	100 m	4243 m	47°05,6 N	017°26,7 W	
		9:40	MSN	700 m	4255 m	47°05,4 N	017°26,8 W	
		11:53	MSN	2500 m	4370 m	47°05,9 N	017°27,9 W	
		13:36	APN	60 m	73 m	47°05,9 N	017°28,0 W	
		14:03	CTD	700 m	4374 m	47°05,9 N	017°28,2 W	
		17:23	XBT-76 drop		4085 m	46°35,9 N	017°27,4 W	

Date	Station	Time [UTC]	Device	Depth of device (m)	Water depth (m)	Geographical Position Latitude	Longitude	Remarks
		19:55	XBT-77 drop		4517 m	46°05,9 N	017°27,4 W	
	359	22:46 - 23:26	CTD	3 x 200 m, 1 x 700 m	4659 m	45°35,9 N	017°27,4 W	JoJo
04.10.1996		0:12	MSN	100 m	4659 m	45°35,9 N	017°27,3 W	
		0:46	MSN	700 m	4661 m	45°36,0 N	017°27,3 W	
		1:41	MSN	500 m	4660 m	45°35,9 N	017°27,3 W	
		2:11	APN	60 m	4662 m	45°35,9 N	017°27,2 W	
02:18 End of station work, departure to Vigo.								

Abbreviations:

CTD:	CTD Sensor with rosette system
MUC:	Multicorer
MSN:	Multinet
APN:	Apstein net
RN:	Ring-net
OS:	Optic sensor
RM:	Radiometer

7.5.2 Water Sample Data Summary Database

id	stn	cast	niskin	depth	salt (ctd)	salt (som)	ct	
365001	xbt1	0	uw	5	35,800	35,656	2035,00	1
365002	xbt1a	0	uw	5	35,800	35,673	2040,43	2
365003	xbt1b	0	uw	5	35,800	35,704	2045,31	3
365004	xbt2	0	uw	5	35,800	35,652	2043,87	4
365005	xbt2a	0	uw	5	35,800	35,714	2046,74	5
365006	xbt2b	0	uw	5	35,800	35,720	2047,00	6
365007	xbt3	0	uw	5	35,800	35,731	2035,17	7
365008	xbt3a	0	uw	5	35,800	35,737	2042,80	8
365009	xbt3b	0	uw	5	35,800	35,711	2039,33	9
365010	xbt4	0	uw	5	35,800	35,703	2043,58	10
365011	xbt4a	0	uw	5	35,800	35,742	2042,42	11
365012	298-1	1	2	90	35,980	35,889	2111,29	12
365013	298-1	1	2	90	35,980	35,876	2111,70	13
365014	298-1	1	3	84	35,990	35,852	2111,45	14
365015	298-1	1	6	54	35,980	36,144	2108,70	15
365016	298-1	1	9	40	35,900	35,803	2081,72	16
365017	298-1	1	12	29	35,840	35,760	2060,21	17
365018	298-1	1	15	29	35,820	35,816	2060,33	18
365019	298-1	1	18	22	35,850	35,754	2047,20	19
365020	298-1	1	21	13	35,850	35,800	2043,85	20
365021	298-1	1	21	13	35,850	35,729	2043,38	21
365022	xbt5	1	uw	5	35,800	35,699	2042,20	22
365023	299-3	1	1	90	35,810	35,821	2109,96	23
365024	299-3	1	1	90	35,810	35,727	2111,34	24
365025	299-3	1	2	67	35,780	35,671	2106,71	25
365026	299-3	1	3	59	35,760	35,625	2105,42	26
365027	299-3	1	6	52	35,740	35,682	2103,10	27
365028	299-3	1	8	39	35,750	35,582	2091,15	28
365029	299-3	1	11	28	35,730	35,651	2060,69	29
365030	299-3	1	14	21	35,760	35,620	2050,80	30
365031	299-3	1	17	15	35,780	35,682	2049,26	31
365032	299-3	1	20	10	35,780	35,659	2049,18	32
365033	299-4	1	2	700	35,250	35,129	2170,57	33
365034	299-4	1	2	700	35,250	35,172	2170,56	34
365035	299-4	1	6	500	35,430	35,335	2142,80	35
365036	299-4	1	10	300	35,580	35,454	2128,43	36
365037	299-4	1	14	150	35,770	35,687	2120,15	37
365038	299-4	1	15	100	35,820	35,644	2121,02	38
365039	xbt6	1	uw	5	35,800	35,872	2048,83	39
365040	300-5	1	2	700	35,192	35,205	2167,72	40

id	stn	cast	niskin	depth	salt (ctd)	salt (som)	ct	
365041	300-5	1	2	700	35,192	34,984	2169,13	41
365042	300-5	1	6	500	35,422	35,308	2149,66	42
365043	300-5	1	10	300	35,645	35,599	2126,10	43
365044	300-5	1	14	150	35,784	35,690	2117,74	44
365045	300-5	1	16	100	35,860	35,753	2112,25	45
365046	300-5	1	19	40	35,786	35,692	2074,65	46
365047	300-5	1	23	10	35,795	35,719	2050,65	47
365048	xbt8	1	uw	5	35,800	35,615	2048,73	48
365049	301-6	1	20	45	35,840	35,792	2106,80	49
365050	301-6	1	22	20	35,710	35,697	2068,45	50
365051	xbt9	1	uw	5	35,800	35,649	2049,35	51
365052	302-7	1	1	700	35,407	35,360	2159,38	52
365053	302-7	1	1	700	35,407	35,307	2159,50	53
365054	302-7	1	2	550	35,579	35,378	2140,87	54
365055	302-7	1	3	400	35,668	35,597	2124,66	55
365056	302-7	1	4	250	35,789	35,821	2119,61	56
365057	302-7	1	6	99	35,933	35,857	2110,70	57
365058	302-7	1	8	72	35,917	35,829	2106,23	58
365059	302-7	1	10	62	35,912	35,858	2102,49	59
365060	302-7	1	12	52	35,878	35,875	2100,44	60
365061	302-7	1	15	42	35,841	35,794	2086,44	61
365062	302-7	1	17	32	35,804	35,721	2066,81	62
365063	302-7	1	19	24	35,864	35,754	2046,66	63
365064	302-7	1	21	18	35,874	35,788	2043,19	64
365065	302-7	1	23	10	35,880	35,689	2043,95	65
365066	302-7	1	23	10	35,880	35,749	2042,65	66
365067	xbt10	1	uw	5	35,800	35,858	2037,39	67
365068	303-8	1	16	58	35,824	35,704	2098,18	68
365069	303-8	1	20	10	35,903	35,783	2046,40	69
365070	xbt11	1	uw	5	35,800	35,788	2040,27	70
365071	xbt11	1	uw	5	35,800	35,866	2039,44	71
365072	xbt11a	1	uw	5	35,800	35,890	2039,21	72
365073	xbt11b	1	uw	5	35,800	35,808	2042,79	73
365074	304-9	1	1	700	35,400	35,285	2161,25	74
365075	304-9	1	4	600	35,500	35,415	2148,16	75
365076	304-9	1	5	500	35,550	35,437	2142,66	76
365077	304-9	1	7	400	35,720	35,656	2123,46	77
365078	304-9	1	10	300	35,810	35,664	2118,32	78
365079	304-9	1	14	150	35,920	35,837	2115,92	79
365080	304-9	1	18	80	35,950	35,892	2108,65	80
365081	304-9	1	20	40	35,900	35,845	2069,29	81
365082	304-9	1	24	10	35,920	35,941	2042,85	82

id	stn	cast	niskin	depth	salt (ctd)	salt (som)	ct	
365083	xbt12	1	uw	5	35,800	35,796	2046,10	83
365084	305-12	1	1	4450	35,047	34,925	2201,34	84
365085	305-10	1	1	100	35,816	35,629	2108,58	85
365086	305-10	1	4	65	35,936	35,943	2104,65	86
365087	305-10	1	7	42	35,922	35,872	2086,30	87
365088	305-10	1	11	31	35,829	35,731	2050,90	88
365089	305-10	1	14	23	35,835	35,738	2044,28	89
365090	305-10	1	17	17	35,835	35,660	2042,91	90
365091	305-10	1	20	10	35,835	35,772	2043,92	91
365092	305-12	1	1	4450	35,047	34,941	2202,31	92
365093	305-12	1	2	4100	35,052	34,941	2198,88	93
365094	305-12	1	3	3800	35,057	34,932	2197,39	94
365095	305-12	1	4	3500	35,066	34,916	2191,04	95
365096	305-12	1	8	3000	35,088	34,973	2178,20	96
365097	305-12	1	9	2700	35,095	34,979	2168,53	97
365098	305-12	1	10	2400	35,080	35,028	2158,11	98
365099	305-12	1	11	2100	35,065	34,867	2154,67	99
365100	305-12	1	12	1800	35,044	34,904	2154,54	100
365101	305-12	1	13	1500	35,117	34,996	2160,45	101
365102	305-12	1	14	1200	35,236	35,082	2169,09	102
365103	305-12	1	15	900	35,268	35,088	2173,04	103
365104	305-12	1	17	700	35,528	35,328	2158,00	104
365105	305-12	1	19	500	35,636	35,527	2130,08	105
365106	305-12	1	19	500	35,636	35,563	2130,01	106
365107	305-12	1	21	300	35,756	35,631	2122,38	107
365108	305-12	1	21	300	35,756	35,816	2123,45	108
365109	105a	1	uw	5	35,800	35,658	2038,38	109
365110	xbt13	1	uw	5	35,800	35,635	2043,16	110
365111	306-13	1	1	150	35,872	35,800	2118,33	111
365112	306-13	1	2	95	35,942	35,914	2114,20	112
365113	306-13	1	3	70	35,957	35,785	2110,16	113
365114	306-13	1	6	46	35,938	35,861	2107,23	114
365115	306-13	1	8	40	35,938	35,813	2106,66	115
365116	306-13	1	11	30	35,927	35,799	2103,74	116
365117	306-13	1	14	22	35,756	35,678	2076,89	117
365118	306-13	1	17	17	35,794	35,672	2052,41	118
365119	306-13	1	20	10	35,783	35,695	2047,52	119
365120	xbt14	1	uw	5	35,800	35,651	2044,13	120
365121	307-14	1	19	50	35,718	35,656	2097,62	121
365122	307-14	1	23	10	35,785	35,722	2048,56	122
365123	xbt15	1	uw	5	35,800	35,577	2040,68	123
365124	308-15	1	1	700	35,460	35,062	2161,07	124

id	stn	cast	niskin	depth	salt (ctd)	salt (som)	ct	
365125	308-15	1	1	700	35,460	35,087	2162,31	125
365126	308-15	1	2	600	35,510	35,545	2149,03	126
365127	308-15	1	3	500	35,580	35,366	2140,13	127
365128	308-15	1	5	400	35,620	35,732	2131,04	128
365129	308-15	1	7	300	35,660	35,612	2127,69	129
365130	308-15	1	11	200	35,710	35,223	2123,32	130
365131	308-15	1	11	200	35,710	35,591	2123,74	131
365132	308-15	1	13	150	35,740	35,577	2123,00	132
365133	308-15	1	15	100	35,780	35,734	2117,45	133
365134	308-15	1	17	45	35,740	35,452	2099,73	134
365135	308-15	1	19	20	35,770	35,843	2044,96	135
365136	308-15	1	21	10	35,780	35,734	2045,93	136
365137	xbt16	1	uw	5	35,800	35,698	2046,74	137
365138	309-16	1	1	700	35,440	35,303	2173,66	138
365139	309-16	1	1	700	35,440	35,124	2173,60	139
365140	309-16	1	5	500	35,480	35,388	2153,70	140
365141	309-16	1	9	300	35,590	35,554	2133,79	141
365142	309-16	1	15	100	35,730	35,757	2118,80	142
365143	309-16	1	17	60	35,710	35,690	2099,69	143
365144	309-16	1	19	10	35,840	35,779	2037,84	144
365145	xbt17	1	uw	5	35,800	35,409	2038,70	145
365146	310-17	1	1	700	35,542	35,848	2168,58	146
365147	310-17	1	3	600	35,431	35,414	2157,37	147
365148	310-17	1	6	400	35,609	35,625	2136,15	148
365149	310-17	1	10	200	35,777	35,981	2121,45	149
365150	310-17	1	12	100	35,853	35,677	2111,48	150
365151	310-17	1	15	80	35,806	35,828	2107,52	151
365152	310-17	1	17	60	35,776	35,360	2101,34	152
365153	310-17	1	20	40	35,880	35,941	2058,51	153
365154	310-17	1	22	10	35,871	35,607	2042,04	154
365155	xbt18	1	uw	5	35,800	35,517	2038,00	155
365156	311-18	1	19	10	35,815	35,850	2034,65	156
365157	xbt21	1	uw	5	35,800	35,707	2039,26	157
365158	312-19	1	1	4100	35,007	34,921	2200,90	158
365159	312-19	1	1	4100	35,007	34,902	2200,99	159
365160	312-19	1	2	4000	35,068	34,755	2199,48	160
365161	312-19	1	3	3800	35,041	34,905	2198,99	161
365162	312-19	1	4	3500	35,079	34,804	2194,08	162
365163	312-19	1	8	3000	35,100	34,975	2179,33	163
365164	312-19	1	9	2800	35,107	34,985	2176,31	164
365165	312-19	1	10	2500	35,113	34,896	2165,72	165
365166	312-19	1	11	2200	35,101	34,931	2159,00	166

id	stn	cast	niskin	depth	salt (ctd)	salt (som)	ct	
365167	312-19	1	11	2200	35,101	35,020	2157,47	167
365168	312-19	1	12	1800	35,055	35,037	2152,81	168
365169	312-19	1	13	1500	35,084	35,081	2156,39	169
365170	312-19	1	14	1200	35,277	34,938	2168,42	170
365171	312-19	1	15	800	35,589	35,485	2176,08	171
365172	312-19	1	16	500	35,519	35,498	2144,95	172
365173	312-19	1	17	400	35,589	35,386	2139,47	173
365174	312-19	1	18	300	35,633	35,549	2131,73	174
365175	312-19	1	19	200	35,705	35,468	2125,01	175
365176	312-20	1	3	67	35,746	35,574	2099,70	176
365177	312-20	1	6	52	35,731	35,659	2101,13	177
365178	312-20	1	6	52	35,731	35,369	2100,80	178
365179	312-20	1	8	43	35,728	35,523	2094,96	179
365180	312-20	1	11	32	35,799	35,655	2042,09	180
365181	312-20	1	14	24	35,812	35,717	2039,23	181
365182	312-20	1	20	15	35,809	35,662	2039,07	182
365182	313-21	1	16	100	35,760	35,725	2112,46	183
365183	313-21	1	18	45	35,750	35,327	2075,84	184
365185	313-21	1	20	20	35,780	35,653	2045,35	185
365186	313-21	1	22	15	35,770	35,559	2044,87	186
365187	314-22	1	1	4300	35,070	34,972	2200,97	187
365188	314-22	1	1	4300	35,070	34,900	2200,80	188
365189	314-22	1	2	4000	35,074	34,984	2199,74	189
365190	314-22	1	3	3800	35,078	34,992	2198,02	190
365191	314-22	1	4	3500	35,087	34,919	2193,30	191
365192	314-22	1	5	3000	35,108	34,940	2183,61	192
365193	xbt22	1	uw	5	35,800	35,711	2035,38	193
365194	314-22	1	7	2500	35,112	35,067	2163,63	194
365195	314-22	1	8	2200	35,097	35,035	2156,33	195
365196	314-22	1	9	1800	35,067	35,007	2154,21	196
365197	314-22	1	10	1500	35,111	34,999	2160,13	197
365198	314-22	1	11	1200	35,292	35,190	2170,71	198
365199	314-22	1	12	800	35,449	35,302	2169,96	199
365200	314-22	1	12	800	35,449	35,413	2170,39	200
365201	314-22	1	13	500	35,598	35,416	2136,33	201
365202	314-22	1	14	400	35,670	35,785	2127,13	202
365203	314-22	1	15	300	35,729	35,446	2123,04	203
365204	314-22	1	16	200	35,767	35,496	2120,89	204
365205	314-22	1	17	100	35,881	35,758	2113,25	205
365206	314-22	1	18	50	35,837	35,713	2093,06	206
365207	314-22	1	20	20	35,807	35,872	2038,17	207
365208	315-23	1	17	40	35,840	35,709	2102,40	208

id	stn	cast	niskin	depth	salt (ctd)	salt (som)	ct	
365209	315-23	1	22	15	35,780	35,663	2034,73	209
365210	xbt23	1	uw	5	35,800	35,665	2046,70	210
365211	316-24	1	3	58	35,979	35,839	2111,58	211
365212	316-24	1	6	35	35,916	35,907	2098,11	212
365213	316-24	1	11	26	35,816	35,769	2057,94	213
365214	316-24	1	14	19	35,792	35,677	2047,41	214
365215	316-24	1	17	15	35,788	35,728	2043,35	215
365216	316-24	1	17	15	35,788	35,641	2043,15	216
365217	316-25	1	1	4300	35,070	34,985	2203,09	217
365218	316-25	1	2	4000	35,076	34,941	2200,54	218
365219	316-25	1	2	4000	35,076	34,937	2200,15	219
365220	316-25	1	4	3500	35,091	34,948	2194,26	220
365221	316-25	1	5	3000	35,113	35,029	2179,96	221
365222	316-25	1	7	2500	35,113	34,948	2161,10	222
365223	316-25	1	7	2500	35,113	34,963	2161,58	223
365224	316-25	1	8	2200	35,086	35,006	2154,57	224
365225	316-25	1	9	1800	35,061	34,936	2154,60	225
365226	316-25	1	11	1200	35,279	35,231	2170,31	226
365227	316-25	1	12	800	35,363	35,261	2172,20	227
365228	316-25	1	13	500	35,562	35,462	2140,66	228
365229	316-25	1	14	400	35,634	35,595	2131,37	229
365230	316-25	1	16	200	35,873	35,793	2120,60	230
365231	316-25	1	17	100	35,971	35,906	2113,73	231
365232	316-25	1	20	20	35,776	35,713	2043,38	232
365233	317-26	1	19	45	35,840	35,808	2104,65	233
365234	317-26	1	22	20	35,750	35,689	2048,14	234
365235	318-27	1	19	50	35,834	35,732	2101,59	235
365236	318-27	1	22	20	35,801	35,681	2051,09	236
365237	319-28	1	18	40	35,846	35,725	2098,80	237
365238	319-28	1	21	20	35,751	35,674	2039,66	238
365239	xbt27	1	uw	5	35,800	35,710	2041,86	239
365240	320-29	1	3	64	36,010	35,845	2109,87	240
365241	320-29	1	6	48	35,960	35,820	2106,24	241
365242	320-29	1	11	30	35,900	35,758	2088,32	242
365243	320-29	1	21	15	35,790	35,554	2049,26	243
365244	320-29	1	21	15	35,790	35,729	2049,09	244
365245	320-30	1	1	4050	35,084	34,977	2200,25	245
365246	320-30	1	1	4050	35,084	34,959	2199,73	246
365247	320-30	1	3	3500	35,100	34,947	2191,86	247
365248	320-30	1	5	2800	35,128	35,024	2169,41	248
365249	320-30	1	7	2200	35,098	34,996	2154,40	249
365250	320-30	1	9	1500	35,121	35,106	2157,95	250

id	stn	cast	niskin	depth	salt (ctd)	salt (som)	ct	
365251	320-30	1	11	800	35,500	35,454	2171,32	251
365252	320-30	1	13	400	35,675	35,526	2130,04	252
365253	320-30	1	13	400	35,675	35,533	2128,28	253
365254	320-30	1	15	200	35,826	35,760	2120,48	254
365255	320-30	1	18	100	35,902	35,834	2113,93	255
365256	320-30	1	20	50	35,931	35,782	2101,67	256
365257	320-30	1	24	20	35,805	35,702	2046,99	257
365258	xbt28	1	uw	5	35,800	35,779	2045,50	258
365259	321-31	1	17	50	35,970	35,848	2104,39	259
365260	321-31	1	22	15	35,790	35,753	2043,08	260
365261	xbt29	1	uw	5	35,800	35,629	2049,85	261
365262	322-32	1	1	4500	35,084	34,978	2201,62	262
365263	322-32	1	2	4000	35,091	34,990	2198,17	263
365264	322-32	1	4	3500	35,104	34,897	2191,58	264
365265	322-32	1	5	3000	35,125	35,023	2179,08	265
365266	322-32	1	10	2500	35,137	34,976	2165,31	266
365267	322-32	1	11	2200	35,117	34,890	2156,60	267
365268	322-32	1	12	1800	35,102	34,940	2155,35	268
365269	322-32	1	13	1500	35,208	35,190	2162,49	269
365270	322-32	1	14	1200	35,402	35,247	2174,60	270
365271	322-32	1	15	800	35,635	35,439	2165,54	271
365272	322-32	1	16	500	35,651	35,490	2130,64	272
365273	322-32	1	18	300	35,743	35,620	2122,75	273
365274	322-32	1	20	150	35,876	35,849	2118,66	274
365275	322-33	1	3	58	35,779	35,571	2105,04	275
365276	322-33	1	6	45	35,824	35,710	2098,63	276
365277	322-33	1	8	35	35,843	35,728	2066,20	277
365278	322-33	1	11	26	35,825	35,779	2050,20	278
365279	322-33	1	14	19	35,822	35,719	2048,31	279
365280	322-33	1	18	15	35,822	35,728	2047,91	280
365281	323-34	1	18	45	35,825	35,769	2116,65	281
365282	323-34	1	22	20	35,799	35,707	2093,99	282
365283	324-35	1	18	50	35,772	35,638	2092,03	283
365284	324-35	1	22	20	35,787	35,696	2042,98	284
365285	325-36	1	3	600	35,474	35,374	2156,03	285
365286	325-36	1	5	500	35,575	35,505	2144,61	286
365287	325-36	1	5	500	35,575	35,441	2143,92	287
365288	325-36	1	7	400	35,606	35,484	2138,57	288
365289	325-36	1	9	300	35,711	35,598	2128,89	289
365290	325-36	1	11	250	35,765	35,636	2125,65	290
365291	325-36	1	13	200	35,835	35,739	2122,24	291
365292	325-36	1	15	150	35,905	35,767	2120,01	292

id	stn	cast	niskin	depth	salt (ctd)	salt (som)	ct	
365293	325-36	1	17	100	35,987	35,876	2114,93	293
365294	325-36	1	19	40	35,858	35,761	2081,28	294
365295	325-36	1	22	20	35,812	35,693	2050,77	295
365296	325-36	1	1	700	35,380	35,242	2167,91	296
365297	325-36	1	1	700	35,380	35,228	2167,49	297
365298	326-37	1	3	57	36,017	35,911	2106,59	298
365299	326-37	1	6	35	35,865	35,809	2087,38	299
365300	326-37	1	11	25	35,805	35,714	2054,83	300
365301	326-37	1	14	18	35,803	35,678	2053,87	301
365302	326-37	1	17	15	35,803	35,700	2054,48	302
365303	326-37	1	17	15	35,803	35,657	2055,24	303
365304	326-38	1	1	4400	35,088	34,965	2202,83	304
365305	326-38	1	3	3800	35,110	34,987	2197,96	305
365306	326-38	1	5	3200	35,133	34,998	2181,84	306
365307	326-38	1	5	3200	35,133	35,008	2182,99	307
365308	326-38	1	7	2500	35,140	34,991	2162,43	308
365309	326-38	1	8	2200	35,110	34,986	2156,56	309
365310	326-38	1	9	1800	35,100	34,992	2156,21	310
365311	326-38	1	10	1500	35,100	35,019	2160,56	311
365312	326-38	1	11	1200	35,230	35,094	2168,08	312
365313	326-38	1	12	800	35,420	35,296	2175,52	313
365314	326-38	1	13	500	35,560	35,430	2138,70	314
365315	326-38	1	14	400	35,610	35,487	2136,89	315
365316	326-38	1	16	200	35,810	35,700	2125,68	316
365317	326-38	1	18	100	35,990	35,939	2114,13	317
365318	327-39	1	20	35	35,743	35,764	2053,19	318
365319	327-39	1	22	15	35,736	35,544	2051,50	319
365320	328-40	1	19	40	35,810	35,542	2086,59	320
365321	328-40	1	22	15	35,790	35,754	2053,05	321
365322	329-41	1	19	35	35,822	35,738	2050,52	322
365323	329-41	1	22	15	35,817	35,605	2049,32	323
365324	330-42	1	1	85	35,972	35,775	2112,17	324
365325	330-42	1	1	85	35,972	35,914	2112,03	325
365326	330-42	1	3	60	35,982	35,828	2108,80	326
365327	330-42	1	5	51	35,964	35,779	2107,96	327
365328	330-42	1	9	31	35,866	35,795	2075,38	328
365329	330-42	1	12	23	35,826	35,763	2056,14	329
365330	330-42	1	15	16	35,797	35,757	2053,29	330
365331	330-42	1	18	12	35,792	35,783	2053,94	331
365332	330-43	1	1	4200	35,100	34,964	2201,15	332
365333	330-43	1	2	3800	35,100	34,989	2199,93	333
365334	330-43	1	2	3800	35,100	34,919	2198,76	334

id	stn	cast	niskin	depth	salt (ctd)	salt (som)	ct	
365335	330-43	1	3	3500	35,120	34,929	2192,92	335
365336	330-43	1	7	3000	35,140	35,035	2177,46	336
365337	330-43	1	9	2500	35,140	35,028	2161,42	337
365338	330-43	1	10	2200	35,160	34,956	2154,20	338
365339	330-43	1	11	1800	35,096	34,959	2154,61	339
365340	330-43	1	12	1500	35,140	34,958	2159,42	340
365341	330-43	1	13	1200	35,310	35,171	2170,90	341
365342	330-43	1	13	1200	35,310	35,244	2171,24	342
365343	330-43	1	14	800	35,310	35,457	2172,62	343
365344	330-43	1	15	600	35,570	35,479	2145,72	344
365345	330-43	1	16	300	35,770	35,685	2123,74	345
365346	330-43	1	17	150	35,920	35,761	2119,25	346
365347	330-43	1	18	100	35,980	35,930	2115,67	347
365348	330-43	1	19	50	35,996	35,894	2110,00	348
365349	330-43	1	24	20	35,780	35,742	2052,64	349
365350	331-44	1	3	102	36,050	35,964	2112,25	350
365351	331-44	1	8	72	36,020	35,898	2109,50	351
365352	331-44	1	10	62	35,970	35,898	2105,11	352
365353	331-44	1	12	52	35,950	35,975	2102,16	353
365354	331-44	1	15	38	35,940	35,775	2068,37	354
365355	331-44	1	17	28	35,920	35,882	2053,22	355
365356	331-44	1	19	20	35,920	35,759	2051,39	356
365357	331-44	1	21	15	35,900	35,828	2051,09	357
365358	331-44	1	23	10	35,920	35,823	2050,55	358
365359	332-46	1	22	10	35,870	35,867	2053,91	359
365360	332-46	1	19	40	35,870	35,875	2054,11	360
365361	333-47	1	1	4350	35,107	34,975	2200,70	361
365362	333-47	1	2	4000	35,111	34,942	2198,97	362
365363	333-47	1	2	4000	35,111	35,131	2200,54	363
365364	333-47	1	4	3500	35,126	34,981	2190,70	364
365365	333-47	1	6	3000	35,147	34,877	2176,84	365
365366	333-47	1	8	2500	35,149	35,013	2161,07	366
365367	333-47	1	9	2200	35,120	35,047	2154,16	367
365368	333-47	1	10	1800	35,101	34,957	2153,35	368
365369	333-47	1	11	1500	35,144	35,083	2158,92	369
365370	333-47	1	12	1200	35,254	35,169	2167,25	370
365371	333-47	1	13	800	35,296	35,197	2171,02	371
365372	333-47	1	14	500	35,620	35,427	2140,83	372
365373	333-47	1	14	500	35,620	35,534	2141,35	373
365374	333-47	1	16	300	35,858	35,690	2121,17	374
365375	333-47	1	18	200	35,912	35,724	2119,07	375
365376	333-47	1	19	150	35,995	36,038	2113,83	376

id	stn	cast	niskin	depth	salt (ctd)	salt (som)	ct	
365377	333-47	1	19	150	35,995	35,891	2114,37	377
365378	333-47	1	20	100	36,069	36,117	2111,69	378
365379	333-47	1	21	80	36,029	35,951	2108,95	379
365380	333-47	1	22	50	35,976	35,999	2093,45	380
365381	333-47	1	23	30	35,878	35,830	2053,60	381
365382	333-47	1	24	10	35,884	35,833	2053,14	382
365383	334-48	1	19	40	35,940	35,850	2050,17	383
365384	334-48	1	22	20	35,940	35,822	2049,99	384
365385	335-49	1	19	40	35,772	35,615	2061,44	385
365386	335-49	1	22	20	35,773	35,703	2047,80	386
365387	336-50	1	19	35	35,914	35,879	2052,54	387
365388	336-50	1	21	20	35,925	35,815	2051,06	388
365389	337-51	1	1	97	35,990	35,788	2114,51	389
365390	337-51	1	3	70	35,920	35,684	2108,27	390
365391	337-51	1	5	60	35,860	35,712	2099,42	391
365392	337-51	1	8	37	35,950	35,860	2052,87	392
365393	337-51	1	12	27	35,950	35,882	2052,56	393
365394	337-51	1	15	20	35,950	35,917	2053,23	394
365395	337-51	1	18	14	35,950	35,909	2053,13	395
365396	337-51	1	21	8	35,950	35,726	2052,92	396
365397	337-52	1	1	4150	35,114	34,956	2199,52	397
365398	337-52	1	1	4150	35,114	34,924	2200,05	398
365399	337-52	1	3	3800	35,122	35,047	2196,39	399
365400	337-52	1	5	3200	35,147	34,957	2178,32	400
365401	337-52	1	7	2800	35,150	35,027	2163,56	401
365402	337-52	1	8	2500	35,145	34,992	2158,36	402
365403	337-52	1	9	2200	35,120	34,937	2153,48	403
365404	337-52	1	10	1800	35,110	34,928	2152,90	404
365405	337-52	1	11	1500	35,150	35,036	2158,92	405
365406	337-52	1	12	1200	35,250	35,101	2168,94	406
365407	337-52	1	13	800	35,470	35,353	2167,14	407
365408	337-52	1	14	500	35,640	35,508	2137,78	408
365409	337-52	1	15	400	35,710	35,521	2129,66	409
365410	337-52	1	17	200	35,860	35,760	2121,55	410
365411	337-52	1	17	200	35,860	35,729	2121,22	411
365412	337-52	1	19	100	35,880	35,700	2105,25	412
365413	338-53	1	19	40	35,910	35,747	2061,16	413
365414	338-53	1	22	10	35,890	35,750	2054,96	414
365415	339-54	1	1	94	36,016	35,867	2111,46	415
365416	339-54	1	3	69	35,992	35,825	2107,76	416
365417	339-54	1	5	60	35,963	35,837	2102,50	417
365418	339-54	1	9	37	35,820	35,698	2057,41	418

id	stn	cast	niskin	depth	salt (ctd)	salt (som)	ct	
365419	339-54	1	12	27	35,813	35,661	2054,60	419
365420	339-54	1	15	19	35,812	35,655	2055,33	420
365421	339-54	1	18	14	35,813	35,682	2054,89	421
365422	339-54	1	21	8	35,813	35,723	2056,43	422
365423	339-54	1	21	8	35,813	35,757	2055,35	423
365424	339-55	1	1	4200	35,120	34,987	2200,87	424
365425	339-55	1	3	3800	35,125	34,957	2197,18	425
365426	339-55	1	22	20	35,820	35,666	2053,60	426
365427	339-55	1	5	3000	35,160	35,007	2175,82	427
365428	339-55	1	7	2500	35,150	35,044	2159,50	428
365429	339-55	1	8	2200	35,130	35,016	2154,52	429
365430	339-55	1	9	1800	35,110	34,940	2154,37	430
365431	339-55	1	10	1500	35,140	35,052	2156,44	431
365432	339-55	1	11	1200	35,230	35,104	2166,23	432
365433	339-55	1	12	1000	35,290	35,124	2172,00	433
365434	339-55	1	13	850	35,300	35,171	2172,77	434
365435	339-55	1	14	650	35,420	35,295	2158,11	435
365436	339-55	1	15	500	35,600	35,446	2134,46	436
365437	339-55	1	16	300	35,820	35,725	2123,19	437
365438	339-55	1	18	150	35,990	35,905	2115,80	438
365439	340-56	1	21	30	35,760	35,626	2051,53	439
365439	340-56	1	21	30	35,760	35,626	2051,53	439
365439	340-56	1	21	30	35,760	35,626	2051,53	439
365439	340-56	1	21	30	35,760	35,626	2051,53	439
365439	340-56	1	21	30	35,760	35,626	2051,53	439
365440	340-56	1	23	15	35,760	35,612	2052,25	440
365441	341-57	1	1	3600	35,130	34,948	2195,44	441
365442	341-57	1	1	3600	35,130	34,995	2195,59	442
365443	341-57	1	3	3000	35,160	35,059	2177,16	443
365444	341-57	1	5	2500	35,160	34,988	2161,15	444
365445	341-57	1	6	2200	35,140	35,013	2155,85	445
365446	341-57	1	7	1800	35,110	34,984	2153,67	446
365447	341-57	1	8	1500	35,130	34,979	2156,78	447
365448	341-57	1	9	1200	35,240	35,068	2165,76	448
365449	341-57	1	10	1000	35,320	35,156	2171,24	449
365450	341-57	1	10	1000	35,320	35,172	2170,50	450
365451	341-57	1	11	850	35,320	35,174	2172,83	451
365452	341-57	1	13	500	35,460	35,343	2153,18	452
365453	341-57	1	15	300	35,630	35,490	2131,77	453
365454	341-57	1	17	150	35,760	35,646	2126,12	454
365455	341-57	1	19	50	35,200	35,714	2106,93	455
365456	341-57	1	22	20	35,750	35,677	2051,99	456

id	stn	cast	niskin	depth	salt (ctd)	salt (som)	ct	
365457	341-58	1	1	108	35,840	35,733	2121,46	457
365458	341-58	1	3	76	35,840	35,716	2112,84	458
365459	341-58	1	5	63	35,860	35,700	2108,53	459
365460	341-58	1	8	39	35,770	35,674	2055,87	460
365461	341-58	1	11	29	35,760	35,642	2051,21	461
365462	341-58	1	18	20	35,760	35,681	2052,09	462
365463	342-59	1	1	102	35,990	35,802	2111,77	463
365464	342-59	1	3	72	35,930	35,793	2102,67	464
365465	342-59	1	5	62	35,900	35,748	2093,46	465
365466	342-59	1	8	47	35,860	35,735	2063,90	466
365467	342-59	1	11	38	35,860	35,701	2059,63	467
365468	342-59	1	14	27	35,860	35,771	2059,83	468
365469	342-59	1	17	20	35,860	35,742	2059,35	469
365470	342-59	1	20	15	35,860	35,771	2059,28	470
365471	342-59	1	20	15	35,860	35,768	2060,70	471
365472	343-60	1	1	700	35,350	35,200	2168,68	472
365473	343-60	1	1	700	35,350	35,140	2169,87	473
365474	343-60	1	3	600	35,410	35,228	2160,66	474
365475	343-60	1	5	500	35,510	35,392	2146,05	475
365476	343-60	1	7	400	35,640	35,508	2131,47	476
365477	343-60	1	9	300	35,740	35,719	2127,77	477
365478	343-60	1	11	200	35,840	35,669	2121,69	478
365479	343-60	1	13	150	35,890	35,848	2119,80	479
365480	343-60	1	15	100	35,940	35,882	2112,92	480
365481	343-60	1	17	80	35,940	35,793	2110,48	481
365482	343-60	1	19	50	35,890	35,795	2078,99	482
365483	343-60	1	21	35	35,860	35,736	2058,65	483
365484	343-60	1	23	20	35,860	35,731	2058,65	484
365485	344-61	1	19	30	35,910	35,823	2059,58	485
365486	344-61	1	22	20	35,910	35,761	2058,59	486
365487	xbt58	1	uw	5	35,920	35,780	2053,49	487
365488	345-62	1	1	96	36,070	35,957	2112,16	488
365489	345-62	1	1	96	36,070	35,941	2112,55	489
365490	345-62	1	4	70	36,080	35,817	2111,21	490
365491	345-62	1	7	59	35,980	35,940	2107,71	491
365492	345-62	1	10	36	35,940	35,817	2102,59	492
365493	345-62	1	13	26	35,940	35,797	2052,63	493
365494	345-62	1	16	20	35,940	35,785	2051,95	494
365495	xbt59	1	uw	5	35,940	35,718	2049,95	495
365496	346-63	1	1	700	35,450	35,299	2161,09	496
365497	346-63	1	5	500	35,650	35,375	2148,56	497
365498	346-63	1	9	300	35,860	35,581	2125,70	498

id	stn	cast	niskin	depth	salt (ctd)	salt (som)	ct	
365499	346-63	1	17	100	36,040	35,785	2116,29	499
365500	346-63	1	19	50	35,950	35,928	2111,92	500
365501	346-63	1	21	40	35,940	35,773	2049,99	501
365502	346-63	1	23	20	35,940	35,831	2049,21	502
365503	xbt60	1	uw	5	35,930	35,726	2047,53	503
365504	347-64	1	17	80	36,050	35,767	2110,77	504
365505	347-64	1	19	50	35,930	35,807	2096,06	505
365506	347-64	1	21	35	35,940	35,788	2049,93	506
365507	347-64	1	23	20	35,920	35,825	2049,66	507
365508	347-64	1	23	20	35,920	35,759	2049,56	508
365509	xbt61	1	uw	5	35,940	35,766	2054,19	509
365510	348-65	1	1	20	35,940	35,774	2053,14	510
365511	348-65	1	1	20	35,940	35,834	2052,06	511
365512	348-65	1	3	700	35,510	35,336	2156,24	512
365513	348-65	1	5	600	35,580	35,433	2146,15	513
365514	348-65	1	7	500	35,740	35,606	2129,86	514
365515	348-65	1	9	400	35,800	35,666	2122,98	515
365516	348-65	1	13	250	35,896	35,844	2120,61	516
365517	348-65	1	17	150	35,950	35,835	2118,60	517
365518	348-65	1	19	100	36,040	35,915	2113,45	518
365519	348-65	1	22	50	35,970	35,854	2094,18	519
365520	348-65	1	pump	5	35,940	35,747	2051,98	520
365521	xbt62	1	uw	5	35,900	35,810	2056,11	521
365522	349-66	1	17	100	36,020	35,937	2108,32	522
365523	349-66	1	19	60	35,990	35,757	2057,27	523
365524	349-66	1	21	40	35,850	35,756	2055,38	524
365525	349-66	1	23	15	35,860	35,734	2054,94	525
365526	xbt63	1	uw	5	35,800	35,565	2049,06	526
365527	350-67	1	17	100	35,930	35,765	2113,02	527
365528	350-67	1	19	60	35,930	35,799	2105,08	528
365529	350-67	1	21	45	35,850	35,696	2077,73	529
365530	350-67	1	23	15	35,660	35,537	2047,03	530
365531	xbt64	1	uw	5	35,700	35,580	2049,51	531
365532	351-68	1	1	700	35,310	35,115	2168,98	532
365533	351-68	1	1	700	35,310	35,106	2170,71	533
365534	351-68	1	3	600	35,430	35,336	2163,26	534
365535	351-68	1	5	500	35,480	35,380	2150,60	535
365536	351-68	1	7	400	35,620	35,495	2140,99	536
365537	351-68	1	9	300	35,740	35,647	2130,31	537
365538	351-68	1	13	200	35,940	35,823	2119,17	538
365539	351-68	1	15	150	36,020	35,897	2114,06	539
365540	351-68	1	17	100	35,990	35,879	2111,67	540

id	stn	cast	niskin	depth	salt (ctd)	salt (som)	ct	
365541	351-68	1	18	60	35,910	35,777	2104,00	541
365542	351-68	1	19	50	35,870	35,761	2086,09	542
365543	351-68	1	20	40	35,750	35,608	2053,69	543
365544	351-68	1	23	15	35,750	35,623	2051,00	544
365545	351-69	1	1	99	35,890	35,708	2112,11	545
365546	351-69	1	1	99	35,890	35,770	2112,28	546
365547	351-69	1	3	74	35,920	35,840	2106,54	547
365548	351-69	1	5	64	35,900	35,790	2101,86	548
365549	351-69	1	8	59	35,910	35,816	2095,13	549
365550	351-69	1	10	39	35,760	35,619	2052,66	550
365551	351-69	1	13	28	35,740	35,635	2051,76	551
365552	351-69	1	16	21	35,750	35,631	2052,60	552
365553	351-69	1	19	15	35,740	35,635	2051,77	553
365554	xbt65	1	uw	5	35,760	35,608	2053,50	554
365555	352-70	1	16	100	36,030	35,764	2110,61	555
365556	352-70	1	18	50	35,950	35,752	2086,92	556
365557	352-70	1	20	40	35,790	35,642	2058,15	557
365558	352-70	1	22	15	35,790	35,617	2056,62	558
365559	xbt66	1	uw	5	35,820	35,658	2057,85	559
365560	353-71	1	17	100	36,040	35,876	2110,08	560
365561	353-71	1	19	50	35,860	35,677	2062,75	561
365562	353-71	1	21	35	35,860	35,755	2063,06	562
365563	353-71	1	23	15	35,860	35,715	2060,57	563
365564	xbt67	1	uw	5	35,820	35,681	2060,78	564
365565	354-72	1	1	700	35,360	35,247	2170,18	565
365566	354-72	1	1	700	35,360	35,229	2170,13	566
365567	354-72	1	3	600	35,420	35,247	2162,80	567
365568	354-72	1	5	500	35,470	35,390	2151,42	568
365569	354-72	1	7	400	35,570	35,437	2135,94	569
365570	354-72	1	9	300	35,650	35,491	2131,41	570
365571	354-72	1	13	200	35,760	35,622	2124,11	571
365572	354-72	1	15	150	35,800	35,709	2116,79	572
365573	354-72	1	15	150	35,800	35,603	2116,39	573
365574	354-72	1	17	100	35,850	35,754	2112,73	574
365575	354-72	1	19	50	35,780	35,672	2070,39	575
365576	354-72	1	21	35	35,780	35,718	2061,89	576
365577	354-72	1	23	15	35,780	35,725	2062,00	577
365578	355-73	1	1	97	35,910	35,786	2112,25	578
365579	355-73	1	3	69	35,890	35,844	2108,96	579
365580	355-73	1	5	60	35,880	35,730	2105,44	580
365581	355-73	1	8	50	35,870	35,689	2075,44	581
365582	355-73	1	11	37	35,870	35,807	2062,64	582

id	stn	cast	niskin	depth	salt (ctd)	salt (som)	ct	
365583	355-73	1	14	27	35,870	35,755	2061,48	583
365584	355-73	1	17	20	35,870	35,808	2061,54	584
365585	355-73	1	20	15	35,870	35,811	2060,81	585
365586	xbt68	1	uw	5	35,800	35,642	2059,77	586
365587	xbt69	1	uw	5	35,800	35,680	2063,61	587
365588	xbt70	1	uw	5	35,800	35,649	2054,14	588
365589	xbt71	1	uw	5	35,800	35,719	2058,49	589
365590	xbt72	1	uw	5	35,800	35,657	2055,05	590
365591	xbt73	1	uw	5	35,800	35,663	2053,06	591
365592	356-74	1	1	3000	35,180	35,027	2181,26	592
365593	356-74	1	1	3000	35,180	35,009	2181,47	593
365594	356-74	1	3	2500	35,190	35,048	2166,80	594
365595	356-74	1	4	2200	35,170	34,984	2157,80	595
365596	356-74	1	5	2000	35,150	35,038	2155,25	596
365597	356-74	1	7	1600	35,170	34,990	2158,95	597
365598	356-74	1	9	1200	35,410	35,287	2172,63	598
365599	356-74	1	10	1000	35,580	35,389	2177,02	599
365600	356-74	1	11	800	35,510	35,363	2168,68	600
365601	356-74	1	12	700	35,540	35,433	2158,53	601
365602	356-74	1	13	600	35,570	35,427	2148,17	602
365603	356-74	1	14	500	35,650	35,480	2135,38	603
365604	356-74	1	15	400	35,680	35,566	2130,26	604
365605	356-74	1	16	300	35,730	35,620	2124,62	605
365606	356-74	1	17	200	35,790	35,629	2128,19	606
365607	356-74	1	18	150	35,820	35,605	2122,69	607
365608	356-74	1	19	100	35,860	35,713	2117,95	608
365609	356-74	1	20	50	35,830	35,644	2105,23	609
365610	356-74	1	21	40	35,800	35,730	2075,07	610
365611	356-74	1	23	15	35,750	35,605	2054,45	611
365612	356-74	1	23	15	35,750	35,633	2055,97	612
365613	357-75	1	11	100	35,930	35,776	2119,54	613
365614	357-75	1	11	100	35,930	35,876	2118,78	614
365615	357-75	1	13	70	35,990	35,900	2115,45	615
365616	357-75	1	15	50	35,970	35,828	2109,53	616
365617	357-75	1	17	30	35,780	35,717	2058,73	617
365618	357-75	1	21	15	35,780	35,673	2054,42	618
365619	358-76	1	11	100	35,880	35,735	2118,25	619
365620	358-76	1	13	70	35,850	35,703	2109,80	620
365621	358-76	1	15	50	35,880	35,628	2091,66	621
365622	358-76	1	18	40	35,890	35,833	2056,68	622
365623	358-76	1	22	15	35,880	35,775	2056,29	623
365624	358-76	1	22	15	35,880	35,867	2056,44	624

id	stn	cast	niskin	depth	salt (ctd)	salt (som)	ct	
365625	356-muc	1	muc	4800	35,000	35,326	2177,82	625
365626	359-78	1	11	100	35,970	35,817	2114,16	626
365627	359-78	1	13	70	35,920	35,820	2105,94	627
365628	359-78	1	15	50	35,870	35,673	2095,55	628
365629	359-78	1	17	35	35,870	35,749	2052,31	629
365630	359-78	1	21	15	35,870	35,745	2048,69	630

7.5.3 Stations and Depths Analysed

The pH and alkalinity was analysed in:

station 300 10,40,100,150,300,500 and 700 m.
station 302 10,18,24,32,42,52,62,72,99,250,400,550 and 700 m.
station 303 10,20,58,100,300,500 and 700 m.
station 305 42, 100, 150, 200, 300, 400, 500, 600 and 700 m.
station 307 10, 20, 50, 100, 150, 200, 250, 300, 400, 500, 600 and 700 m.
station 308 10, 20, 45, 100, 150, 200, 250, 300, 400, 500, 600 and 700 m.
station 312 200, 300, 400, 500, 800, 1200, 1500, 1800, 2200, 2500, 2800, 3000, 4000 and 4100 m.
station 314 7, 20, 50, 100, 200, 300, 400, 500, 800, 1200, 1500, 1800, 2000, 2500, 2800, 3000, 3500, 3800, 4000 and 4300 m.
station 320 20, 50, 100, 150, 200, 300, 400, 500, 800, 1500, 2200, 2800, 3500 and 4050 m.
station 321 7, 15, 20, 50, 100, 150, 200, 300, 400, 500, 600 and 700 m.
station 322 15, 150, 200, 300, 400, 500, 1200, 1500, 1800, 2500, 2800, 3000, 3500, 3800, 4000 and 4500 m.
station 326 7, 20, 40, 50, 100, 150, 200, 300, 400, 500, 800, 1200, 1500, 1800, 2200, 2500, 2800, 3200, 3800, 4000 and 4400 m.
staion 330 7, 20, 38, 50, 100, 150, 300, 600, 800, 1200, 1500, 1800, 2200, 2500, 2800, 3000, 3500, 3800 and 4200 m.
station 333 7, 10, 30, 50, 80, 100, 150, 200, 250, 300, 400, 500, 800, 1200, 1500, 1800, 2200, 2500, 2800, 3000, 3200, 3800, 4000 and 4350 m.
station 337 35, 50, 80, 100, 150, 200, 300, 400, 500, 800, 1200, 1500, 1800, 2200, 2500, 2800, 3000, 3200, 3500, 3800, 4000 and 4150 m.
station 339 7, 20, 50, 150, 200, 300, 500, 650, 850, 1000, 1200, 1500, 1800, 2200, 2500, 2800, 3000, 3800, 4000 and 4200 m.
station 341 7, 20, 50, 100, 150, 200, 300, 400, 500, 650, 850, 1000, 1200, 1500, 1800, 2200, 2500, 2800, 3000, 3300 and 3600 m.
station 351 7, 15, 40, 50, 60, 100, 150, 200, 250, 300, 400, 500, 600 and 700 m.
station 354 7, 15, 35, 50, 100, 150, 200, 250, 300, 400, 500, 600 and 700 m.
station 356 7, 15, 40, 50, 100, 150, 200, 300, 400, 500, 600, 700, 800, 1000, 1200, 1600, 2000, 2200, 2500 and 3000 m.
station 358 7, 15, 40, 50, 70, 100, 150, 200, 300, 500 and 700 m.
station 359 7, 15, 35, 50, 70, 100, 150, 200, 300, 500 and 700 m.

Only the pH was analysed in:

station 298 7, 13, 22, 29, 40, 54, 84 and 90 m.
station 299 7, 10, 15, 21, 28, 39 , 52, 59, 67 and 90 m.
station 323 7, 20, 45, 100, 150, 200, 250, 300, 400, 500, 600 and 700 m.
station 324 20, 50, 100, 150, 200, 300, 400, 500, 600 and 700 m.

7.5.4 Samples Collected at Stations

Station	Depth	Species	# of Specimens
298	0-100	universa	4
298	0-100	universa	3
298	0-30	universa	8
298	0-30	ruber (white)	4
298	0-30	sacculifer	3
298	0-30	universa	7
298	0-30	siphonifera	6
298	0-30	ruber (white)	12
298	0-30	universa	10
298	0-30	ruber (white)	18
298	0-30	sacculifer	6
298	0-30	siphonifera	8
298	0-30	ruber (white)	4
298	0-30	dutertrei	7
303	0-30	inflata	2
303	0-30	incompta	4
303	0-30	sacculifer	6
303	0-100	sacculifer	51
303	0-100	ruber	18
303	0-100	universa	53
303	0-100	universa	17
305	0-100	sacculifer	25
305	0-100	ruber	11
305	0-100	universa	26
305	2500-2000	UFO's (TypII)	2
316	0-50	bulloides	13
316	0-50	universa	16
320	0-50	ruber	21
320	0-50	dutertrei	18
320	0-50	inflata	11
327	0-50	dutertrei	7
342	0-50	bulloides	31
342	0-50	siphonifera	18
354	100-0	falconensis	1
354	100-0	dutertrei	10
354	100-0	bulloides	10
354	100-0	incompta	10
356	100-0	bulloides	25
356	100-0	ruber	5

Station	Depth	Species	# of Specimens
356	100-0	quinqueloba	5
356	100-0	falconensis	1
356	100-0	incompta	1
356	100-0	quinqueloba	26
356	100-0	sacculifer	1
357	100-0	incompta	1
357	100-0	dutertrei	1
358	100-0	dutertrei	2
358	100-0	inflata	1
358	100-0	incompta	4
358	100-0	ruber	4
358	100-0	universa	7
358	100-0	sacculifer	3
358	100-0	universa	7
358	100-0	sacculifer	8

7.6 Leg M 36/6

7.6.1 Pore Water Profiles

MC-36#369	
Depth (cm)	**SiO_2 [µM]**
0	47.8
-0.25	57.6
-0.75	82.6
-1.25	116.7
-1.75	
-2.25	145.5
-2.75	
-3.25	175.2
-3.75	
-4.25	192.4
-4.75	
-5.5	207.6
-6.5	210.8
-7.5	212.6
-8.5	228.1
-9.5	231.9
-11	231.0
-15	225.7
-19	217.7
-23	209.3
-27	219.1
-30.75	201.9

MC-50#395	
Depth (cm)	**SiO_2 [µM]**
0	15.0
-0.25	48.0
-0.75	74.9
-1.5	89.9
-2.5	125.9
-3.5	155.8
-4.5	122.9
-5.5	170.8
-6.5	161.8
-7.5	173.8

MC-56#399	
Depth (cm)	**SiO_2 [µM]**
-8.5	155.8
0	31.1
-0.25	60.2
-0.75	69.5
-1.5	104.8
-2.5	138.5
-3.5	169.7
-4.5	188.3
-5.5	190.4
-6.5	194.0

MC-59#405							
Depth (cm)	**SiO_2 [µM]**	**NO_3 [µM]**	**NH_4 [µM]**	**PO_4 [µM]**	**N/P**	**pH**	**TA [mmol/kg]**
0	48.2	21.7	0.0	2.1	10.1		2.3
-0.25	81.8		3.8	1.9			
-0.75	113.9	33.3	5.9	1.9	20.5		2.2
-1.5	138.2	37.1	3.5	2.4	17.1		2.2
-2.5	176.6	37.3	2.6	2.6	15.3	7.6	2.2
-3.5	215.9	40.7	4.7	3.0	15.3	7.7	2.3
-4.5	229.4	42.8	6.8	4.5	10.9	7.6	
-5.5	236.6	41.9	3.2	3.2	14.0	7.6	2.3
-6.5	247.0	43.9	4.7	3.5	14.1	7.6	
-7.5	245.9	41.4	5.3	3.7	12.7	7.6	
-8.5	244.4	38.5	4.7	3.8	11.3	7.6	
-9.5	242.8	39.6	6.8	3.8	12.2	7.7	
-11.5	227.8	37.1	7.1	3.8	11.6	7.7	
-14.5	222.1	30.3	5.3	3.8	9.3	7.7	

KG-10#405							
Depth (cm)	**SiO_2 [µM]**	**NO_3 [µM]**	**NH_4 [µM]**	**PO_4 [µM]**	**N/P**	**pH**	**TA [mmol/kg]**
0	23.4	7.9	2.1	0.7	14.0		
-0.25	74.6	38.8	13.2	2.3	23.0	7.6	2.3
-0.75	93.7	29.4	8.8	2.3	16.9	7.7	2.3
-1.5	141.9	26.9	3.2	1.9	15.8	7.6	2.2
-2.5	154.8	31.0	3.5	2.4	14.5	7.7	2.4
-3.5	183.3	44.4	3.5	2.9	16.8	7.6	2.3
-4.5	199.9	33.7	7.1	3.3	12.2	7.7	2.5
-5.5	207.1	34.0	4.1	3.6	10.7	7.7	2.5
-6.5	210.7	31.0	4.7	4.0	8.8	7.8	2.5
-7.5	209.7	33.0	4.1	3.6	10.4	7.8	
-8.5	206.1	31.2	5.3	4.2	8.8	7.8	
-9.5	207.6	29.9	6.2	4.6	7.8	7.8	
-11.5	210.2	30.3	7.1	4.9	7.6	7.8	
-14.5	211.3	28.5	4.7	4.5	7.3	7.7	2.6
-17.5	210.7	24.2	6.5	4.4	7.0	7.7	2.4
-20.5	223.2	25.1	4.1	5.0	5.8	7.7	2.4
-23.5	233.5	26.0	5.0	5.1	6.1	7.6	2.3
-26.5	239.2	22.4	2.4	5.6	4.4	7.7	2.6
-29.5	236.6		3.2	5.6		7.6	2.6
0	42.0	24.0	2.4	2.0	13.1		
-0.25	63.0	28.7		1.7	16.8	7.7	2.3
-0.75	76.2	31.8	6.4	1.6	24.6	7.8	2.2
-1.5	98.5	30.8	7.7	1.8	20.9	7.7	2.1
-2.5	121.5	31.8	4.3	2.0	18.0	7.7	2.1
-3.5	120.8	35.6	5.9	2.2	18.7	7.8	2.2
-4.5	158.2	34.4	8.5	2.8	15.4	7.7	2.2
-5.5	171.4	34.3	5.8	2.8	14.4	7.5	2.3
-6.5	179.9	34.7	6.6	2.9	14.3	7.5	2.2
-7.5	181.2	33.3	5.3	3.0	12.9	7.6	2.3
-8.5	181.9		5.9			7.5	2.1
-9.5	183.8					7.7	2.3
-11.5	180.6	32.4		3.7	8.7	7.6	2.4
-14.5	173.3	30.7	7.2	3.7	10.2	7.6	2.3
-17.5	197.0	29.5	7.2	3.9	9.5	7.6	2.3

MC-34#362					
Depth (cm)	**SiO_2 [μM]**	**NO_3 [μM]**	**NH_4 [μM]**	**PO_4 [μM]**	**N/P**
0					
-0.25					
-0.75	109.0				
-1.5	114.2	32.5		2.7	11.8
-2.5	158.2	36.6	5.8	1.9	21.8
-3.5	172.0				
-4.5	188.4	36.5	7.1	2.3	18.7
-5.5	197.6	35.9	3.3	2.2	17.8
-6.5	200.9	35.8	5.6	2.8	14.6
-7.5	206.2	35.5	4.4	2.4	16.4
-8.5	212.1	35.8	4.1	2.9	13.8
-9.5	160.9	35.3	8.2	3.5	12.5
-11.5	210.8	34.4	4.4	3.0	12.8
-14.5	206.8	33.1	5.8	3.3	11.9
-17.5	208.1	29.8	4.4	3.5	9.7

MC-46#388					
Depth (cm)	**SiO_2 [μM]**	**NO_3 [μM]**	**NH_4 [μM]**	**PO_4 [μM]**	**N/P**
0					
-0.25	68.3	27.8	57.4	6.5	13.2
-0.75	83.4	29.8	24.4	3.2	16.8
-1.5	120.0	30.9	7.6	1.9	20.1
-2.5	157.2	33.4	8.2	2.6	15.8
-3.5	183.4	33.4	9.7	3.3	12.9
-4.5	193.1	35.2	10.3	3.0	15.2
-5.5	191.0	35.0	9.7	3.2	13.8
-6.5	202.7	36.8	7.4	3.3	13.2
-7.5	209.6	36.1	6.8	3.5	12.4
-8.5	215.1	34.8	6.5	3.9	10.4
-9.5	209.6	35.2		4.8	7.4
-11.5	215.8	30.9	11.2	3.8	11.0
-14.5	218.6	33.6	5.3		

7.6.2 List of Stations

Station	Time (UTC)	Device	Date	Geographical Position		Water depth (m)	Wire length (m)
				latitude	longitude		
test	09.22	CTD	11.10.1996	47°58.80'	15°25.10'	4799	4300
360	19.55	MUC	11.10.1996	48°58.08'	16°27.83'	4802	4846
	22.45	MUC	11.10.1996	48°58.01'	16°27.94'	4802	4855
	01.57	MUC	12.10.1996	48°58.03'	16°27.93'	4804	4857
	04.50	MUC	12.10.1996	48°58.05'	16°28.01'	4804	4860
361	08.40	SF	12.10.1996	48°55.56'	16°35.07'	4802	
362	10.30	MUC	12.10.1996	48°58.00'	16°27.98'	4802	4867
	13.43	MUC	12.10.1996	48°58.01'	16°28.00'	4804	4869
363	16.24	RK	12.10.1996	48°58.40'	16°21.20'	4806	
364	18.15	MUC	12.10.1996	48°49.90'	16°21.10'	4802	541
365	12.24	CTD	14.10.1996	48°58.12'	16°27.75'	4800	800
	13.56	MSN	14.10.1996	48°57.90'	16°27.90'	4803	700
366	09.40	CTD	16.10.1996	48°58.00'	16°28.70'	4802	4750
367	12.45	RK	16.10.1996	48°58.00'	16°20.80'	4803	
	13.15	MSN	16.10.1996	48°57.90'	16°21.10'	4800	100
368	16.00	FFR	16.10.1996	48°59.10'	16°24.80'	4803	
369	17.54	MUC	16.10.1996	48°58.01'	16°28.04'	4806	4858
	20.46	MUC	16.10.1996	48°58.02'	16°28.05'	4804	4866
	23.41	MUC	16.10.1996	48°58.03'	16°27.01'	4804	4857
370	06.41	MOC	17.10.1996	48°46.20'	16°18.30'	4803	7632
371	14.19	BWS	17.10.1996	48°42.37'	16°19.29'	4796	4850
372	19.50	MUC	17.10.1996	48°58.00'	16°28.00'	4804	4862
	23.02	GKG	17.10.1996	48°58.00'	16°27.90'	4803	4851
	02.21	MUC	18.10.1996	48°58.00'	16°28.00'	4805	4852
	07.18	MUC	18.10.1996	48°58.01'	16°27.72'	4803	4870
373	07.59	MUC	19.10.1996	48°58.05'	16°27.96'	4802	4854
374	10.28	RK	19.10.1996	48°55.30'	16°27.80'	4803	
375	13.44	MSN	19.10.1996	48°58.30'	16°27.80'	4802	2500
	16.55	CTD	19.10.1996	48°57.85'	16°27.32'	4800	4796
	19.03	MSN	19.10.1996	48°57.20'	16°25.90'	4803	100
	19.56	MSN	19.10.1996	48°57.60'	16°27.10'	4803	700
376	23.50	FTV	19.10.1996	48°51.80'	16°29.10'	4801	5601
	00.42	FTV	20.10.1996	48°50.40'	16°29.60'	4802	6410
377	10.43	SF	20.10.1996	48°55.30'	16°34.70'	4802	
378	13.38	FFR	20.10.1996	48°59.80'	16°24.30'	4802	
379	16.41	RK	20.10.1996	48°55.50'	16°27.40'	4802	
380	19.06	MSN	20.10.1996	48°58.10'	16°28.00'	4803	2500

Station	Time (UTC)	Device	Date	Geographical Position		Water depth (m)	Wire length (m)
				latitude	longitude		
	22.52	CTD	20.10.1996	48°57.84'	16°27.84'	4803	4839
	00.59	MSN	21.10.1996	48°57.90'	16°28.10'	4802	100
	01.44	MSN	21.10.1996	48°57.50'	16°28.10'	4803	700
381	05.47	BWS	21.10.1996	48°57.99'	16°27.73'	4801	4855
382	15.10	MOC	21.10.1996	48°54.20'	16°20.20'	4802	6793
383	23.38	XBT	21.10.1996	48°35.88'	17°27.39	4305	
384	07.51	XBT	22.10.1996	48°05.64'	17°27.40'	4416	
385	16.40	XBT	22.10.1996	47°35.78'	17°27.71'	4154	
386	12.41	CTD	23.10.1996	47°10.93'	19°33.79'	4568	800
387	15.25	SF	23.10.1996	47°07.70'	19°40.40'	4516	
	14.57	MSN	23.10.1996	47°07.70'	19°40.40'	4520	100
388	18.14	MUC	23.10.1996	47°10.95'	19°34.10'	4565	4612
	21.02	MUC	23.10.1996	47°11.20'	19°33.84'	4565	4611
	23.48	MUC	23.10.1996	47°11.00'	19°34.00'	4565	4604
	02.55	MUC	24.10.1996	47°12.00'	19°34.00'	4564	4607
	05.58	MUC	24.10.1996	47°11.99'	19°34.99'	4562	4606
	08.59	MUC	24.10.1996	47°12.02'	19°35.13'	4564	4616
389	11.18	RK	24.10.1996	47°09.90'	19°37.80'	4559	
390	11.56	MSN	24.10.1996	47°11.10'	19°33.90'	4567	100
	13.41	MSN	24.10.1996	47°10.80'	19°34.50'	4565	2500
	16.41	MSN	24.10.1996	47°10.80'	19°34.80'	4564	700
391	18.04	FFR	24.10.1996	47°15.00'	19°32.90'	4557	
392	20.21	CTD	24.10.1996	47°12.04'	19°34.92'	4566	4586
	00.21	XBT	25.10.1996	47°23.40'	19°13.70'	4545	
393	02.40	CTD	25.10.1996	47°35.28'	18°51.73'	4138	700
	05.38	XBT	25.10.1996	47°50.80'	18°30.40'	4515	
394	08.27	CTD	25.10.1996	48°05.83	18°90.49'	4434	700
395	20.51	MUC	25.10.1996	47°11.25'	19°33.92'	4564	4622
	23.29	MUC	25.10.1996	47°11.00'	19°34.00'	4564	4610
	02.23	MUC	26.10.1996	47°10.96'	19°33.90'	4567	4607
	05.17	MUC	26.10.1996	47°11.10'	19°33.92'	4567	4593
396	11.15	RK	28.10.1996	47°09.90'	19°37.50'	4561	
397	12.39	CTD	28.10.1996	47°10.80'	19°33.97'	4566	700
398	16.53	MUC	28.10.1996	47°28.27'	19°40.50'	4530	4596
399	21.33	MUC	28.10.1996	47°11.65'	19°34.14'	4565	4620
	00.26	MUC	29.10.1996	47°10.90'	19°33.86	4565	4601
	03.27	MUC	29.10.1996	47°10.90'	19°34.18'	4567	4610
	06.10	MUC	29.10.1996	47°11.11'	19°34.14'	4566	4603
400	09.39	FFR	29.10.1996	47°14.94'	19°34.25'	4554	

Station	Time (UTC)	Device	Date	Geographical Position		Water depth (m)	Wire length (m)
				latitude	longitude		
401	12.48	SF	29.10.1996	47°08.70'	19°40.30'	4491	
402	16.52	BWS	29.10.1996	47°11.20'	19°32.75'	4565	4615
403	00.09	MOC	30.10.1996	47°14.40'	19°25.10'	4557	6514
404	08.01	CTD	30.10.1996	47°11.05'	19°33.95'	4567	4595
405	11.13	GKG	30.10.1996	47°11.10'	19°33.90'	4565	4609
	13.56	MUC	30.10.1996	47°11.02'	19°34.02'	4565	4609
	16.39	MUC	30.10.1996	47°11.03'	19°34.08'	4566	4632
	19.26	MUC	30.10.1996	47°11.07'	19°34.02'	4566	4623
406	00.06	BWS	31.10.1996	47°10.99'	19°33.99'	4565	4622
407	03.42	CTD	31.10.1996	47°10.93'	19°33.91'	4564	2500
	05.06	APN	31.10.1996	47°11.00'	19°34.00'	4566	70
	05.24	MSN	31.10.1996	47°11.00'	19°34.00'	4564	100
	07.12	MSN	31.10.1996	47°11.00'	19°34.00'	4566	2500
	10.03	MSN	31.10.1996	47°11.00'	19°34.00'	4565	700
408	13.13	MUC	31.10.1996	47°22.00'	19°42.00'	3877	3941
	18.00	XBT	31.10.1996	46°53.10'	18°52.40'	4567	
409	20.32	CTD	31.10.1996	46°35.17'	18°52.64'	4612	700
	21.17	APN	31.10.1996	46°34.50'	18°51.80'	4611	70
	23.07	XBT	31.10.1996	46°20.90'	18°21.90'	3711	
410	01.25	CTD	01.11.1996	46°05.83'	18°09.54'	4116	700
	02.09	APN	01.11.1996	46°05.70'	18°08.80'	4157	70
	04.26	XBT	01.11.1996	45°50.90'	17°48.60'	4005	
411	06.45	CTD	01.11.1996	45°35.94'	17°27.46	4651	700
	07.28	APN	01.11.1996	45°36.10'	17°27.40'	4659	70
	07.42	MUC	01.11.1996	45°35.94'	17°27.46'	4657	4718

Abbreviations:

BWS:	Bottom Water Sampler
GKG:	Box corer
MUC:	Multicorer
CTD:	CTD system with rosette system
APN:	Apstein net
MSN:	Multinet
FFR:	Free Fall Respirometer
RK:	Reusenkette
XBT:	Expandable Bathythermograph
SF:	Sinkstoffalle

8 Concluding Remarks and Acknowledgements

The 36th voyage of RV Meteor served six legs and five major research programmes in which 37 institutes worked together multidisciplinary. The sampling and survey programmes have successfully completed and no loss of equipment has been reported.

It is noteworthy to mention the increasing importance in international inter-laboratory comparability of data sets. For example, currently different international standards are used in order to quantify the oceanic uptake in CO_2. An at-sea intercomparison during the first Meteor Leg 36/1 provided an ideal setting to overcome uncertainties in different underway pCO_2 systems. Such comparisons are important to ascertain a high standard of marine research. Another important aspect of environmental research is the mooring work in physical oceanography, where one of the few long-term current meter stations has been tracked for 16 years. Long term stations also served the Sonderforschungsbereich 313 in recording seasonal changes in the planktonic and benthic faunal assemblages in relation to changes in surface productivity in the Norwegian Sea. A rarely observable chlorophyll-rich layer on the sediment surface was detected. This provides clear evidence for an intense plankton-blooming event in the surface waters.

Long term stations are now investigated in several national and European programmes where, for example, an intermediate nepholoid layer was detected, which is most likely created by the breaking of internal waves on the continental slope. Also, the ocean summer conditions and later, their changes to an autumn situation were documented resembling an early spring bloom which may have supported a CO_2 sink situation during the autumn. Finally, new benthic chamber lander systems for deep-water investigations were moored for several days. They are used for example for in-situ determination of benthic oxygen consumption. In-situ devices are becoming increasingly important not only for biological studies, but also for geophysical studies of the sea floor properties. The High-Frequency Ocean Bottom Hydrophones (HF-OBH) have successfully been deployed in areas where gas hydrates have been identified on seismic records. The HF-OBH data make it possible to obtain a more detailed velocity record from which one can infer the distribution of hydrates in the sediment column. In the future more in-situ deep-water instruments for both short and long-term studies are necessary for a better understanding of the ocean - climate coupling.

The success of the Meteor Legs 1-6 was on one hand due to the captains and their crew who gave support and advice around the clock and provided immeasurable help during the work on deck. On the other hand, the METEOR Leitstelle with Captain Schmickler and the R&F team ensured good organisation of the cruise legs together with the dedication of the scientists. We would like to thank Manon Wilken, Keiko Kähler-Mähl, Marcia Schwartz and Ute Brennwald for helping to complete the cruise report and all the individual teams for their contributions. Finally, the funding by the Deutsche Forschungsgemeinschaft in particular and other funding agencies which allowed to carry out the research are gratefully acknowledged.

9 References

BARNETT, P.R.O., J. WATSON, and D. CONNELLY (1984): A multiple corer for taking virtually undisturbed samples from shelf, bathyal and abyssal sediments. Oceanol. Acta, **7**, 399-408.

BILLETT, D.M.S.,R.S. LAMPITT, A.L. RICE, and R.F.C. MANTOURA (1983): Seasonal sedimentation of phytoplankton to the deep-sea benthos. Nature (Lond.), **302**, 520-522.

BUGGE, T. (1983): Submarine slides on the Norwegian continental margin, with special emphasis on the Storegga area. IKU Publication, 110.

CHESTER R. and K.J.T MURPHY (1990): Metals in the marine atmosphere. In: Heavy metals in the marine environment (P.S. Rainbow and R.W. Furness, Eds.) CRC Press, Boca Raton, Florida, 27-49.

CHRISTIANSEN, B. (1996): Bait-attending amphipods in the deep sea: A comparison of 3 localities in the NE Atlantic. J. mar. biol. Ass. U.K., **76**, 345-360.

CHRISTIANSEN, B. and V. NUPPENAU (in press): The IHF Fototrawl: experiences with a television-controlled, deep-sea epibenthic sledge. Deep-Sea Res.

COWIE G.L. and J.I. HEDGES (1992): Sources and reactivities of amino acids in a coastal marine environment. Limnol. Oceanogr., **37**, 703-724.

DAMUTH, J.E. (1978): Echo character of the Norwegian-Greenland Sea: relationship to Quaternary sedimentation. Marine Geology, **28**, 1-36.

DICKSON, A.G. (1993): pH buffers for sea water media based on the total hydrogen ion concentrations scale. Deep-Sea Res. I, **40**, 107-118.

DOE (1994): Handbook of methods for the analysis of the various parameters of the carbon dioxide system in sea water, Version 2, A.G. Dickson and C. Goyet (Eds.), ORNL/CDIAC-74.

GRASSHOF, M., K. EHRHARDT, and K. KREMLING (1983): Methods of seawater analysis, 2nd edition, Verlag Chemie, Weinheim, 419 pp.

HONJO, S. and S.J. MANGANINI (1993): Annual biogenic particle fluxes to the interior of the North Atlantic Ocean; studied at 34°N 21°W and 48°N 21°W. Deep-Sea Res. I, **40**, 587-607.

JOHNSON K.M, K.D. WILLS, D.B. BUTLER, W.K. JOHNSON, and C.S. WONG (1993): Coulometric total carbon dioxide analysis for marine studies: automation and calibration. Mar. Chem., **44**, 167-187.

JOHNSON, K.M., A. KÖRTZINGER, L. MINTROP, and J.C. DUINKER: Coulometric total carbon dioxide analysis for marine studies: The feasibility of continuous unattended measurements aboard stationary or underway platforms, in prep., to be submitted to Mar. Chem.

KEIL R. G. and D.L. KIRCHMAN (1991): Contribution of dissolved free amino acids and ammonium to the nitrogen requirements of heterotrophic bacterioplankton. Mar. Ecol. Prog. Ser., **73**, 1-10.

KENYON, N.H. (1987): Mass-wasting features on the continental slope of northwest Europe. Marine Geology, **74**, 57-77.

KING, E.L., H.P. SEJRUP, H. HAFLIDASON, A. ELVERHOI, and I. AARSETH (1996): Quaternary seismic stratigraphy of the North Sea Fan: glacially-fed gravity flow aprons, hemipelagic sediments, and large submarine slides. Marine Geology, **130**, 293-315.

KÖRTZINGER A., H. THOMAS, B. SCHNEIDER, N. GRONAU, L. MINTROP, and J.C. DUINKER (1996): At-sea intercalibration of two newly designed underway pCO_2 systems - Encouraging results. Mar. Chem., **52**, 133-145.

KÖRTZINGER A., L. MINTROP and J.C. DUINKER (1997): On the penetration depth and inventory of anthropogenic CO_2 in the North Atlantic Ocean, J. Geophys. Res. (submitted).

KREMLING K. and P. STREU (1993): Saharan dust influenced trace element fluxes in deep North Atlantic subtropical waters, Deep-Sea Res., **40**, 1155-1168.

LOCHTE, K. (1992): Bacterial standing stock and consumption of organic carbon in the benthic boundary layer of the abyssal North Atlantic - In: Deep-sea food chains and the global carbon cycle. G.T. Rowe and V. Pariente (Eds.), Kluwer Academic Publishers, 1-10.

LOCHTE, K. (1993): Mikrobiologie von Tiefseesedimenten. In: Mikrobiologie des Meeresbodens. Meyer-Reil, L.A. and M. Köster (Eds.), Jena, G. Fischer Verlag, 258-282.

LUNDGREEN U. (1996): Aminosäuren im Nordatlantik: Partikelzusammensetzung und Remineralisierung. Kiel, Berichte aus dem Institut für Meerskunde an der Christian-Albrechts-Universität Kiel, 128.

MARTIN J.H. and G.A. KNAUER (1973): The elemental composition of plankton. Geochim. Cosmochim. Acta, **37**, 1639-1653.

MCINTYRE, A. and A.H.W. BÉ (1967): Modern Coccolithophoridae of the Atlantic Ocean. In: Placoliths and Cyrtoliths. Deep Rea Res., **14**, 561-597.

MILLERO F. J., J.Z. ZHANG, K. LEE, and D.M. CAMPBELL (1993): Titration alkalinity of seawater. Mar. Chem., **44**, 153-165.

MINTROP L.: The VINDTA manual, Version 2.0 (June 1996), unpubl.

MÜLLER, P.J. (1977): C/N ratios in Pacific deep-sea semiments: Effect of inorganic ammonium and organic nitrogen compounds sorbed by clays. Geochim. Cosmochim. Acta, **41**, 765-776.

PFANNKUCHE, O. (1992): Organic flux through the benthic community in the temperature abyssal Northeast Atlantic. In: Deep-sea food chains and the global carbon cycle, G.T. Rowe and V. Pariente (Eds.), Kluwer Academic Publishers, 183-198.

PFANNKUCHE, O. (1993): Benthic response to the sedimentation of particulate organic matter at the BIOTRANS station, 47°N, 20°W. Deep-Sea Res. II, **40**, 135-149.

REID, G.S.and D. HAMILTON (1990): A reconnaissance survey of the Whittatrd Sea Fan, Southwestern Approaches, British Isles. Marine Geology, **92**, 69-86.

SAMBROTTO R.N., G. SAVIDGE, C. ROBINSON, P. BOYD, T. TAKAHASHI, D.M. KARL, C. LANGDON, D. CHIPMAN, J. MARRA, and L. CODISPOTI (1993): Elevated consumption of carbon relative to nitrogen in the surface ocean. Nature **363**, 248-250.

SCHÜSSLER U. and K. KREMLING (1993): A pumping system for underway sampling of dissolved and particulate trace elements in near-surface waters, Deep-Sea Res., **40**, 257-266.

SEJRUP, H.P., E.L. KING, I. AARSETH, H. HAFLIDASON, and A. ELVERHOI: Quaternary erosion and depositional processes: Western Norwegian fjords, Norwegian Channel and North Sea Fan. Special Publication of the Geological Society of London (in press).

SPENCER D. W. and P.L. SACHS (1970): Some aspects of the distribution, chemistry, and mineralogy of suspended matter in the Gulf of Maine, Mar. Geol., **9**, 117-136.

STOKER, M.S., K. HITCHEN, and C.C. GRAHAM (1993): United Kingdom offshore regional report: the geology of the Hebrides and West Shetland shelves, and adjacent deep-water areas. (London: HMSO for the British Geological Survey).

TENGBERG, A., F. de BOVEE, P. HALL, W. BERELSON, G. CICCERI, P. CRASSOUS, A. DEVOL, S. EMERSON, R. GLUD, F. GRAZIOTTIN, J. GUNDERSEN, D. HAMMOND, W. HELDER, R. JAHNKE, AQ. KHRIPOUNOFF, V. NUPPENAU, O. PFANNKUCHE, C. REIMERS, G. ROWE, A. SAHAMI, F. SAYLES, M. SCHUSTER, B. WEHRLI, and P. de WILDE (1995): Benthic chamber and profile landers in oceanography - A review of design, technical solutions and functioning. Prog. Oceanography, **35**, 253-294.

WIEBE, P.H., A.W. MORTON, A.M. BRADLEY, R.H. BACKHUS, J.E. CRADDOCK, V. BARBER, T.J. COWLES, and G.R. FLIERL (1985): New developments in the MOCNESS, an apparatus for sampling zooplankton and micronekton. Mar. Biol., **87**, 313-323.

WILLIAMS P.J. le B.T. Berman, and O. HOLM-HANSEN (1976): Amino acid uptake and respiration by marine heterotrophs. Mar. Biol., **35**, 41-47.

Publications from METEOR expeditions in other reports

Gerlach, S.A., J. Thiede, G. Graf und F. Werner (1986): Forschungsschiff Meteor, Reise 2 vom 19. Juni bis 16. Juli 1986. Forschungsschiff Poseidon, Reise 128 vom 7. Mai bis 8. Juni 1986. Ber. Sonderforschungsbereich 313, Univ. Kiel, 4, 140 S.

Siedler, G., H. Schmickler, T.J. Müller, H.-W. Schenke und W. Zenk (1987): Forschungsschiff Meteor, Reise Nr. 4, Kapverden - Expedition, Oktober - Dezember 1986. Ber. Inst. f. Meeresk., 173, Kiel, 123 S.

Wefer, G., G.F. Lutze, T.J. Müller, O. Pfannkuche, W. Schenke, G. Siedler und W. Zenk (1988): Kurzbericht über die Meteor - Expedition Nr. 6, Hamburg - Hamburg, 28. Oktober 1987 - 19. Mai 1988. Berichte, Fachbereich Geowissenschaften, Universität Bremen, 4, 29 S.

Müller T.J., G. Siedler und W. Zenk (1988): Forschungsschiff Meteor, Reise Nr. 6, Atlantik 87/88, Fahrtabschnitte Nr. 1 - 3, Oktober - Dezember 1987. Ber. Inst. f. Meeresk., 184, Kiel, 77 S.

Lutze, G.F., C.O.C. Agwu, A. Altenbach, U. Henken-Mellies, C. Kothe, N. Mühlhan, U. Pflaumann, C. Samtleben, M. Sarnthein, M. Segl, Th. Soltwedel, U. Stute, R. Tiedemann und P. Weinholz (1988): Bericht über die "Meteor" -Fahrt 6-5, Dakar - Libreville, 15.1.-16.2.1988.Berichte - Reports, Geol. Paläont. Inst., Univ. Kiel, 22, 60 S.

Wefer, G., U. Bleil, P.J. Müller, H.D. Schulz, W.H.Berger, U. Brathauer, L. Brück, A. Dahmke, K. Dehning, M.L. Durate-Morais, F. Fürsich, S. Hinrichs, K. Klockgeter, A. Kölling, C. Kothe, J.F. Makaya, H. Oberhänsli, W. Oschmann, J. Posny, F. Rostek, H. Schmidt, R. Schneider, M. Segl, M. Sobiesiak, T. Soltwedel und V. Spieß (1988): Bericht über die Meteor - Fahrt M 6-6, Libreville - Las Palmas, 18.2.1988 - 23.2.1988. Berichte, Fachbereich Geowissenschaften, Universität Bremen, 3, 97 S.

Hirschleber, H., F. Theilen, W. Balzer, B. v. Bodungen und J. Thiede (1988): Forschungsschiff Meteor, Reise 7, vom 1. Juni bis 28. September 1988, Ber. Sonderforschungsbereich 313, Univ. Kiel, 10, 358 S.

METEOR-Berichte
List of publications

89-1	(1989) Meincke, J., Quadfasel, D.	GRÖNLANDSEE 1988-Expedition, Reise Nr. 8, 27. Oktober 1988 - 18. Dezember 1988. Universität Hamburg, 40 S.
89-2	(1989) Zenk, W., Müller, T.J., Wefer, G.	BARLAVENTO-Expedition, Reise Nr. 9, 29. Dezember 1988 - 17. März 1989. Universität Hamburg, 238 S.
90-1	(1990) Zeitschel, B., Lenz, J., Thiel, H., Boje, R., Stuhr, A., Passow, U.	PLANKTON'89 - BENTHOS'89, Reise Nr. 10, 19. März - 31. August 1989. Universität Hamburg, 216 S.
90-2	(1990) Roether, W., Sarnthein, M., Müller, T.J., Nellen, W., Sahrhage, D.	SÜDATLANTIK-ZIRKUMPOLARSTROM, Reise Nr. 11, 3. Oktober 1989 - 11. März 1990. Universität Hamburg, 169 S.
91-1	(1991) Wefer, G., Weigel, W., Pfannkuche	OSTATLANTIK 90 - EXPEDITION, Reise Nr. 12, 13. März - 30. Juni 1990. Universität Hamburg, 166 S.
91-2	(1991) Gerlach, S.A., Graf, G.	EUROPÄISCHES NORDMEER, Reise Nr. 13, 6. Juli - 24. August 1990. Universität Hamburg, 217 S.
91-3	(1991) Hinz, K., Hasse, L., Schott, F.	SUBTROPISCHER & TROPISCHER ATLANTIK, Reise Nr. 14/1-3, Maritime Meteorologie und Physikalische Ozeanographie, 17. September - 30. Dezember 1990. Universität Hamburg, 58 S.
91-4	(1991) Hinz, K.	SUBTROPISCHER & TROPISCHER ATLANTIK, Reise Nr. 14/3, Geophysik, 31. Oktober - 30. Dezember 1990. Universität Hamburg, 94 S.
92-1	(1992) Siedler, G., Zenk, W.	WOCE Südatlantik 1991, Reise Nr. 15, 30. Dezember 1990 - 23. März 1991. Universität Hamburg, 126 S.
92-2	(1992) Wefer, G., Schulz, H.D., Schott, F., Hirschleber, H. B.	ATLANTIK 91 - EXPEDITION, Reise Nr. 16, 27. März - 8. Juli 1991. Universität Hamburg, 288 S.

92-3	(1992) Suess, E., Altenbach, A.V.	EUROPÄISCHES NORDMEER, Reise Nr. 17, 15. Juli - 29. August 1991. Universität Hamburg, 164 S.
93-1	(1993) Meincke, J., Becker, G.	WOCE-NORD, Cruise No. 18, 2. September - 26. September 1991. NORDSEE, Cruise No. 19, 30 September - 12 October 1991. Universität Hamburg, 105 pp.
93-2	(1993) Wefer, G., Schulz, H.D.	OSTATLANTIK 91/92 - EXPEDITION, Reise Nr. 20, M 20/1 und M 20/2, 18. November 1991 - 3. Februar 1992. Universität Hamburg, 248 S.
93-3	(1993) Wefer, G., Hinz, K., Roeser, H.A.	OSTATLANTIK 91/92 - EXPEDITION, Reise Nr. 20, M 20/3, 4. Februar - 13. März 1992. Universität Hamburg, 145 S.
93-4	(1993) Pfannkuche, O., Duinker, J.C., Graf, G., Henrich, R., Thiel, H., Zeitschel, B.	NORDATLANTIK 92, Reise Nr. 21, 16. März - 31. August 1992. Universität Hamburg, 281 S.
93-5	(1993) Siedler, G., Balzer, W., Müller, T.J., Rhein, M., Onken, R., Zenk, W.	WOCE South Atlantic 1992, Cruise No. 22, 22 September 1992 - 31 January 1993. Universität Hamburg, 131 pp.
94-1	(1994) Bleil, U., Spieß, V., Wefer, G.	Geo Bremen SOUTH ATLANTIC 1993, Cruise No. 23, 4 February - 12 April 1993. Universität Hamburg, 261 pp.
94-2	(1994) Schmincke, H.-U., Rihm, O.	OZEANVULKAN 1993, Cruise No. 24, 15 April - 9 May 1993. Universität Hamburg, 88 pp.
94-3	(1994) Hieke, W., Halbach, P., Türkay, M., Weikert, H.	MITTELMEER 1993, Cruise No. 25, 12 May - 20 August 1993. Universität Hamburg, 243 pp.
94-4	(1994) Suess, E., Kremling, K., Mienert, J.	NORDATLANTIK 1993, Cruise No. 26, 24 August - 26 November 1993. Universität Hamburg, 256 pp.

94-5	(1994) Bröckel, K. von, Thiel, H., Krause, G.	ÜBERFÜHRUNGSFAHRT, Reise Nr. 0, 15. März - 15. Mai 1986. ERPROBUNGSFAHRT, Reise Nr. 1, 16. Mai - 14. Juni 1986. BIOTRANS IV, Skagerrak 86, Reise Nr. 3, 21. Juli - 28. August 1986. Universität Hamburg, 126 S.
94-6	(1994) Pfannkuche, O., Balzer, W., Schott, F.	CARBON CYCLE AND TRANSPORT OF WATER MASSES IN THE NORTH ATLANTIC - THE WINTER SITUATION, Cruise No. 27, 29 December - 26 March 1994. Universität Hamburg, 134 pp.
95-1	(1995) Zenk, W., Müller, T.J.	WOCE Studies in the South Atlantic, Cruise No. 28, 29 March - 14 June 1994. Universität Hamburg, 193 pp.
95-2	(1995) Schulz, H., Bleil, U., Henrich, R., Segl, M.	Geo Bremen SOUTH ATLANTIC 1994, Cruise No. 29, 17 June - 5 September 1994. Universität Hamburg, 323 pp.
96-1	(1996) Nellen, W., Bettac, W., Roether, W., Schnack, D., Thiel, H., Weikert, H., Zeitschel, B.	MINDIK (Band I), Reise Nr. 5, 2. Januar - 24. September 1987. Universität Hamburg, 275 S.
96-2	(1996) Nellen, W., Bettac, W., Roether, W., Schnack, D., Thiel, H., Weikert, H., Zeitschel, B.	MINDIK (Band II), Reise Nr. 5, 2. Januar - 24. September 1987. Universität Hamburg, 179 S.
96-3	(1996) Koltermann, K.P., Pfannkuche, O., Meincke, J.	JGOFS, OMEX and WOCE in the North Atlantic 1994, Cruise No. 30, 7 September - 22 December 1994. Universität Hamburg, 148 pp.
96-4	(1996) Hemleben, Ch., Roether, W., Stoffers, P.	Östliches Mittelmeer, Rotes Meer, Arabisches Meer, Cruise No. 31, 30 December 1994 - 22 March 1995. Universität Hamburg, 282 pp.

96-5	(1996) Lochte, K., Halbach, P., Flemming, B.W.	Biogeochemical Fluxes in the Deep-Sea and Investigations of Geological Structures in the Indian Ocean, Cruise No. 33, 22 September - 30 December 1995. Universität Hamburg, 160 pp.
96-6	(1996) Schott, F., Pollehne, F., Quadfasel, D., Stramma, L., Wiesner, M., Zeitzschel, B.	ARABIAN SEA 1995, Cruise No. 32, 23 March - 19 September 1995. Universität Hamburg, 163 pp
97-1	(1997) Wefer, G. Bleil, U. Schulz, H. Fischer, G.	Geo Bremen SOUTH ATLANTIC 1996 (Volume I), Cruise No. 34, 3 January - 18 February 1996. Universität Hamburg, 254 pp.
97-2	(1997) Wefer, G. Bleil, U. Schulz, H. Fischer, G.	Geo Bremen SOUTH ATLANTIC 1996 (Volume II), Cruise No. 34, 21 February - 15 April 1996. Universität Hamburg, 268 pp.
97-3	(1997) Wefer, G.	10 Jahre Forschungsschiff METEOR (1986 - 1996) - Dokumentation der Fahrten M0 - M34 (Volume I), Cruise No. 0-17. Universität Hamburg, 269 pp.
97-4	(1997) Wefer, G.	10 Jahre Forschungsschiff METEOR (1986 - 1996) - Dokumentation der Fahrten M0 - M34 (Volume II), Cruise No. 18-34. Universität Hamburg, 236 pp.
98-1	(1998) Wefer, G. Müller, T.J.	Canary Islands 1996/97, Cruise No. 37, 4 December 1996 - 22 January 1997. Universität Hamburg, 134 pp.
98-2	(1998) Mienert, J. Graf, G. Hemleben, C. Kremling, K. Pfannkuche, O. Schulz-Bull, D.	Nordatlantik 1996, Cruise No. 36, 6 June 1996 - 4 November 1996. Universität Hamburg, 302 pp.